

Durham E-Theses

*A study of the ring opening metathesis polymerization
of polycyclic aromatic monomers and cyclopentenes
with well defined initiators*

Keiji Sugawara

How to cite:

Sugawara, Keiji (1994) A study of the ring opening metathesis polymerization of polycyclic aromatic monomers and cyclopentenes with well defined initiators. Doctoral thesis, Durham University.

Use policy

The full-text may be used and/or reproduced, and given to third parties in any format or medium, without prior permission or charge, for personal research or study, educational, or not-for-profit purposes provided that:

- a full bibliographic reference is made to the original source
- a <https://etheses.durham.ac.uk/id/eprint/5143/> is made to the metadata record in Durham E-Theses
- the full-text is not changed in any way

The full-text must not be sold in any format or medium without the formal permission of the copyright holders.

Please consult the [full Durham E-Theses policy](#) for further details.

**A study of the ring opening metathesis polymerization
of polycyclic aromatic monomers and cyclopentenes
with well defined initiators**

by
Keiji Sugawara

The copyright of this thesis rests with the author.
No quotation from it should be published without
his prior written consent and information derived
from it should be acknowledged.

A thesis submitted to the University of Durham for the degree of
Doctor of philosophy

July 1994



12 SEP 1994

Abstract

A Study of the Ring Opening Metathesis Polymerisation of Polycyclic Aromatic Monomers and Cyclopentenes with Well Defined Initiators

This thesis describes studies into the ring opening metathesis polymerisation (ROMP) of polycyclic aromatic monomers and cyclopentenes.

Chapter 1 reviews general aspects of ring opening metathesis polymerisation of relevance to the themes of this thesis.

Chapter 2 describes the synthesis of polycyclic aromatic monomers, the endo and the exo Diels-Alder adducts of acenaphthylene and cyclopentadiene.

Chapter 3 reports a study on the polymerisation of these monomers using well defined initiators and classical catalyst systems.

Chapter 4 describes the synthesis of a substituted cyclopentene.

Chapter 5 reports an investigation of polymerisation of cyclopentene using a variety of well defined initiators of general formula $M(=NAr)(-OR)_2(=CHR)$ where $M=Mo$ or W .

Chapter 6 presents a study on the polymerisation of a substituted cyclopentene, 4-methylcyclopentene, using a series of well defined initiators, and the characterisations of the polymers obtained using infrared, 1H , and ^{13}C n.m.r. spectroscopy, differential scanning calorimetry, and gel permeation chromatography and an analysis of detailed microstructure with respect to meso/racemic configurations in the polymer chain.

Finally, Chapter 7 summarises the conclusions and makes some suggestions for future work.

Acknowledgements

This work and thesis would not have been possible without the contribution and help of many colleagues whom I would like to thank.

Professor W. J. Feast for his continuous patient guidance, support and encouragement to my work and life.

Dr. B. Wilson and Dr. E. Khosravi for their helpful advice; Dr. P. Dounis for his helpful advice about experimental technique and encouragement; Dr. A. Kenwright for help with interpretation and presentation of the n.m.r. spectra and Mrs. J. Say for recording them. Mr. G. Forrest for his help with the GPC and DSC. Mr. R. Hart and Mr. G. Haswell for providing the glassware, and all the staff of the Chemistry Department for their assistance. All my colleagues in the IRC for their help and kindness.

NKK Corporation for giving me a chance to study in the IRC.

My wife Etsuko and mother Michiko and father Kazumasa for their love and consideration.

Memorandum

The work reported in this thesis was carried out at the Interdisciplinary Research Centre in Polymer Science and Technology at Durham University between August 1992 and July 1994. This work has not been submitted for any other degree and is the original work of the author except where acknowledged by reference.

Copyright

The copyright of this thesis rests with the author. No quotation from it should be published without his prior written consent and information derived from it should be acknowledged.

CONTENTS

	<i>page</i>
Abstract	<i>ii</i>
Acknowledgments	<i>iii</i>
Memorandum	<i>iii</i>
Copyright	<i>iii</i>
Contents	<i>iv</i>
CHAPTER 1: General introduction and background	<i>1</i>
1.1 The origins and background of olefin metathesis	<i>1</i>
1.2 Metathesis polymerisation	<i>2</i>
1.3 Catalyst systems for metathesis polymerisation	<i>4</i>
1.3.1 Survey of catalyst systems	<i>4</i>
(a) Heterogeneous catalysts	<i>4</i>
(b) Homogeneous catalysts	<i>5</i>
b (i) Two or three component systems involving cocatalysts and / or promoters	<i>5</i>
b (ii) Compounds that do not contain a pregenerated metal carbene, a metallacyclobutane or an alkyl, aryl or allyl containing species.	<i>6</i>
b (iii) Carbene catalyst systems	<i>7</i>
b (iv) Metallacyclobutane catalyst systems	<i>10</i>
1.3.2 Classical catalyst systems and well defined initiator systems for polymerisation	<i>11</i>
1.4 Mechanism of metathesis polymerisation	<i>13</i>
1.5 Termination of ring opening metathesis polymerisation	<i>17</i>

1.6 Chain transfer reaction	18
1.7 Thermodynamic arguments and polymerisability of monocyclic alkenes	19
1.8 Microstructure and stereochemistry of ring opening metathesis polymerisations	20
(i) Cis / trans double bond isomerism	21
(ii) Tacticity effects	21
(iii) Head/tail isomerism	23

CHAPTER 2: Synthesis of acenaphthylene-cyclopentadiene Diels-Alder adducts 25

2.1 Introduction	25
2.2 Synthesis of acenaphthylene-cyclopentadiene Diels-Alder adducts	25
2.3. Experimental	30

CHAPTER 3: The ring opening metathesis polymerisation of the Diels-Alder adducts of cyclopentadiene and acenaphthylene 32

3.1 Introduction	32
3.2 Polymerisation of the endo-adduct using well defined initiators	34
3.3 Characterization of the polymer of endo-adduct obtained using well defined initiators	43
3.3.1 Infrared spectroscopy	43
3.3.2 Nuclear magnetic resonance spectroscopy	43
3.4 Attempted polymerisation of the exo-adduct	46
3.5 Polymerisation of endo and exo adducts mixture	47
3.6 Summary and Discussion	51

3.7 Experimental	53
a) Polymerisation using well defined initiators	53
b) Polymerisation using classical catalysts	54
(b-i) Polymerisation initiated by tungsten catalyst	54
(b-ii) Polymerisation initiated by molybdenum catalyst	54
CHAPTER 4: Synthesis of 4-methylcyclopentene	55
4.1 Introduction	55
4.2 Results and discussion	55
4.2.1 Synthesis of 3-cyclopentene-1-carboxylic acid	58
4.2.2 Synthesis of 4-hydroxymethylcyclopentene	62
4.2.3 Synthesis of 3-cyclopentenemethyl p-toluenesulfonate	62
4.2.4 Synthesis of 4-methylcyclopentene	64
4.3 Experimental	66
Dimethyl 3-cyclopentene-1,1-dicarboxylate	66
3-Cyclopentene-1,1-dicarboxylic acid	67
3-Cyclopentenecarboxylic acid	67
4-Hydroxymethylcyclopentene	68
3-Cyclopentenemethyl p-toluenesulfonate	69
4-Methylcyclopentene	70
CHAPTER 5: Polymerisation of cyclopentene and characterisation of the polymers obtained	71
5.1 Introduction	71
5.2 Polymerisation of cyclopentene	73

5.2.1	Reproducibility in the polymerisation of cyclopentene	74
5.2.2	Polymerisation of cyclopentene under various conditions	76
a)	Polymerisation using the t-butoxy molybdenum initiator	77
b)	Polymerisation using the trifluorinated butoxy molybdenum initiator	79
c)	Polymerisation using the t-butoxy tungsten initiator	80
5.3	Characterisation of the polymers obtained	83
5.3.1	Characterisation by infrared spectroscopy	83
5.3.2	Characterisation by ^1H nuclear magnetic resonance spectroscopy	83
5.3.3	Introduction to characterisation of polyalkenamers by ^{13}C nuclear magnetic resonance spectroscopy	84
5.3.4	Reproducibility of the microstructure of the polymers produced	86
5.3.5	Characterisation of the polymers by ^{13}C n.m.r. spectroscopy as a function of reaction conditions in synthesis	89
a)	Examination of the polymerisation using the t-butoxy molybdenum initiator	89
b)	Examination of the polymerisation using the fluorinated butoxy molybdenum initiator	90
c)	Examination using t-butoxy tungsten initiator	90
5.3.6	Thermal characterisation	91
5.4	Summary and discussion	92
5.5	Experimental	94
 CHAPTER 6: Polymerisation of 4-methylcyclopentene		97
6.1	Introduction	97
6.2	Polymerisation of 4-methylcyclopentene	98
6.3	Characterisation of the polymers obtained	100
6.3.1	Characterisation by infrared spectroscopy	100

6.3.2	Characterisation by ^1H n.m.r. spectroscopy	101
6.3.3	Characterisation by ^{13}C n.m.r. spectroscopy	102
6.4	Hydrogenation of the polymer obtained	105
6.5	The detailed examination of the microstructures of poly(4-methyl-1-pentenylene) and poly(1-methylpentamethylene)	107
6.6	Thermal properties of the polymers obtained	115
6.7	Discussion	116
6.7.1	Thermodynamics	116
6.7.2	Microstructure	120
6.8	Experimental	122
 CHAPTER 7: Conclusion and proposals for future work		 123

APPENDIXES

APPENDIX 1	General procedures, equipment and instrumentation
APPENDIX 2	Analytical data for Chapter 2
APPENDIX 3	Analytical data for Chapter 3
APPENDIX 4	Analytical data for Chapter 4
APPENDIX 5	Analytical data for Chapter 5
APPENDIX 6	Analytical data for Chapter 6
APPENDIX 7	References
APPENDIX 8	Lectures and conferences attended

CHAPTER 1: General introduction and background

1.1 The origins and background of olefin metathesis

In the presence of a variety of catalysts, most commonly containing tungsten, molybdenum or rhenium with either organotin or aluminium compounds, alkenes undergo the metathesis reaction in accordance with Figure 1.1. The reaction may be considered as a bond-reorganization process and proceeds via the cleavage and reformation of the double bonds.

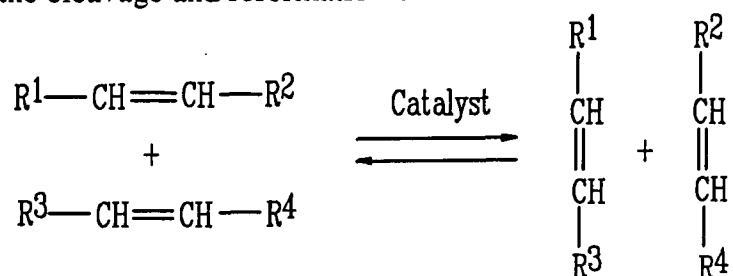


Figure 1.1. General equation for the metathesis of an acyclic alkene

This reaction is characterized by the fact that the total number and types of chemical bonds remains unchanged during the transformation of the reactants into products. There has been major development of the metathesis reaction of alkenes in the field of hydrocarbon chemistry during the last three decades. The versatility of the metathesis reaction gives not only a novel method for organic synthesis but also some new developments for the chemical industry.

In 1964, Banks and Bailey¹ reported the first example of the metathesis reaction of linear alkenes. The reaction was described as "olefin disproportionation" and it converted an unsymmetrical linear olefin into equimolar amounts of higher and lower molecular weight olefins. They used heterogeneous catalysts made from molybdenum or tungsten hexacarbonyls deposited on alumina and they examined linear olefins with three to eight carbon

atoms. This early work opened the way for the development and study of a very important new field of organic chemistry and especially gave an impetus for better understanding of the reactivity of organometallic compounds in polymerisation. The metathesis reaction has been investigated intensively and many kinds of reactant types have been studied, including alkenes, dienes, polyenes, alkynes, and cycloalkenes. The last mentioned reactants giving rise to interesting polymeric and/or macrocyclic products as shown in Figure 1.2.

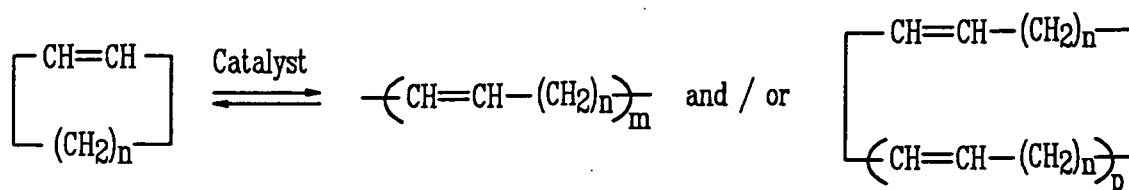


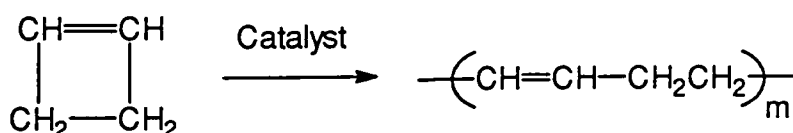
Figure 1.2. Formation of polymer and macrocyclic alkenes

1.2 Metathesis polymerisation

In 1968 Calderon² and Wassermann³ recognized this ring opening polymerisation as a special case of olefin metathesis. In fact the first description of an olefin metathesis reaction catalysed by a transition metal compound had been reported by Anderson and Merckling^{4,5} in 1955, when they successfully polymerised bicyclo[2.2.1]hept-2-ene (norbornene) to a high molecular weight polymer using a mixture of ethyl magnesium bromide and titanium tetrachloride. Initially the structure of the polymer was not appreciated, but later Truett and co-workers^{6,7} demonstrated that the catalyst system used by Anderson and Merckling resulted in ring opening polymerisation. In 1963 Eleuterio^{8,9} reported the ring opening polymerisation of a variety of cycloolefins, using a catalyst derived from molybdenum oxide on alumina, activated by hydrogen reduction and further reacted with aluminium hydride. He polymerised cycloalkenes such as, bicyclo[2.2.1]hept-2-ene, tricyclo[5.2.1.0^{2,6}]dec-8-ene, that is, the partially

hydrogenated dimer of cyclopentadiene, and cyclopentene. In the case of cyclopentene, trans-poly(1-pentenylene) was formed with a high degree of stereoregularity but only low yield. In 1963, Dall'Asta and Natta,^{5,10} demonstrated the possibility of producing stereoregular polymers from cycloalkenes using different catalyst systems and reaction conditions; some of their results are listed in Table 1.1., by way of illustration.

Table 1.1. Polymerisation of cyclobutene¹⁰



Catalyst system	Polymer structure
TiCl ₄ /Et ₃ Al/n-heptane	mainly cis
TiCl ₄ /R ₃ Al/toluene	mainly trans
MoCl ₅ /Et ₃ Al/toluene	mainly cis
RuCl ₃ /H ₂ O	cis:trans = 50:50
RuCl ₃ /EtOH	trans

In 1964 the same authors^{7,11} investigated tungsten and molybdenum halides in combination with organoaluminium compounds as catalysts, cyclopentene was polymerised by ring opening under mild conditions, again stereoselectivity was demonstrated. In 1967 Calderon et al.^{9,10,12,13} were the first to use the term "olefin metathesis" for the overall result of the reaction in which they converted 2-pentene into a mixture containing, at equilibrium, a 25:50:25 molar ratio of 2-butene, 2-pentene and 3-hexene respectively: the catalyst system used was WCl₆/EtAlCl₂/EtOH. This result was very important in the evolution of the metathesis concept because it demonstrated that ring opening reactions and the

reactions of acyclic olefins belonged to the same class of reaction and were effected by similar catalysts. This observation was the beginning of the big increase in the number of papers concerned with metathesis reactions, and already many reviews of the expanding literature of this subject have been published.¹⁴⁻¹⁸

1.3 Catalyst systems for metathesis polymerisation

A number of catalyst systems are known to initiate olefin metathesis, the most important are the organometallic compounds which contain the Group IVA, VA, VIA, VIIA, and VIII transition metals shown in Table 1.2. Molybdenum, tungsten and rhenium generally provide most effective catalyst systems. Although non-transition metal compounds, such as $Al_2O_3/EtAlCl_2$, have been reported to be catalysts for olefin metathesis, the number of examples of such systems is restricted.

Table 1.2. Transition metals used in catalyst systems for metathesis

IVA	VA	VIA	VIIA	VIII
Ti	V	Cr		
Zr	Nb	Mo		Ru Rh
Hf	Ta	W	Re	Os Ir

1.3.1 Survey of catalyst systems

The catalysts are generally classified into two types; namely, either heterogeneous or homogeneous systems.

(a) Heterogeneous catalysts comprise of two main components; a support, such as alumina or silica, with a high surface-area on which transition metal promoters

such as oxides, sulfides or carbonyls of metals are deposited. Usually a third component is introduced to reduce the poisoning of the catalyst and increase the reactivity or to reduce side reactions such as double bond migration.¹⁹ The catalysts derived from oxides and carbonyls of molybdenum, tungsten and rhenium have the greatest activity,^{1,20-22} whilst the remainder are less effective.²³ Sulfides of molybdenum and tungsten provide poor catalysts,²⁴ but in special conditions MoS₂ alone can be quite active.²⁵ The preparation of heterogeneous catalysts may be carried out in many ways. The three main methods are: (i) dry mixing, (ii) coprecipitation and (iii) impregnation of the support with a precursor compound that decomposes at high temperature to leave the catalyst. The catalysts are activated in an inert atmosphere and used with cocatalysts and/or promoters. The selectivity of these reactions is always below 100% due to the numerous side reactions that occur, for example, polymerisation and isomerisation, which can be minimized to a certain extent by the addition of alkali²⁶ or alkaline earth²⁷ metals or copper or silver²⁸ before catalyst activation. Heterogeneous catalysts can promote metathesis of acyclic olefins but they are rarely used for ring opening polymerisation.

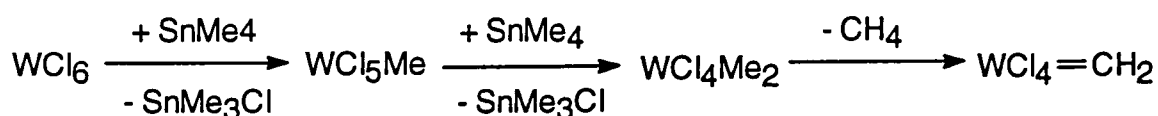
(b) Homogeneous catalysts are usually used in the liquid phase, either in neat monomer or dissolved in a solvent, and although they are termed homogeneous catalysts, some of them may react as finely divided heterogeneous catalysts.

The classical supposedly homogeneous catalyst systems can be divided into four main categories:

b (i) Two or three component systems involving cocatalysts and/or promoters.

This type of classical initiator usually consists of two main components, a transition metal compound (most often the chloride) of tungsten, molybdenum, rhenium or tantalum and a co-catalyst which is usually an organometallic

compound from groups I to IV, in some cases addition of a third component which can be an oxygenated compound such as an alcohol, an ether, a peroxide or water, improves the effectiveness of the catalyst system.²⁹ The metal carbene is generated by the reaction between the two main components. Ultra-violet spectroscopic studies of the WCl_6/Me_4Sn system led to the proposed mechanism for metal carbene formation shown below. The reaction is complex and many side reactions are possible.



In 1967 Calderon and Scott¹³ were the first to describe homogeneous catalysts for olefin metathesis. At that time tungsten compounds gave the most efficient catalysts for ring opening polymerisation of cyclic olefins, and a large number of catalysts were derived from WCl_6 combined with suitable co-catalysts. These kinds of reactions are usually conducted in the liquid phase in neat monomer, or in a solvent. Developments of these initial observations included the use of photochemically activated catalysts such as $W(CO)_6$,³⁰ WCl_6 ,³¹ and $TiCl_4$ ³² and the observation that metal carbenes such as $(CO)_5W=CPh_2$ are active in the ring opening polymerisation of cycloalkenes.

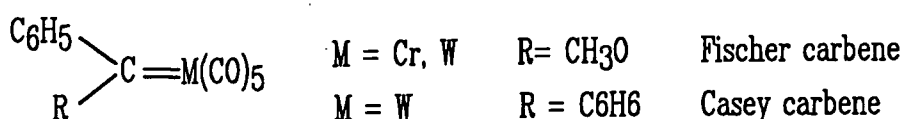
b (ii) Compounds that do not contain a pregenerated metal carbene, a metallacyclobutane or an alkyl, aryl or allyl containing species.

Examples of this kind of system are the transition metal halides: WCl_6 , $ReCl_5$, $RuCl_3$, $OsCl_3$ and $IrCl_3$. This kind of initiator is presumed to generate a metal carbene *in situ* by the reaction of the transition metal halide with monomer, although activators are sometimes required, for example, oxygen, water or ethanol.

Ruthenium, osmium and iridium hydrated trichlorides ($XCl_3 \cdot H_2O$) are unique in that they were found to initiate ring opening metathesis polymerisation in protic media (water and ethanol), unlike most other metathesis catalysts, which are destroyed by such solvents. These aqueous initiators are capable of polymerising strained ring monocyclic olefins (e.g. cyclobutene, substituted norbornenes and 7-oxanorbornenes) in alcoholic and emulsified aqueous systems between 20-100°C.

b (iii) Carbene catalyst systems

Since the discovery of metal carbenes in 1964,³³ a number of this type of organometallic complex have been synthesised and examined, and many of these have been shown to be capable of inducing the olefin metathesis reaction. The first isolated metal carbene species, the Fischer carbene,³⁴ was a heteroatom stabilized complex and was shown to be reactive in olefin metathesis. It reacted with strained olefins such as cyclobutene and norbornene derivatives,³⁵ while the diphenyl carbene complex first synthesized by Casey and Burkhardt in 1973, which wasn't stabilized by an heteroatom, was much more reactive and can initiate the polymerisation of less strained cyclic olefins.^{36,37}



Recently, four coordinate alkylidene complexes of tungsten and molybdenum were isolated which were highly active in olefin metathesis.^{38,39} The general structure of these complexes is $[\text{M}(\text{CHBu})(\text{NAr})(\text{OR})_2]$ and they possess the bulky imido ligand (2,6-diisopropylphenyl imido) and alkoxide groups as well as the active alkylidene. Substitution of the methyl groups on the alkoxides with the more electronegative trifluoromethyl groups makes this complex more active since the trifluoro groups draw electron density away from the metal centre, which makes the metal centre of the complex more electrophilic

and a better acceptor for the incoming olefin which can be regarded as a π -donor.^{40,41} This effect is demonstrated by the observation that when OR is OMe(CF₃)₂ the tungsten complex will readily metathesis acyclic olefins but when OR is O-t-Bu it does not react with acyclic olefins readily. Several examples of this kind of metal carbene are shown in Figure 1.3. and an outline of the synthesis of such a metal carbene is shown in Figure 1.4. overleaf.

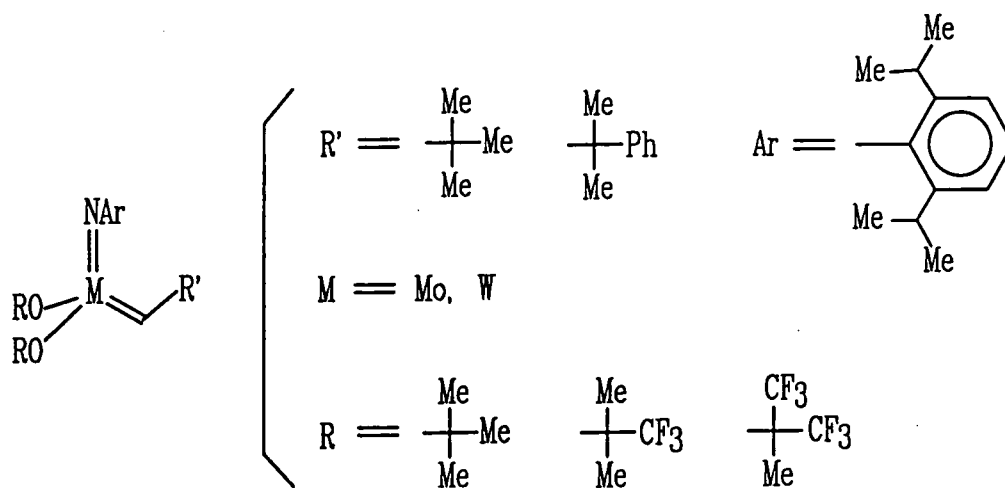
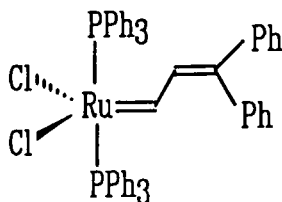


Figure 1.3. Some Schrock-type metal carbene complexes used for metathesis

Investigations of the use of such well defined metal carbenes in metathesis reactions have been very fruitful during the last decade and this phenomena looks likely to continue. For example Grubbs⁴² recently reported the preparation of a stable ruthenium metal carbene complex, shown below, which is able to initiate the living ring opening metathesis polymerisation of strained cyclic olefins, even in the presence of protic solvents such as ethanol or water.



Ruthenium carbene reported by Grubbs

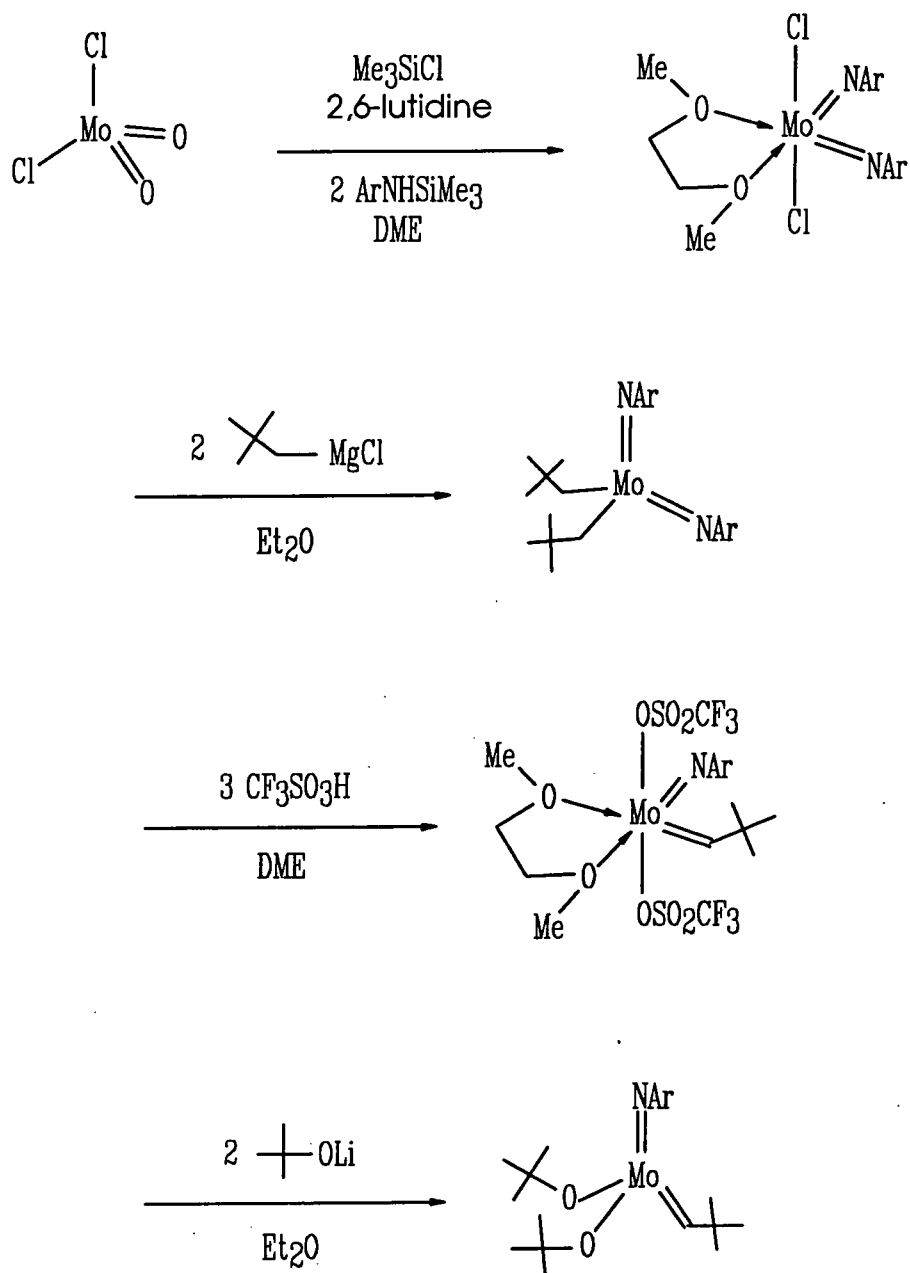


Figure 1.4. Outline of the synthetic route to the metal carbene



b (iv) Metallacyclobutane catalyst systems

The first well defined metallacyclo complexes isolated and found to be active as metathesis catalysts were prepared by Grubbs and co-workers. They reported that the reaction of Tebbe reagent with various olefins in the presence of nitrogen bases resulted in the formation of titanacyclobutane complexes,^{43,44} and it has been shown that these titanacycles readily exchange with added olefins⁴⁵ via a rate-determining loss of olefin from the titanacyclobutane ring to generate the transition metal methylene species $\text{Cp}_2\text{Ti}=\text{CH}_2$ which is active in metathesis as shown in Figure 1.5.

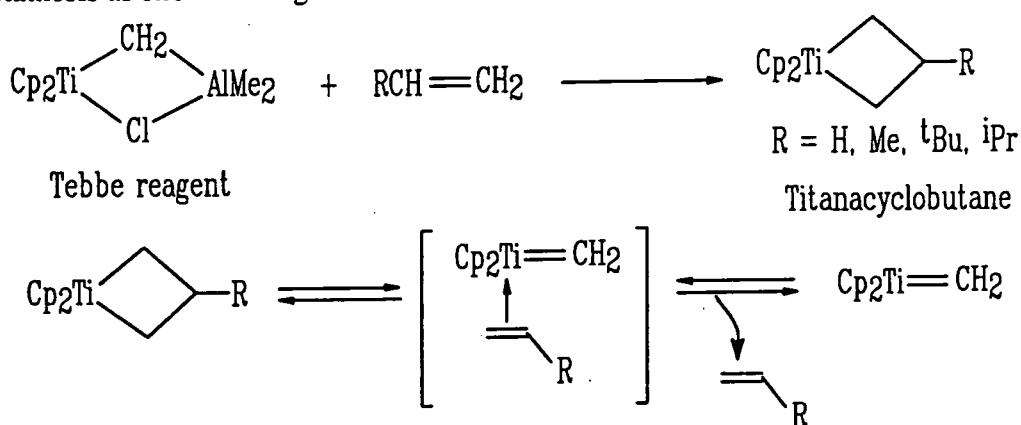


Figure 1.5. Formation of metallacyclobutane and methylene species

They also demonstrated that this type of catalyst is able to polymerise norbornene and produce living polynorbornene with a narrow molecular weight distribution.⁴⁶ These initiators are remarkable amongst catalyst systems since the metallacyclobutane is the stable, "resting", chain carrying species rather than the metal carbene.

As described above, Schrock and Grubbs have reported a series of transition metal carbenes or metallacyclobutanes, which are able to initiate living ring opening metathesis polymerisation of cyclic olefins, and these complexes are generally called well defined initiators.

1.3.2 Classical catalyst systems and well defined initiator systems for polymerisation

The well defined initiators described above have many advantages compared to classical catalyst systems. In the case of polymerisation using classical catalyst systems :-

(i) There is a lack of molecular weight control, due to the generally high activity of the $M=C$ bond which tends to react with the $C=C$ bonds in the polymer chain producing linear and cyclic oligomers and a broadening of the molecular weight distribution.

(ii) There is an element of irreproducibility because the production of the initiating carbene tends to be dependent on physical parameters such as temperature, concentration and mixing rates. There may also be more than one kind of metal carbene present.

(iii) Stereoregular polymers are rarely produced.

(iv) Alkylidene complexes are produced only in low yield and those that are formed are relatively unstable and decompose easily.

(v) They also have limited tolerance towards functional groups. Most classical initiators for example, are destroyed by oxygen, water and oxygen containing monomers and solvents.

By contrast well defined initiators are, in favorable cases, able to produce highly stereoregular monodisperse polymers from cyclic olefins and furthermore these living systems allow preparation of well defined block copolymers when a second monomer is added to the reaction mixture after the first one has been consumed.

Because such remarkable advantages had been demonstrated using well defined initiators, and these recently commenced investigations had provided

many fruitful developments in metathesis polymerisation, we considered that the examination of the metathesis polymerisation of aromatic monomers might be useful and interesting. In fact, the polymerisation of several aromatic monomers has been examined using classical catalyst systems. The monomers investigated are shown in Figure 1.6.^{47,48,49,50} Of these monomers only I has been examined using a well defined initiator.⁵¹ Some investigations of the polymerisation of aromatic compounds using well defined initiators form the basis of Chapter 3. of this thesis.

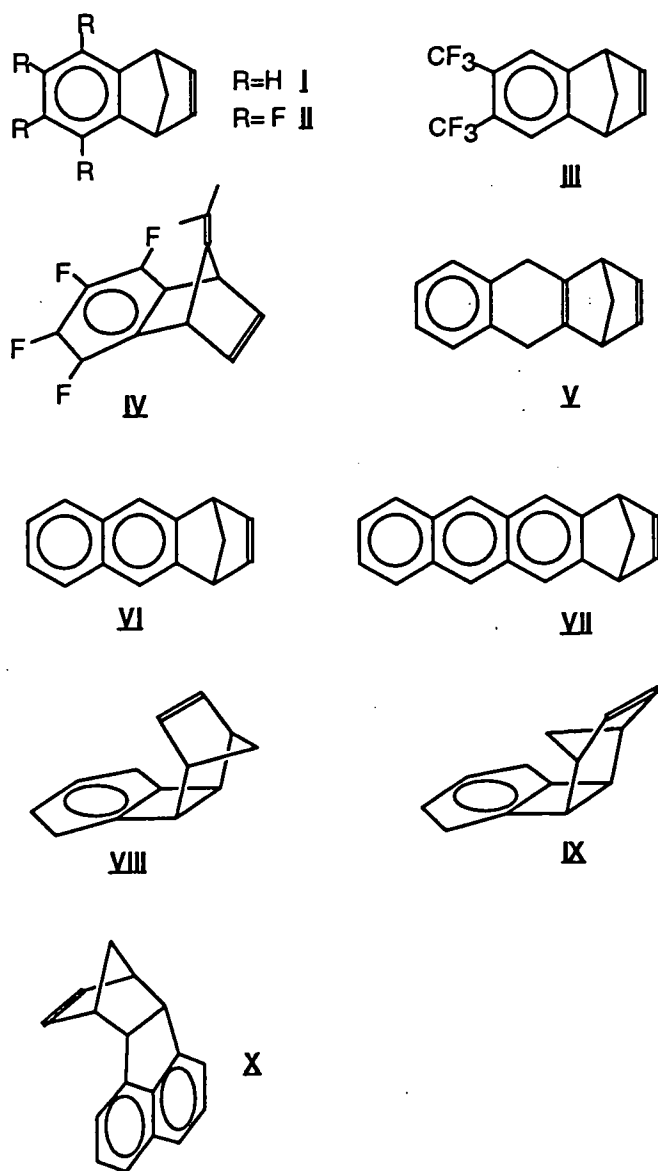


Figure 1.6. Aromatic monomers polymerised using classical catalyst systems

1.4 Mechanism of metathesis polymerisation

The mechanism of the metathesis reaction has been the subject of many investigations and much discussion.

Calderon² first proposed the transalkylidenation scheme for the mechanism of ring opening polymerisation of cycloalkenes and ruled out Natta's¹¹ earlier proposal of transalkylation. Later, Dall'Asta and Motroni^{52,53} provided direct experimental evidence that in the ring opening polymerisation of cycloalkenes the cleavage occurs at the double bond. These authors proved this by copolymerisation of cyclooctene and cyclopentene where the cyclopentene double bond was labelled with ¹⁴C, then the resulting polymer may have two types of unit depending on whether cleavage takes place at the double bond or at the carbon single bond adjacent to the double bond as shown in Figure 1.7.

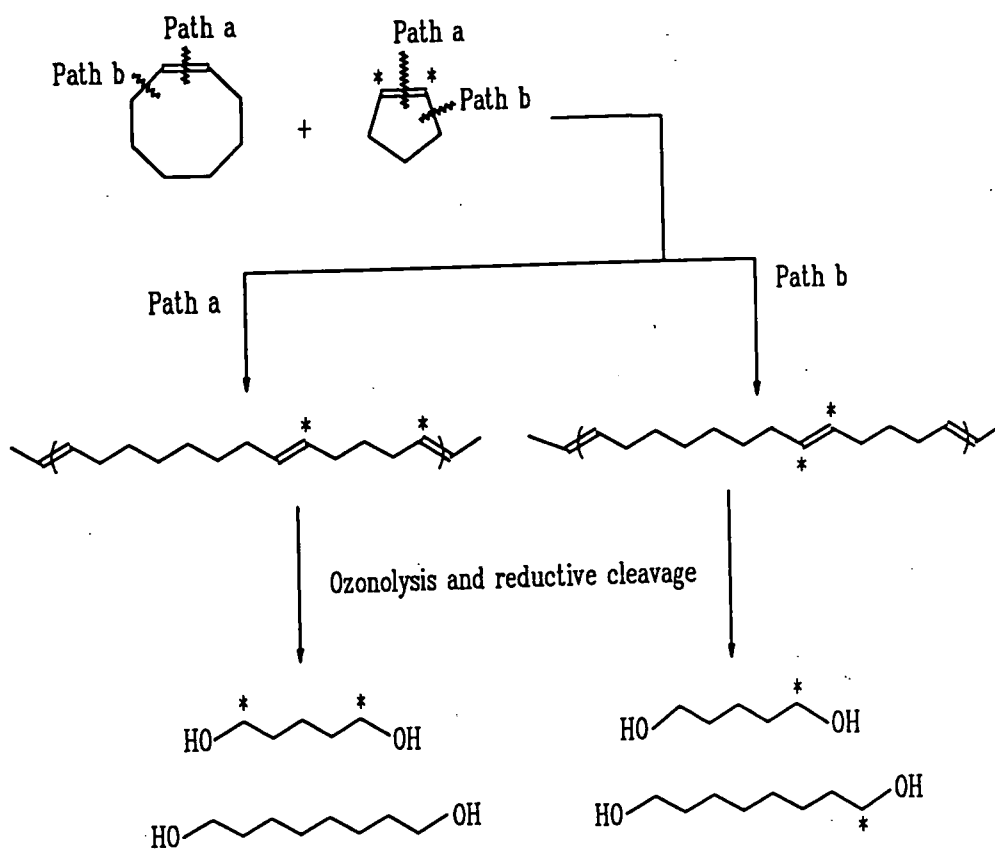


Figure 1.7. Copolymerisation of cyclooctene and labelled cyclopentene
 Key: * denotes ¹⁴C labelling,
 Path a : Double bond cleavage, Path b : Single bond cleavage

Ozonolysis of the copolymer followed by reductive cleavage and radiochemical analysis of the resulting diols showed that all the radioactive carbon atoms were contained in the 1,5-diol, proving that ring opening polymerisation had proceeded via cleavage of the double bond (Path a).

The question of the detailed mechanistic pathway is much more complicated and difficult to establish definitely. Several mechanistic proposals have been put forward, and the area is still one of active discussion.

The outline mechanistic sequence which is generally accepted now for olefin metathesis and ring opening metathesis polymerisation was initially proposed by Herrisson and Chauvin⁵⁴ in 1970 after a detailed study of the products of cross metathesis between a series of cycloalkenes and linear unsymmetrical alkenes. Essentially the same rationalization was put forward independently by Lappert and co-workers.⁵⁵

The proposed mechanism involves transalkylidenation via the cleavage of the C=C double bond and the involvement of a transition metal carbene which possesses a vacant coordination site as the chain carrier. As outlined in Figure 1.8., this mechanism of ring opening metathesis polymerisation consists of a cycle of four steps.

(i) The C=C double bond of monomer first coordinates to the vacant site on the metal of carbene complex forming a metal π -complex, which carries the propagating species as a carbene ligand.

(ii) The second step is the conversion of the complex to the metallacyclobutane intermediate via a 2+2 cycloaddition.

(iii) The metallacyclobutane cleaves either degeneratively or productively to form a new metal carbene complex and a new π -complex of a C=C double bond, which possesses the carbene ligand of the propagating species and which is one degree of polymerisation higher.

(iv) The final step is the decooordination of the C=C double bond of the end monomeric unit of the growing chain to form a new metal carbene with a vacant site; namely, regeneration of the active species.

All steps are reversible so the outcome of the metathesis of acyclic alkenes and of ring opening polymerisation depends on reaction conditions, such as temperature, concentration, reaction duration, the nature of the olefin and the nature of the propagating polymer chain end.

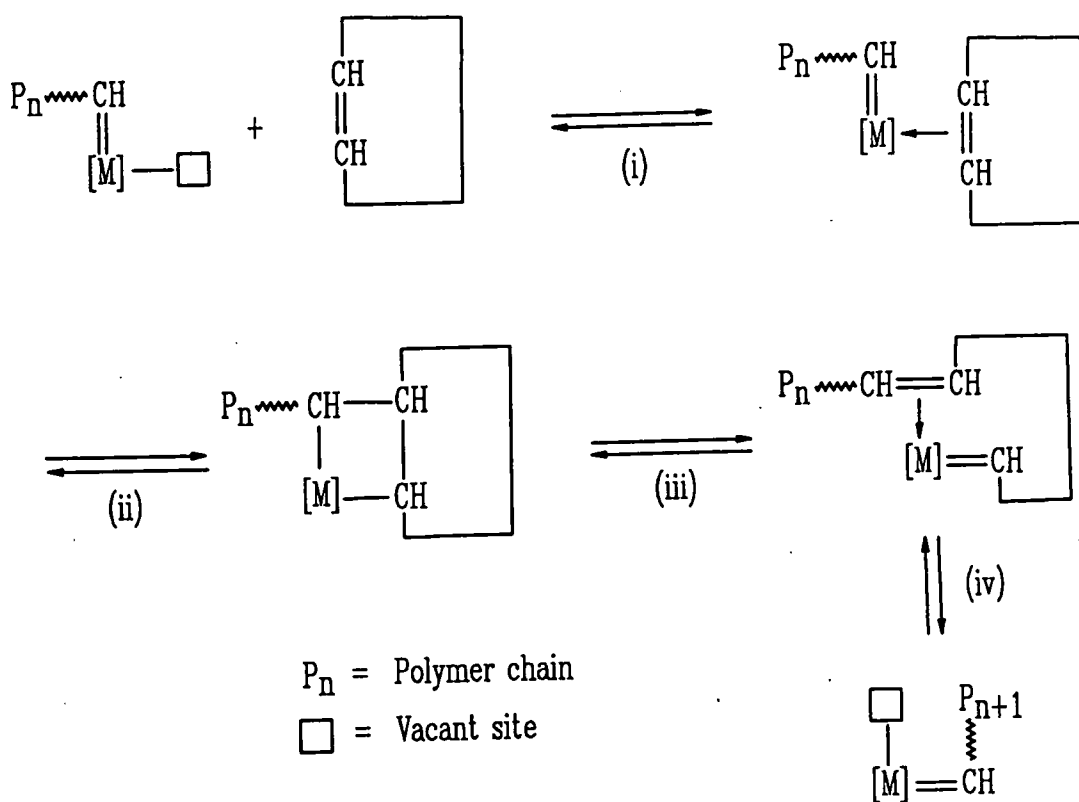
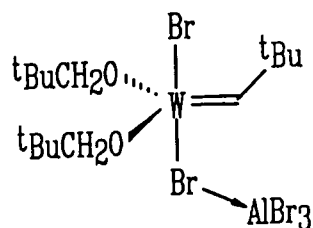


Figure 1.8. Scheme for ring opening metathesis polymerisation (ROMP)

This scheme was supported by the existence of metal carbenes, stable at low temperatures, such as the Casey and the Fischer carbenes, and the isolation of stable metallacyclobutanes derived from Tebbe reagent, both of which were shown to initiate the metathesis polymerisation of strained cyclic olefins. Further evidence of a metallacyclobutane intermediate was reported by Green⁵⁶ who showed that stable metallacyclobutanes produced metal carbenes and alkenes as a

result of thermolysis or photolysis. Osborn provided the final confirmation when he observed the simultaneous occurrence and inter conversion of a tungsten metal carbene and tungsten metallacyclobutane during the ring opening polymerisation of norbornene with the Osborn catalyst shown below.



Osborn catalyst

More recently Schrock and co-workers have identified, by n.m.r. spectroscopy, a metallacyclobutane from the reaction of a tungsten carbene initiator and a fluorinated norbornadiene derivative, as shown in Figure 1.9.⁵¹

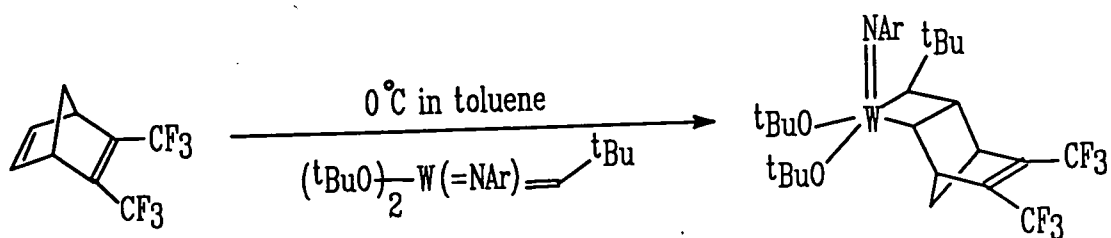


Figure 1.9. The metallacyclobutane identified by Schrock and co-workers

They also isolated a metal carbene species, namely the first insertion product of a potential polymerisation reaction, by reacting a well defined molybdenum metal carbene with the norbornadiene compound shown in Figure 1.10., in this case the structure of the 1:1 adduct was established by X-ray crystallography.⁵¹

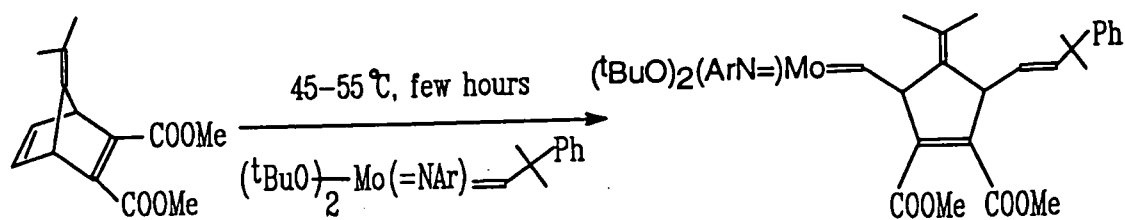
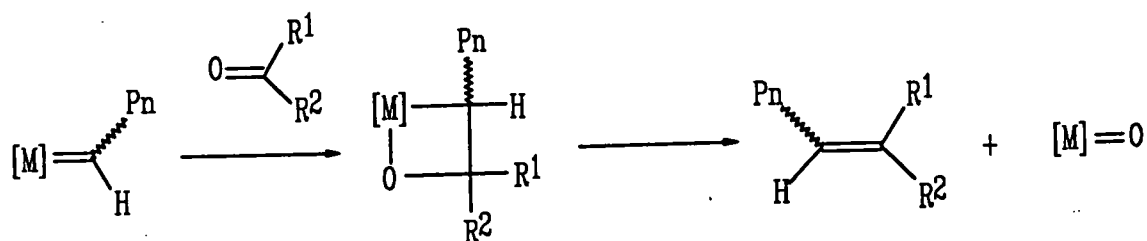


Figure 1.10. 1:1 Metal carbene : monomer adduct isolated by Schrock and co-workers

1.5 Termination of ring opening metathesis polymerisation

Wittig-like reaction and β -elimination reaction are known as characteristic reactions of metal carbene complexes. In fact, ring opening polymerisations, where metal carbenes are supposed to be the propagating species, are often terminated by adding carbonyl compounds such as acetone or benzaldehyde as shown in Figure 1.11.



Pn = Polymer chain

Figure 1.11. Reaction of a metal carbene with a carbonyl compound

Although alcohols and water destroy some active initiators presumably adding to the reactive metal carbene, some initiators are inert towards protic solvents. These generalized termination processes apply to both well defined and classical initiators.

1.6 Chain transfer reaction

Chain transfer reactions can occur between the propagating metal carbene and a C=C double bond in another polymer chain as shown in Figure 1.12. The polymer C=C double bonds compete with those in the monomer for the active metal carbene species resulting in the reduction the availability of these species.

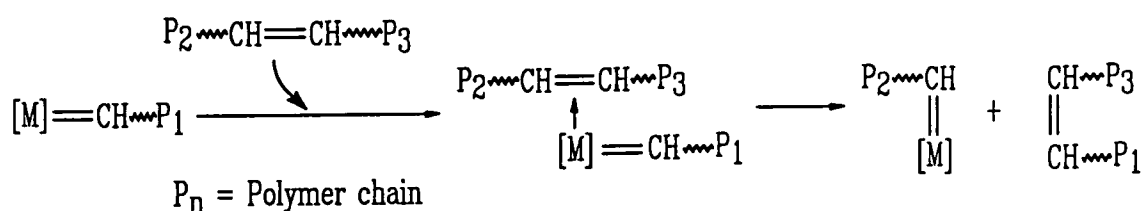


Figure 1.12. Chain Transfer reaction in ring opening metathesis polymerisation

A similar reaction can take place intermolecularly between the active metal carbene and the C=C double bonds from the same polymer chain resulting in the formation of cyclic oligomers as shown in Figure 1.13.

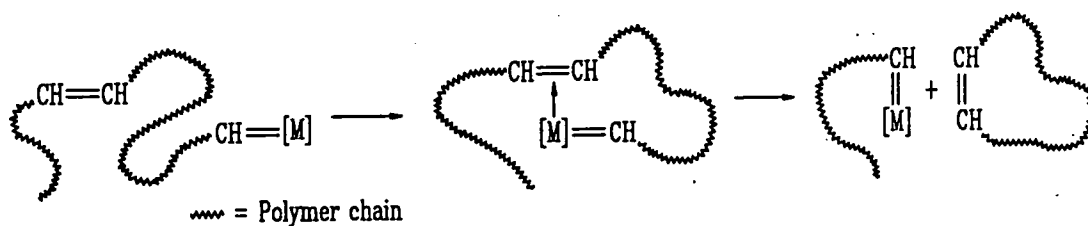


Figure 1.13. Backbiting reaction in ring opening metathesis polymerisation

This is known as a back biting reaction and can result in a lower molecular weight and higher dispersity of the resulting polymer. If the initial concentration of monomer $[M_0]$ is below a certain critical value then an equilibrium is established between the high molecular weight polymer and the low molecular weight cyclic oligomers. Higher concentration results in a higher proportion of high molecular weight polymer at equilibrium. The lower molecular weight cyclic oligomers are produced under conditions of relatively low concentration.

If $[M_0]$ is below the critical value then high molecular weight polymer is not formed.

1.7 Thermodynamic arguments and polymerisability of monocyclic alkenes

The thermodynamics and kinetics of ring opening have been a major subject of study in ring opening metathesis polymerisation. Briefly, effective polymerisation requires a low energy barrier between the metal carbene and the metallacyclobutane, and a negative Gibbs free energy of ring opening (ΔG) expressed by the following equation,

$$\Delta G = \Delta H - T\Delta S$$

where T , ΔH and ΔS are the temperature (K), the enthalpy and the entropy of ring opening respectively. The entropy ΔS is always negative since the monomers are combined with each other into macromolecules resulting in the reduction of their freedom. Therefore the entropy term ($-T\Delta S$) is always positive and for a favorable reaction the magnitude of the ΔH term must be greater than the magnitude of $T\Delta S$. As the temperature is increased the entropy term increases and Gibbs free energy eventually becomes positive. The temperature at which $\Delta G=0$, namely $T=\Delta H/\Delta S$, is known as the ceiling temperature, above which polymerisation does not occur.

Ring strain and ring size are important factors in determining whether monocyclic and bicyclic olefins undergo metathesis polymerisation. In the case of 3,4 and 8-12 membered rings, metathesis generally occurs readily, while for 5,6 and 7 membered rings, where ring strain is small, the situation becomes delicately balanced and other physical factors, such as temperature, concentration and pressure, come to affect the polymerisability. According to Gibbs' equation, lower temperature and higher monomer concentration make the entropy term ($-T\Delta S$) smaller, so such reaction conditions are favourable for polymerisation.

Several examples of the polymerisation of 5 and 7 membered monocycloalkenes are known as shown in Table 1.3., but attempts to polymerise substituted monocycloalkenes are restricted to a relatively small number. Chapter 6. of this thesis describes a study of the polymerisation of a substituted cyclopentene.

Table 1.3. Polymerisation of 5 and 7 membered cycloalkenes

Monomer	Catalyst system		Produced polymer
Cyclopentene	MoCl ₅ /Et ₃ Al	-30°C	Cis ⁵⁷
	WCl ₆ /Et ₃ Al	-30°C	Trans ⁵⁸
Cycloheptene	(C ₆ H ₅) ₂ C=W(CO) ₅	40°C	Cis ^{36,59}
	MoCl ₅ /Et ₃ Al	20°C	Trans ⁵⁸

1.8 Microstructure and stereochemistry of ring opening metathesis polymerisations

There are, generally, several ways of incorporating a monomer repeat unit into a polymer chain, changing the microstructure and morphology and hence the physical properties of the polymer. The microstructure can be controlled in favorable cases by changing the catalyst system and the reaction conditions, so that it may be possible to synthesise a polymer with the required physical characteristics for a specific application. The three main factors which define the microstructure of polymers produced by ring opening metathesis polymerisation are:-

- (i) the cis / trans vinylene frequency and distribution,
- (ii) tacticity effects,
- (iii) and the head / head and head / tail frequency and distribution.

A number of polymers from one monomer can exist, in principle, by changing these factors.

(i) Cis / trans double bond isomerism

Monomers such as cyclopentene provide, by ring opening polymerisation, polymers in which only cis / trans double bond isomerism is possible. Each methylene group in the polymer is situated between a cis-cis, a cis-trans, or a trans-trans pair of double bonds as shown in Figure 1.14.

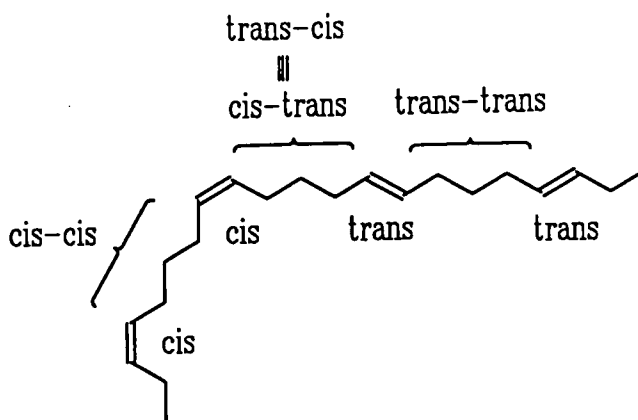


Figure 1.14. Cis / trans isomerism of the polymer obtained by ROMP

The proportion of cis double bonds in a particular polymer, denoted by σ_c , is primarily determined by the catalyst system, concentration, solvent and temperature, and the nature of the monomer may also affect the outcome.

(ii) Tacticity effects

Monomers such as 4-methylcyclopentene or bicyclo[2.2.1]hept-2-ene, norbornene, do not have any chiral centre in themselves but give polymers containing chiral centres. Such polymers may have R or S configuration about the chiral centre. Therefore there is the possibility of two adjacent centres having the same chiralities, resulting in racemic dyads or different chiralities, giving meso dyads as shown in Figure 1.15. and 1.16. Sequences of racemic dyads give syndiotactic polymers and sequences of meso dyads provide isotactic polymers.

Polymers with a random distribution of meso and racemic dyads are called atactic.

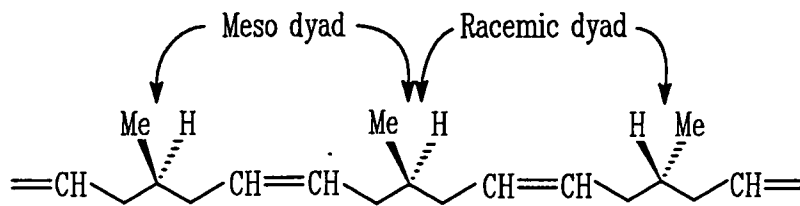


Figure 1.15. Meso and racemic dyads in cis-poly(4-methyl-1-pentenylene) obtained by ROMP

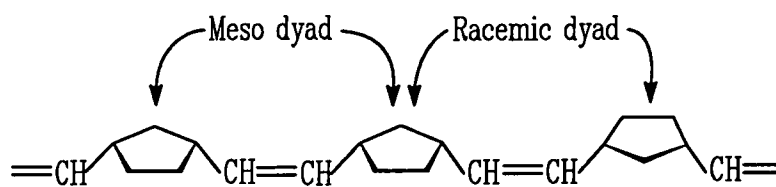


Figure 1.16. Meso and racemic dyads in cis-polybornene obtained by ROMP

Each C=C double bond can have cis or trans geometry, so there are four possible tacticities for each of these polymers. The possible configurations of poly(4-methyl-1-pentenylene) are shown in Figure 1.17. as a typical example.

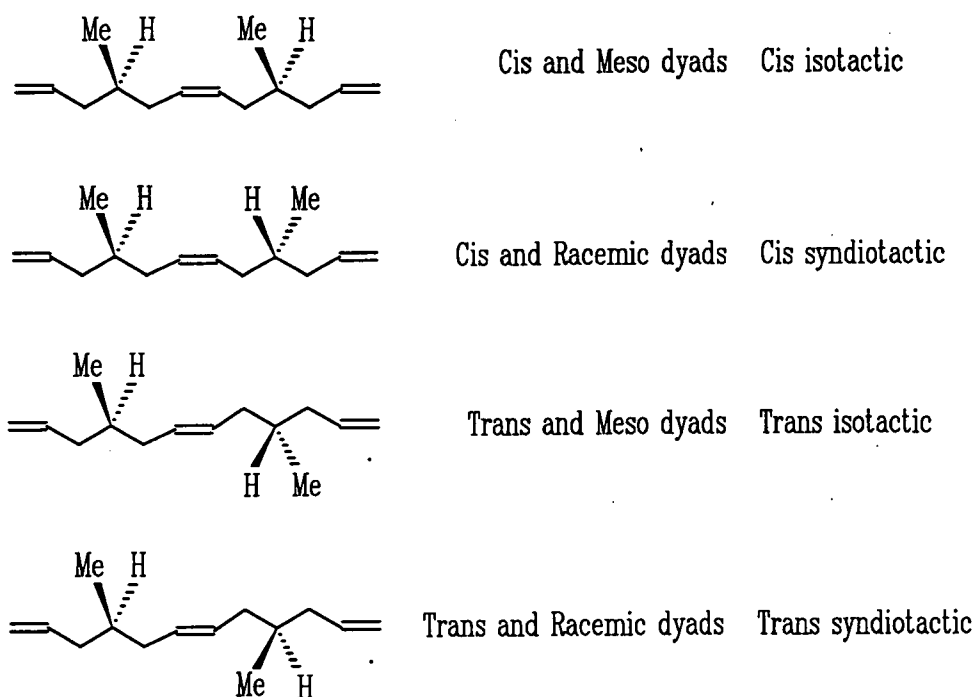


Figure 1.17. Possible configurations of poly(4-methyl-1-pentenylene)

(iii) Head/tail isomerism

In the case of unsymmetrically substituted monomers, such as 4-methylcyclopentene and 5,5-dimethylbicyclo[2.2.1]hept-2-ene polymers with head-head, head-tail and tail-tail structures can occur as shown in Figure 1.18.

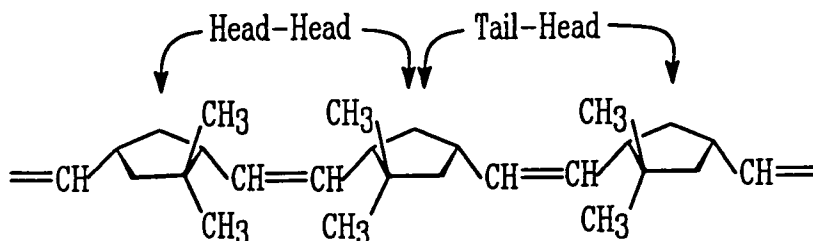


Figure 1.18. Head / tail isomerism of poly(5,5-dimethylbicyclo[2.2.1]hept-2-ene)

Furthermore each of these structures can have meso or racemic dyads and cis/trans isomerism, so a large number of configuration become possible but, even in such cases, some monomers are known to be polymerised to provide stereoregular polymers. For example, 1-methylnorbornene is polymerised with ReCl_5 to give an all cis head-tail syndiotactic polymer, whereas, using OsCl_3 , an high trans head-tail atactic polymer is produced.⁶⁰ It has been suggested that the cis head-head arrangement is not formed with 1-methylnorbornene due to steric hindrance in the metallacyclobutane intermediate. This is a subtle effect, for example, with 5,5-dimethylnorbornene there is less steric hindrance and the cis head-head junction can be formed in polymerisations initiated with ReCl_5 .⁶¹

The microstructures of the polymers produced by ring opening metathesis polymerisation have been intensively studied, especially with regard to cis/trans isomerism. A number of kinds of monomer have been polymerised and the microstructures of the resulting polymers have been established. The examination of meso/racemic dyads (tacticity) is mainly confined to polymers made from 5-substituted norbornenes. The investigation of the microstructures of the superficially simple polymers derived from a substituted cyclopentene might

throw some light on these polymerisation process and this is reported in Chapter 6. of this thesis.

CHAPTER 2:

Synthesis of acenaphthylene-cyclopentadiene Diels-Alder adducts

2.1 Introduction

As discussed in Section 1.3.2 it was thought that an investigation of the polymerisation of aromatic monomers using well defined initiator systems might prove interesting with respect to the synthesis of novel materials and in relation to increasing our understanding of metathesis ring opening polymerisation. We selected the acenaphthylene-cyclopentadiene Diels-Alder adducts as monomers and examined their polymerisation, since it had previously been studied by Feast and El-Saafin with classical catalyst systems.⁵⁰ In this chapter the synthesis of the monomer is described and the examination of the polymerisation is described in the following chapter.

2.2 Synthesis of acenaphthylene-cyclopentadiene Diels-Alder adducts

The Diels-Alder reaction generally tends to provide endo-adducts rather than exo-adducts, this is generally believed to be a consequence of secondary orbital interaction.^{62,63} Cyclic dienophiles such as cyclopropene, cyclopentene, cyclobutadiene, cyclopentadiene, benzocyclobutadiene, maleic anhydride and o- and p-benzoquinone are reported to produce endo-adducts predominantly.^{62,64,65} These endo adducts are the products of kinetic control and in certain cases the reaction can be managed to yield the thermodynamically favourable exo-adduct, for example it was recently demonstrated that some dienophiles containing carbonyl groups produce predominantly exo-adduct by irradiation with ultra violet light,⁶⁶ but more often attempts to regulate the reaction result in the formation of an endo and exo mixture.⁶²

The thermal reaction of acenaphthylene with cyclopentadiene has been studied by Baker and Mason and they reported that the endo-adduct and exo-adduct can be formed in a 3:1 ratio.⁶⁷ We used similar reaction conditions to theirs to synthesise Diels-Alder adducts of acenaphthylene and cyclopentadiene, namely heating acenaphthylene and cyclopentadiene (or cyclopentadiene dimer) at high temperature, see Figure 2.1.

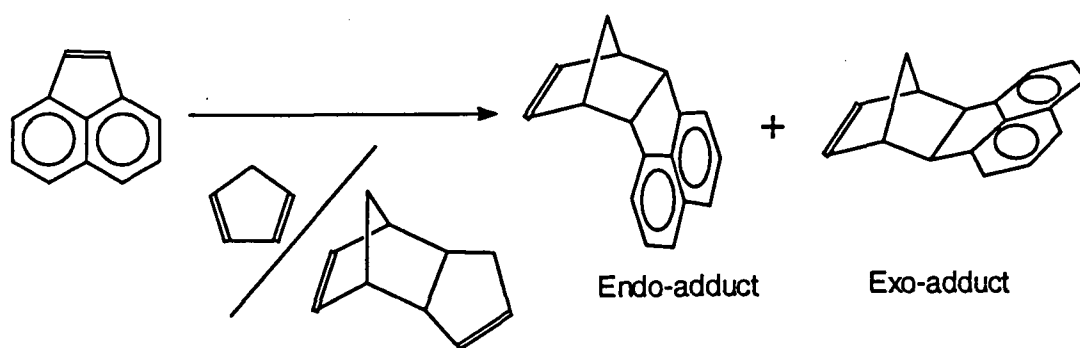


Figure 2.1. Scheme for synthesis of acenaphthylene-cyclopentadiene adducts

The reaction was found to favour the production of endo-adduct as reported, and in addition to endo and exo-adducts, a side product which was probably a 2:1 adduct, since its retention time on gas chromatography was longer than both endo and exo-adducts, was observed also. The effect of reaction duration on the ratio of products was examined. Reaction duration and the percentages of the products, namely endo-adduct, exo-adduct and side product in the reaction mixture, are shown in Table 2.1. for a selection of reactions. The percentages were calculated based on the peak intensities in the gas chromatogram (Appendix 2.1.). A flame ionisation detector was used, for which response factors are a function of "carbon number" so, although the equipment was not calibrated with pure component peaks, the values quoted here are thought to be reliable.

Table 2.1. Reaction duration and the percentages of the yielded compounds

Reaction duration (hr) (185°C, 1atm)	Percentage in the Reaction Mixture a)		
	Endo Isomer	Exo Isomer	Side Product
1	18.2	7.2	0
2	50.8	22.1	3.8
3	46.4	22.0	6.1
4	35.6	24.3	9.4
5	33.6	28.8	10.3

a) The percentages were determined using gas chromatography, starting materials constituted the remainder of the chromatogram. .

As shown in the table, the percentage of the side product and exo-adduct increased with reaction duration. Reaction under high pressure turned out not to favour exo-adduct production, as shown in Table 2.2. Reactions for 2 hours and 5 hours under atmospheric pressure were used to synthesis mixtures of endo and exo-adducts for subsequent separation.

Table 2.2. Reaction conditions and the obtained results

Starting materials ^{a)} (proportion)	Temp. (°C)	Pressure (atm)	Time (hr)	Yields ^{b)} (%)	Endo/Exo ^{c)} (%)
AN / CP (100/115)	177	18	6	17.1	80.1 / 19.9
AN / DCP (100/58)	185	1	2	37.2	73.5 / 26.5
AN / DCP (100/58)	185	1	5	16.5	60.3 / 39.7

a) AN=acenaphthylene, DCP=dicyclopentadiene, CP=cyclopentadiene

b) The yields of the recovered mixture of endo and exo-adducts.

c) The proportions of endo and exo-adducts were determined using gas chromatography after separation from starting materials. .

Although Baker obtained a sample of pure exo-adduct using chromatography on a silver nitrate impregnated silica gel column packing⁶⁷ this method was not available to us, so the isolation of endo and exo-adducts was carried out by means of repeated recrystallization and repeated column chromatography on silica gel. The purity of the samples was checked by gas chromatography (Appendix 2.2. and 2.7.). The pure endo adduct was obtained more easily than the exo adduct but neither was readily accessible by this laborious route, consequently only small amount of pure monomers were available for polymerisation studies.

The infrared spectrum of each adduct (Appendix 2.3. and 2.8.) showed that both had the absorption of aromatic and vinylic C-H over 3000 cm^{-1} as well as the aliphatic below 3000 cm^{-1} and an absorption due to an out-of-plane C-H deformation mode around 730 cm^{-1} as their characteristic absorptions. The spectra were in agreement with literature data.^{50,67} The mass spectrum of the exo-adduct (Appendix 2.9.) confirmed the molecular weight of 218 amu and showed the expected fragments at $m/e=202$ ($M-\text{CH}_4$) and 152 ($M-\text{C}_5\text{H}_6$). Each of ^1H , ^{13}C n.m.r. spectra of endo-adduct (Appendix 2.4. and 2.5.) and ^1H n.m.r. spectrum of exo-adduct (Appendix 2.10.) was also in agreement with published data^{50,67} and the structures and chemical shifts are shown in Figures 2.2., 2.3. and 2.4. respectively.

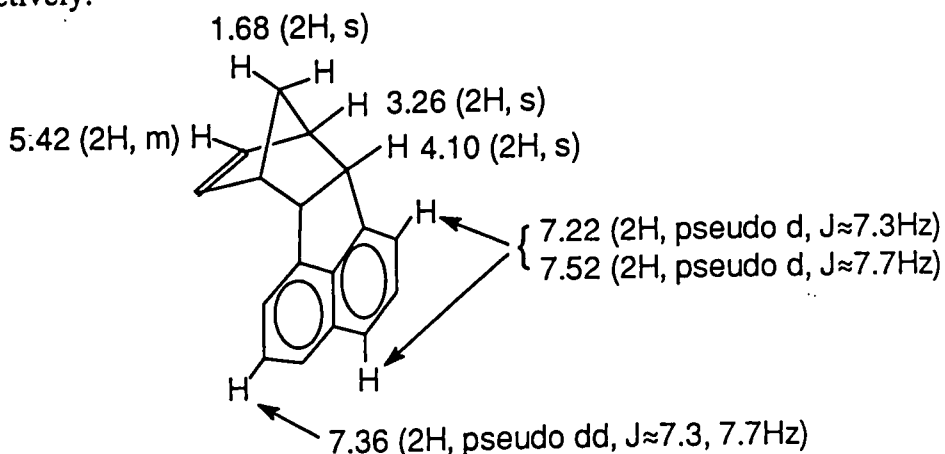


Figure 2.2. ^1H N.m.r. spectral parameters for the endo-adduct (chemical shifts in ppm with respect to TMS)

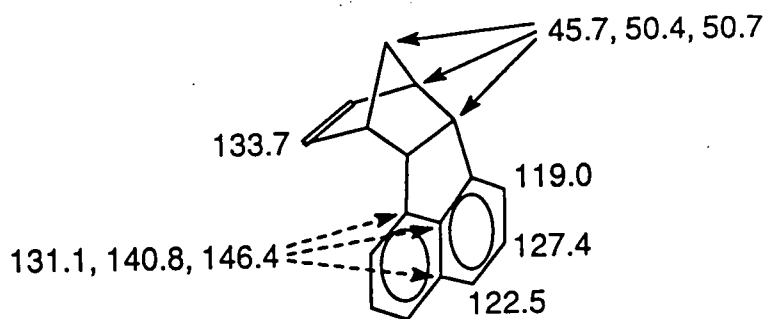


Figure 2.3. ^{13}C N.m.r. spectral parameters for the endo-adduct (chemical shifts in ppm with respect to TMS)

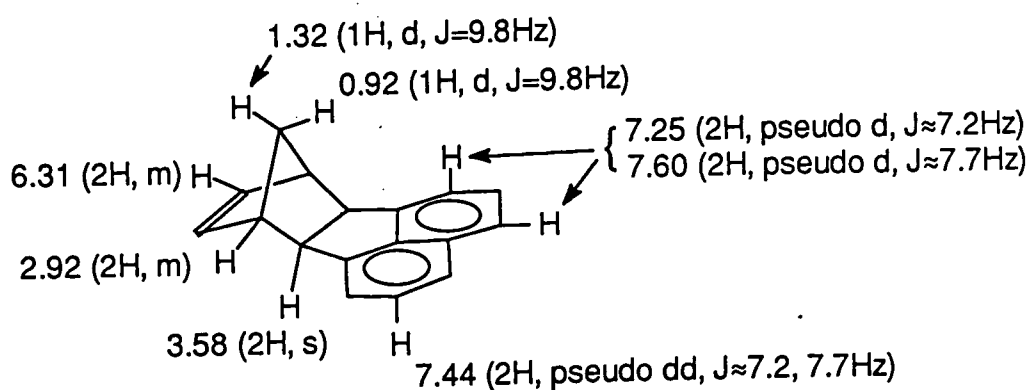


Figure 2.4. ^1H N.m.r. spectral parameters for the exo-adduct (chemical shifts in ppm with respect to TMS)

The ^{13}C -n.m.r. spectrum of the exo adduct (Appendix 2.11.) was assigned by comparison with that of endo adduct as shown in Figure 2.5., since it has not been reported previously.

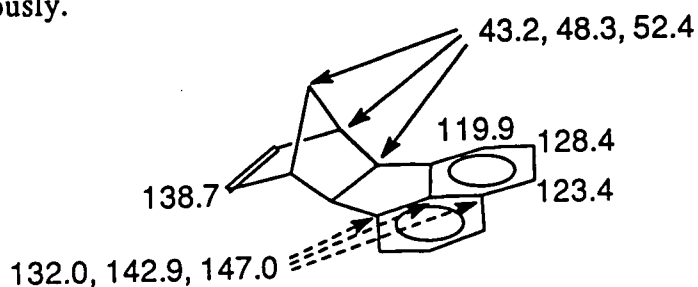


Figure 2.5. ^{13}C N.m.r. spectral parameters for the exo-adduct (chemical shifts in ppm with respect to TMS)

Furthermore, the structure of endo-adduct was confirmed by means of single crystal X-ray diffraction (Appendix 2.6.).

2.3. Experimental

Acenaphthylene, dicyclopentadiene and p-hydroquinone were purchased from Aldrich Chemical Company Ltd. and n-hexane was purchased from BDH Laboratory Supplies (Merck Ltd). All reagents and solvents were used without further purification.

Typical examples of the synthetic procedure and product purification were as follows:-

Acenaphthylene (30g, 0.197 mol), dicyclopentadiene (13g, 0.098 mol) and p-hydroquinone (0.1g) were placed in a round-bottomed flask (200 ml) fitted with a reflux condenser, and the mixture was heated at 185°C with stirring under a nitrogen atmosphere. After 5 hours, the reaction mixture was allowed to cool to room temperature and the resulting brown viscous oil was poured into a twelve-fold excess of a mixture of petroleum ether and toluene (9:1). The precipitated solid was removed by filtration and washed with a seven-fold excess of the petroleum ether toluene mixture. The filtrate was concentrated under reduced pressure and the yellow oil obtained was vacuum-distilled to give a pale yellow viscous oil (16g, 0.0729 mol, 37%), collected in the boiling range 112-128°C/0.5-0.6mmHg. The oil contained both of endo and exo-adducts.

The variation in the ratio of products with reaction duration was obtained on the basis of gas chromatographic analysis of several samples taken from the reaction mixture after the prescribed reaction duration.

For the reaction under high pressure, the starting materials were put in a sealed glass tube and heated at 177°C for 6 hours. The work-up was carried out by a similar method to that described above.

Each pure sample of endo and exo adduct was obtained by means of recrystallization and column chromatography. The mixture of endo and exo adducts obtained by distillation was recrystallised from hexane solution. The

crystalline product still contained both endo and exo-adducts, although recrystallization did result in some enrichment in the endo-adduct. Both the endo-rich crystals and the exo-rich solution were subjected to silica gel column chromatography using n-hexane as the eluent. The exo-adduct was eluted faster than the endo-adduct but the separation was very poor ($R_{f_{\text{endo}}}=0.21$, $R_{f_{\text{exo}}}=0.26$). The column chromatography was repeated until both the endo and the exo adduct was purified. Pure samples of endo and exo-adducts were obtained as colourless hexagonal crystals and a pale yellow oil, respectively.

Endo-adduct IR 3037, 2966, 1602, 1494, 1364, 1338, 1120, 828, 780, 734, 676 cm^{-1} ; ^1H n.m.r. (CDCl_3) δ 1.68 (2H, s), 3.26 (2H, s), 4.10 (2H, s) 5.42 (2H, m), 7.22 (2H, d, $J=7.3\text{Hz}$), 7.36 (2H, t, $J=7.6\text{Hz}$), 7.52 ppm (2H, d, $J=7.7\text{Hz}$); ^{13}C n.m.r. (CDCl_3 , offresonance) δ 45.7, 50.4, 50.7, 119.0, 122.5, 127.4, 131.1, 133.7, 140.8, 146.4 ppm.

Exo-adduct IR 3060, 2966, 1602, 1367, 1326, 1014, 820, 779, 726, 673 cm^{-1} ; MS 218 (M^+), 202 ($\text{M}-\text{CH}_4$), 152 ($\text{M}-\text{C}_5\text{H}_6$); ^1H n.m.r. (CDCl_3) δ 0.92 (1H, d, $J=9.8\text{Hz}$), 1.32 (1H, d, $J=9.8\text{Hz}$), 2.92 (2H, m), 3.58 (2H, s), 6.31 (2H, m), 7.25 (2H, d, $J=7.2\text{Hz}$), 7.44 (2H, t, $J=7.7\text{Hz}$), 7.60 ppm (2H, d, $J=7.7\text{Hz}$); ^{13}C n.m.r. (CDCl_3 , offresonance) δ 43.2, 48.3, 52.4, 119.9, 123.4, 128.4, 132.0, 138.7, 142.9, 147.0 ppm.

CHAPTER 3: The ring opening metathesis polymerisation of the Diels-Alder adducts of cyclopentadiene and acenaphthylene

3.1 Introduction

The ring opening metathesis polymerisation of the Diels-Alder adducts of cyclopentadiene and acenaphthylene was studied previously by Feast and El-Saafin.⁵⁰ The examination was carried out using the endo-adduct as the monomer and classical catalyst systems for the initiation of the polymerisation. The results shown in Table 3.1. were obtained. As shown in the table, the classical catalyst systems used provided the polymer with 50% of cis and 50% of trans double bonds in the main chain. The control over the polymerisation was limited and the reproducibility was poor.

Table 3.1. Polymerisation of endo-adduct using classical catalyst systems⁵⁰

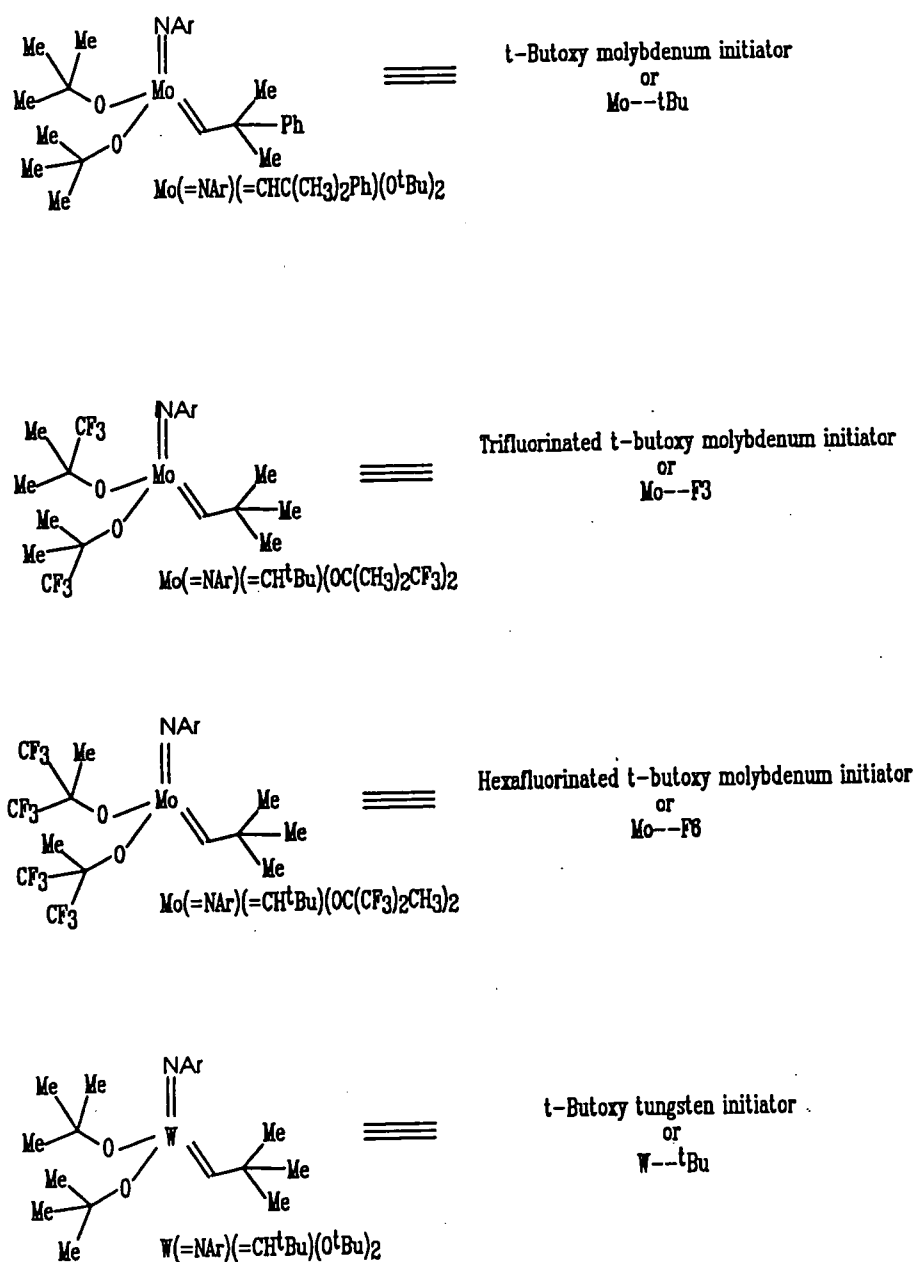
Co-catalyst	W:Sn:Monomer	Time	Yield (%)	Ratio Cis / Trans
SnPh ₄	1 : 2 : 60	5 sec	100 ^{a)}	--
	1 : 2 : 139	20 hr	100	50 / 50
	1 : 2 : 35	20 hr	100	
SnMe ₄	1 : 2 : 60	1.5 min	82	
	1 : 2 : 139	20 hr	100	
	1 : 2 : 35	20 hr	100	

a) The whole mass solidified and could not be redissolved.

In this work we investigated the polymerisation of endo and exo-adducts of acenaphthylene and cyclopentadiene using well defined initiators to explore the differences in microstructure between the polymers obtained with classical

catalyst systems and well defined initiator systems, and the differences in the polymerisation of endo and exo-adducts.

The well defined initiators used in the work described in this thesis are represented by the symbols as shown in Figure 3.1. The examination discussed in this chapter was carried out using t-butoxy molybdenum initiator and trifluorinated t-butoxy molybdenum initiator.



(Ar = 2,6-diisopropylphenyl)

Figure 3.1. Well defined initiators used in the work described in this thesis

3.2 Polymerisation of the endo-adduct using well defined initiators

A typical polymerisation procedure was as follows. 1) The monomer solution was added into the initiator solution under an inert atmosphere at ambient temperature. 2) After stirring at ambient temperature for 1 minute, the reaction mixture become viscous and was quenched by adding benzaldehyde. 3) The produced end capped polymer was isolated by reprecipitation or removing the quenched initiator from the reaction solution by passing the solution down a short alumina column, followed concentration and drying. The outline of the polymerisation process is shown in Figure 3.2.

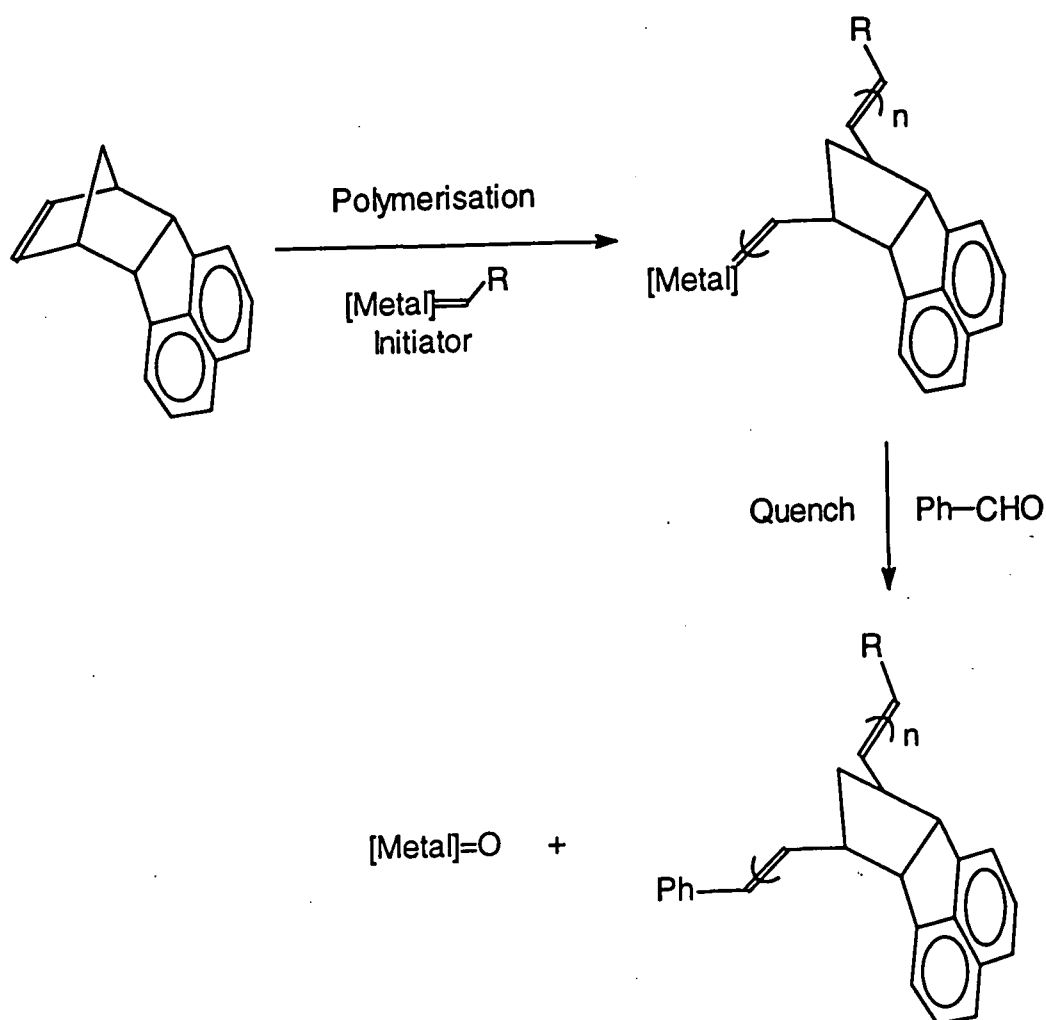


Figure 3.2. The outline of the polymerisation of the endo-adduct

The number average molecular weights and polydispersities (PDI) of the polymers obtained were measured by gel permeation chromatography. The results are shown in Table 3.2.

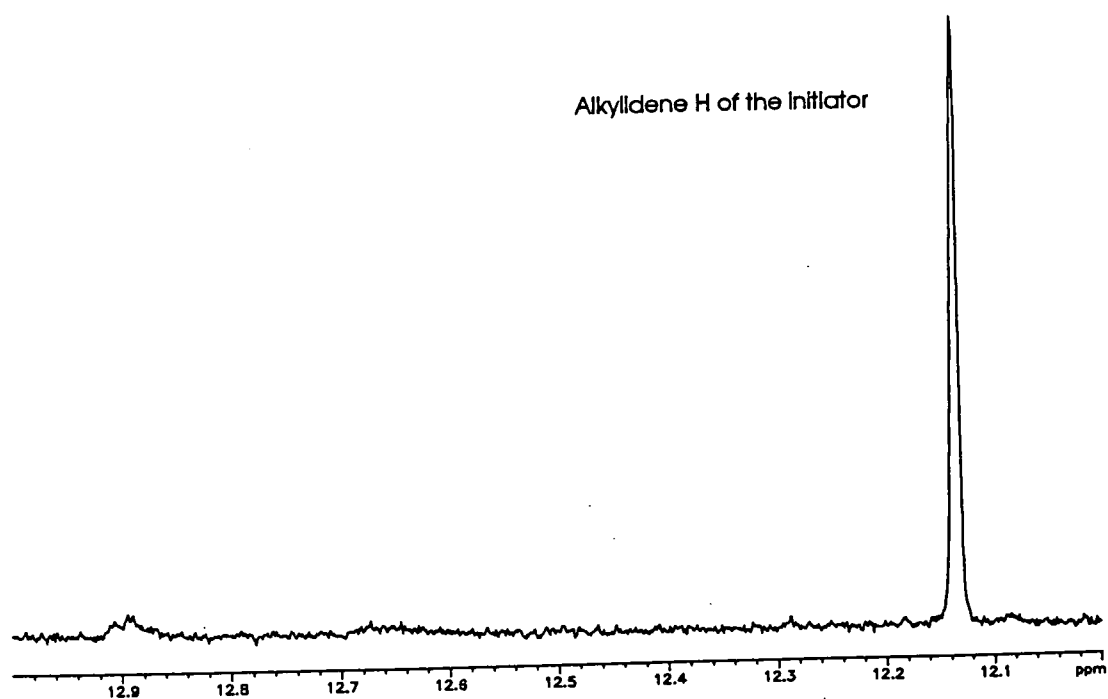
Table 3.2. Results of the polymerisation of the endo-adduct

No.	Initiator	Solvent	Ratio Monomer/Initiator	M _n (10 ³)		PDI
				Observed	Theoretical	
P3-1	Mo-- ^t Bu	C ₆ D ₆	20 / 1	8	4.36	1.4
P3-2		C ₆ D ₆	50 / 1	32	10.9	1.7
P3-3		C ₆ D ₆	50 / 1 a)	32	10.9	1.8
P3-4		CHCl ₃	50 / 1 b)	28	10.9	1.9
P3-5		Toluene	50 / 1 b)	--c)		
P3-6	Mo--F3	C ₆ D ₆	20 / 1	15	4.36	1.8

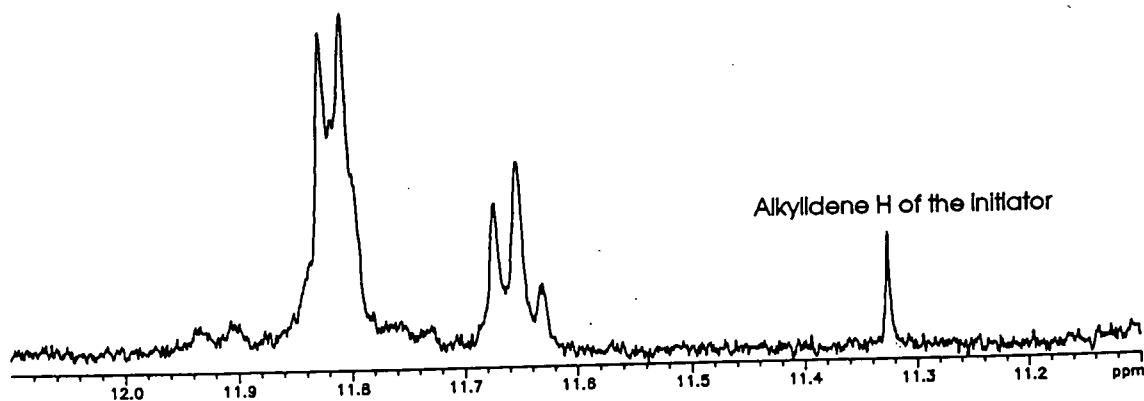
- a) The monomer solution was added to the initiator solution over 1 hour.
 b) The monomer solution was added to the initiator solution at -40°C and the mixture was allowed to warm up to ambient temperature.
 c) Precipitation occurred during the polymerisation reaction.

If the polymerisation progressed completely in a typical living manner, it would be expected that the number average molecular weight would be roughly equal to the theoretical value and that the polydispersity would be close to 1. However, as shown in the table, both of the number average molecular weight and the polydispersity were much larger than the expected values, computed on the assumption of perfect living polymerisation, and increased with the initial ratio of the monomer to the initiator (P3-1,2) and with changing to a more reactive initiator (P3-1,6), and were not essentially affected by change either of the method of mixing the monomer and initiator solutions or of the solvent (P3-2,3,4).

The observations recorded above seemed to suggest that the polymerisation progressed in a classical manner; but, after all monomer had been consumed, the alkylidene protons of the propagating polymer chain ends were observed by ^1H n.m.r. as shown in Figure 3.3. Such observations are good indicators of living propagating chain ends in ring opening metathesis polymerisation, as shown in Figure 3.4.



(b) P3-6



(a) P3-1

Figure 3.3. The ^1H n.m.r. spectra of the alkylidene regions for

(a) P3-1 and (b) P3-6

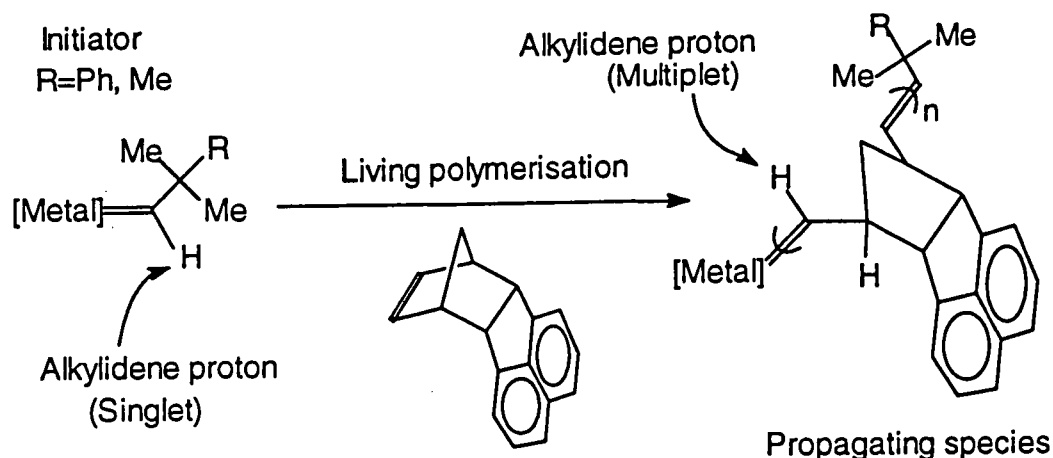


Figure 3.4. The observed alkylidene protons in a living polymerisation

The signals at 11.32 ppm in Figure 3.3.a and at 12.13 ppm in Figure 3.3.b are the alkylidene protons of *t*-butoxy molybdenum and trifluorinated *t*-butoxy molybdenum initiators respectively. Four sets of doublet signals (11.62-11.96 ppm) due to the alkylidene protons of the propagating species were observed in the ^1H n.m.r. spectrum of P3-1 since the signal due to the alkylidene proton should be a doublet, although only a poorly resolved multiplet (12.84-12.92 ppm) was observed in case of P3-6. Such a complex set of alkylidene resonances is possibly explained by the isomerism about the propagating polymer chain end, such as *syn/anti* isomerism of metal-carbene double bond and *cis/trans* isomerism about the next carbon-carbon double bond in the propagating species, as shown in Figure 3.5.

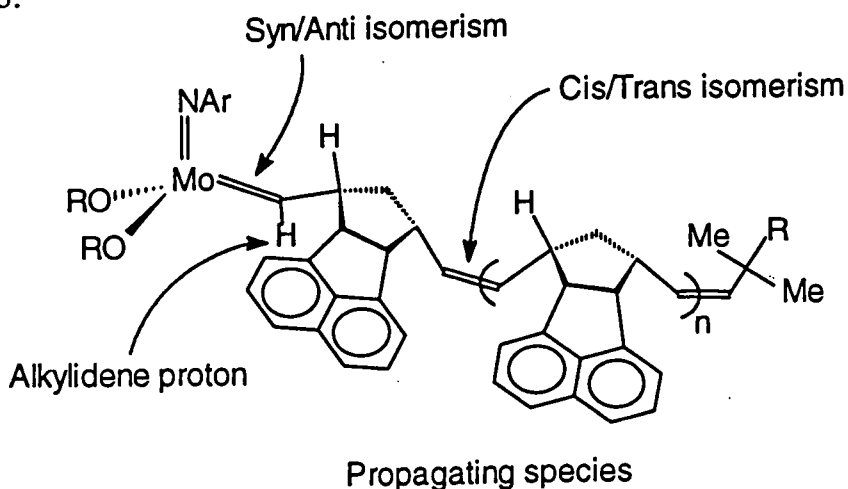


Figure 3.5. Isomerism in the propagating polymer chain end

Bazan and co-workers have reported that a complex set of alkylidene resonances were observed for the living chain end alkylidene in the polymerisation of benzonorbornadiene (see Figure 3.6.), regardless with the fact that those observed in the polymerisations of both 2,3-dicarbomethoxynorbornadiene and of 2,3-bis(trifluoromethyl)norbornadiene were well resolved and simple, and explained this on the basis that when an aromatic ring is present the alkylidene protons become more sensitive to the cis or trans configuration of at least the next double bond in the chain.^{51,68} If this is so, a similar effect might be operating in the polymerisation discussed above.

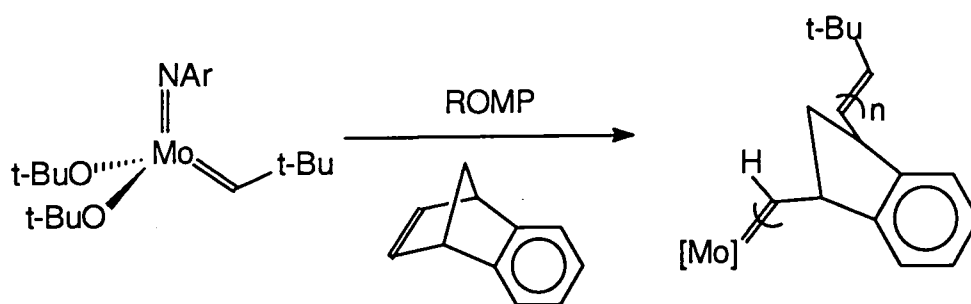


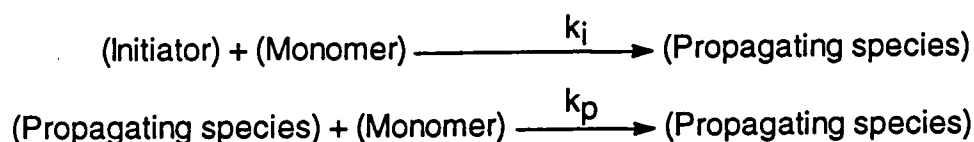
Figure 3.6. The polymerisation of benzonorbornadiene

It was seen that relatively more initiator remained in the polymerisation using trifluorinated molybdenum butoxy initiator than that using t-butoxy molybdenum initiator after all monomer had been consumed, as shown in Figure 3.3. and it seemed to be consistent with the fact that the trifluorinated molybdenum t-butoxy initiator is much more reactive than t-butoxy molybdenum initiator. In both cases a considerable amount of initiator remained, which suggested that the rate of propagation was much faster than that of initiation in these polymerisations. So the ratio of the propagation rate (k_p) to the initiation rate (k_i) was examined in the polymerisation using t-butoxy molybdenum initiator.

The monomer, the endo-adduct, was reacted with the t-butoxy molybdenum initiator under the same conditions as used in the polymerisations

described above. The ratio k_p/k_i was calculated from the signal intensities observed by ^1H n.m.r. after the consumption of all monomer was confirmed. The calculation method was similar to that used by Bazan and co-workers⁵¹ and is described below.

If the rate of the propagating process is not dependent on the degree of polymerisation then the initiation process and propagation process are expressed by the following set of equations.



Where the initial concentration of the monomer and the initiator and the concentration of the monomer, the initiator and the propagating species and the reaction time are $[M_0]$, $[I_0]$, $[M]$, $[I]$, $[P]$ and t respectively, the following set of equation can be constructed to describe the situation.

$$\begin{aligned} -d[I]/dt &= k_i[I][M] \\ -d[M]/dt &= k_i[I][M] + k_p[P][M] \\ [P] &= [I_0] - [I] \end{aligned}$$

Where the concentration of remaining initiator is $[I_R]$, the following equation is given by solving the above differential equation from $[M] = [M_0]$ to $[M] = 0$, namely from $[I] = [I_0]$ to $[I] = [I_R]$.

$$(k_p/k_i) \{ 1 + \ln([I_R]/[I_0]) - [I_R]/[I_0] \} = 1 - [I_R]/[I_0] - [M_0]/[I_0]$$

The ^1H n.m.r. of the resulting solution is shown in Figure 3.7. (Appendix 3.3.1.).

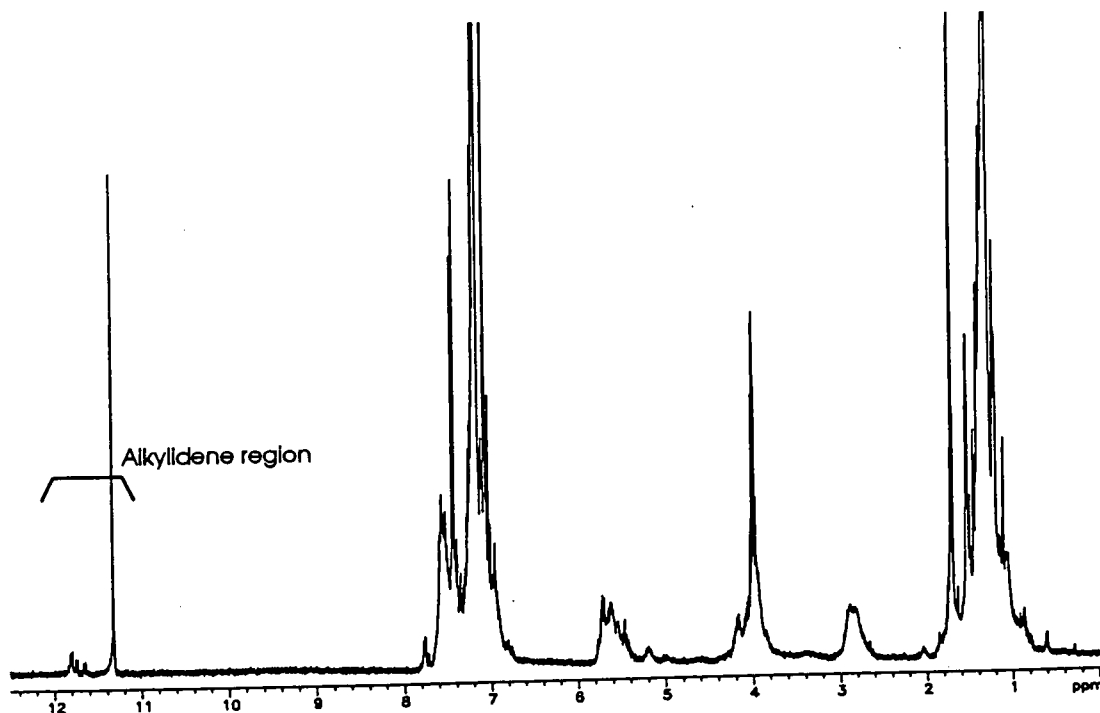


Figure 3.7. The ^1H n.m.r. spectrum of the resulting solution (reaction of the endo-adduct with *t*-butoxy molybdenum initiator)

The ^1H n.m.r. spectrum confirmed that all the monomer, i.e. the endo-adduct, had been consumed. In the spectrum, the broad signal in the range of 2.6 to 3.1 ppm was due to the allylic protons in the propagating chain and the multiplet in the range of 3.8 to 4.3 ppm was due to the benzylic protons in the propagating chain and the methine protons of isopropyl group of the imide ligand on the metal as shown in Figure 3.8. overleaf. The value for $[\text{M}_0]/[\text{I}_0]$ was calculated based on the signal intensities in these two regions. The resonances due to alkylidene protons of the initiator and the propagating species were observed at 11.32 ppm and in the region of 11.62 to 11.96 ppm, so the value for $[\text{I}_\text{R}]/[\text{I}_0]$ was calculated based on the signal intensities in these two regions. The value obtained for k_p/k_i was 34.

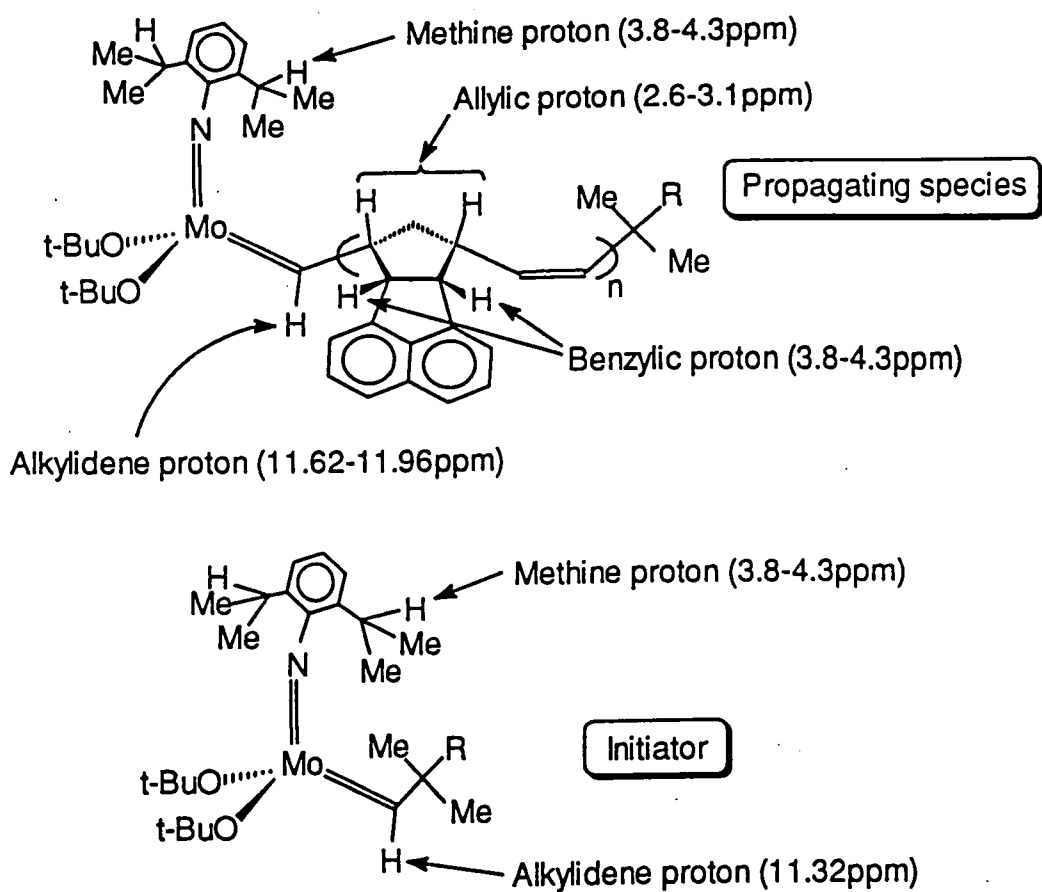


Figure 3.8. Chemical shifts of protons in propagating species and initiator

The GPC trace of P3-2 and the peak molecular weight are shown in Figure 3.9. as a typical example. As shown in the figure the trace had a shoulder on the high molecular weight side of the main peak and a tail in the low molecular weight region.

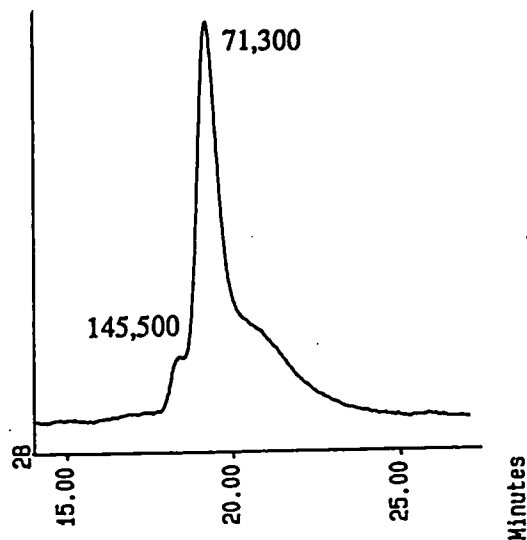


Figure 3.9. The GPC trace of P3-2

The peak molecular weight of the shoulder was roughly twice of that of the main peak. Feast and co-workers have reported that a trace of dioxygen introduced at the termination stage induced bimolecular dimerisation of the living polymer to give a component at twice the molecular weight of the main peak in ring opening metathesis polymerisations, and suggested the mechanism shown in Figure 3.10.⁶⁹ So the minor high molecular weight component of P3-2 was considered as a consequence of such dimerisation reaction induced by the impurity, dioxygen.

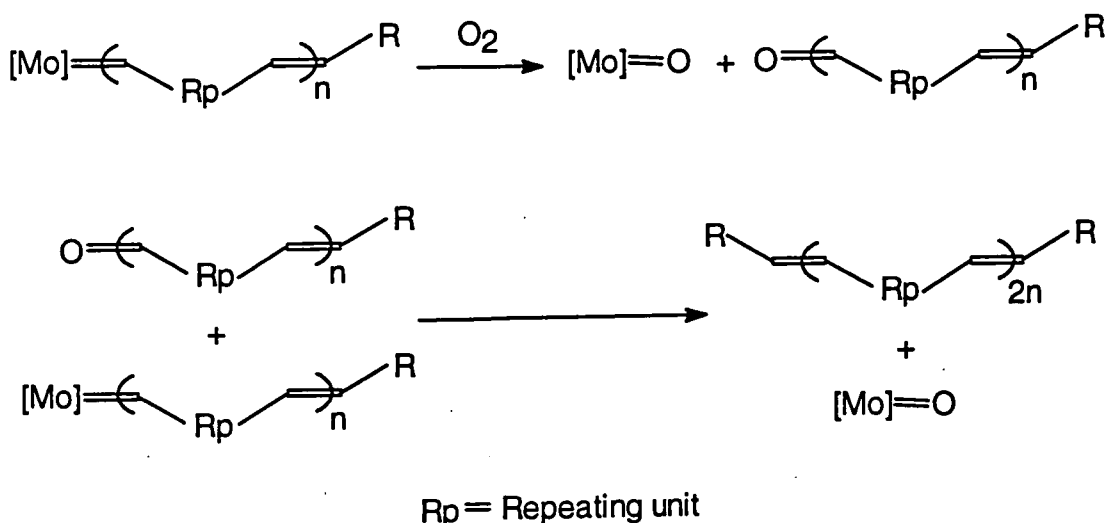


Figure 3.10 The mechanism of the dimerisation of living polymer during termination of ring opening metathesis polymerisation

As for the tail at low molecular weight, it was concluded that this was probably a consequence of mixing efficiency, considering the fact that the rate of the propagation was much faster than that of initiation.

These two factors make the number average molecular weight and polydispersity of the polymers obtained larger than expected and such an explanation is consistent with the limited data recorded in Table 3.2. Thus, under the same conditions the larger initial concentration ratio of the monomer to the initiator and more reactive initiator produced the broader molecular weight distributions in the product polymers (P3-1,2 and 6).

3.3 Characterization of the polymer of endo-adduct obtained using well defined initiators

3.3.1 Infrared spectroscopy

The infrared spectra of the polymers obtained (P3-3,6; Appendix 3.2.1.,2.) showed the absorption of aromatic and vinylic C-H stretching over 3000 cm^{-1} as well as the aliphatic below 3000 cm^{-1} and the skeletal vibration of aromatic ring at 1600 cm^{-1} , C-H deformation at 1447 cm^{-1} , and out-of-plane C-H deformation of benzene ring at 820 cm^{-1} . The absorption due to out-of-plane C-H deformation of trans CH=CH unit was observed around 980 cm^{-1} , although the absorption due to cis unit was not distinguished from other absorptions.

3.3.2 Nuclear magnetic resonance spectroscopy

Nuclear magnetic resonance spectroscopy especially ^{13}C n.m.r. spectroscopy provides a powerful analytical method to examine the cis / trans content of unsaturated polymers. Ivin and co-workers have investigated the ^{13}C n.m.r. spectra of many polymers prepared by ring opening of cyclic and bicyclic olefins, such as poly(1-pentenylene),⁷⁰ poly(1,3-cyclopentenylene vinylene)⁷¹ and related norbornene derivatives.⁷²⁻⁷⁶ The problem they looked at was that of defining the relative proportion of cis and trans double bond. As mentioned above, this question can also be answered by analysis of intensities of the out-of-plane C-H deformation of modes of vinylic C-H bonds, however work by Ivin's group established that ^{13}C n.m.r. spectroscopy provides a more reliable quantitative analysis than infrared spectroscopy.

The ^1H n.m.r. and ^{13}C n.m.r. spectra were similar amongst the polymers obtained (Appendix 3.3.2.-5.). So the assignments of the spectra of P3-3 (endo capped polymer) are shown in Figure 3.11. and 3.12, as typical examples.

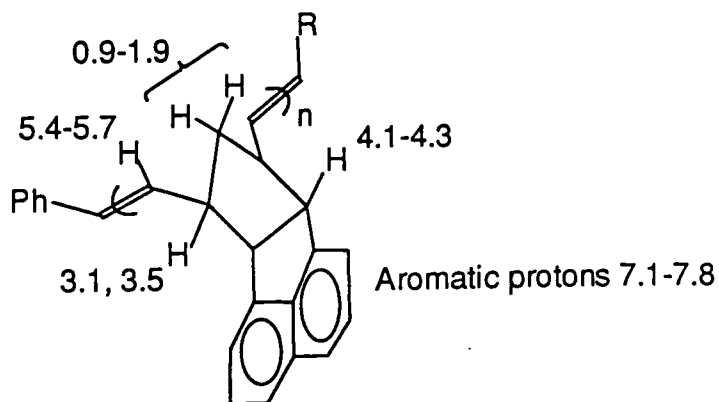


Figure 3.11. The assignment of the chemical shifts in the ^1H n.m.r. spectrum of P3-3 (ppm with respect to TMS)

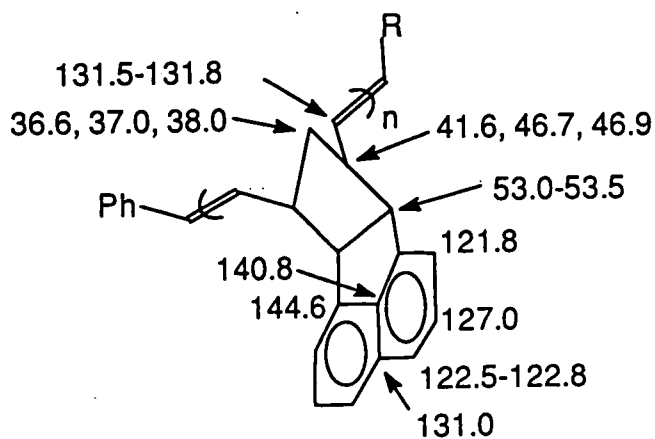


Figure 3.12. The assignment of the chemical shifts in the ^{13}C n.m.r. spectrum of P3-3 (ppm with respect to TMS)

In Figure 3.13., ^{13}C n.m.r. spectrum in the region of 30 to 60 ppm of P3-3 is shown.

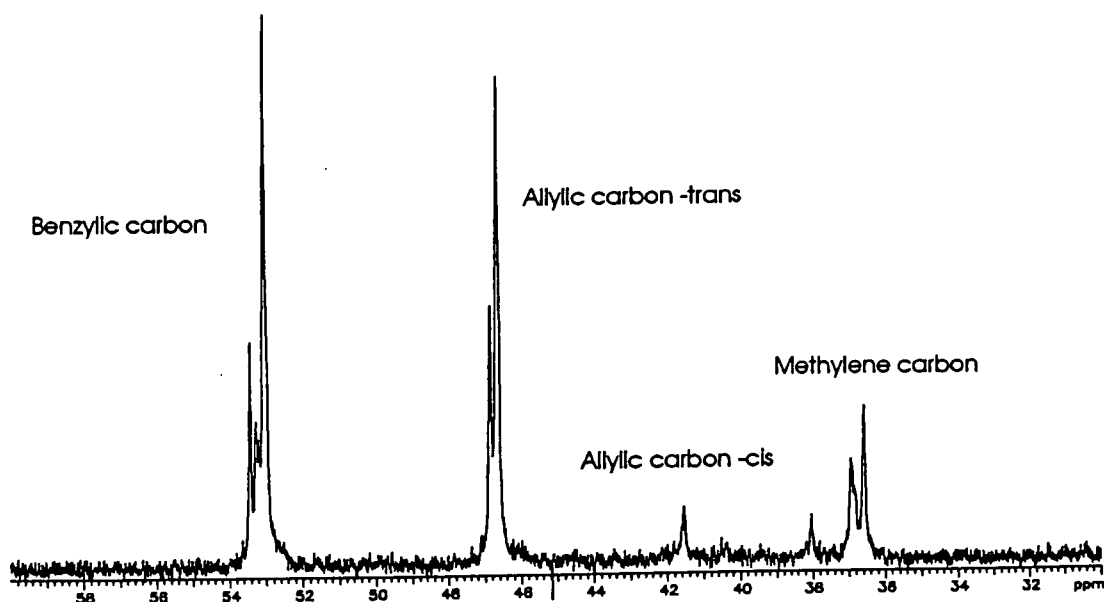


Figure 3.13 ^{13}C n.m.r. spectrum (30-60 ppm) of P3-3

The signal at 41.6 ppm and both signals at 46.7 and 46.9 ppm are assigned to the allylic carbons adjacent to cis and trans double bonds, considering the fact that in simple alkenes the allylic carbon atoms next to a cis-double bond always appear about 5 ppm upfield from those next to a trans double bond.⁷⁷ The signals at 46.7 and 46.9 ppm were considered to corresponding to the isomerism of the next nearest double bond. The methylene, vinylic, benzylic and aromatic carbon resonances were not well resolved and could not be assigned in detail.

The ratio of cis to trans double bonds in the polymer main chain were determined on the basis of the signal intensities of the allylic carbons. Living polymers were observed by ^{13}C n.m.r. before quenching, since the termination reaction turned out to be highly sensitive to oxygen, and, for some polymers, the ratio in the end capped polymers were also obtained for comparison. The results are shown in Table 3.3.

Table 3.3. Cis / trans ratio of double bonds in the polymers produced from the endo-adduct

No.	Initiator	Ratio Monomer / Initiator	Ratio Cis/ Trans	
			Living polymer	Capped polymer
P3-1	Mo--O ^t Bu	20 / 1	16 / 84	--
P3-2		50 / 1	17 / 83	18 / 82
P3-3		50 / 1 a)	11 / 89	9 / 91
P3-6	Mo--F3	20 / 1	80 / 20	77 / 23

a) The monomer solution was added to the initiator solution over 1 hour.

As shown in the table t-butoxy molybdenum initiator produced a high trans content polymer while trifluorinated butoxy molybdenum initiator provided a high cis content polymer.

3. 4 Attempted polymerisation of the exo-adduct

The polymerisation of the exo-adduct was attempted using the t-butoxy molybdenum initiator. The results are shown in Table 3.4.

Table 3.4. The results of the polymerisation of the exo-adduct

No.	Solvent	Ratio (Monomer / Initiator)	Polymer obtained
P3-7	C ₆ D ₆	20 / 1	Insoluble polymer
P3-8	C ₆ D ₆	3 / 1	Insoluble polymer
P3-9	THF-d ₈	20 / 1	Insoluble polymer

Under the same condition as those used for the endo-adduct polymerisation, the monomer solution became very viscous and solidified like a

gel 10 seconds after mixing the monomer and the initiator solutions (P3-7). The material could not be redissolved even in boiling dimethylsulfoxide. As this result seemed to suggest the activity of the initiator was too vigorous to induce reasonable ring opening metathesis polymerisation, polymerisation using tetrahydrofuran as solvent was attempted, since tetrahydrofuran was expected to reduce the activity of the initiator. However, it again produced a gel like material (P3-9). The formation of this insoluble gel might be due to either cross linking or the character of the product polymer, such as crystallinity. Polymerisation with a smaller ratio of monomer to initiator was tried because both the crystalline character of the polymer and the chance of cross linking were expected to be reduced in low molecular weight oligomers, but, even in this case, the obtained material was like gel (P3-9).

The infrared spectrum of P3-7 is recorded in Appendix 3.2.3. as a typical example. It was similar to those of the polymers of the endo-adduct and showed the absorptions due to out-of-plane C-H deformation of cis CH=CH unit and trans unit around 760 and 980 cm^{-1} respectively, although the proportion of cis and trans double bonds could not be determined because of the poor resolution and the possibility of overlap with other absorptions, particularly aromatic ring modes around 700~740 cm^{-1} .

3.5 Polymerisation of endo and exo adducts mixture

As the exo-adduct behaved in the unexpected manner described above in polymerisations using a well defined initiator, the polymerisation of an endo- and exo-adduct mixture was examined using both a well defined initiator and classical catalyst systems. The ratio of endo- to exo-adduct was 73:27. The results are shown in Table 3.5.

Table 3.5. The results of the polymerisation of the mixture of endo/exo-adducts

	No.	Cat., Co-cat., Additive (Ratio) ^{a)}	Solvent b)	Reaction duration (min)	Yields (%)		GPC	
					Gel	Soluble	M _n (10 ³)	PDI
Well-defined initiator	P3-10	Mo--O ^t Bu (5)	C ₆ D ₆	10	0	100		
Classical catalyst system	P3-11	WCl ₆ , Me ₄ Sn (2, 4)	T	16	70	1.5	-	-
	P3-12	MoCl ₅ , Et ₂ AlI, AcOEt (1, 4, 60)	T	60	30	0	-	-
	P3-13	MoCl ₅ , Et ₂ AlI, AcOEt, 1-Octene (1, 4, 60, 4.7)	T+C	60	0	22	100	2.1

a) The ratio to 100 of monomer

b) T = toluene, C = chlorobenzene

The mixture of the endo and exo-adducts was polymerised readily using *t*-butoxy molybdenum initiator under the same reaction conditions as were used in the polymerisation of endo-adduct (P3-10), the presence of the resonances due to propagating alkylidene protons in the downfield region of the ¹H n.m.r. spectrum (Appendix 3.3.6.a) confirmed that the polymerisation progressed in a living manner.

The polymerisation of the endo/exo mixture using similar condition to that used by El Saafin and co-workers for the polymerisation of the endo-adduct resulted in a production of insoluble polymer (P3-11), while they obtained a

soluble polymer. The reaction using a classical molybdenum catalyst system which was supposed to be a milder system than the tungsten catalyst also produced insoluble polymers (P3-12). Soluble polymer was obtained by using the chain transfer reagent (1-octene) although the yield was low (P3-13), the catalyst system and the chain transfer reagent used in this case were previously patented as a method to produce gel-free alkylnorbornene polymers by ring opening metathesis polymerisation.⁷⁸

The resonances between 40 and 60 ppm due to methine carbons observed in the ^{13}C DEPT spectrum of P3-10 are shown in Figure 3.14. (Appendix 3.3.6.b).

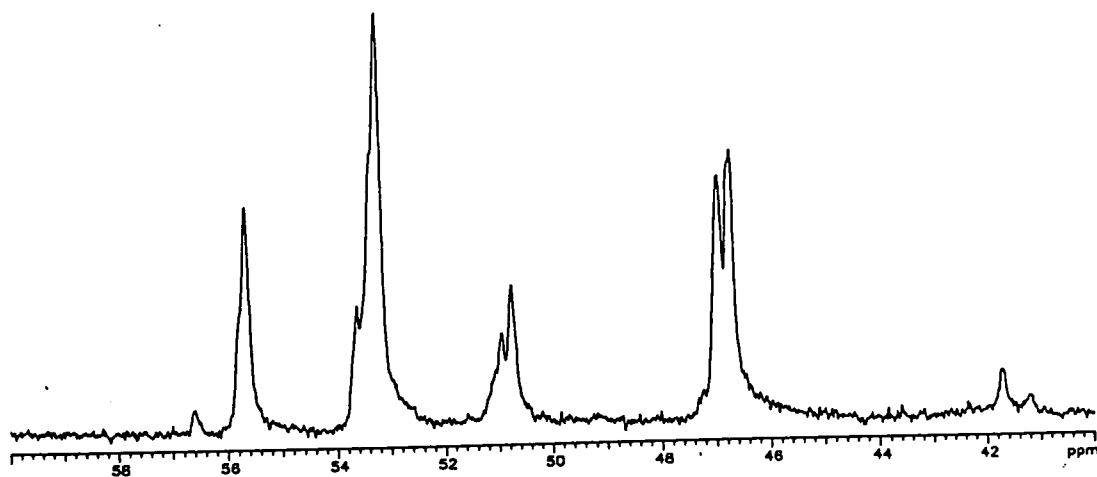


Figure 3.14. DEPT spectrum (40-60 ppm) of methine carbon

The resonances at 46.7, 47.0 and 41.7 ppm seemed to be due to the allylic carbons of endo-adduct unit adjacent to trans and cis double bond in the polymer chain and the resonance at 53.3 ppm was assigned to the resonance due to benzylic carbons of the endo-adduct unit since the chemical shifts are similar to those of the polymer of endo-adduct (see Figure 3.12.) and the intensity of the resonance at 53.3 ppm is roughly equal to the total intensity of the resonances at 46.7, 47.0 and 41.7 ppm. If this is correct the cis/trans ratio for the endo-adduct

derived repeat unit is 16:84. The resonances at 55.7 and 50.8 ppm might be due to the allylic carbons in the exo-adduct units adjacent to trans and cis double bonds since these resonances were also separated by about 5 ppm but the cis/trans ratio can not be determined since the resonance due to the benzylic carbons of the exo-adduct unit was possibly overlapping on either of these two resonances. No other provisional assignments could be made because of the complexity of the spectrum.

As shown in Table 3.6. (Appendix 3.3.7.a), the ^1H n.m.r. spectrum of P3-13 showed that the proportion of each region, namely aromatic, vinylic, benzylic, allylic, and methylene region was roughly the expected ratio (6:2:2:2:2), although the sample contained a small amount of unremoved monomer as an impurity. However a more detailed analysis was not possible because of poor resolution of spectrum.

Table 3.6. The proportion of each region in ^1H n.m.r. of P3-13 (ppm)

Region	Aromatic	Vinylic	Benzylic	Allylic	Methylene
Obtained result	7.0-7.8	5.2-6.1	3.6-4.4	2.3-3.3	1.0-2.3
(Proportion)	(6)	(2)	(2)	(2)	(2)

The ^{13}C n.m.r. spectrum (Appendix 3.3.7.b) showed similar resonances to those of P3-10, but the detailed assignment was again difficult because of poor resolution and the complexity of the spectrum.

As described above the exo-adduct was polymerised to give soluble copolymers using a well defined initiator and an exo-/endo-adduct mixture and using classical catalyst system by using a chain transfer reagent and it was confirmed that the produced polymer contained both endo and exo-adduct units in the polymer chain.

3.6 Summary and Discussion

It turned out that the t-butoxy molybdenum initiator polymerised the endo-adduct to give a high trans content polymer and the more reactive trifluorinated butoxy molybdenum initiator provided a high cis content polymer, while the classical catalyst system, tungsten hexachloride and tetramethyltin, produced a non-stereoregular polymer. The difference in the behavior of the initiators was similar to that in the polymerisation of 2,3-bis(trifluoromethyl)bicyclo[2.2.1]hepta-2,5-diene reported by Feast and co-workers,⁷⁹ and it is consistent with the mechanism of ring opening metathesis polymerisation using well defined initiator described by Bazan and co-workers.⁵¹ Namely, it can be explained as follows:-

(see Figure 3.15. overleaf)

- (1) If a monomer approaches and reacts with a syn rotamer of the propagating species then a trans double bond and an anti rotamer of propagating species would be formed.
- (2) If a next incoming monomer reacts with the propagating species before it converts to a syn rotamer then cis double bond would be formed.
- (3) But if the initiator is not so reactive then the propagating species would convert to the syn rotamer before the next propagation step.
- (4) The syn rotamer then reacts with the next incoming monomer to form trans double bond. As a consequence the more reactive initiator, the trifluorinated butoxy molybdenum initiator, produced more cis content polymer than t-butoxy molybdenum initiator.

In this study the polymerisation of exo-adduct using a well defined initiator did not provided well defined soluble polymer but insoluble gel. The examination using classical catalysts, which are more Lewis acidic than well defined initiators, seemed to show that the polymerisation process for the exo-adduct was highly sensitive to Lewis acidity. So it is suggested that the

polymerisation of the exo-adduct is strongly affected by even small amount of Lewis acid to produce some cross linking which made the polymer insoluble. The gelation was avoided by copolymerisation with the endo-adduct and by using a chain transfer agent to limit the molecular weight. However further investigation is required to unambiguously clarify the reason for gel production.

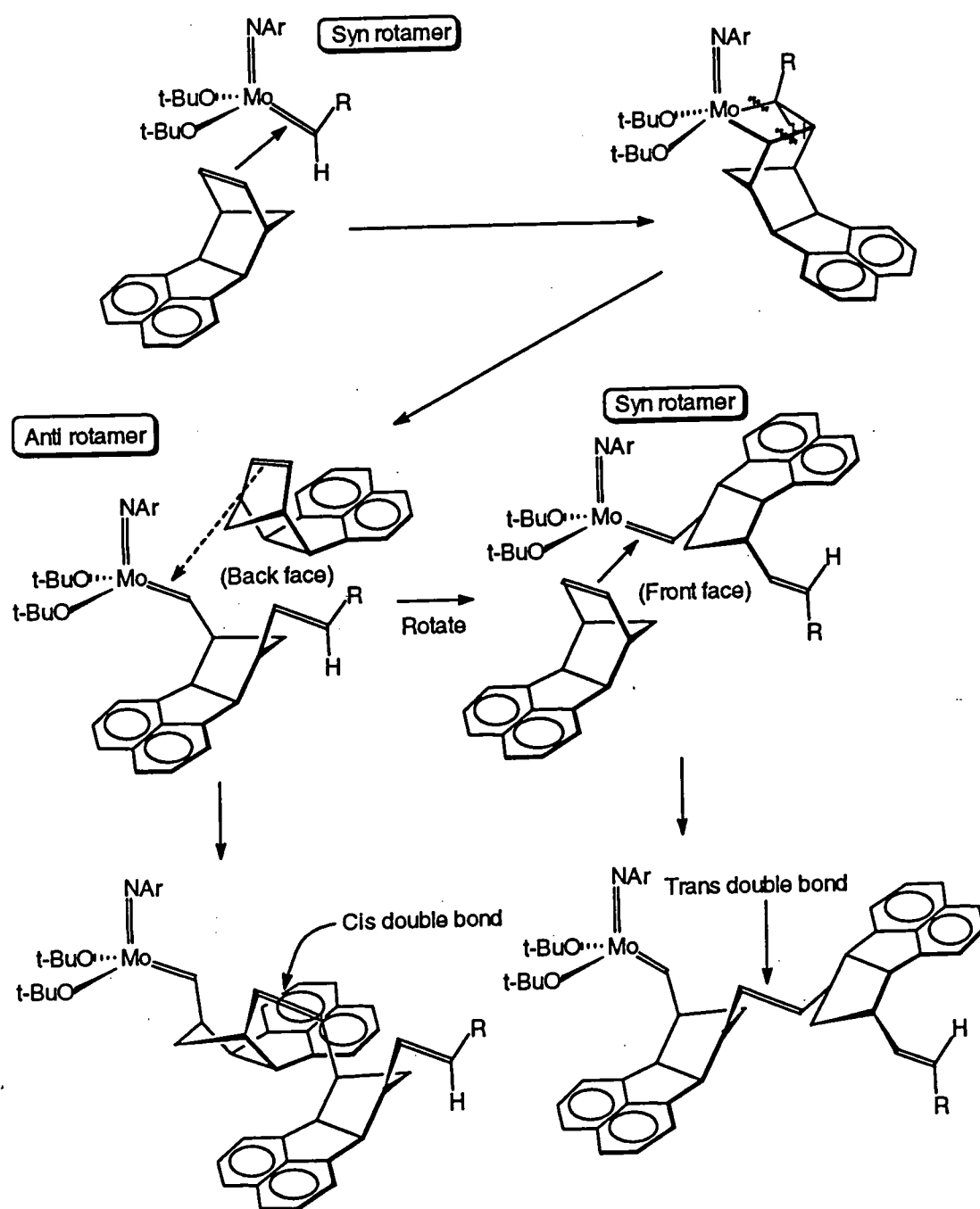


Figure 3.15. The probable mechanism of the polymerisation

3.7 Experimental

The initiators used throughout this work and following work were prepared either in the research group of Prof. V. C. Gibson or in the IRC laboratories by Dr. E. Khosravi and used as supplied in solid form under an inert atmosphere. The adducts were dried over molecular sieves, chloroform was dried over phosphorus pentoxide, benzaldehyde was dried over molecular sieves and toluene and tetrahydrofuran were dried over sodium-benzophenone until the mixture remained purple on stirring overnight, then these were vacuum-transferred into dry ampoules following deoxygenation by means of the freeze-thaw-pump technique. The solvents were passed through a short column (c.a. 4 cm) of oven dried neutral alumina in a glove box before use. Typical examples of the polymerisation method are described below.

a) Polymerisation using well defined initiators

The following procedure was performed in a glove box, where the concentration of oxygen was below 8 ppm and moisture was below 7 ppm.

The endo-adduct of acenaphthylene with cyclopentadiene (79mg, 0.36 mmol) was dissolved in perdeuterobenzene (0.45 ml) and t-butoxy molybdenum initiator (10mg, 0.018 mmol) was dissolved in the same solvent (0.45 ml). Each solution was stirred for 1 minute and then the monomer solution was added to the initiator solution. The mixture was placed in a n.m.r.-tube after stirring for 1 minute. The n.m.r.-tube was sealed and taken out the glove box. The n.m.r. was observed immediately.

For obtaining end capped polymers, an excess of benzaldehyde was added to the reaction mixture 1 minute after mixing the monomer and initiator solutions and the resulting solution was stirred for 10 hours. Then the mixture was taken out the glove box and the polymer obtained was precipitated from benzene into methanol under a dry oxygen free nitrogen atmosphere, and dried under vacuum.

In case of the polymerisation of exo-adduct of acenaphthylene and cyclopentadiene, the reaction mixture became very viscous and produced gel like material 10 seconds after mixing the monomer and the initiator solutions. The material was not soluble in ordinary solvents.

b) Polymerisation using classical catalysts

All manipulation was carried out under a nitrogen atmosphere.

(b-i) Polymerisation initiated by tungsten catalyst

To a toluene solution of tungsten hexachloride (0.18 M, 1 ml), tetramethyltin (0.066g, 0.37 mmol) dissolved in toluene (9 ml) was added. After the colour changed from blue-black to brown-black (17 minutes), a toluene solution of the endo and exo-adducts (2.56 M, 3.5 ml) was added. The mixture was stirred for 16 minutes then methanol (1 ml) was added to the mixture. The resulting mixture was added into excess amount of methanol and the precipitate was collected by filtration. The precipitate was stirred in an excess of toluene at 80° C for 2 hours then filtered. The soluble product was obtained by concentrating the filtrate and insoluble product was obtained by drying the remaining solid.

(b-ii) Polymerisation initiated by molybdenum catalyst

To a toluene solution of a mixture of endo and exo-adducts of acenaphthylene with cyclopentadiene (2.56 M, 3.9 ml), 1-octene (0.053g, 0.47 mmol), chlorobenzene (9.5 ml) and diethylaluminium iodide dissolved in toluene (0.25M, 1.6ml) were added. After stirring the mixture for 24 minutes a mixture of molybdenum pentachloride (0.1 mmol) and ethyl acetate (6.0 mmol) dissolved in toluene (2 ml) was added and the resulting solution was stirred for 1 hour, then methanol (1 ml) was added to the solution. The mixture was added to an excess of methanol and the precipitated material was recovered by filtration, washed with methanol and dried under vacuum for 14 hours.

CHAPTER 4: Synthesis of 4-methylcyclopentene

4.1 Introduction

As described in Chapter 1, one of the objectives of this study was to examine the polymerisability of a symmetrically substituted cyclopentene and to establish the microstructures of the product polymers. 4-Methylcyclopentene is one of the simplest of such monomers but, even in this case, the microstructural possibilities for the resulting polymers are numerous since every repeat unit has one double bond and one chiral centre. Analysis of the microstructures of the polymers obtained from this simple monocyclic olefin has not been reported and, if it could be accomplished, might help to understand the mechanism(s) of such polymerisations.

In this chapter, the synthesis of 4-methylcyclopentene and related molecules is described. The polymerisation of the monomer and examination of the structures and properties of the resulting polymers is discussed in Chapter 6.

4.2 Results and discussion

4-Methylcyclopentene was synthesized following the route shown in Figure 4.1.

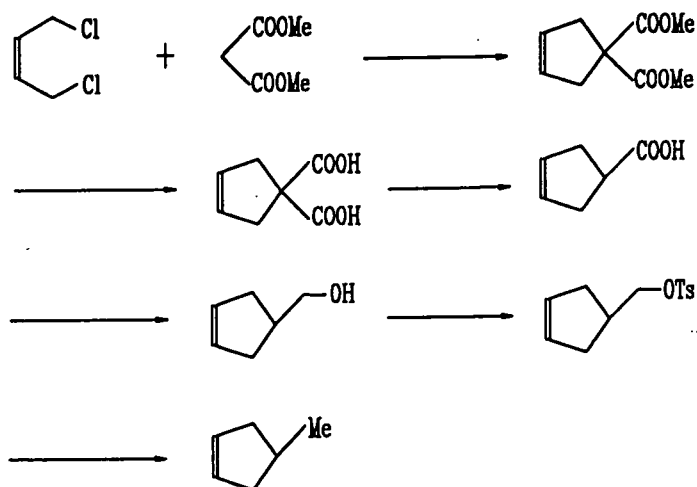
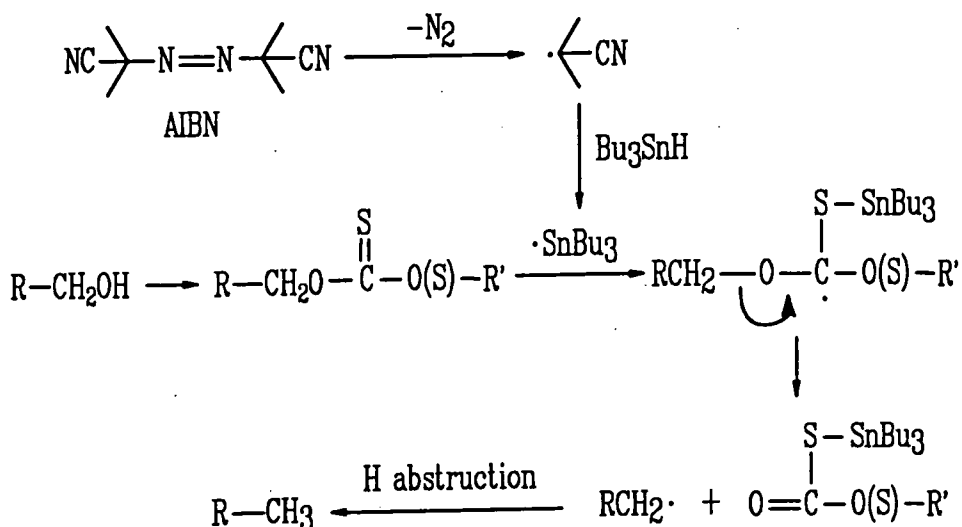
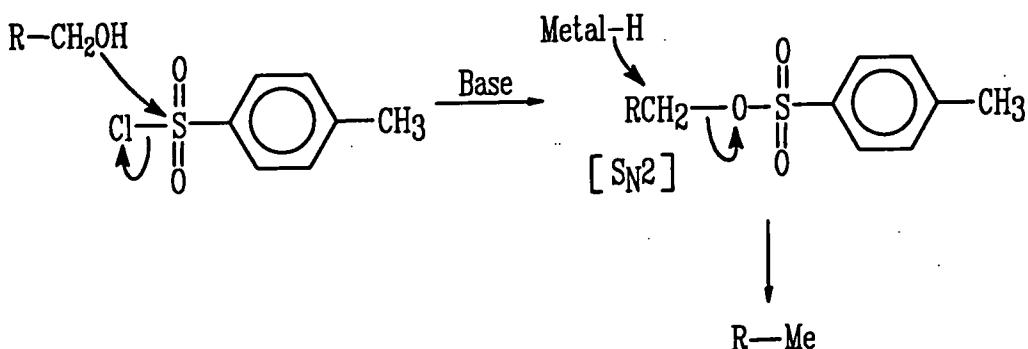


Figure 4.1. Scheme for the synthesis of 4-methylcyclopentene



c) The conversion of the alcohol to the p-toluenesulfonate and subsequent reduction by metal hydride.⁸⁰



In procedure (a), the bromination is believed to proceed not only via $\text{S}_\text{N}2$ displacement of the protonated hydroxyl, but also via an $\text{S}_\text{N}1$ mechanism to some extent. Consequently an intermediate alkyl cation may be formed during the process of bromination. In the case of procedure (b), an alkyl radical is formed after radical deoxygenation. Both these reaction intermediates have the potential to induce side reactions or isomerisation of the carbon skeleton. In order to obtain the desired product it is necessary to avoid such side reactions and to control the reaction completely so as to proceed via an $\text{S}_\text{N}2$ mechanism during the displacement step. Consequently procedure (c) was selected to convert the alcohol to the corresponding alkane, as shown in Figure 4.1.

4.2.1 Synthesis of 3-cyclopentene-1-carboxylic acid

Four routes (Murdock's,^{83,84} Schmid's,^{85,86} Cremer's^{87,88} and Greene's⁸⁹ procedures) are known for the synthesis of 3-cyclopentene-1-carboxylic acid. Murdoc made this product by the condensation of cis-1,4-dichloro-2-butene with malonic ester followed by saponification and decarboxylation (Figure 4.2).^{83,84} However this procedure resulted in the formation of 2-vinylcyclopropane-1,1-dicarboxylate as a side product and the yield of the desired acid was poor (19-33%).

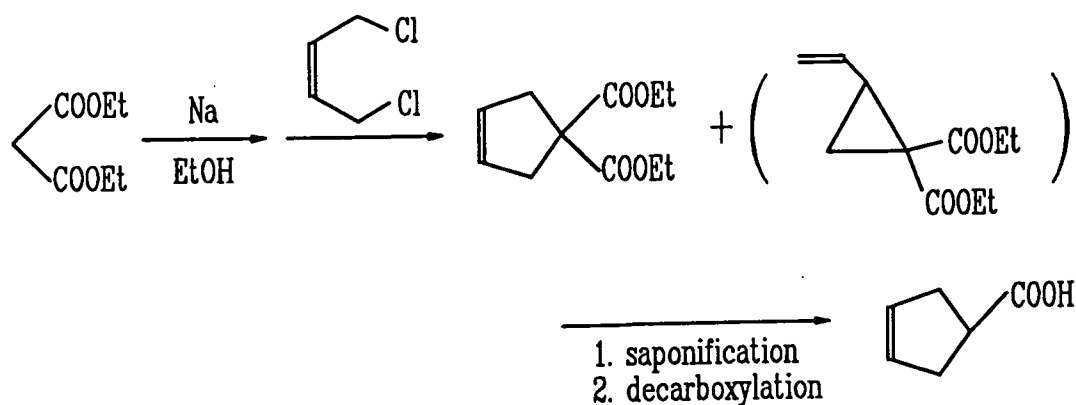


Figure 4.2. Murdock's scheme for the synthesis of 3-cyclopentene-1-carboxylic acid^{83,84}

Schmid accomplished the conversion of the 2-vinylcyclopropane-1,1-dicarboxylate side product to the desired 3-cyclopentene-1,1-dicarboxylate by means of a thermal rearrangement. He pyrolyzed the mixture produced by the condensation of the but-2-ene dichloride and malonic ester at 400-425°C and obtained 3-cyclopentene-1-carboxylic acid in 32% overall yield (Figure 4.3.) after saponification and decarboxylation.^{85,86}

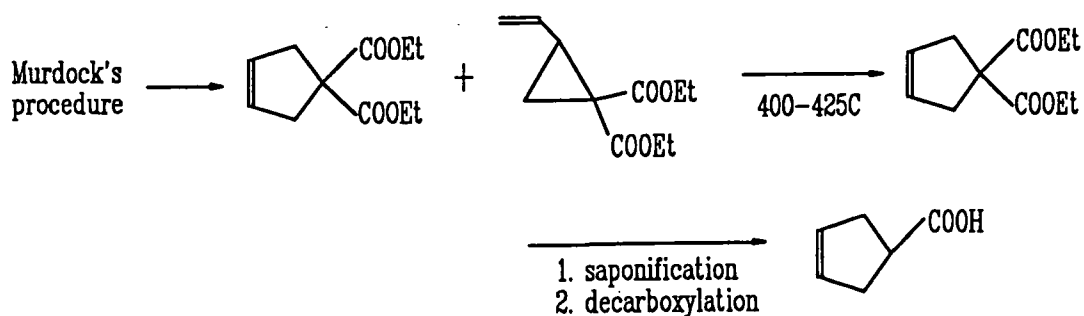


Figure 4.3. Schmid's improvement of Murdock's procedure for the synthesis of 3-cyclopentene-1-carboxylic acid^{85,86}

Cremer obtained the acid in 44% overall yield using cyclopentadiene as a starting material (Figure 4.4.).^{87,88}

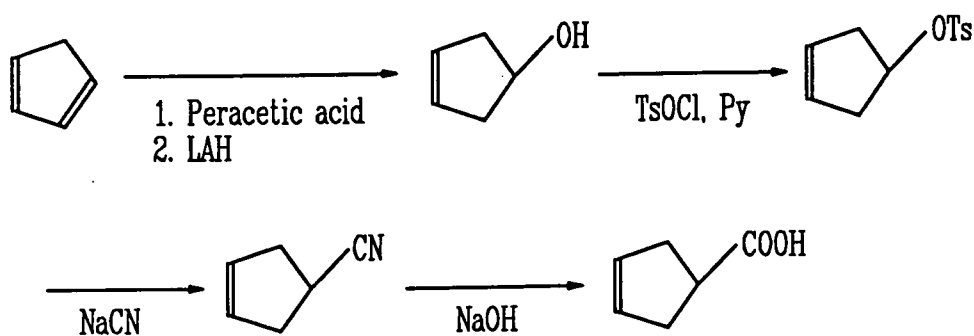


Figure 4.4. Cremer's route to 3-cyclopentene-1-carboxylic acid^{87,88}

An improvement of Murdock's procedure was accomplished by Greene,⁸⁹ who found the formation of 2-vinylcyclopropane-1,1-dicarboxylate in the condensation between the *cis*-1,4-dichloro-2-butene and malonic ester to be highly sensitive to changes in the base, the solvent and the R groups of the starting malonic ester. The desired acid was obtained in 70% overall yield by this improved procedure using dimethyl malonate under the conditions indicated in Figure 4.5.

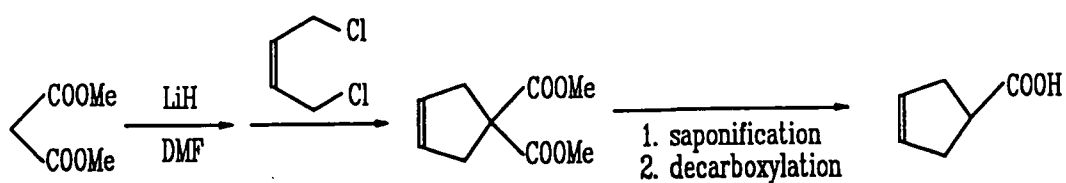


Figure 4.5. Greene's optimised route to 3-cyclopentene-1-carboxylic acid⁸⁹

We used Greene's procedure to synthesize 3-cyclopentene-1-carboxylic acid in this work because of its high yield.

Dimethyl 3-cyclopentene-1,1-dicarboxylate was synthesized by the condensation of dimethyl malonate and cis-1,4-dichloro-2-butene. The ester was reacted with lithium hydride as base in dimethylformamide as solvent, and condensed with the chloride at ambient temperature. The material obtained consisted of two components in a ratio of about 95:5 according to analytical gas chromatography (Appendix 4.1.1.). The minor component was not identified but was probably dimethyl 2-vinylcyclopropane-1,1-dicarboxylate; Greene obtained it in similar ratio to dimethyl 3-cyclopentene-1,1-dicarboxylate. The major component was purified by recrystallisation from n-hexane (Appendix 4.1.2), the yield was 67%.

The infrared spectrum of the purified product (Appendix 4.1.3) was consistent with expectation and showed a vinylic C-H stretching absorption at 3004 cm^{-1} , aliphatic C-H stretching at 2955 cm^{-1} , C=O stretching of the ester groups at 1732 cm^{-1} , a C-H deformation at 1435 cm^{-1} , the C-O stretching of the ester groups at 1258 cm^{-1} , and the out-of-plane C-H deformation of the cis CH=CH double bond at 700 cm^{-1} . The mass spectrum (Appendix 4.1.4) confirmed the molecular weight of 184 amu, and showed the expected fragments at 152 ($M^+ - \text{CH}_3\text{OH}$), 124 ($M^+ - \text{HCOOCH}_3$), 65 (C_5H_5^+), and 39 (C_3H_3^+). The ^1H n.m.r. spectrum (Appendix 4.1.5.a) showed four methylene (3.03 ppm ,s), six methyl (3.74 ppm ,s) and two vinylic (5.62 ppm ,s) signals as would be expected. The infrared and ^1H n.m.r. spectrum were in agreement with the spectra reported by Greene. The ^{13}C -n.m.r. spectrum (Appendix 4.1.5.b) showed a methylene carbon at 40.84 ppm, a methoxy carbon at 52.73 ppm, a quaternary carbon at 58.65 ppm, a vinyl carbon at 127.70 ppm, and a carbonyl carbon at 172.54 ppm; again completely consistent with expectation.

Dimethyl 3-cyclopentene-1,1-dicarboxylate was converted to the free acid by means of hydrolysis. The infrared spectrum (Appendix 4.1.6.) showed the

characteristic absorption for C=O stretching of a carboxylic acid group at 1698 cm^{-1} , the O-H deformation mode at 1405 cm^{-1} , the C-O stretching of a carboxylic acid group at 1281 cm^{-1} , a O-H deformation at 924 cm^{-1} , and the out-of-plane C-H deformation of the cis CH=CH unit at 688 cm^{-1} as well as the strong broad absorption typical of O-H of free carboxylic acid around 2900 cm^{-1} . The ^1H n.m.r. spectrum (Appendix 4.1.7.) showed four methylene (3.10 ppm, s) and two vinyl (5.65 ppm, s) signals, and confirmed that the solvolysis was complete as the signal of the methyl group had completely disappeared.

The decarboxylation of the diacid was carried out by heating it at 180°C for 1 hour. The sample was purified by vacuum distillation, and its purity was confirmed by gas chromatography (Appendix 4.1.8.). The yield from dimethyl 3-cyclopentene-1,1-dicarboxylate was 91%. The boiling point and the yield based on dimethyl malonate turned out to be $75^\circ\text{C}/1\text{mmHg}$ and 61%, which are similar to the literature values of $70^\circ\text{C}/1\text{mmHg}$ and 70%.⁸⁹ The infrared spectrum (Appendix 4.1.9.) showed the carboxylic acid C=O group stretching absorption at 1707 cm^{-1} , a O-H deformation at 1420 cm^{-1} , the C-O stretching of the carboxylic acid group at 1296 cm^{-1} , a O-H deformation at 947 cm^{-1} , and the out-of-plane C-H deformation of the cis CH=CH unit at 691 cm^{-1} as well as the strong broad absorption of the O-H of free carboxylic acid around 2900 cm^{-1} . The mass spectrum (Appendix 4.1.10.) confirmed the molecular weight of 112 amu and showed expected fragments at 97 (M^+-OH) and 67 (M^+-COOH). The ^1H n.m.r. spectrum (Appendix 4.1.11.a) showed four methylene (2.69 ppm, m), one methine (3.16 ppm, m), two vinyl (5.67 ppm, s), and one carboxylic acid signals (11.2 ppm, broad). These infrared and ^1H n.m.r. spectroscopic data were in agreement with those reported by Greene.⁸⁹ The ^{13}C -n.m.r. spectrum (Appendix 4.1.11.b) showed methylene, methine, vinyl and carbonyl carbon signals at 36.2, 41.4, 128.9, 183.0 ppm respectively.

4.2.2 Synthesis of 4-hydroxymethylcyclopentene

4-Hydroxymethylcyclopentene was synthesised by metal hydride reduction of 3-cyclopentenecarboxylic acid, according to Hutchison's procedure⁹⁰ with minor modification. The acid was reduced by three equivalents of lithium aluminium hydride in diethyl ether at reflux temperature. The yield of purified sample was 95%. The purity of the sample was confirmed by gas chromatography (Appendix 4.1.12.).

The infrared spectrum (Appendix 4.1.13.) showed the O-H stretching absorption at 3332 cm^{-1} , the vinylic C-H stretching at 3054 cm^{-1} , the aliphatic C-H stretching at 2927 cm^{-1} , C-H deformations at 1471 cm^{-1} and 1442 cm^{-1} , C-O stretching and O-H deformation at 1074 cm^{-1} and 1038 cm^{-1} , and the out-of-plane C-H deformation of the cis CH=CH unit at 672 cm^{-1} . The mass spectrum (Appendix 4.1.14.) showed expected fragments at 81 ($M^+ - \text{OH}$), 80 ($M^+ - \text{H}_2\text{O}$), and 67 ($M^+ - \text{CH}_2\text{OH}$), but the molecular ion peak was not detected. The ^1H n.m.r. spectrum (Appendix 4.1.15.a) showed the four methylene hydrogens of the cyclopentene ring, one methine and one hydroxy hydrogen between 2.05~2.60 ppm, as a complex overlapping multiplet, a methylene (3.52 ppm, d $J=6\text{Hz}$) and two vinyl hydrogen (5.64 ppm, s) signals as expected. The ^{13}C -nmr spectrum (Appendix 4.1.15.b) showed the methylenes of the cyclopentene ring, the methine, a methylene, and vinyl carbons at 35.5, 39.1, 67.0, and 129.5 ppm respectively.

4.2.3 Synthesis of 3-cyclopentenemethyl p-toluenesulfonate

3-Cyclopentenemethyl p-toluenesulfonate was synthesised by esterification of 4-hydroxymethylcyclopentene using p-toluenesulfonyl chloride in pyridine at low temperature. The purity of the sample obtained was confirmed by

gas chromatography (Appendix 4.1.16.). The yield was 92% and the melting point was 31-32°C.

The infrared spectrum (Appendix 4.1.17.) showed a vinylic C-H stretching absorption at 3056 cm^{-1} , aliphatic C-H stretching modes at 2926 cm^{-1} and 2852 cm^{-1} , a skeletal vibration of the benzene ring at 1599 cm^{-1} , a C-H deformation at 1443 cm^{-1} , the S=O stretching modes of the sulfonate group at 1361 cm^{-1} and 1175 cm^{-1} , the out-of-plane C-H deformation of the benzene ring at 815 cm^{-1} and the out-of-plane C-H deformation of the cis CH=CH unit at 665 cm^{-1} . The chemical shifts from the ^1H and ^{13}C n.m.r. spectra (Appendix 4.1.18.a and b) are shown in Figure 4.6.a. and 4.6.b. respectively, the chemical shifts observed were consistent with the assigned structure.

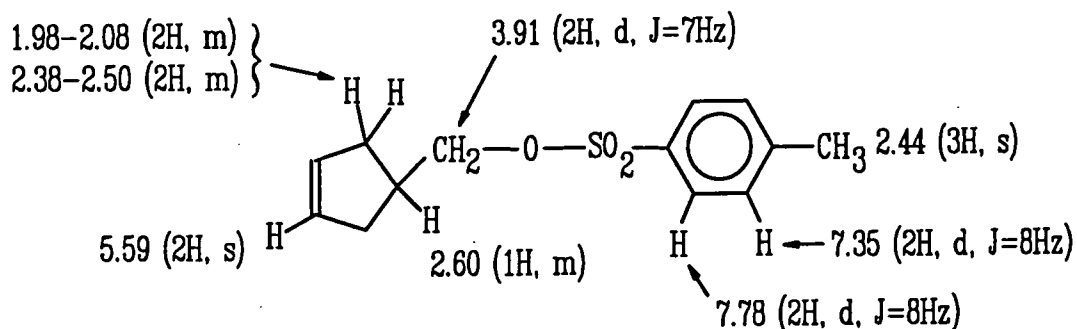


Figure 4.6.a. The chemical shifts from the ^1H n.m.r. spectrum of 3-cyclopentenemethyl sulfonate (ppm with respect to TMS)

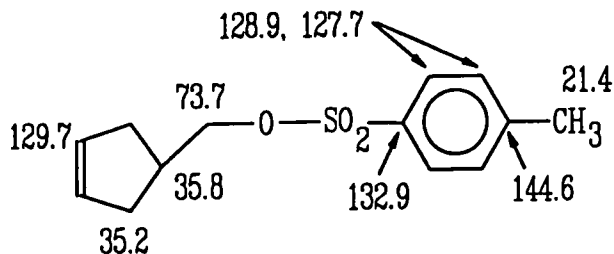


Figure 4.6.b. The chemical shifts from the ^{13}C n.m.r. spectrum of 3-cyclopentenemethyl sulfonate (ppm with respect to TMS)

4.2.4 Synthesis of 4-methylcyclopentene

Sodium borohydride (NaBH_4) in dimethyl sulfoxide, sodium trimethoxyborohydride ($\text{NaBH}(\text{OMe})_3$) in dimethyl sulfoxide, lithium triethylborohydride (LiEt_3BH) and lithium aluminium hydride (LiAlH_4) are known as suitable reagents to reduce the p-toluenesulfonates of alcohols to the corresponding alkanes. In the case of sodium borohydride, the borane produced in the process may react further with the double bond via hydroboration to yield side products,⁹¹ this reagent was therefore considered unsuitable for the reduction of 3-cyclopentenemethyl p-toluenesulfonate. Sodium trimethoxyborohydride can be used to avoid such side reaction⁹¹ but was not commercially available. Lithium triethylborohydride is known to reduce even hindered p-toluenesulfonates via a completely $\text{S}_{\text{N}}2$ mechanism without any hydroboration of double bonds,⁹² but it was commercially available only as a tetrahydrofuran solution. The boiling point of our anticipated product, 4-methylcyclopentene, was expected to be similar to that of tetrahydrofuran (b.p.=67°C), by comparison with the boiling point of cyclopentene, which is 44°C; if this assumption were valid it would be difficult to isolate the product after the completion of the reaction. Lithium aluminium hydride was therefore selected as the reagent to convert 3-cyclopentene p-toluenesulfonate to 4-methylcyclopentene; this reducing reagent is cheap and readily available.

The reduction of 4-methylcyclopentene in diethyl ether using six equivalents of lithium aluminium hydride was attempted first; although gas chromatography of the reaction mixture confirmed the starting material was completely converted after four hours, the product could not be isolated from the reaction mixture because of small difference between the boiling points of the product and the solvent. Diglyme, boiling point 162°C, was used in the next attempt. It is inert towards lithium aluminium hydride although the rate of reduction of p-toluenesulfonates with lithium aluminium hydride in diglyme is known to be much slower than that in diethyl ether.⁹³ In this case the product was distilled from the reaction mixture over eight

hours. The gas chromatogram (Appendix 4.1.19.) and GC-mass spectroscopy confirmed that the first peak in the chromatogram was chloroform (used as solvent for injection) and the later one was 4-methylcyclopentene. The yield was 75%. The material obtained was used as a sample for analysis and polymerisation studies. The infrared spectrum (Appendix 4.1.20.) showed the vinylic C-H stretching absorption at 3055 cm^{-1} , the aliphatic C-H stretching modes at 2955 cm^{-1} , 2925 cm^{-1} and 2842 cm^{-1} , a C-H deformation at 1458 cm^{-1} , and an out-of-plane C-H deformation of the cis CH=CH double bond at 670 cm^{-1} . The mass spectrum (Appendix 4.1.21.) confirmed the molecular weight 82 amu and showed expected fragments at 67 ($\text{M}^+ - \text{CH}_3$), 65 (C_5H_5^+), and 39 (C_3^+). The signals of the ^1H n.m.r. spectrum (Appendix 4.1.22.a) were assigned as shown in Figure 4.7.a., using the integration value and the splitting pattern for each signal. The signals of the ^{13}C n.m.r. spectrum (Appendix 4.1.22.b) were assigned as shown in Figure 4.7.b., using the chemical shifts of each signal and DEPT analysis (Appendix 4.1.22.c).

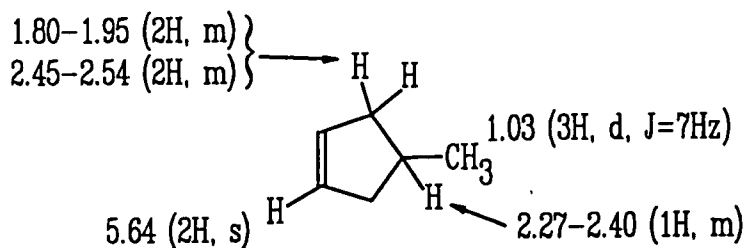


Figure 4.7.a. The chemical shifts from the ^1H n.m.r. spectrum of 4-methylcyclopentene (ppm with respect to TMS)

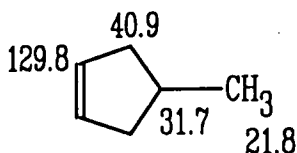


Figure 4.7.b. The chemical shifts from the ^{13}C n.m.r. spectrum of 4-methylcyclopentene (ppm with respect to TMS)

4.3 Experimental

Dimethyl 3-cyclopentene-1,1-dicarboxylate

Methyl malonate (98%), cis-1,4-dichloro-2-butene (95%), N,N-dimethylformamide (water<0.005%) and lithium hydride (95%) were purchased from Aldrich Chemical Co. Dimethyl malonate and cis-1,4-dichloro-2-butene were dried over molecular sieves for two days before use.

Dry dimethyl formamide (920 ml) and dimethyl malonate (87.4g, 0.649 mol) were placed in a two-necked round-bottomed flask (2 l), one neck was fitted with a reflux condenser which was attached to a nitrogen inlet and another was closed with a stopper. After the apparatus was purged with dry nitrogen, the mixture in the flask was cooled in an ice-water bath. To the stirred mixture lithium hydride (13.8g, 1.64 mol, 1.26 equivalents) was added in several portions against a dry nitrogen flow. After the evolution of hydrogen ceased (2 hour), cis-1,4-dichloro-2-butene (97.6g, 0.742 mol, 1.14 equivalents) was added and the mixture was then allowed to warm to room temperature. After 91 hours, the resulting mixture was divided into three portions and each portion was worked up using the same procedure. Cold water (400 ml) was added to each portion and the mixture extracted with diethyl ether (400 ml) and n-hexane (400 ml). The organic layer was washed with water (400 ml) and brine (400 ml). The accumulated aqueous layer was then extracted with diethyl ether (400 ml) and n-hexane (400 ml) again, and the second organic layer was washed with water (400 ml) and brine (400 ml). These two organic layers were combined and dried over anhydrous magnesium sulfate. After the solid was removed by filtration, the three filtrates obtained from the three portions were combined and the solvents were removed by vacuum evaporation, to give a mixture (104.74g) of dimethyl 3-cyclopentene-1,1-dicarboxylate and dimethyl 2-vinylcyclopropane-1,1-dicarboxylate in a ca. 95:5 ratio, as a white-brown solid. Recrystallization of this mixture from n-hexane afforded the desired ester (80.60g, 0.438 mol, 67%) as

white crystals. An additional recrystallization produced an analytical sample of the dimethyl 3-cyclopentene-1,1-dicarboxylate; mp 57-58°C; IR 3004, 2955, 1732, 1435, 1258, 1194, 1167, 1075, 974, 700 cm^{-1} ; MS 184 (M^+), 152, 124, 93, 79, 65, 59, 39; $^1\text{H-n.m.r.}$ (CDCl_3) δ 3.03 (4H, s), 3.74 (6H, s), 5.62 ppm (2H, s); $^{13}\text{C-n.m.r.}$ (CDCl_3 , offresonance) δ 40.84, 52.73, 58.65, 127.70, 172.54 ppm.

3-Cyclopentene-1,1-dicarboxylic acid

Dimethyl 3-cyclopentene-1,1-dicarboxylate (80.11g, 0.435 mol) and 80% aqueous ethanol (860 ml) were placed in a round-bottomed flask (2 l) fitted with a reflux condenser. To the stirred mixture was added potassium hydroxide (77.90g, 1.18 mol, 1.4 equivalents). The mixture was stirred for 22 hours at 55~60°C and then concentrated by vacuum evaporation to remove ethanol. To the liquid obtained water (330 ml) was added and the mixture was washed with 20% diethyl ether in n-hexane (500 ml). The resulting mixture was cooled in an ice-water bath and cautiously treated with concentrated sulfuric acid (71 ml). The acidified aqueous phase was extracted four times with ethyl acetate (600 ml), and the organic phase was dried over anhydrous magnesium sulfate. After the solid was removed by filtration, the solution was concentrated by vacuum evaporation to give 3-cyclopentene-1,1-dicarboxylic acid (67.82g, 0.435 mol, ca. 100%) as a pale yellow solid. The material obtained was used as the starting material for the following step without further purification since the diester was confirmed to be converted completely by $^1\text{H n.m.r.}$; IR 2893 (broad), 2665, 1698, 1405, 1281, 1214, 924, 688 cm^{-1} ; $^1\text{H-n.m.r.}$ (CDCl_3) δ 3.10 (4H, s), 5.65 (2H, s) ppm.

3-Cyclopentenecarboxylic acid

3-Cyclopentene-1,1-dicarboxylic acid (67.82g, 0.435 mol) was placed in a round-bottomed flask (250 ml) fitted with a reflux condenser and a nitrogen inlet.

The flask was purged with dry nitrogen, and the flask was heated in an oil bath at 180°C. After 1 hour, gas evolution ceased and the residual oil was distilled under reduced pressure to give 3-cyclopentenecarboxylic acid (44.2g, 0.394 mol, 91% yield from dimethyl 3-cyclopentene-1,1-dicarboxylate) as a colourless oil; bp 75°C/1mmHg; IR 3060 (broad), 2928, 2654, 1707, 1420, 1296, 1233, 947, 691 cm⁻¹; MS 112 (M⁺), 97, 67; ¹H-n.m.r. (CDCl₃) δ 2.69 (4H, m), 3.16 (1H, m), 5.67 (2H, s), 11.2 ppm (1H, broad s); ¹³C-n.m.r. (CDCl₃, offresonance) δ 36.2, 41.4, 128.9, 183.0 ppm.

4-Hydroxymethylcyclopentene

Lithium aluminium hydride (95%) was purchased from Aldrich Chemical Co. Ltd. Diethyl ether was dried over sodium-benzophenone until it turned purple.

Lithium aluminium hydride (2 g, 50.8 mmol, 1.5 equivalents) and dry ether (77 ml) were placed in a two necked round-bottomed flask (250 ml) fitted with a reflux condenser to which was attached to a nitrogen inlet. 3-Cyclopentenecarboxylic acid (5.0g, 44.6 mmol) in dry ether (20 ml) was slowly added to the mixture so as to maintain a gentle reflux. After the addition was completed, the mixture was stirred at room temperature for 14 hours. To the mixture was added lithium aluminium hydride (2.13g, 54.1 mmol, 1.6 equivalents) in several portions against a dry nitrogen flow, and the mixture was refluxed for an additional 8 hours under a nitrogen atmosphere. After the reaction was completed the mixture was allowed to cool and was then carefully quenched with water (1.1 ml) followed by sodium hydroxide solution (5 ml, 40%). The precipitated white hydroxides were removed by filtration, the clear ether layer was dried over anhydrous magnesium sulfate and the solvent evaporated under reduced pressure. The resulting liquid was distilled under vacuum to give 4-hydroxymethylcyclopentene (4.16g, 42.4 mmol, 95% yield); bp 70°C/15mmHg; IR 3332, 3054, 2927, 1616, 1471, 1442, 1353, 1074, 1038, 945,

672 cm^{-1} ; MS 81 (M^+ -OH), 80, 67; ^1H -n.m.r. (CDCl_3) δ 2.05-2.38 (3H, m), 2.40-2.60 (3H, m), 3.52 (2H, d $J=6\text{Hz}$), 5.64 ppm (2H, s); ^{13}C -n.m.r. (CDCl_3 , offresonance) δ 35.5, 39.1, 67.0, 129.5 ppm.

3-Cyclopentenemethyl p-toluenesulfonate

p-Toluenesulfonyl chloride (99%) and pyridine were purchased from Aldrich Chemical Co. Ltd. and pyridine was dried over sodium hydroxide and distilled before use.

4-Hydroxymethylcyclopentene (7.92g, 80.8 mmol) and dry pyridine (22 ml) were placed in a round-bottomed flask (100 ml) fitted with a drying tube which contained sodium hydroxide pellets. The mixture was cooled to 0°C and dry p-toluenesulfonyl chloride (16.4g, 86.0 mmol 1.06 equivalents) was added in several portions. After the addition was complete the mixture was stirred for 3 hours at 0°C and put in a refrigerator (-5°C) for 17 hours. Cool water (55.5 ml) was added to the resulting mixture and the product p-toluenesulfonate was extracted with chloroform (3 x 80 ml). The chloroform extract was washed with water (200 ml) twice, hydrochloric acid (0.22N, 200 ml) twice, sodium hydrogen carbonate solution (200 ml) twice, and water (200 ml) twice to get rid of the last trace of pyridine. The washed chloroform layer was dried over anhydrous magnesium sulfate and the solvent was evaporated under reduced pressure. The resulting solid was dried under vacuum for 5 hours to give 3-cyclopentenemethyl p-toluenesulfonate (19.7g, 78.1 mmol, 97% yield); mp $31\text{-}32^\circ\text{C}$; IR 3056, 2926, 2852, (1924, 1718), 1599, 1443, 1361, 1175, 1097, 970, 942, 815, 665, 555 cm^{-1} ; ^1H -n.m.r. (CDCl_3) δ 1.98-2.08 (2H, m), 2.38-2.50 (2H, m), 2.44 (3H, s), 2.60 (1H, m), 3.91 (2H, d $J=7\text{Hz}$), 5.59 (2H, s), 7.35 (2H, d $J=8\text{Hz}$), 7.78 ppm (2H, d $J=8\text{Hz}$); ^{13}C -n.m.r. (CDCl_3 , offresonance) δ 21.4, 35.2, 35.8, 73.7, 127.7, 128.9, 129.7, 132.9, 144.6 ppm.

4-Methylcyclopentene

Lithium aluminium hydride and dry diethyl ether were obtained as described above.

Lithium aluminium hydride (3.52g, 93.2 mmol 3.4 equivalents), was placed in a two necked round-bottomed flask (100 ml) fitted with a fractionating column to which was attached a distillation head with a receiver. After purging with nitrogen the flask was cooled down at 0°C and dry diglyme (33 ml) was carefully placed in the flask. The mixture was stirred at 0°C for 10 minutes and allowed to warm up to room temperature. The receiver was cooled down to -78°C with a solid carbon dioxide/acetone bath. To the mixture in the flask 3-cyclopentene p-toluenesulfonate (7.0g, 27.8 mmol) dissolved in dry diglyme (7 ml) was added using a syringe. The mixture was stirred at room temperature for 30 minutes and then heated up to 110°C over 90 minutes using an oil bath, then kept at that temperature for 7 hours. The liquid collected in the receiver was distilled to give 4-methylcyclopentene (1.56g, 19.0 mmol, 68% yield); bp 60°C/760mmHg; IR 3055, 2955, 2925, 2842, 1617, 1458, 975, 911, 670 cm⁻¹; MS 82 (M⁺), 81, 79, 67, 65, 39; ¹H-n.m.r. (CDCl₃) δ 1.03 (3H, d J=7Hz), 1.80-1.95 (2H, m), 2.27-2.40 (1H, m), 2.45-2.54 (2H, m), 5.64 ppm (2H, s); ¹³C-n.m.r. (CDCl₃, offresonance) δ 21.8, 31.7, 40.9, 129.8 ppm.

CHAPTER 5: Polymerisation of cyclopentene and characterisation of the polymers obtained

The behavior of various initiators in the polymerisation of cyclopentene was examined before starting the investigation of the polymerisation of 4-methylcyclopentene. This sequence was adopted partly to gain some familiarity with the experimental procedures involved and partly to check the validity of some literature claims. Cyclopentene is cheap and readily available and so is an appropriate monomers to learn technique with. In this chapter the polymerisation of cyclopentene and the characterisation of the polymers obtained are discussed, and the study using the less readily accesible 4-methylcyclopentene is discussed in the next chapter.

5.1 Introduction

Ever since the first discovery of ring opening polymerisation of cyclopentene⁹ the potential commercial importance of this elastomeric product has stimulated the examination of the details of its polymerisation. A very large number of catalyst systems, mostly based on tungsten compounds, have been evaluated for this polymerisation and this work has resulted in many patents and articles.⁹⁴⁻⁹⁹

In the case of ring opening polymerisation of cyclopentene, the polymerisation reaches equilibrium between monomer, cyclic oligomers, and linear polymer as shown in Figure 5.1. overleaf. The sign of the Gibbs free energy for ring opening of five membered rings is close to zero in most cases and consequently relatively small changes in reaction conditions can alter the position of the equilibrium quite dramatically.

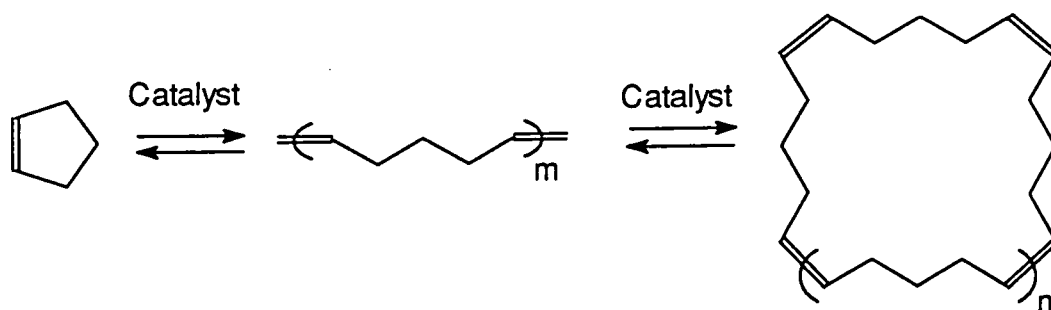


Figure 5.1. Equilibrium of ring opening polymerisation of cyclopentene

A large number of catalyst systems have been reported and examined. A selection of examples of the classical catalyst systems, chosen because of their remarkable selectivity, are shown in Table 5.1.

Table 5.1. Examples of classical catalyst systems for the polymerisation of cyclopentene

Catalyst systems				Produced polymers
WCl ₆ / Et ₃ Al	-30°C	bulk monomer		high trans 58
WCl ₆ / <i>i</i> Bu ₃ Al				high trans 100
WCl ₆ / Et ₄ Sn (1 / 4)	-30°C	in toluene		high cis 101,102
WCl ₆ / (CH ₂ =CHCH ₂) ₄ Si	-30°C			high cis 103
WCl ₆		UV		high cis 104
WF ₆ / Et ₃ Al ₂ Cl ₃ (2 / 1)	-30°C	in toluene		high cis 105
Ph ₂ C=W(CO) ₅	40°C			high cis 106
(π -C ₄ H ₇) ₄ W / AlBr ₃	30°C	in benzene		high trans 107
MoCl ₅ / Et ₃ Al	-30°C			high cis 57

As described in Chapter 1, well defined initiators have several advantages in ring opening metathesis polymerisation as compared to classical catalyst systems, however the investigation of the polymerisation of monocyclic alkenes using well defined initiator systems have started comparatively recently¹⁰⁸ and

the accumulation of data is still restricted to some extent by the limited availability of well defined initiators. It was decided to examine the polymerisation of cyclopentene using well defined initiators in order to try to add to this basic knowledge of the system..

5.2 Polymerisation of cyclopentene

For the polymerisation experiments in this chapter, the initial monomer concentration and the ratio of the monomer to the initiator were fixed as follows:-

- Initial monomer concentration = 4.0 mol / 1 l of solvent
- Molar ratio of Monomer / Initiator = 400 / 1

This ratio, assuming 100% initiation and perfect living polymerisation, should give a polypentenamer with a number average molecular weight of 27,200.

As discussed in Section 1.7., low reaction temperature and high monomer concentration work in favour of polymerisation of less strained monomers, such as 5, 6 and 7 membered cycloalkenes. Therefore all polymerisation experiments throughout this investigation were carried out at low reaction temperature and high initial monomer concentration.

A typical polymerisation procedure was as follows.

- 1) The cooled monomer solution was added to the cooled initiator solution at the low temperature and under a nitrogen atmosphere.
- 2) After the mixture was stirred for the prescribed time benzaldehyde solution was added to the resulting mixture to quench the living polymer.
- 3) The polymer was isolated by reprecipitation or removing the quenched initiator from the reaction solution by absorption on a short alumina column, followed by concentration and drying.

An outline of the polymerisation process is shown in Figure 5.2.

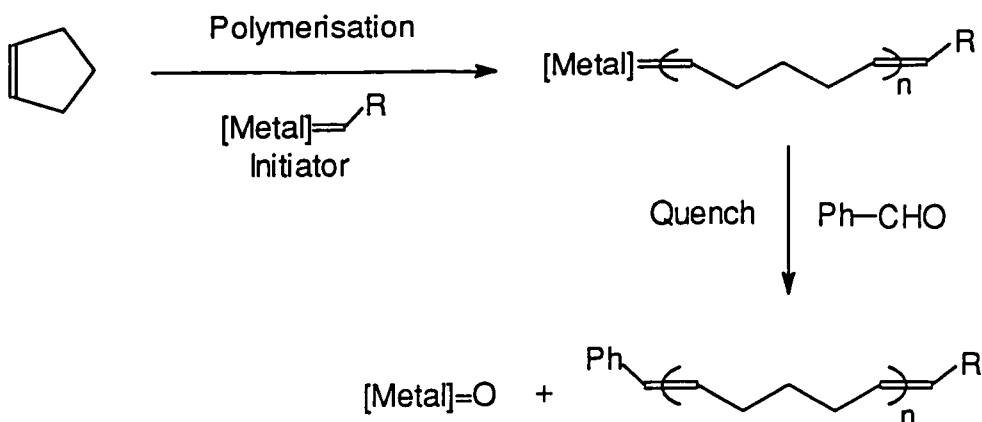


Figure 5.2. Outline of the polymerisation process for cyclopentene initiated by a well defined metal carbene

The average molecular weights and polydispersities of the polymers obtained were calculated based on the results of gel permeation chromatography. The gel permeation chromatograms of the obtained polymers (P5-1~P5-20) are shown in Appendix 5.1.1.-5.1.20. The apparatus was calibrated with respect to polystyrene and the molecular weight quoted are "polystyrene equivalent".

5.2.1 Reproducibility in the polymerisation of cyclopentene

At the beginning of this study, the reproducibility of the polymerisation using well defined initiators was investigated.

Cyclopentene was polymerised under the same condition several times, and the recovered yields, average molecular weight (M_n) and polydispersity (PDI) of the polymers obtained were examined. Schrock type initiators based on molybdenum and tungsten carrying *t*-Butoxy ligands were used in the initial investigation.

The results of polymerisations of cyclopentene using *t*-butoxy molybdenum initiator and *t*-butoxy tungsten initiator are shown in Table 5.2. and 5.3., and GPC traces of the polymers obtained are shown in Figure 5.3. and 5.4., respectively.

Table 5.2. Polymerisation of cyclopentene using the t-butoxy molybdenum initiator

No.	Solvent	Temp (°C)	Time (hr)	Recovered Yield(%)	Mn ($\times 10^3$)	PDI
P5-1	Chloroform	-55	3	30	86	1.8
P5-2	Chloroform	-55	3	33	78	1.9
P5-3	Chloroform	-55	3	28	92	1.9
P5-4	Chloroform	-55	3	27	91	1.8

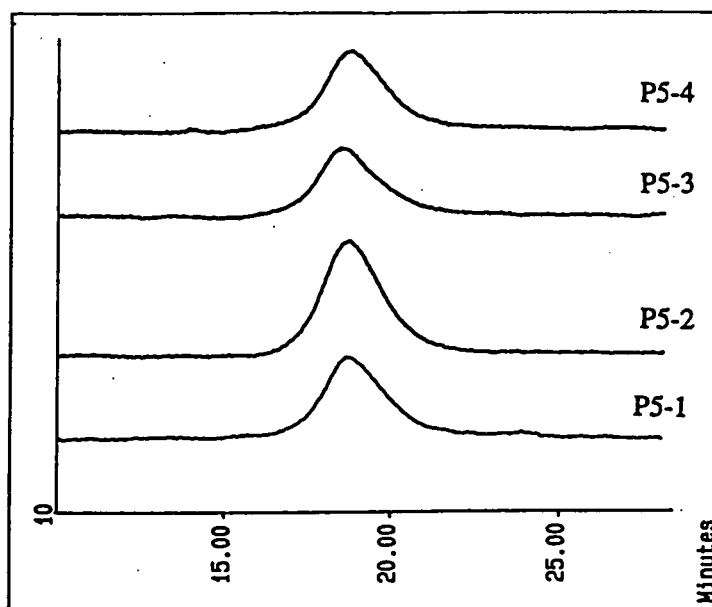


Figure 5.3. GPC traces of the polymers obtained using the t-butoxy molybdenum initiator

Table 5.3. Polymerisation of cyclopentene using the t-butoxy tungsten initiator

No	Solvent	Temp (°C)	Time (hr)	Recovered Yield(%)	Mn ($\times 10^3$)	PDI
P5-16	Chloroform	-55	18	32	31	1.2
					169	1.5
P5-17	Chloroform	-55	18	35	28	1.2
					198	1.7

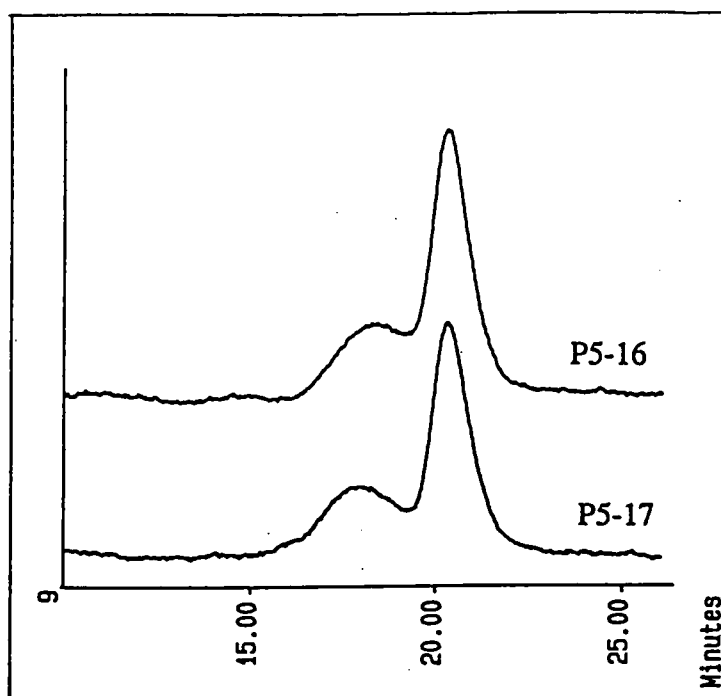


Figure 5.4. GPC traces of the polymers obtained using the t-butoxy tungsten initiator

These experiments established that under the protocol adopted in this work well defined initiators polymerise cyclopentene with good reproducibility, since the polymerisation under the same conditions produced similar results in both cases. It should be noted that the GPC traces are consistent with experimental error and that the tungsten based initiator gave a bimodal distribution.

5.2.2 Polymerisation of cyclopentene under various conditions

As the reproducibility of the method was established, the effects of reaction conditions on the polymerisation were examined next. The recovered

yields, average molecular weights and polydispersities of the polymers obtained were examined as a function of reaction time, reaction temperature and solvent.

a) Polymerisation using the t-butoxy molybdenum initiator

Chloroform, toluene and tetrahydrofuran (THF) were used as solvents. The results are shown in Table 5.4. The GPC traces of the obtained polymers, P5-1, 5 and 6, are shown in Figure 5.5.

Table 5.4. Polymerisation of cyclopentene using the t-butoxy molybdenum initiator

No.	Solvent	Temp (°C)	Time (hr)	Recovered Yield(%)	Mn ($\times 10^3$)	PDI
P5-1	Chloroform	-55	3	30	86	1.8
P5-5	Chloroform	-55	18	86	109	1.9
P5-6	Chloroform	-55	48	100	123	1.8
P5-7	Chloroform	-45	1.5	33	60	1.8
P5-8	Chloroform	-35	17	83	88	1.6
P5-9	Toluene	-55	2	35	113	1.9
P5-10	THF	-55	3	< 2 a)	238	1.6
P5-11 ^{b)}	THF	-55	6	7	41	1.5
					691	2.0

a) The recovered polymer contained decomposed initiator which could not be removed by elution through an alumina column. b) The produced polymers had a bimodal distribution. The recorded molecular weights and polydispersities were calculated for the high mass and low mass components individually.

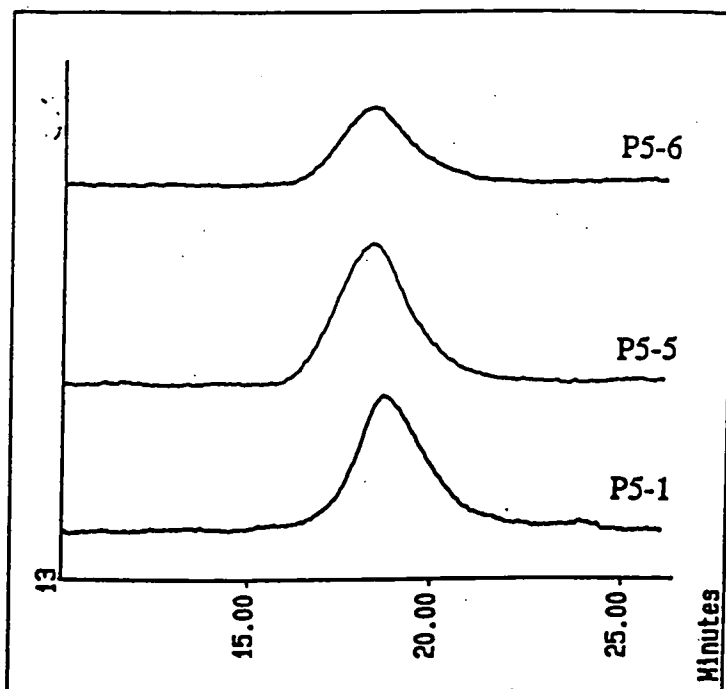


Figure 5.5. GPC traces of the polymers (P5-1, 5 and 6)

Noteable features are:

both the yields and the average molecular weights increased with the reaction time, (compare P5-1,5,6, P5-10,11); higher reaction temperature gave higher yield, (compare P5-1,7); polymerisation seemed to proceed faster in toluene than in chloroform. (compare P5-1,9); in the case of tetrahydrofuran, the polymerisation was very slow and produced bimodal polymer with the overwhelming mass of the product associated with the lower molecular weight component. This last observation may suggest that an interaction of the t-butoxy molybdenum initiator with tetrahydrofuran occurred resulting in a small amount of a more reactive chain end which competed with the original initiator.

The recorded polydispersities, around two under all conditions, are characteristic of a polymerisation which proceeds in a classical chain growth manner rather than a living well defined process. All other features of these

polymerisations are consistent with this picture, which also agrees with the results of Dounis who found that tungsten based initiators used at low temperature and for as short a reaction time as was acceptable gave the best results in his attempts to make living and low polydispersity polypentenamers.¹⁰⁸

b) Polymerisation using the trifluorinated butoxy molybdenum initiator

Polymerisation of cyclopentene using the trifluorinated butoxy molybdenum initiator was investigated. The obtained results are shown in Table 5.5. Cyclopentene was polymerised very rapidly when initiated by the trifluorinated t-butoxy molybdenum initiator. The reaction mixture became very viscous within three minutes of mixing the initiator and monomer solutions, and it could not be stirred (using a conventional magnetic stirrer follower) after eight minutes. Consequently polymerisation initiated by the hexafluorinated t-butoxy initiator was not attempted since that initiator is even more reactive.

Table 5.5 Polymerisation of cyclopentene using the trifluorinated t-butoxy molybdenum initiator

No.	Solvent	Temp (°C)	Time (min)	Recovered Yield(%)	Mn ($\times 10^3$)	PDI
P5-12	Chloroform	-55	3	15	223	2.0
P5-13	Chloroform	-55	8	63	264	2.0

Thus, this initiator polymerised the monomer much faster than the t-butoxy molybdenum initiator; it also produced the polymer in higher yield and higher average molecular weight. The polymerisation seemed to proceed in a

classical chain growth manner, as was observed for the polymerisation initiated with the t-butoxy molybdenum initiator, as shown by polydispersities around two.

c) Polymerisation using the t-butoxy tungsten initiator

Polymerisation of cyclopentene using t-butoxy tungsten initiator was investigated. The results obtained are shown in Table 5.6. and the GPC traces of some of the polymers obtained (P5-14,15,16) are shown in Figure 5.6.

Table 5.6. Polymerisation of cyclopentene using the t-butoxy tungsten initiator

No.	Solvent	Temp (°C)	Time (hr)	Recovered Yield(%)	Mn ($\times 10^3$)	PDI a)
P5-14	Chloroform	-55	3	11	6	1.3
					65	1.2
P5-15	Chloroform	-55	4.5	11	9	1.3
					82	1.3
P5-16	Chloroform	-55	18	32	31	1.2
					169	1.5
P5-18	Chloroform	-45	4.5	33	23	1.1
					113	1.2
P5-19	Toluene	-55	6	24	22	1.2
					173	1.2
P5-20	Toluene	-40	2	21	33	1.2
					144	1.1

a) The polymers produced all had bimodal distributions. The described average molecular weights and polydispersities were calculated for the high mass and low mass components individually.

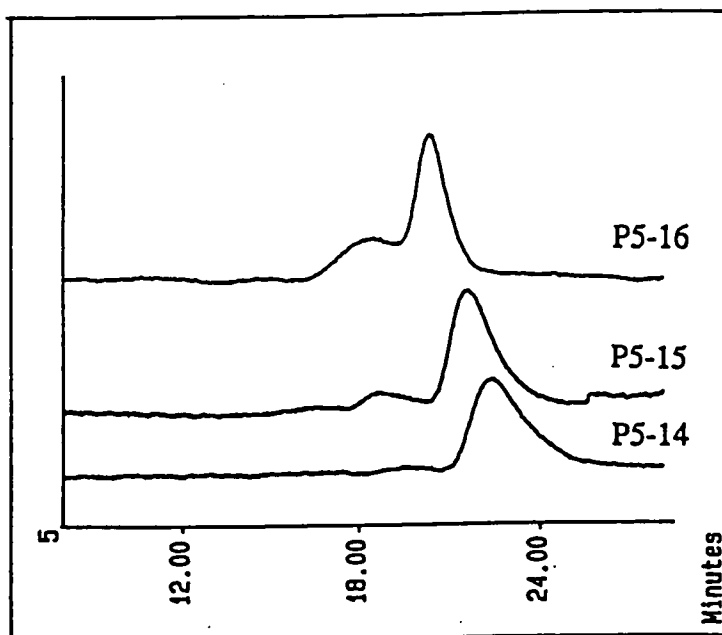


Figure 5.6. GPC traces of the polymers (P5-14,15,16)

This initiator gave a much slower rate of polymerisation than the t-butoxy molybdenum initiator, and the yield and average molecular weight of the polymers produced (P5-14,15,16) increased with the reaction time as shown in Table 5.6. and Figure 5.6. The polymers produced had a bimodal distribution in molecular weight. The average molecular weights and polydispersities calculated for the high mass and low mass components individually were around 1.2, from which it can be inferred that this polymerisation proceeded in a reasonably well defined manner. The average molecular weights of the high mass components were more than five times higher than those of low mass components. It is known that a small amount of oxygen introduced into the reaction mixture at the termination stage can result in dimerisation of the living polymer to produce the twofold polymer. The molecular weights of these high mass components are far too high to be considered as the consequence of dimerisation of living polymer. The GPC analysis of these materials was carried out by injecting 0.2% solution of the sample in chloroform into the instrument. P5-16 was injected at the higher

concentration of 1.3% to see if this made a difference to the relative intensity of the high and low mass components, since it was considered as a possibility that aggregation of polymer in solution might be the cause of the high mass peak on the GPC trace (see Figure 5.7.). A sample of 0.2% concentration in tetrahydrofuran was also analysed by GPC (see Figure 5.8.). No detectable difference in the bimodal distribution was seen in all these cases and, since the level of aggregation can be expected to be solvent and concentration dependent, there was no support for an aggregation based explanation of this observation.

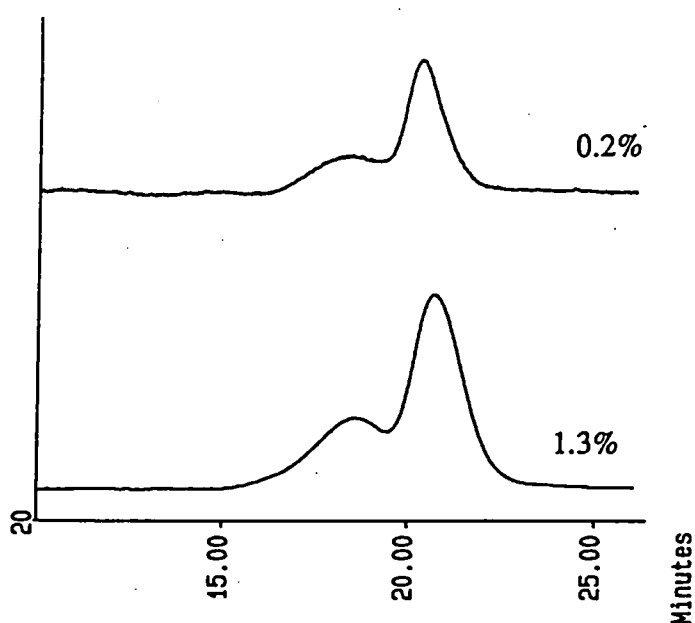


Figure 5.7. GPC traces of P5-16 as a function of concentration in chloroform

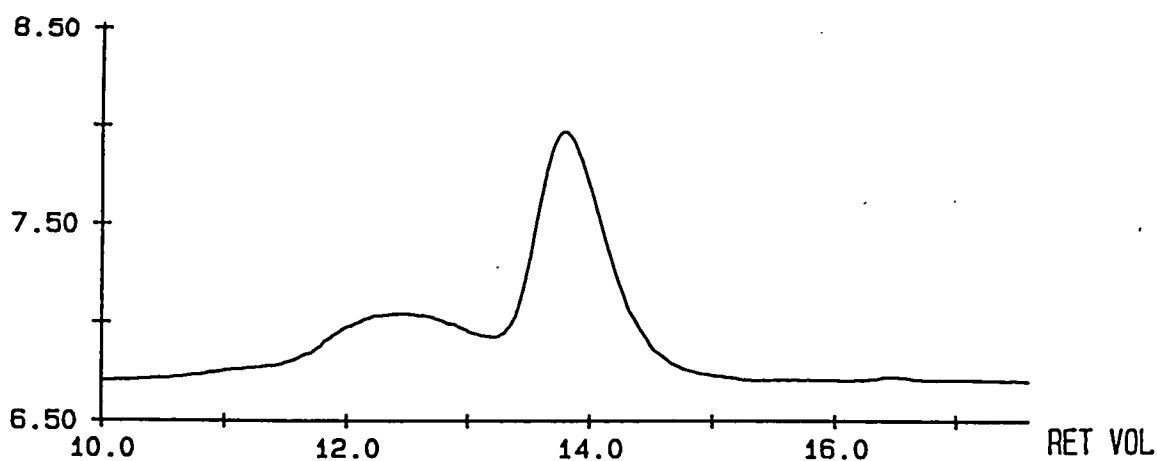


Figure 5.8. GPC traces of P5-16 using tetrahydrofuran as solvent

5.3 Characterisation of the polymers obtained

This section describes the characterisation of the polymers whose synthesis was discussed in section 5.2. The characterisation of the polymers was carried out by means of infrared spectroscopy, ^1H and ^{13}C nuclear magnetic resonance spectroscopy, thermogravimetry and differential scanning calorimetry.

The infrared, ^1H n.m.r. and ^{13}C n.m.r. spectra of the polymers (P5-1~20) are shown in Appendices 5.2.1. to 20., Appendices 5.3.1. to 20. and Appendices 5.4.1. to 20., respectively.

5.3.1 Characterisation by infrared spectroscopy

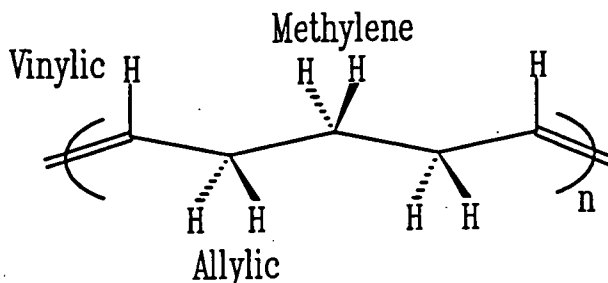
All the spectra showed the expected absorption for vinylic C-H stretching above 3000 cm^{-1} , aliphatic C-H stretching absorptions in the $2800\text{-}3000\text{ cm}^{-1}$ region, C-H deformation around 1450 cm^{-1} , out-of-plane C-H deformation of trans CH=CH unit around 965 cm^{-1} . The absorption around 715 cm^{-1} is regarded as the overlapping absorption of out-of-plane C-H deformation for cis double bonds and a $(\text{CH}_2)_n$ skeletal vibration and it is consequently unreliable for diagnostic purposes.

5.3.2 Characterisation by ^1H nuclear magnetic resonance spectroscopy

The ^1H n.m.r. spectra of the polymers were in agreement with the structures proposed. The spectra of polymers (P5-1 to P5-20) all showed a similar pattern, with signals due to vinylic, allylic and methylene protons as expected. The parameters for sample P5-1 are shown in Table 5.7. as a typical example.

Table 5.7. ^1H n.m.r. spectral parameters for P5-1

Position of H	vinylc	allylic	methylene
Chemical shift (ppm)	5.33-5.42	1.94-2.08	1.40
Signal pattern	multiplet	multiplet	quintet ($J=7.2$ Hz)
Ratio of intensities	2	4	2

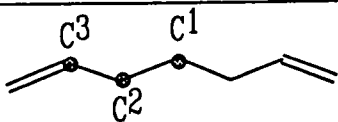
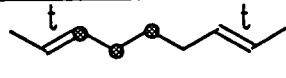
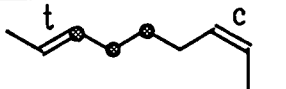
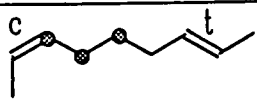
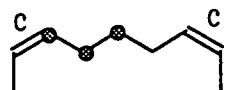


5.3.3 Introduction to characterisation of polyalkenamers by ^{13}C nuclear magnetic resonance spectroscopy

As mentioned in Chapter 2., Ivin and co-workers have demonstrated the effectiveness of ^{13}C n.m.r. spectroscopy for the analysis of unsaturated polymers, especially for determining the relative proportion of cis and trans double bonds in the polymer chain. They also showed that ^{13}C n.m.r. spectroscopy allows several different independent measurements of the cis / trans content to be made and the internal consistency of these measurements may be taken as good evidence of their accuracy. The number of signals observed by them for poly(1-pentenylene) can not be explained simply by the fact that the chemical shifts of the C^1 (methylene), C^2 (allyl) and C^3 (vinyl) carbon atoms are sensitive to the geometrical isomerism about the nearest double bond, but requires that they are also sensitive to the geometrical isomerism about the next nearest double bond. Therefore, four peaks should be observed for the C^2 carbon atom of poly(1-pentenylene) containing both cis and trans double bonds, that is $\text{C}^{2\text{tt}}$, $\text{C}^{2\text{tc}}$, $\text{C}^{2\text{ct}}$ and $\text{C}^{2\text{cc}}$ (the first letter represents the configuration of the nearest double bond

and the second letter represents that of the next nearest double bond). For the C¹ carbon atom, which is symmetrically situated between two double bonds, three signals should be expected corresponding to C¹_{tt}, C¹_{tc}=C¹_{ct} and C¹_{cc}. Using this argument, and the fact that in simple alkenes the allylic carbon atoms next to cis-double bond always appear about 5 ppm upfield from those next to trans double bond,⁷⁷ together with a comparison of the ¹³C n.m.r. spectra of different cis content polymers, the signals at 32.06, 32.19, 26.76, and 26.90 ppm were assigned to C²_{tt}, C²_{tc}, C²_{ct} and C²_{cc}, respectively, and three peaks at 29.56, 29.73 and 29.84 ppm were assigned to C¹_{tt}, C¹_{tc}=C¹_{ct} and C¹_{cc}, respectively, as shown in Table 5.8.^{70,109}

Table 5.8. ¹³C Chemical shift assignments for poly(1-pentenylene)⁷⁰

	C ¹	C ²	C ³
			
tt 	29.56	32.06	
tc 	29.73	32.19	130.32
ct 		26.76	129.85
cc 	29.84	26.90	

The relative intensities of these signals may be used to calculate the amount of cis and trans double bonds in the polymer using the formulae for the determination of the fraction of cis double bonds, σ_c , for each set of signals as shown below and compared with the value obtained from the intensities of the signals due to cis C³ and trans C³, i.e. the vinyl carbons, where:-

$$\sigma_c = C^3_c / (C^3_c + C^3_t) \quad \text{Vinyl carbon atom}$$

$$\sigma_c = (C^2_{ct} + C^2_{cc}) / (C^2_{tt} + C^2_{tc} + C^2_{ct} + C^2_{cc}) \quad \text{Allyl carbon atom}$$

$$\sigma_c = (C^1_{cc} + 0.5(C^1_{tc} \equiv C^1_{ct})) / (C^1_{tt} + (C^1_{tc} \equiv C^1_{ct}) + C^1_{cc}) \quad \text{Methylene carbon atom}$$

Ivin and co-workers reported that for a range of polymers the relative proportion of cis double bond (σ_c) determined from the C^1 , C^2 and C^3 signals in each polymer were in good agreement internally.

Furthermore the blockiness about the cis / trans double bond isomerism of the polymers can be calculated by the following argument based on the ^{13}C signal intensities.

If the cis and trans double bonds on a given polymer chain are distributed at random, the chance of a given double bond being cis is the same, regardless of the cis or trans structure of adjacent double bonds. This means that the ratios represented by $r_t = tt/tc$ and $1/r_c = ct/cc$ should be the same ; in other words, $r_t r_c$ should tend to one. Values of $r_t r_c$ less than unity would mean a tendency to alternation of cis and trans double bond, while values greater than unity would mean a tendency towards a blocky distribution. In fact the ratios tt/tc and ct/cc are not always equal, especially in high cis content polymers.⁷² Ivin and co-workers concluded that this requires interpretation in terms of two kinetically distinct propagating species.

5.3.4 Reproducibility of the microstructure of the polymers produced

At first, the reproducibility of the polymerisation using well defined initiators was examined from the microstructural point of view. Several polymers obtained using t-butoxy molybdenum initiator and t-butoxy tungsten initiator under the same conditions as described in Section 5.2.1. were characterised by ^{13}C n.m.r. The ^{13}C n.m.r. spectra of the polymers produced

were essentially same, the ^{13}C n.m.r. spectrum and the assignment of each signal for sample P5-1 are shown in Figure 5.9. and Table 5.9. as typical examples. The comparison with the literature values are also shown in Table 5.9. The obtained results showed good agreement with the literature values.

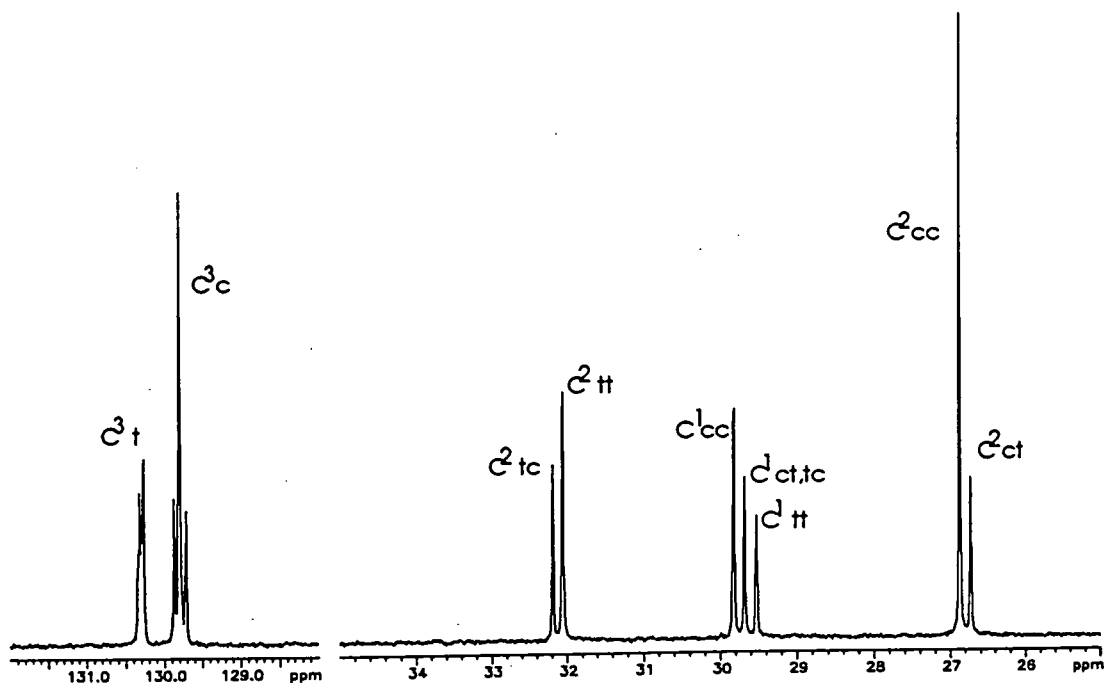
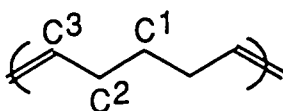


Figure 5.9. ^{13}C n.m.r. spectrum of P5-1

Table 5.9. Assignment of ^{13}C n.m.r. spectrum of P5-1 and literature values

	(ppm)								
	C ¹			C ²				C ³	
	tt	tc=ct	cc	tt	tc	ct	cc	t	c
P5-1	29.53	29.69	29.82	32.06	32.19	26.73	26.88	130.30	129.81
lit. ⁷⁰	29.56	29.73	29.84	32.06	32.19	26.76	26.90	130.32	129.85



The cis double bond content, σ_c , and the blockiness for the obtained polymers calculated by the method described above are shown in Table 5.10. for samples produced using t-butoxy molybdenum initiator and in Table 5.11. for samples produced using t-butoxy tungsten initiator.

Table 5.10. Cis / trans ratio and blockiness of the polymers produced with the t-butoxy molybdenum initiator

No.	Solvent	Temp (°C)	Time (hr)	Cis/Trans Ratio ^a			Blocki- ness ^b
				C ³	C ¹	C ²	
P5-1	Chloroform	-55	3	63 / 37	59 / 41	61 / 39	4.6
P5-2	Chloroform	-55	3	65 / 35	61 / 39	62 / 38	4.4
P5-3	Chloroform	-55	3	64 / 36	62 / 38	62 / 38	4.9
P5-4	Chloroform	-55	3	64 / 36	62 / 38	62 / 38	4.6

a) The cis / trans ratios were calculated based on the signal intensities of each carbon (C¹, C², C³). b) Blockiness is measured by r_{TC} , see text.

Table 5.11. Cis / trans ratio and blockiness of the polymers produced with the t-butoxy tungsten initiator

No.	Solvent	Temp. (°C)	Time (hr)	Cis/Trans Ratio ^a			Blocki- ness ^b
				C ³	C ¹	C ²	
P5-16	Chloroform	-55	18	76 / 24	72 / 28	72 / 28	8.4
P5-17	Chloroform	-55	18	79 / 21	74 / 26	75 / 25	9.8

a) The cis / trans ratios were calculated based on the signal intensities of each carbon (C¹, C², C³). b) Blockiness is measured by r_{TC} , see text.

As shown in Table 5.10. and 5.11., polymers produced under the same experimental conditions had similar cis double bond content and blockiness, which can be taken to mean that, with the limits of experimental control and

analysis, well defined initiators provided reproducible polymerisation from the microstructural point of view.

5.3.5 Characterisation of the polymers by ^{13}C n.m.r. spectroscopy as a function of reaction conditions in synthesis

Cyclopentene was polymerised under various conditions using the t-butoxy molybdenum initiator, the trifluorinated t-butoxy molybdenum initiator and the t-butoxy tungsten initiator, and the differences in the microstructures of the polymers produced were investigated by means of ^{13}C n.m.r spectroscopy.

a) Examination of the polymerisation using the t-butoxy molybdenum initiator

The results for the polymers produced with t-butoxy molybdenum initiator are shown in Table 5.12.

Table 5.12. Cis / trans ratio and blockiness of the polymers produced with the t-butoxy molybdenum initiator under different conditions

No.	Solvent	Temp (°C)	Time (hr)	Cis/Trans Ratio ^a			Blocki- ness ^b
				C ³	C ¹	C ²	
P5-1	Chloroform	-55	3	63 / 37	59 / 41	61 / 39	4.6
P5-5	Chloroform	-55	18	62 / 38	59 / 41	60 / 40	4.3
P5-6	Chloroform	-55	48	54 / 46	50 / 50	51 / 49	4.3
P5-7	Chloroform	-45	1.5	56 / 44	57 / 43	55 / 45	3.6
P5-8	Chloroform	-35	17	42 / 58	41 / 59	39 / 61	2.7
P5-9	Toluene	-55	2	72 / 28	69 / 31	69 / 31	5.5
P5-10	THF	-55	3	69 / 31	65 / 35	69 / 31	7.6
P5-11	THF	-55	6	74 / 26	76 / 24	72 / 28	7.7

a) The cis / trans ratios were calculated based on the signal intensities of each carbon (C¹, C², C³). b) Blockiness is measured by r_{TC} , see text.

Longer reaction duration favoured the production of higher trans content polymers (P-5-1,5,6), and higher reaction temperatures also tended to produce higher trans content polymers (P5-1,7,8). The polymerisation produced higher cis content polymers in toluene and tetrahydrofuran than in chloroform.

b) Examination of the polymerisation using the fluorinated butoxy molybdenum initiator

The results for the polymers produced with the trifluorinated t-butoxy molybdenum initiator are shown in Table 5.13.

Table 5.13. Cis / trans ratio and blockiness of the polymers produced with the trifluorinated t-butoxy molybdenum initiator

No.	Solvent	Temp (°C)	Time (min)	Cis/Trans Ratio ^a			Blocki- ness ^b
				C ³	C ¹	C ²	
P5-12	Chloroform	-55	3	87 / 13	82 / 18	86 / 14	10.5
P5-13	Chloroform	-55	8	78 / 22	73 / 27	74 / 26	6.6

a) The cis / trans ratios were calculated based on the signal intensities of each carbon (C¹, C², C³). b) Blockiness is measured by r_{TC} , see text.

This initiator produced much more cis content and more highly blocky polymers than the t-butoxy molybdenum initiator did under the same conditions. As before, prolonged reaction duration yielded more trans vinylene content in the polymer.

c) Examination using t-butoxy tungsten initiator

The examination was carried out using chloroform and toluene as solvents, since t-butoxy tungsten initiator is known to react with tetrahydrofuran. The results are shown in Table 5.14.

Table 5.14. Cis / trans ratio and blockiness of the polymers produced with the t-butoxy tungsten initiator under different conditions

No.	Solvent	Temp. (°C)	Time (hr)	Cis/Trans Ratio ^a			Blocki- ness ^b
				C ³	C ¹	C ²	
P5-14	Chloroform	-55	3	72 / 28	72 / 28	70 / 30	7.6
P5-15	Chloroform	-55	4.5	74 / 26	76 / 24	73 / 27	8.2
P5-16	Chloroform	-55	18	76 / 24	72 / 28	72 / 28	8.4
P5-18	Chloroform	-45	4.5	64 / 36	63 / 37	62 / 38	7.8
P5-19	Toluene	-55	6	86 / 14	80 / 20	82 / 18	9.7
P5-20	Toluene	-40	2	70 / 30	64 / 36	65 / 35	7.5

a) The cis / trans ratios were calculated based on the signal intensities of each carbon (C¹, C², C³). b) Blockiness is measured by r_{trC} , see text.

No significant change in the microstructure of the polymers produced was observed with reaction duration in the range in which the examination was carried out (P5-14,15,16). This initiator produced slightly more cis content and more highly blocky polymers than t-butoxy molybdenum initiator. Higher reaction temperature produced more trans content polymer (P5-15,18 and P5-19,20), and the effect of changing solvent was similar to that mentioned above (P5-14,19), namely that toluene favoured higher cis content and increased blockiness.

5.3.6 Thermal characterisation

Thermal properties, such as decomposition temperature (Td), glass transition temperature (Tg) and melting temperature (Tm), of some obtained polymers were examined by thermal gravimetry and differential scanning calorimetry. The results are shown in Table 5.15. DSC traces are shown in Appendices 5.5.1. to 4.

Table 5.15. Td, Tg and Tm of some obtained polymers

	Cis / Trans	TGA	DSC	
	Ratio (C ²)	Td (°C)	Tg (°C)	Tm (°C)
P5-8	39 / 61	368	-97	-57
P5-6	51 / 49	366	-100	-60
P5-1	61 / 39	368	-101	not observed
P5-12	86 / 14	365	-104	not observed

The results showed that all the polymers examined had similar decomposition temperatures, and the higher the cis content in the polymer the lower the glass transition temperature and melting temperature, although the melting temperature of the polymer which was more than 60% cis content was not observed. This tendency is consistent with the reported one, which is that the glass transition temperature and melting temperature of high trans content poly(1-pentenylene) are -90°C and 23°C, and those of high cis content polymer are -114°C and -41°C, respectively.^{95,112}

5.4 Summary and discussion

The work described above confirmed that well defined initiators polymerise cyclopentene with good reproducibility to produce the expected polymers in reasonable yields, at least the range of -35°C to -55°C. The effect of changing solvent is relatively small, except that tetrahydrofuran seemed to induce a side reaction.

The higher reaction temperature works in favour the production of higher trans content polymer, which is consistent with observations on the polymerisation of cyclopentene using tungsten classical catalyst system by Oreshkin.¹⁰³ Longer reaction duration also gives a higher trans content polymer.

This is considered to be the consequence of secondary metathesis reactions for the following reasons. Secondary metathesis reactions, such as chain transfer and the formation of cyclic oligomers, is known to tend to happen at cis double bonds in the polymer chain because of both electronic and steric effects. For example, the chain transfer constants decrease in the order shown below.¹¹⁰

But-1-ene > cis-But-2-ene > trans-But-2-ene > Isobutene

Tanaka and co-workers reported that the double bonds in polycyclooctadiene produced with classical catalyst undergo rapid secondary metathesis leading a fall in the cis content below 50% from the 80% observed initially.¹¹¹

The order of the reactivity of initiators in the polymerisation turned to be as follows:-

Trifluorinated t-butoxy molybdenum initiator
> t-Butoxy molybdenum initiator
> t-Butoxy tungsten initiator

The selectivity order of initiators for the production of cis content in the polymer was follows:-

Trifluorinated t-butoxy molybdenum initiator
> t-Butoxy tungsten initiator
> t-Butoxy molybdenum initiator

As for the living behavior of these initiators, these results indicate that under these conditions the t-butoxy and trifluorinated t-butoxy molybdenum initiators polymerise the monomer in classical manner since the polymers produced were mono-modal and had polydispersities of about 2 which is characteristic of classical chain growth polymerisation and not consistent with a living process of chain growth. While the t-butoxy tungsten initiator seemed to induce products more indicative of living polymerisation, but it also produced a minor high molecular weight component, as well as normal narrow distributed

polymer as the major component. Schrock and co-workers have reported that the *t*-butoxy tungsten initiator polymerised cyclopentene to give narrow distribution mono-modal polymer and the replacement of the n.m.r. signal of the alkylidene proton of the initiator by that of the propagating species was also observed. They concluded this reaction roceed in living manner.^{113,114} Their polymerisations were carried out at -40°C in toluene, the initial monomer concentration was 4.0 mol/l1 of solvent, and the ratio of the monomer to the initiator was 234:1. A possible reason for the observed difference between this work and that reported by Schrock might be that a backbiting reaction produced high molecular weight cyclic polymer like catenanes in the large ratio of monomer/initiator we used, the hypothesis is shown in Figure 5.10. However, much further investigation would be required to establish the mechanism of this side reaction since even a very small amount of cross linking or branching reaction might be sufficient to account for such a minor high molecular weight component.

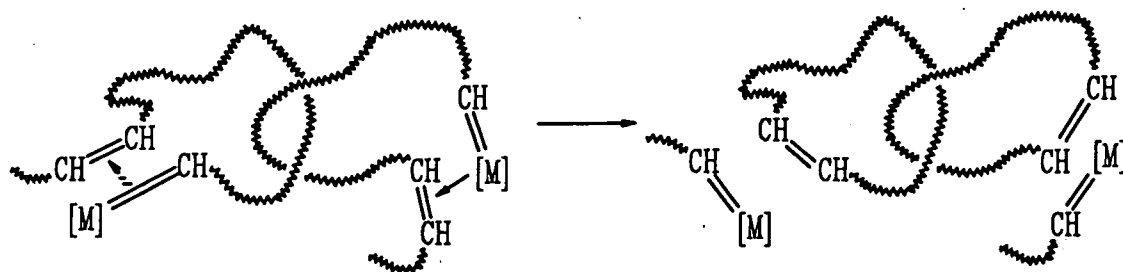


Figure 5.10. A possible backbiting reaction to form catenanes

5.5 Experimental

A typical example of the procedure adopted for the polymerisation of cyclopentene is described below. The initiators used throughout this work and in the following chapter's work were prepared either in the research group of Prof.

V. C. Gibson or in the IRC laboratories by Dr. E. Khosravi and used as supplied in solid form in inert atmosphere. Cyclopentene, chloroform (99.9%, HPLC grade), calcium hydride, sodium, benzaldehyde, benzophenone and neutral alumina were purchased from Aldrich Chemical Ltd. Tetrahydrofuran, toluene, methanol, and phosphorous pentoxide were purchased from B. D. H. Chemical Supplies (Merk Ltd.). Cyclopentene was dried over calcium hydride, chloroform was dried over phosphorus pentoxide, benzaldehyde was dried over molecular sieves and toluene and tetrahydrofuran were dried over sodium-benzophenone until the mixture remained purple on stirring overnight, then these were vacuum-transferred into dry ampoules following deoxygenation by means of the freeze-thaw-pump technique. The solvents were passed through a short column (c.a. 4 cm) of oven dried neutral alumina in a glove box before use.

The solutions of initiator, monomer, and benzaldehyde were made up in a glove box, where the concentration of oxygen was below 8 ppm and moisture was below 7 ppm. The initiator (0.011 mmol) was dissolved in solvent (0.5 ml) and the solution was transferred into a ampoule (5 ml). Cyclopentene (0.3 g, 4.4 mmol), giving a molar ratio of monomer to initiator of 400:1, was dissolved in solvent (0.6 ml) and transferred into a sample vial (5 ml). Benzaldehyde (c.a. 50 mg, 0.047 mmol) was dissolved in solvent (1 ml) and transferred into a sample vial. The ampoule was sealed with a Young's valve, and the sample vials were sealed with rubber serum caps, and they were taken out from the glove box and cooled to the prescribed temperature in the cooling bath. The Young's valve of the ampoule was replaced with rubber cap under positive pressure of nitrogen. Then the monomer solution was added to the stirred initiator solution through a canular by pressurising with dry nitrogen. After the prescribed reaction duration the benzaldehyde solution was added to the reaction mixture by the technique described above. The resulting solution was stirred for one hour and allowed to warm up to the ambient temperature. After stirring for few hours, the mixture was precipitated from chloroform into methanol, recovered and dried under

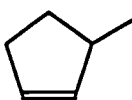
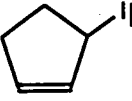
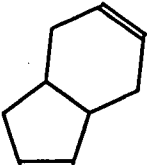
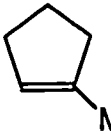
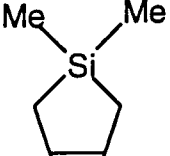
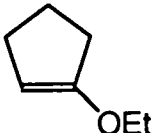
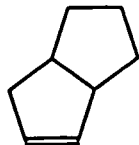
vacuum. For the mixture from which the polymer could not be isolated by precipitation the mixture was passed through a short column (c.a. 4 cm) of oven dried neutral alumina to get rid of decomposed initiator and the eluted solution was concentrated and dried.

CHAPTER 6: Polymerisation of 4-methylcyclopentene

6.1 Introduction

As described in Chapter 1, 4-substituted cyclopentenes are expected to be interesting monomers in ring opening metathesis polymerisation with regard to both the thermodynamics of the reaction and the microstructure of the polymers produced. Several substituted cyclopentenes have been subjected to study for their polymerisability in ring opening metathesis polymerisation, as shown in Table 1.1.

Table 1.1. The reported polymerisabilities of substituted cyclopentenes

Polymerisable	Not polymerisable
 105)	 105)
 a) 117)	 115)
 119)	 116)
	 118)

a) Only the 5-membered ring opens.

As shown in the table, bicyclo[4.3.0]nona-3,7-diene has been shown to be polymerisable. In this compound the cyclopentene ring is supposed to be strained due to the cyclohexene ring fused with it so as to become more favourable to ring opening. By contrast, bicyclo[3.3.0]oct-2-ene has been reported to be non-polymerisable although it might be expected to be subject to strain as well. 3-Methylcyclopentene was also reported to be polymerisable, as was the 4,4-dimethyl-4-silacyclopentene, however, the effect of substitution on polymerisability in cyclopentenenes is not very clear.

6.2 Polymerisation of 4-methylcyclopentene

The polymerisations of 4-methylcyclopentene were carried out using similar conditions and procedures (Figure 6.1.) to those described in Chapter 5. Chloroform was used as solvent and the initial monomer concentration and the ratio of the monomer to the initiator were fixed as follows:-

- Initial monomer concentration = 4.0 mol / 1 l of solvent
- Monomer / Initiator = 400 / 1

This ratio would provide a polymer with a molecular weight of 32,800 if the polymerisation proceeded with 100% initiation and in a completely living manner.

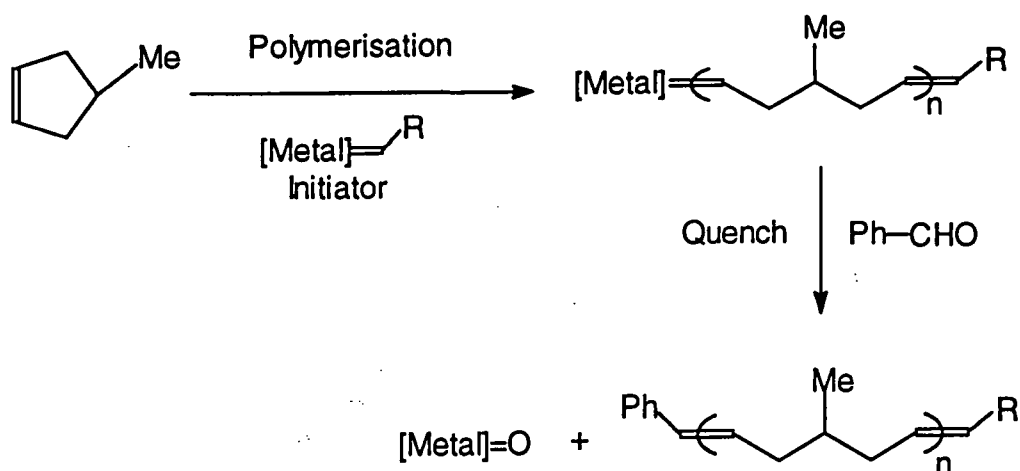


Figure 6.1. Outline of the polymerisation process

The average molecular weights and polydispersities of the polymers obtained were calculated based on gel permeation chromatography calibrated by polystyrene standards and are shown in Table 6.2. The gel permeation chromatograms of the polymers obtained (P6-2,4,5) are shown in Appendices 6.1.1. to 6.1.3.

Table 6.2. The Mn and PDI of the polymers obtained by ROMP of 4-methylcyclopentene

No.	Initiator ^{a)}	Temp (°C)	Reaction duration	Recovered Yield (%)	Mn (10 ³)	PDI
P6-1	Mo-- ^t Bu	-55	20 hr	~0	--	--
P6-2	Mo--F ₃	-55	4 hr	20	145	2.1
P6-3	Mo--F ₃	-35	20 hr	<2	--	--
P6-4	Mo--F ₆	-55	10 min	32	131	1.9
P6-5	Mo--F ₆	-55	15 min	51	142	2.3
P6-6	W-- ^t Bu	-55	20 hr	~0	--	--

a) Mo--^tBu, Mo--F₃, Mo--F₆ and W--^tBu are the t-butoxy molybdenum initiator, the trifluorinated-t-butoxy molybdenum initiator, the hexafluorinated-t-butoxy molybdenum initiator and the t-butoxy tungsten initiator respectively.

As shown in the table, neither the t-butoxy molybdenum initiator nor the t-butoxy tungsten initiator were able to polymerise the monomer (compare P6-1 and 6), although they polymerised cyclopentene under the same condition in yields of 86 and 32% respectively. This difference between the polymerisability of 4-methylcyclopentene and cyclopentene using the t-butoxy molybdenum and tungsten initiators might be a consequence of a kinetically unfavourable polymerisation for 4-methylcyclopentene compared to that of cyclopentene.

However 4-methylcyclopentene was polymerised with the trifluorinated butoxy molybdenum initiator at -55°C in 20% yield and at -35°C in less than 2% (compare P6-2 and 3), while, as described in Chapter 5, cyclopentene was polymerised using the t-butoxy molybdenum initiator at -55°C after 3 hours in 30% yield and at -35°C after 17 hours in 83%. This fact suggested that the polymerisation of 4-methylcyclopentene was thermodynamically much less favourable than that of cyclopentene, as was expected. The hexafluorinated molybdenum initiator also polymerised 4-methylcyclopentene faster than the trifluorinated molybdenum initiator (compare P6-2 and 3 with P6-4 and 5). All the polymers produced displayed polydispersities around 2 which suggests that the polymerisations proceeded via a classical chain growth manner rather than a well defined living process, as was observed for the polymerisations of cyclopentene using molybdenum centred initiators.

6.3 Characterisation of the polymers obtained

6.3.1 Infrared spectroscopy

The infrared spectra of P6-2, 4 and 5 are shown in Appendices 6.2.1. to 3. All spectra showed a vinylic C-H stretching absorption above 3000 cm^{-1} , aliphatic C-H stretching absorptions in the region of $2800\text{-}3000\text{ cm}^{-1}$, a C-H deformation at 1455 cm^{-1} , the out-of-plane C-H deformation of the trans CH=CH double bond around 968 cm^{-1} . The absorption around 708 cm^{-1} is regarded as the overlapping absorption of the out-of-plane C-H deformation of cis double bond and CH_2 skeletal vibrations.

6.3.2 Characterisation by ^1H n.m.r. spectroscopy

The ^1H n.m.r. spectra of P6-2~5 are shown in Appendices 6.3.1. to 4. and are consistent with the expected structure. The assignment of the spectrum for P6-4 is shown in Figure 6.2. as a typical example since the spectra of all polymers were similar.

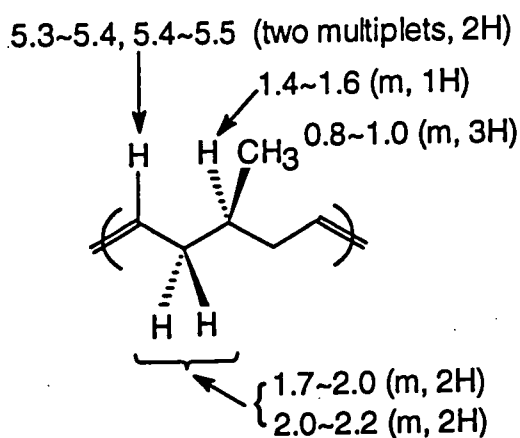


Figure 6.2. The chemical shifts from the ^1H n.m.r. of P6-4
(ppm with respect to TMS)

Two resonances at 5.3~5.4 and 5.4~5.5 ppm were assigned to vinylic ^1H attached to trans and cis double bonds, but it was not possible to determine by ^1H n.m.r. spectroscopy by itself which resonance corresponded to which vinylic ^1H . However the resonance at higher chemical shifts was shown to be due to cis vinylic ^1H , on the basis of the analysis of the ^{13}C n.m.r. spectrum which is discussed in the following section. The proportions of cis and trans double bonds in the polymers obtained, determined on the basis of the assignments given above, are shown in Table 6.3. It is clear that higher temperature and longer reaction time favours the generation of trans vinylenes.



Table 6.3. The ratio of the cis/trans double bonds in the polymers obtained

(based on ^1H n.m.r. spectra)

No.	Initiator a)	Temp ($^{\circ}\text{C}$)	Reaction duration	Ratio (cis / trans)
P6-2	Mo--F ₃	-55	4 hr	65 / 35
P6-3	Mo--F ₃	-35	20 hr	29 / 71
P6-4	Mo--F ₆	-55	10 min	60 / 40
P6-5	Mo--F ₆	-55	15 min	55 / 45

6.3.3 Characterisation by ^{13}C n.m.r. spectroscopy

As in the case of the polymers of cyclopentene, four peaks should be observed for the polymers containing both cis and trans double bonds for the C² (allyl) carbon atoms (see Figure 6.3. for the numbering of carbon atoms), i.e. C²_{tt}, C²_{tc}, C²_{ct} and C²_{cc} (the first letter represents the configuration of the nearest double bond and the second letter represents that of the next nearest double bond) and for C¹ (methine) and C⁴ (methyl) carbon atoms, which are symmetrically situated between two double bonds, three signals should be expected corresponding to C¹_{tt}, C¹_{tc}=C¹_{ct}, C¹_{cc} and C⁴_{tt}, C⁴_{tc}=C⁴_{ct}, C⁴_{cc}, respectively.

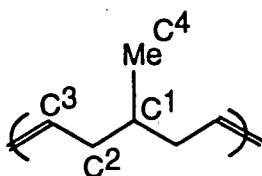


Figure 6.3. The numbering of the carbon atoms in poly(4-methyl-1-pentenylene)

However the ^{13}C n.m.r. spectra of the polymers obtained did not show the patterns expected so, in an attempt to clarify the situation, DEPT spectra of the polymers were recorded. The ^{13}C n.m.r. and DEPT spectra of P6-2~5 are shown

in Appendices 6.4.1. to 4. and 6.5.1. to 3. respectively. For P6-3 a DEPT spectrum was not possible because not enough of the sample was obtained. As the spectra of all the polymers were similar, only the DEPT spectrum for P6-4 is shown in Figure 6.4. as a typical example. As shown in Figure 6.4. the DEPT spectra proved that the signals due to C^{2ct} and C^{1cc} appeared at the same chemical shift (34.2 ppm). The assignment of the ^{13}C signals based on the DEPT analysis of P6-4 is shown in Table 6.4.

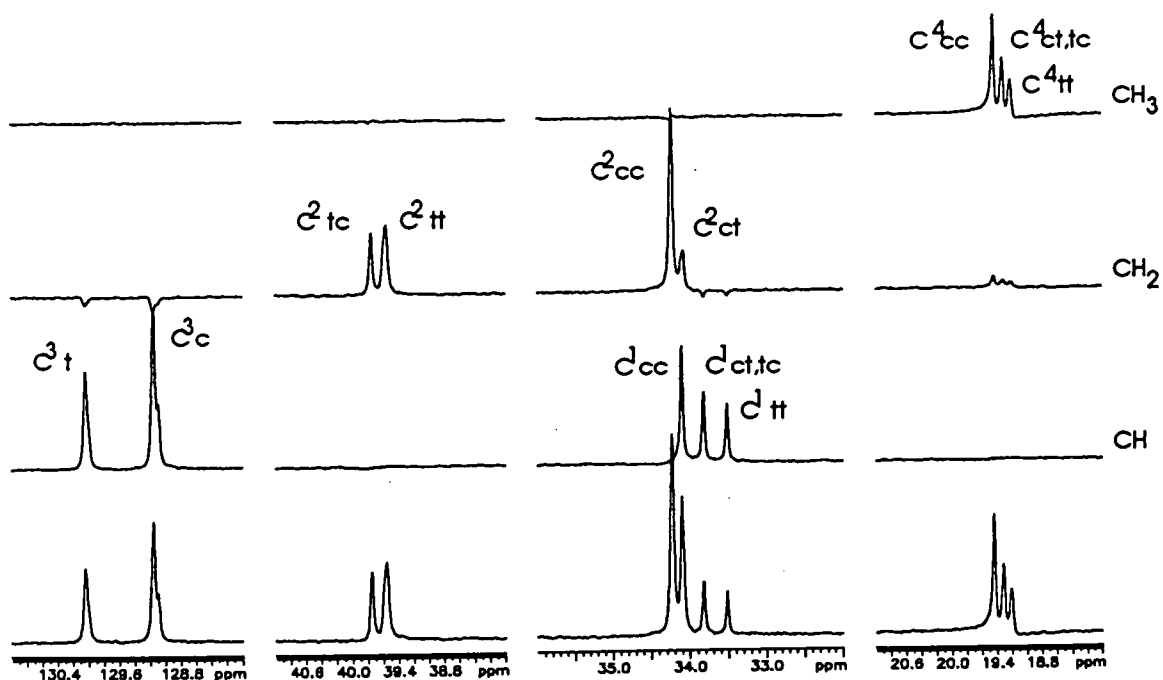


Figure 6.4. The DEPT spectra of P6-4 (ppm with respect to TMS)

Table 6.4. Assignment for ^{13}C n.m.r. spectrum of 6-4 (ppm with respect to TMS)

	C^1 (methine)			C^2 (methylene)				C^3 (vinyl)	
	tt	tc=ct	cc	tt	tc	ct	cc	t	c
P6-4	33.64	33.94	34.22	39.68	39.87	34.22	34.35	130.15	129.27

	C^4 (methyl)		
	tt	tc=ct	cc
P6-4	19.33	19.43	19.56

The ratio of cis/trans double bonds for the polymers obtained were determined on the basis of the assignments recorded above; they are shown in Table 6.5.

Table 6.5. The ratio of cis to trans double bonds for polymers of 4-methylcyclopentene

(based on ^{13}C n.m.r. spectra)

No.	Initiator a)	Temp (°C)	Reaction duration	Ratio (Cis / Trans)				Blocki- ness
				C1	C2	C3	C4	
P6-2	Mo--F ₃	-55	4 hr	63 / 37	61 / 39	66 / 34	62 / 38	8.8
P6-3	Mo--F ₃	-35	20 hr	--b)	--b)	32 / 68	35 / 65	--b)
P6-4	Mo--F ₆	-55	10 min	60 / 40	60 / 40	63 / 37	60 / 40	6.3
P6-5	Mo--F ₆	-55	15 min	57 / 43	53 / 47	57 / 43	56 / 44	7.4

a) Mo--F₃ and Mo--F₆ are the trifluorinated-t-butoxy molybdenum initiator and the hexafluorinated-t-butoxy molybdenum initiator respectively.

b) These values could not be determined since DEPT analysis was not available because of the small amount of sample obtained.

As shown in the table the cis/trans ratios were consistent with those obtained from the ^1H n.m.r. spectra. The trifluorinated molybdenum initiator produced a greater cis vinylene content (see P6-2) at -55°C than the polymer produced at -35°C after longer reaction duration (see P6-3). This might be explained on the basis that higher temperature and long reaction duration are favourable to production of the more stable trans vinylene units in the polymer, which is in agreement with our observation of the polymerisation of cyclopentene. The hexafluorinated molybdenum initiator produced polymer with similar cis content to that of the polymer produced using the trifluorinated molybdenum initiator (compare P6-4 and 2), and longer reaction duration seemed to make the

cis content slightly lower (compare P6-4 and 5). So the secondary metathesis reaction, which is likely to produce more of the more stable trans content polymer, appears to occur from an early stage which is probably due to the reactivity of living polymer in metathesis with double bonds in the chain.

A more detailed examination of the microstructures of the polymers obtained is discussed in Section 6.5.

6.4 Hydrogenation of the poly(4-methyl-1-pentenylenes)

As the microstructural analysis of poly(4-methyl-1-pentenylene) was difficult on the basis of the spectra of the polymers available, the hydrogenation of the poly(4-methyl-1-pentenylene) was carried out since it was possible that the spectrum of the hydrogenated polymer, poly(1-methylpentamethylene), might provide additional information to help with the analysis. The polymer (P6-4, $M_n=131,000$, $PDI=1.9$) was hydrogenated using p-toluenesulfonyl hydrazide in p-xylene at reflux temperature for 6 hours; this procedure is a well established method for syn hydrogenation of C=C double bonds.¹²⁰⁻¹²³ The scheme for the hydrogenation is shown in Figure 6.5. The hydrogenated polymer (P6-7) was isolated by precipitation from hot p-xylene into cool methanol.

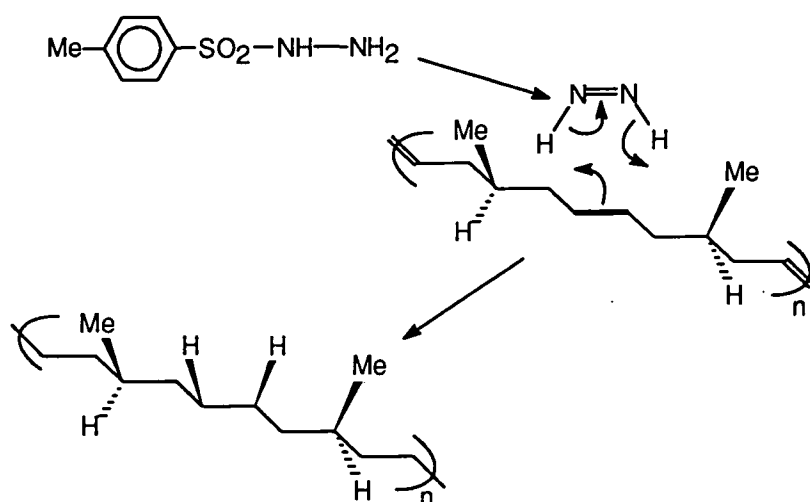


Figure 6.5. The scheme for the hydrogenation of poly(4-methyl-1-pentenylene)

The yield from the hydrogenation was 91%. The gel permeation chromatogram of the hydrogenated polymer (Appendix 6.1.4.) showed the number average molecular weight was 99,000 and PDI was 1.7; both were smaller than those of the polymer before hydrogenation. Thus, it appears that under these conditions the polymer molecules of the hydrogenated polymer occupy a smaller hydrodynamic volume than those of poly(4-methyl-1-pentenylene). The infrared spectrum of the polymer (Appendix 6.2.4) showed characteristic aliphatic C-H stretching absorptions in the region of 2800-3000 cm^{-1} but the absorptions due to vinylic C-H stretching mode, which were observed in poly(4-methyl-1-pentenylene) had disappeared, confirming the completion of the hydrogenation. The ^1H n.m.r. spectrum of the polymer (Appendix 6.3.5.) showed two resonances, 0.84 ppm (3H, d, $J=6.4\text{Hz}$) and 1.0-1.5 ppm(9H, m) and the resonance in the starting material due to the vinylic ^1H was not observed. The assignments of the ^{13}C n.m.r. spectrum of the polymer (Appendix 6.4.5.) was carried out using DEPT analysis (Appendix 6.5.4.), and is shown in Figure 6.6.

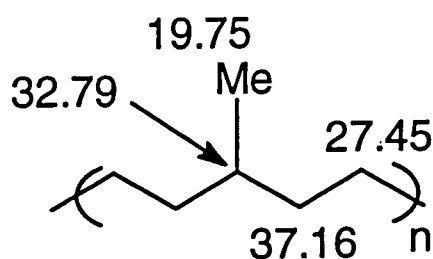


Figure 6.6 The assignments of the ^{13}C n.m.r. chemical shifts of the hydrogenated polymer (P6-7)

6.5 The detailed examination of the microstructures of poly(4-methyl-1-pentenylene) and poly(1-methylpentamethylene)

As was described in Chapter 1, polymers which have a chiral centre in each repeating unit may have R or S configuration about the chiral centre, and consequently there is the possibility of two adjacent centres having the same chiralities, resulting in racemic dyads or different chiralities, giving meso dyads. The microstructure due to trans/cis isomerism of the double bonds for poly(1-pentenylene)s was analysed as discussed in Section 6.3., but the microstructure due to the R/S configuration effects of the repeating units could not be analysed since further detailed microstructure of each signal in the ^{13}C n.m.r. spectra was not accessible by an ordinary treatment of the free induction decay (FID) signals acquired. However, it was found that microstructural information for each signal became distinguishable by treating the FID signals with a resolution enhancement procedure. In this section the discussion of the microstructures of poly(4-methyl-1-pentenylene) and poly(1-methylpentamethylene), based on spectra treated by the resolution enhancement procedure (Appendices 6.6.1. to 5.), is described.

For the determination of tacticity, the microstructure of the hydrogenated polymer (P6-7) was examined since the ^{13}C n.m.r. spectrum was expected to be simple for the hydrogenated polymer which did not have cis/trans isomerism. The resolution-enhanced resonances of each ^{13}C signal of the polymer are shown in Figure 6.7. As shown in the figure it was observed that the signal due to C^1 consisted of three peaks (the intensity ratio was 1:2:1; the differences in the chemical shifts was 0.012 ppm), C^2 signal consisted of four equivalent peaks (the differences in the chemical shifts was 0.013 ppm), C^3 signal consisted of two nearly equivalent peaks (the differences in the chemical shifts was 0.017 ppm) and C^4 signal consisted of three peaks (the intensity ratio was 1:2:1; the differences in the chemical shifts was 0.02 ppm).

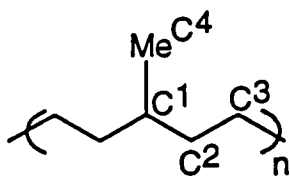
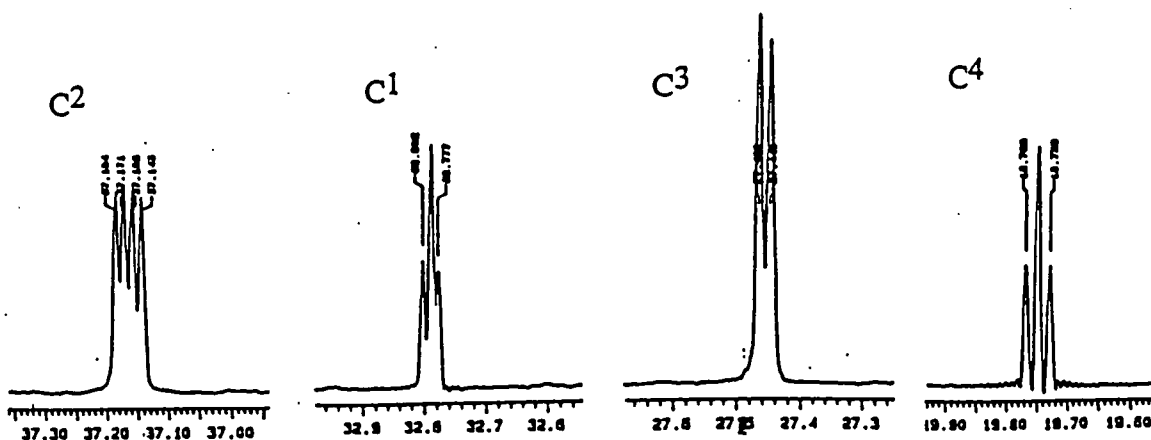


Figure 6.7. The resolution enhanced spectra of C¹, C², C³ and C⁴ of the hydrogenated polymer (P6-7)

These observation could be explained as follows: if the polymer contains both R and S configurations then there should be two possible configuration for a dyad, meso and racemic, and if the effect of configurational differences are apparent over a longer range, the possible triad configurations should be four as shown in Figure 6.8.¹²⁴ Thus, in a triad, there are potentially four different environments for the carbon atoms which are unsymmetrically situated in the repeating unit, that is C² and C³, while for the carbon atoms symmetrically situated, such as C¹ and C⁴, there should be three different environments because the racemic-meso triad and the meso-racemic triad provides same environment.

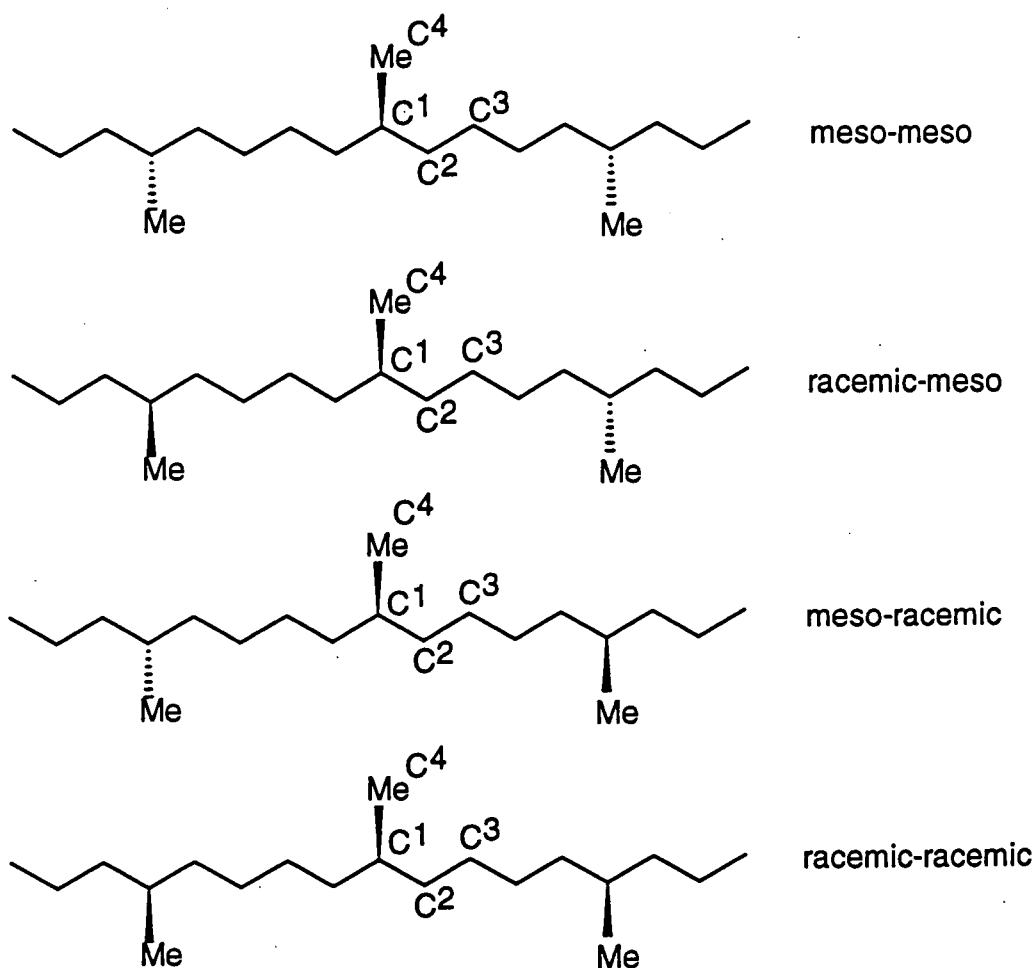


Figure 6.8. Possible configurations for triad

In practice, it turned out that C^1 , C^2 and C^4 were more sensitive to the surrounding configurations than C^3 which was affected only by the configurations of the dyad, and strangely C^4 was more sensitive to the configurations of the triads than C^1 which is nearer to the chiral centres on either side. The chemical shift difference resulting from the effect of the meso/racemic configurations of the nearest dyad on C^2 was 0.026 ppm whereas the next nearest dyad configurations provided a shift difference of 0.013 ppm. The intensity ratios of the peaks, namely 1:2:1 for C^1 , 1:1:1:1 for C^2 , 1:1 for C^3 and 1:2:1 for C^4 , proved that all possible triad configurations, meso-meso, racemic-meso, meso-racemic and racemic-racemic, were equally probable in the polymer chain, which

means that this hydrogenated polymer was atactic. Although the fully hydrogenated polymer was completely atactic, it is possible that the ratios of meso to racemic dyads in poly(4-methyl-1-pentenylene) could be different in segments of the chain having different cis or trans sequences. During hydrogenation the dyad information in such sequences must be retained, that is, a meso dyad in the unsaturated polymer will generate a meso dyad in the saturated polymer via a syn addition of hydrogen from diimide (see Figure 6.5.) irrespective of the stereochemistry of the vinylene unit. Thus, while it is possible, for example, that some all-cis sequences have a different tacticity than all-trans sequences, the overall distribution of meso and racemic dyads leads to an overall atactic saturated polymer and overall an atactic distribution of meso and racemic dyads must be present in the unsaturated polymer. The author believed that the probability of tactic sequences in different parts of the molecular chain of the unsaturated polymer exactly balancing each other so as to lead to an atactic hydrogenated polymer from partially tactic sequences in the precursor is very small, if this assumption is true then poly(4-methyl-1-pentenylene) must be atactic, although it has to be admitted that this can not be unambiguously proved on the basis of the available data.

Acting on the assumption that the poly(4-methyl-1-pentenylene) obtained was atactic, a detailed analysis of the spectrum of the polymer was carried out by comparison with spectra of poly(1-pentenylene) with differing cis/trans ratios. The resolution-enhanced spectra due to C^3 , C^{2trans} and C^{2cis} of P5-2, P5-12 and P6-4 are shown in Table 6.6., 6.7. and 6.8. respectively.

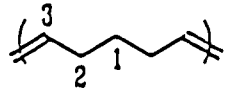
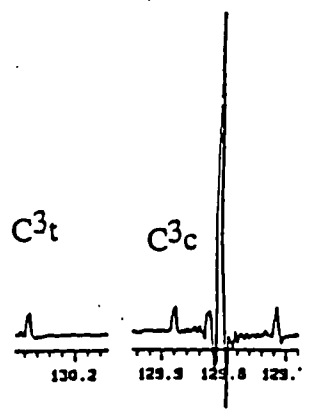
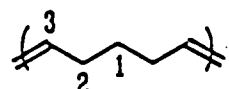
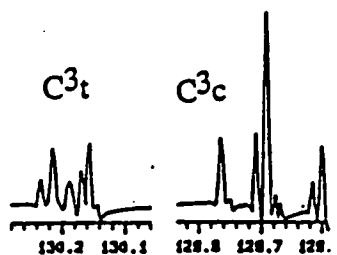
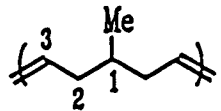
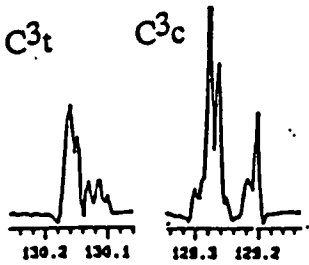
P5-2 = poly(1-pentenylene) cis/trans(calculated using signal intensities of

$$C^2)=62/38$$

P5-12 = poly(1-pentenylene) cis/trans(C^2)=86/14

P6-4 = poly(4-methyl-1-pentenylene) cis/trans(C^2)=60/40

Table 6.6. The resolution-enhanced resonances due to C³ of P5-2, P5-12 and P6-4

No.		Cis/Trans ^{a)}	Resolution enhanced resonances
P5-12		86/14	
P5-2		62/38	
P6-4		60 / 40	

a) The ratios of cis/trans were calculated based on the signal intensities due to C² in the unenhanced ¹³C n.m.r. spectra.

Considering the data recorded in Table 6.6., the complex resonance pattern for C^3 of P5-2 was not observed in the resonance of P5-12 which has a higher cis content. The observed complexity in this case was assigned to the effects of the cis/trans isomer sequence, that is to say a particular vinyl carbon is sensitive to nearest, next nearest and possibly further neighbours, the similar complexity observed in the vinyl-resonances of P6-4 was assigned as being due to the same reason.

Table 6.7. The resolution-enhanced resonances due to C^{2trans} of P5-2, P5-12 and P6-4

No.		Cis/Trans ^{a)}	Resolution enhanced resonances
P5-12		86/14	C^{2tc} C^{2tt} 32.25 32.15 32.05 31.95
P5-2		62/38	C^{2tc} C^{2tt} 32.15 32.05 31.95
P6-4		60 / 40	C^{2tc} C^{2tt} 33.85 33.75 33.65

a) The ratios of cis/trans were calculated based on the signal intensities due to C^2 in the unenhanced ^{13}C n.m.r. spectra.

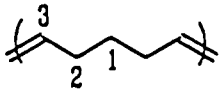
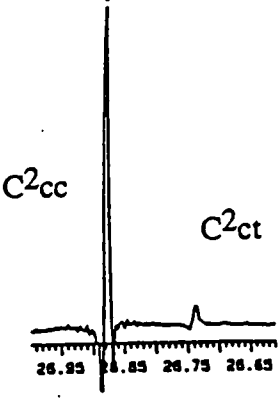
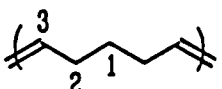
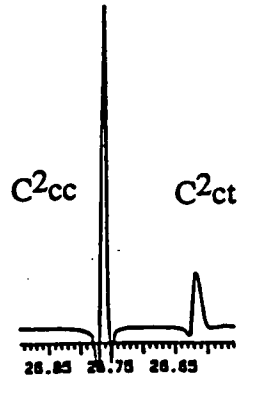
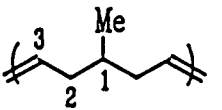
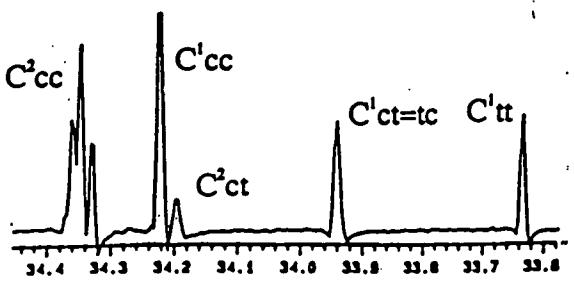
As shown in Table 6.7., the resonance due to C^{2tt} of P6-4 consisted of at least four signals and C^{2tc} consisted of two signals, while the resonances due to

both C^{2tt} and C^{2tc} of both P5-2 and P5-12 consisted of single signals. Therefore the splitting observed in the C^{2tt} and C^{2tc} resonances of P6-4 should be due to a reason other than the cis/trans isomerism and it would seem that these signals are sensitive to meso/racemic configuration effects. The signal for C^{2tc} was sensitive to the configurations of the dyad, providing two equivalent signals, which means that the meso/racemic dyads connected with the trans double bonds occur with equal frequency. The C^{2tt} signal was apparently sensitive to triad effects and consequently provided four signals, ideally these should occur in equal intensity if the meso/racemic distribution occurs with equal frequency, the data is not clear on this matter.

In Table 6.8., overleaf, the resonance due to C^{2cc} of P6-4 is shown, under resolution enhancement, to consist of three signals. The resonances due to C^{2ct} (34.2 ppm) was overlapping with the resonance due to C^{1cc} as discussed previously, while the resonances due to both C^{2cc} and C^{2ct} of both P5-2 and P5-12 consisted of single signals. Therefore the splitting observed in the C^{2cc} resonance of P6-4 should be due to meso/racemic configuration effects. It is assumed that there is overlap of two pairs of signals due to the configurations of triads leading to the observation of three resonances.

As described above it turned out that the resolution-enhanced spectrum of the poly(4-methyl-1-pentenylene) obtained contained the information about both the cis/trans isomerism and the tacticity due to the meso/racemic configurations and they became distinguishable by comparison with the spectra of poly(1-pentenylene). The analysis of the spectra of poly(4-methyl-1-pentenylene) and the hydrogenated polymer obtained from it suggests that both polymers are atactic.

Table 6.8. The resolution-enhanced resonances due to C^{2cis} of P5-2, P5-12 and P6-4

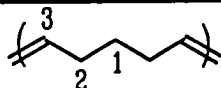
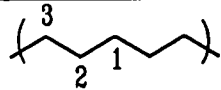
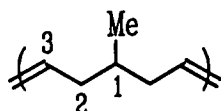
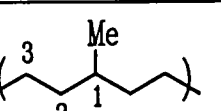
No.		Cis/Trans ^{a)}	Resolution enhanced resonances
P5-12		86/14	
P5-2		62/38	
P6-4		60 / 40	

a) The ratios of cis/trans were calculated based on the signal intensities due to C^2 in the unenhanced ^{13}C n.m.r. spectra.

6.6 Thermal properties of the polymers obtained

The decomposition temperature (T_d), the glass transition temperature (T_g) and the melting temperature (T_m) of the polymers (P6-4 and 7) obtained were examined using thermal gravimetric analysis and differential scanning calorimetry (Appendices 6.7.1. and 2.). The results are shown in Table 6.9. with those for poly(1-pentenylene) and hydrogenated poly(1-pentenylene), polyethylene, (Appendices 5.5.1. and 6.7.3.) for the comparison. The polyethylene (P5-1H) was obtained by hydrogenation of P5-1, poly(1-pentenylene), using a similar method to that used for the hydrogenation of poly(4-methyl-1-pentenylene).

Table 6.9. Thermal characterisation parameters, T_d , T_g and T_m , observed for the polymers obtained

No.	Polymer	Cis / Trans Ratio ^a	TG ^b		DSC ^b	
			T_d (°C)	T_g (°C)	T_m (°C)	
P5-1		61 / 39	368	-101	not observed	
P5-1H		--	421	-125 ^c	130	
P6-4		60 / 40	370	-72	not observed	
P6-7		--	419	-59	not observed	

- a) The ratios of cis/trans were calculated based on the signal intensities due to C^2 .
 b) See Appendix 1. for details.
 c) The value for the T_g of P5-1H was the literature value for T_g of polyethylene.¹²⁵

The poly(4-methyl-1-pentenylene) (P6-4) and poly(1-methylpentamethylene) (P6-7) obtained were not highly crystalline polymer since the melting temperatures

were not observed. As shown in the table, the introduction of a methyl group into each of poly(1-pentenylene) and polyethylene raised the glass transition temperature of each polymer (6-4 and 7).

6.7 Discussion

6.7.1 Thermodynamics

It turned out that 4-methylcyclopentene can be polymerised by ring opening metathesis although the monomer was less easily polymerised than cyclopentene. As discussed in Chapter 1, polymerisability by ring opening is dependent on the sign of the Gibbs free energy (ΔG) and is largely affected by enthalpy (ΔH) term. As shown in Table 6.10., the enthalpies of ring opening polymerisation for various cyclopentenes were reported as estimated values and they are supposed to parallel the polymerisabilities; namely, ring opening with larger negative enthalpy is more likely to occur, since the entropy terms ($T\Delta S$) in these ring opening polymerisations should be similar.

Table 6.10. ΔH for the polymerisation of liquid cycloalkanes and cycloalkene by ring opening to give solid amorphous polymers at 25°C (kcal/mol)

Monomer	ΔH
Cyclopentane	-5.3 ^a ,125
Methylcyclopentane	-4.1 ^b ,125
1,1-Dimethylcyclopentane	-3.2 ^b ,125
Cyclopentene (--> cis polymer)	-3.8 ^b ,126
Cyclopentene (--> trans polymer)	-4.8 ^b ,126

a) Experimental value, b) Semi-empirical estimate

However the value for substituted cyclopentene had not been reported. So the enthalpies for substituted cyclopentenenes were estimated based on the heat of formation energies which were obtained using semi-empirical molecular orbital calculations. In order to determine an appropriate calculation method for the heats of formation the values for several compounds were computed by three methods (PM3, AM1 and MNDO on the MOPAC program via "Insight II" of the Biosym Technologies Ltd package) and compared with the experimental values.

Table 6.11. The heat of formation for some compounds estimated using semi-empirical molecular orbital calculations (kcal/mol)

Compound	Experimental value	Semi-empirical MO calculation		
		PM3	AM1	MNDO
Cyclopentane	-18.5	-23.89	-28.79	-30.3
Cyclohexane	-29.4	-31.03	--	--
Ethane	-20.2	-18.13	--	--
Ethylene	12.5	16.63	16.47	15.40
Heptane	-44.9	-45.32	--	--
Cyclopentene	--	3.02	2.98	-0.33
4-Methylcyclopentene	--	-3.01	-2.29	-3.06

As shown in Table 6.11. the values obtained using PM3 showed relatively good correlations with the experimental values, so the following calculations were carried out using PM3. Enthalpies for ring opening (ΔH_{Op}) were calculated for several cyclic compounds according to the following equation.

$$\Delta H_{Op} = (HF_P - HF_C) - HF_M$$

where HF_M , HF_P and HF_C are the heats of formation calculated for cyclic compound "M" and compounds "P" and "C" respectively. An example of compounds "M", "P" and "C" are shown in Figure 6.9.

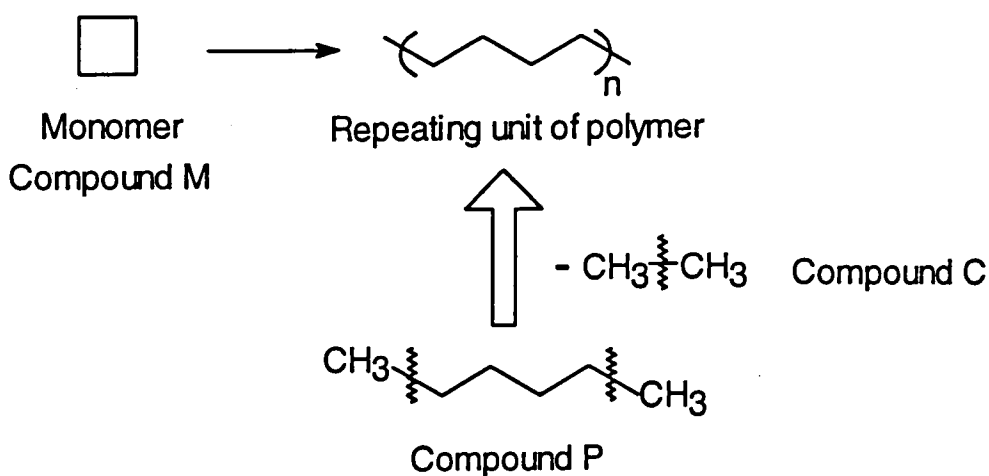


Figure 6.9. An example of compounds "M", "P" and "C"

The values calculated for HF_M , HF_P , HF_C and $\Delta\text{H}_{\text{OP}}$ are shown in Table 6.12. overleaf. As shown in the table, the correlations between the enthalpies for ring opening of cyclopentanes and cyclopentene were roughly similar to those shown in Table 6.10., and the order of the enthalpies for ring opening of cycloalkanes predicted was








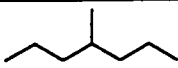




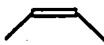

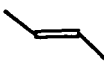
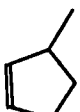
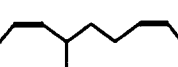

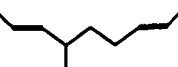
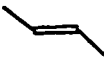
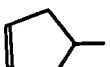
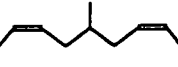

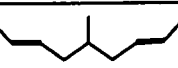



which was consistent with the polymerisability predicted on the basis of thermochemical calculations by Ivin.¹⁷ The estimates were also consistent with the fact that a substituted group on a cyclic compound makes ring opening more difficult. It was estimated that for the cyclopentenes ring opening reactions producing trans polymers were more favourable than those producing cis polymers and the order of the polymerisability was



however, the enthalpy for 4-methylcyclopentene was still negative. So, these estimates help to rationalise the results described in Section 6.2.; namely, that 4-methylcyclopentene was polymerised with reasonable yield at -55°C but the yield at -35°C was very small, while cyclopentene was more readily polymerised under the same conditions.

Table 6.12. The heats of formation and ring opening enthalpies calculated for various cyclic compounds (kcal/mol)^a

M	HF _M	P	HF _P	C	HF _C	ΔH _{OP}
	-3.79		-39.90	Ethane	-18.13	-18.0
	-31.03		-50.74	Ethane	-18.13	-1.6
	-23.89		-45.32	Ethane	-18.13	-3.3
	-29.92		-50.12	Ethane	-18.13	-2.1
	-35.87		-54.21	Ethane	-18.13	-0.2
	3.02		-2.77		-3.56	-2.2
			-4.01		-3.77	-3.2
	-2.60		-7.75		-3.56	-1.6
			-9.32		-3.77	-3.0
	-3.01		-7.34		-3.56	-0.7
			-9.43		-3.77	-2.6

a) HF_M, HF_P and HF_C are the heat formation energies calculated for cyclic compound "M" and olefin "P" and "C" respectively.

6.7.2 Microstructure

As discussed in Section 6.5., the tacticity of poly(4-methyl-1-pentenylene) obtained, P6-4, in this work was atactic. Although the polymerisation turned out to proceed in a classical manner, a potential mechanism for the production of racemic and meso dyads in the polymerisation of 4-methylcyclopentene can be postulated as follows.

In the case where the incoming 4-methylcyclopentene reacts with the metal alkylidene complex at the propagating chain end to produce a metallacyclobutane in which the chain and the cyclopentane ring have a cis relationship there are two possible stereochemistries. In Figure 6.10. these possibilities are labelled "Front face approach" and "Back face approach" and assume that the methyl in the monomer points away from the plane of the alkylidene. If this is true, Front face approach will produce a racemic dyad and Back face approach a meso dyad, as shown in the figure. In this proposition the steric interaction between the incoming monomer and the propagating chain end is supposed to be a major factor influencing the outcome. If the steric interaction is large enough Front face approach would be disfavoured over Back face approach consequently predominantly meso dyads would be expected in association with cis carbon-carbon double bonds.

Since a similar argument can be applied to the case of forming trans metallacyclobutane intermediates, racemic dyads might be expected to be associated with trans carbon-carbon doubles.

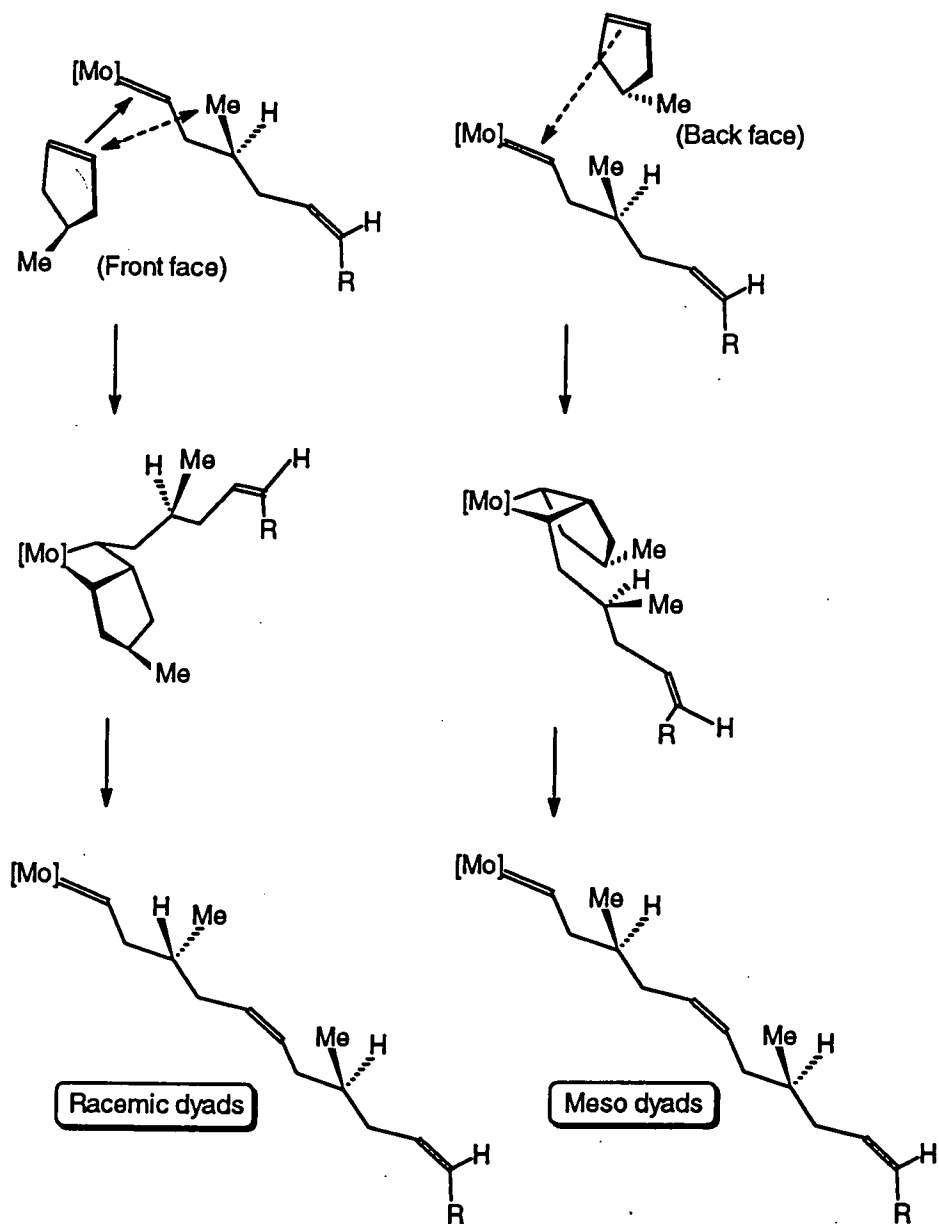


Figure 6.10. A mechanism suggested for the production of racemic/meso dyads in the metathesis polymerisation of 4-methylcyclopentene

In our examination the poly(4-methyl-1-pentenylene) obtained was atactic, although the number of attempts was restricted. This suggests that the polymerisations studied here proceeded without any control over the formation of racemic or meso configurations. So, it can be concluded that the steric interaction between the incoming monomer and the propagating chain end are too small to cause a difference between

reaction paths, of which the Front face approach and Back face approach discussed above constitute an example.

6.8 Experimental

The polymerisations were carried out using similar procedures to those for the polymerisations of cyclopentene described in Chapter 5.

The method for the hydrogenation is described below.

The polymer (P6-4) obtained (70mg, 0.85 repeat unit mmol) and p-xylene (11 ml) were placed in a two necked round-bottomed flask (50 ml) fitted with a reflux condenser and a nitrogen inlet. The flask was purged with a dry nitrogen, and heated in an oil bath at 150°C. Then p-toluenesulfonyl hydrazide (1.6g, 8.5 mmol, 10 equivalents) was carefully added to the flask in several portions against a nitrogen flow. After 5 hours, the hot mixture was slowly poured into cool methanol (100 ml) and a fine powder was precipitated after 15 hours. The white precipitate obtained by filtration was dried under vacuum for 5 hours. The yield was 91%.

CHAPTER 7: Conclusion and proposals for future work

As discussed in Chapter 3 the endo Diels-Alder adduct of acenaphthylene and cyclopentadiene was readily polymerised to provide high trans content polymer by the *t*-butoxy molybdenum initiator and high cis content polymer by the trifluorinated *t*-butoxy molybdenum initiator. Thus well defined initiators polymerise this monomer stereoregularly, while classical systems did not. The polymerisation proceeded in a living manner although the molecular weights of the polymers obtained were not very narrowly distributed because of the high k_p/k_i ratio.

In the polymerisation of the exo-adduct soluble polymer was not obtained although a mixture of the endo and the exo adducts was polymerised using a well defined initiator and using a classical molybdenum catalyst system with a chain transfer reagent. The propagating process of the exo-adduct was concluded to be highly sensitive to Lewis acid. Examination using the block copolymerisation technique is suggested as a future experiment to investigate the polymerisation of the exo-adduct. As mentioned above an endo/exo mixture was readily polymerised using a well defined initiator, so it might be possible to synthesise a block copolymer consisting of a first block whose structure had been well established, such as polynorbornene, and a poly(exo-adduct) block with a relatively small number of the repeat unit, as shown in Figure 7.1., namely by a ring opening polymerisation of norbornene using a well defined initiator, such as the *t*-butoxy molybdenum initiator, to produce living polymer and subsequent chain propagation using the exo-adduct.

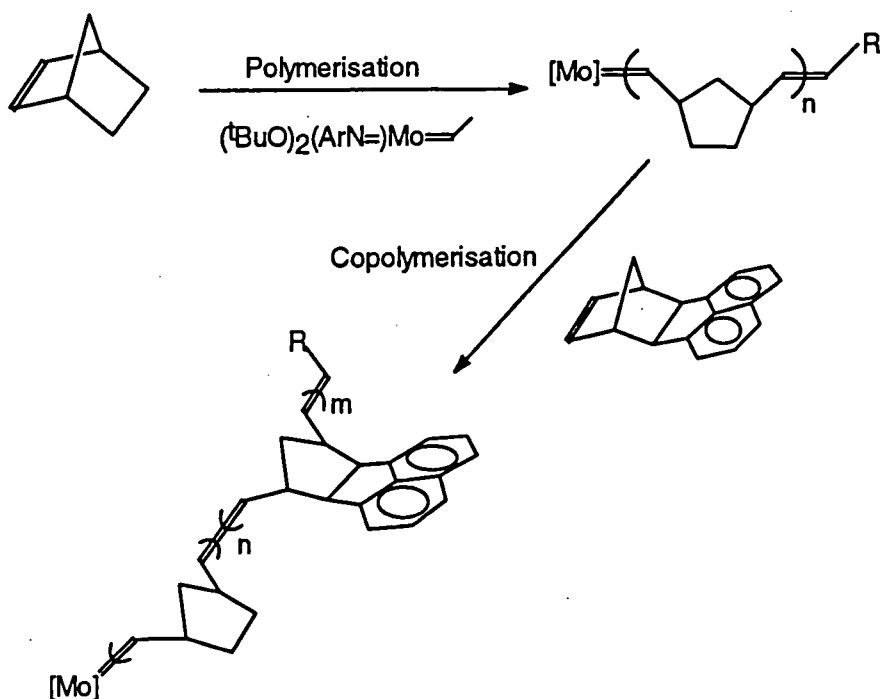


Figure 7.1. A possible scheme for a production of a copolymer containing a poly(exo-adduct) block

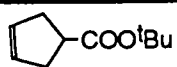
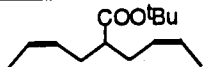

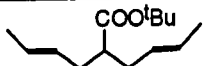
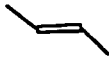
If such polymer can be synthesised then it would be soluble and the analysis of the poly(exo-adduct) might become possible.

In Chapter 5, the effects of various reaction conditions on the polymerisation of cyclopentene using several well defined initiators were discussed, along with the microstructures of the resultant polymers. The molybdenum centred initiators polymerised cyclopentene in a classical manner and well defined tungsten centred initiator polymerised it mainly in a well defined manner but a side reaction occurred to produce a much higher molecular weight component.

In Chapter 6, the investigation of the polymerisation and the polymers obtained using 4-methylcyclopentene, as an example of a monomer having a substituent group on the cyclopentene ring which leads to polymers having chiral centres in the main chain, is described. 4-Methylcyclopentene was

confirmed to be polymerisable using the well defined initiators, but the monomer was significantly less favoured with respect to the ring opening metathesis polymerisation than cyclopentene. The reaction conditions, such as the reaction temperature and the reaction duration, affected the polymerisation in a similar manner to the polymerisation of cyclopentene. It was confirmed that information about the racemic/meso configurations in poly(4-methyl-1-pentenylene) and the poly(1-methylpentamethylene) obtained from it can be established by ^{13}C n.m.r. spectroscopy, although each methyl substituent group is five bonds away from next one. Both polymers were shown to be atactic. As discussed in Section 6.7.2., it was concluded that the methyl substituent group is too small to cause an effective steric interaction, which would control the reaction direction, in the transition state of the propagating process. So, it is suggested as a further work to examine the microstructures of the polymers obtained from a monomer with larger substituent group. *t*-Butyl 3-cyclopentene-1-carboxylate is proposed as such a monomer since it has a sterically bulky *t*-butyl group which may be expected to have a bigger effect on the control of the reaction path than methyl. The enthalpy values estimated by same method described in Section 6.7. for the ring opening of *t*-butyl 3-cyclopentene-1-carboxylate are shown in Table 7.1.

Table 7.1. The heats of formation and enthalpies calculated for ring openings of *t*-butyl 3-cyclopentene-1-carboxylate (kcal/mol)^a

M	HF _M	P	HF _P	C	HF _C	ΔH _{OP}
	-90.26		-94.86		-3.56	-1.0
			-96.19		-3.77	-2.2

a) HF_M, HF_P and HF_C are the heats of formation calculated for cyclic compound "M" and olefin "P" and "C" respectively.

Although it might be expected that the bulky t-butyl group would make the polymerisability much lower, the enthalpies calculated were similar to those for 4-methylcyclopentene, from which it may be inferred that t-butyl 3-cyclopentene-1-carboxylate is still polymerisable. The reason is possibly that the t-butyl group is not situated close to the cyclopentene ring. Thus the polymerisation of t-butyl 3-cyclopentene-1-carboxylate might provide further progress in the examination of the tacticity of the polymers produced by ring opening metathesis polymerisation of substituted cyclopentenes.

APPENDIX 1

General procedures, equipment and instrumentation

General experimental procedures

The glove box used throughout this work was a modified Miller Howe dry box with a fitted freezer (-40°C), the inert gas was oxygen-free nitrogen and the working conditions were 2~10 ppm oxygen and 2~10 ppm moisture. Apparatus was transferred in and out of the box via two vacuum / nitrogen ports.

The vacuum / nitrogen line was fitted with Young valves and greaseless joints to allow handling of materials either under nitrogen or under vacuum. Vacuum was provided by an Edwards 5 Two Stage pump and dry oxygen-free nitrogen was supplied through a double P₂O₅ column.

The thermostated cooling bath used for the polymerisation of cyclopentenes was a HAAKE F3-Q model and the cooling fluid used was methylated spirits.

Instrumentation and procedures for measurements

Gas Chromatography was carried out using a Hewlett Packard 5890A GC (capillary column: SE 30 crosslinked methyl silicone column 25m x 0.32mm x 0.25µ ID).

Infrared spectra were recorded on a Perkin Elmer 1600 series FTIR. The spectra were recorded as solvent (chloroform) cast films or KBr pellets.

¹H and ¹³C Nuclear Magnetic Resonance spectra were recorded on a Varian VXR 400 NMR spectrometer at 399.953 MHz (¹H) and 100.577 MHz (¹³C) and a Varian Gemini 200 NMR spectrometer at 199.532 MHz (¹H) and 50.289 MHz (¹³C). Perdeuterobenzene or deutrochloroform was used as the solvent.

Mass Spectra were recorded on a VG Analytical Model 7070E Mass Spectrometer.

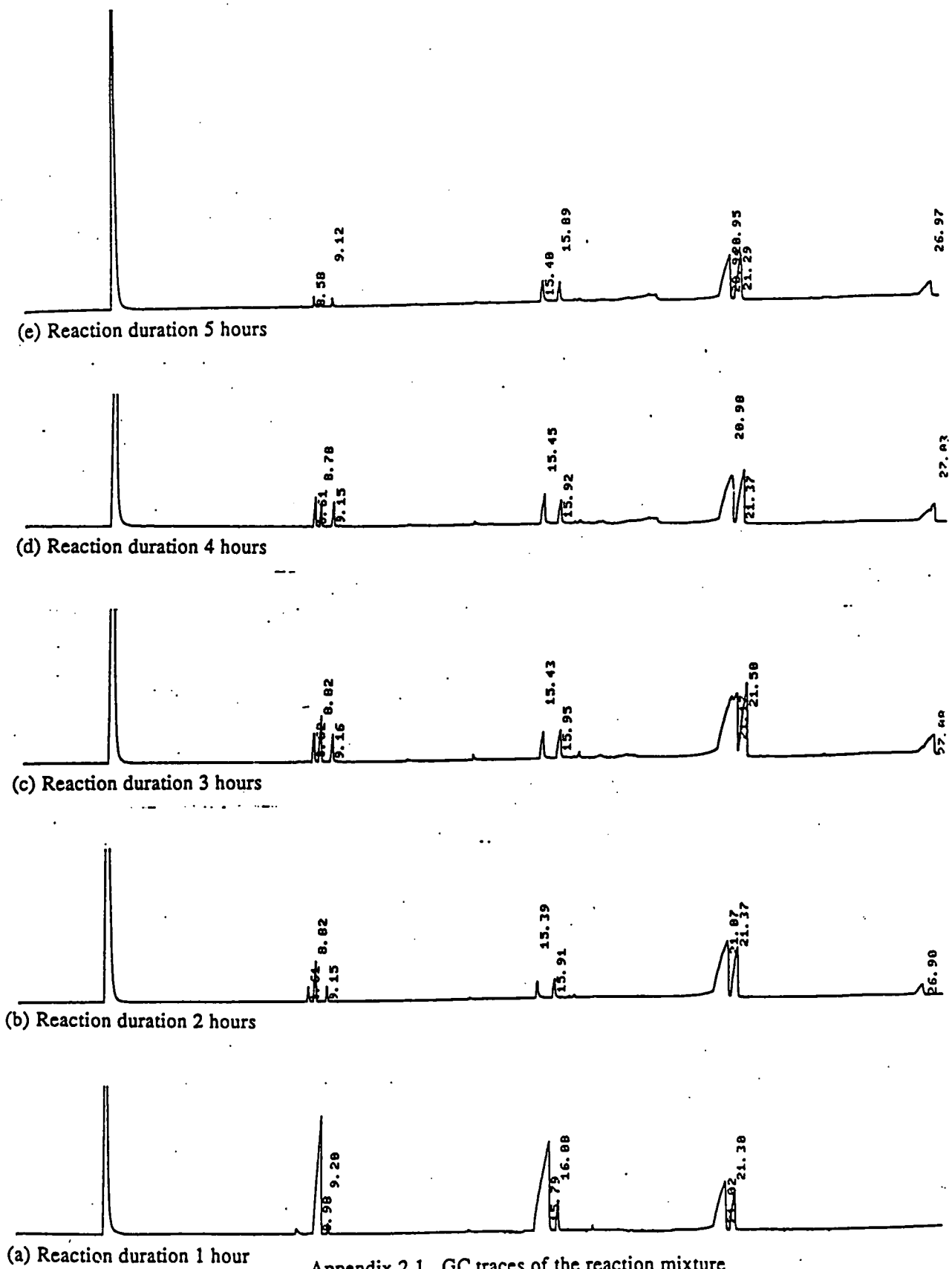
Gel Permeation Chromatography was carried out using a Waters Model 590 (refractometer, column packing PL_{gel} 5 μ mixed styrene-divinyl benzene beads, solvent: chloroform) and a Viscotek Differential Refractometer/Viscometer Model 200 (column packing PL_{gel} 10 μ mixed styrene-divinyl benzene beads, solvent: tetrahydrofuran). The concentration of the samples was 0.2% unless it is mentioned in the text.

Thermogravimetric Analysis was performed using a Stanton Redcroft TG760 thermobalance. TGA traces were recorded by increasing the sample temperature by 10°C per minute under a nitrogen atmosphere and the 2% weight loss temperature was taken as decomposition temperature.

Differential Scanning Calorimetry was performed using a Perkin Elmer DSC 7 differential scanning calorimeter. The glass transition temperature was examined for each sample by first running from -120°C to 350°C under a nitrogen atmosphere. Then a virgin sample was annealed at 20°C above its glass transition temperature for one hour, and cooled down to -120°C and DSC traces were recorded with increasing temperature by 10°C per minute from -120°C to 350°C under a nitrogen atmosphere. The T_g recorded was the mid point of the transition in the base line associated with the glass transition process.

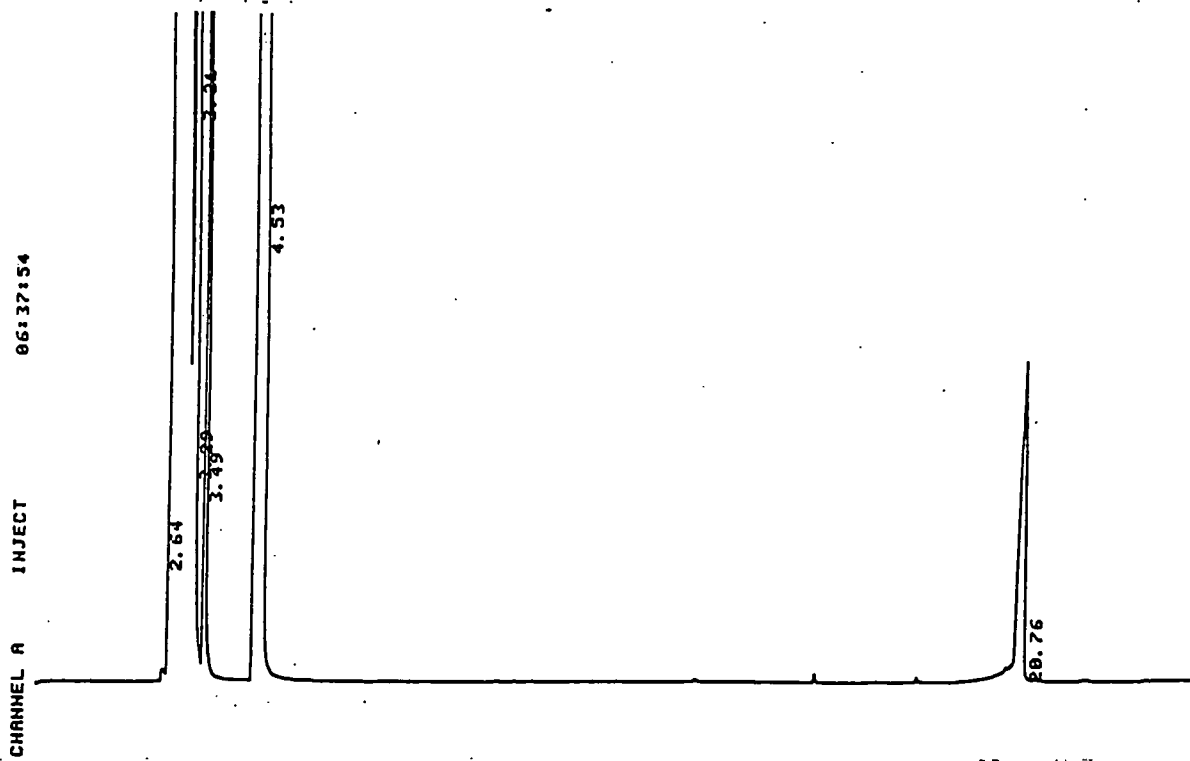
APPENDIX 2

Analytical data for Chapter 2

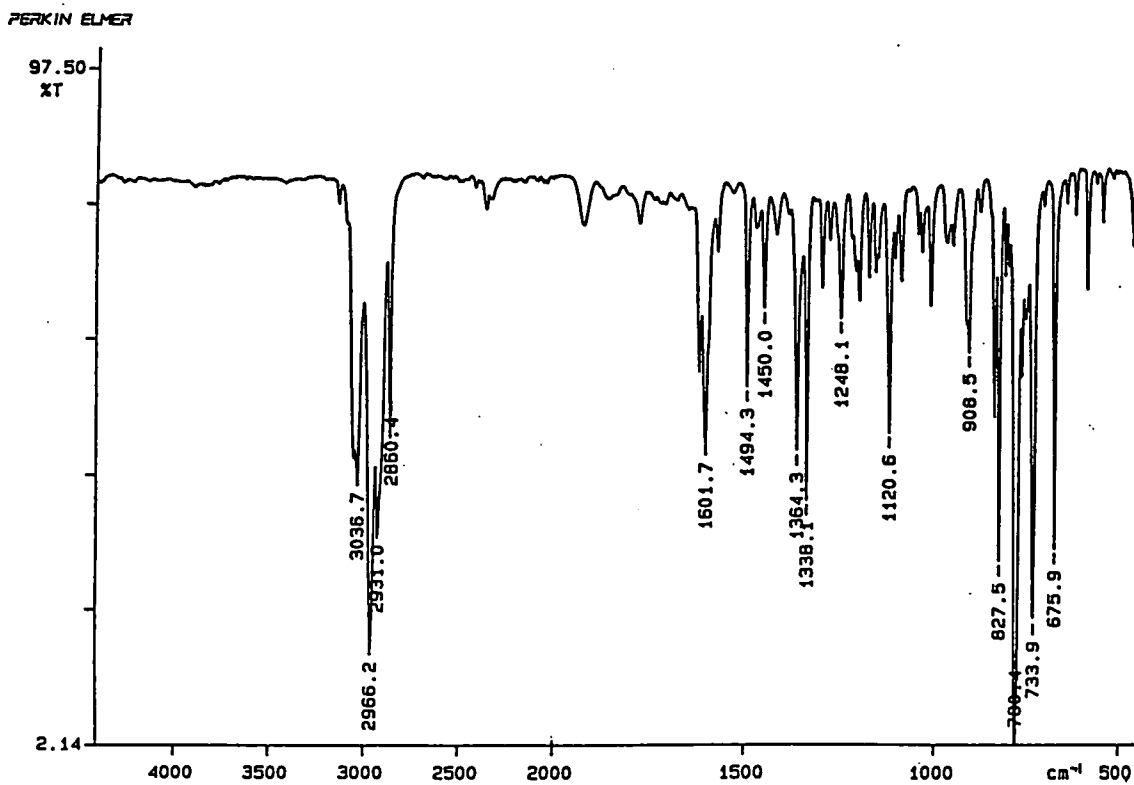


Appendix 2.1. GC traces of the reaction mixture

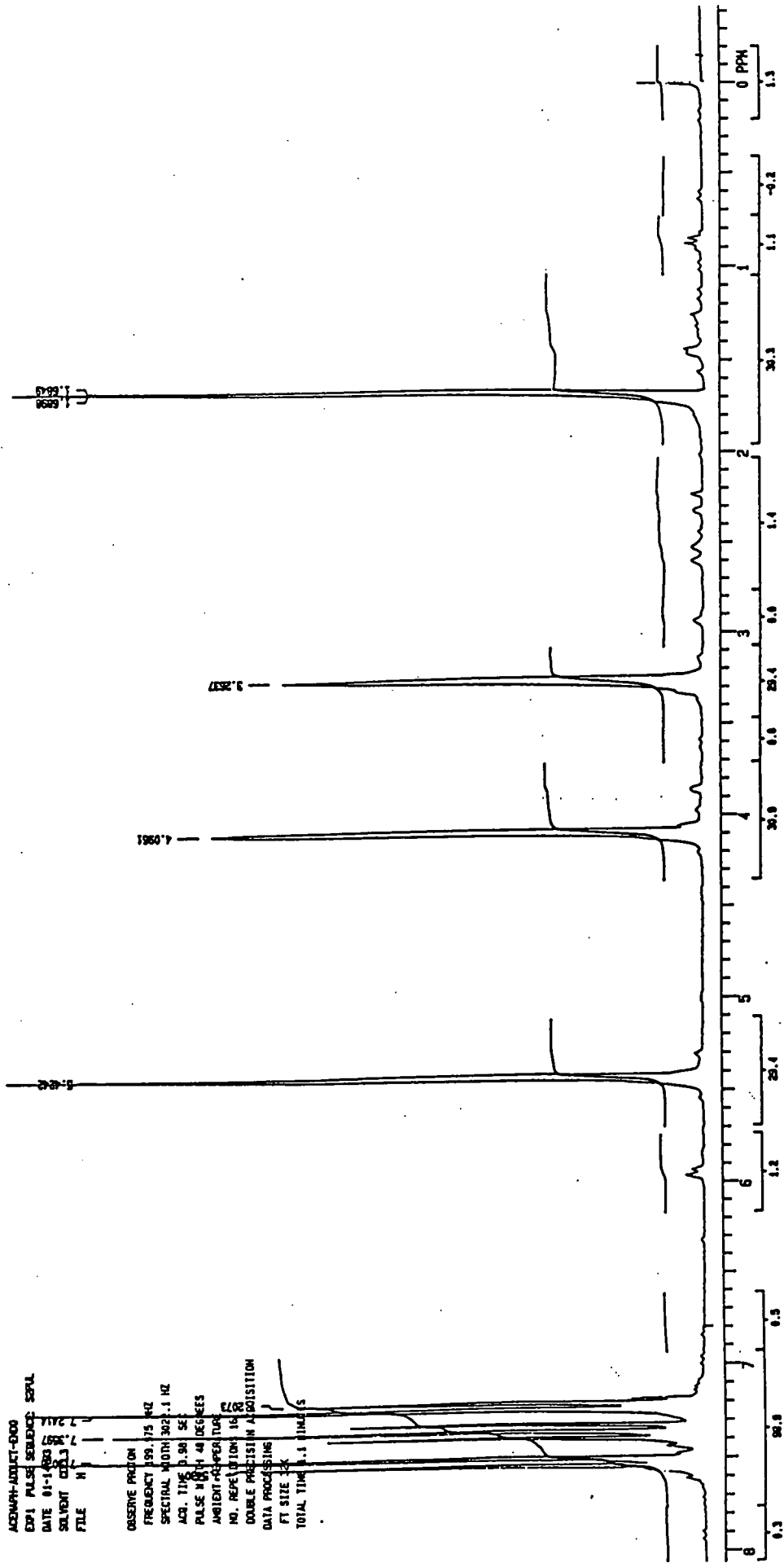
(Diels-Alder reaction between acenaphthylene and cyclopentadiene)



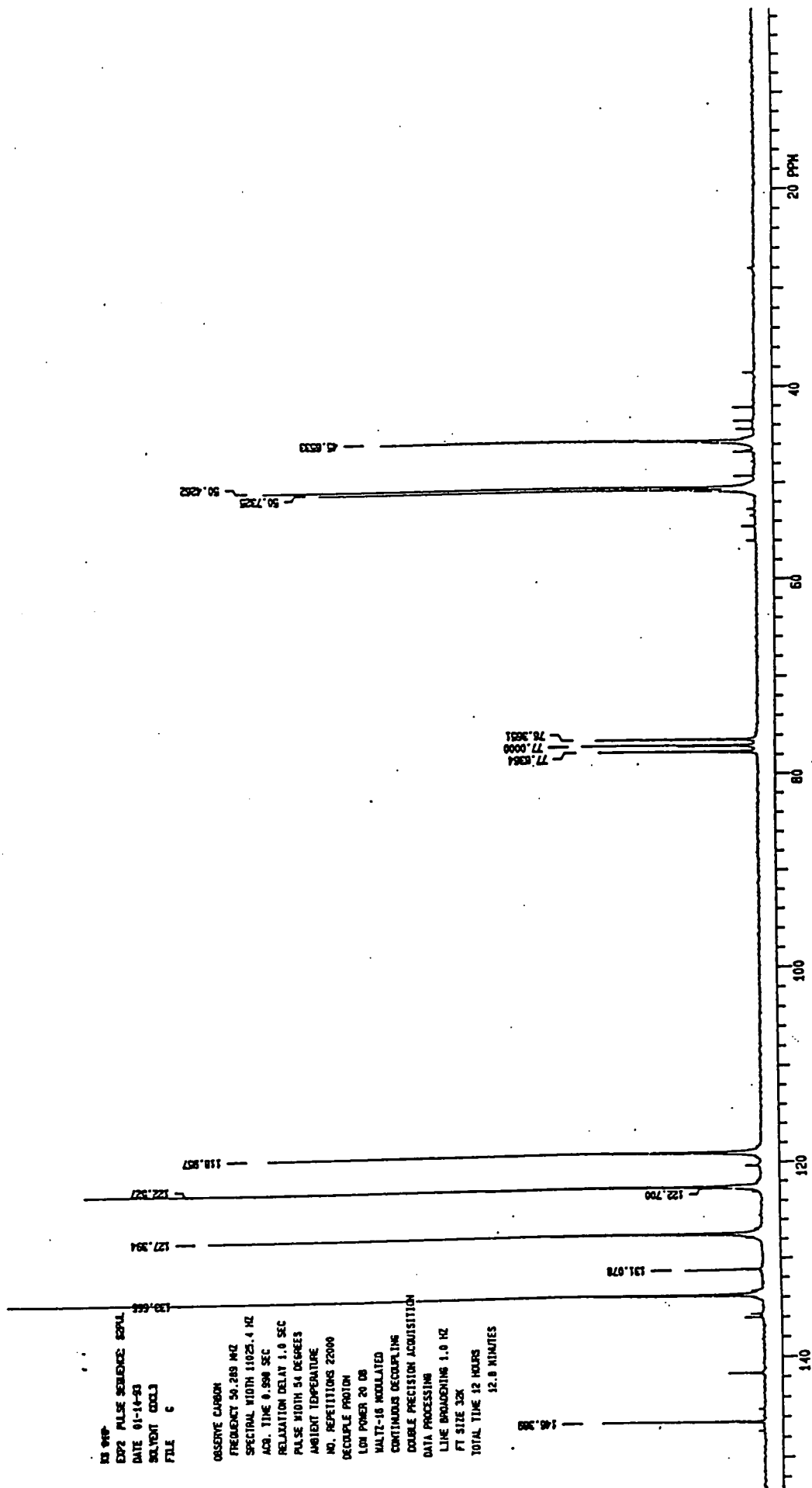
Appendix 2.2. GC trace of endo Diels-Alder adduct of acenaphthylene and cyclopentadiene



Appendix 2.3. Infrared spectrum of endo Diels-Alder adduct of acenaphthylene and cyclopentadiene



Appendix 2.4. ^1H n.m.r. spectrum of endo Diels-Alder adduct of acenaphthylene and cyclopentadiene



Appendix 2.5. ¹³C n.m.r. spectrum of endo Diels-Alder adduct of acenaphthylene and cyclopentadiene

Appendix 2.6. Single crystal X-ray diffraction data of endo Diels-Alder adduct of acenaphthylene and cyclopentadiene

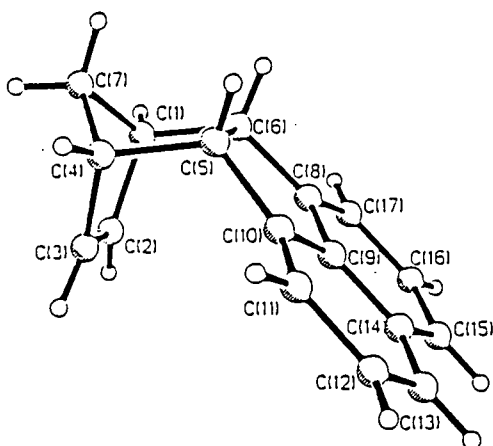


Table 2. Bond lengths (Å).

C(01)-C(02)	1.514 (3)	C(01)-C(06)	1.566 (3)
C(01)-C(07)	1.538 (3)	C(02)-C(03)	1.326 (3)
C(03)-C(04)	1.510 (3)	C(04)-C(05)	1.569 (3)
C(04)-C(07)	1.537 (3)	C(05)-C(06)	1.578 (2)
C(05)-C(010)	1.510 (2)	C(06)-C(08)	1.512 (2)
C(08)-C(09)	1.413 (2)	C(08)-C(017)	1.372 (3)
C(09)-C(010)	1.412 (2)	C(09)-C(014)	1.410 (2)
C(010)-C(011)	1.370 (3)	C(011)-C(012)	1.420 (3)
C(012)-C(013)	1.374 (3)	C(013)-C(014)	1.418 (3)
C(014)-C(015)	1.422 (3)	C(015)-C(016)	1.376 (3)
C(016)-C(017)	1.422 (3)	C(1)-C(2)	1.515 (3)
C(1)-C(6)	1.566 (3)	C(1)-C(7)	1.539 (3)
C(2)-C(3)	1.330 (3)	C(3)-C(4)	1.516 (3)
C(4)-C(5)	1.565 (3)	C(4)-C(7)	1.538 (3)
C(5)-C(6)	1.577 (2)	C(5)-C(10)	1.513 (3)
C(6)-C(8)	1.507 (2)	C(8)-C(9)	1.409 (2)
C(8)-C(17)	1.376 (2)	C(9)-C(10)	1.418 (2)
C(9)-C(14)	1.405 (2)	C(10)-C(11)	1.374 (3)
C(11)-C(12)	1.422 (3)	C(12)-C(13)	1.374 (3)
C(13)-C(14)	1.417 (3)	C(14)-C(15)	1.421 (3)
C(15)-C(16)	1.373 (3)	C(16)-C(17)	1.416 (3)

Table 3. Bond angles (°)

C(02)-C(01)-C(06)	106.8(1)	C(02)-C(01)-C(07)	100.5(2)
C(06)-C(01)-C(07)	99.7(1)	C(01)-C(02)-C(03)	107.6(2)
C(02)-C(03)-C(04)	107.9(2)	C(03)-C(04)-C(05)	106.7(1)
C(03)-C(04)-C(07)	100.7(2)	C(05)-C(04)-C(07)	99.4(1)
C(04)-C(05)-C(06)	102.5(1)	C(04)-C(05)-C(010)	117.1(1)
C(06)-C(05)-C(010)	105.0(1)	C(01)-C(06)-C(05)	102.2(1)
C(01)-C(06)-C(08)	117.9(1)	C(05)-C(06)-C(08)	104.7(1)
C(01)-C(07)-C(04)	93.9(1)	C(06)-C(08)-C(09)	108.7(1)
C(06)-C(08)-C(017)	132.6(2)	C(09)-C(08)-C(017)	118.7(2)
C(08)-C(09)-C(010)	112.8(2)	C(08)-C(09)-C(014)	123.7(2)
C(010)-C(09)-C(014)	123.4(2)	C(05)-C(010)-C(09)	108.7(1)
C(05)-C(010)-C(011)	132.7(2)	C(09)-C(010)-C(011)	118.6(2)
C(010)-C(011)-C(012)	119.0(2)	C(011)-C(012)-C(013)	122.4(2)
C(012)-C(013)-C(014)	120.1(2)	C(09)-C(014)-C(013)	116.5(2)
C(09)-C(014)-C(015)	116.0(2)	C(013)-C(014)-C(015)	127.5(2)
C(014)-C(015)-C(016)	120.3(2)	C(015)-C(016)-C(017)	122.4(2)
C(08)-C(017)-C(016)	118.9(2)	C(2)-C(1)-C(6)	107.6(1)
C(2)-C(1)-C(7)	100.0(1)	C(6)-C(1)-C(7)	99.6(1)
C(1)-C(2)-C(3)	107.8(2)	C(2)-C(3)-C(4)	107.5(2)
C(3)-C(4)-C(5)	106.9(1)	C(3)-C(4)-C(7)	100.0(1)
C(5)-C(4)-C(7)	100.4(1)	C(4)-C(5)-C(6)	102.3(1)
C(4)-C(5)-C(10)	118.1(1)	C(6)-C(5)-C(10)	104.7(1)
C(1)-C(6)-C(5)	102.5(1)	C(1)-C(6)-C(8)	117.4(1)
C(5)-C(6)-C(8)	104.8(1)	C(1)-C(7)-C(4)	93.9(1)
C(6)-C(8)-C(9)	109.2(1)	C(6)-C(8)-C(17)	132.1(2)
C(9)-C(8)-C(17)	118.6(2)	C(8)-C(9)-C(10)	112.4(2)
C(8)-C(9)-C(14)	123.8(2)	C(10)-C(9)-C(14)	123.8(2)
C(5)-C(10)-C(9)	108.8(1)	C(5)-C(10)-C(11)	133.0(2)
C(9)-C(10)-C(11)	118.2(2)	C(10)-C(11)-C(12)	118.9(2)
C(11)-C(12)-C(13)	122.6(2)	C(12)-C(13)-C(14)	120.0(2)
C(9)-C(14)-C(13)	116.4(2)	C(9)-C(14)-C(15)	116.2(2)
C(13)-C(14)-C(15)	127.4(2)	C(14)-C(15)-C(16)	120.1(2)
C(15)-C(16)-C(17)	122.6(2)	C(16)-C(17)-C(16)	118.7(2)

Table 4. Atomic coordinates and equivalent isotropic displacement coefficients (Å²)

	x	y	z	U(eq)
C(01)	0.0921(1)	-0.3432(2)	0.0781(1)	0.037(1)
C(02)	0.1786(1)	-0.3109(2)	0.0931(2)	0.041(1)
C(03)	0.2068(1)	-0.2793(2)	0.0099(2)	0.041(1)
C(04)	0.1405(1)	-0.2902(2)	-0.0627(1)	0.036(1)
C(05)	0.0837(1)	-0.1662(2)	-0.0447(1)	0.030(1)
C(06)	0.0499(1)	-0.2033(2)	0.0543(1)	0.030(1)
C(07)	0.0922(1)	-0.4078(2)	-0.0208(1)	0.041(1)
C(08)	0.0696(1)	-0.0798(2)	0.1158(1)	0.029(1)
C(09)	0.1097(1)	0.0184(2)	0.0618(1)	0.027(1)
C(010)	0.1204(1)	-0.0253(2)	-0.0317(1)	0.028(1)
C(011)	0.1589(1)	0.0605(2)	-0.0914(1)	0.034(1)
C(012)	0.1862(1)	0.1903(2)	-0.0575(1)	0.035(1)
C(013)	0.1752(1)	0.2335(2)	0.0333(1)	0.033(1)
C(014)	0.1357(1)	0.1472(2)	0.0970(1)	0.028(1)
C(015)	0.1191(1)	0.1756(2)	0.1925(1)	0.035(1)
C(016)	0.0807(1)	0.0794(2)	0.2455(1)	0.038(1)
C(017)	0.0552(1)	-0.0496(2)	0.2080(1)	0.035(1)
C(1)	0.3599(1)	-0.6017(2)	0.2998(1)	0.031(1)
C(2)	0.3793(1)	-0.4545(2)	0.2732(1)	0.031(1)
C(3)	0.3889(1)	-0.4511(2)	0.1807(1)	0.033(1)
C(4)	0.3770(1)	-0.5965(2)	0.1436(1)	0.033(1)
C(5)	0.4491(1)	-0.6837(2)	0.1800(1)	0.030(1)
C(6)	0.4361(1)	-0.6899(2)	0.2893(1)	0.028(1)
C(7)	0.3139(1)	-0.6475(2)	0.2103(1)	0.036(1)
C(8)	0.5111(1)	-0.6343(2)	0.3339(1)	0.026(1)
C(9)	0.5630(1)	-0.5988(2)	0.2627(1)	0.027(1)
C(10)	0.5302(1)	-0.6226(2)	0.1712(1)	0.028(1)
C(11)	0.5750(1)	-0.5922(2)	0.0952(1)	0.034(1)
C(12)	0.6525(1)	-0.5417(2)	0.1116(1)	0.036(1)
C(13)	0.6846(1)	-0.5220(2)	0.2005(1)	0.035(1)
C(14)	0.6394(1)	-0.5487(2)	0.2804(1)	0.030(1)
C(15)	0.6630(1)	-0.5333(2)	0.3766(1)	0.034(1)
C(16)	0.6121(1)	-0.5662(2)	0.4461(1)	0.034(1)
C(17)	0.5356(1)	-0.6178(2)	0.4264(1)	0.031(1)

* Equivalent isotropic U defined as one third of the trace of the orthogonalized U_{ij} tensor

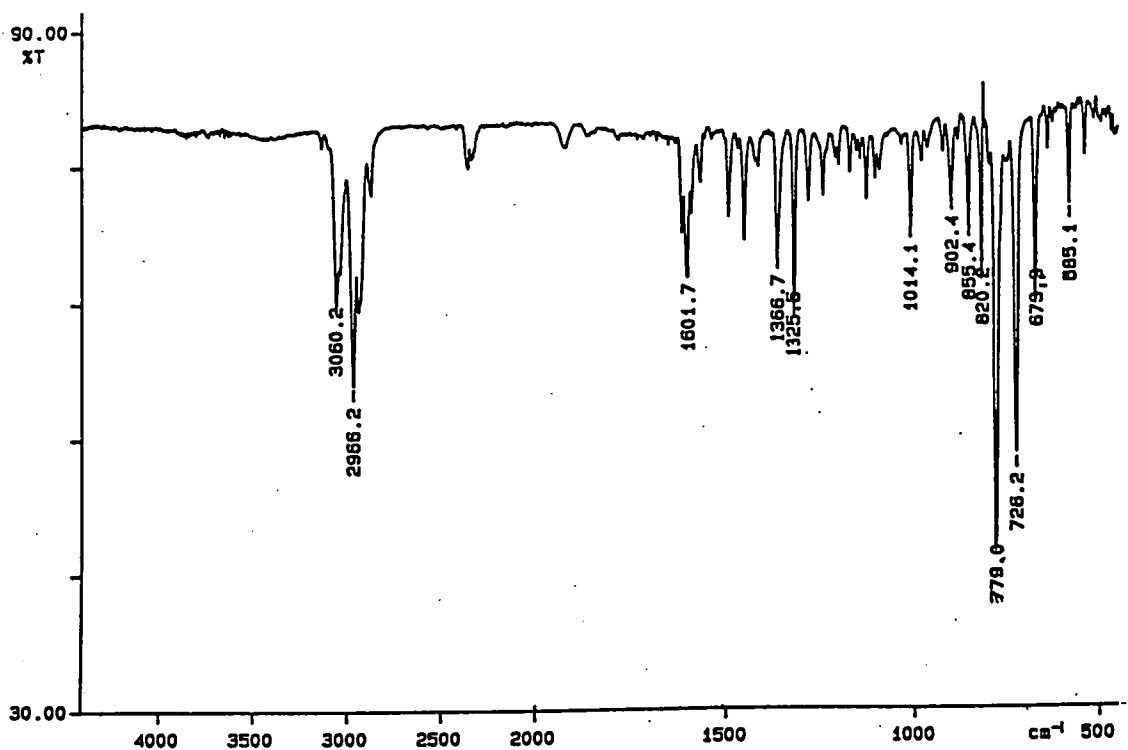
Table 5. Atom coordinates and isotropic displacement coefficients (Å²)

	x	y	z	U
H(01A)	0.0690	-0.3984	0.1260	0.043(6)
H(02A)	0.2078	-0.3132	0.1519	0.059(7)
H(03A)	0.2599	-0.2530	-0.0018	0.050(6)
H(04A)	0.1556	-0.3032	-0.1266	0.040(5)
H(05A)	0.0425	-0.1630	-0.0923	0.036(5)
H(06A)	-0.0059	-0.2161	0.0493	0.032(5)
H(07A)	0.1186	-0.4953	-0.0220	0.044(6)
H(07B)	0.0406	-0.4157	-0.0493	0.037(5)
H(011)	0.1670	0.0330	-0.1553	0.037(5)
H(012)	0.2130	0.2504	-0.0994	0.043(6)
H(013)	0.1946	0.3218	0.0542	0.041(5)
H(015)	0.1350	0.2616	0.2207	0.047(6)
H(016)	0.0705	0.1001	0.3100	0.052(6)
H(017)	0.0286	-0.1149	0.2466	0.040(5)
H(1A)	0.3333	-0.6130	0.3578	0.041(6)
H(2A)	0.3840	-0.3771	0.3152	0.046(6)
H(3A)	0.4013	-0.3713	0.1439	0.045(6)
H(4A)	0.3641	-0.6041	0.0775	0.034(5)
H(5A)	0.4472	-0.7746	0.1531	0.038(5)
H(6A)	0.4274	-0.7832	0.3092	0.029(5)
H(7A)	0.2649	-0.5997	0.2013	0.042(6)
H(7B)	0.3058	-0.7455	0.2069	0.037(5)
H(11A)	0.5541	-0.6049	0.0322	0.044(6)
H(12A)	0.6838	-0.5209	0.0584	0.029(5)
H(13A)	0.7375	-0.4889	0.2084	0.040(5)
H(15A)	0.7143	-0.4981	0.3927	0.036(5)
H(16A)	0.6295	-0.5547	0.5106	0.042(6)
H(17A)	0.5012	-0.6406	0.4763	0.034(5)

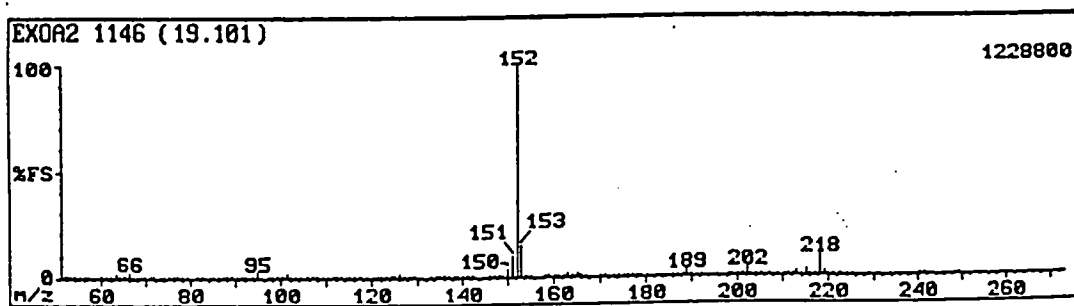


Appendix 2.7. GC trace of exo Diels-Alder adduct of acenaphthylene and cyclopentadiene

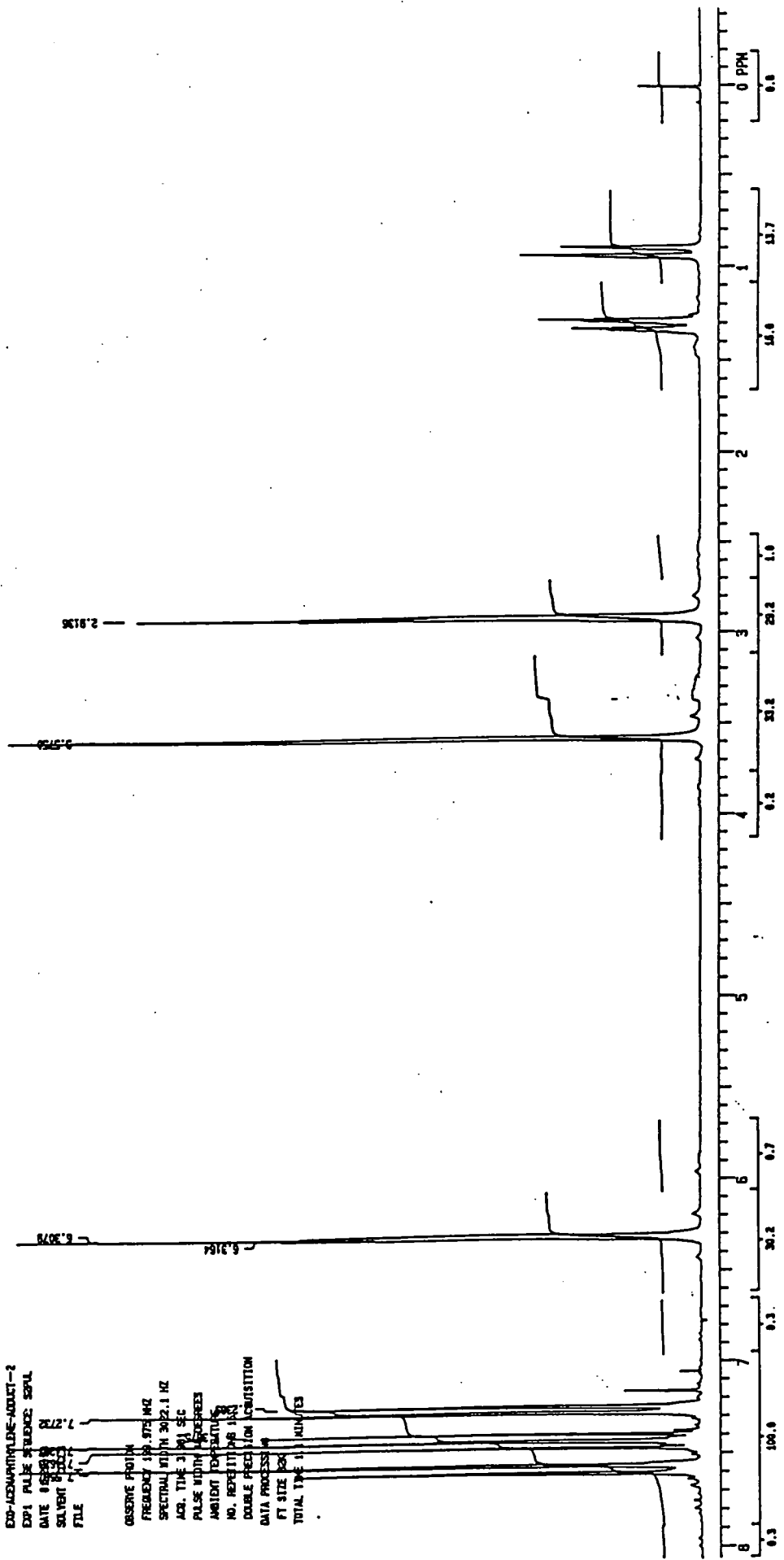
PERKIN ELMER



Appendix 2.8. Infrared spectrum of exo Diels-Alder adduct of acenaphthylene and cyclopentadiene



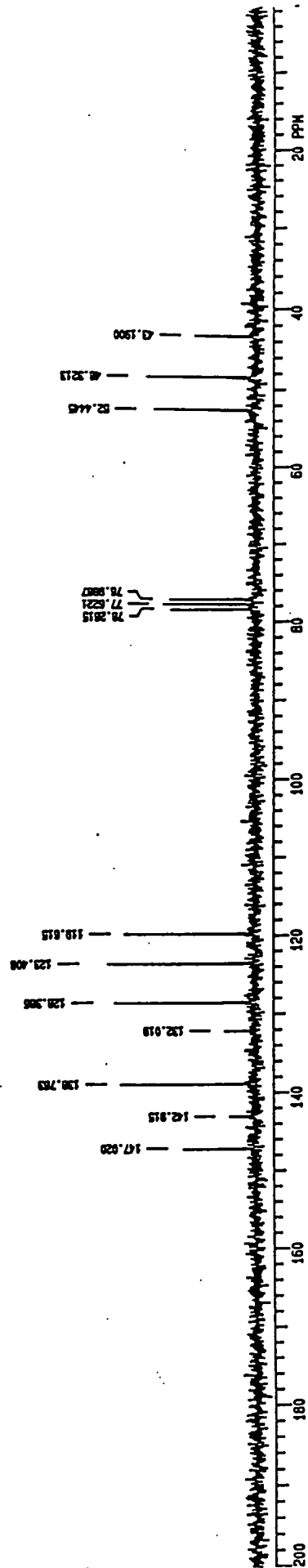
Appendix 2.9. Mass spectrum of exo Diels-Alder adduct of acenaphthylene and cyclopentadiene



Appendix 2.10. ¹H n.m.r. spectrum of exo Diels-Alder adduct of acenaphthylene and cyclopentadiene

EXO-ACENAPHTHYLENE-ADDUCT-2
EPR2 PULSE SEQUENCE: EPR1
DATE 01-20-93
SOLVENT CDCL3
FILE 6

OBSERVE CARBON
FREQUENCY 50.269 MHZ
SPECTRAL WIDTH 11025.4 HZ
ACQ. TIME 0.998 SEC
RELAXATION DELAY 1.0 SEC
PULSE WIDTH 35 DEGREES
AMBIENT TEMPERATURE
NO. REPETITIONS 16
DECUPLE PROTON
LOW POWER 20 DB
MULTI-16 MODULATED
CONTINUOUS DECOUPLING
DOUBLE PRECISION ACQUISITION
DATA PROCESSING
LINE BROUDDING 1.0 HZ
FT SIZE 32K



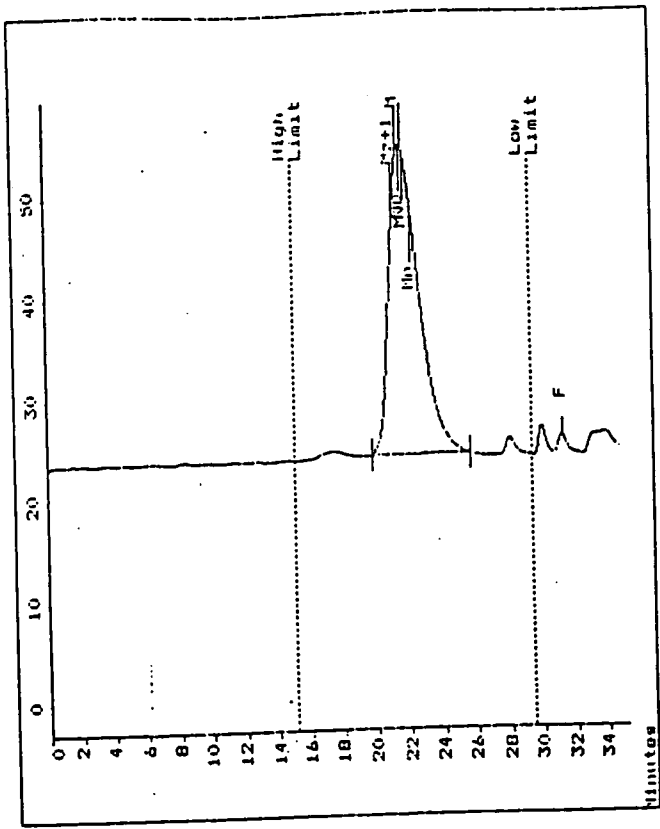
Appendix 2.11. ¹³C n.m.r. spectrum of exo Diels-Alder adduct of acenaphthylene and cyclopentadiene

APPENDIX 3

Analytical data for Chapter 3

Polymer Laboratories
 GPC Data Station Ver 4.0
 Unknown L0017.037
 Acquired GPC Data Station Ver 4.0
 Date: Fri Mar 05 1993

Concentration :
 Injection Volume :
 Solvent : TRICHLOROETHYLENE
 Column Set :
 Method : 1
 Calibration Using Narrow Standards Curve Used 3rd Order Polynomial
 Calibration Limits : 15.15 to 29.43 Mins
 Flow Rate Marker : TOLUENE found at 30.78 Mins
 Broad Peak Start : 19.83 End : 25.68 Mins
 In Standards at 31.00 Mins

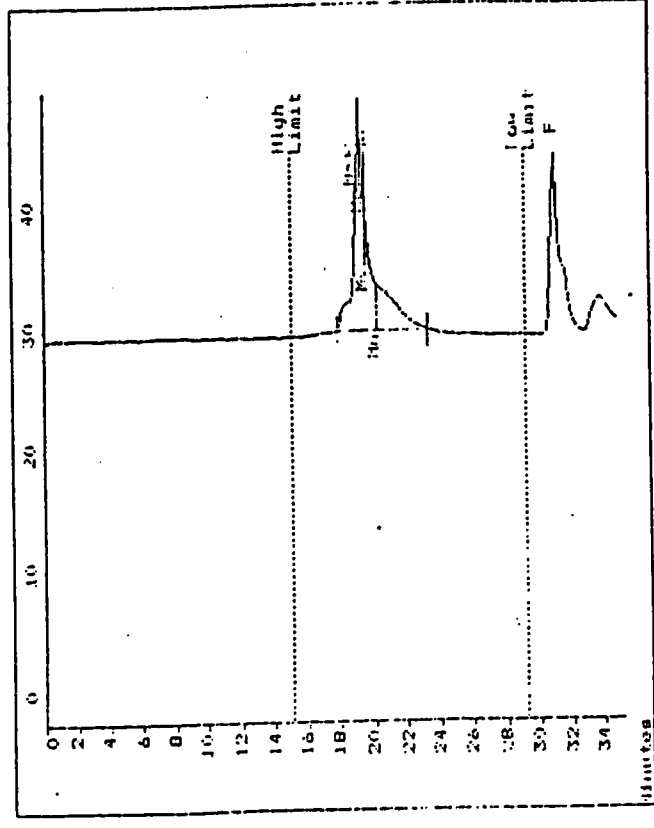


Molecular Weight Averages
 M_n = 15523.9 M_w = 15582.2
 M_v = 8482. M_z = 10937.7
 M_w = 12044.7 M_v = 11527.0
 Polydispersity = 1.420

Appendix 3.1.1. GPC trace of P3-1

Polymer Laboratories
 GPC Data Station Ver 4.0
 Unknown L0043.011
 Acquired GPC Data Station Ver 4.0
 Date: Fri Jun 18 1993

Concentration :
 Injection Volume :
 Solvent : TRICHLOROETHYLENE
 Column Set :
 Method : 1
 Calibration Using Narrow Standards Curve Used 3rd Order Polynomial
 Calibration Limits : 15.13 to 29.17 Mins
 Flow Rate Marker : TOLUENE found at 31.05 Mins
 Broad Peak Start : 17.83 End : 23.57 Mins
 In Standards at 31.00 Mins



Molecular Weight Averages
 M_n = 69627.8 M_w = 73015.2
 M_v = 32144.0 M_z = 88315.5
 M_w = 54604.1 M_v = 51582.1
 Polydispersity = 1.099

Appendix 3.1.2. GPC trace of P3-2

Polymer Laboratories
GPC Data Station Ver 4.0

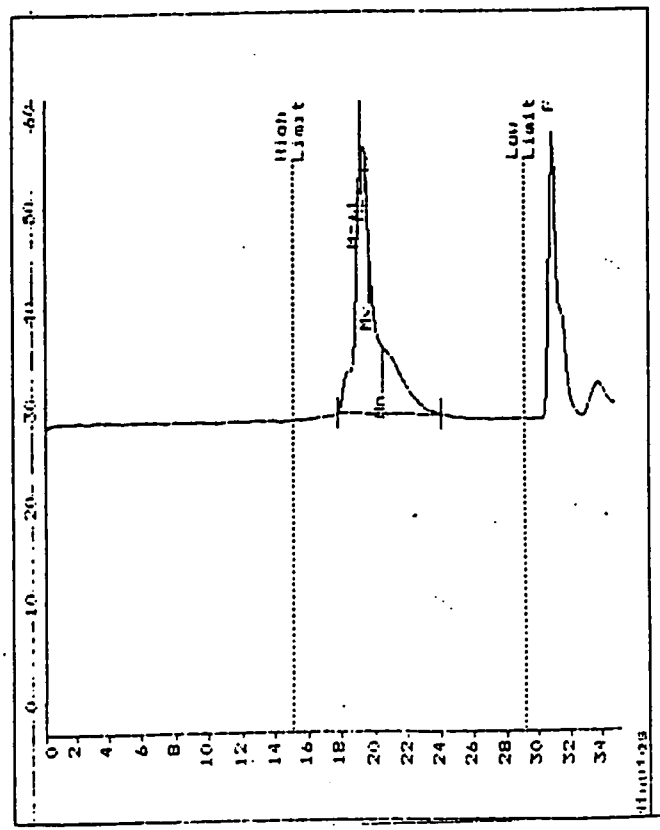
16155 Thu Jun 17 1993

Unknown U0033.009 acquired GPC Data Station Ver 4.0

Concentration :
Injection Volume :
Solvent : TRICHLOROETHANE
Column Set :
Method : 1
Detector :
Temperature :
Flow Rate :
Standards :

Calibration Using Narrow Standards Curve Used 3rd Order Polynomial
Calibration Limits 15.13 to 29.15 Mins

Flow Rate Marker : TOLUENE found at 31.05Mins
in Standards at 30.98Mins
Flow Peak Start : 17.82 End : 24.12 Mins



Molecular Weight Averages
Mn = 56456.6 Mz = 70671.2
Mw = 27315.5 Mz+1 = 87287.2
Mv = 31036.4 Mv = 45588.5
Polydispersity = 1.855

Appendix 3.1.4. GPC trace of P3-4

Polymer Laboratories
GPC Data Station Ver 4.0

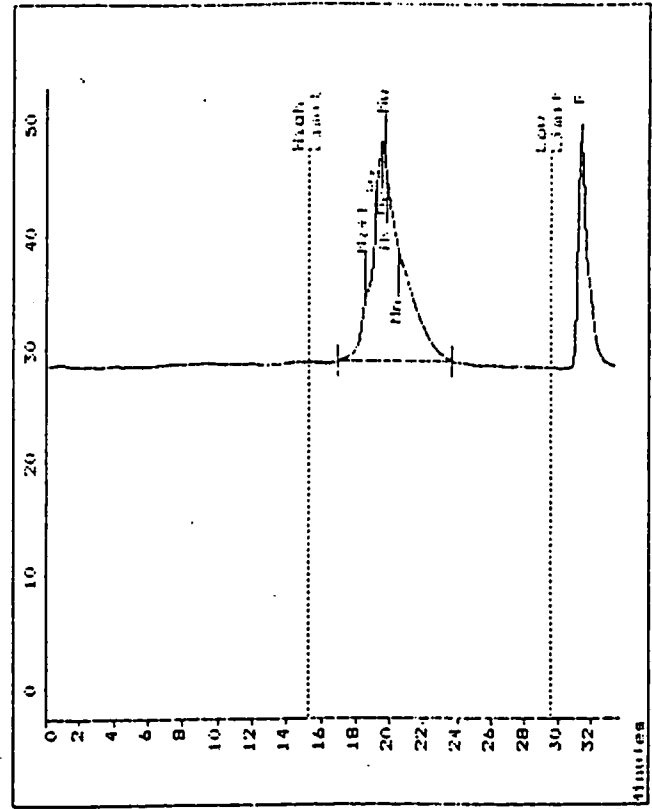
16155 Fri Jun 11 1993

Unknown U0032.005 acquired GPC Data Station Ver 4.0

Concentration :
Injection Volume :
Solvent : TRICHLOROETHANE
Column Set :
Method : 1
Detector :
Temperature :
Flow Rate :
Standards :

Calibration Using Narrow Standards Curve Used 3rd Order Polynomial
Calibration Limits 15.33 to 29.45 Mins

Flow Rate Marker : TOLUENE found at 31.05Mins
in Standards at 31.03Mins
Flow Peak Start : 17.00 End : 23.68 Mins

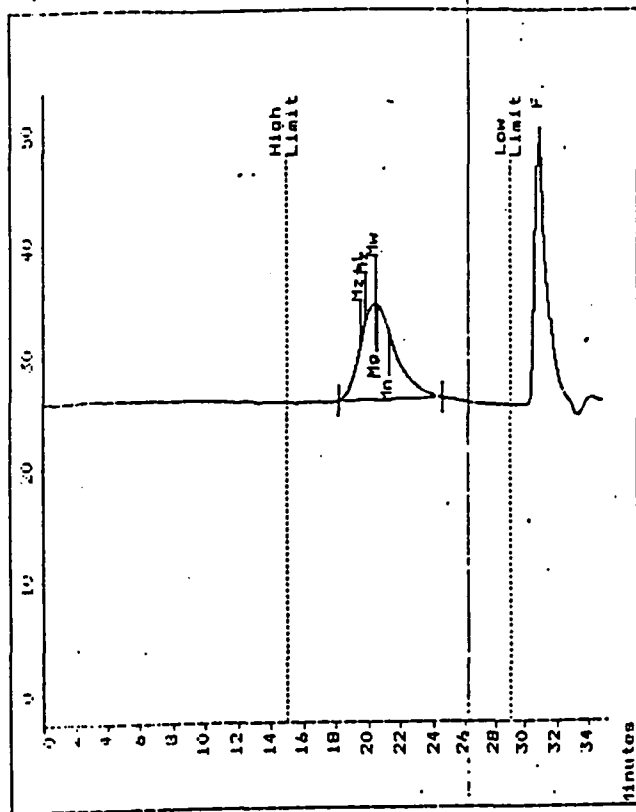


Molecular Weight Averages
Mn = 67436.7 Mz = 91146.0
Mw = 32077.4 Mz+1 = 141187.5
Mv = 57076.6 Mv = 82949.8
Polydispersity = 1.779

Appendix 3.1.3. GPC trace of P3-3

Polymer Laboratories
 GPC Data Station Ver 4.0
 16:38 Fri Aug 13 1993
 Unknown LC038.044 acquired GPC Data Station Ver 4.0

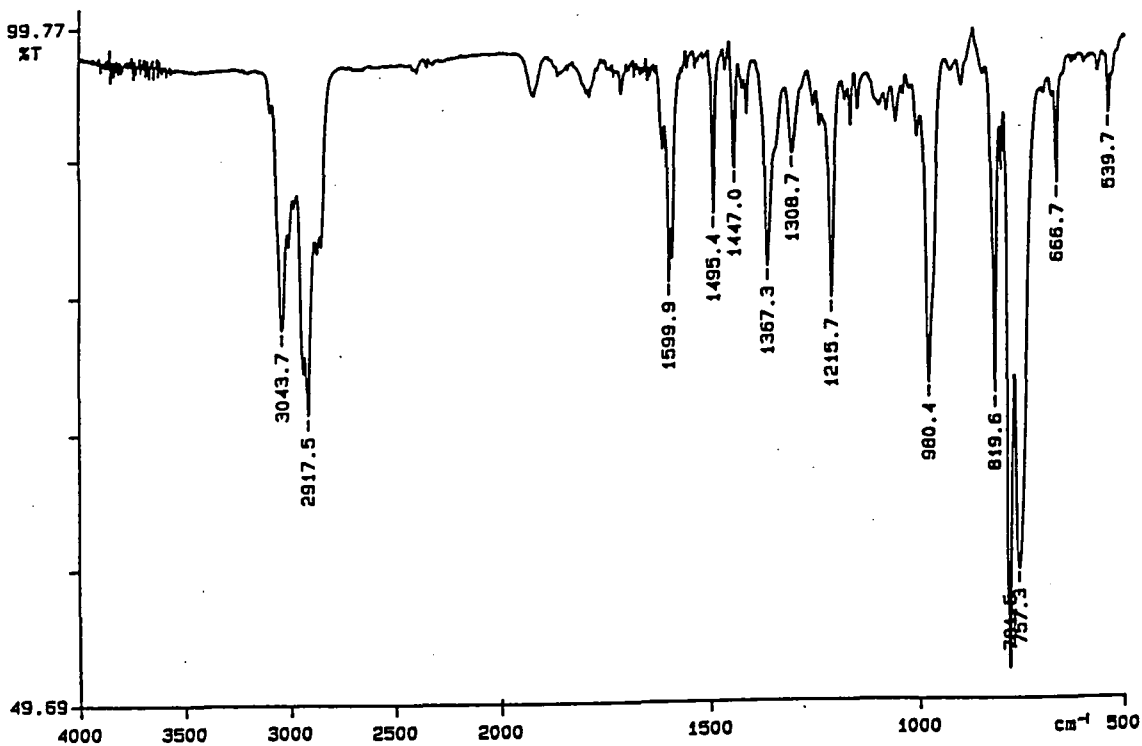
Concentration :
 Injection Volume :
 Solvent : TRICHLOROMETHANE
 Column Set :
 Detector :
 Temperature :
 Flow Rate :
 Standards :
 Method : 1
 Calibration Using Narrow Standards Curve Used 3rd Order Polynomial
 Calibration Limits 15.08 to 29.08 Mins
 Flow Rate Marker : TOLUENE found at 31.03Mins
 in Standards at 30.90Mins
 Broad Peak Start : 18.27 End : 24.47 Mins



Molecular Weight Averages
 Mo = 26003.0 Mz = 38872.7
 Mn = 14720.9 Mz+1 = 52244.0
 Mw = 25637.3 Mw = 24079.4
 Polydispersity = 1.755

Appendix 3.1.5. GPC trace of P3-6

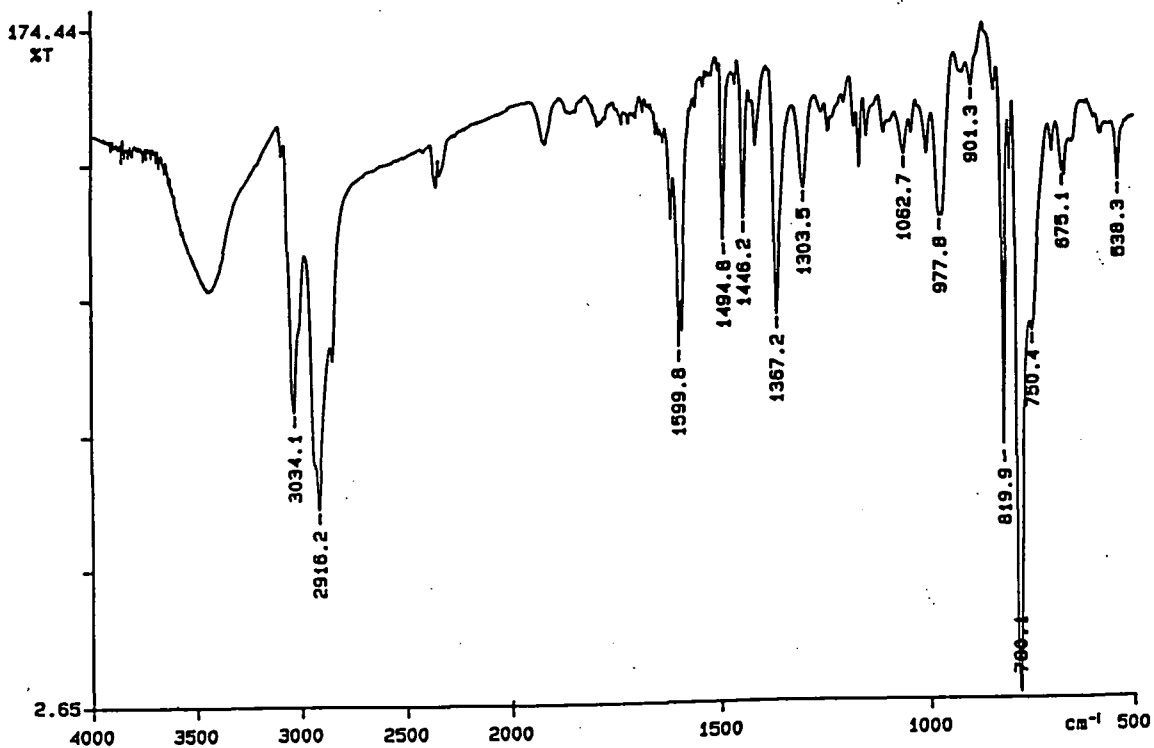
PERKIN ELMER



93/08/04 12:35
X: 16 scans, 4.0 cm^{-1} .

Appendix 3.2.1. Infrared spectrum of P3-3

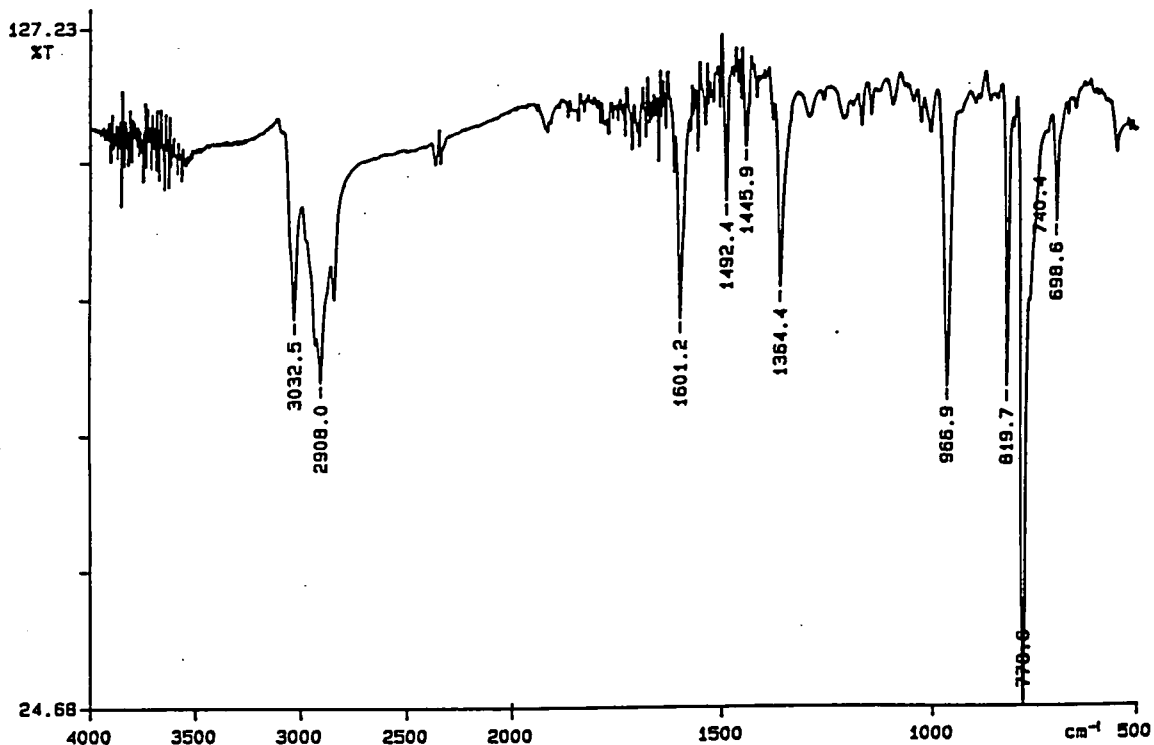
PERKIN ELMER



93/08/11 10:46
X: 16 scans, 4.0 cm^{-1} , flat

Appendix 3.2.2. Infrared spectrum of P3-6

PERKIN ELMER

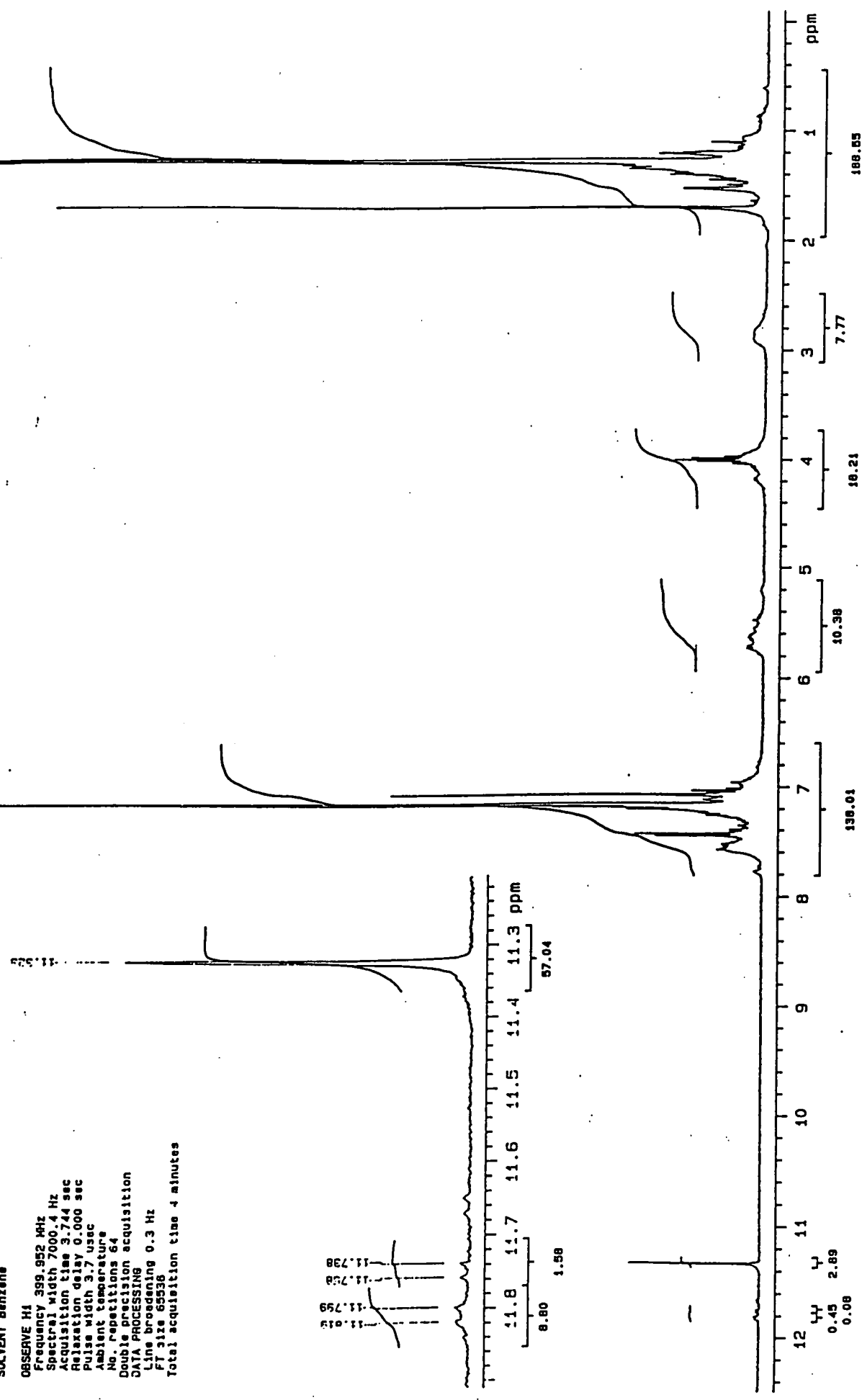


93/08/05 09:07
X: 16 scans, 4.0cm-1, flat
s-22-4 after acetone-wash

Appendix 3.2.3. Infrared spectrum of P3-7

FILE /data/cvrdat/kse12j01a.fid
 RUN ON JUL 12 93
 SOLVENT Benzene

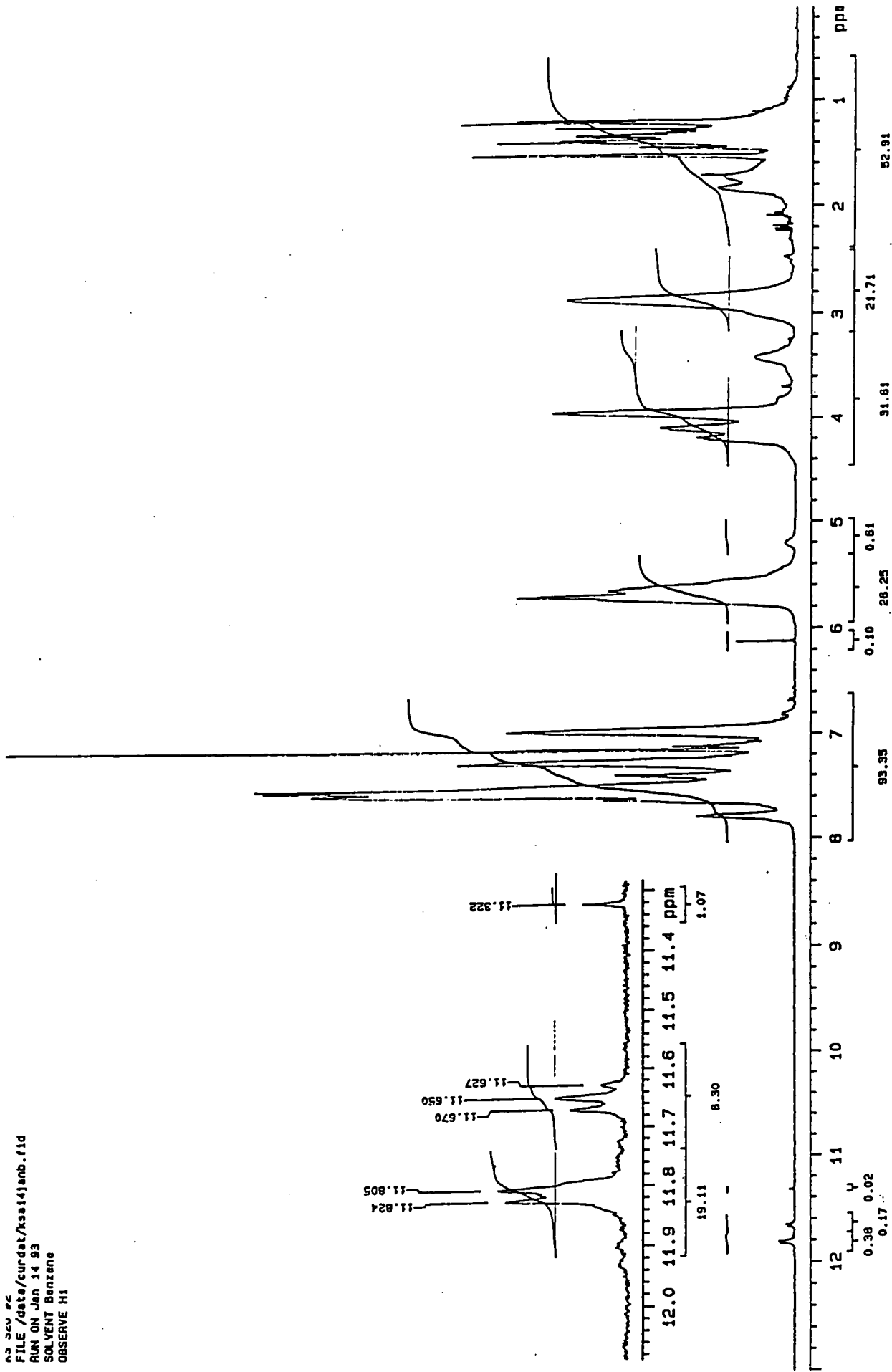
OBSERVE H1
 Frequency 399.952 MHz
 Spectral width 7000.4 Hz
 Acquisition time 3.744 sec
 Relaxation delay 0.000 sec
 Pulse width 3.7 usec
 Ambient temperature
 No. repetitions 64
 Double precision acquisition
 DATA PROCESSING
 Line broadening 0.3 Hz
 FI size 65536
 Total acquisition time 4 minutes



Appendix 3.3.1. 1H n.m.r. spectrum of the reaction mixture

(reaction of the endo-adduct with t-butoxy molybdenum initiator in 1:1 molar ratio)

n3 sev #2
 FILE /data/curdat/kas14jamb.fid
 RUN ON Jan 14 93
 SOLVENT Benzene
 OBSERVE H1

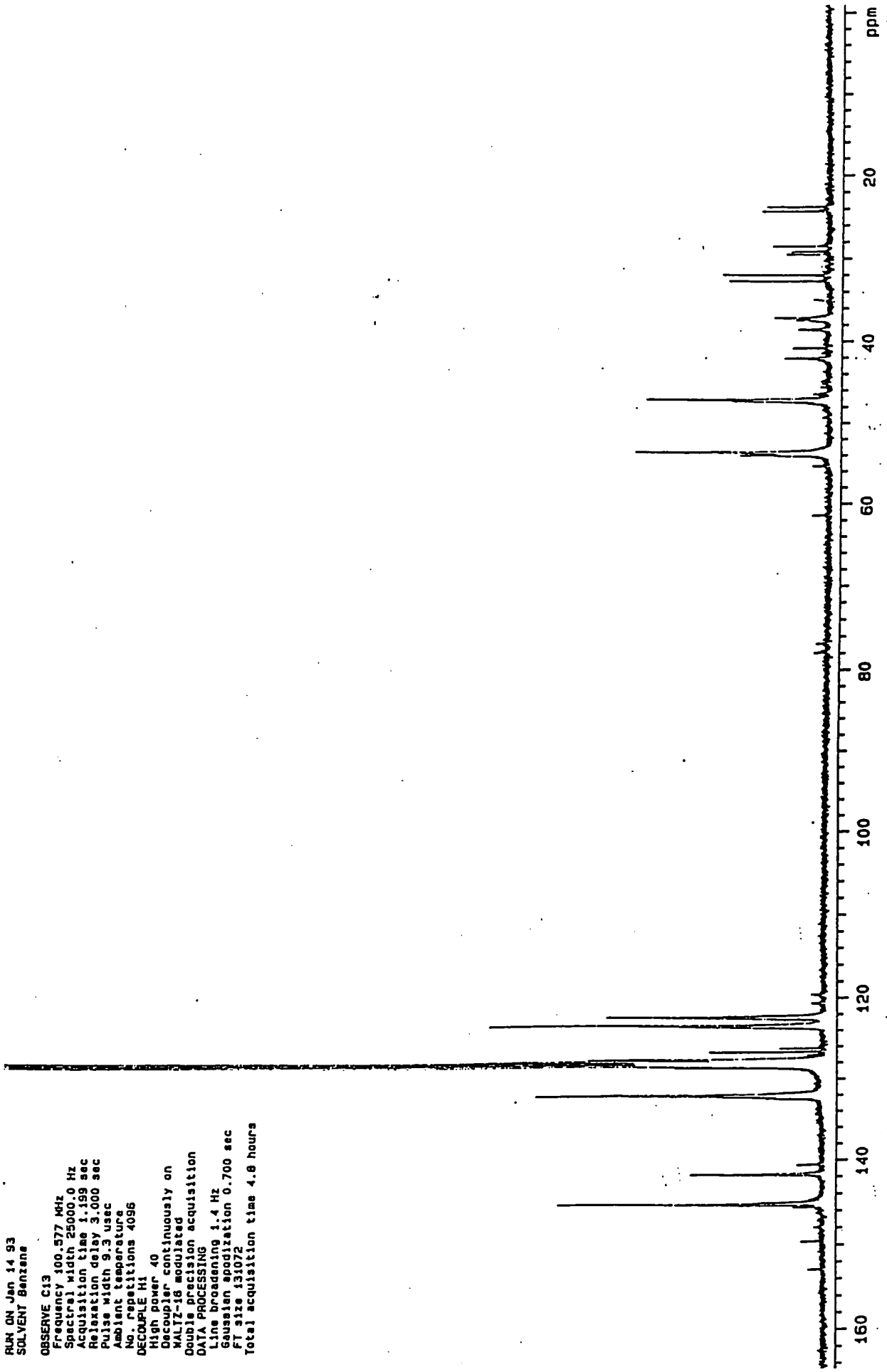


Appendix 3.3.2.a ¹H n.m.r. spectrum of P3-1 (living polymer)

RUN ON Jan 14 93
SOLVENT Benzene

OBSERVE C13

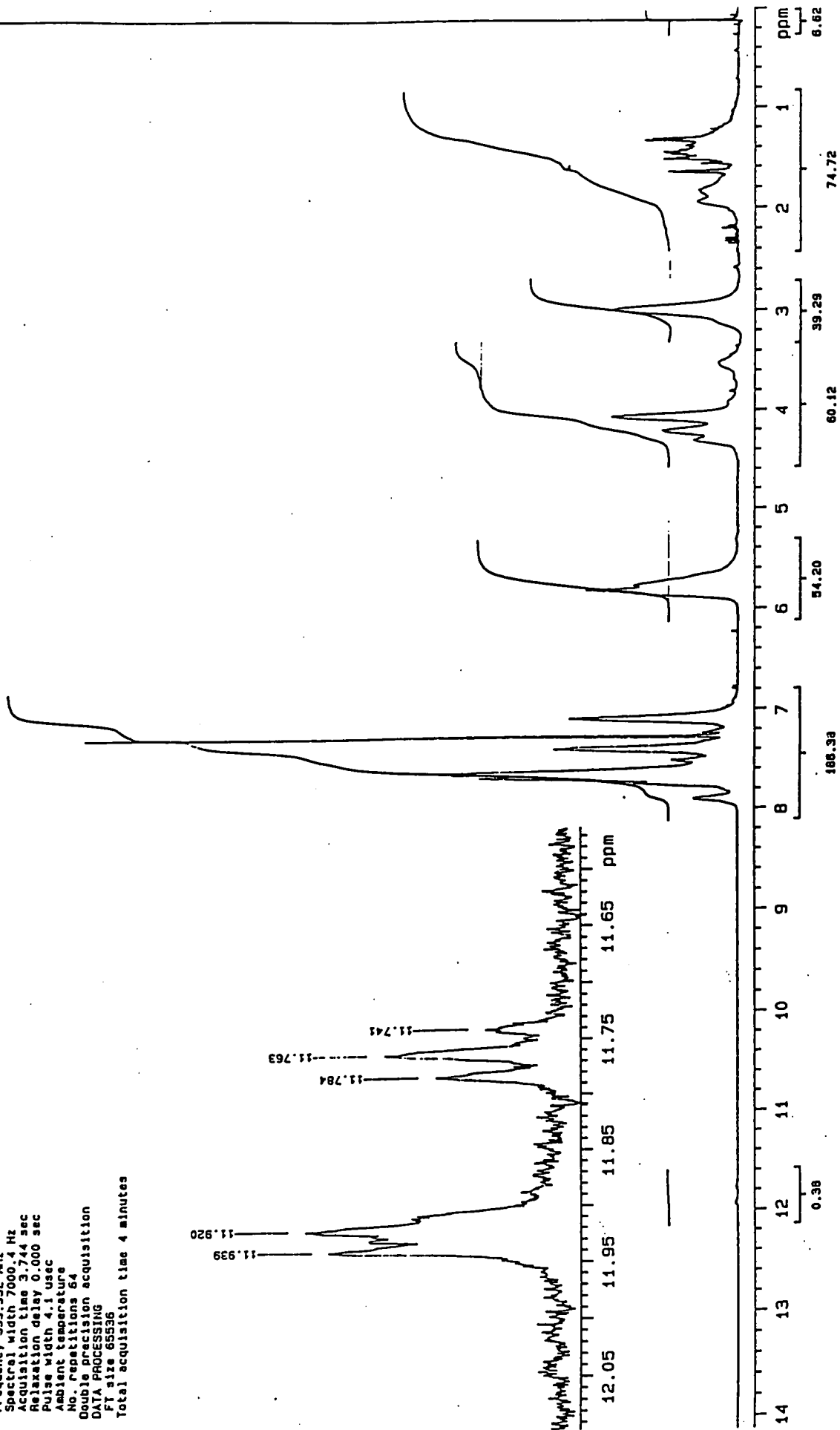
Frequency 100.577 MHz
Spectral width 25000.0 Hz
Acquisition time 1.199 sec
Relaxation delay 3.000 sec
Pulse width 9.3 usec
Ambient temperature
No. repetitions 4096
DECUPLE H1
High power 40
Decoupler continuously on
WALTZ-16 modulated
Double precision acquisition
DATA PROCESSING
Line broadening 1.4 Hz
Gaussian apodization 0.700 sec
FT size 131072
Total acquisition time 4.8 hours



Appendix 3.3.2.b ¹³C n.m.r. spectrum of P3-1 (living polymer)

KS S24 41
FILE /data/curdatt/ksa26fabb.f1d
RUN ON Feb 26 93
SOLVENT Benzene

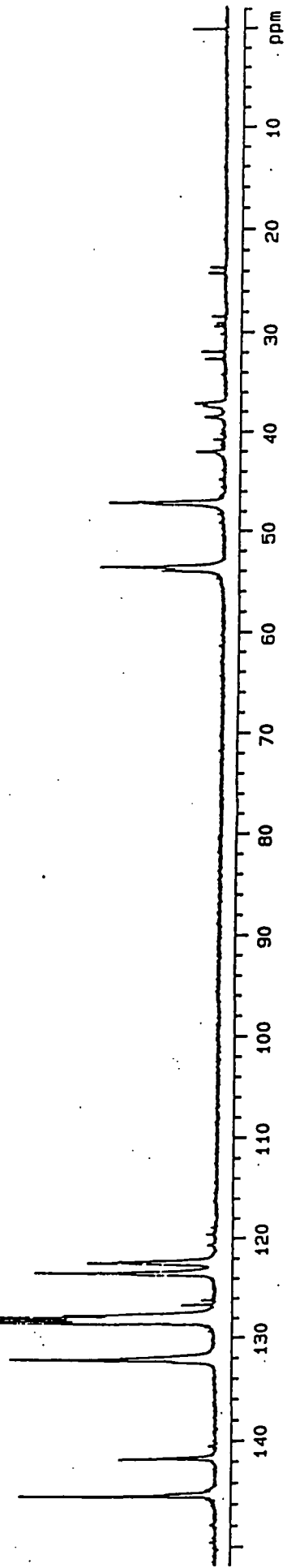
OBSERVE H1
Frequency 399.952 MHz
Spectral width 7000.4 Hz
Acquisition time 3.744 sec
Relaxation delay 0.000 sec
Pulse width 4.1 usec
Ambient temperature
No. repetitions 64
Double precision acquisition
DATA PROCESSING
F1 size 65536
Total acquisition time 4 minutes



Appendix 3.3.3.a ^1H n.m.r. spectrum of P3-2 (living polymer)

FILE /data/curdatt/kss26fabd.fid
RUN ON Feb 26 93
SOLVENT Benzene

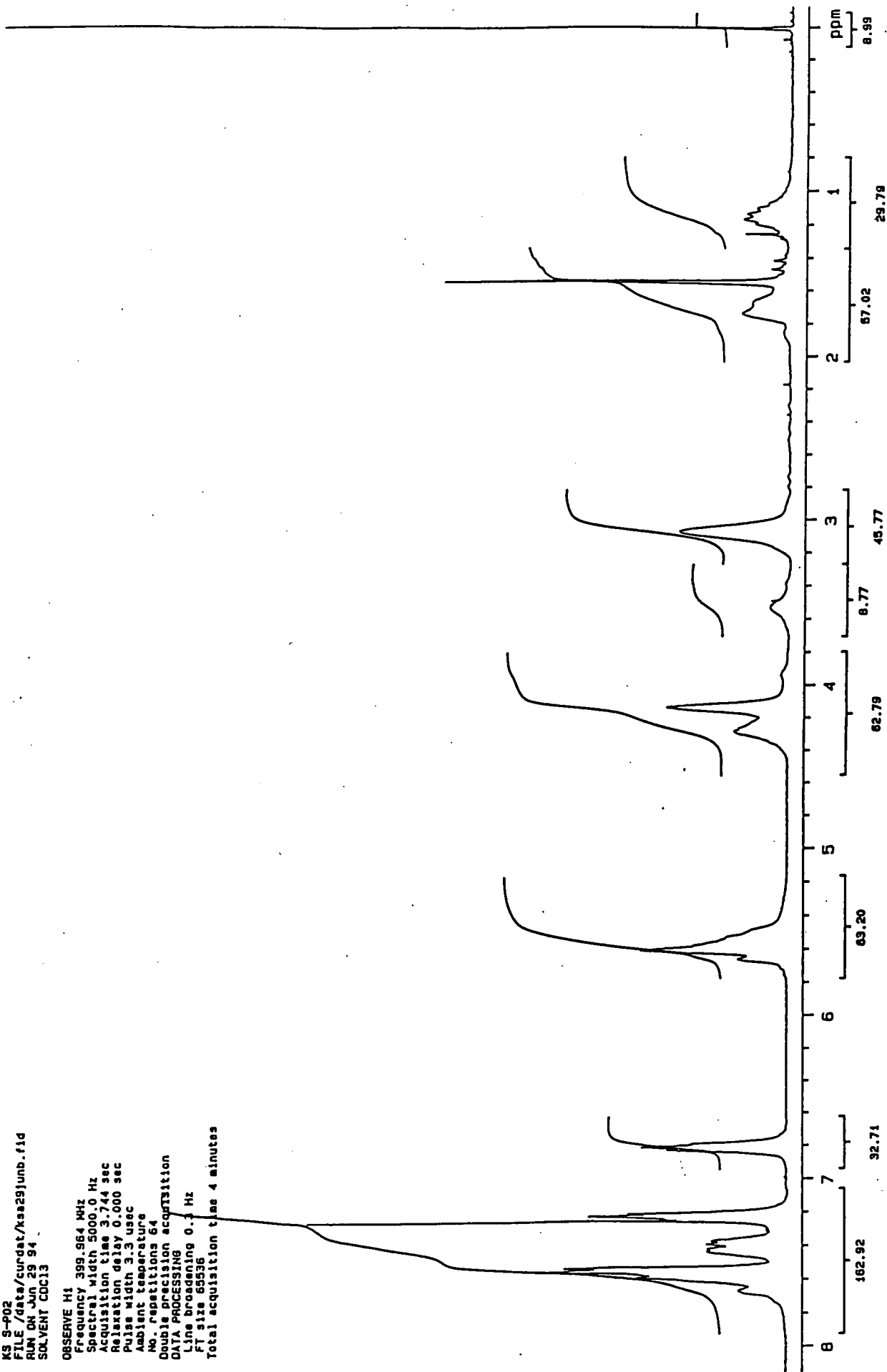
OBSERVE C13
Frequency 100.577 MHz
Spectral width 25000.0 Hz
Acquisition time 1.199 sec
Relaxation delay 3.000 sec
Pulse width 9.3 usec
Ambient temperature
No. repetitions 4096
DECOUPLE H1
High power 40
Decoupler continuously on
MALTZ-16 modulated
Double precision acquisition
DATA PROCESSING
Line broadening 1.7 Hz
Gaussian apodization 0.600 sec
FT size 131072
Total acquisition time 4.8 hours



Appendix 3.3.3.b ¹³C n.m.r. spectrum of P3-2 (living polymer)

K3 S-902
FILE /data/curdat/ksa29jmb.fid
RUN ON JUN 29 94
SOLVENT CCl3

OBSERVE H1
Frequency 399.964 MHz
Spectral width 5000.0 Hz
Acquisition time 3.744 sec
Relaxation delay 0.000 sec
Pulse width 3.3 usec
Ambient temperature
No. repetitions 64
Double precision acquisition
DATA PROCESSING
Line broadening 0.3 Hz
FT size 65536
Total acquisition time 4 minutes

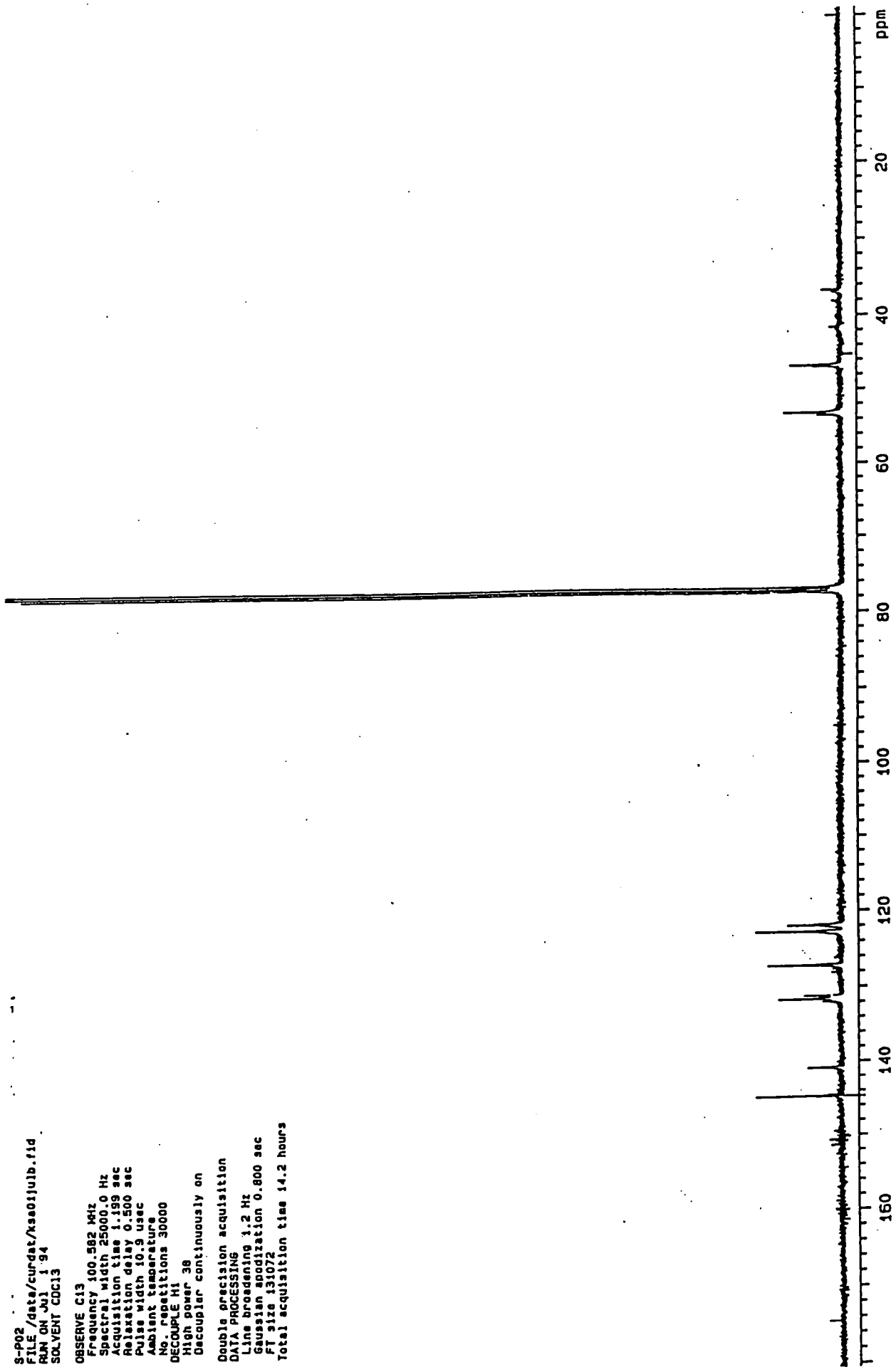


Appendix 3.3.3.c 1H n.m.r. spectrum of P3-2 (end-capped polymer)

S-P02
FILE /data/curdat/vsa01julb.f1d
RAN ON Jul 1 94
SOLVENT CCl3

OBSERVE C13
Frequency 100.582 MHz
Spectral width 25000.0 Hz
Acquisition time 1.199 sec
Relaxation delay 0.500 sec
Pulse width 10.9 usec
Ambient temperature
No. repetitions 30000
DECOUPLE H1
High power 38
Decoupler continuously on

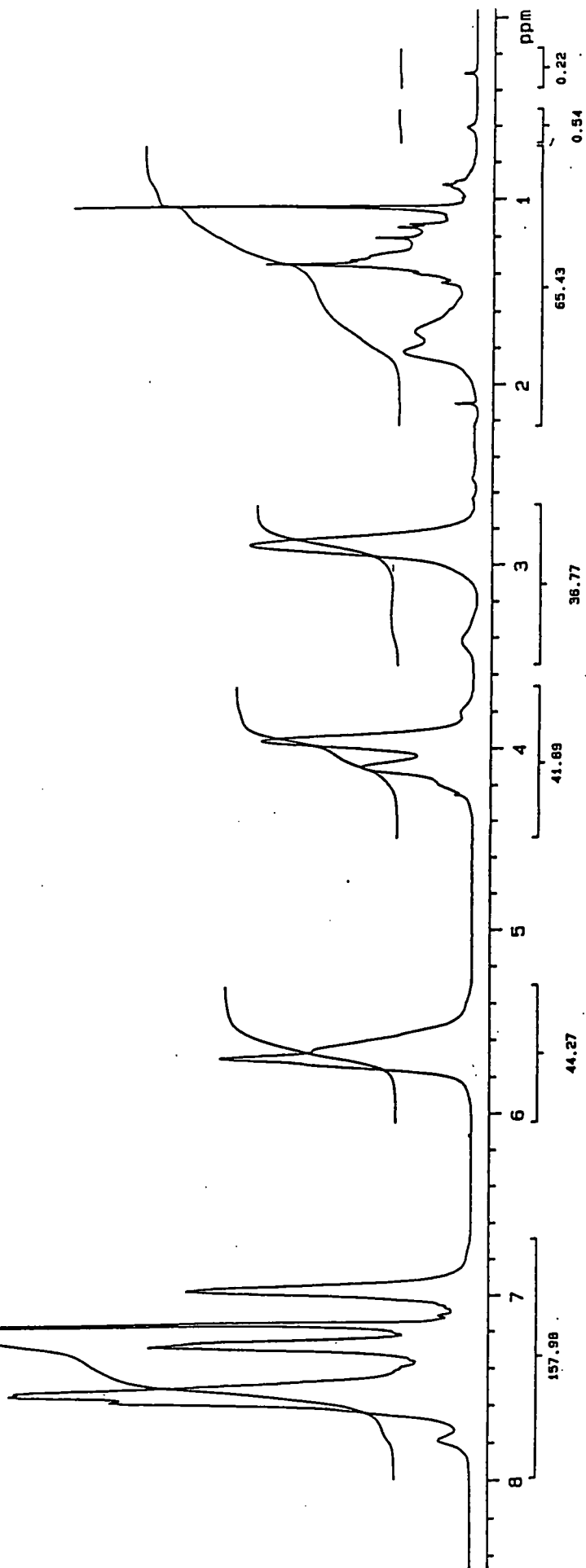
Double precision acquisition
DATA PROCESSING
Line broadening 1.2 Hz
Gaussian smodization 0.800 sec
FT size 131072
Total acquisition time 14.2 hours



Appendix 3.3.3.d 13C n.m.r. spectrum of P3-2 (end-capped polymer)

KS 926-2
FILE /date/cundat/ks03jmb.f1d
RUN ON Jun 3 93
SOLVENT Benzene

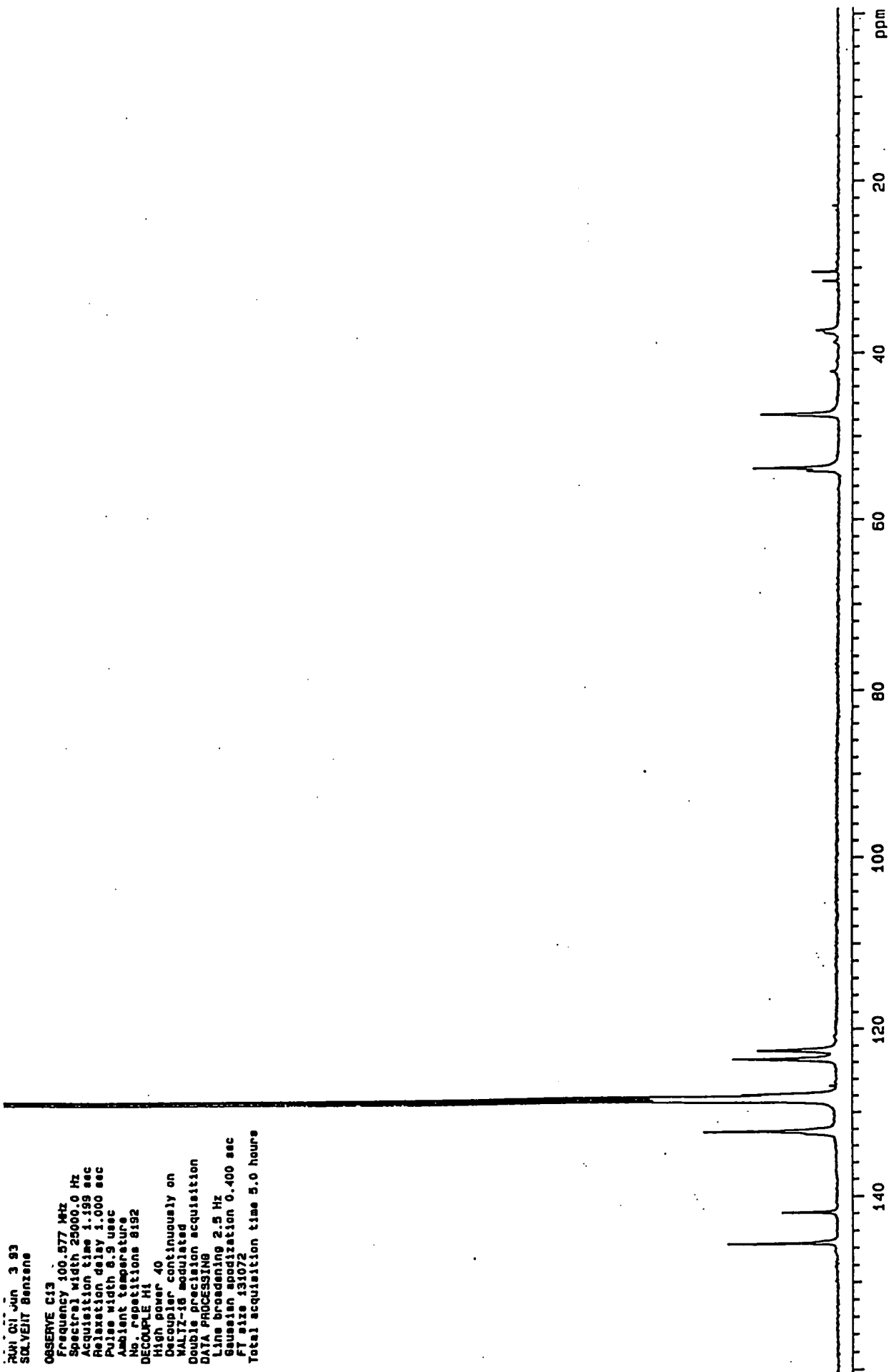
OBSERVE H1
Frequency 399.952 MHz
Spectral width 5000.0 Hz
Acquisition time 3.744 sec
Relaxation delay 0.000 sec
Pulse width 3.7 usec
Ambient temperature
No. repetitions 64
Double precision acquisition
DATA PROCESSING
Line broadening 0.7 Hz
Gaussian smodization 1.500 sec
FT size 65536
Total acquisition time 4 minutes



Appendix 3.3.4.a ^1H n.m.r. spectrum of P3-3 (living polymer)

RUN 01 JUN 3 93
SOLVENT Benzene

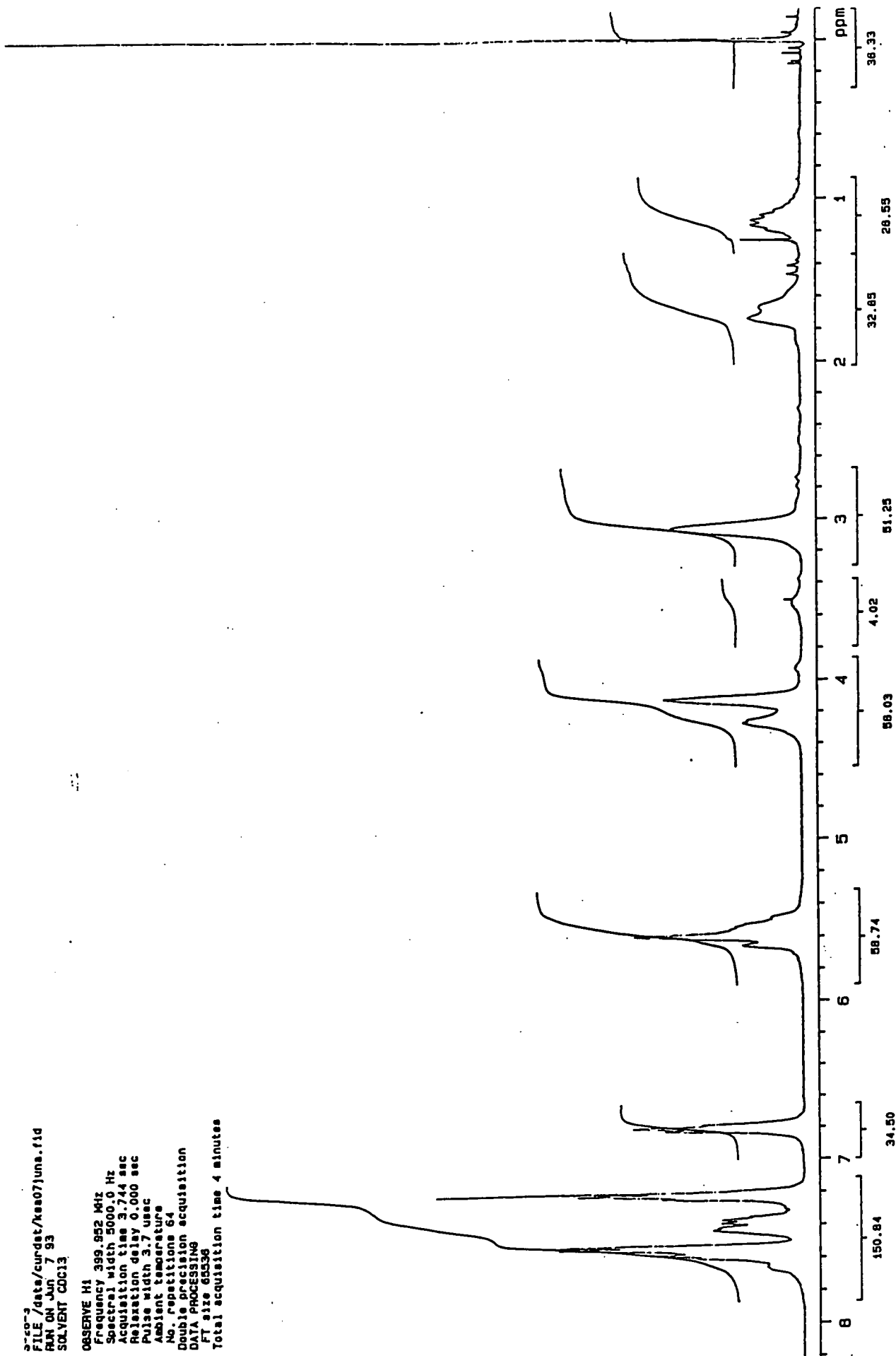
OBSERVE C13
Frequency 100.627 MHz
Spectral width 25000.0 Hz
Acquisition time 1.195 sec
Relaxation delay 1.000 sec
Pulse width 6.9 usec
Ambient temperature
No. repetitions 8192
DECOUPLE H1
High power 40
Decoupler continuously on
WALTZ-16 modulated
Double precision acquisition
DATA PROCESSING
Line broadening 2.5 Hz
Gaussian apodization 0.400 sec
FT size 131072
Total acquisition time 5.0 hours



Appendix 3.3.4.b 13C n.m.r. spectrum of P3-3 (living polymer)

3-co-3
FILE /data/curdet/ks07juna.fid
RUN ON Jun 7 93
SOLVENT C0C13

OBSERVE H1
Frequency 399.952 MHz
Spectral width 5000.0 Hz
Acquisition time 3.744 sec
Relaxation delay 6.000 sec
Pulse width 3.7 usec
Ambient temperature
No. repetitions 64
Double precision acquisition
DATA PROCESSING
FT size 65536
Total acquisition time 4 minutes

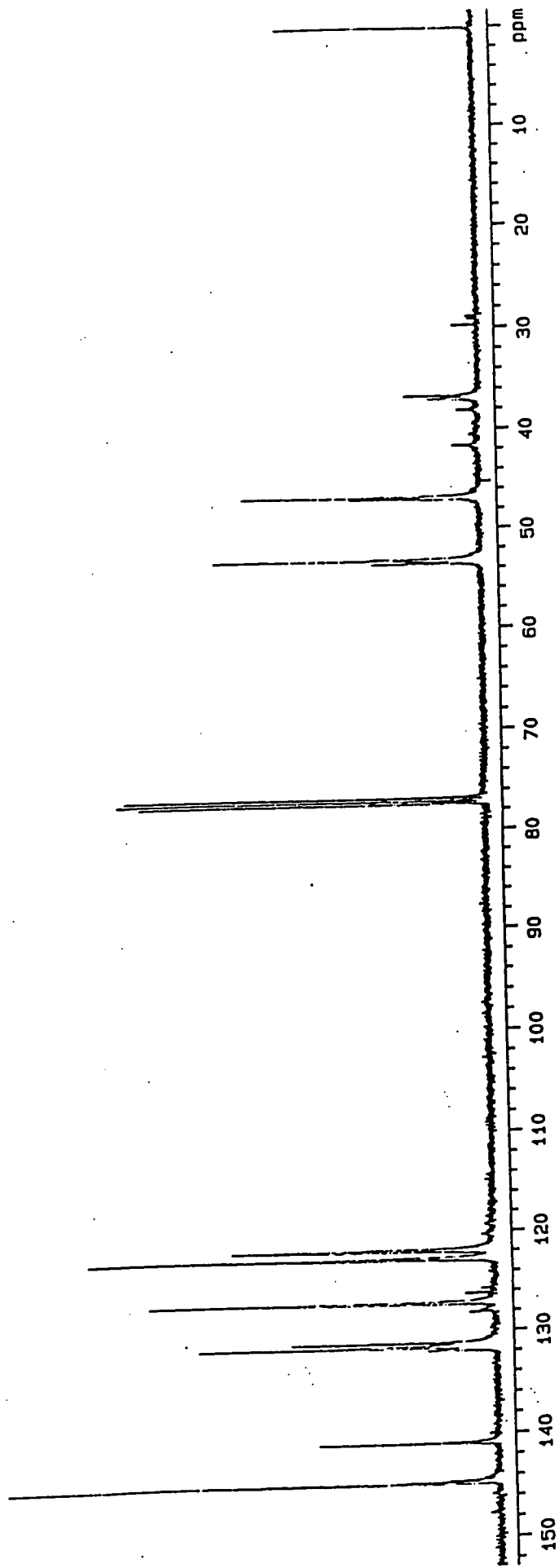


Appendix 3.3.4.c 1H n.m.r. spectrum of P3-3 (end-capped polymer)

8-26-3
FILE /data/curdat/ksa07junb.fid
RUN ON JUN 7 93
SOLVENT CDCl3

OBSERVE C13

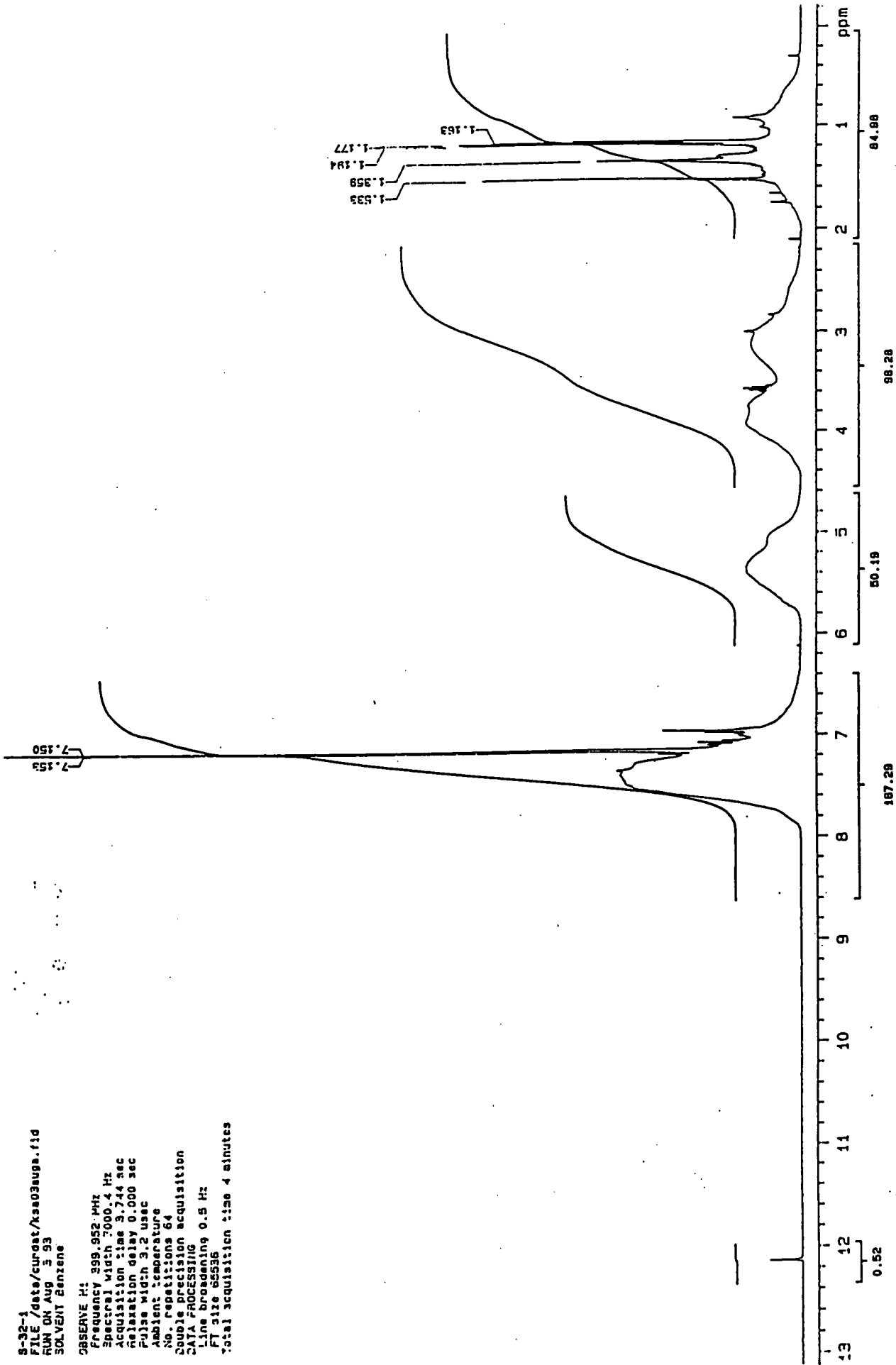
Frequency 100.577 MHz
Spectral width 25000.0 Hz
Acquisition time 1.159 sec
Relaxation delay 1.000 sec
Pulse width 9.9 usec
Ambient temperature
No. repetitions 5000
DECOUPLE H1
High power 40
Decoupler continuously on
WALTZ-16 modulated
Double precision acquisition
DATA PROCESSING
Line broadening 1.2 Hz
Gaussian apodization 0.800 sec
F1 size 131072
Total acquisition time 3.1 hours



Appendix 3.3.4.d ¹³C n.m.r. spectrum of P3-3 (end-capped polymer)

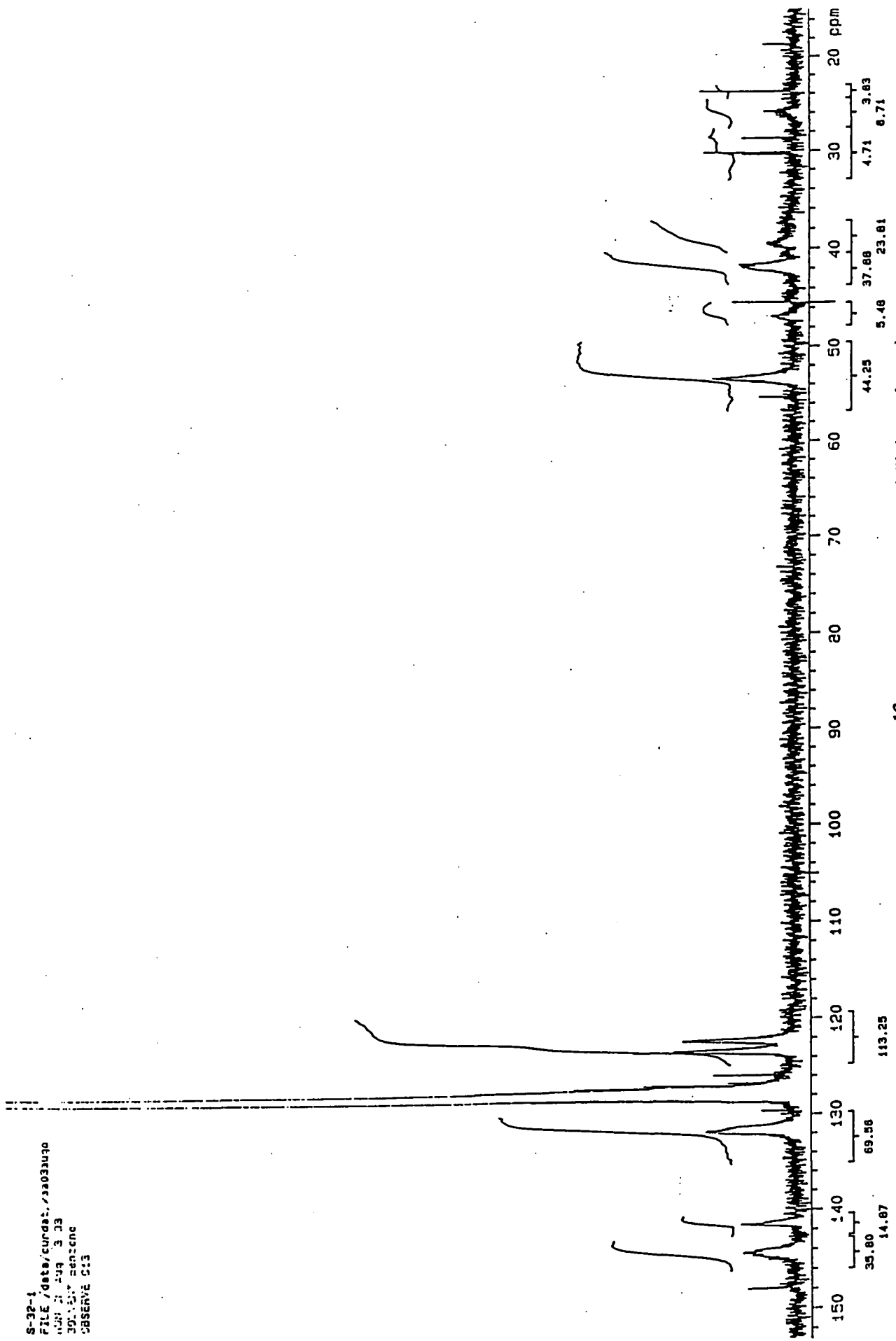
8-32-1
FILE /data/cupdat/ksa03augb.fid
RUN ON Aug 5 93
SOLVENT Benzene

OBSERVE H:
Frequency 399.952 MHz
Spectral width 7000.4 Hz
Acquisition time 3.744 sec
Relaxation delay 0.000 sec
Pulse width 3.2 usec
Ambient temperature
No. repetitions 64
Double precision acquisition
DATA PROCESSING
Line broadening 0.5 Hz
F1 size 85536
Total acquisition time 4 minutes



Appendix 3.3.5.a ¹H n.m.r. spectrum of P3-6 (living polymer)

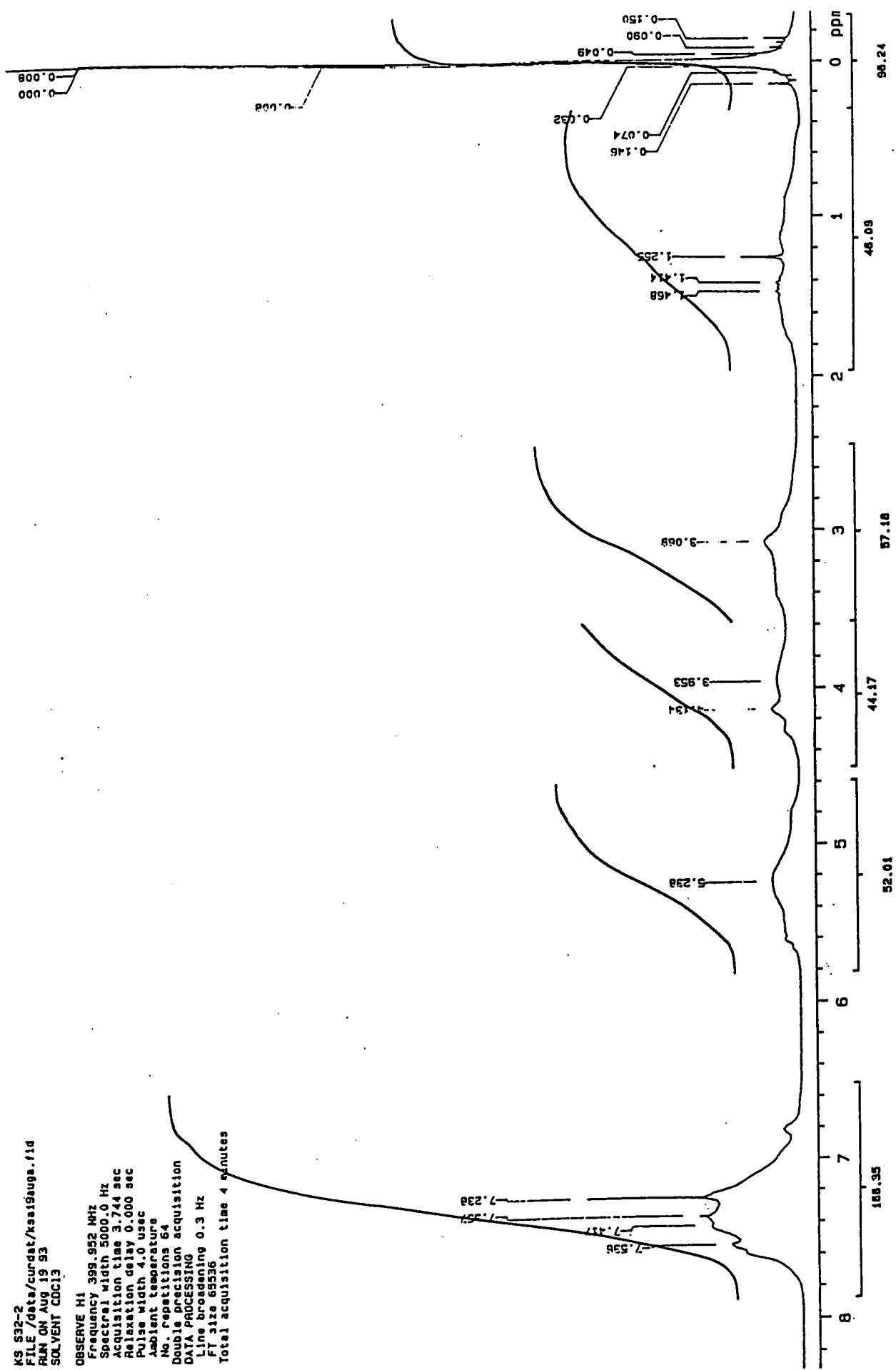
S-32-1
FILE /data/curdat./j3a03a9a
MAY 21 199 3 33
30.137 BENZENE
OBSERVE C13



Appendix 3.3.5.b ^{13}C n.m.r. spectrum of P3-6 (living polymer)

KS 532-2
 FILE /data/curdat/ksa19aug.11d
 RUN ON Aug 19 93
 SOLVENT CDCl3

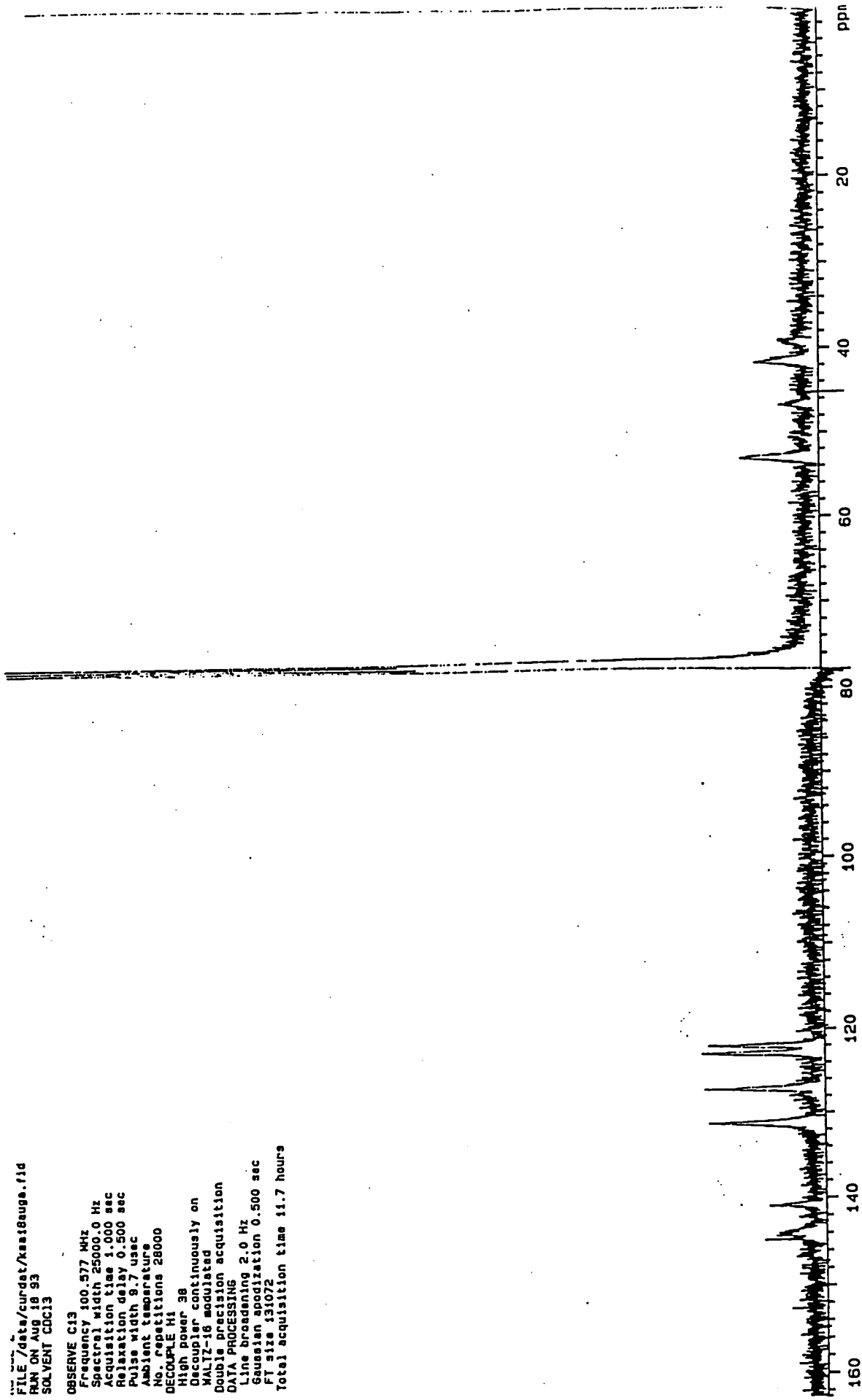
OBSERVE H1
 Frequency 399.952 MHz
 Spectral width 5000.0 Hz
 Acquisition time 3.744 sec
 Relaxation delay 0.000 sec
 Pulse width 4.0 usec
 Ambient temperature
 No. repetitions 64
 Double precision acquisition
 DATA PROCESSING
 Line broadening 0.3 Hz
 FI size 65536
 Total acquisition time 4 minutes



Appendix 3.3.5.c 1H n.m.r. spectrum of P3-6 (end-capped polymer)

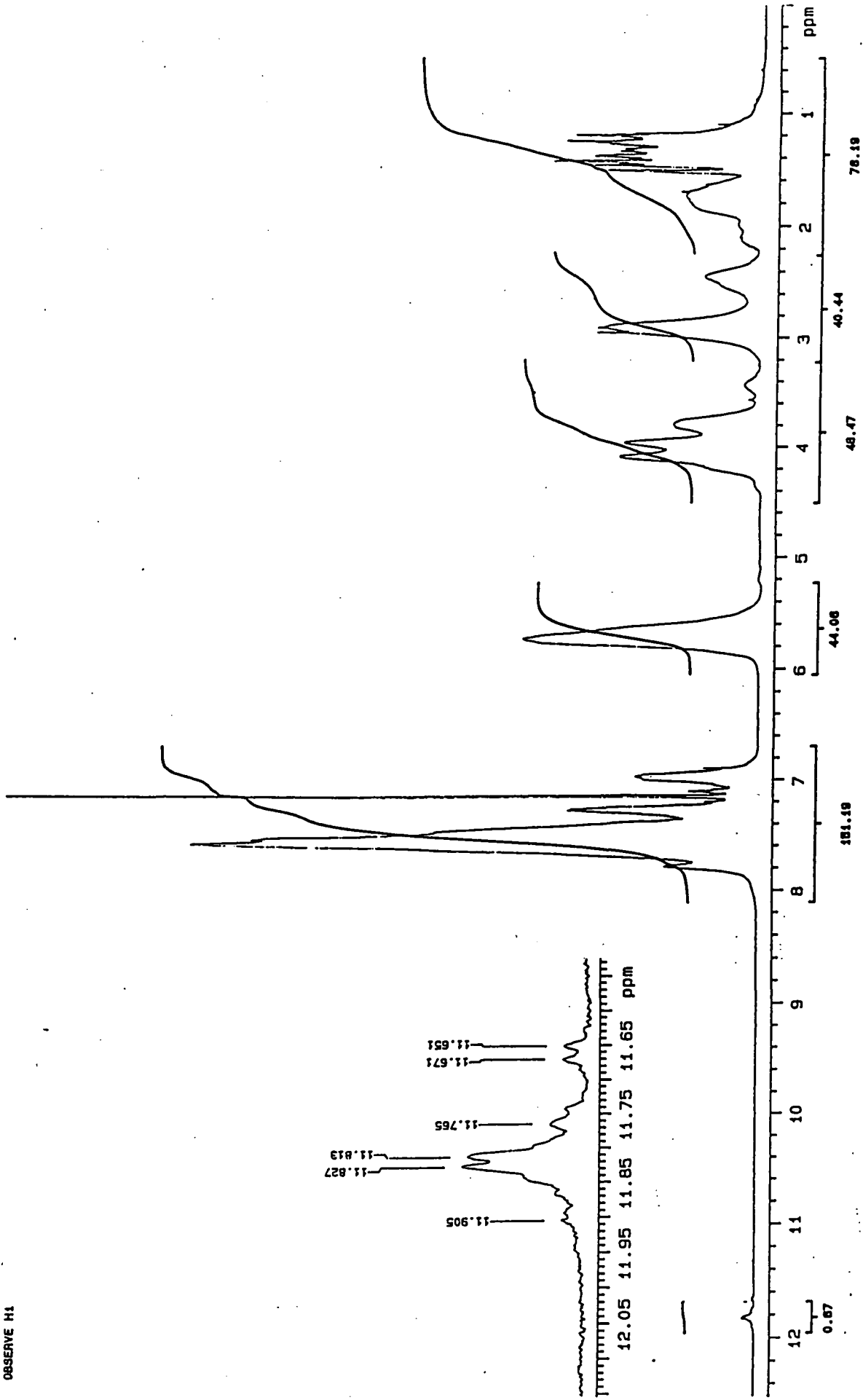
FILE /data/curdst/kas18aug.11d
RUN ON Aug 18 93
SOLVENT CDCl3

OBSERVE C13
Frequency 100.577 MHz
Spectral width 25000.0 Hz
Acquisition time 1.000 sec
Relaxation delay 0.500 sec
Pulse width 9.7 usec
Ambient temperature
No. repetitions 28000
DECOUPLE H1
High power 38
Decoupler continuously on
WALTZ-16 modulated
Double precision acquisition
DATA PROCESSING
Line broadening 2.0 Hz
Gaussian apodization 0.500 sec
FT size 131072
Total acquisition time 11.7 hours



Appendix 3.3.5.d ¹³C n.m.r. spectrum of P3-6 (end-capped polymer)

K9 939
FILE /data/curdat/ksa14dec.11d
RUN ON Dec 14 92
SOLVENT Benzene
OBSERVE H1



Appendix 3.3.6.a 1H n.m.r. spectrum of P3-10 (living polymer)

K9
FILE /data/curdet/ks18dec.f1d
RUN ON Dec 18 92
SOLVENT Benzene
OBSERVE C13

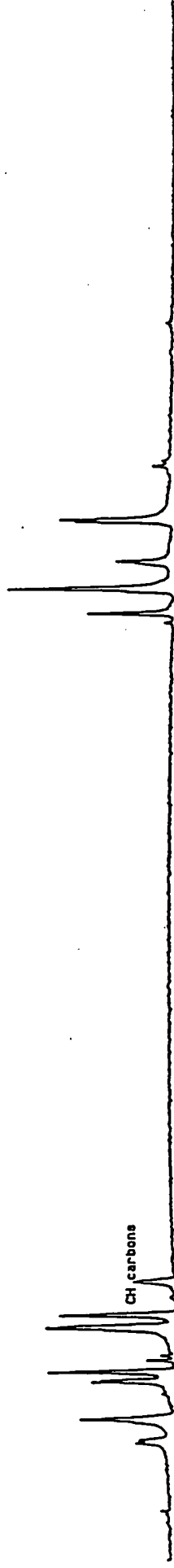
CH3 carbons



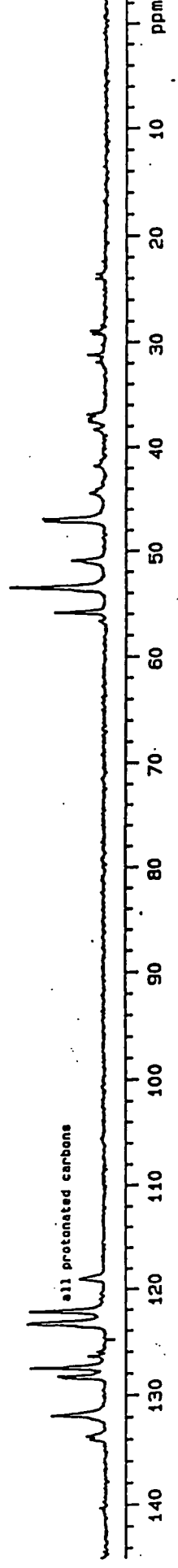
CH2 carbons



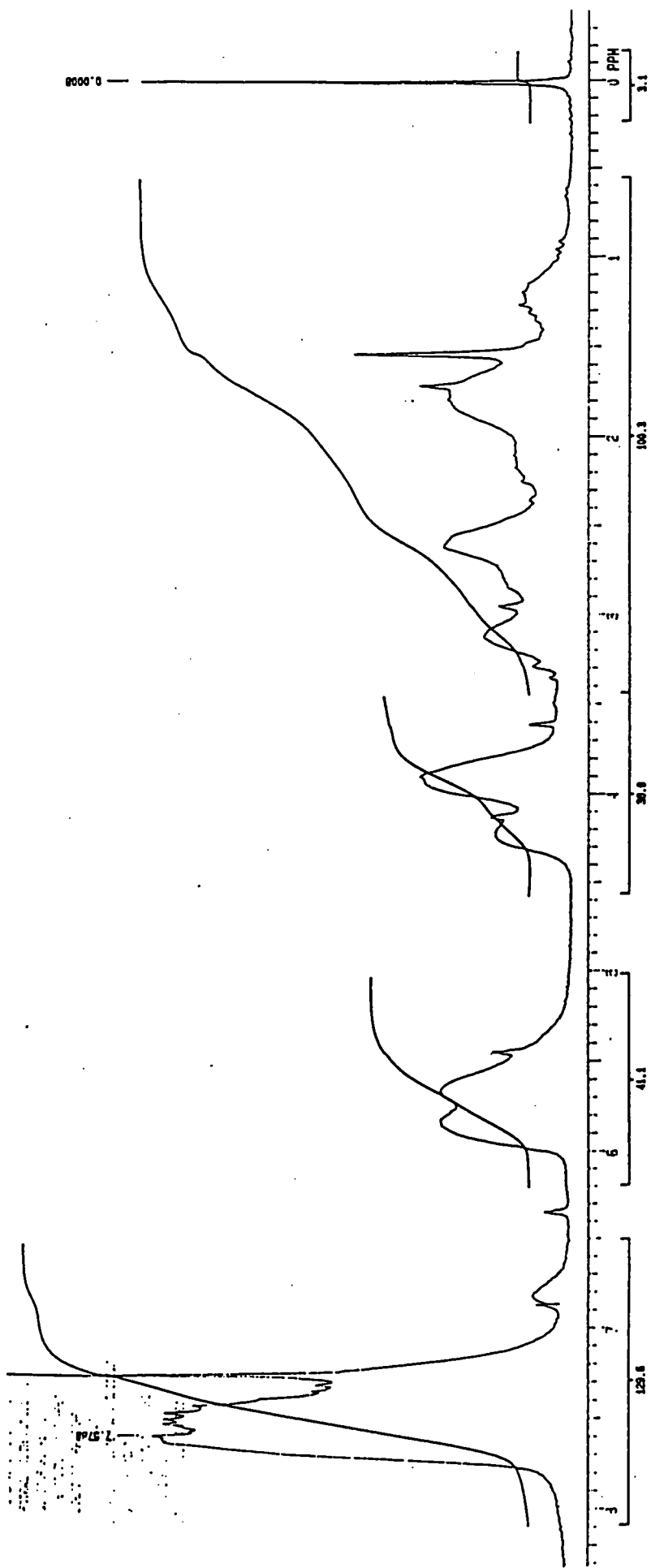
CH carbons



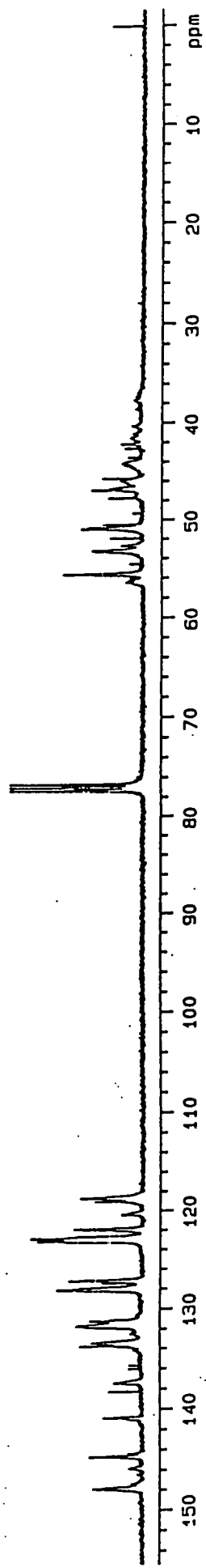
all protonated carbons



Appendix 3.3.6.b DEPT spectrum of P3-10 (living polymer)

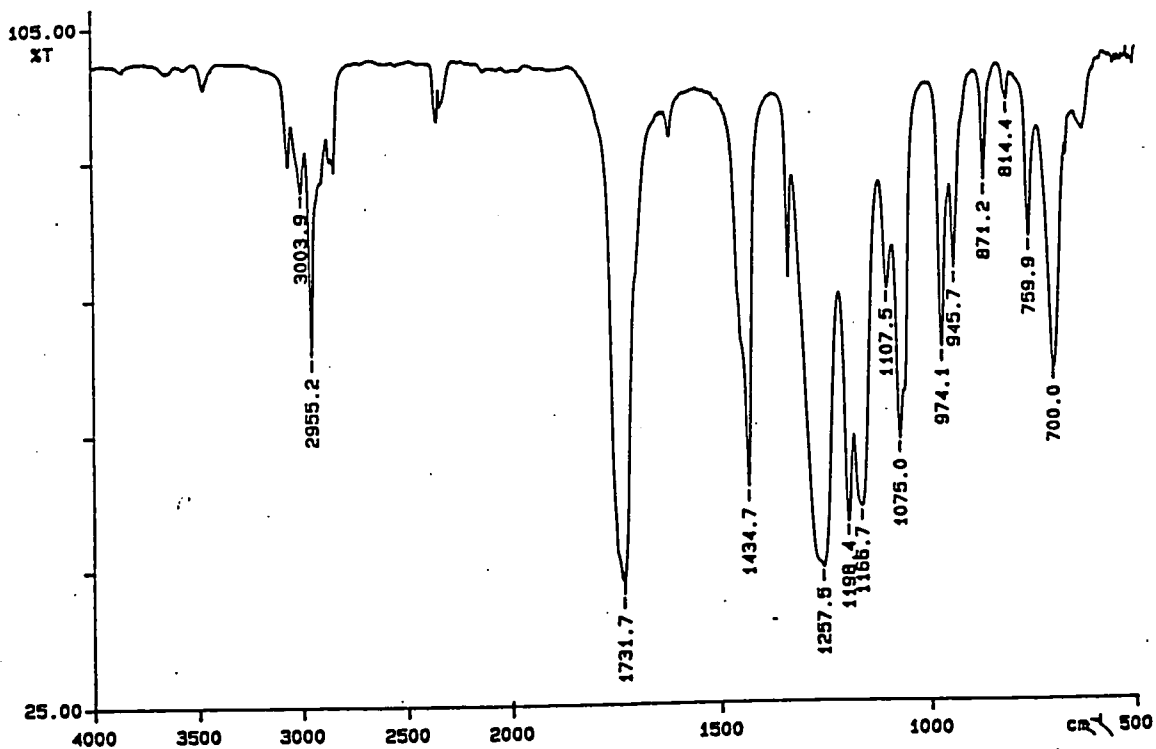


Appendix 3.3.7.a ^1H n.m.r. spectrum of P3-13



Appendix 3.3.7.b ^{13}C n.m.r. spectrum of P3-13

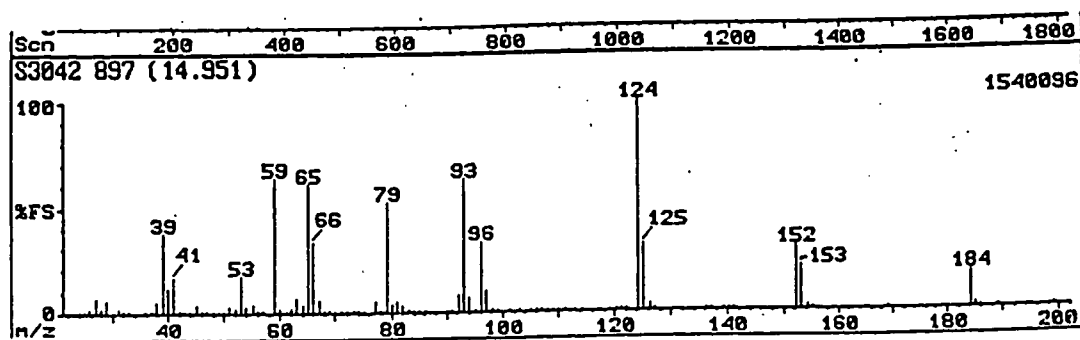
PERKIN ELMER



93/10/22 15:18

X: 16 scans, 4.0cm-1, flat

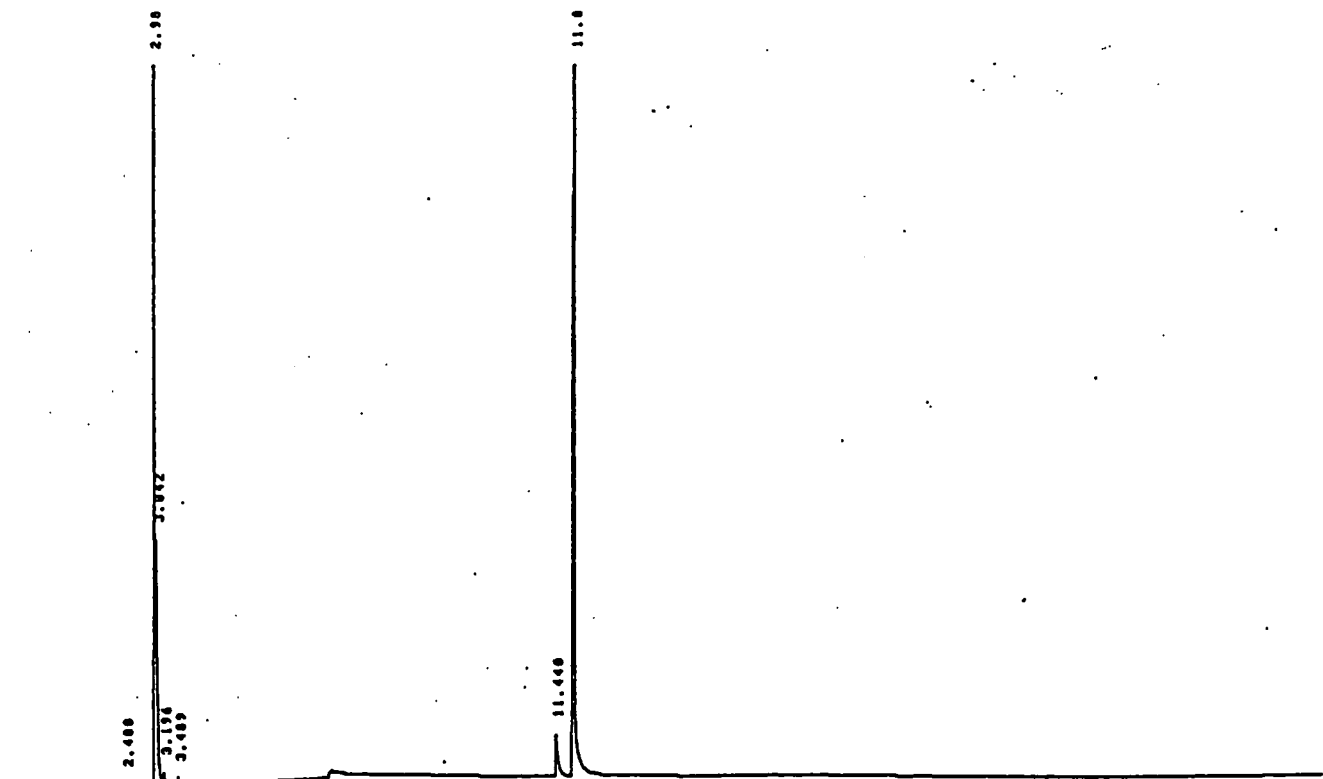
Appendix 4.1.3. Infrared spectrum of dimethyl 3-cyclopentene-1,1-dicarboxylate



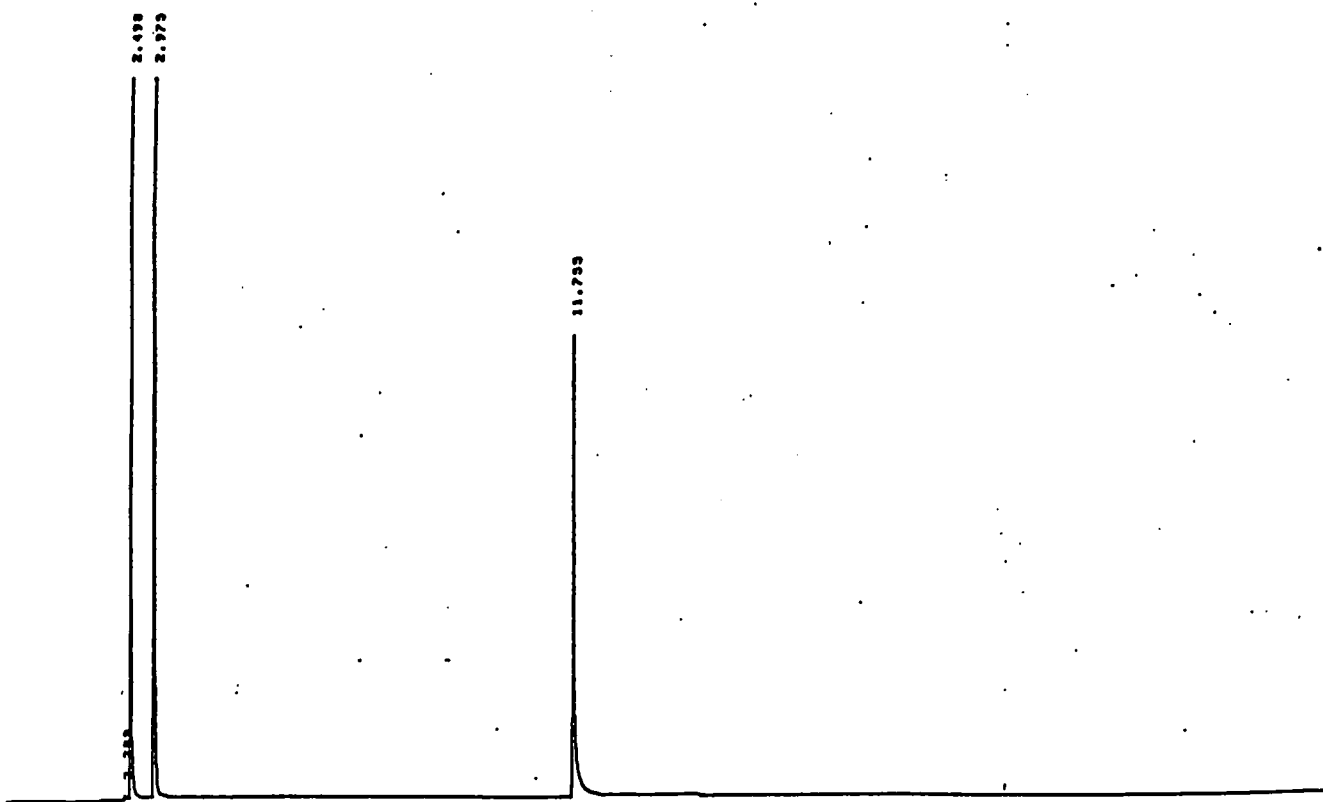
Appendix 4.1.4. Mass spectrum of dimethyl 3-cyclopentene-1,1-dicarboxylate

APPENDIX 4

Analytical data for Chapter 4



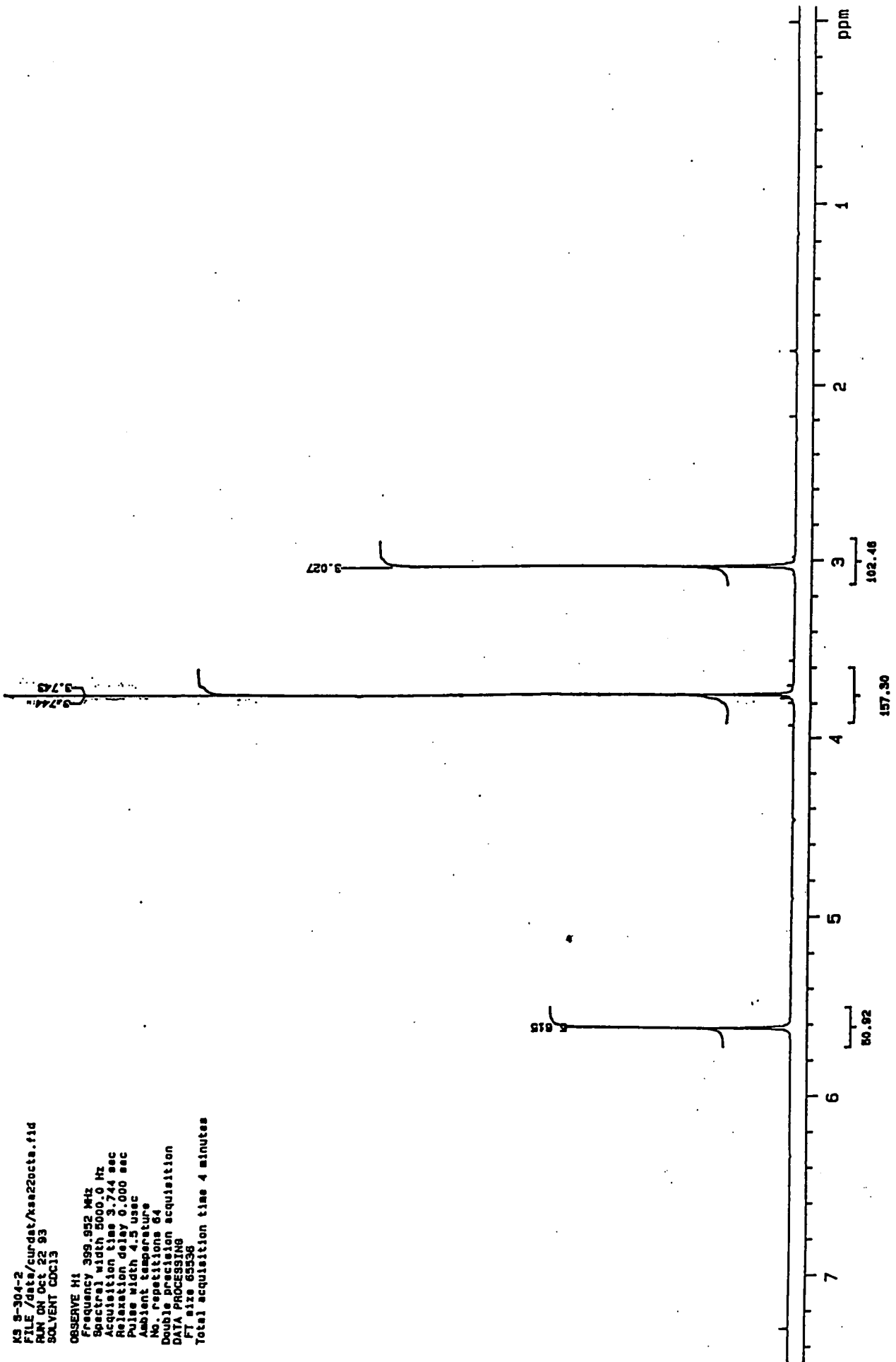
Appendix 4.1.1. GC trace of the material obtained by the condensation of cis-1,4-dichloro-2-butene and dimethyl malonate



Appendix 4.1.2. GC trace of dimethyl 3-cyclopentene-1,1-dicarboxylate

K5 8-304-2
FILE /data/curdst/kas2octa.f1d
RUN ON Oct 22 83
SOLVENT CCl4

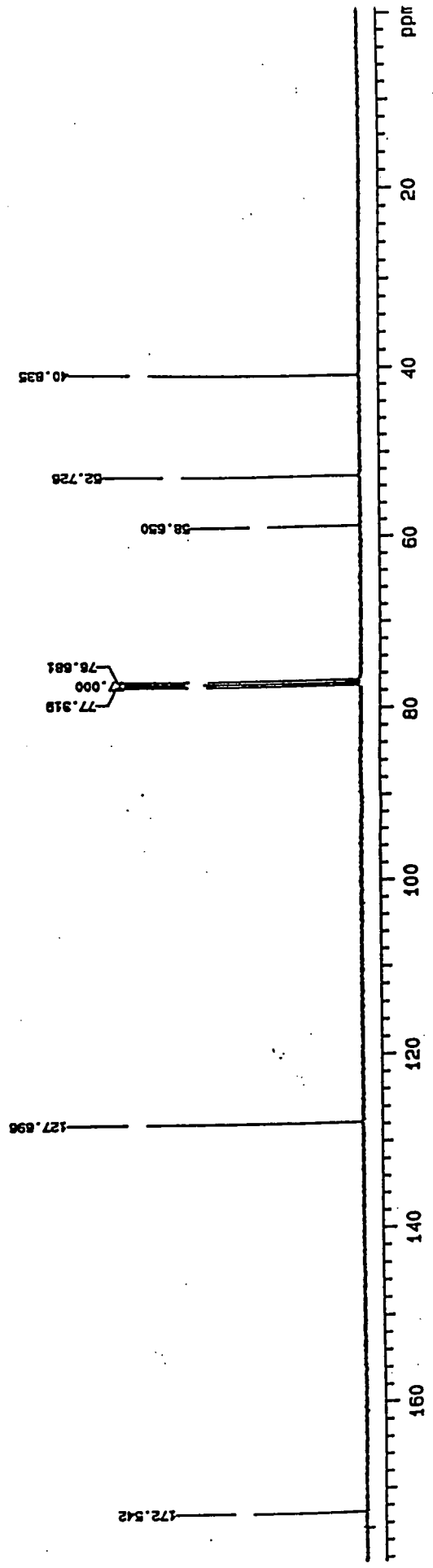
OBSERVE H1
Frequency 399.952 MHz
Spectral width 5000.0 Hz
Acquisition time 3.744 sec
Relaxation delay 0.000 sec
Pulse width 4.5 usec
Ambient temperature
No. repetitions 64
Double precision acquisition
DATA PROCESSING
FT size 65536
Total acquisition time 4 minutes



Appendix 4.1.5.a 1H n.m.r. spectrum of dimethyl 3-cyclopentene-1,1-dicarboxylate

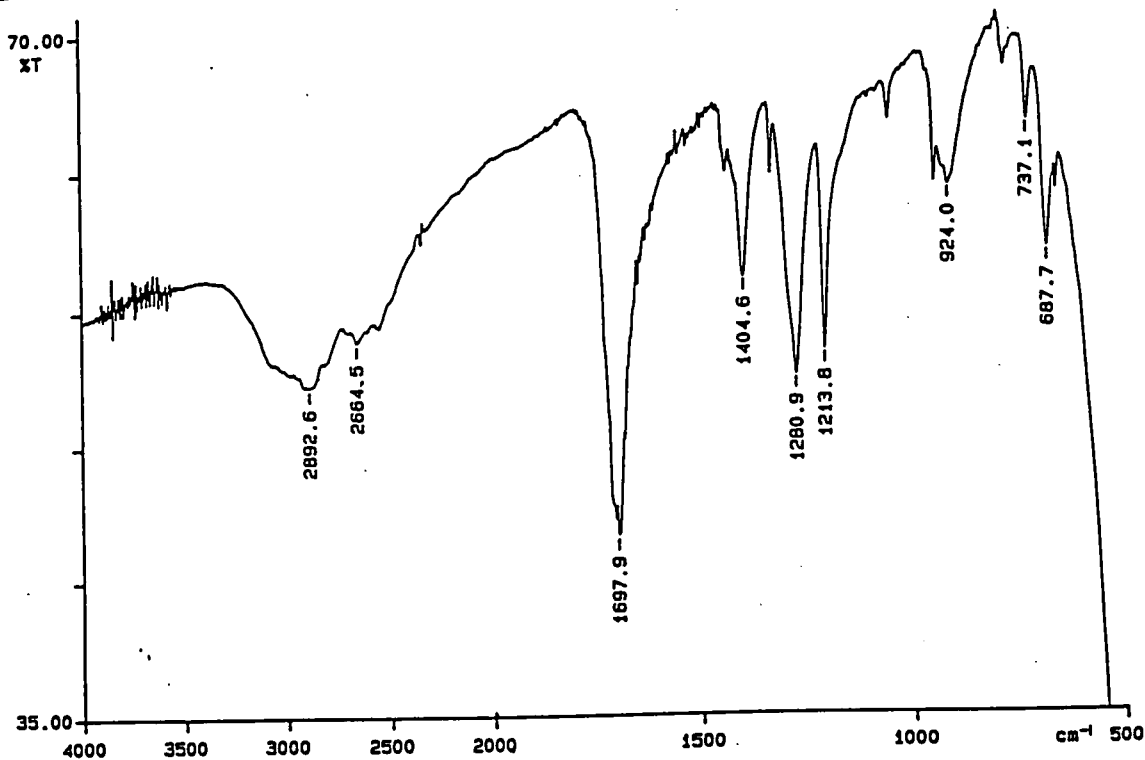
KS 9-304-2
FILE /date/curdnt/ksa22octb.fid
RUN ON Oct 22 93
SOLVENT CDCl3

OBSERVE C13
Frequency 100.677 MHz
Spectral width 25000.0 Hz
Acquisition time 1.199 sec
Relaxation delay 3.000 sec
Pulse width 9.3 usec
Ambient temperature
No. repetitions 1024
DECOUPLE H1
High power 40
Decoupler continuously on
MULTI-16 modulated
Double precision acquisition
DATA PROCESSING
Line broadening 0.8 Hz
FT size 131072
Total acquisition time 71 minutes



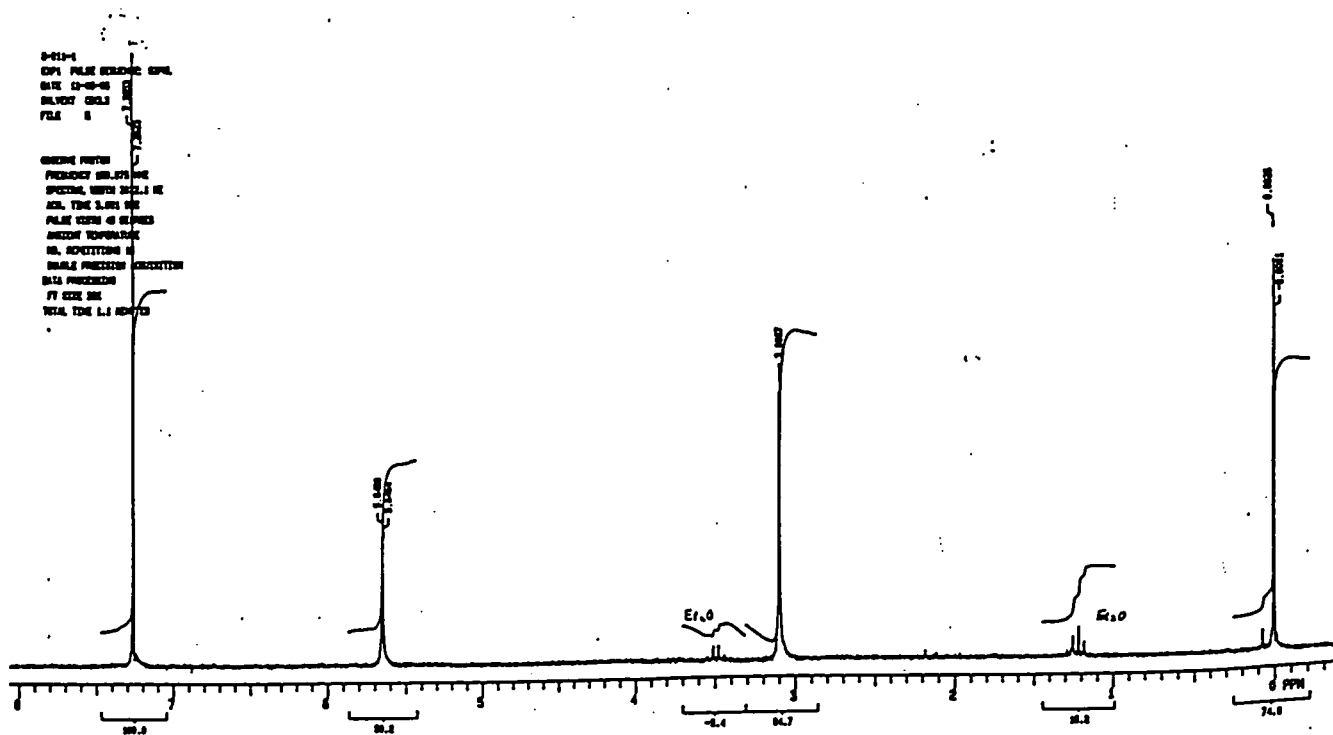
Appendix 4.1.5.b ¹³C n.m.r. spectrum of dimethyl 3-cyclopentene-1,1-dicarboxylate

PERKIN ELMER

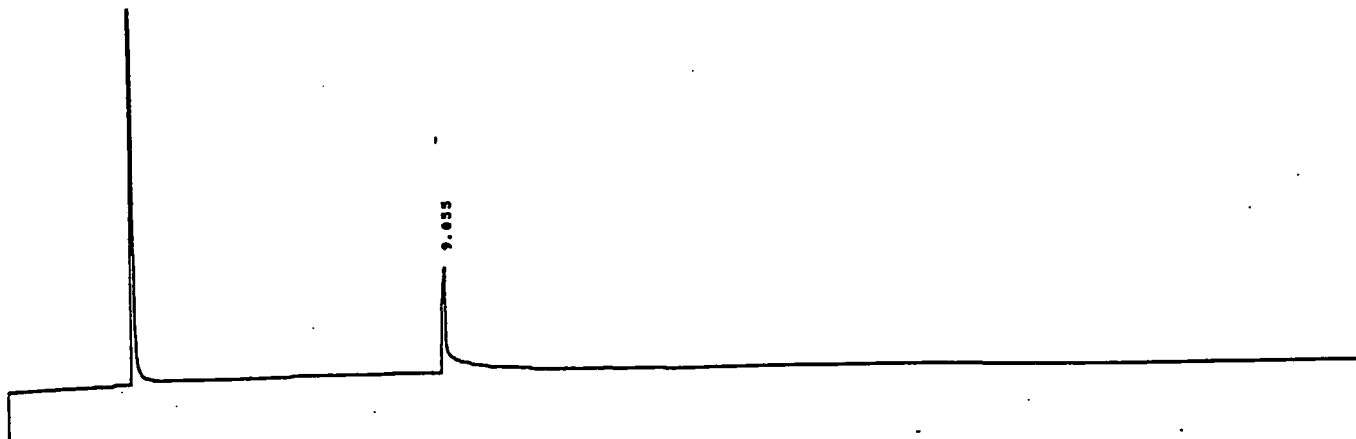


94/05/17 15:11 red
X: 16 scans, 4.0cm⁻¹

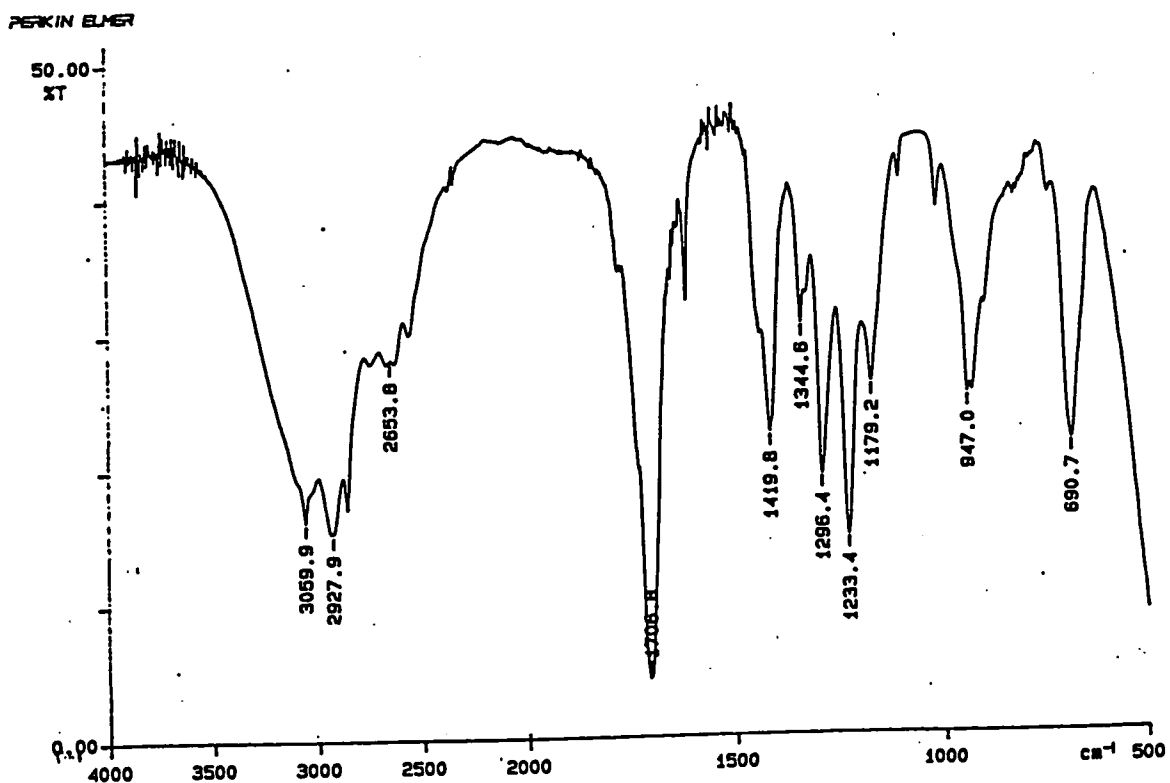
Appendix 4.1.6. Infrared spectrum of 3-cyclopentene-1,1-dicarboxylic acid



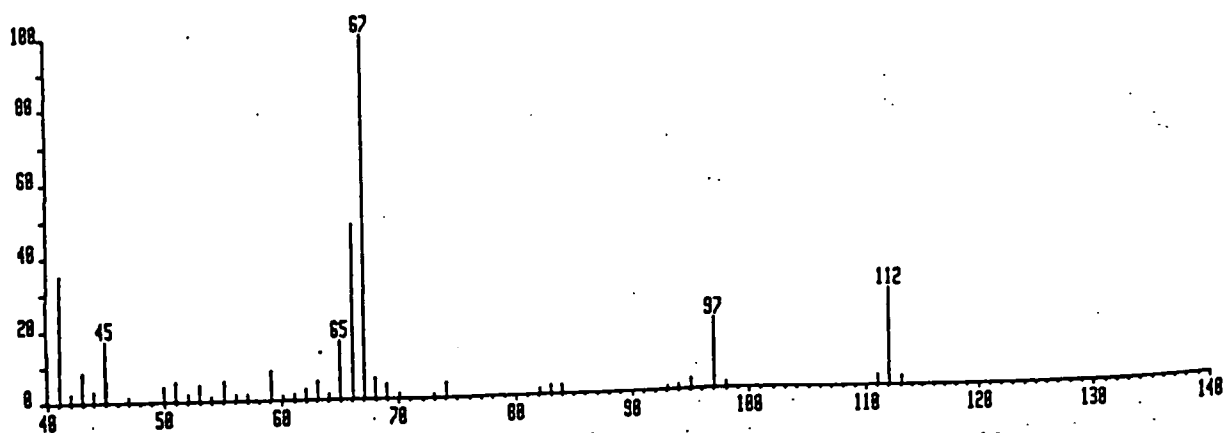
Appendix 4.1.7. ¹H n.m.r. spectrum of 3-cyclopentene-1,1-dicarboxylic acid



Appendix 4.1.8. GC trace of 3-Cyclopentenecarboxylic acid



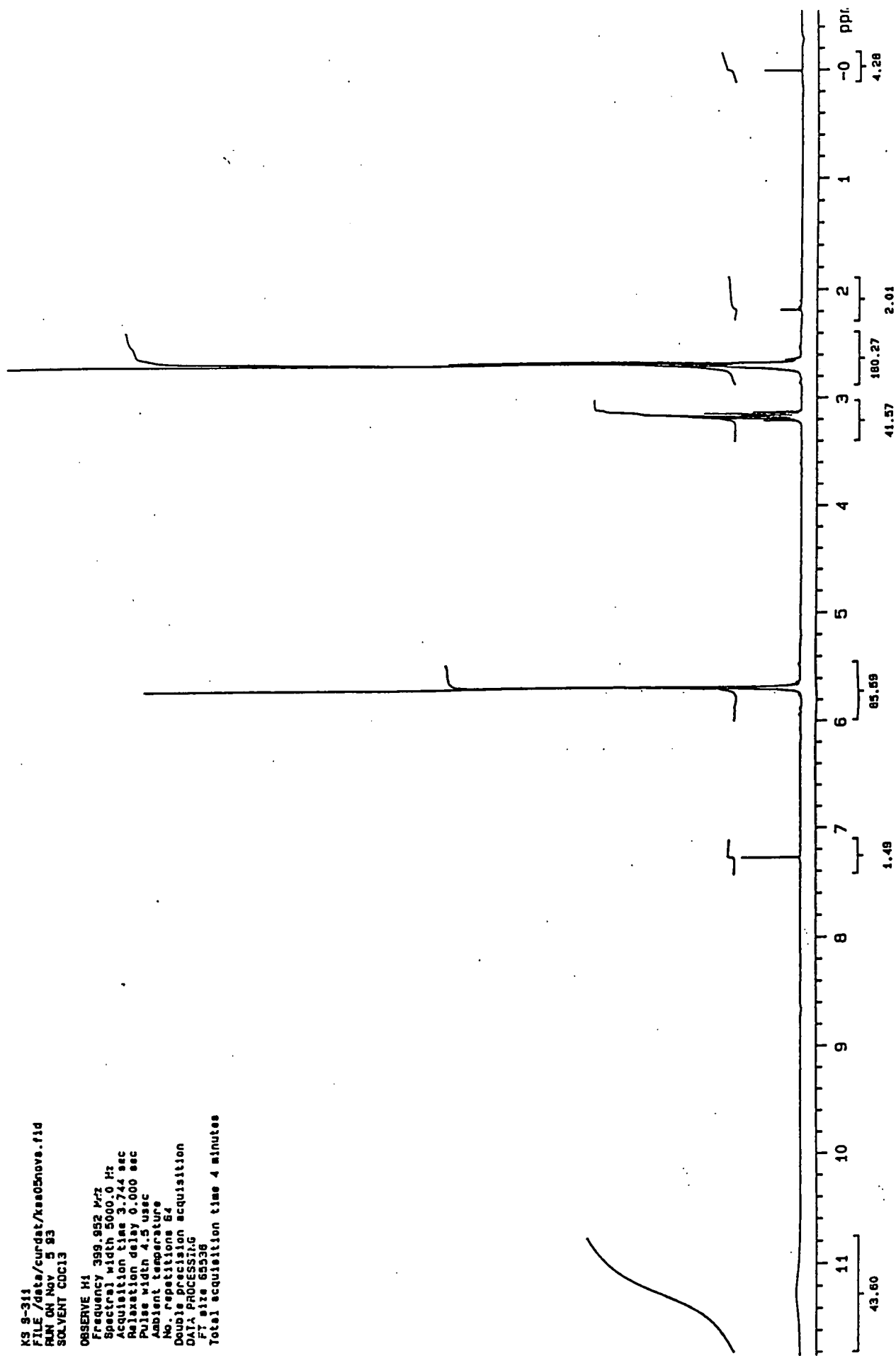
Appendix 4.1.9. Infrared spectrum of 3-Cyclopentenecarboxylic acid



Appendix 4.1.10. Mass spectrum of 3-Cyclopentenecarboxylic acid

KS 9-311
FILE /data/curdat/ks05nov8.fid
RUN ON Nov 5 93
SOLVENT CDCl3

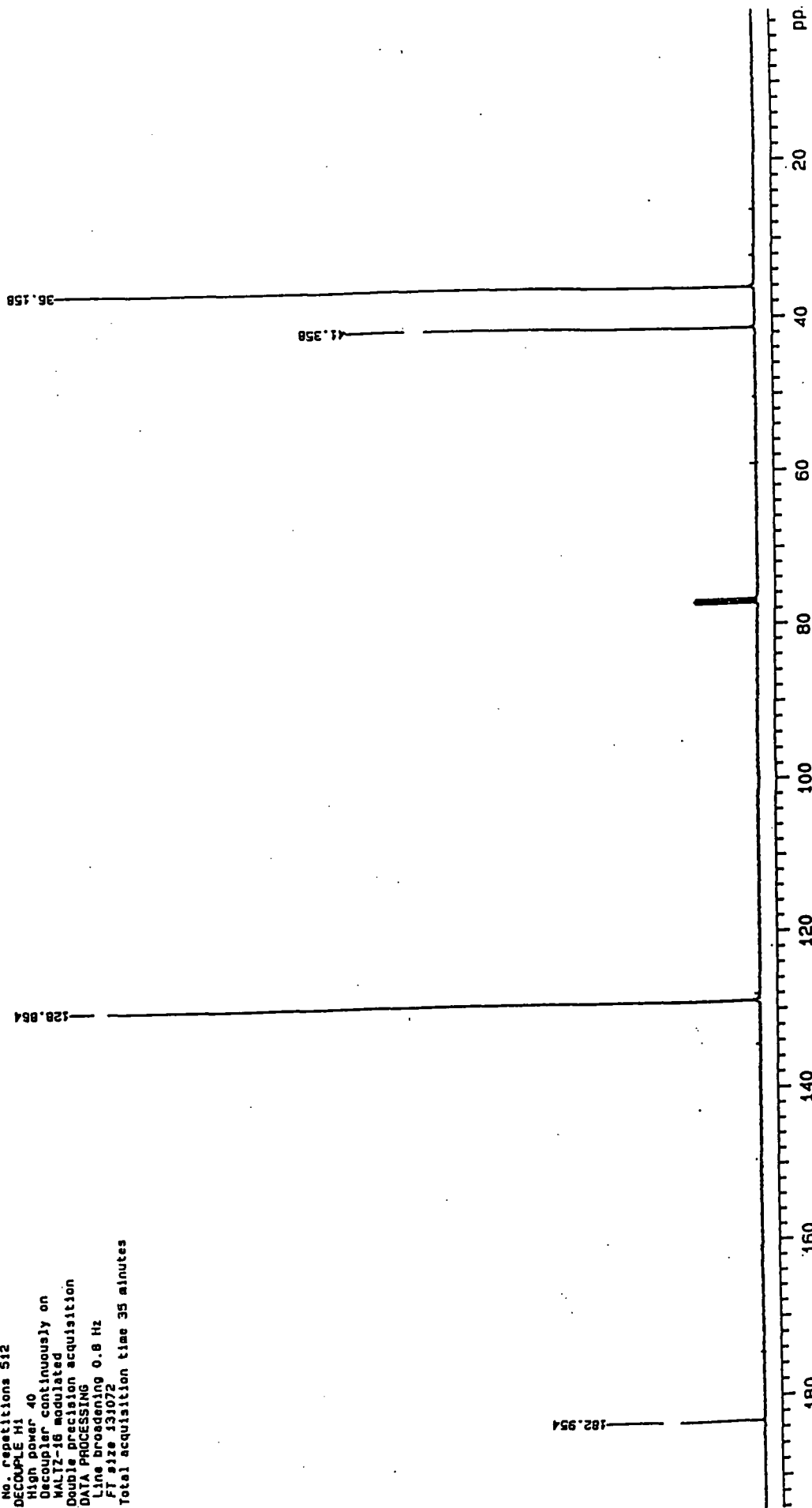
OBSERVE H1
Frequency 399.952 Mhz
Spectral width 5000.0 Hz
Acquisition time 3.744 sec
Relaxation delay 0.000 sec
Pulse width 4.5 usec
Ambient temperature
No. repetitions 64
Double precision acquisition
DATA PROCESSING
F1 size 65536
Total acquisition time 4 minutes



Appendix 4.1.11.a 1H n.m.r. spectrum of 3-Cyclopentenecarboxylic acid

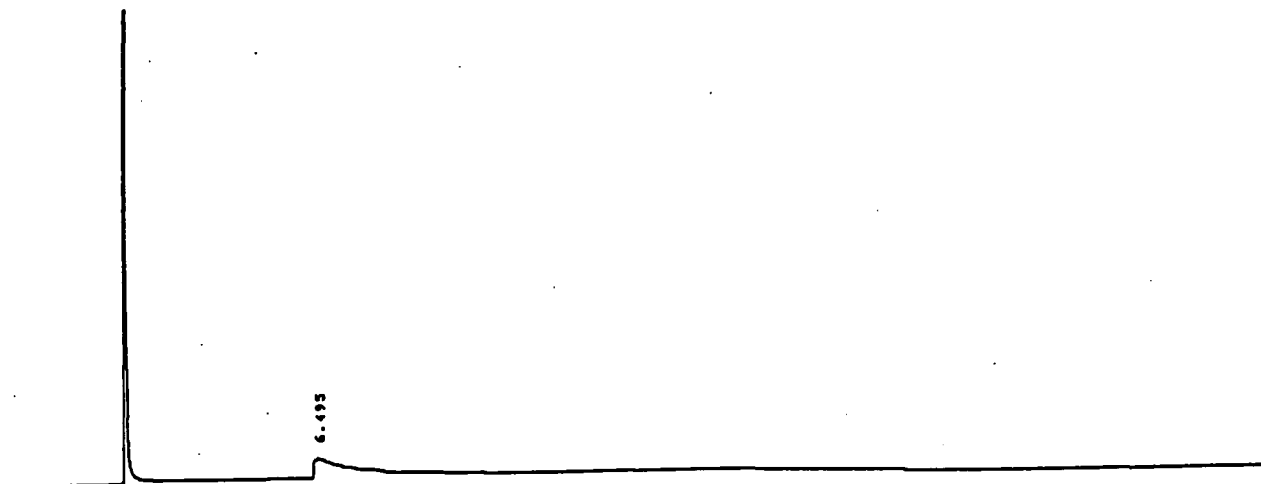
KS S-311
FILE /data/curdat/ksa05novb.fid
RUN ON Nov 5 93
SOLVENT CDCl3

OBSERVE C13
Frequency 100.577 MHz
Spectral width 25000.0 Hz
Acquisition time 1.199 sec
Relaxation delay 3.000 sec
Pulse width 10.0 usec
Ambient temperature
No. repetitions 512
DECOUPLE H1
High power 40
Decoupler continuously on
MALZ-18 modulated
Double precision acquisition
DATA PROCESSING
Line broadening 0.8 Hz
FT size 131072
Total acquisition time 35 minutes

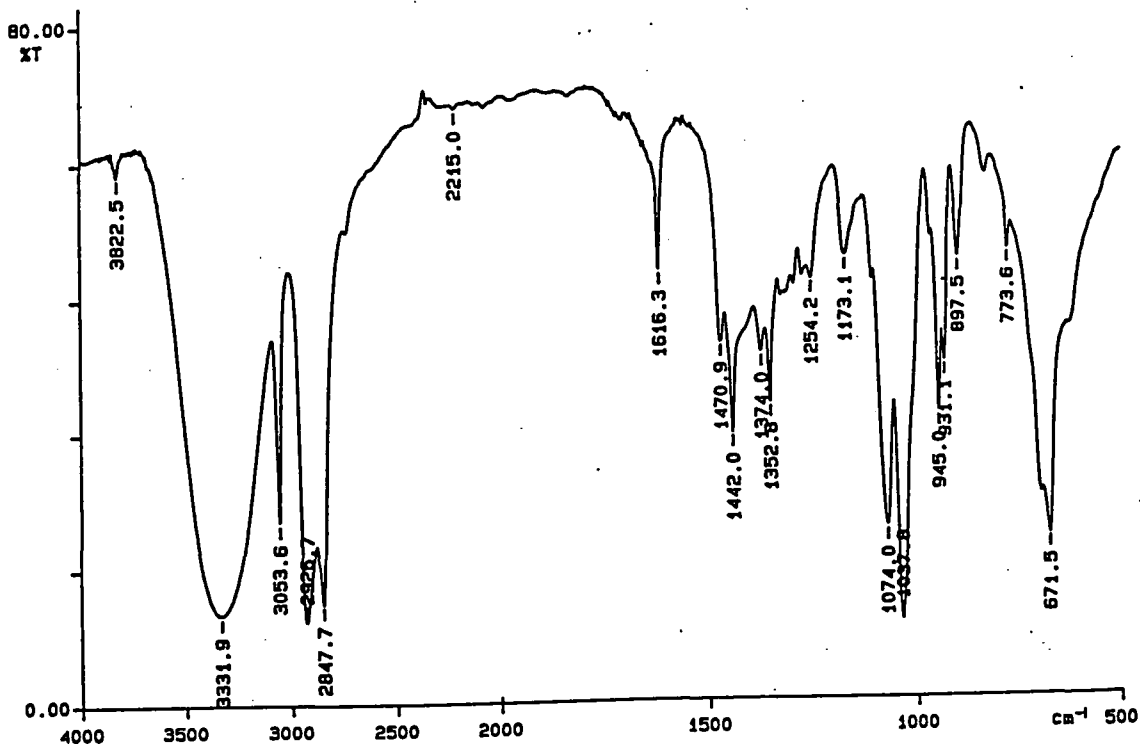


Appendix 4.1.11.b ¹³C n.m.r. spectrum of 3-Cyclopentenecarboxylic acid

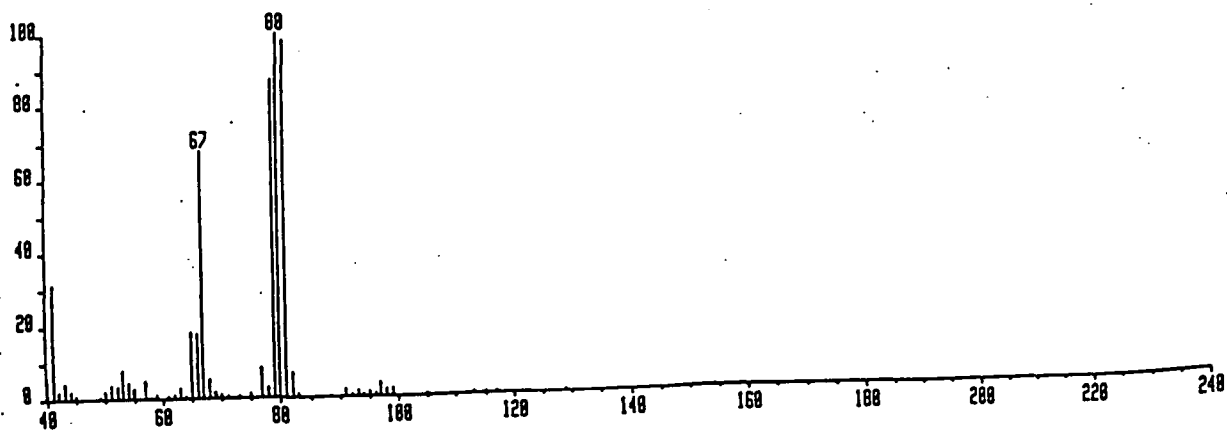
• RUN 8 7 JAN 19, 1994 13109104
START



Appendix 4.1.12. GC trace of 4-hydroxymethylcyclopentene



Appendix 4.1.13. Infrared spectrum of 4-hydroxymethylcyclopentene

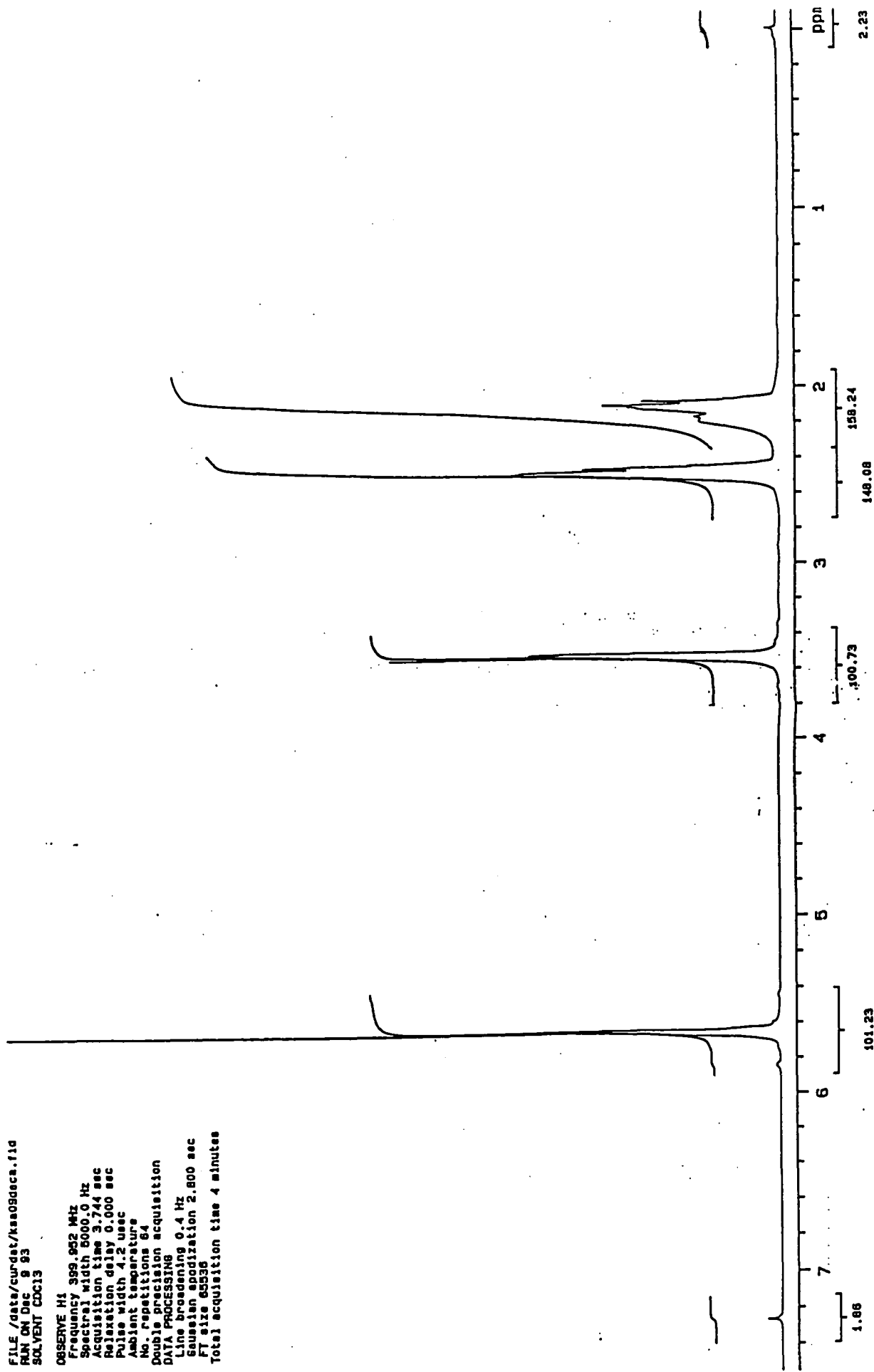


Appendix 4.1.14. Mass spectrum of 4-hydroxymethylcyclopentene

FILE /data/cwrdet/kas09dca.f10
RUN ON Dec 9 93
SOLVENT CDCl3

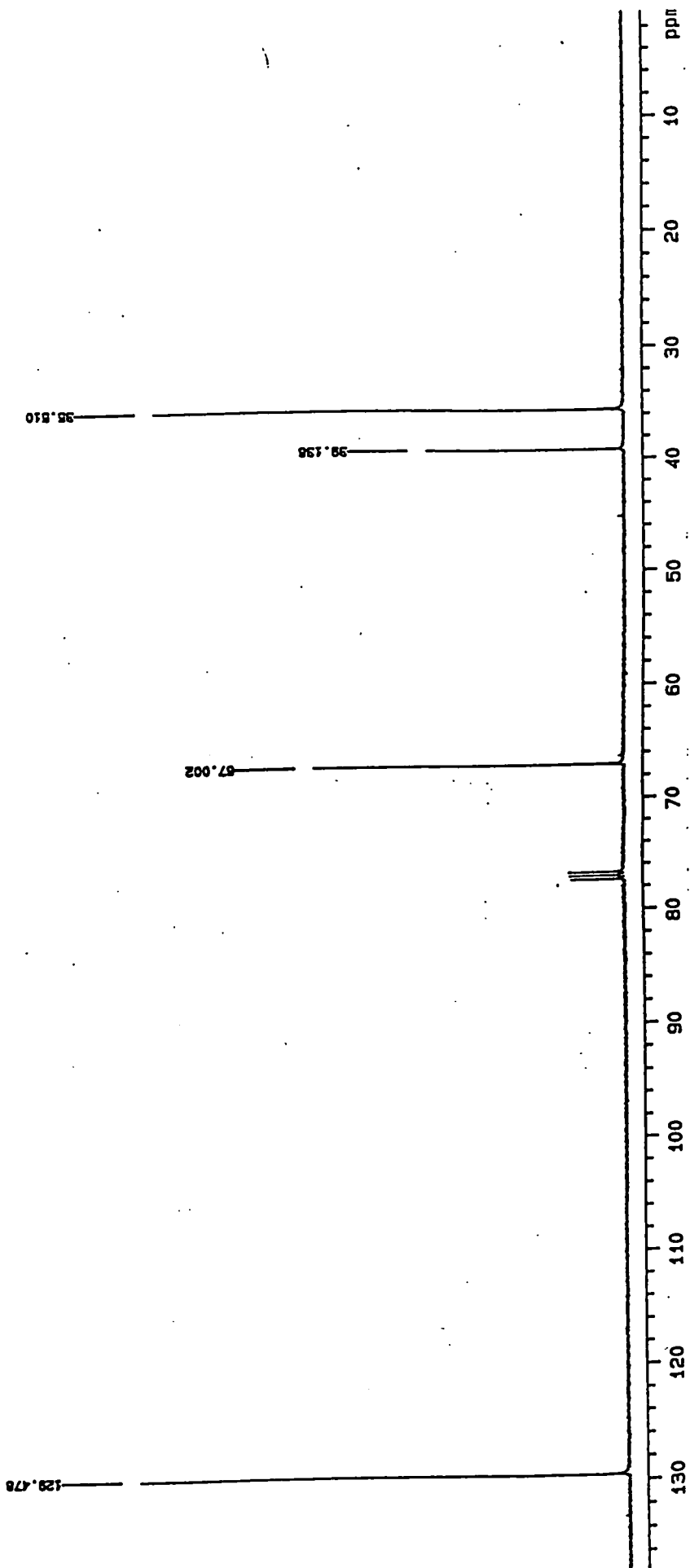
OBSERVE H1

Frequency 399.952 MHz
Spectral width 5000.0 Hz
Acquisition time 3.744 sec
Relaxation delay 0.000 sec
Pulse width 4.2 usec
Ambient temperature
No. Repetitions 64
Double precision acquisition
DATA PROCESSING
Line broadening 0.4 Hz
Gaussian apodization 2.800 sec
FT size 65536
Total acquisition time 4 minutes

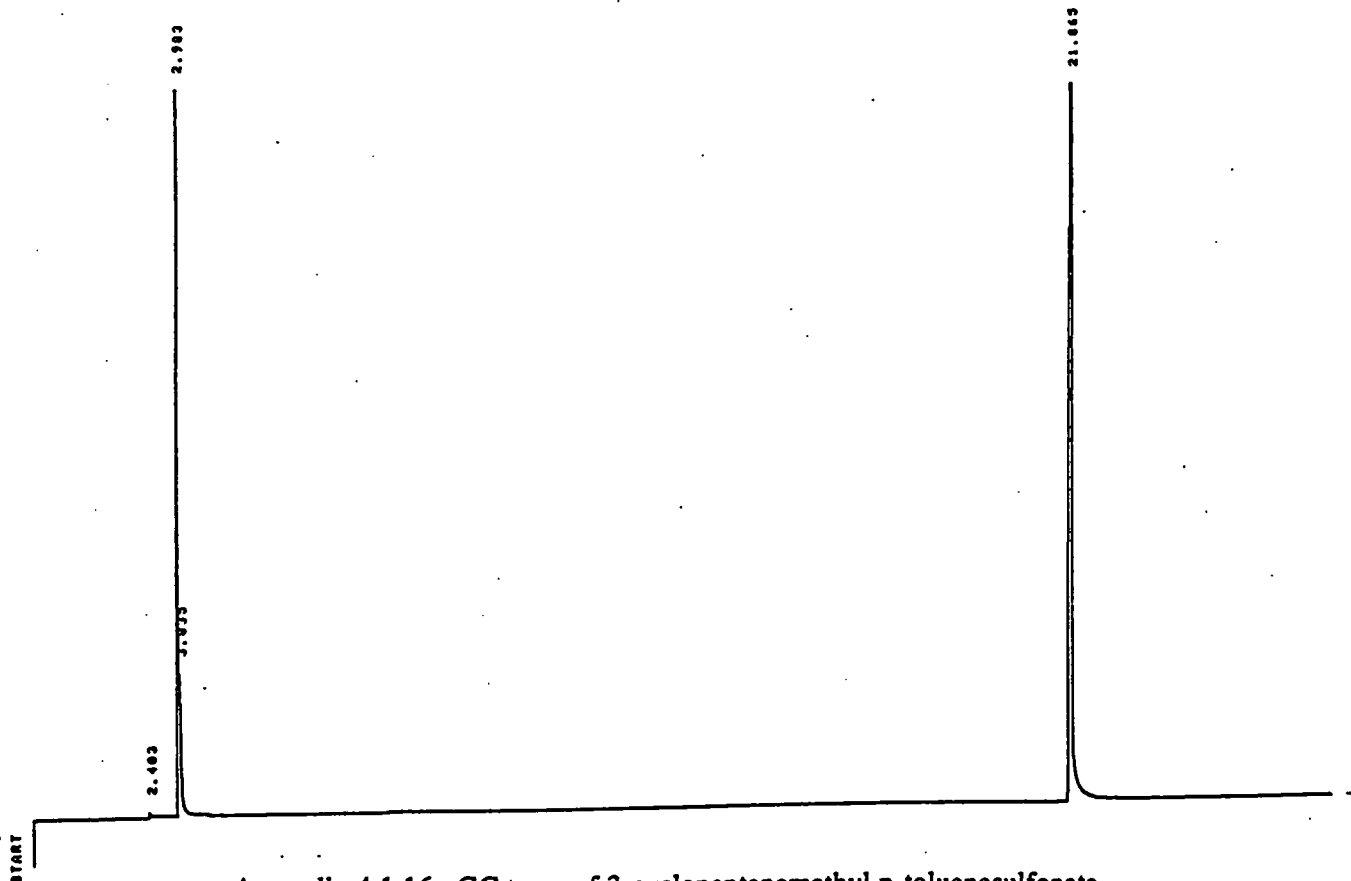


Appendix 4.1.15.a 1H n.m.r. spectrum of 4-hydroxymethylcyclopentene

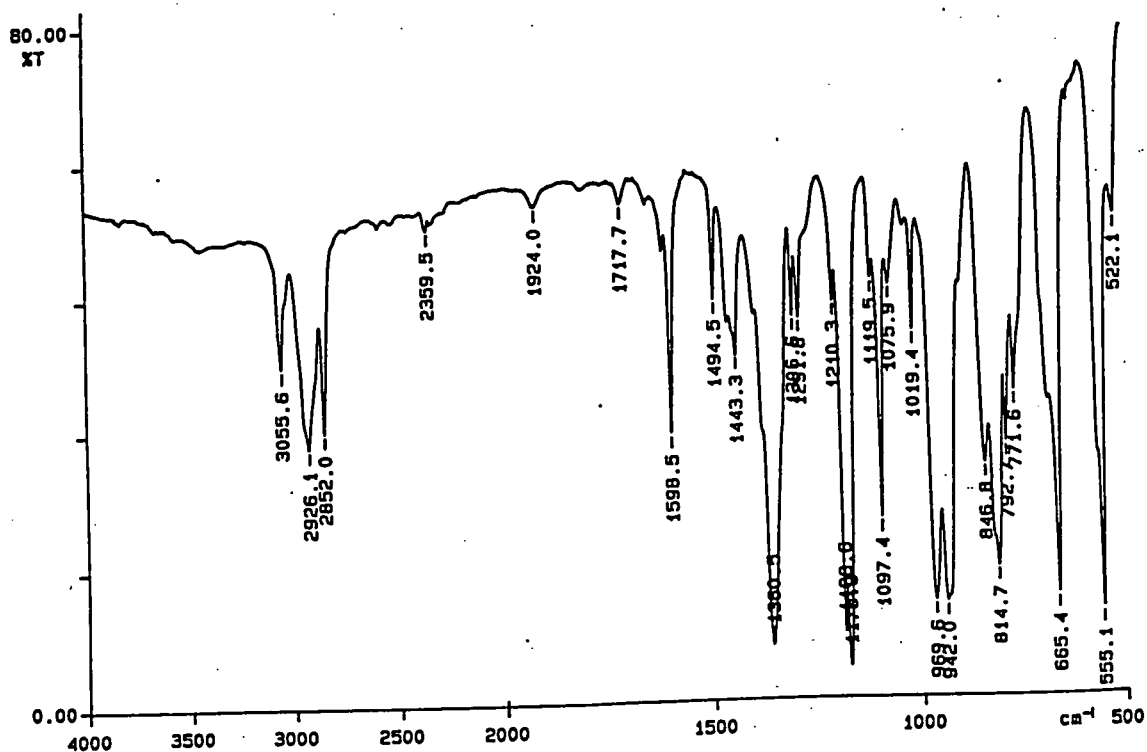
K3 8323
FILE /data/curdat/kss09decb.fid
RUN ON Dec 9 83
SOLVENT CDCl3
OBSERVE C13



Appendix 4.1.15.b ¹³C n.m.r. spectrum of 4-hydroxymethylcyclopentene



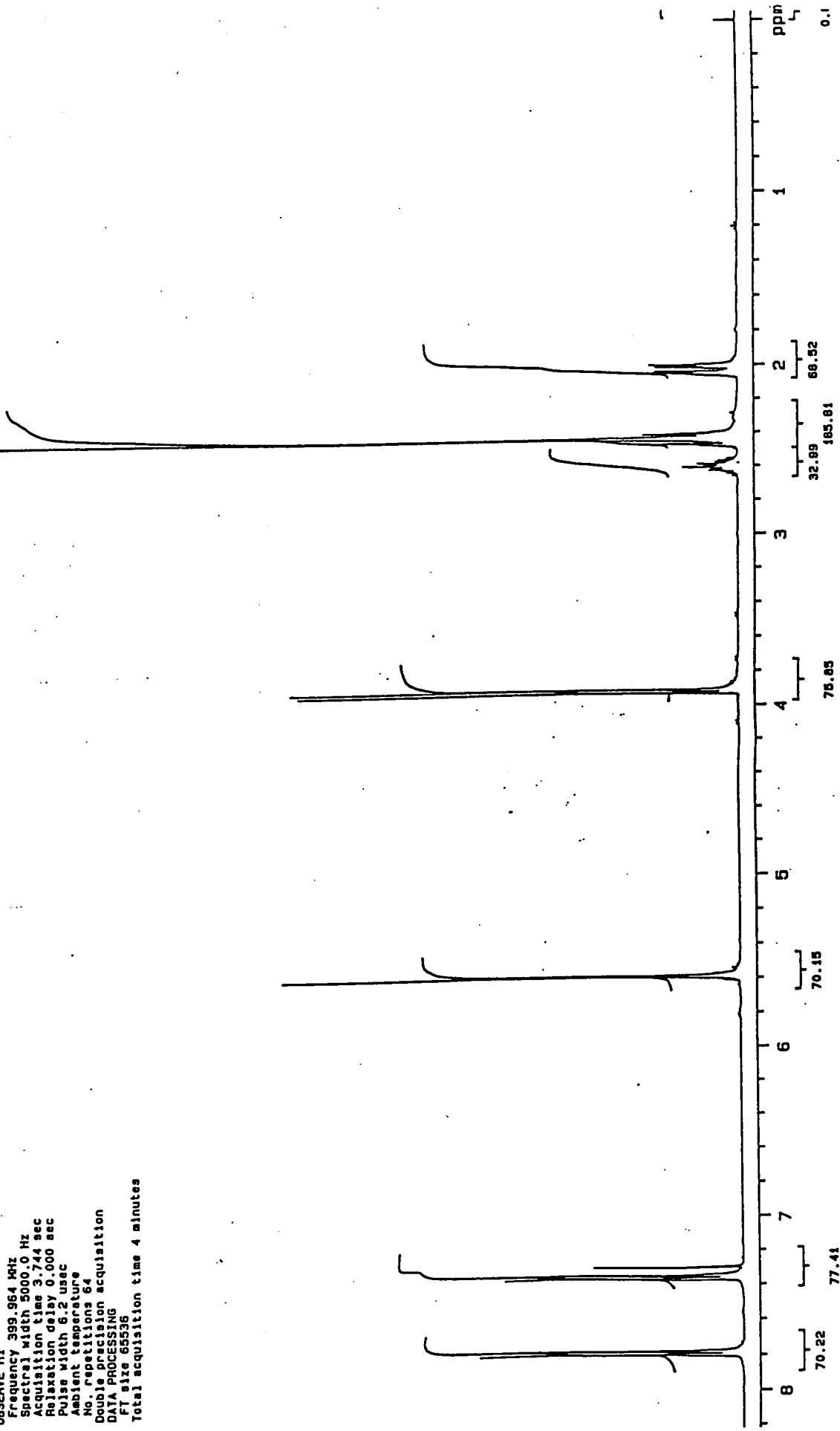
Appendix 4.1.16. GC trace of 3-cyclopentenemethyl p-toluenesulfonate



Appendix 4.1.17. Infrared spectrum of 3-cyclopentenemethyl p-toluenesulfonate

S-329
FILE /data/curdad/ksa14janc.fid
RUN ON Jan 14 94
SOLVENT CCl3

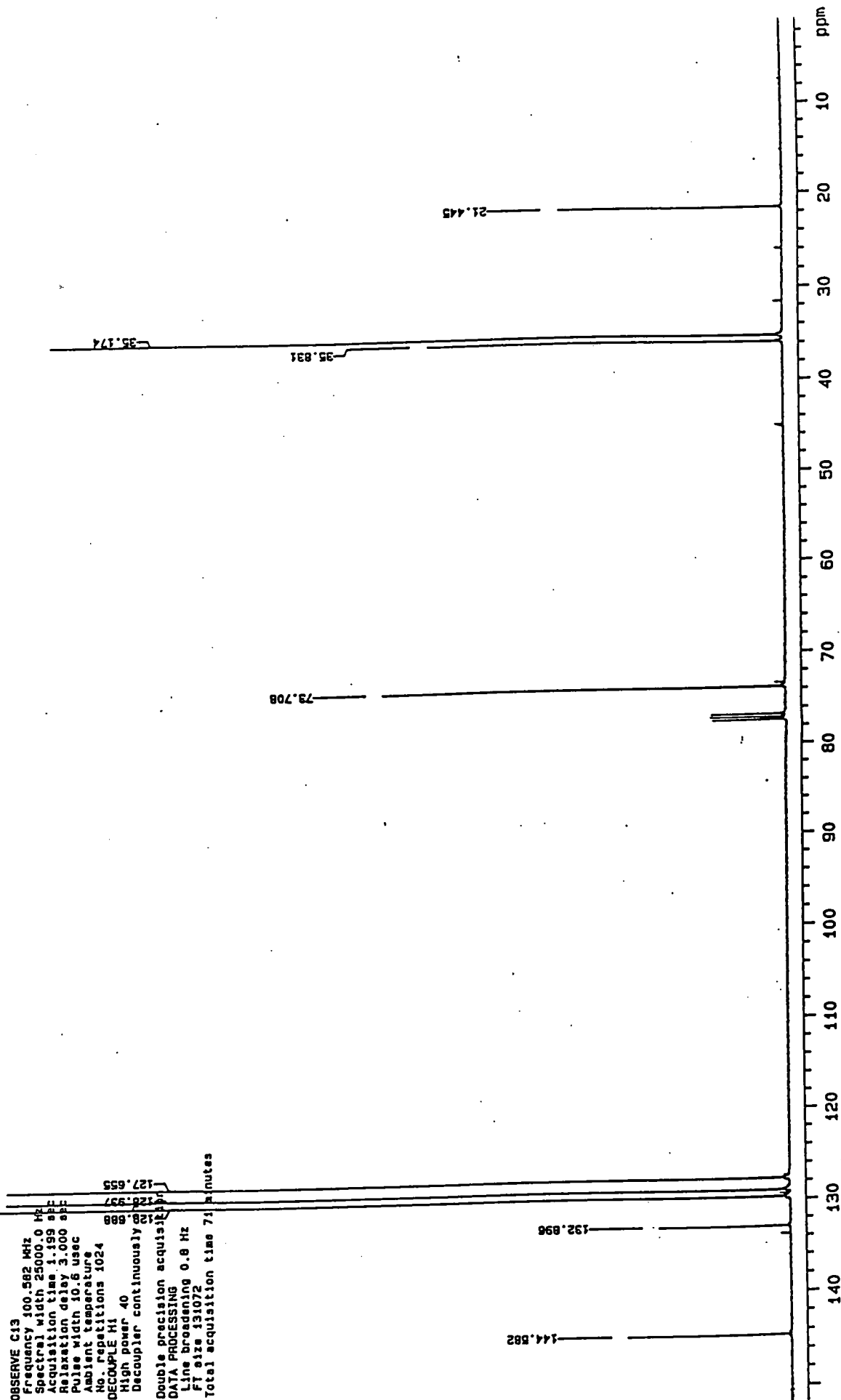
OBSERVE H1
Frequency 399.964 MHz
Spectral width 5000.0 Hz
Acquisition time 3.744 sec
Relaxation delay 0.000 sec
Pulse width 6.2 usec
Ambient temperature
No. repetitions 64
Double precision acquisition
DATA PROCESSING
F1 size 65536
Total acquisition time 4 minutes



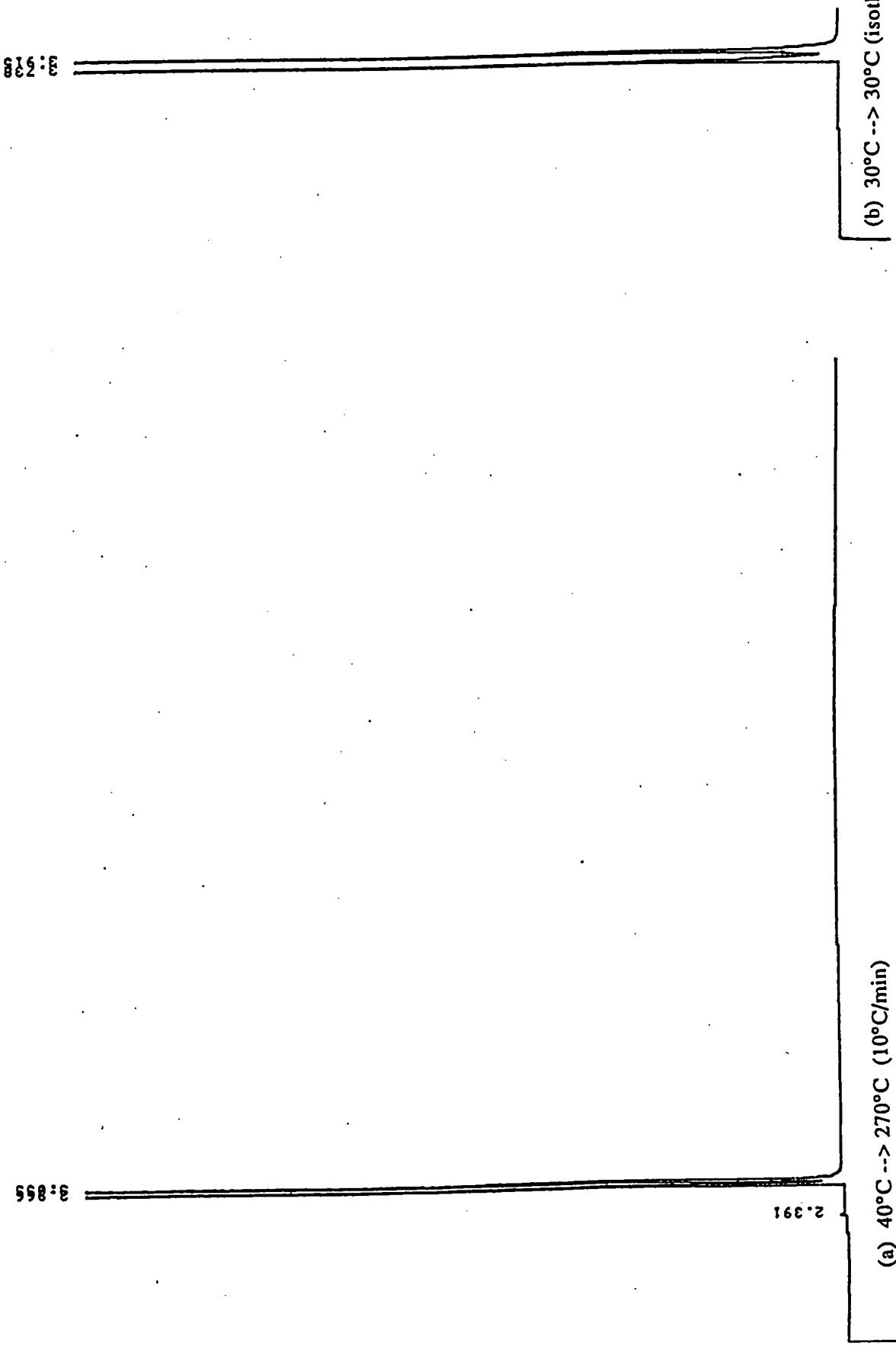
Appendix 4.1.18.a 1H n.m.r. spectrum of 3-cyclopentenemethyl p-toluenesulfonate

8-328
FILE /data/curdat/ksa141and.11d
RUN ON Jan 14 94
SOLVENT CDCl3

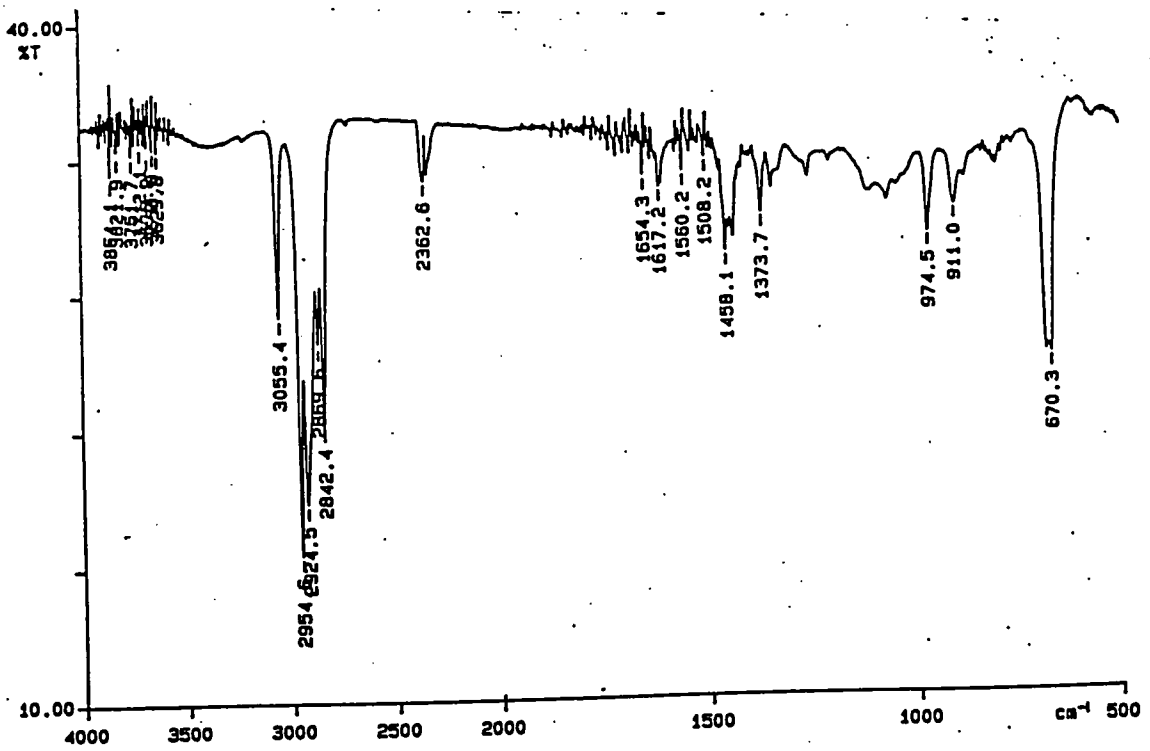
OBSERVE C13
Frequency 100.582 MHz
Spectral width 25000.0 Hz
Acquisition time 1.199 spt
Relaxation delay 3.000 spt
Pulse width 10.6 usec
Ambient temperature
No. repetitions 1024
DECOUPLE H1
High power 40
Decoupler continuously
Double precision acquisition
DATA PROCESSING
Line broadening 0.8 Hz
F1 size 131072
Total acquisition time 71 minutes



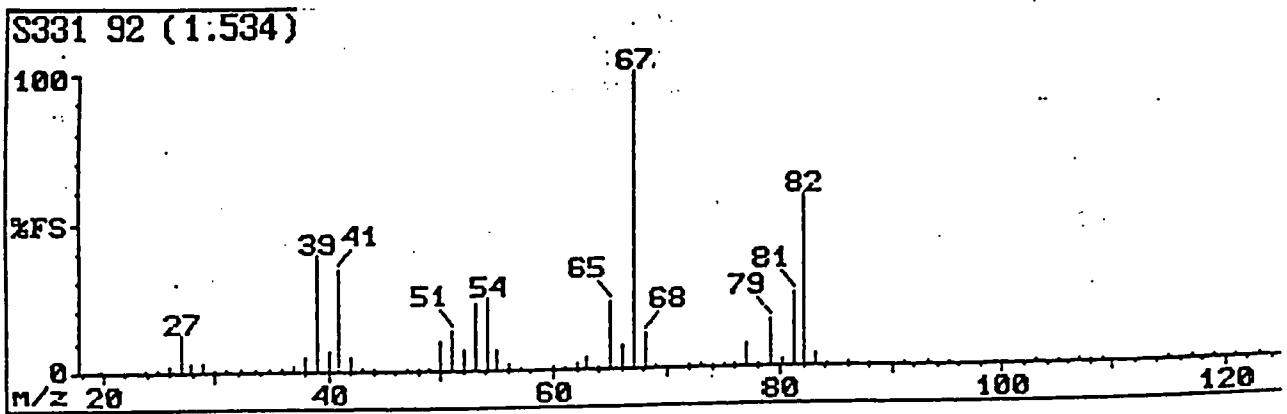
Appendix 4.1.18.b ¹³C n.m.r. spectrum of 3-cyclopentenemethyl p-toluenesulfonate



Appendix 4.1.19. GC traces of 4-methylcyclohexene



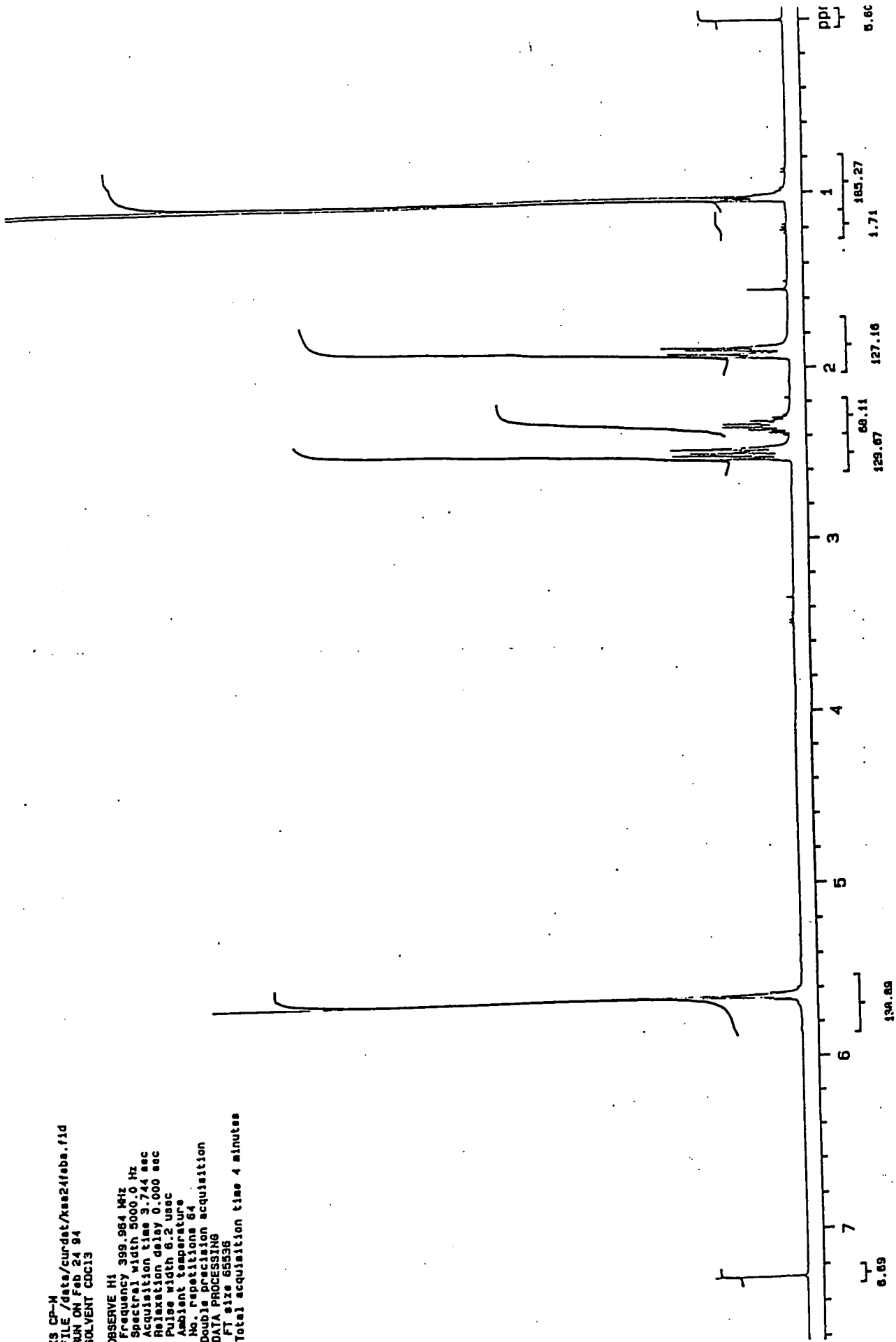
Appendix 4.1.20. Infrared spectrum of 4-methylcyclopentene



Appendix 4.1.21. Mass spectrum of 4-methylcyclopentene

KS CP-M
FILE /data/curdat/kas24feb.fid
RUN ON Feb 24 94
SOLVENT CCl3

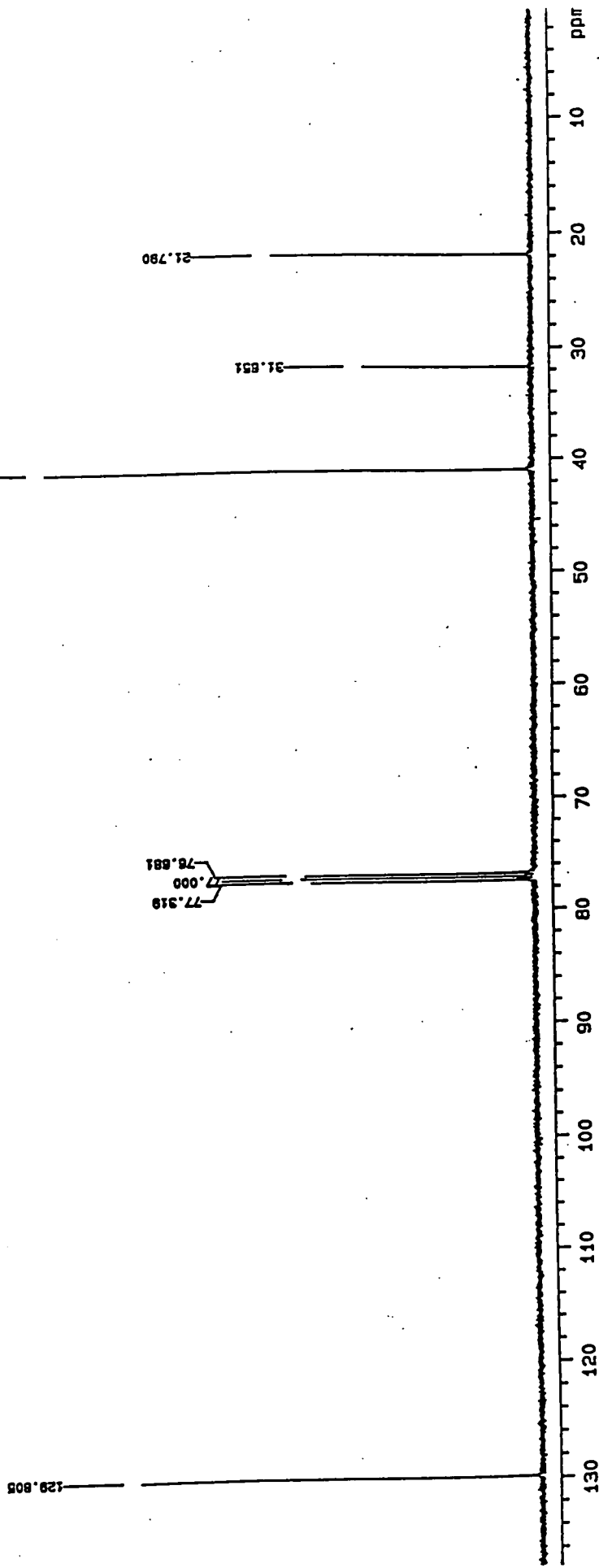
OBSERVE H1
Frequency 399.984 MHz
Spectral width 5000.0 Hz
Acquisition time 3.744 sec
Relaxation delay 0.000 sec
Pulse width 6.2 usec
Ambient temperature
No. repetitions 64
Double precision acquisition
DATA PROCESSING
F1 size 65836
Total acquisition time 4 minutes



Appendix 4.1.22.a 1H n.m.r. spectrum of 4-methylcyclopentene

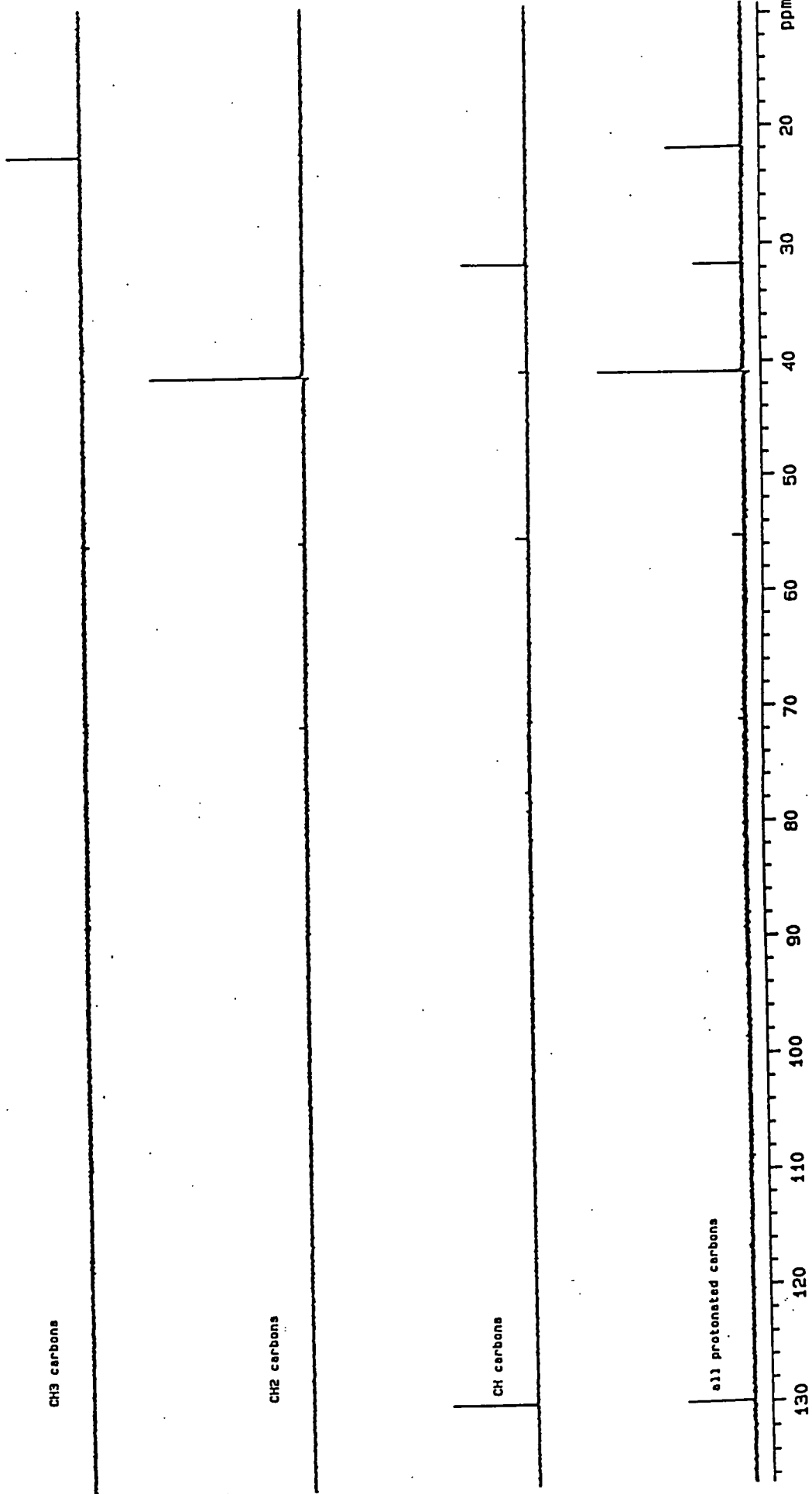
K5 CP-H
FILE /data/curdat/kas24feb.fid
RUN ON Feb 24 84
SOLVENT CDCl3

OBSERVE C13
Frequency 100.626 MHz
Spectral width 25000.0 Hz
Acquisition time 1.199 sec
Relaxation delay 3.000 sec
Pulse width 10.000 usec
Ambient temperature
No. repetitions 512
DECOUPLE H1
High power 40
Decoupler continuously on
Double precision acquisition
DATA PROCESSING
Line broadening 0.8 Hz
FT size 131072
Total acquisition time 35 minutes



Appendix 4.1.22.b ¹³C n.m.r. spectrum of 4-methylcyclopentene

KS CP-H
FILE /data/curdat/ksa24fabc.fid
RUN ON Feb 24 84
SOLVENT CCl3
OBSERVE C13



Appendix 4.1.22.c DEPT spectrum of 4-methylcyclopentene

APPENDIX 5

Analytical data for Chapter 5

Polymer Laboratories
GPC Data Station Ver 4.0

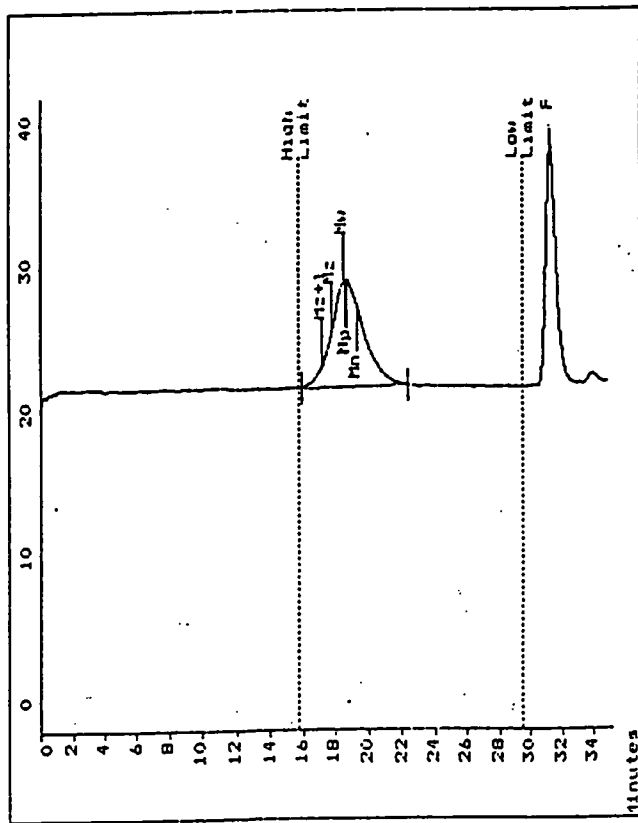
13/19 Fri Mar 11 1994

Unknown CC065.039 acquired GPC Data Station Ver 4.0

Concentration :
Injection Volume :
Solvent : TRICHLOROMETHANE
Column Set :
Method 1
Detector :
Temperature :
Flow Rate :
Standards :

Calibration Using Narrow Standards Curve Used 3rd Order Polynomial
Calibration Limits 15.73 to 29.47 Mins

Flow Rate Marker 1 TOLUENE found at 30.90Mins
Broad Peak Start 1 15.92 End 1 22.43 Mins
found in Standards at 31.28Mins



Molecular Weight Averages
Mn = 123521.9 Mz = 258955.8
Mw = 77759.3 Mz+1 = 435399.3
Mw = 145029. MV = 132698.1
Polydispersity = 1.865

Appendix 5.1.2. GPC trace of P5-2

Polymer Laboratories
GPC Data Station Ver 4.0

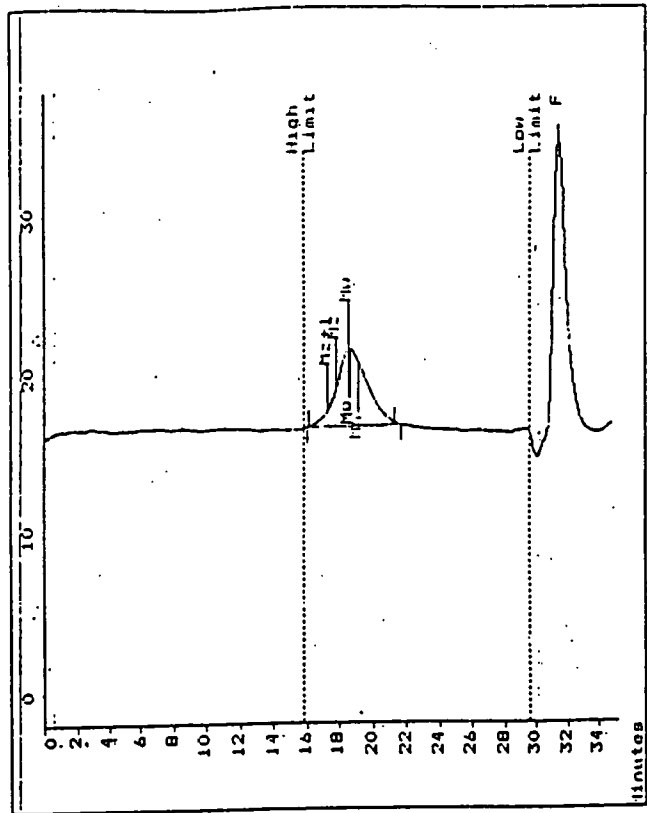
10/17 Tue Mar 22 1994

Unknown CC066.011 acquired GPC Data Station Ver 4.0

Concentration :
Injection Volume :
Solvent : TRICHLOROMETHANE
Column Set :
Method 1
Detector :
Temperature :
Flow Rate :
Standards :

Calibration Using Narrow Standards Curve Used 3rd Order Polynomial
Calibration Limits 15.90 to 29.58 Mins

Flow Rate Marker 1 TOLUENE found at 31.52Mins
Broad Peak Start 1 16.22 End 1 21.33 Mins
found in Standards at 31.47Mins



Molecular Weight Averages
Mn = 145537.0 Mz = 276001.1
Mw = 85731.1 Mz+1 = 478220.1
Mw = 150623. MV = 137732.6
Polydispersity = 1.757

Appendix 5.1.1. GPC trace of P5-1

Polymer Laboratories
GPC Data Station Ver 4.0

11:33 Tue Mar 22 1994

Unknown CC066,012 acquired GPC Data Station Ver 4.0

Concentration :
Injection Volume :
Solvent : TRICHLOROMETHANE
Column Set :
Method : 1
Calibration Using Narrow Standards Curve Used 3rd Order Polynomial
Calibration Limits 15.95 to 29.67 Mins
Flow Rate Marker : TOLUENE found in Standards at 31.32mins
Broad Peak Start : 16.08 End : 21.30 Mins found in Standards at 31.53mins

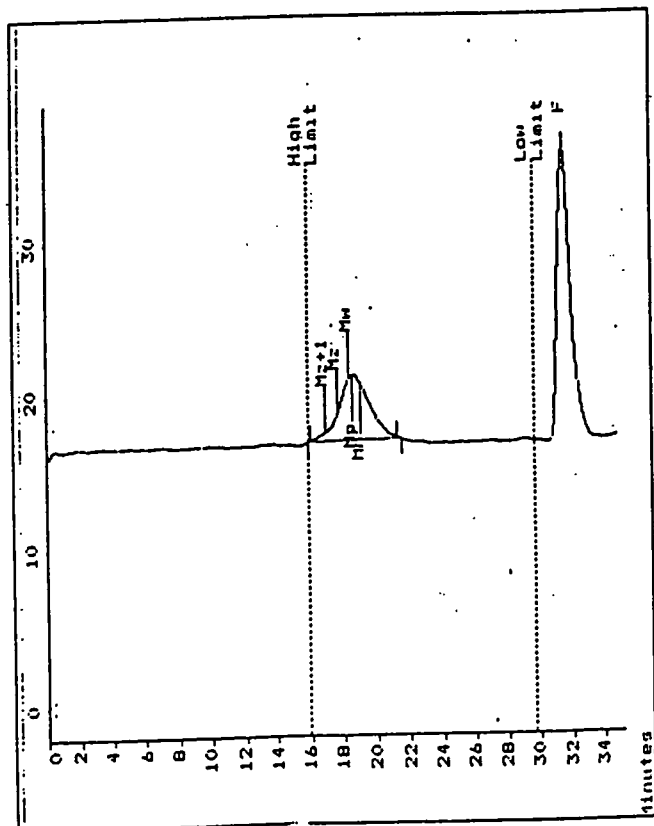
Concentration :
Injection Volume :
Solvent : TRICHLOROMETHANE
Column Set :
Method : 1
Calibration Using Narrow Standards Curve Used 3rd Order Polynomial
Calibration Limits 15.95 to 29.67 Mins
Flow Rate Marker : TOLUENE found in Standards at 31.32mins
Broad Peak Start : 16.02 End : 21.60 Mins

Polymer Laboratories
GPC Data Station Ver 4.0

09:51 Tue Mar 22 1994

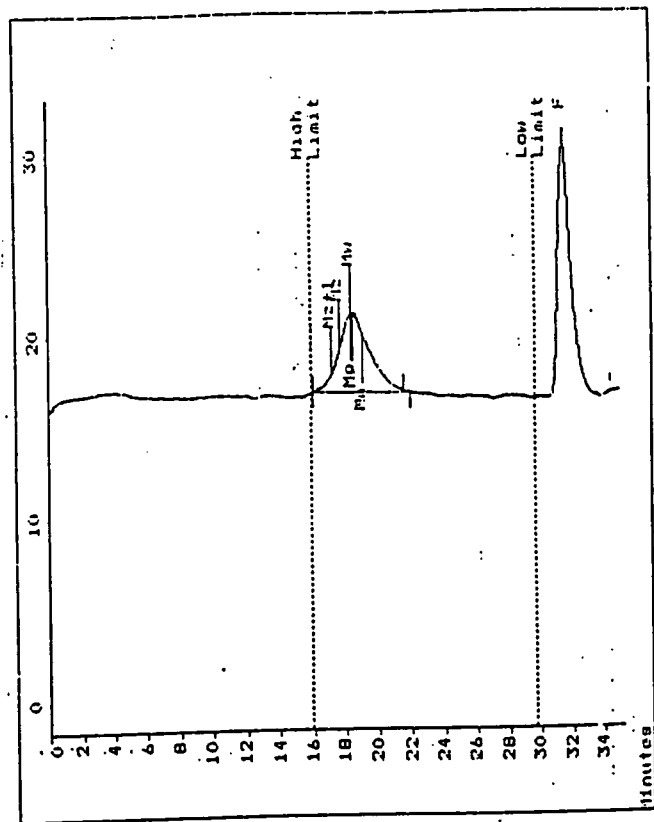
Unknown CC066,010 acquired GPC Data Station Ver 4.0

Concentration :
Injection Volume :
Solvent : TRICHLOROMETHANE
Column Set :
Method : 1
Calibration Using Narrow Standards Curve Used 3rd Order Polynomial
Calibration Limits 15.95 to 29.67 Mins
Flow Rate Marker : TOLUENE found in Standards at 31.32mins
Broad Peak Start : 16.02 End : 21.60 Mins



Appendix 5.1.4. GPC trace of P5-4

Molecular Weight Averages
Mp = 141330.4 Mz = 331234.0
Mn = 90319.3 Mz+1 = 630381.0
Mw = 163410. Mv = 147879.1
Polydispersity = 1.803



Appendix 5.1.3. GPC trace of P5-3

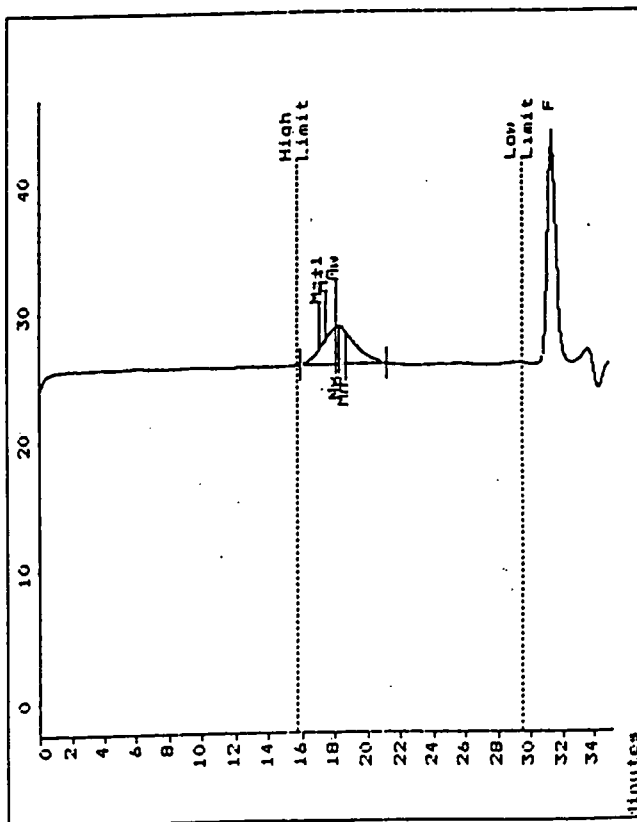
Molecular Weight Averages
Mp = 163180.4 Mz = 313433.8
Mn = 91937.0 Mz+1 = 527893.4
Mw = 171499. Mv = 156279.4
Polydispersity = 1.874

Unknown CC065.041 acquired GPC Data Station Ver 4.0

Concentration :
Injection Volume :
Solvent : TRICHLOROMETHANE
Column Set :
Detector :
Temperature :
Flow Rate :
Standards :

Method 1
Calibration Using Narrow Standards Curve Used 3rd Order Polynomial
Calibration Limits 15.77 to 29.52 Mins

Flow Rate Marker : TOLUENE found at 30.90Mins
Broad Peak Start : 15.97 End : 21.15 Mins in Standards at 31.33Mins



Molecular Weight Averages
Mp = 175092.6 Mz = 345421.0
Mn = 123315. Mz+1 = 498124.8
Mw = 214218. Mw = 198117.5
Polydispersity = 1.737

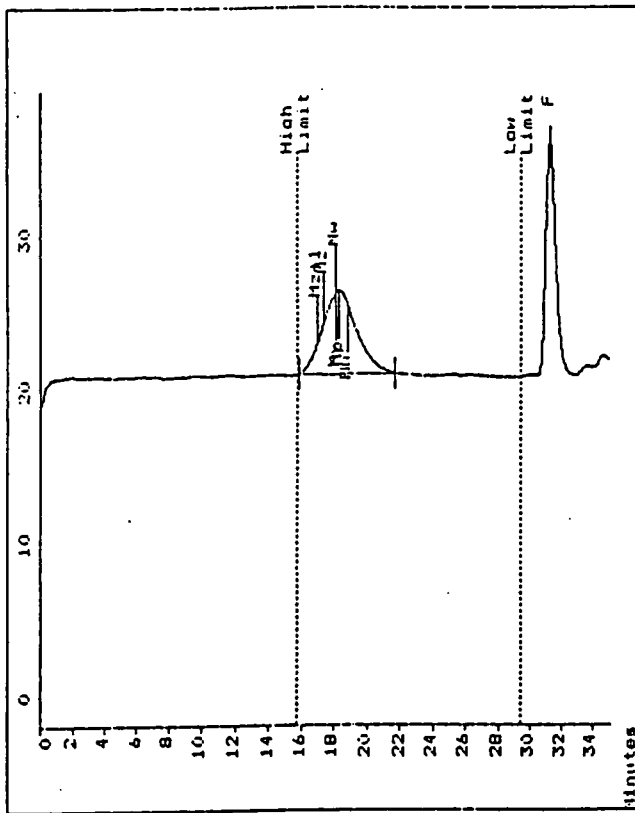
Appendix 5.1.6. GPC trace of P5-6

Unknown CC065.038 acquired GPC Data Station Ver 4.0

Concentration :
Injection Volume :
Solvent : TRICHLOROMETHANE
Column Set :
Detector :
Temperature :
Flow Rate :
Standards :

Method 1
Calibration Using Narrow Standards Curve Used 3rd Order Polynomial
Calibration Limits 15.72 to 29.43 Mins

Flow Rate Marker : TOLUENE found at 30.96Mins
Broad Peak Start : 15.88 End : 21.73 Mins in Standards at 31.25Mins



Molecular Weight Averages
Mp = 165937.5 Mz = 353071.6
Mn = 107085. Mz+1 = 525131.4
Mw = 206721. Mw = 184231.4
Polydispersity = 1.895

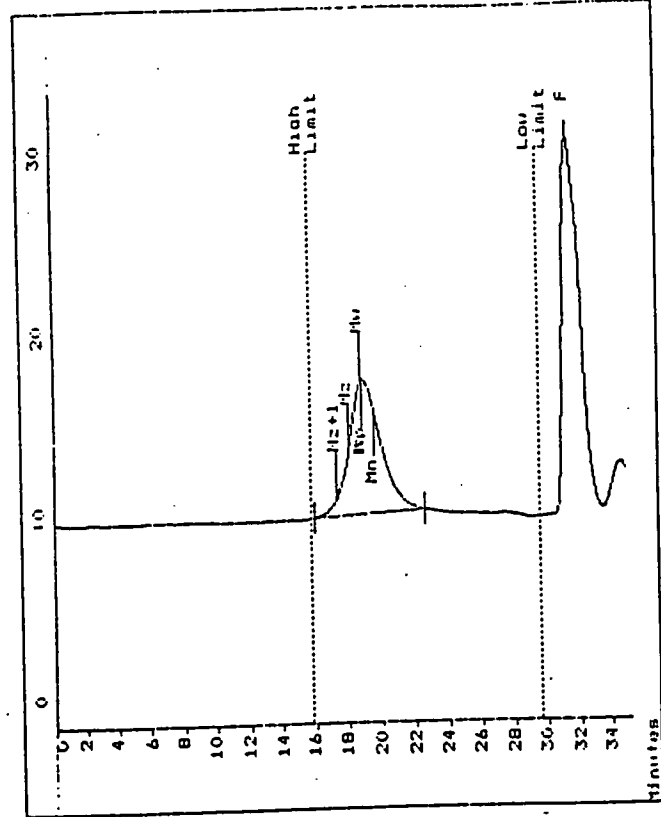
Appendix 5.1.5. GPC trace of P5-5

Polymer Laboratories
 GPC Data Station Ver 4.0
 Unknown CC667.032 acquired GPC Data Station Ver 4.0
 09:20 Wed Mar 30 1994

Concentration :
 Injection Volume :
 Solvent : TRICHLOROETHANE
 Column Set :
 Method 1
 Calibration Using Narrow Standards Curve Used 3rd Order Polynomial
 Calibration Limits 15.90 to 29.58 Mins
 Flow Rate Marker : TOLUENE found at 31.32Mins
 Broad Peak Start : 16.10 End : 22.63 Mins in Standards at 31.47Mins

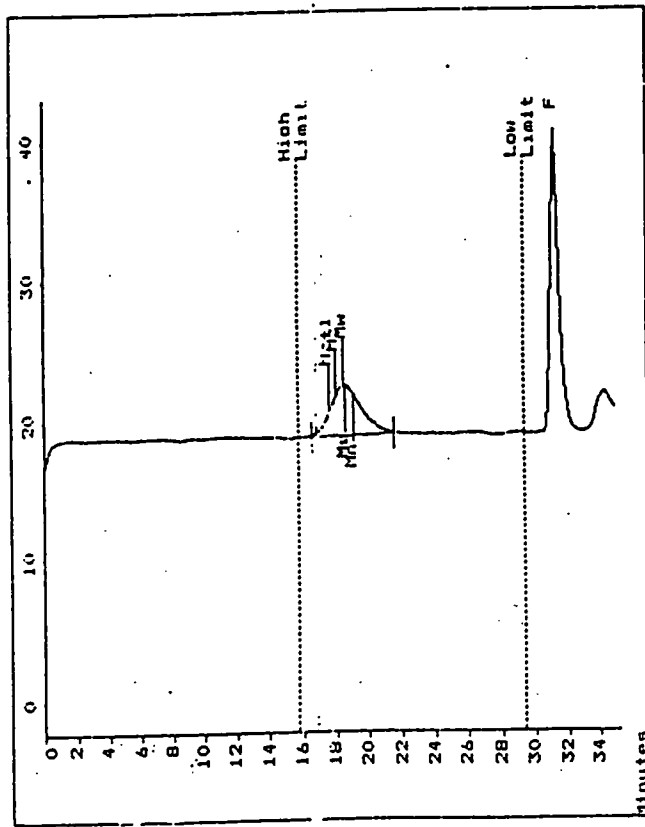
Concentration :
 Injection Volume :
 Solvent : TRICHLOROETHANE
 Column Set :
 Method 1
 Calibration Using Narrow Standards Curve Used 3rd Order Polynomial
 Calibration Limits 15.72 to 29.43 Mins
 Flow Rate Marker : TOLUENE found at 30.90Mins
 Broad Peak Start : 16.55 End : 21.60 Mins in Standards at 31.25Mins

Polymer Laboratories
 GPC Data Station Ver 4.0
 Unknown CC065.019 acquired GPC Data Station Ver 4.0
 11:50 Fri Mar 04 1994



Molecular Weight Averages
 Mp = 105177.3 Mz = 212314.5
 Mn = 60548.4 Mz+1 = 412616.0
 Mw = 110882.0 Mw = 101075.5
 Polydispersity = 1.831

Appendix 5.1.7. GPC trace of P5-7



Molecular Weight Averages
 Mp = 131758.9 Mz = 218853.2
 Mn = 87674.4 Mz+1 = 300429.3
 Mw = 144522.0 Mw = 134450.2
 Polydispersity = 1.648

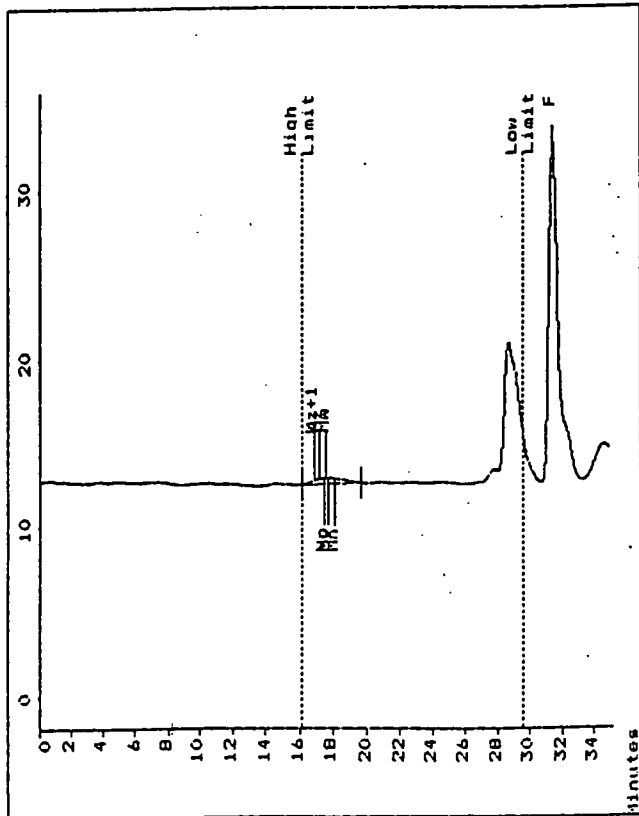
Appendix 5.1.8. GPC trace of P5-8

Polymer Laboratories
GPC Data Station Ver 4.0

Unknown CC071.012 acquired 13:19 Thu May 05 1994 13:17 Fri May 13 1994

Concentration :
Injection Volume :
Solvent : TRICHLOROMETHANE
Column Set :
Method 1
Calibration Using Narrow Standards Curve Used 3rd Order Polynomial
Calibration Limits 16.12 to 29.63 Mins
Flow Rate Marker : TOLUENE found at 31.35Mins
Broad Peak Start : 16.22 End : 19.68 Mins in Standards at 31.48Mins

Detector :
Temperature :
Flow Rate :
Standards :



Appendix 5.1.10. GPC trace of P5-10

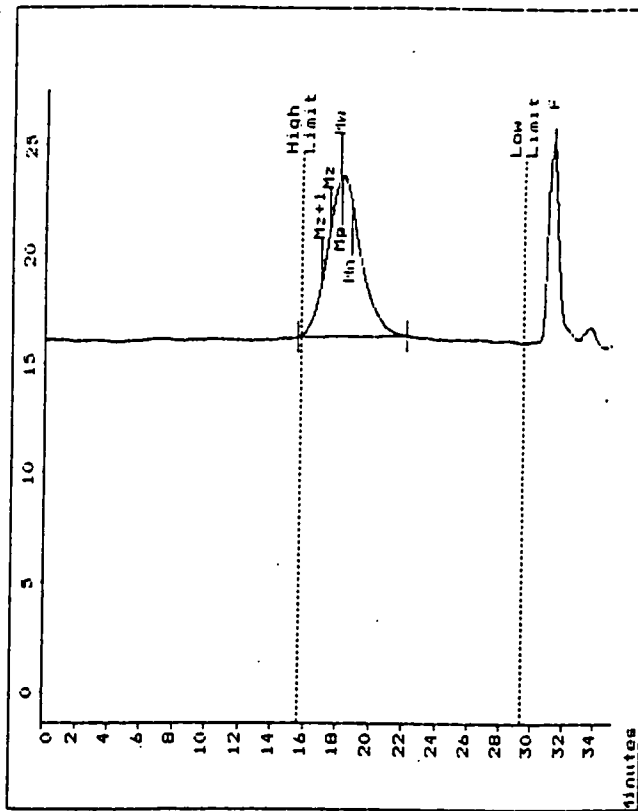
Molecular Weight Averages
Mp = 409054.0 Mz = 562933.9
Mn = 238202.0 Mz+1 = 738436.9
Mw = 379617.0 MV = 355100.6
Polydispersity = 1.594

Polymer Laboratories
GPC Data Station Ver 4.0

Unknown CC069.008 acquired 10:49 Thu Apr 14 1994 12:33 Thu Apr 14 1994

Concentration :
Injection Volume :
Solvent : TRICHLOROMETHANE
Column Set :
Method 1
Calibration Using Narrow Standards Curve Used 3rd Order Polynomial
Calibration Limits 15.68 to 29.45 Mins
Flow Rate Marker : TOLUENE found at 31.28Mins
Broad Peak Start : 15.48 End : 22.15 Mins in Standards at 31.23Mins

Detector :
Temperature :
Flow Rate :
Standards :



Appendix 5.1.9. GPC trace of P5-9

Molecular Weight Averages
Mp = 185781.4 Mz = 360535.8
Mn = 113179.0 Mz+1 = 550149.6
Mw = 212912.0 MV = 195495.2
Polydispersity = 1.881

Polymer Laboratories
 GPC Data Station Ver 4.0
 Unknown CC070.024 acquired 11:45 Wed Apr 27 1994

Polymer Laboratories
 GPC Data Station Ver 4.0
 Unknown CC070.024 acquired 11:45 Wed Apr 27 1994

Concentration :
 Injection Volume :
 Solvent : TRICHLOROMETHANE
 Column Set :

Concentration :
 Injection Volume :
 Solvent : TRICHLOROMETHANE
 Column Set :

Detector :
 Temperature :
 Flow Rate :
 Standards :

Detector :
 Temperature :
 Flow Rate :
 Standards :

Method 1

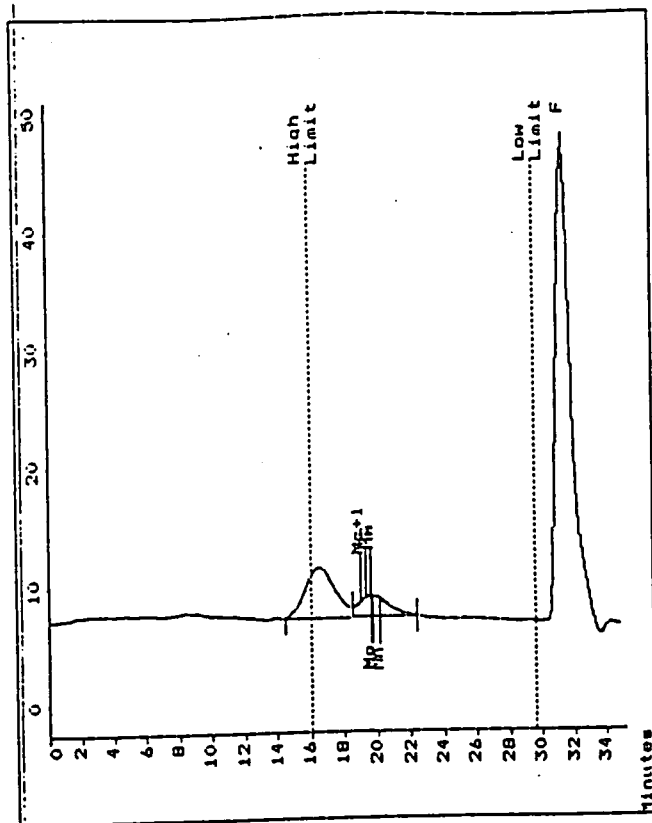
Method 1

Calibration Using Narrow Standards Curve Used 3rd Order Polynomial
 Calibration Limits 16.08 to 29.58 Mins

Calibration Using Narrow Standards Curve Used 3rd Order Polynomial
 Calibration Limits 16.08 to 29.58 Mins

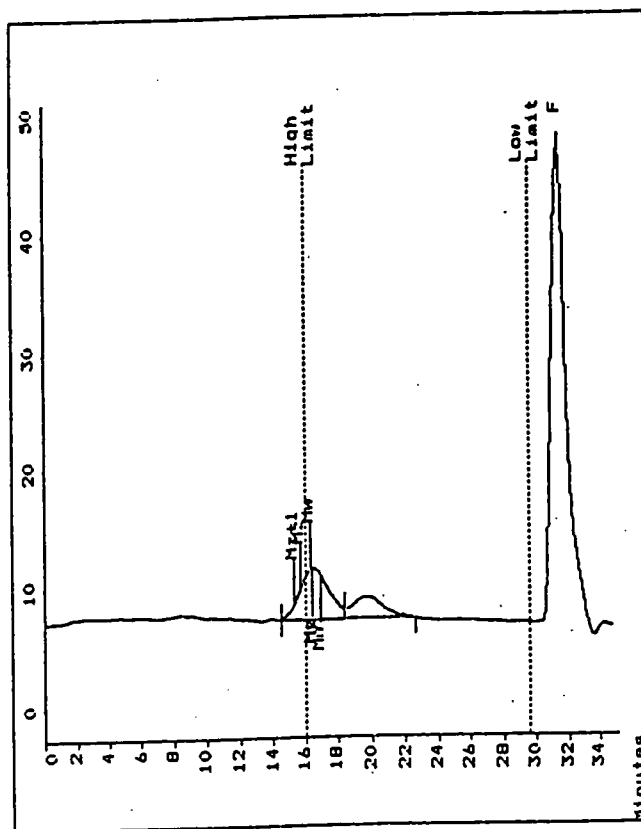
Flow Rate Marker : TOLUENE found at 31.35Mins
 Broad Peak Start : 18.48 End : 22.43 Mins

Flow Rate Marker : TOLUENE found at 31.35Mins
 Broad Peak Start : 14.50 End : 18.43 Mins



Molecular Weight Averages
 Mp = 63271.2 Hz = 80798.7
 Mn = 41247.7 Hz+1 = 99326.7
 Mw = 60111.5 Hz = 57154.0
 Polydispersity = 1.457

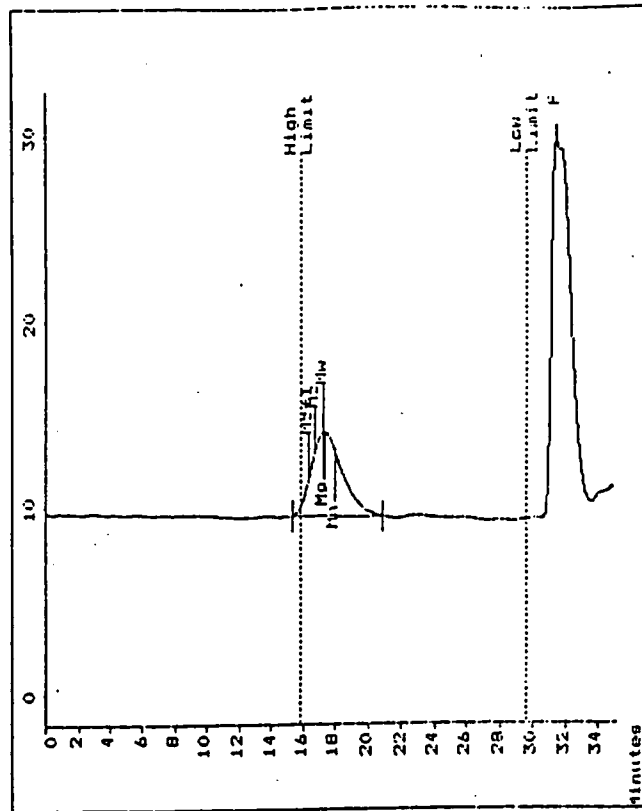
Appendix 5.1.11.a GPC trace of P5-11 (calculation for low mass component)



Molecular Weight Averages
 Mp = 1121591.8 Hz = 2651838.7
 Mn = 690679. Hz+1 = 4393209.4
 Mw = 1359461.3 Hz = 1222404.4
 Polydispersity = 1.968

Appendix 5.1.11.b GPC trace of P5-11 (calculation for high mass component)

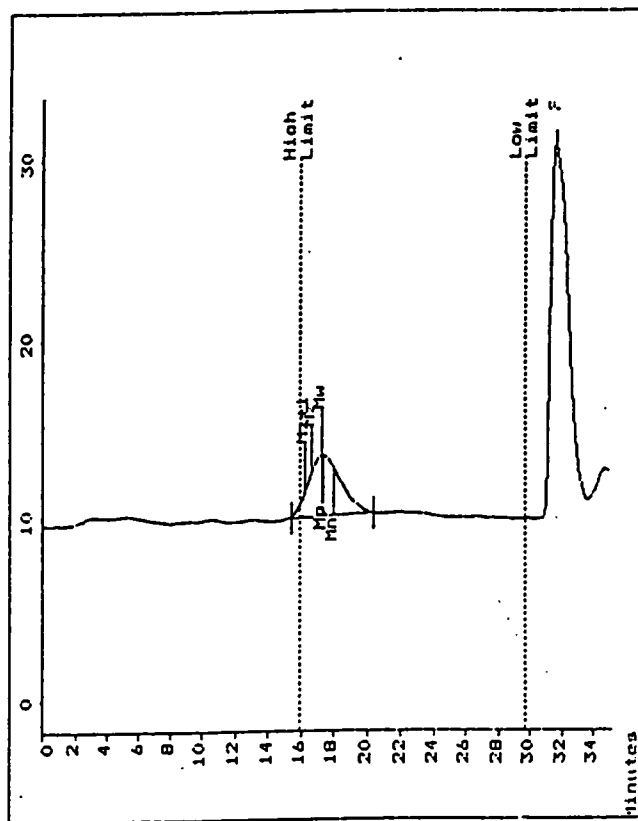
Concentration :
 Injection Volume :
 Solvent : TRICHLOROMETHANE
 Column Set :
 Method 1
 Calibration Using Narrow Standards Curve Used 3rd Order Polynomial
 Calibration Limits 15.88 to 29.57 Mins
 Flow Rate Marker : TOLUENE found at 31.52Min
 Broad Peak Start : 15.32 End : 20.88 Mins found in Standards at 31.48Min



Appendix 5.1.12. GPC trace of P5-12

Molecular Weight Averages
 Mp = 442911.9 Mz = 787318.6
 Mn = 223166. Mz+1 = 1178979.5
 Mw = 451671. MV = 411099.1
 Polydispersity = 2.024

Concentration :
 Injection Volume :
 Solvent : TRICHLOROMETHANE
 Column Set :
 Method 1
 Calibration Using Narrow Standards Curve Used 3rd Order Polynomial
 Calibration Limits 15.98 to 29.73 Mins
 Flow Rate Marker : TOLUENE found at 31.32Mins
 Broad Peak Start : 15.42 End : 20.33 Mins found in Standards at 31.63Mins



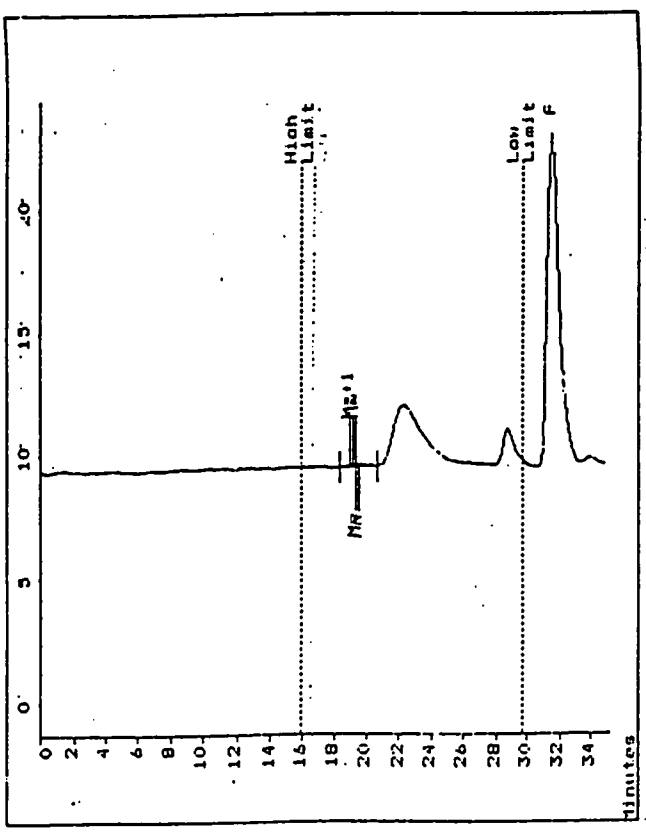
Appendix 5.1.13. GPC trace of P5-13

Molecular Weight Averages
 Mp = 495929.1 Mz = 911802.2
 Mn = 264026. Mz+1 = 1359396.4
 Mw = 519192. MV = 472241.2
 Polydispersity = 1.966

Polymer Laboratories
 GPC Data Station Ver 4.0
 Unknown CC067.043 acquired 11:24 Thu Mar 31 1994

Concentration :
 Injection Volume :
 Solvent : TRICHLOROMETHANE
 Column Set :
 Method 1
 Calibration Using Narrow Standards Curve Used 3rd Order Polynomial
 Calibration Limits 15.93 to 29.68 Mins
 Flow Rate Marker : TOLUENE found at 31.32Mins
 Broad Peak Start : 18.30 End : 20.70 Mins found in Standards at 31.52Mins

Detector :
 Temperature :
 Flow Rate :
 Standards :



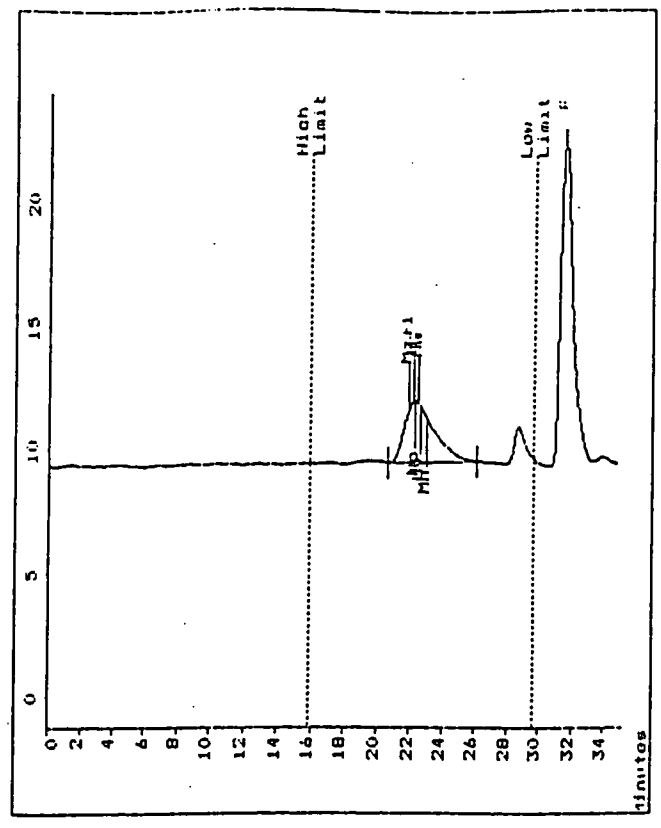
Molecular Weight Averages
 Mp = 76537.8 Mz = 93352.4
 Mn = 65349.2 Mz+1 = 108576.8
 Mw = 78194.3 Mw = 76072.1
 Polydispersity = 1.177

Appendix 5.1.14.b GPC trace of P5-14 (calculation for high mass component)

Polymer Laboratories
 GPC Data Station Ver 4.0
 Unknown CC067.043 acquired 11:24 Thu Mar 31 1994

Concentration :
 Injection Volume :
 Solvent : TRICHLOROMETHANE
 Column Set :
 Method 1
 Calibration Using Narrow Standards Curve Used 3rd Order Polynomial
 Calibration Limits 15.93 to 29.68 Mins
 Flow Rate Marker : TOLUENE found at 31.52Mins
 Broad Peak Start : 20.70 End : 25.09 Mins found in Standards at 31.52Mins

Detector :
 Temperature :
 Flow Rate :
 Standards :

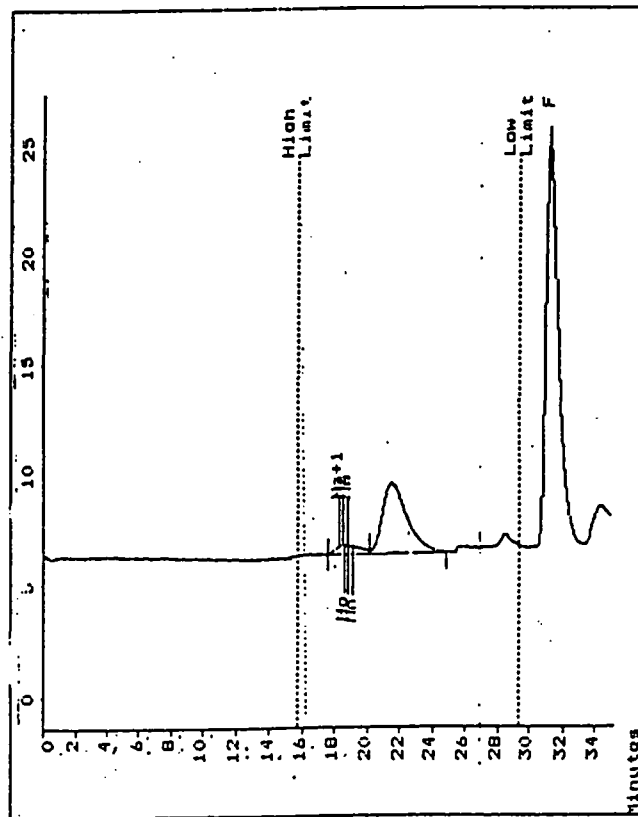


Molecular Weight Averages
 Mp = 9500.5 Mz = 10227.3
 Mn = 5995. Mz+1 = 12110.3
 Mw = 8139. Mw = 7828.4
 Polydispersity = 1.358

Appendix 5.1.14.a GPC trace of P5-14 (calculation for low mass component)

Unknown CC067.040 acquired 15:37 Wed Mar 30 1994

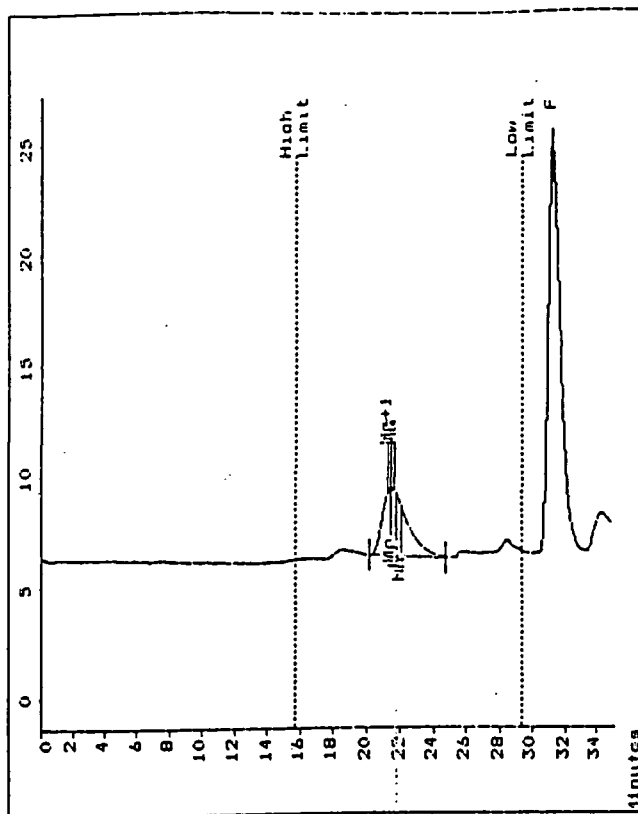
Concentration :
 Injection Volume :
 Solvent : TRICHLOROMETHANE
 Column Set :
 Method 1
 Calibration Using Narrow Standards Curve Used 3rd Order Polynomial
 Calibration Limits 15.78 to 29.38 Mins
 Flow Rate Marker : TOLUENE found at 31.32Mins
 in Standards at 31.25Mins
 Broad Peak Start : 17.62 End : 20.22 Mins



Molecular Weight Averages
 Mo = 11792.0 Mz = 129931.8
 Mn = 82356.9 Mz+1 = 153194.8
 Mw = 104949. HV = 101390.7
 Polydispersity = 1.274

Unknown CC067.040 acquired 15:37 Wed Mar 30 1994

Concentration :
 Injection Volume :
 Solvent : TRICHLOROMETHANE
 Column Set :
 Method 1
 Calibration Using Narrow Standards Curve Used 3rd Order Polynomial
 Calibration Limits 15.78 to 29.38 Mins
 Flow Rate Marker : TOLUENE found at 31.32Mins
 in Standards at 31.25Mins
 Broad Peak Start : 20.22 End : 24.82 Mins



Molecular Weight Averages
 Mp = 13697.1 Mz = 14106.5
 Mn = 9327. Mz+1 = 16042.5
 Mw = 11848.4 HV = 11499.5
 Polydispersity = 1.270

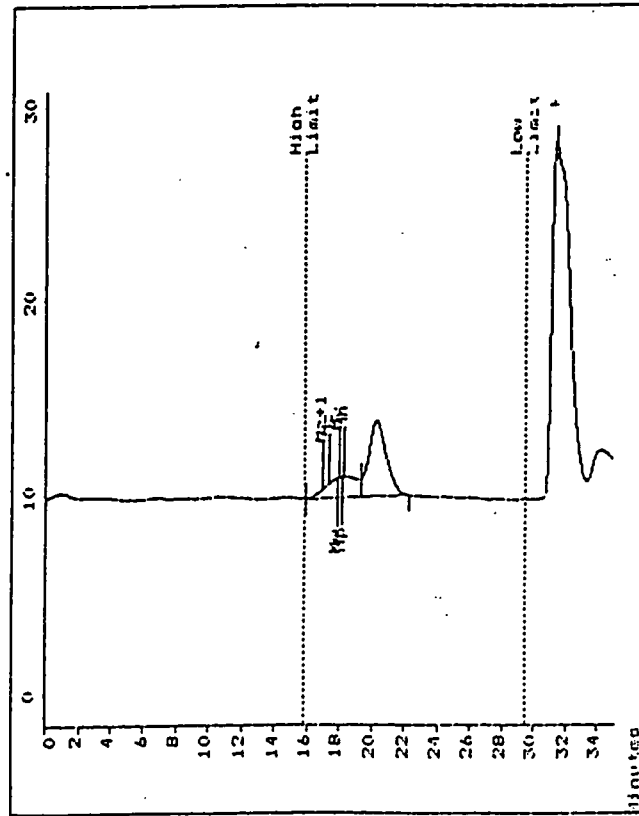
Appendix 5.1.15.a GPC trace of P5-15 (calculation for low mass component)

Appendix 5.1.15.b GPC trace of P5-15 (calculation for high mass component)

Unknown CC067.035 acquired 10:20 Wed Mar 30 1994

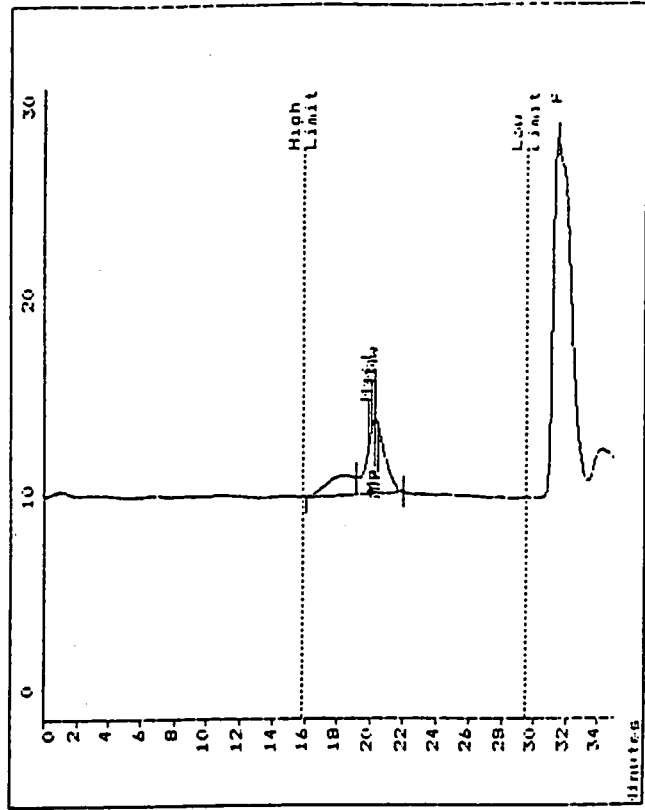
Concentration :
Injection Volume :
Solvent : TRICHLOROMETHANE
Column Set :
Method 1
Calibration Using Narrow Standards Curve Used 3rd Order Polynomial
Calibration Limits 15.87 to 29.53 Mins
Flow Rate Marker : TOLUENE found at 31.32Mins
Broad Peak Start : 18.97 End : 19.30 Mins in Standards at 31.43Mins

Detector :
Temperature :
Flow Rate :
Standards :
Concentration :
Injection Volume :
Solvent : TRICHLOROMETHANE
Column Set :
Method 1
Calibration Using Narrow Standards Curve Used 3rd Order Polynomial
Calibration Limits 15.87 to 29.53 Mins
Flow Rate Marker : TOLUENE found at 31.32Mins
Broad Peak Start : 19.15 End : 22.00 Mins in Standards at 31.43Mins



Molecular Weight Averages
Mn = 181468.3 MZ = 404516.0
Mw = 168735. MZ+1 = 600728.7
Pw = 233255. MZ = 236099.9
Polydispersity = 1.501

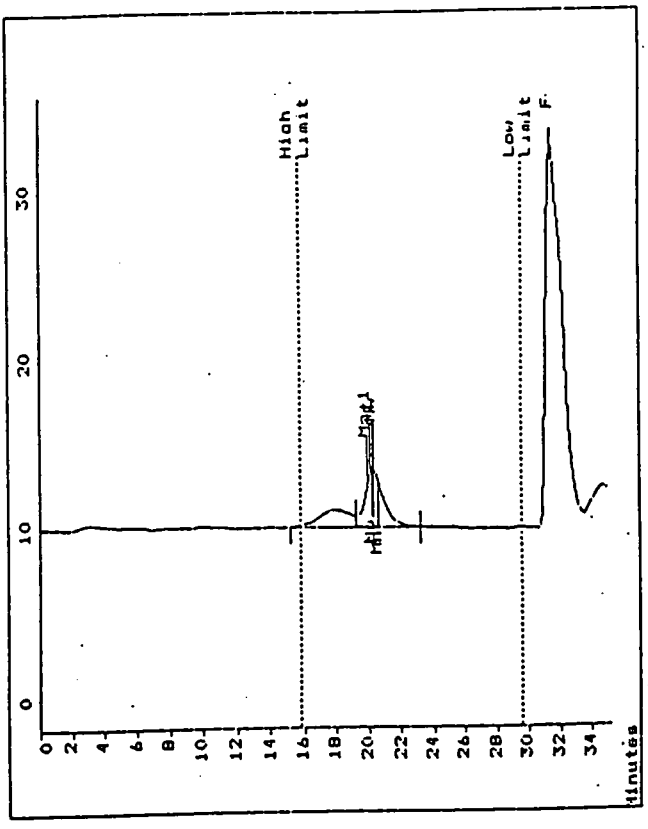
Appendix 5.1.16.a GPC trace of P5-16 (calculation for low mass component)



Molecular Weight Averages
Mn = 36059.2 MZ = 42403.4
Mw = 31302.8 MZ+1 = 48901.9
Pw = 36498.0 MZ = 36656.3
Polydispersity = 1.166

Polymer Laboratories
 GPC Data Station Ver 4.0
 11:02 Wed Mar 30 1994
 Unknown CC067.034 acquired 09:38 Wed Mar 30 1994

Concentration :
 Injection Volume :
 Solvent : TRICHLOROMETHANE
 Column Set :
 Method 1
 Calibration Using Narrow Standards Curve Used 3rd Order Polynomial
 Calibration Limits 15.90 to 29.60 Mins
 Flow Rate Marker : TOLUENE found at 31.32Mins
 in Standards at 31.48Mins
 Broad Peak Start : 19.25 End : 23.23 Mins
 Detector :
 Temperature :
 Flow Rate :
 Standards :

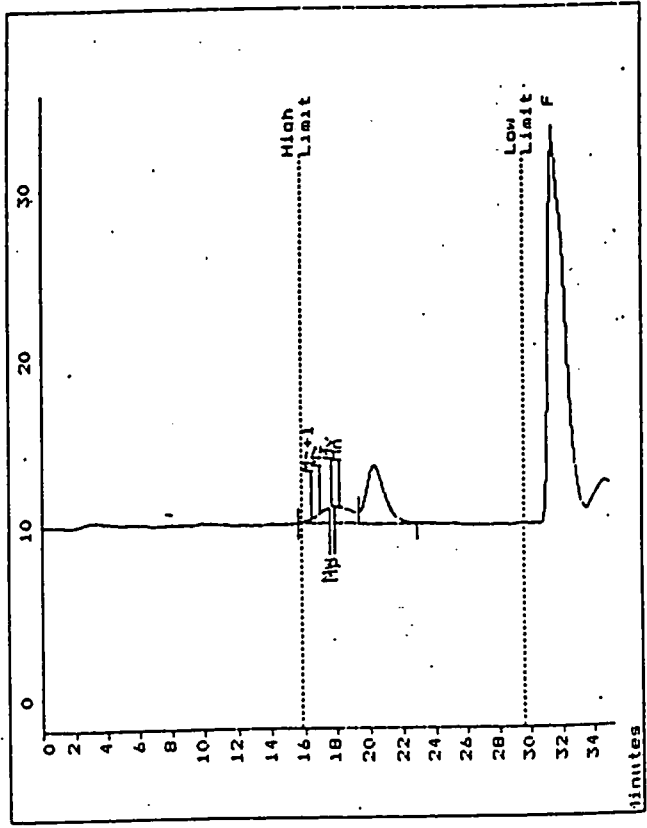


Molecular Weight Averages
 Mp = 36317.9 Mz = 40449.1
 Mn = 28259.2 Mz+1 = 46288.8
 Mw = 34466.3 Mv = 33581.7
 Polydispersity = 1.220

Appendix 5.1.17.a GPC trace of P5-17 (calculation for low mass component)

Polymer Laboratories
 GPC Data Station Ver 4.0
 10:49 Wed Mar 30 1994
 Unknown CC067.034 acquired 09:38 Wed Mar 30 1994

Concentration :
 Injection Volume :
 Solvent : TRICHLOROMETHANE
 Column Set :
 Method 1
 Calibration Using Narrow Standards Curve Used 3rd Order Polynomial
 Calibration Limits 15.90 to 29.60 Mins.
 Flow Rate Marker : TOLUENE found at 31.32Mins
 in Standards at 31.48Mins
 Broad Peak Start : 15.63 End : 19.32 Mins
 Detector :
 Temperature :
 Flow Rate :
 Standards :



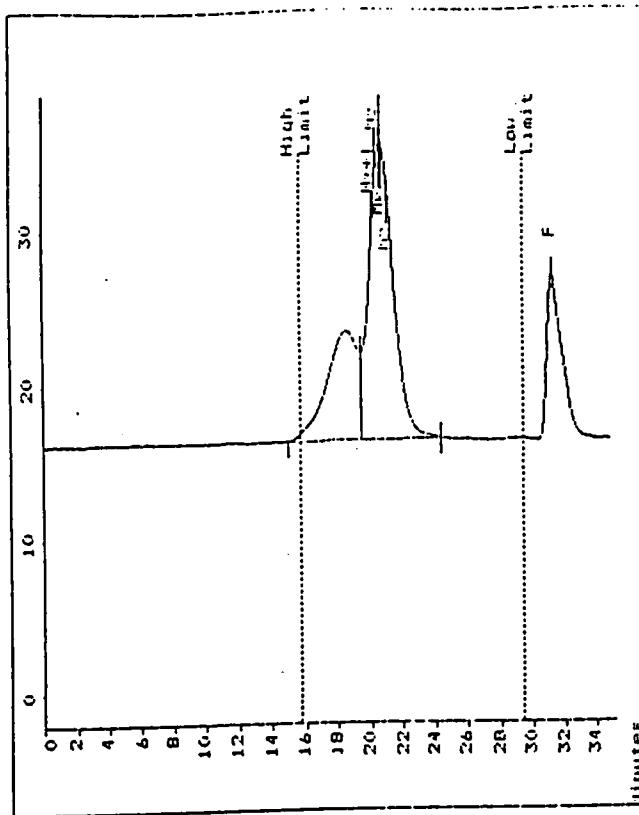
Molecular Weight Averages
 Mp = 257015.0 Mz = 618561.1
 Mn = 197944. Mz+1 = 1028874.9
 Mw = 333314. Mv = 304076.3
 Polydispersity = 1.684

Appendix 5.1.17.b GPC trace of P5-17 (calculation for high mass component)

Polymer Laboratories
 GPC Data Station Ver 4.0
 Unknown K3.001 acquired 11:03 Tue Apr 05 1994

Concentration :
 Injection Volume :
 Solvent : TRICHLOROMETHANE
 Column Set :
 Method 1
 Calibration Using Narrow Standards Curve Used 3rd Order Polynomial
 Calibration Limits 15.78 to 29.38 Mins
 Flow Rate Marker : TOLUENE found at 31.32Mins
 Broad Peak Start : 15.43 End : 24.53 in Standards at 31.25Mins

Detector :
 Temperature :
 Flow Rate :
 Standards :



Molecular Weight Averages
 M_p = 24614.5 M_w = 30614.5
 M_n = 18922.6 M_{w+1} = 25391.4
 M_w = 24691.5 M_w = 23839.4
 Polydispersity = 1.305

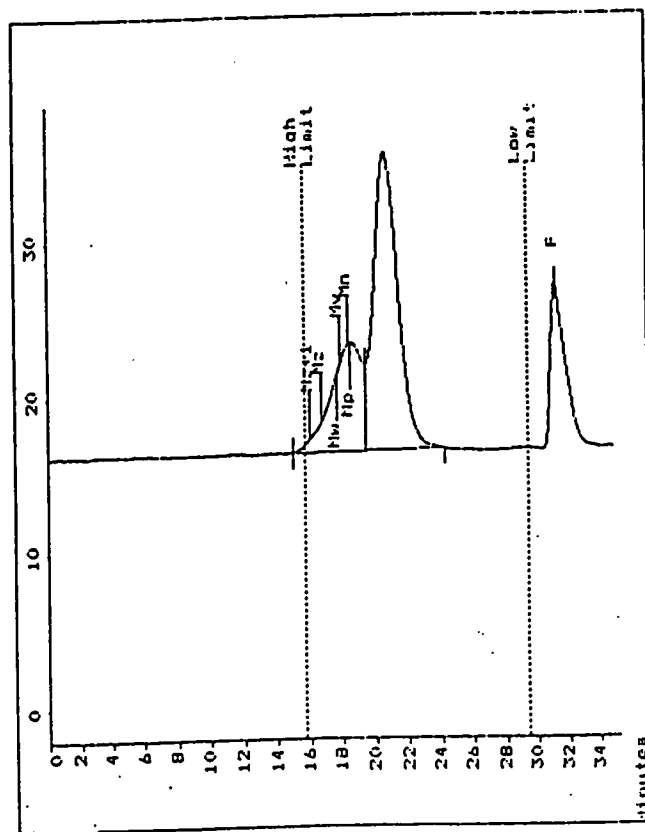
Appendix 5.1.17.c GPC trace of P5-17

(analysis of the sample of 1.3% concentration; calculation for low mass component)

Polymer Laboratories
 GPC Data Station Ver 4.0
 Unknown K3.001 acquired 11:03 Tue Apr 05 1994

Concentration :
 Injection Volume :
 Solvent : TRICHLOROMETHANE
 Column Set :
 Method 1
 Calibration Using Narrow Standards Curve Used 3rd Order Polynomial
 Calibration Limits 15.78 to 29.38 Mins
 Flow Rate Marker : TOLUENE found at 31.32Mins
 Broad Peak Start : 15.07 End : 19.40 in Standards at 31.25Mins

Detector :
 Temperature :
 Flow Rate :
 Standards :



Molecular Weight Averages
 M_p = 129433.7 M_w = 658652.8
 M_n = 145898. M_{w+1} = 1373426.2
 M_w = 264410. M_w = 233559.4
 Polydispersity = 1.812

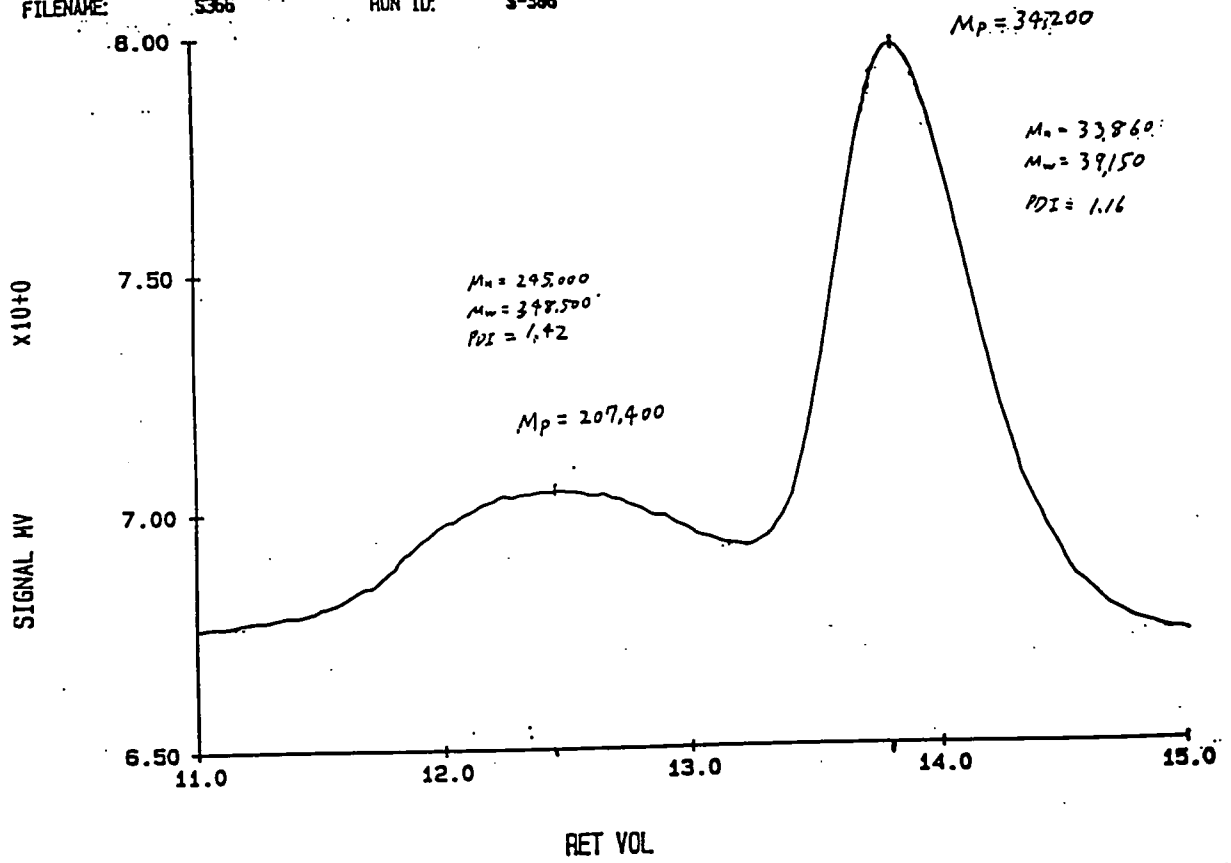
Appendix 5.1.17.d GPC trace of P5-17

(analysis of the sample of 1.3% concentration; calculation for high mass component)

VISCOTEK COHP.
FILENAME: S366

UCAL 4.03
RUN ID: S-366

ENDED: 04/07/94 12:35

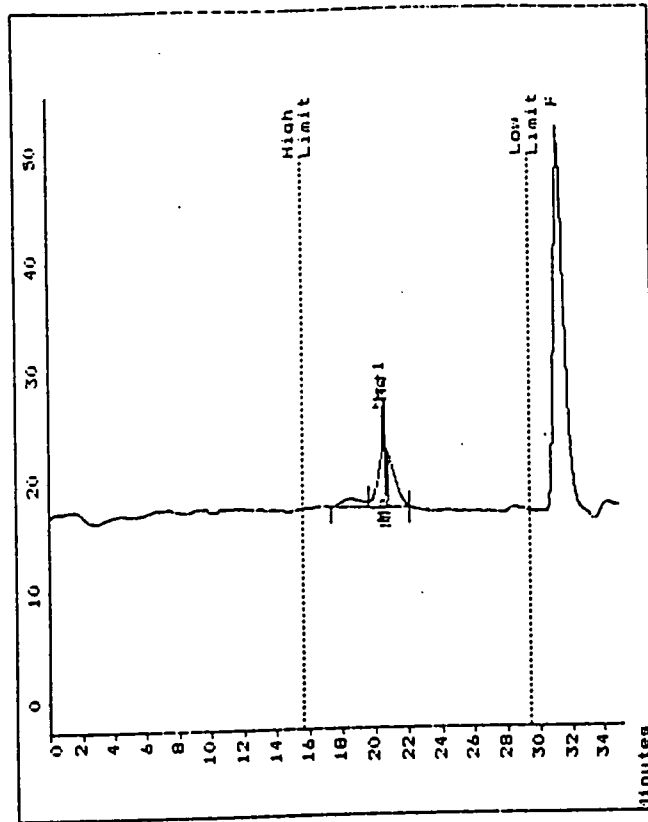


Appendix 5.1.17.e GPC trace of P5-17 (analysis using THF as the eluent)

Polymer Laboratories
 GPC Data Station Ver 4.0
 Unknown CC065.029 acquired 16:31 Wed Mar 09 1994

Concentration :
 Injection Volume :
 Solvent : TRICHLOROMETHANE
 Column Set :
 Method 1
 Calibration Using Narrow Standards Curve Used 3rd Order Polynomial
 Calibration Limits 15.70 to 29.40 Mins
 Flow Rate Marker : TOLUENE found at 30.90Mins
 in Standards at 31.20Mins
 Broad Peak Start : 19.68 End : 22.12 Mins

Appendix 5.1.18.a GPC trace of P5-18 (calculation for low mass component)

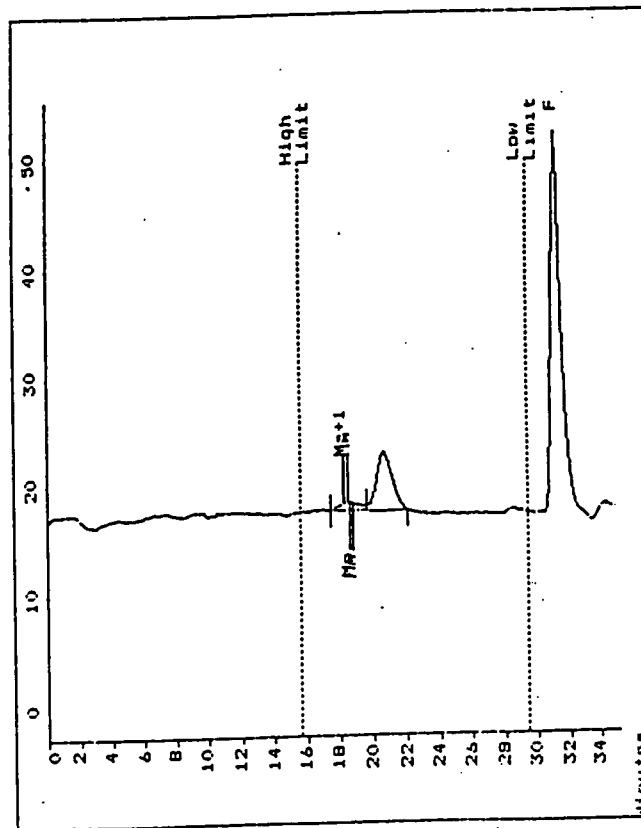


Molecular Weight Averages
 Mo = 26408.9 Mz = 48572.3
 Mn = 23359.8 Mz+1 = 31319.3
 Mw = 25897.9 Mv = 25509.4
 Polydispersity = 1.109

Polymer Laboratories
 GPC Data Station Ver 4.0
 Unknown CC065.029 acquired 16:31 Wed Mar 09 1994

Concentration :
 Injection Volume :
 Solvent : TRICHLOROMETHANE
 Column Set :
 Method 1
 Calibration Using Narrow Standards Curve Used 3rd Order Polynomial
 Calibration Limits 15.70 to 29.40 Mins
 Flow Rate Marker : TOLUENE found at 30.90Mins
 in Standards at 31.20Mins
 Broad Peak Start : 17.48 End : 19.63 Mins

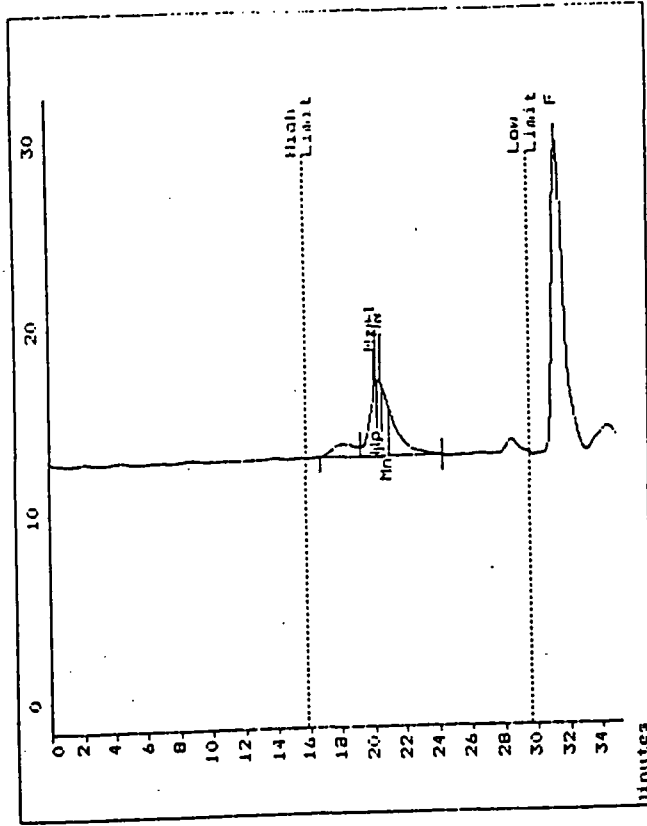
Appendix 5.1.18.b GPC trace of P5-18 (calculation for high mass component)



Molecular Weight Averages
 Mo = 123336.0 Mz = 187618.5
 Mn = 112828.0 Mz+1 = 104987.0
 Mw = 133882.0 Mv = 130496.3
 Polydispersity = 1.187

Polymer Laboratories
 GPC Data Station Ver 4.0
 13:25 Mon Apr 11 1994
 Unknown CC06B.01B acquired 13:13 Mon Apr 11 1994

Concentration :
 Injection Volume :
 Solvent : TRICHLOROMETHANE
 Column Set :
 Method 1
 Calibration Using Narrow Standards Curve Used 3rd Order Polynomial
 Calibration Limits 15.87 to 29.57 Mins
 Flow Rate Marker : TOLUENE found at 31.38Mins
 Broad Peak Start : 19.23 End : 24.23 Mins
 Detector Temperature :
 Flow Rate Standards :

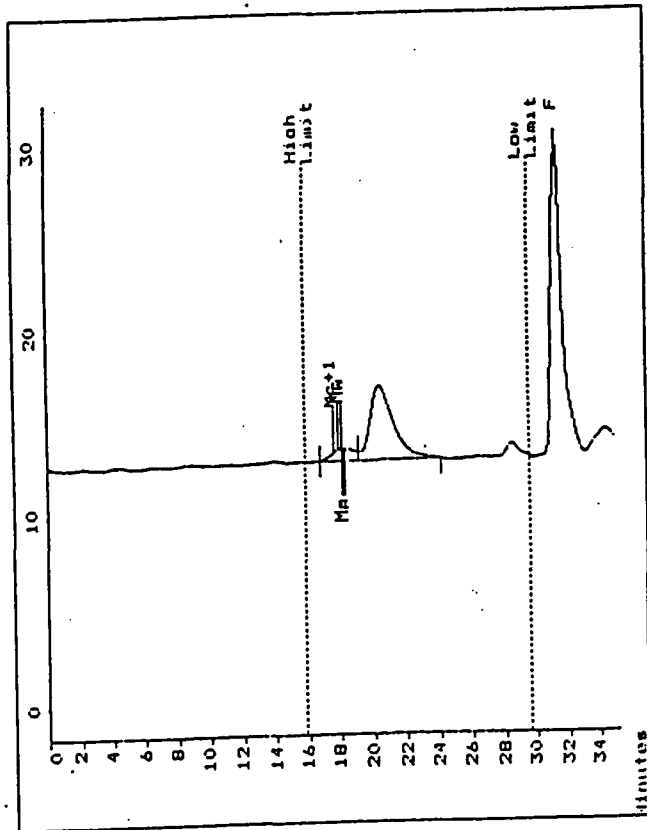


Molecular Weight Averages
 M_w = 35121.7 M_n = 36032.8
 M_w = 21542.9 M_n = 44772.4
 M_w = 30418.2 M_n = 29249.6
 Polydispersity = 1.112

Appendix 5.1.19.a GPC trace of P5-19 (calculation for low mass component)

Polymer Laboratories
 GPC Data Station Ver 4.0
 13:29 Mon Apr 11 1994
 Unknown CC06B.01B acquired 13:13 Mon Apr 11 1994

Concentration :
 Injection Volume :
 Solvent : TRICHLOROMETHANE
 Column Set :
 Method 1
 Calibration Using Narrow Standards Curve Used 3rd Order Polynomial
 Calibration Limits 15.87 to 29.57 Mins
 Flow Rate Marker : TOLUENE found at 31.38Mins
 Broad Peak Start : 16.82 End : 19.18 Mins
 Detector Temperature :
 Flow Rate Standards :



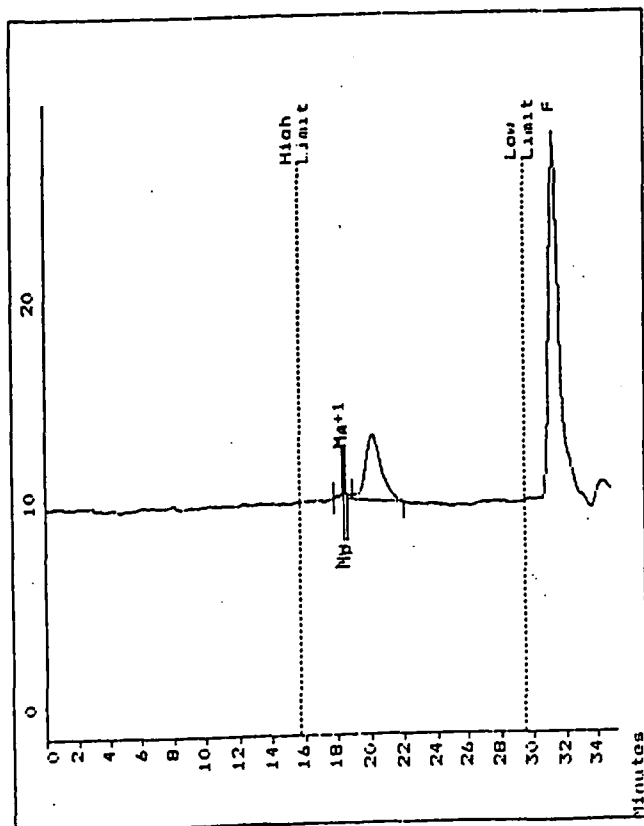
Molecular Weight Averages
 M_w = 195143.4 M_n = 261413.2
 M_w = 172918. M_n = 315211.7
 M_w = 211780. M_n = 205103.3
 Polydispersity = 1.225

Appendix 5.1.19.b GPC trace of P5-19 (calculation for high mass component)

Polymer Laboratories
 GPC Data Station Ver 4.0
 Unknown CC06B.017 acquired 15:19 Fri Apr 08 1994

13:02 Mon Apr 11 1994

Concentration :
 Injection Volume :
 Solvent : TRICHLOROMETHANE
 Column Set :
 Method 1
 Calibration Using Narrow Standards Curve Used 3rd Order Polynomial
 Calibration Limits 15.80 to 29.48 Mins
 Flow Rate Marker : TOLUENE found at 31.38Mins
 in Standards at 31.38Mins
 Broad Peak Start : 17.83 End : 18.97 Mins



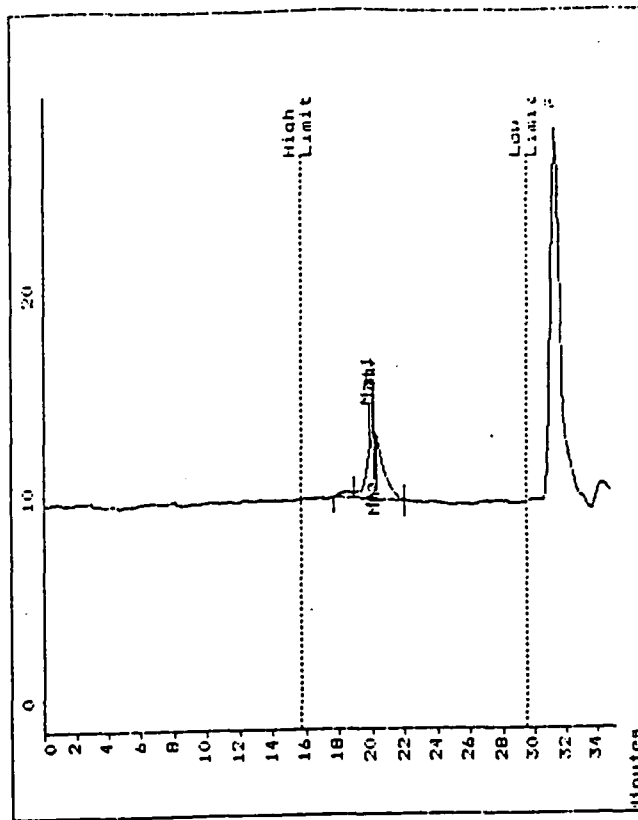
Molecular Weight Averages
 Mp = 135540.1 Mz = 16133.3
 Mn = 144093. Mz+1 = 171021.4
 Mw = 152398. Mv = 151082.0
 Polydispersity = 1.058

Page 1

Polymer Laboratories
 GPC Data Station Ver 4.0
 Unknown CC06B.017 acquired 15:19 Fri Apr 08 1994

12:59 Mon Apr 11 1994

Concentration :
 Injection Volume :
 Solvent : TRICHLOROMETHANE
 Column Set :
 Method 1
 Calibration Using Narrow Standards Curve Used 3rd Order Polynomial
 Calibration Limits 15.80 to 29.48 Mins
 Flow Rate Marker : TOLUENE found at 31.38Mins
 in Standards at 31.38Mins
 Broad Peak Start : 18.98 End : 22.03 Mins



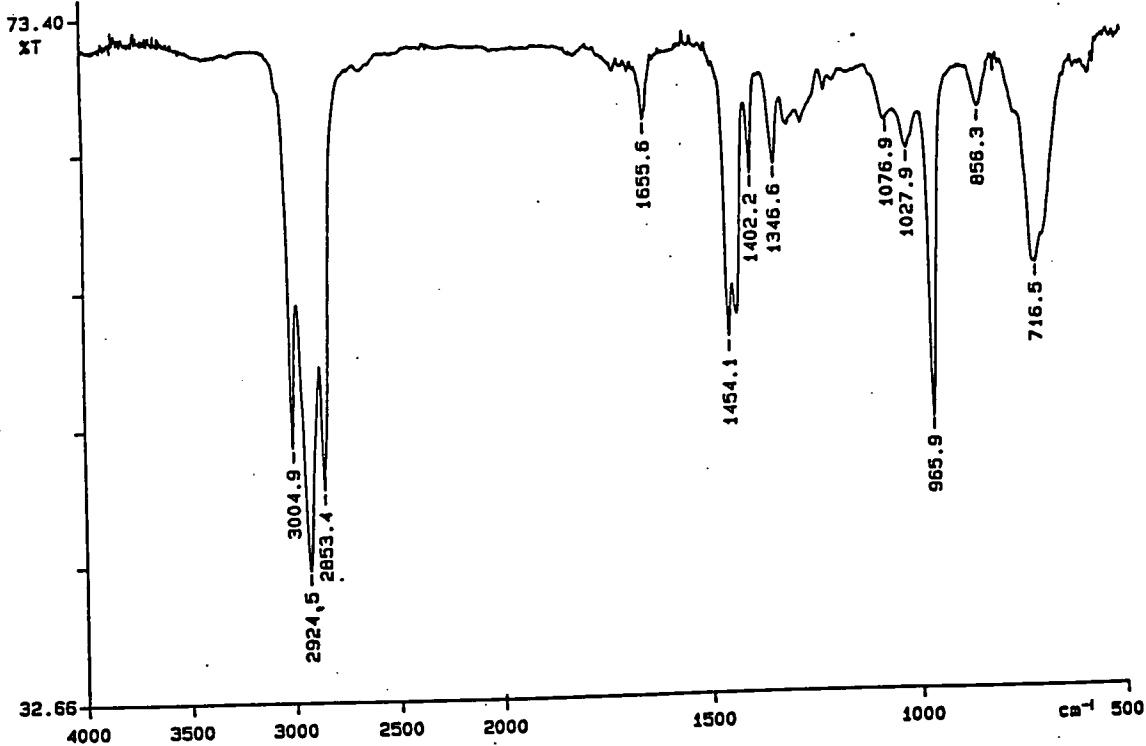
Molecular Weight Averages
 Mp = 38837.1 Mz = 44033.5
 Mn = 33373.9 Mz+1 = 50095.3
 Mw = 38501.0 Mv = 37716.3
 Polydispersity = 1.154

Page 1

Appendix 5.1.20.a GPC trace of P5-20 (calculation for low mass component)

Appendix 5.1.20.b GPC trace of P5-20 (calculation for high mass component)

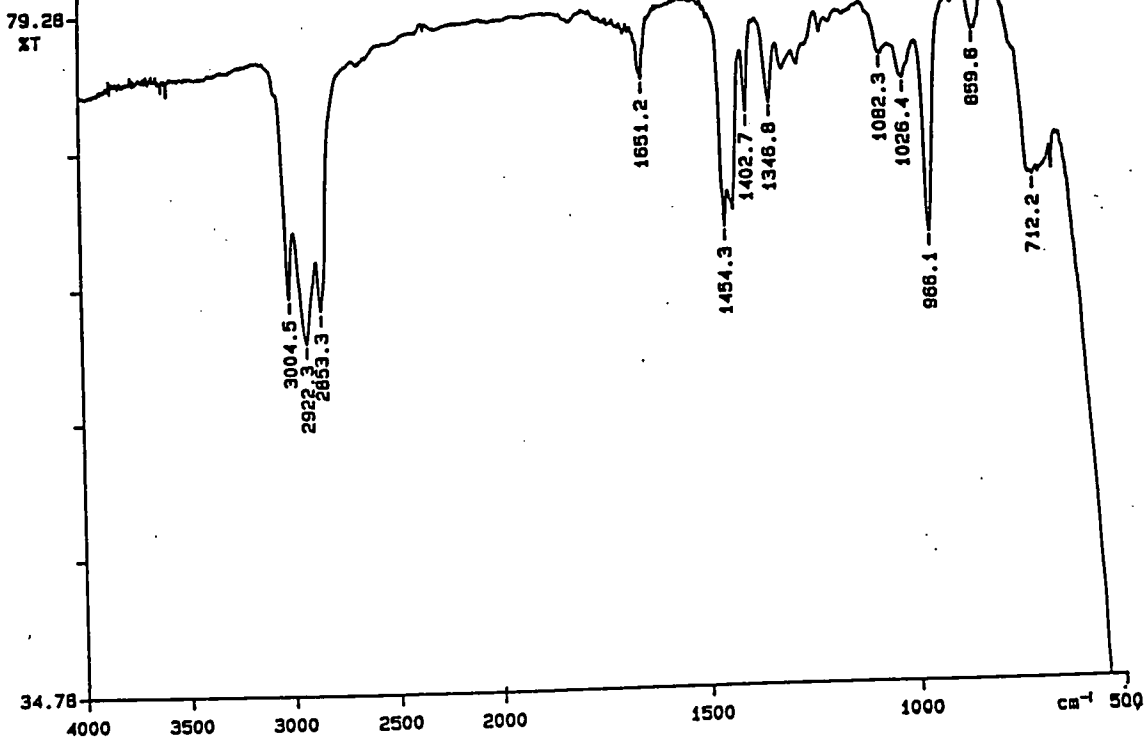
PERKIN ELMER



Appendix 5.2.1. Infrared spectrum of P5-1

94/05/16 10:35 red
X: 4 scans, 4.0 cm^{-1} , flat

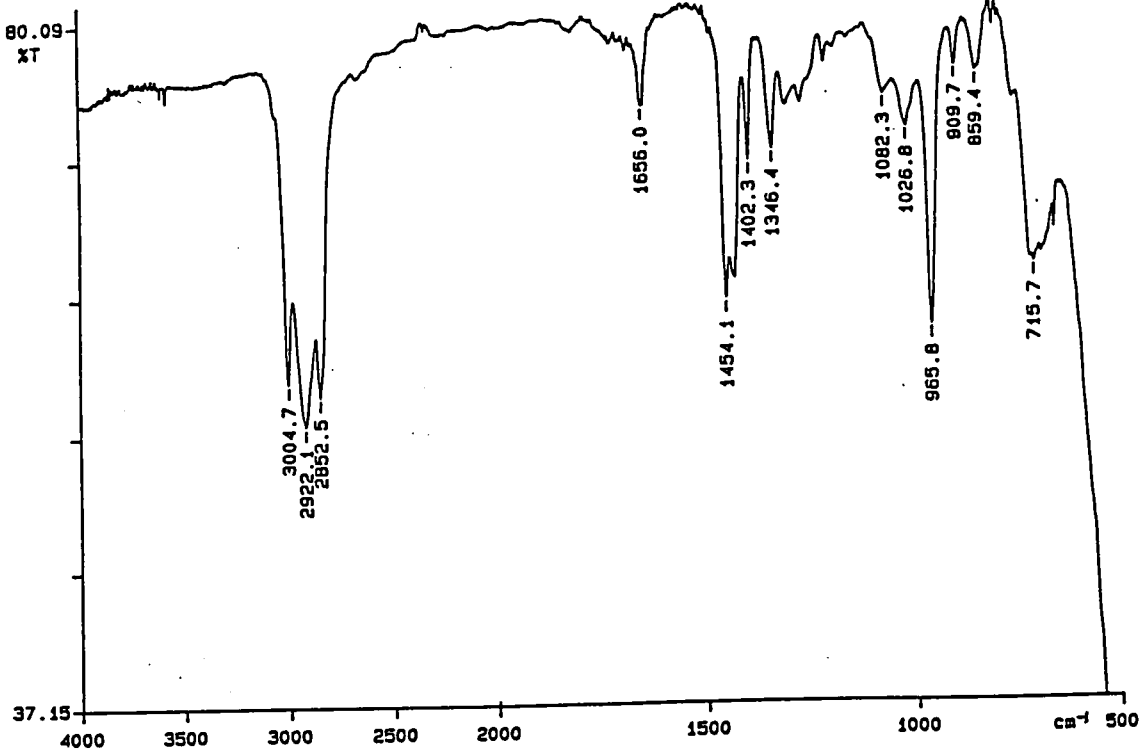
PERKIN ELMER



Appendix 5.2.2. Infrared spectrum of P5-2

94/05/16 10:13 red
X: 4 scans, 4.0 cm^{-1}

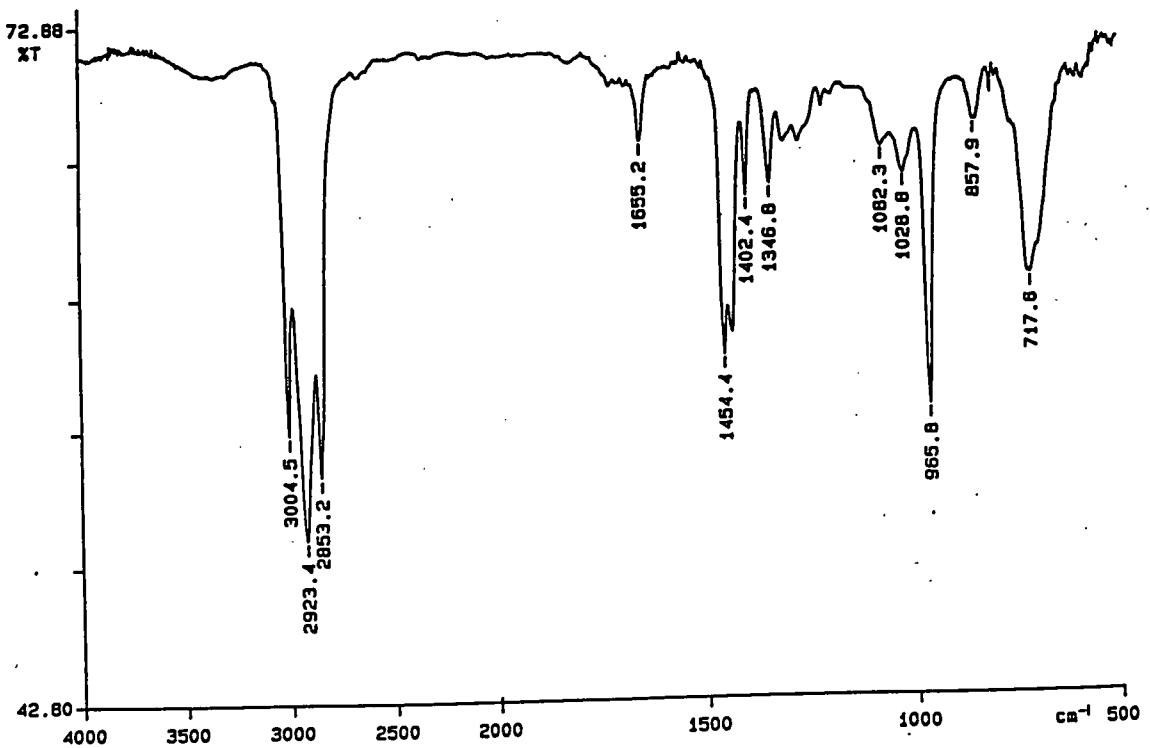
PERKIN ELMER



94/05/16 10:27 red
X: 4 scans, 4.0 cm^{-1}

Appendix 5.2.3. Infrared spectrum of P5-3

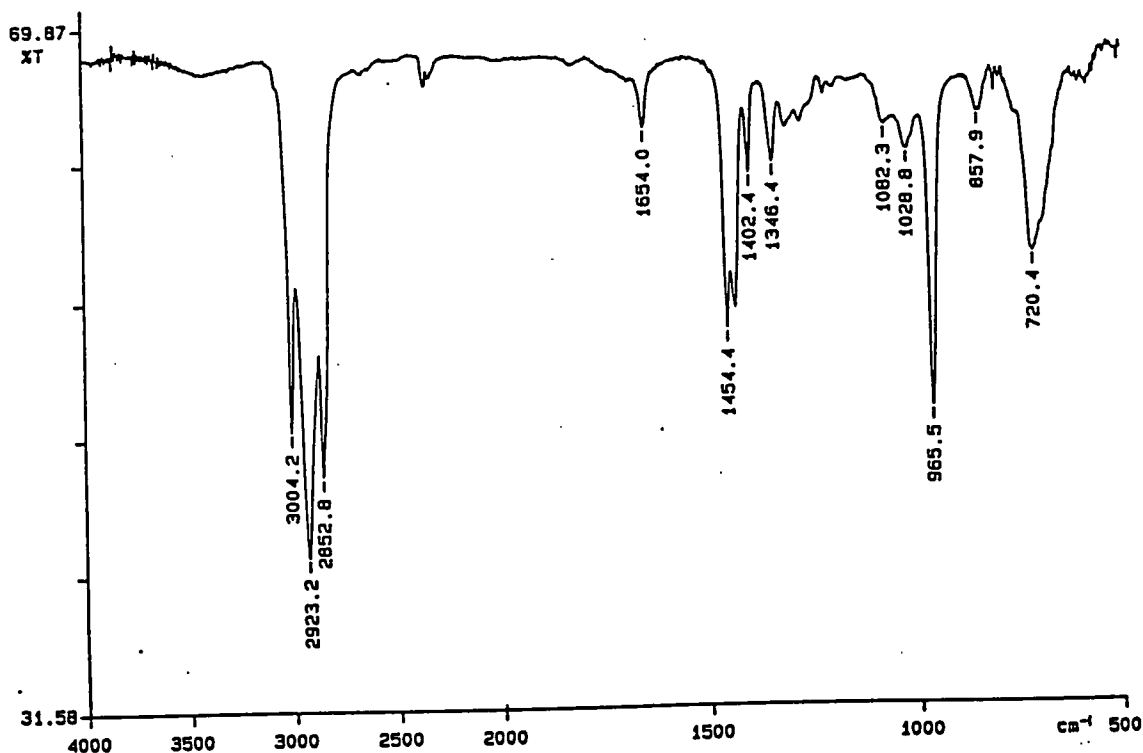
PERKIN ELMER



94/05/16 10:51 red
X: 16 scans, 4.0 cm^{-1} , flat

Appendix 5.2.4. Infrared spectrum of P5-4

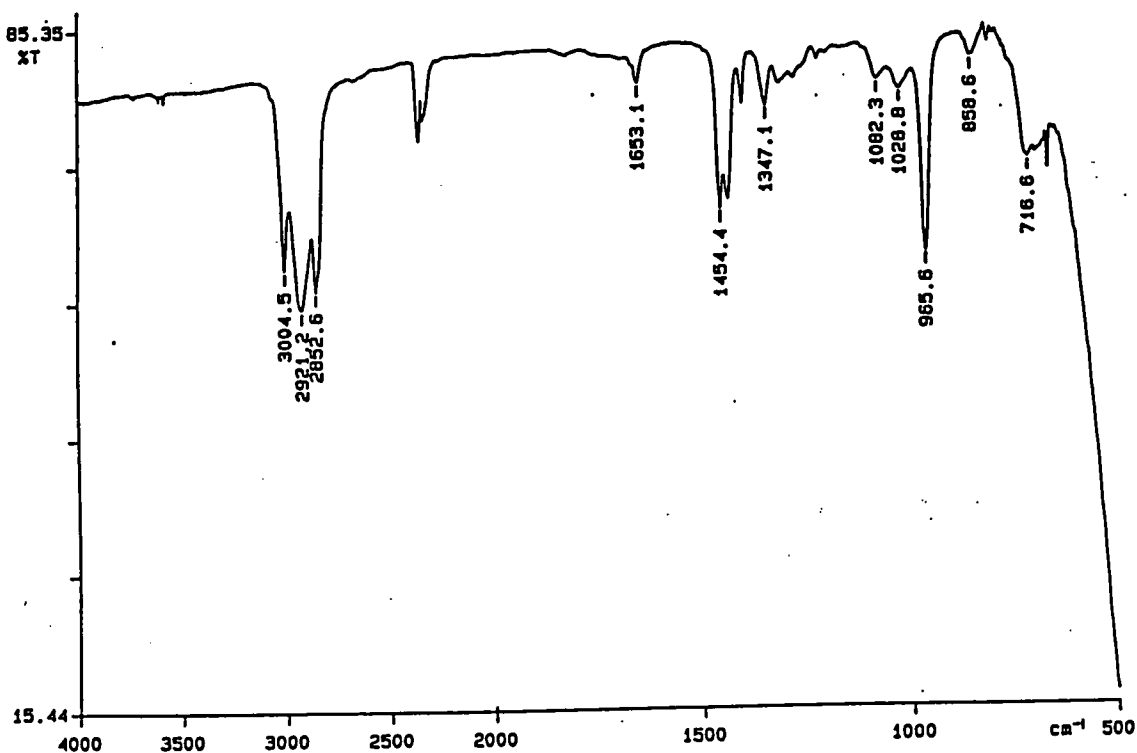
PERKIN ELMER



Appendix 5.2.5. Infrared spectrum of P5-5

94/05/16 09: 57 red
X: 4 scans, 4.0cm-1, flat

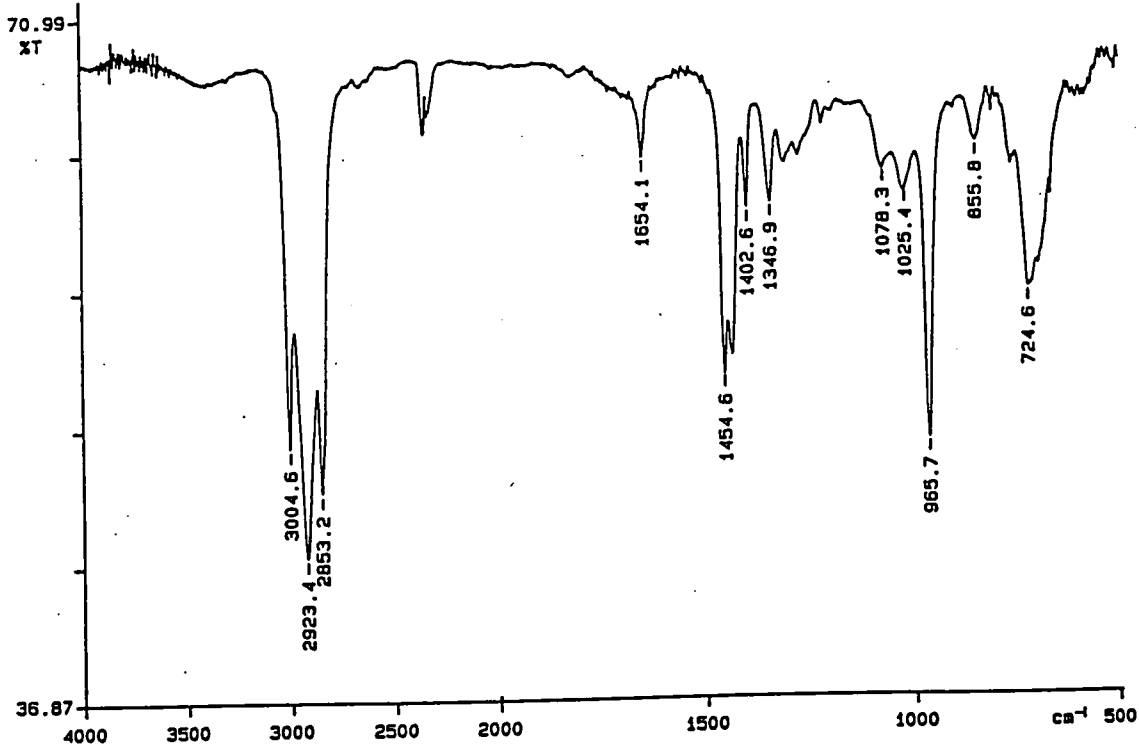
PERKIN ELMER



Appendix 5.2.6. Infrared spectrum of P5-6

94/05/16 09: 54 red
X: 4 scans, 4.0cm-1

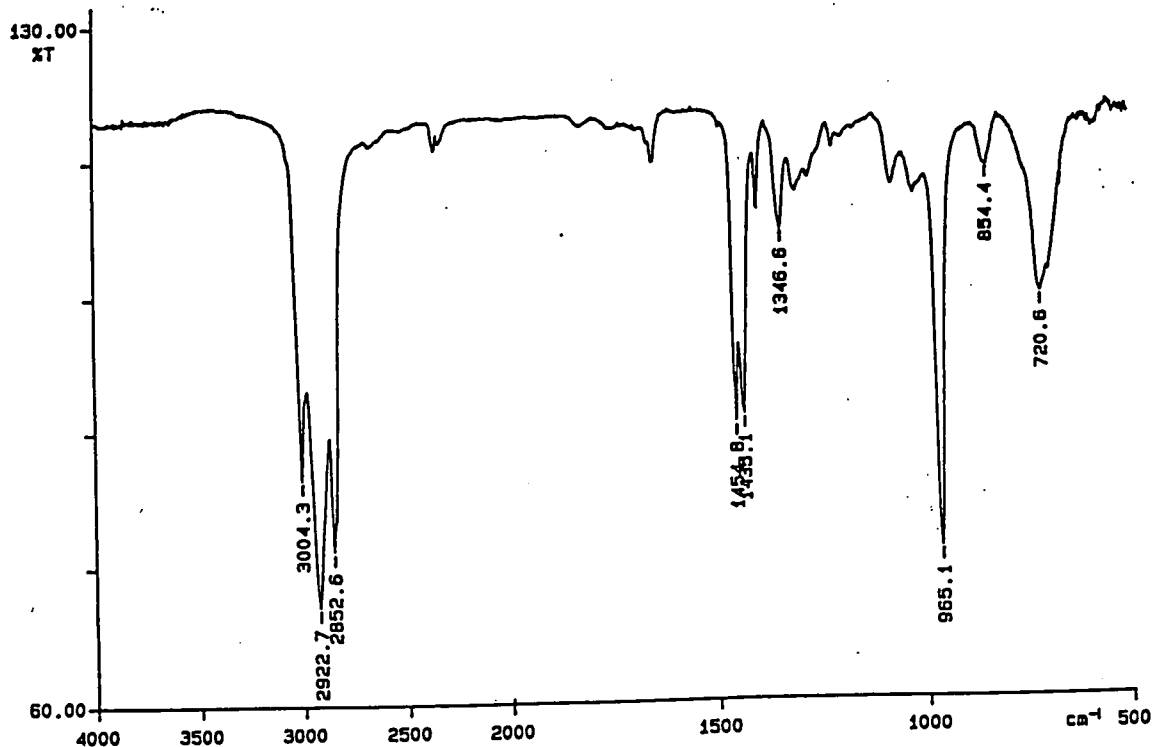
PERKIN ELMER



Appendix 5.2.7. Infrared spectrum of P5-7

94/05/16 10:24 red
s-358: 4 scans, 4.0cm-1. flat

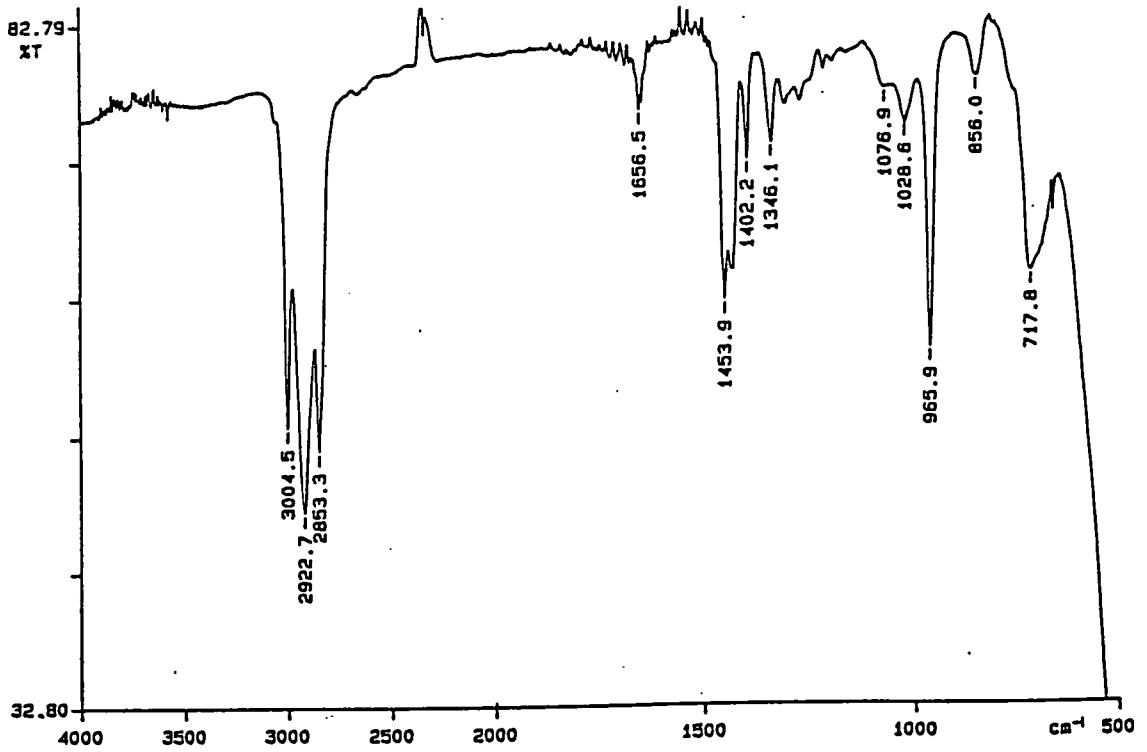
PERKIN ELMER



Appendix 5.2.8. Infrared spectrum of P5-8

94/03/03 16:25 red
X: 16 scans, 2.0cm-1. flat

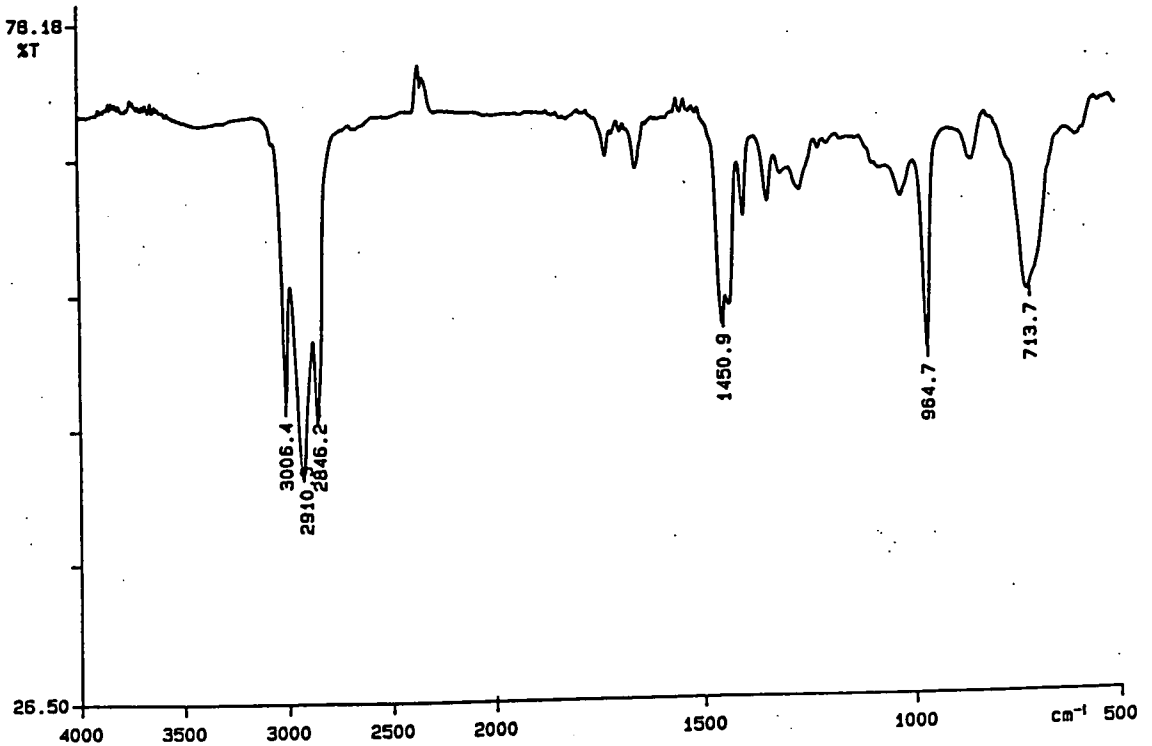
PERKIN ELMER



94/05/16 12:15 red
X: 16 scans, 4.0 cm^{-1}
s-371

Appendix 5.2.9. Infrared spectrum of P5-9

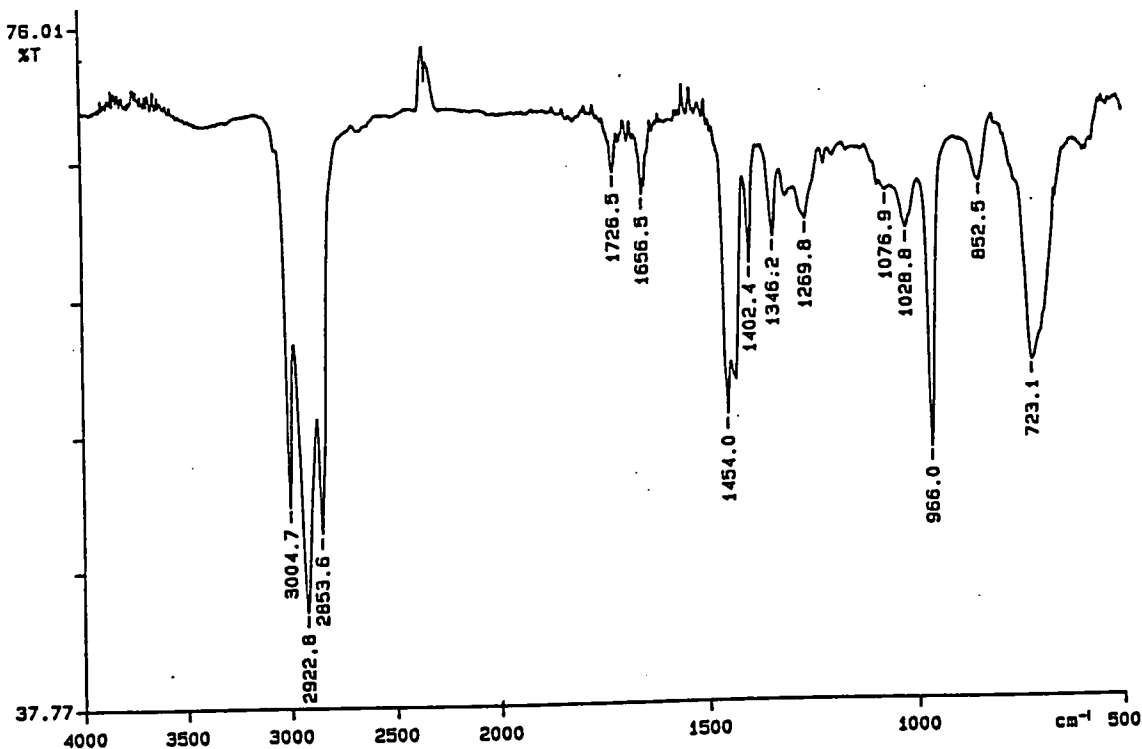
PERKIN ELMER



94/07/19 15:11 s-373
X: 16 scans, 4.0 cm^{-1} , flat, smooth
s-373

Appendix 5.2.10. Infrared spectrum of P5-10

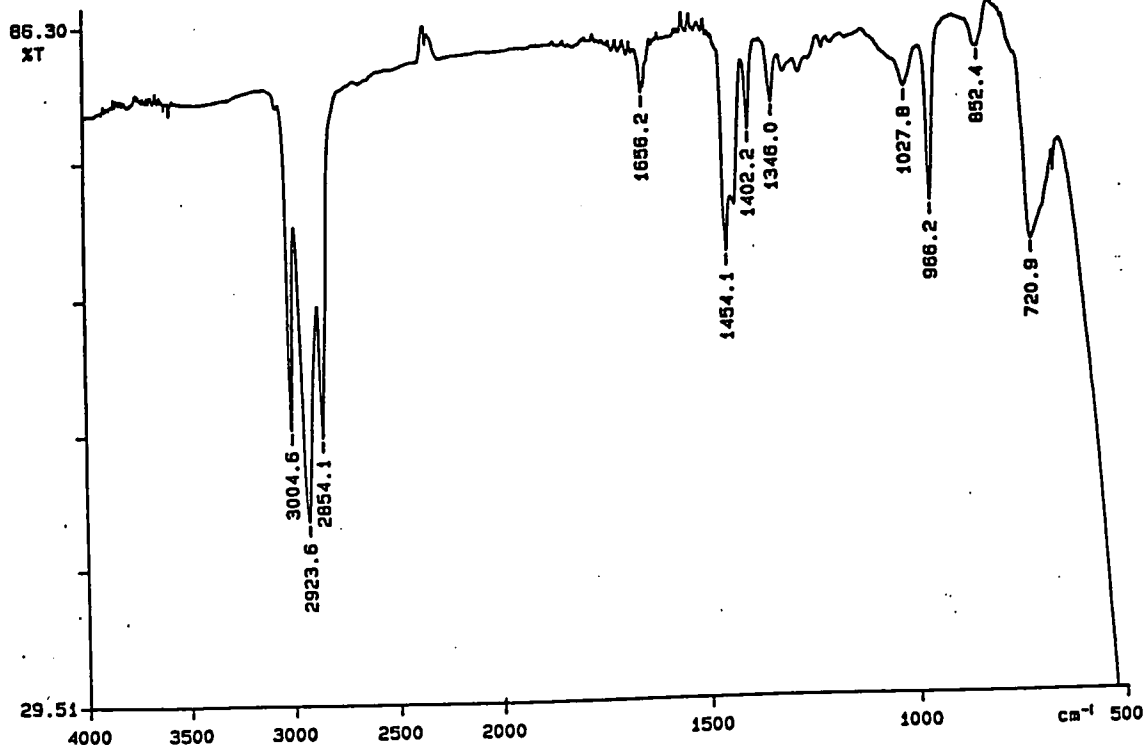
PERKIN ELMER



Appendix 5.2.11. Infrared spectrum of P5-11

94/05/16 12:26 red
X: 16 scans, 4.0 cm^{-1} , flat
s-374

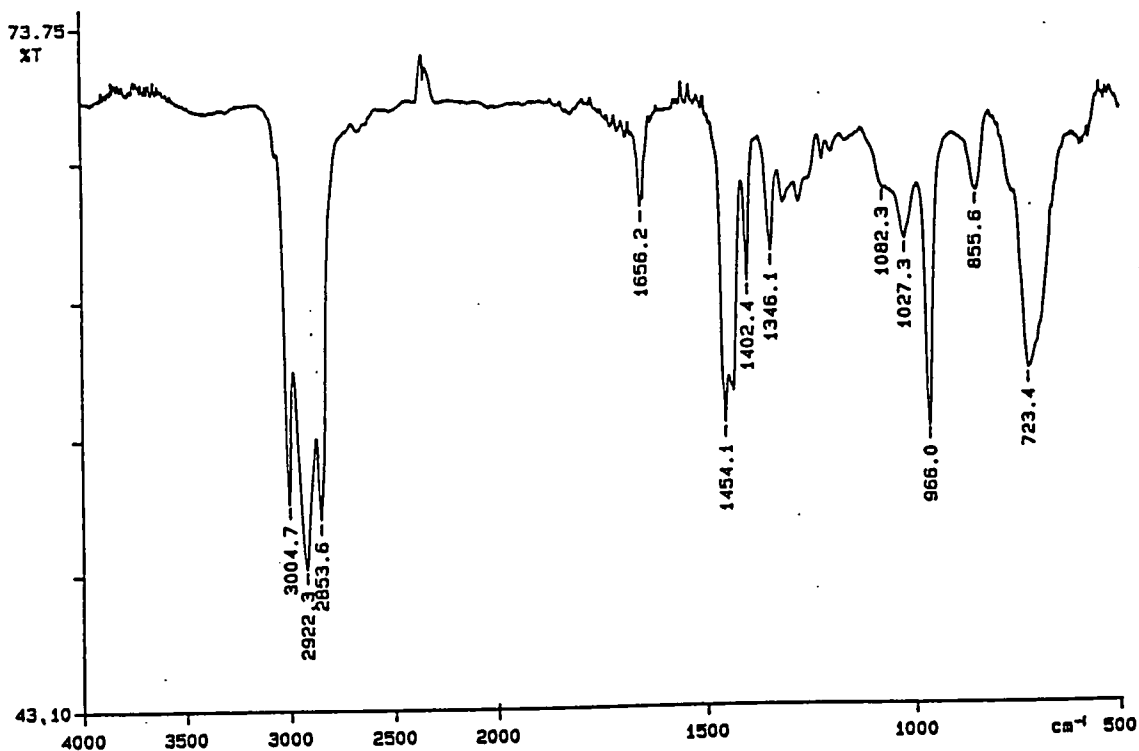
PERKIN ELMER



Appendix 5.2.12. Infrared spectrum of P5-12

94/05/16 11:39 red
X: 16 scans, 4.0 cm^{-1}
s-368

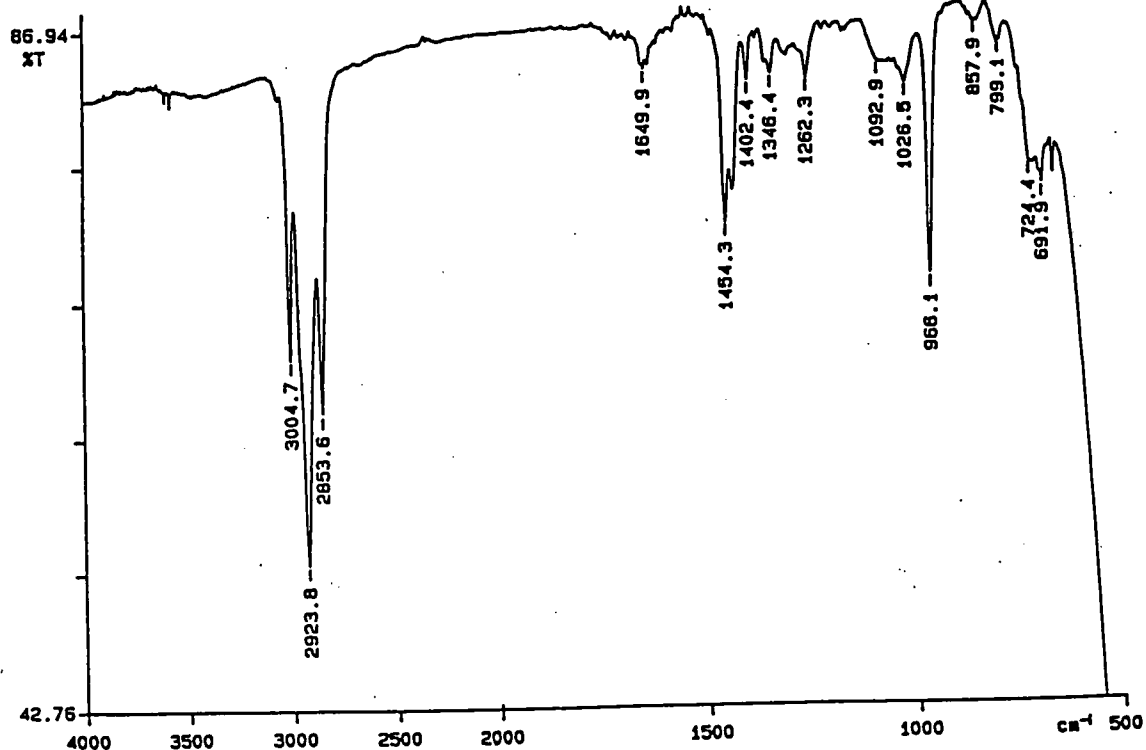
PERKIN ELMER



Appendix 5.2.13. Infrared spectrum of P5-13

94/05/16 11:18 red
X: 16 scans, 4.0cm-1, flat

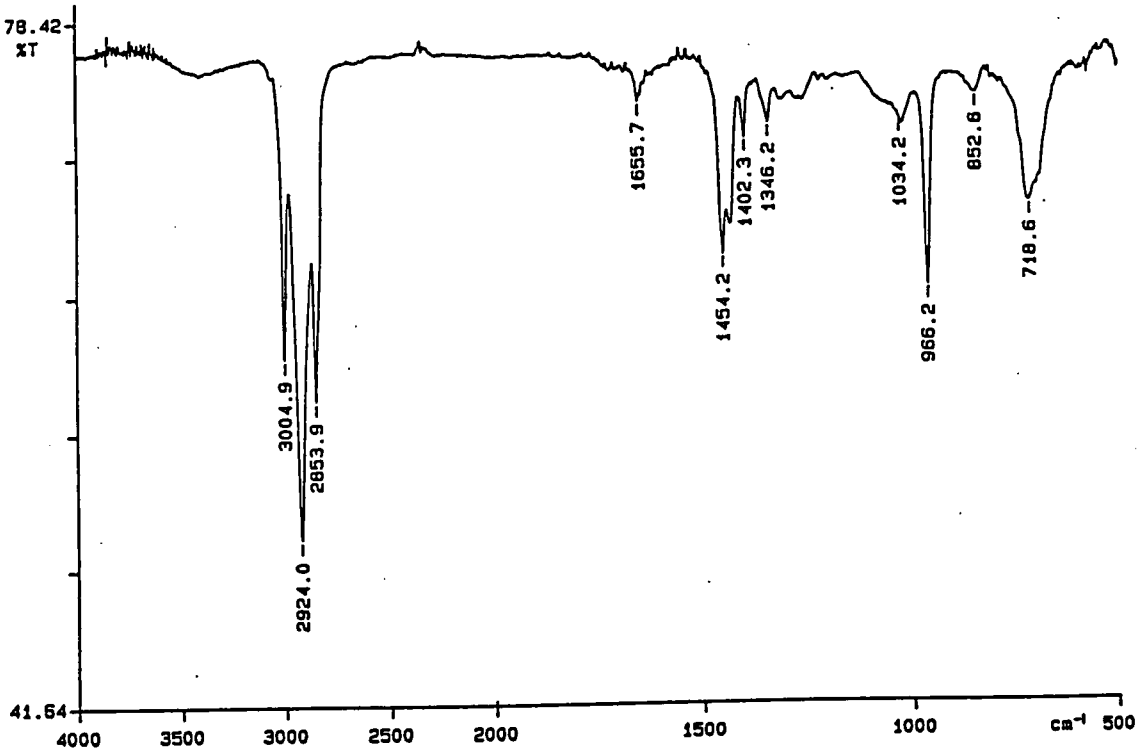
PERKIN ELMER



Appendix 5.2.14. Infrared spectrum of P5-14

94/05/15 11:03 red
X: 16 scans, 4.0cm-1

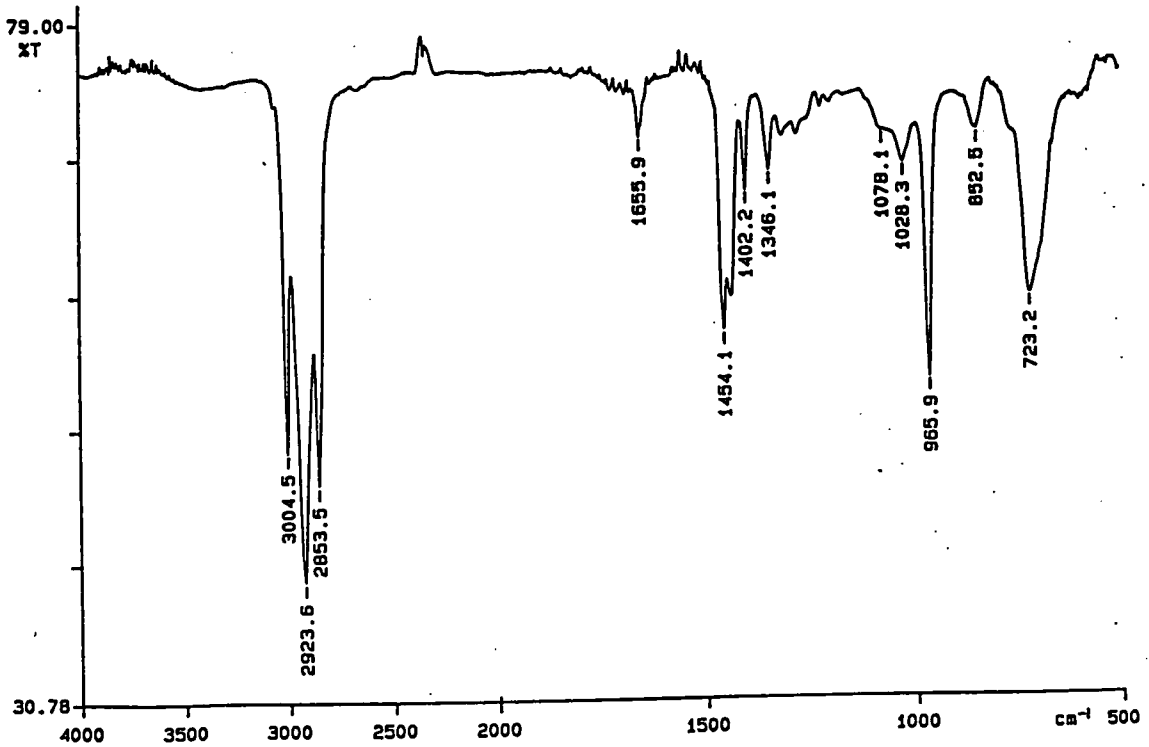
PERKIN ELMER



Appendix 5.2.15. Infrared spectrum of P5-15

94/05/16 11:05 red
X: 16 scans, 4.0 cm^{-1} , flat

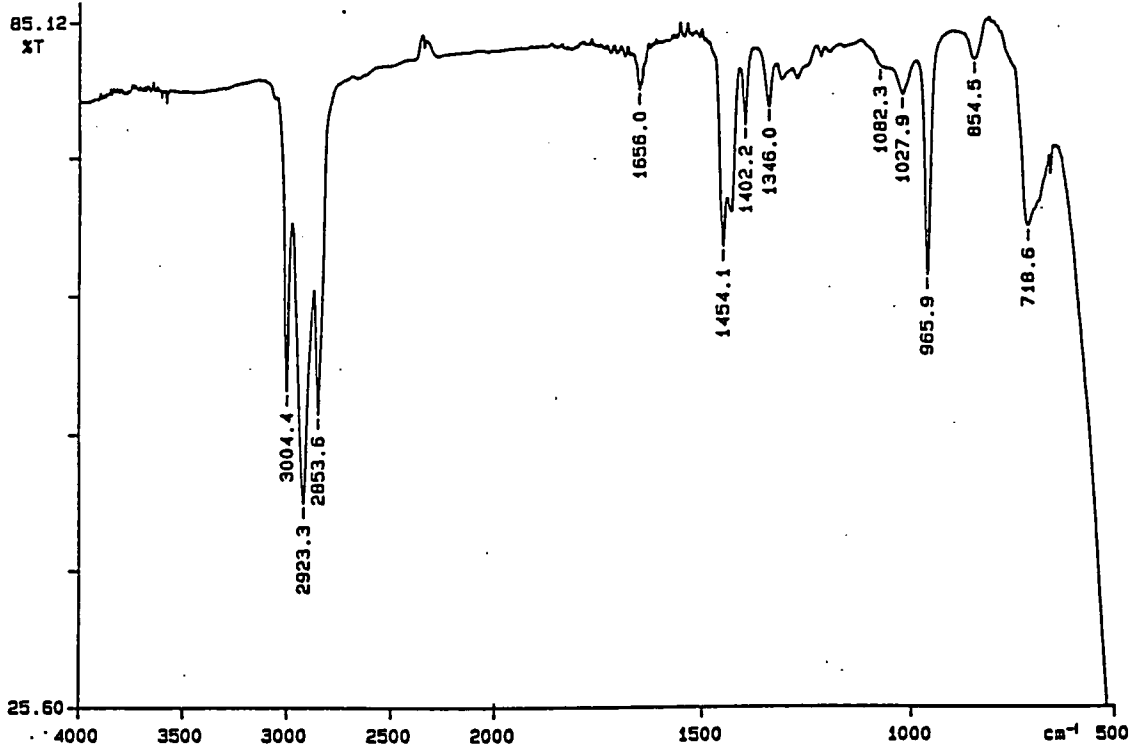
PERKIN ELMER



Appendix 5.2.16. Infrared spectrum of P5-16

94/05/16 11:31 red
s-367: 16 scans, 4.0 cm^{-1} , flat
s-367

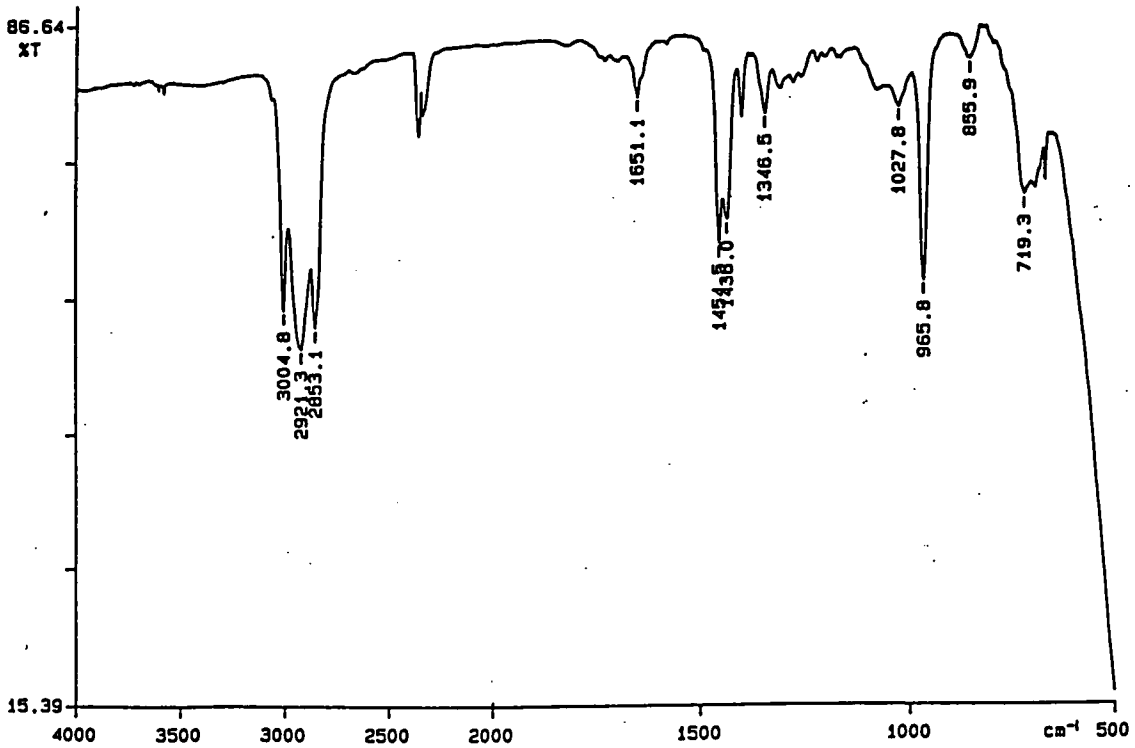
PERKIN ELMER



Appendix 5.2.17. Infrared spectrum of P5-17

94/05/16 11:21 red
X: 16 scans, 4.0 cm^{-1}

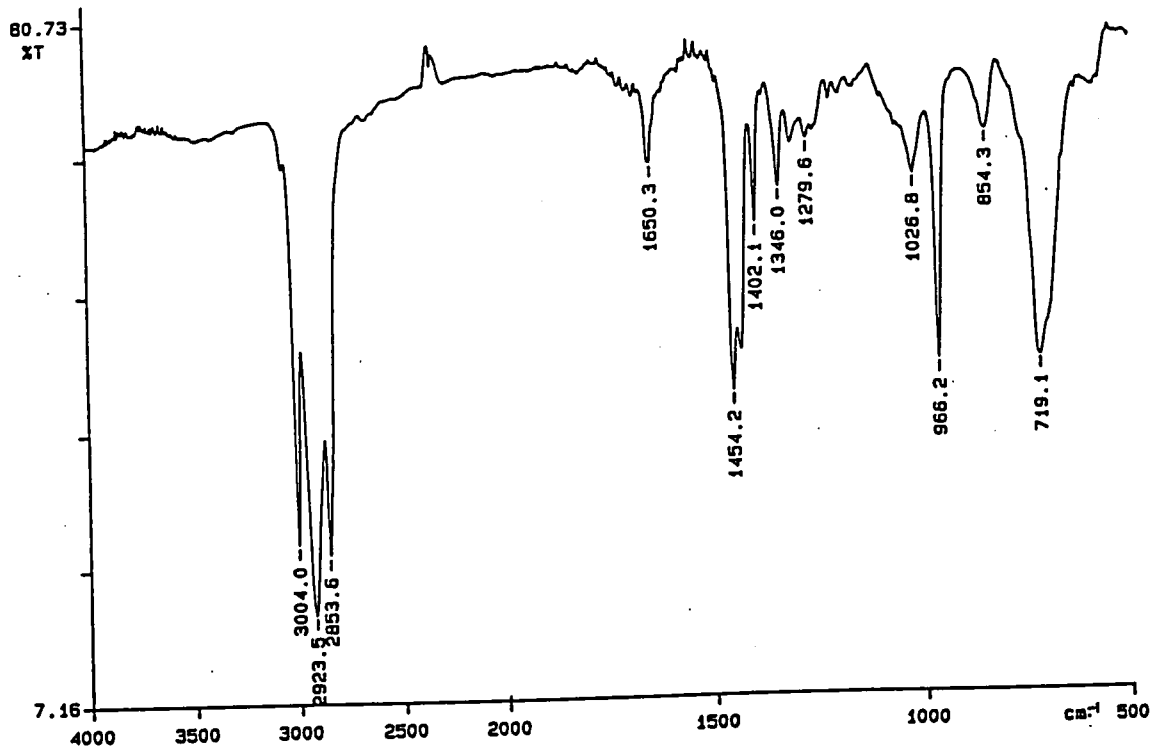
PERKIN ELMER



Appendix 5.2.18. Infrared spectrum of P5-18

94/05/16 09:41 red
X: 4 scans, 4.0 cm^{-1}

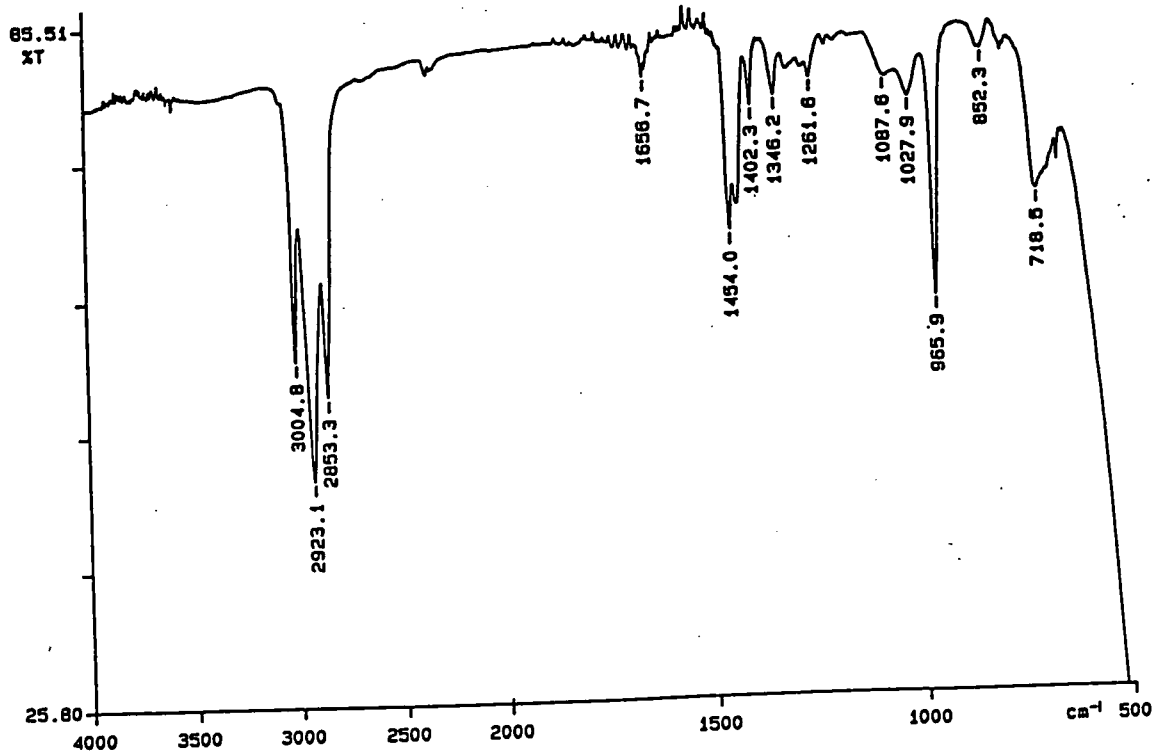
PERKIN ELMER



Appendix 5.2.19. Infrared spectrum of P5-19

94/05/16 12:09 red
X: 16 scans, 4.0 cm^{-1}
9-370

PERKIN ELMER



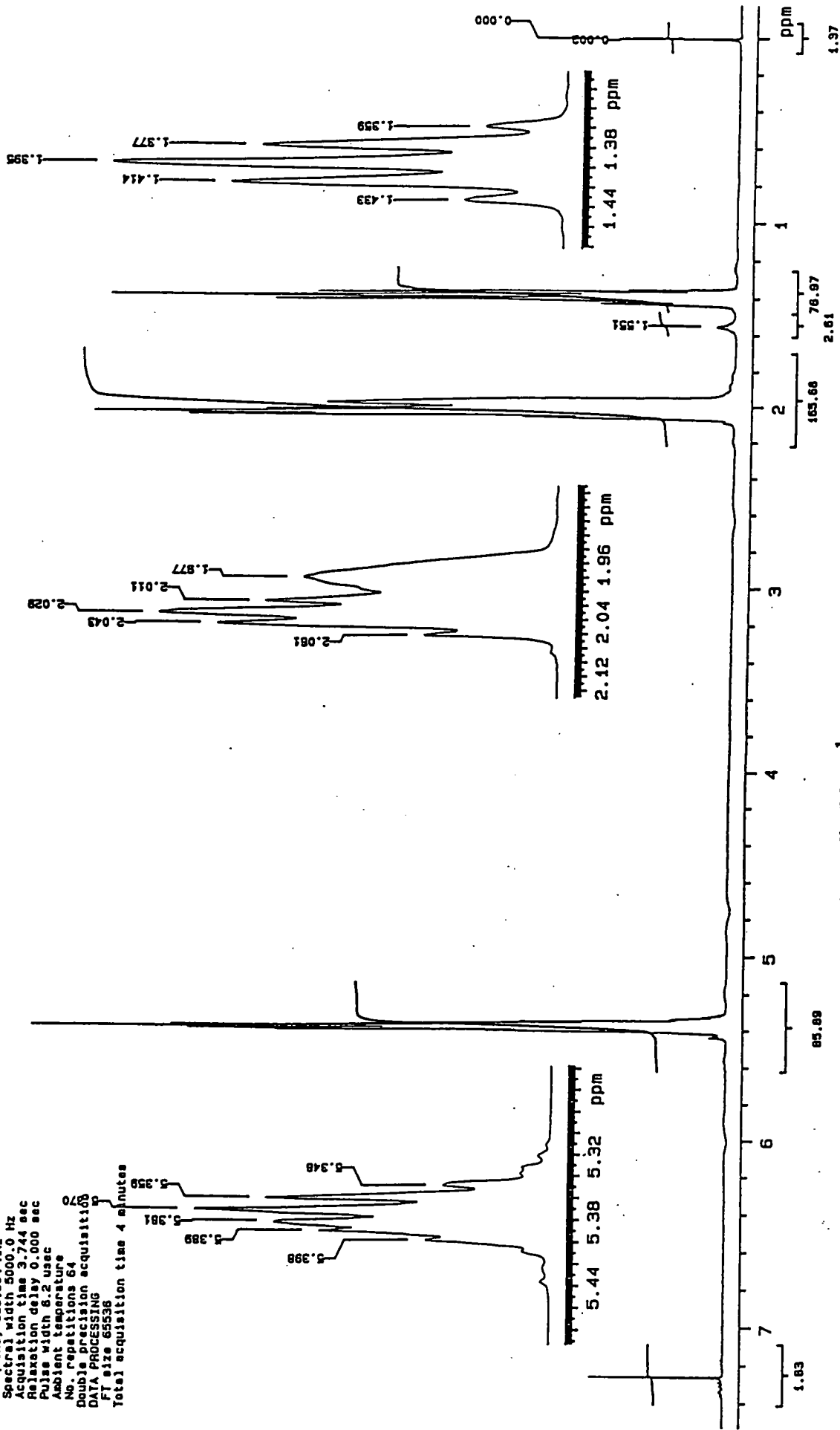
Appendix 5.2.20. Infrared spectrum of P5-20

94/05/16 11:59 red
X: 16 scans, 4.0 cm^{-1}
9-369

8-360
 FILE /data/curdatt/ksa22marc.fid
 RUN ON Mar 22 94
 SOLVENT CDCl3

OBSERVE H1

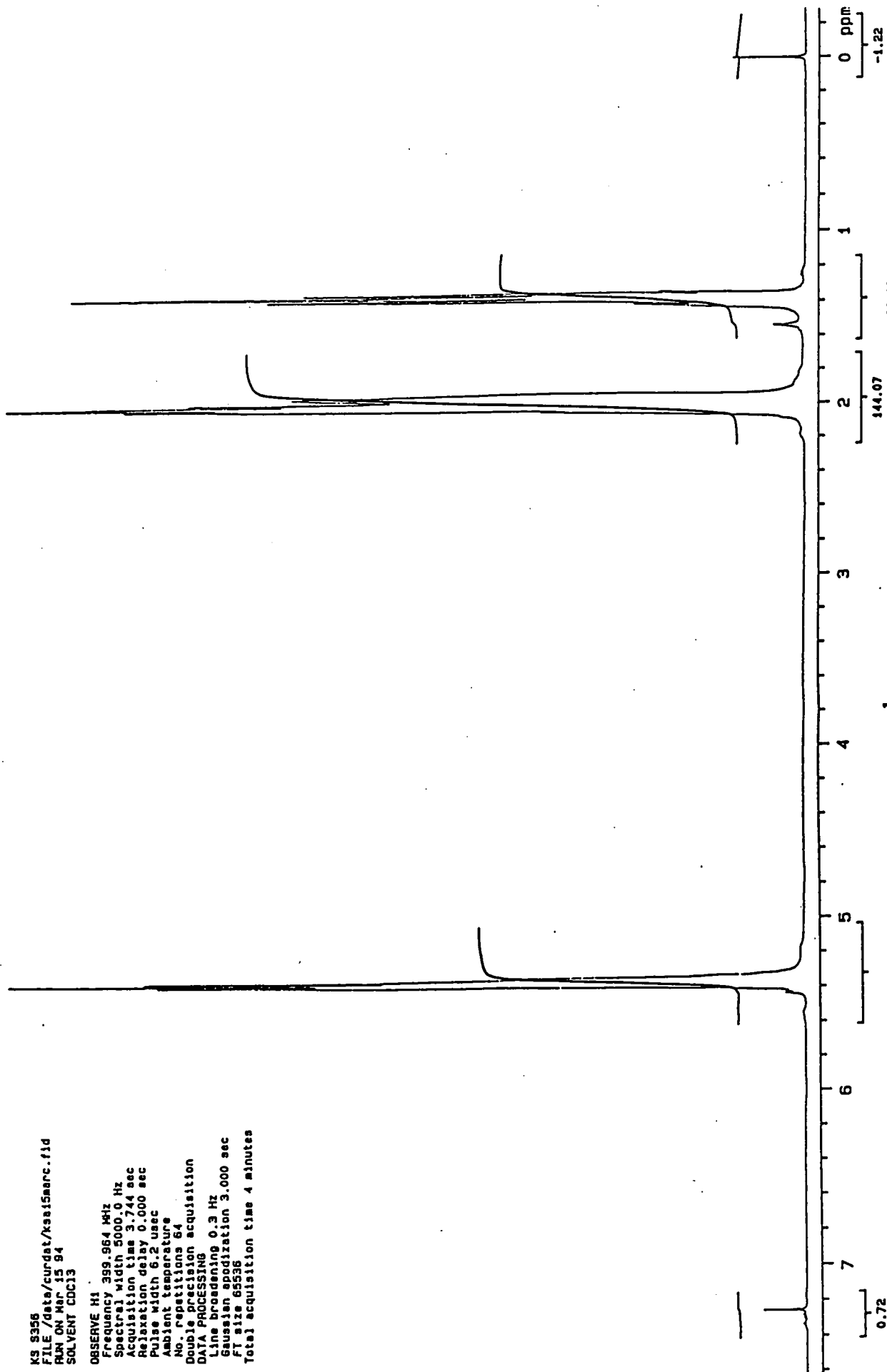
Frequency 399.964 MHz
 Spectral width 5000.0 Hz
 Acquisition time 3.744 sec
 Relaxation delay 0.000 sec
 Pulse width 6.2 usec
 Ambient temperature
 No. repetitions 64
 Double precision acquisition
 DATA PROCESSING
 FT size 65536
 Total acquisition time 4 minutes



Appendix 5.3.1. 1H n.m.r. spectrum of P5-1

KS 8356
FILE /data/curdatt/ksa15marc.fid
RUN ON Mar 15 94
SOLVENT CDC13

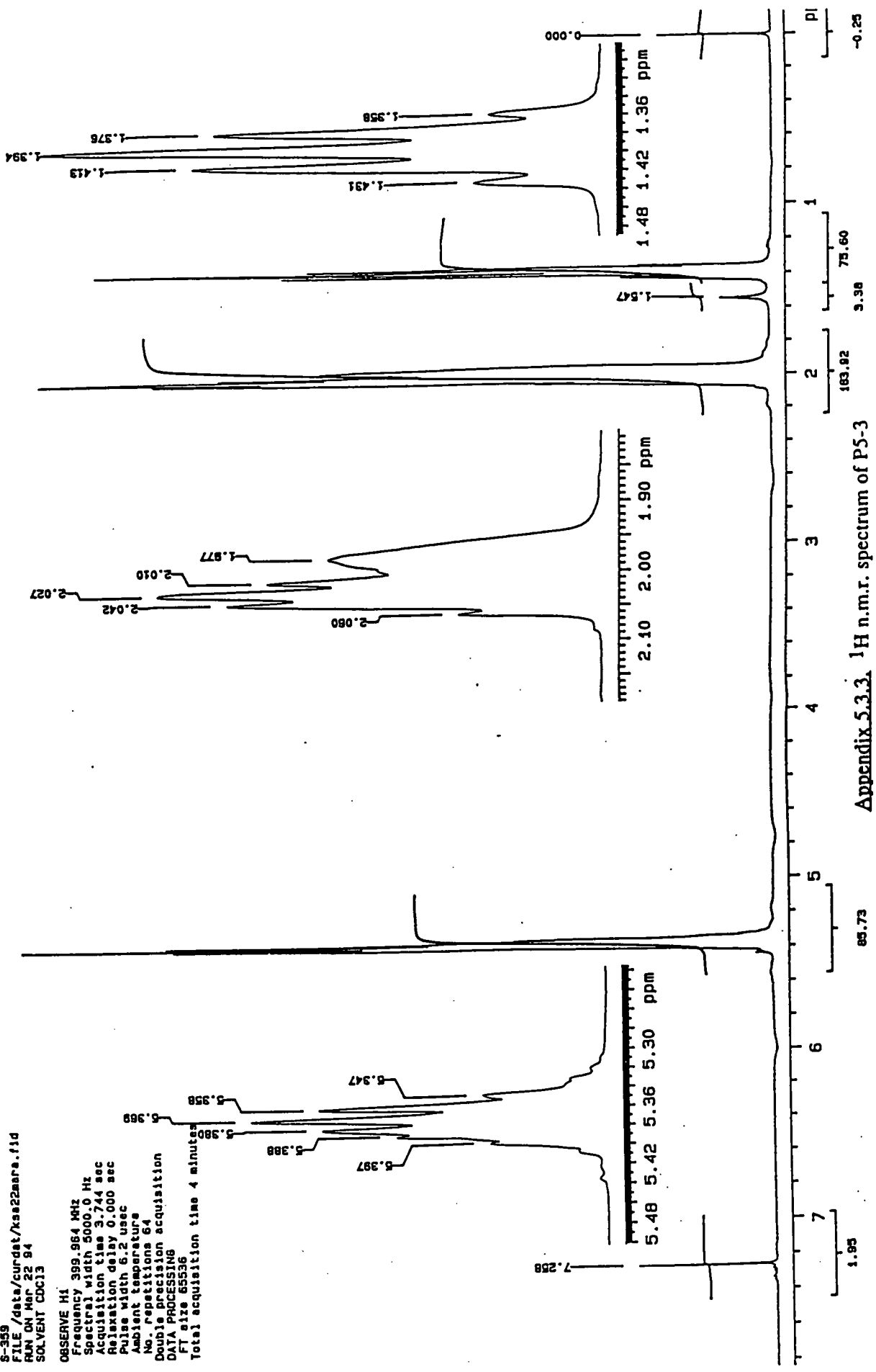
OBSERVE H1
Frequency 399.964 MHz
Spectral width 5000.0 Hz
Acquisition time 3.744 sec
Relaxation delay 0.000 sec
Pulse width 6.2 usec
Ambient temperature
No. repetitions 64
Double precision acquisition
DATA PROCESSING
Line broadening 0.3 Hz
Gaussian apodization 3.000 sec
FT size 65536
Total acquisition time 4 minutes



Appendix 5.3.2. 1H n.m.r. spectrum of P5-2

5-359
 FILE /data/curdst/xsa22mare.fid
 RUN ON Mar 22 94
 SOLVENT CCl3

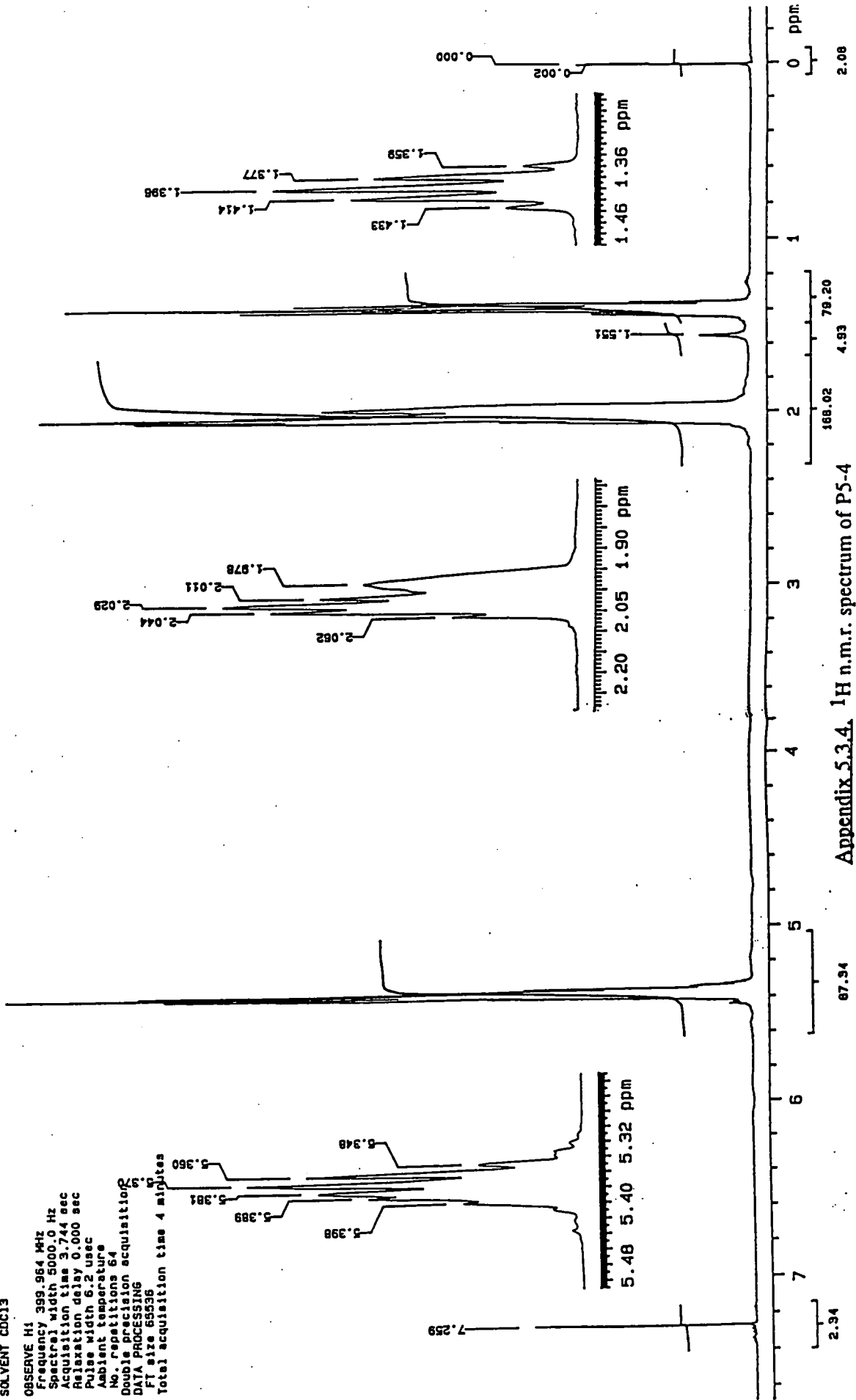
OBSERVE M1
 Frequency 399.964 MHz
 Spectral width 5000.0 Hz
 Acquisition time 3.744 sec
 Relaxation delay 0.000 sec
 Pulse width 6.2 usec
 Ambient temperature
 No. repetitions 64
 Double precision acquisition
 DATA PROCESSING
 FT size 65536
 Total acquisition time 4 minutes



Appendix 5.3.3. 1H n.m.r. spectrum of P5-3

8-361
 FILE /data/curdatt/xse22mare.f1d
 RUN ON Mar 22 94
 SOLVENT CDCl3

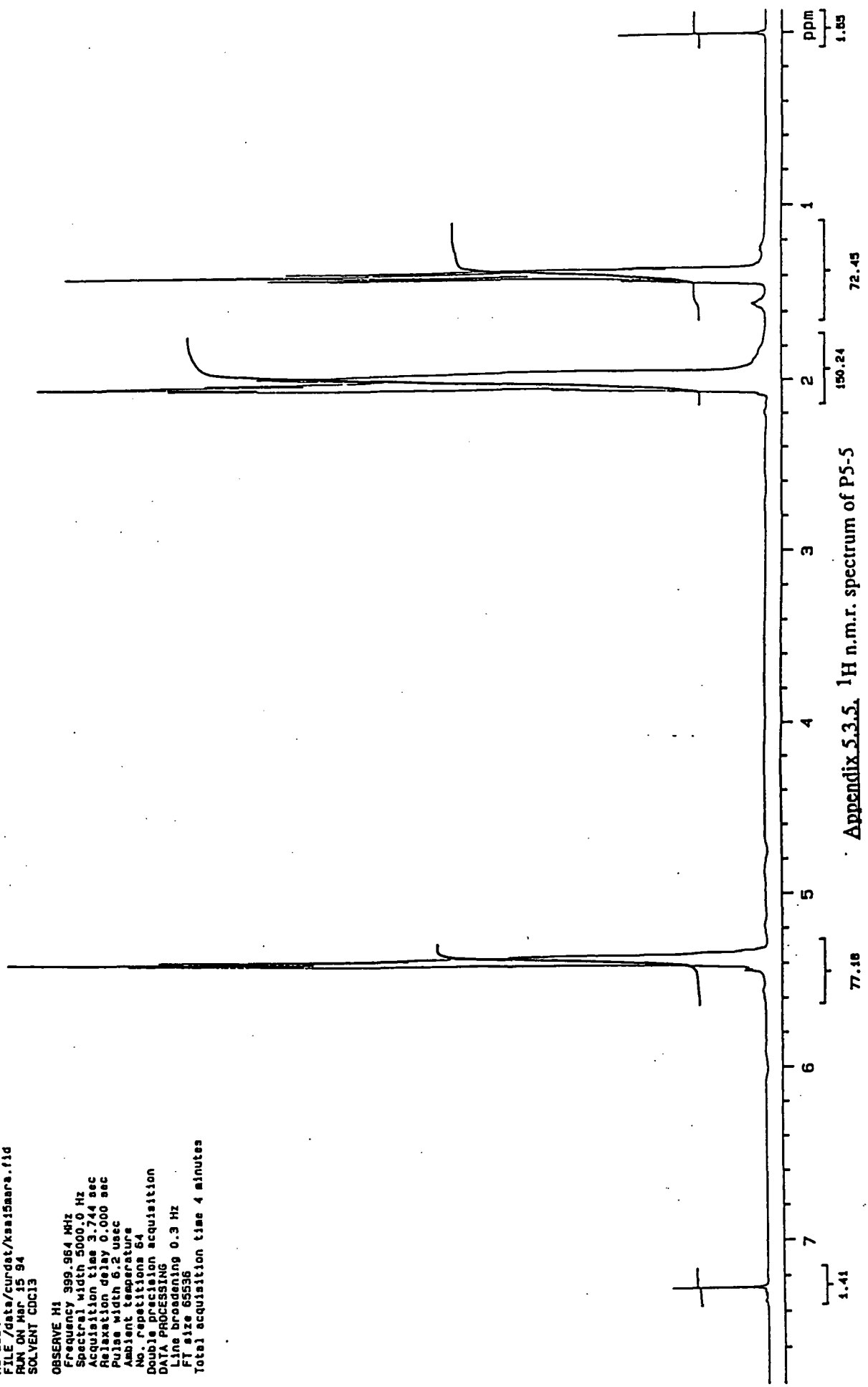
OBSERVE H1
 Frequency 399.964 MHz
 Spectral width 5000.0 Hz
 Acquisition time 3.744 sec
 Relaxation delay 0.000 sec
 Pulse width 6.2 usec
 Ambient temperature
 No. repetitions 64
 Double precision acquisition
 DATA PROCESSING
 FT size 65536
 Total acquisition time 4 minutes



Appendix 5.3.4. ¹H n.m.r. spectrum of P5-4

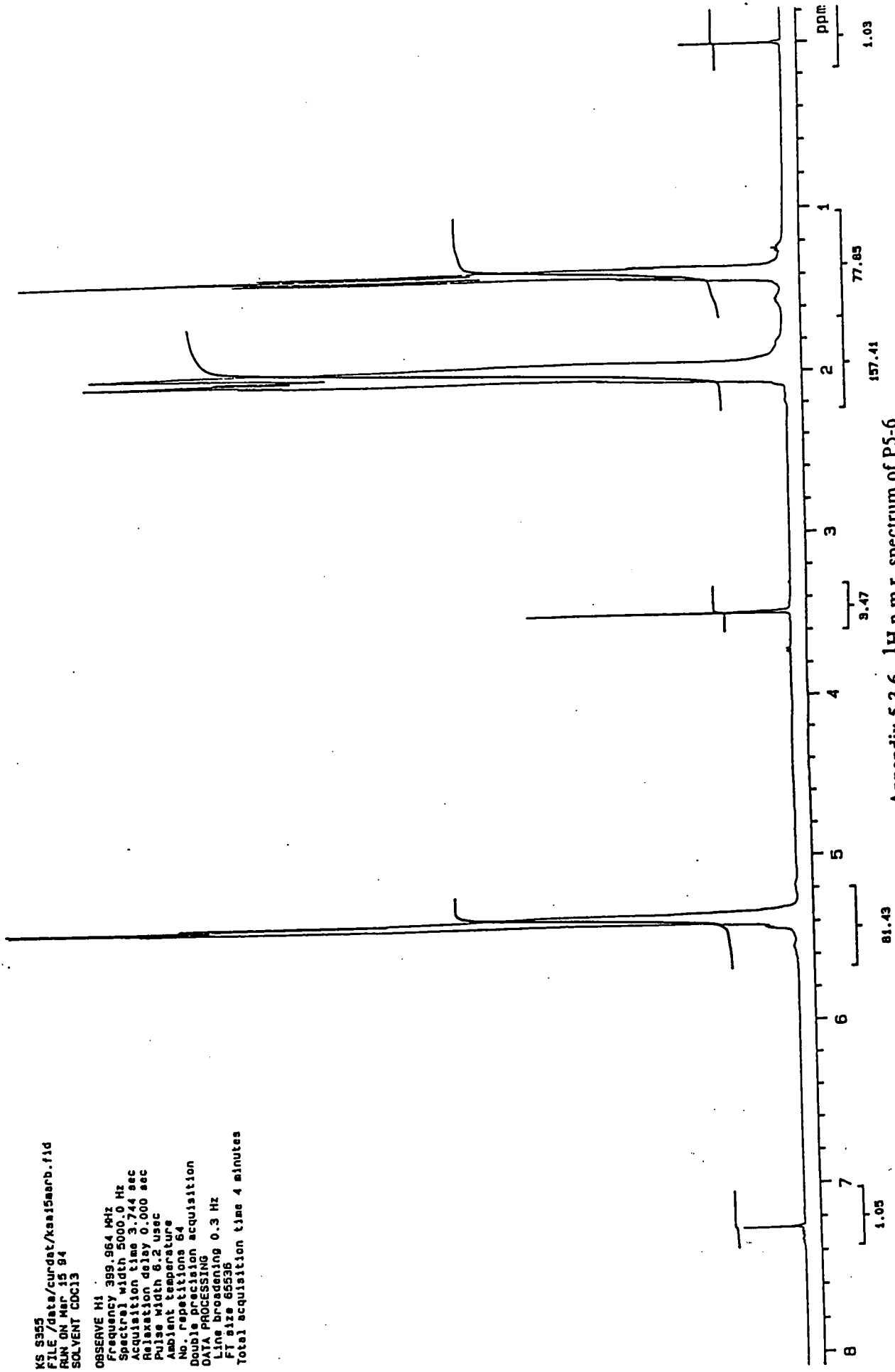
K5 8354
FILE /data/curdat/ksa15mare.fid
RAW ON Mar 15 84
SOLVENT CDCl3

OBSERVE H1
Frequency 999.964 MHz
Spectral width 5000.0 Hz
Acquisition time 3.744 sec
Relaxation delay 0.000 sec
Pulse width 6.2 usec
Ambient temperature
No. repetitions 64
Double precision acquisition
DATA PROCESSING
Line broadening 0.3 Hz
FT size 65536
Total acquisition time 4 minutes



Appendix 5.3.5. 1H n.m.r. spectrum of P5-5

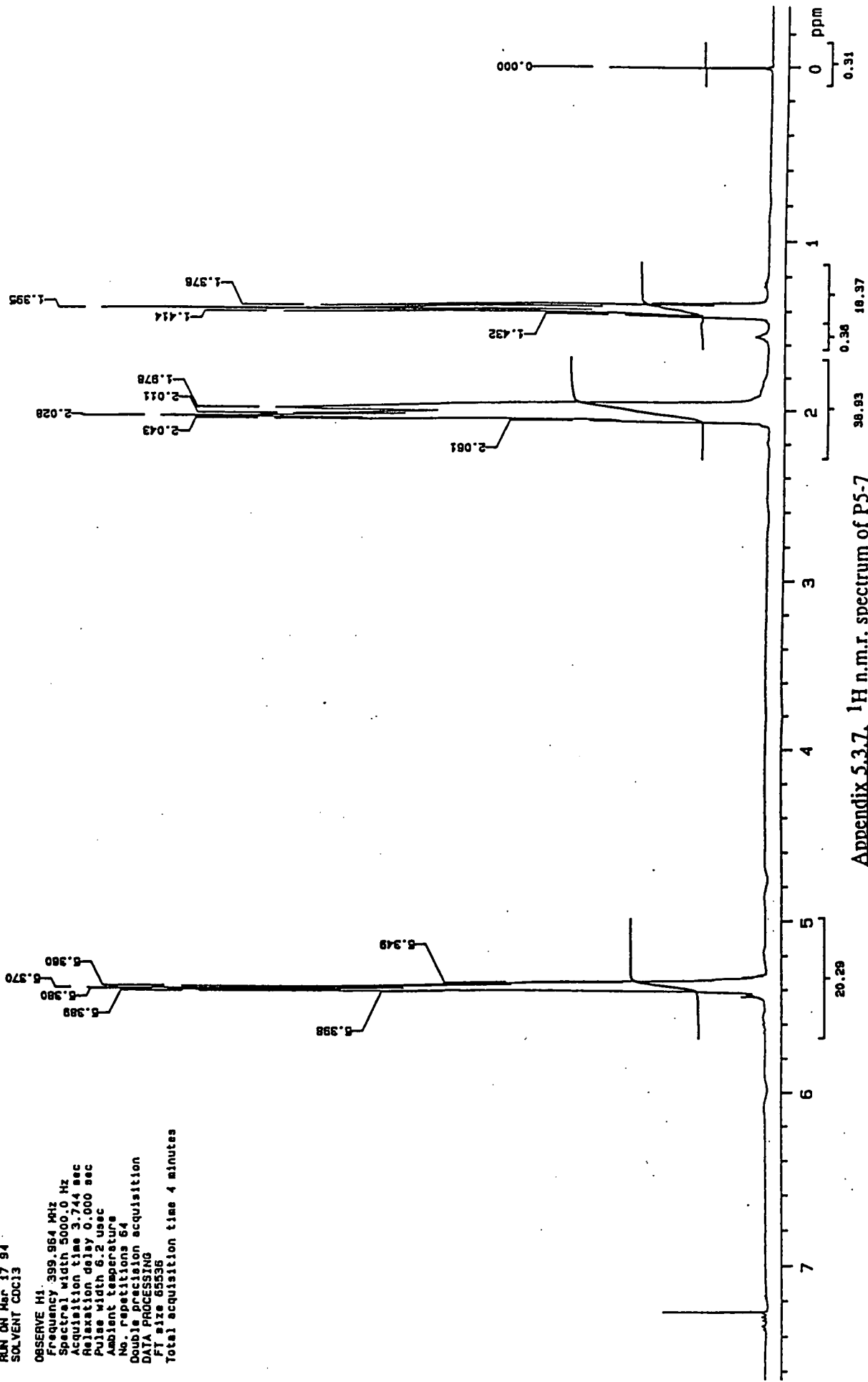
K5 3355
 FILE /data/curdat/kas15marb.fid
 RUN ON Mar 15 84
 SOLVENT CDC13
 OBSERVE M1
 Frequency 399.964 MHz
 Spectral width 5000.0 Hz
 Acquisition time 3.744 sec
 Relaxation delay 0.000 sec
 Pulse width 6.2 usec
 Ambient temperature
 No. repetitions 64
 Double accumulation acquisition
 DATA PROCESSING
 Line broadening 0.3 Hz
 FI size 65536
 Total acquisition time 4 minutes



Appendix 5.3.6. 1H n.m.r. spectrum of P5-6

9-358
RUN ON Mar 17 94
SOLVENT CDCl3

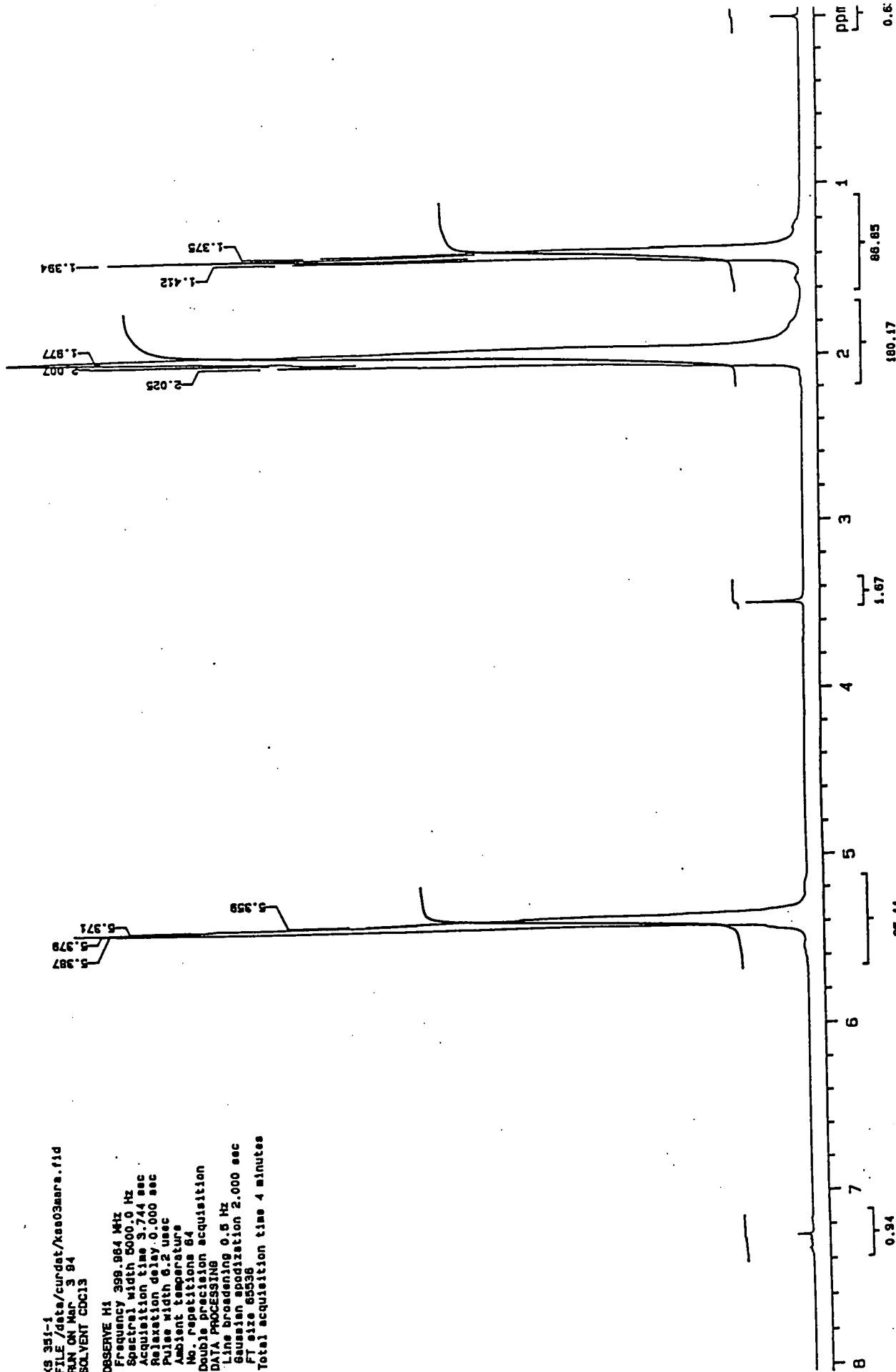
OBSERVE H1
Frequency 399.984 MHz
Spectral width 5000.0 Hz
Acquisition time 3.744 sec
Relaxation delay 0.000 sec
Pulse width 6.2 usec
Ambient temperature
No. repetitions 64
Double repetition acquisition
DATA PROCESSING
F1 size 85536
Total acquisition time 4 minutes



Appendix 5.3.7. 1H n.m.r. spectrum of P5-7

XS 351-1
 FILE /data/cundat/Xse03mars.fid
 RUN ON Mar 3 84
 SOLVENT CDCl3

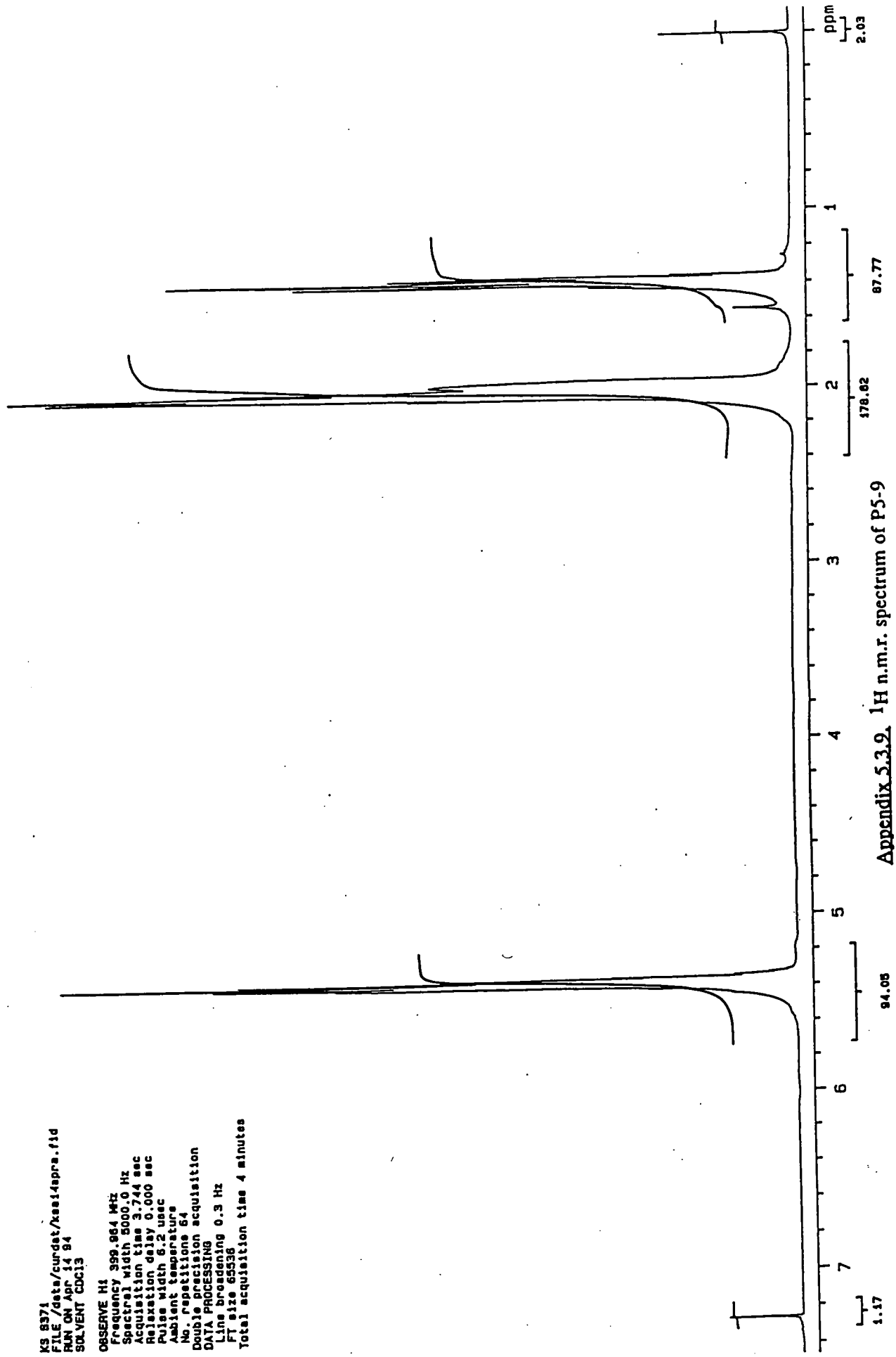
OBSERVE H1
 Frequency 399.964 Mhz
 Spectral width 8000.0 Hz
 Acquisition time 3.744 sec
 Relaxation delay 0.000 sec
 Pulse width 6.2 usec
 Ambient temperature
 No. repetitions 84
 Double precision acquisition
 DATA PROCESSING
 Line broadening 0.5 Hz
 Gaussian apodization 2.000 sec
 FT size 65536
 Total acquisition time 4 minutes



Appendix 5.3.8. 1H n.m.r. spectrum of P5-8

KS 8371
FILE /data/curdat/ks814apr8.fid
RUN ON Apr 14 84
SOLVENT CDCl3

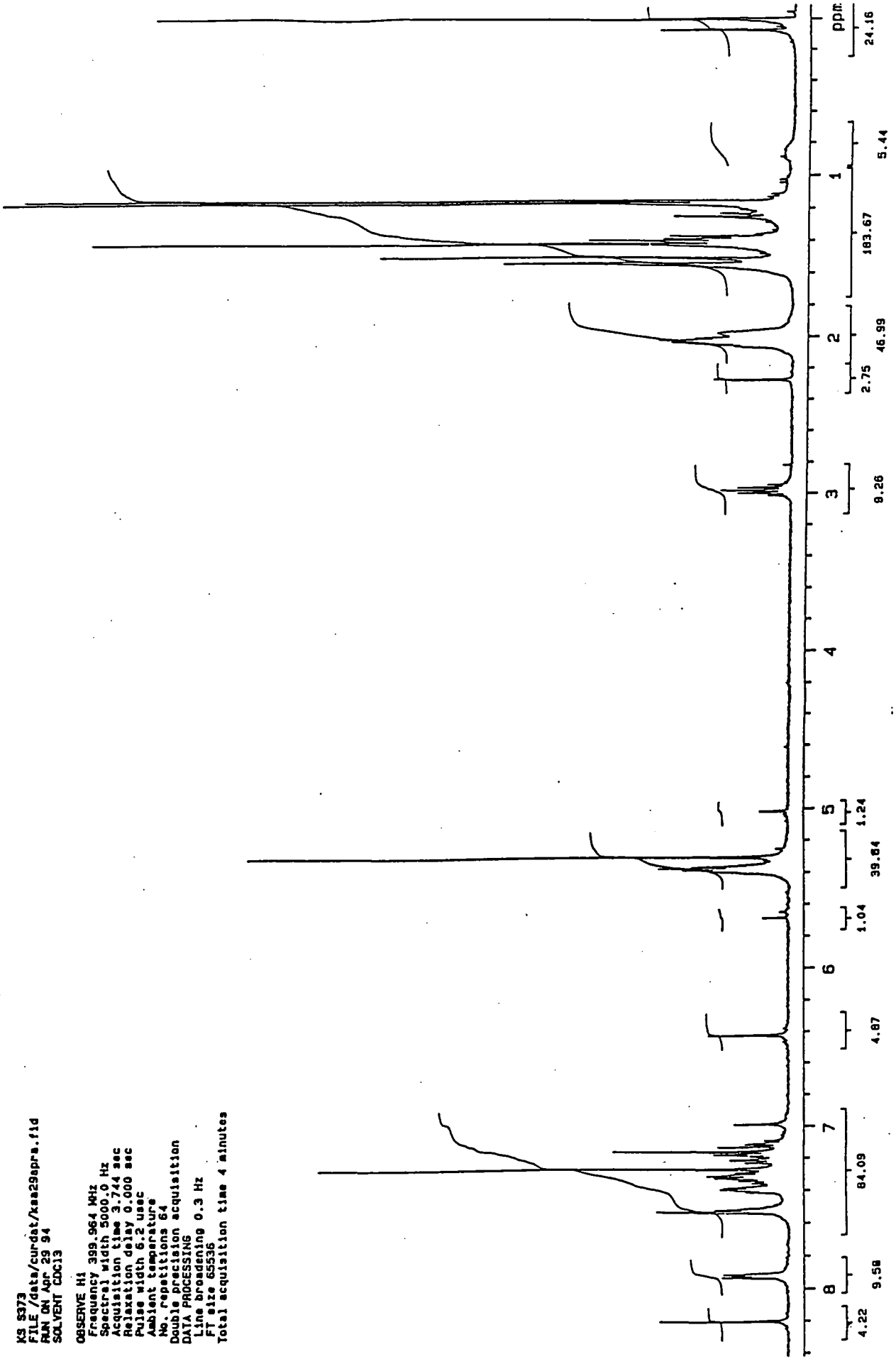
OBSERVE H1
Frequency 399.964 MHz
Spectral width 5000.0 Hz
Acquisition time 3.744 sec
Relaxation delay 0.000 sec
Pulse width 6.2 usec
Ambient temperature
No. repetitions 64
Double precision acquisition
DATA PROCESSING
Line broadening 0.3 Hz
F1 size 65536
Total acquisition time 4 minutes



Appendix 5.3.9. ¹H n.m.r. spectrum of P5-9

KS 8373
FILE /data/curdat/ksa29apra.fid
RUN ON Apr 29 94
SOLVENT CDCl3

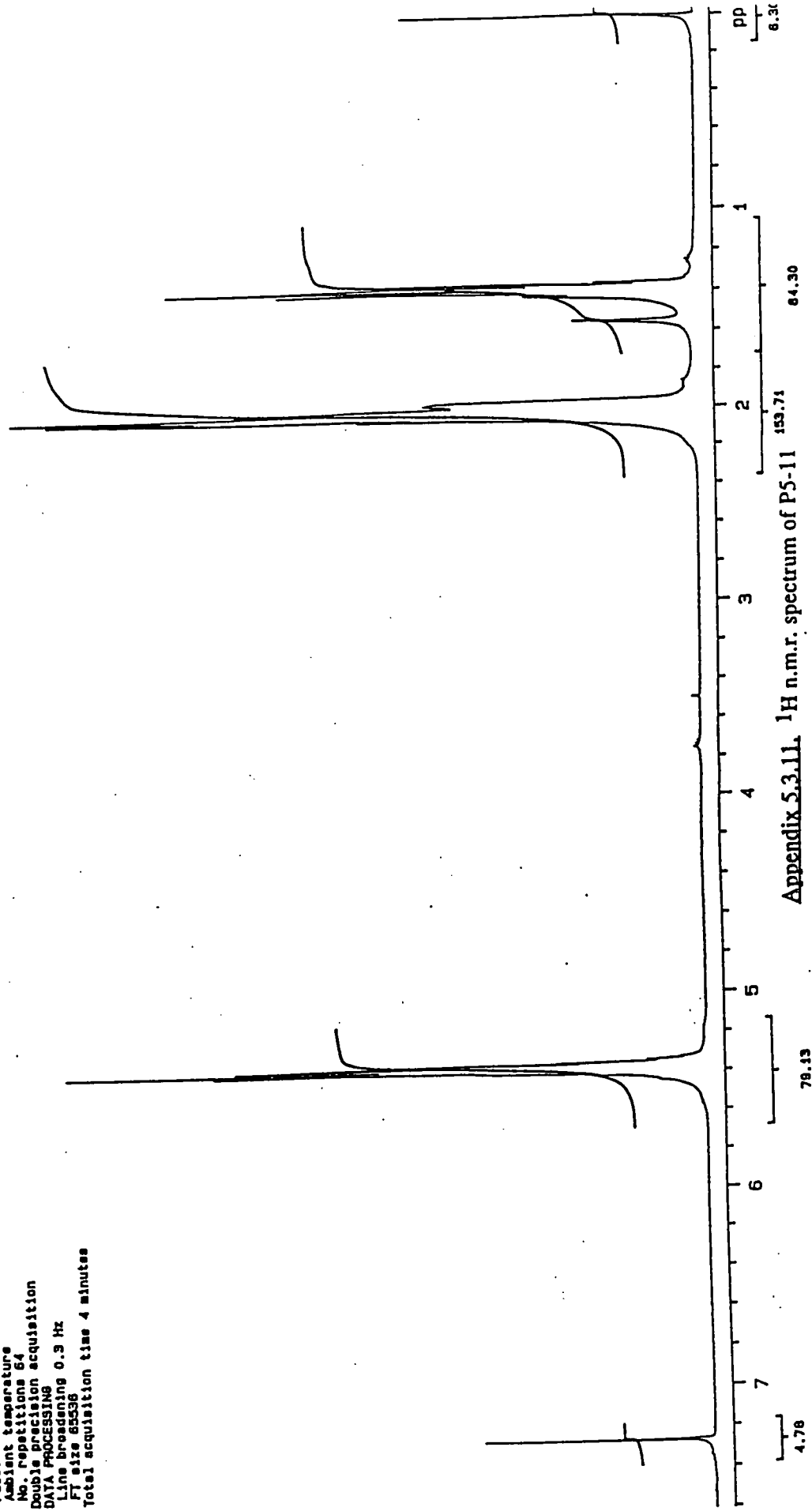
OBSERVE H1
Frequency 300.964 MHz
Spectral width 5000.0 Hz
Acquisition time 3.744 sec
Relaxation delay 0.000 sec
Pulse width 6.2 usec
Ambient temperature
No. repetitions 64
Double precision acquisition
DATA PROCESSING
Line broadening 0.3 Hz
FT size 65536
Total acquisition time 4 minutes



Appendix 5.3.10. ¹H n.m.r. spectrum of P5-10

K9 8374
FILE /data/curdnt/ksa27spr.fid
RUN ON Apr 27 84
SOLVENT CDCl3

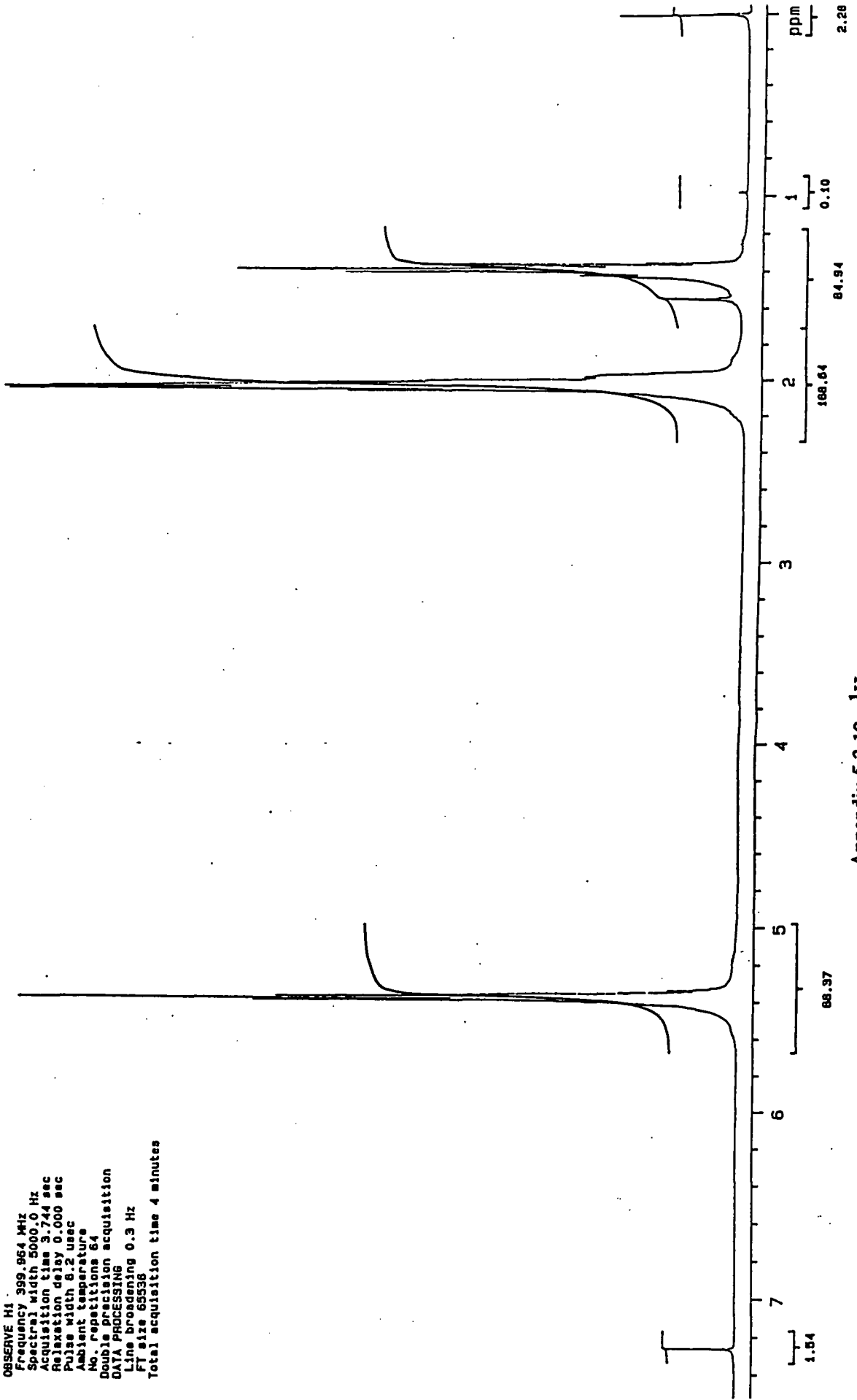
OBSERVE H1
Frequency 300.964 MHz
Spectral width 5000.0 Hz
Acquisition time 3.744 sec
Relaxation delay 0.000 sec
Pulse width 6.2 usec
Ambient temperature
No. repetitions 64
Double precision acquisition
DATA PROCESSING
Line broadening 0.3 Hz
FT size 65536
Total acquisition time 4 minutes



Appendix 5.3.11. 1H n.m.r. spectrum of P5-11

K3 8368
FILE /data/curdet/ksa30mrs.fid
RUN ON Mar 30 84
SOLVENT CCl3

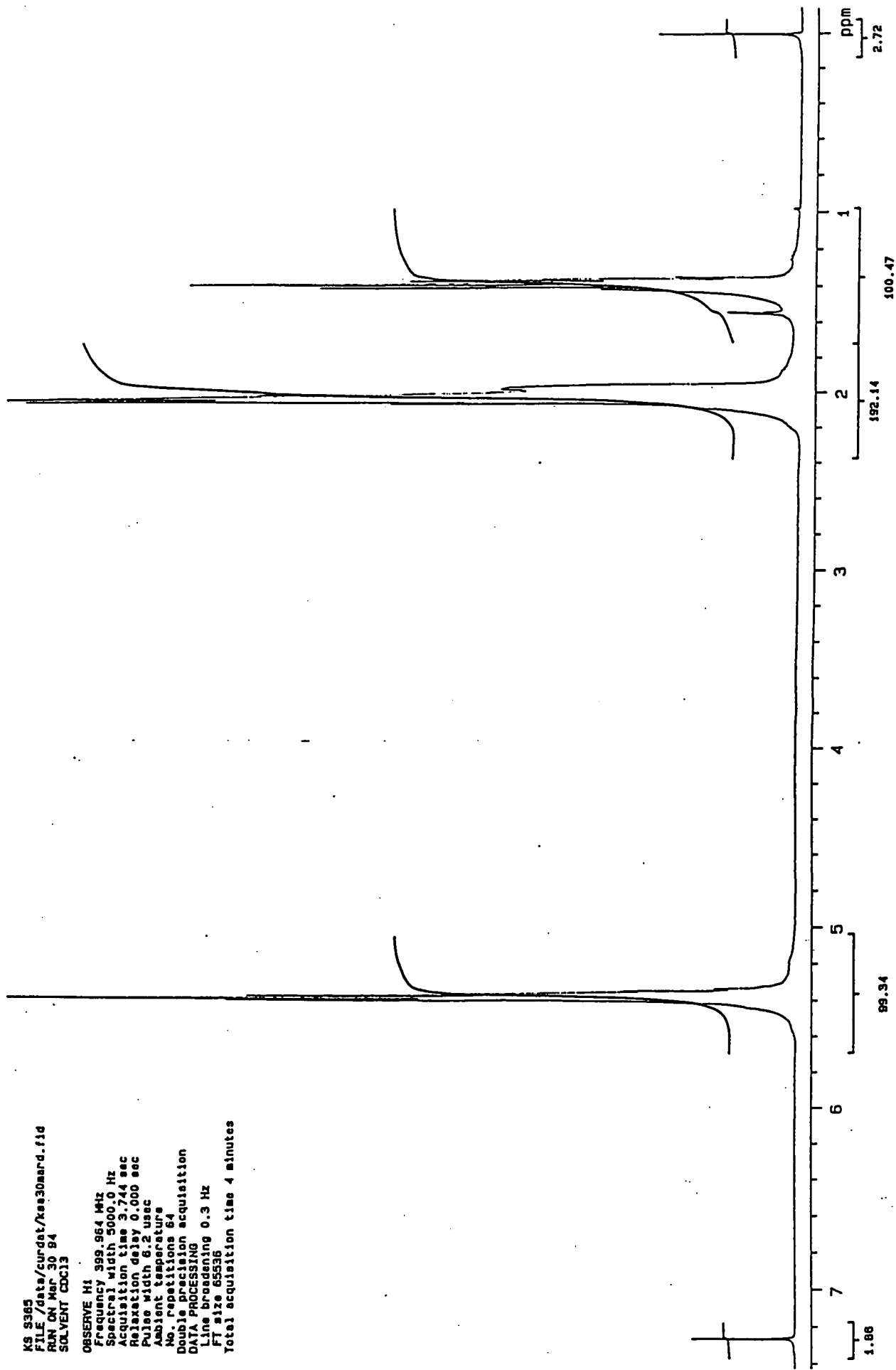
OBSERVE H1
Frequency 399.964 MHz
Spectral width 5000.0 Hz
Acquisition time 3.744 sec
Relaxation delay 0.000 sec
Pulse width 8.2 usec
Ambient temperature
No. repetitions 64
Double precision acquisition
DATA PROCESSING
Line broadening 0.3 Hz
FT size 65536
Total acquisition time 4 minutes



Appendix 5.3.12. ¹H n.m.r. spectrum of P5-12

K5 8365
FILE /data/curdat/kas30aard.fid
RUN ON Mar 30 84
SOLVENT CDC13

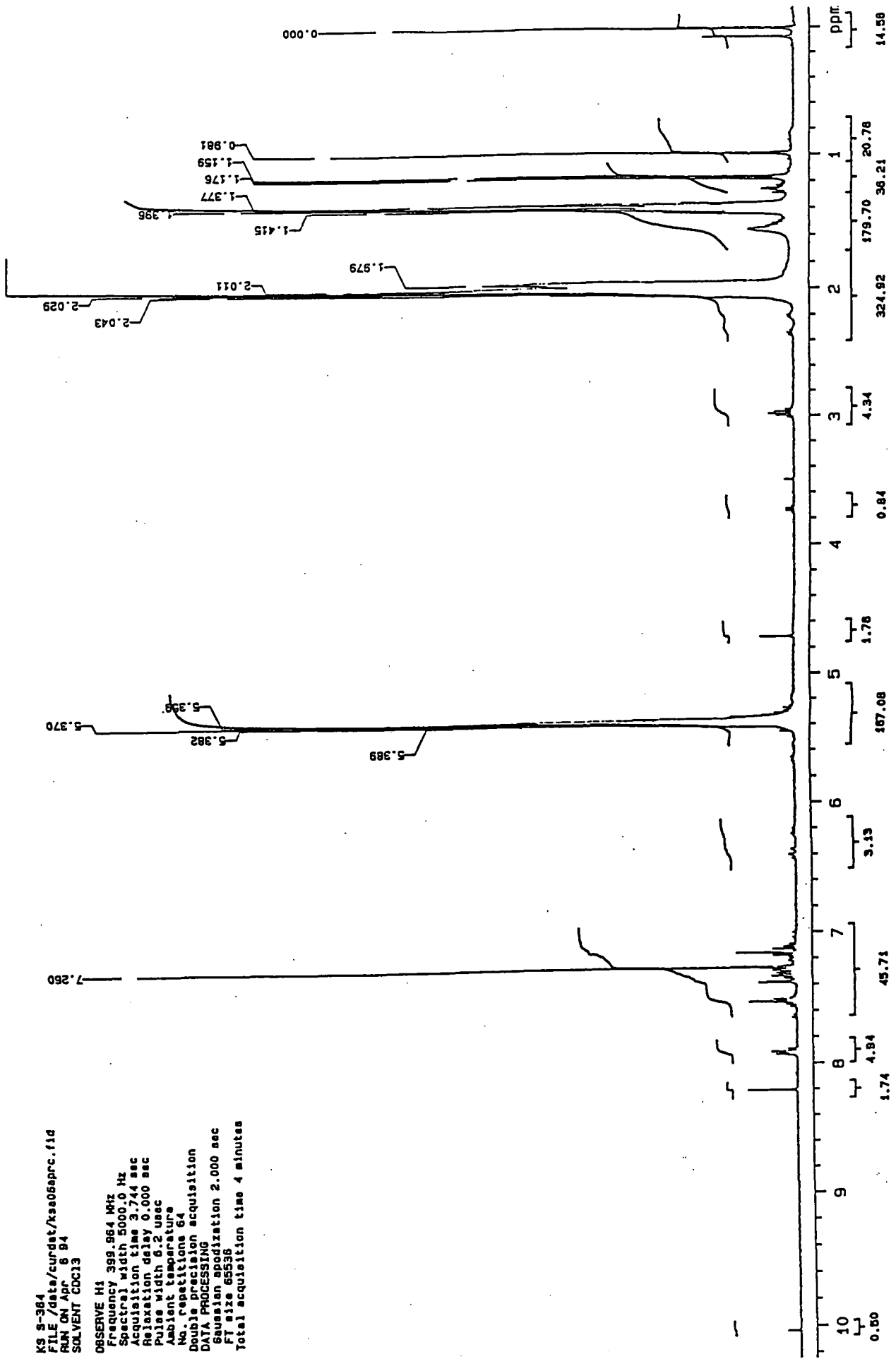
OBSERVE H1
Frequency 399.964 MHz
Spectral width 5000.0 Hz
Acquisition time 3.744 sec
Relaxation delay 0.000 sec
Pulse width 6.2 usec
Ambient temperature
No. repetitions 64
Double precision acquisition
DATA PROCESSING
Line broadening 0.3 Hz
FT size 65536
Total acquisition time 4 minutes



Appendix 5.3.13. ¹H n.m.r. spectrum of P5-13

KS S-364
 FILE /data/curdet/ksa06sprc.fid
 RUN ON Apr 6 94
 SOLVENT CDC13

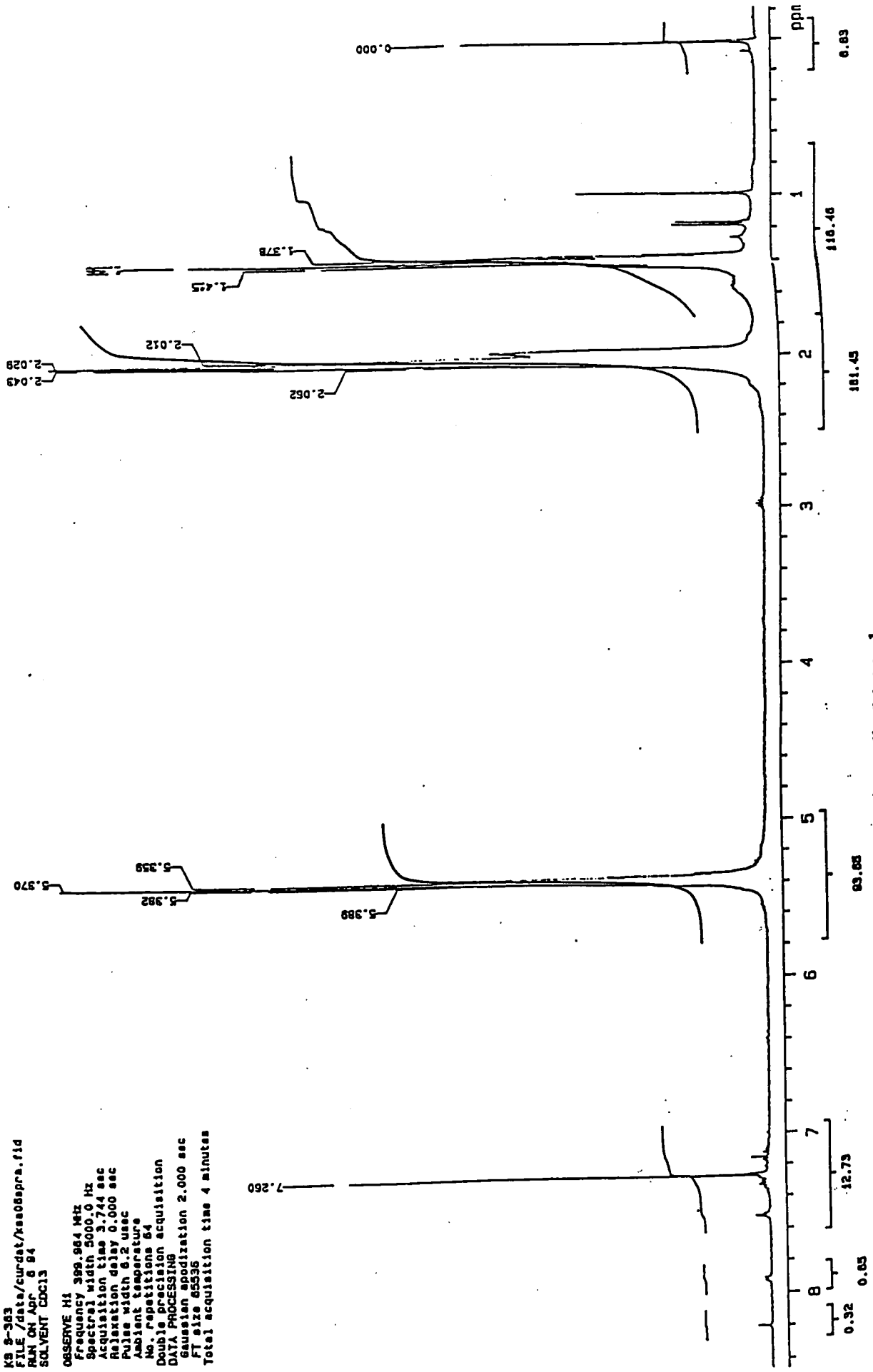
OBSERVE H1
 Frequency 399.964 MHz
 Spectral width 5000.0 Hz
 Acquisition time 3.744 sec
 Relaxation delay 0.000 sec
 Pulse width 6.2 usec
 Ambient temperature
 No. repetitions 64
 Double Precision acquisition
 DATA PROCESSING
 Gaussian modulation 2.000 sec
 F1 size 65536
 Total acquisition time 4 minutes



Appendix 5.3.14. 1H n.m.r. spectrum of P5-14

KB 2-263
 FILE /data/curdnt/ks06apr.fid
 RUN ON APR 6 84
 SOLVENT CDC13

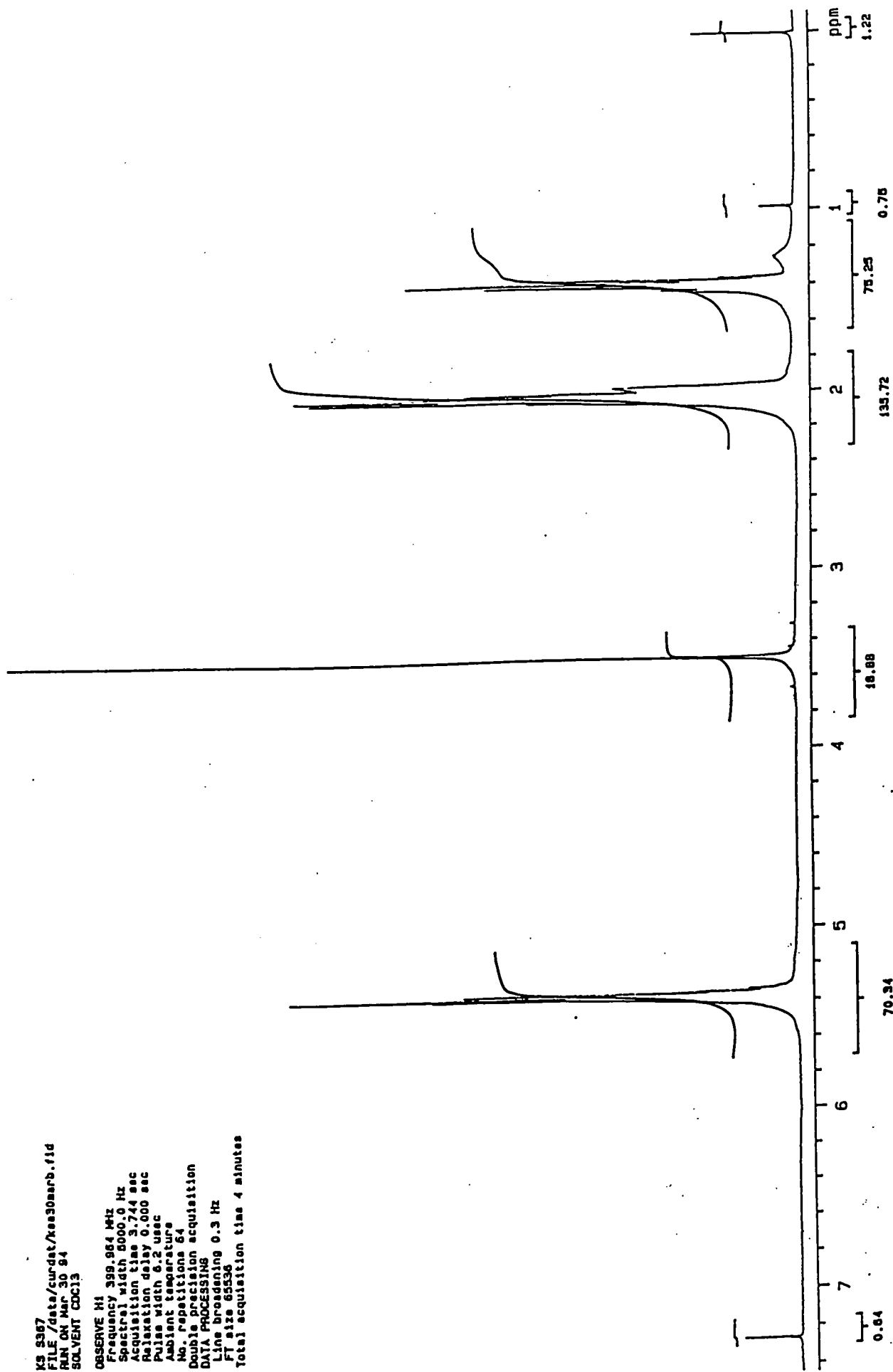
OBSERVE HI
 Frequency 399.964 MHz
 Spectral width 5000.0 Hz
 Acquisition time 3.744 sec
 Relaxation delay 0.000 sec
 Pulse width 6.2 usec
 Ambient temperature
 No. repetitions 64
 Double precision acquisition
 DATA PROCESSING
 Gaussian apodization 2.000 sec
 FT size 65536
 Total acquisition time 4 minutes



Appendix 5.3.15. 1H n.m.r. spectrum of P5-15

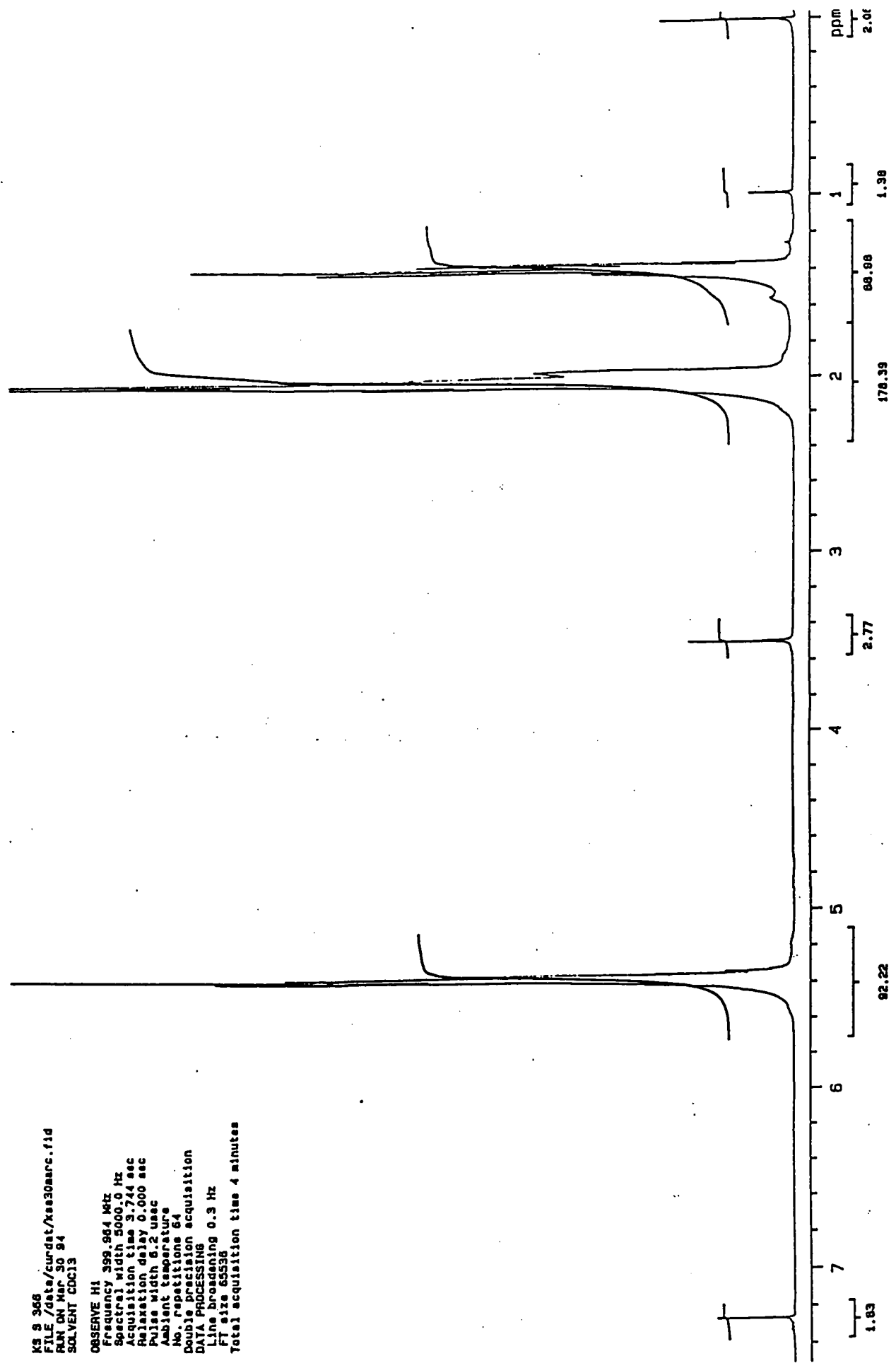
K5 8387
FILE /data/curdatt/nea30narb.11d
RUN ON MP-30 84
SOLVENT CDCl3

OBSERVE H1
Frequency 399.984 MHz
Spectral width 8000.0 Hz
Acquisition time 3.744 sec
Relaxation delay 0.000 sec
Pulse width 6.2 usec
Ambient temperature
No. repetitions 64
Double precision acquisition
DATA PROCESSING
Line broadening 0.3 Hz
FT size 65536
Total acquisition time 4 minutes



Appendix 5.3.16. ¹H n.m.r. spectrum of P5-16

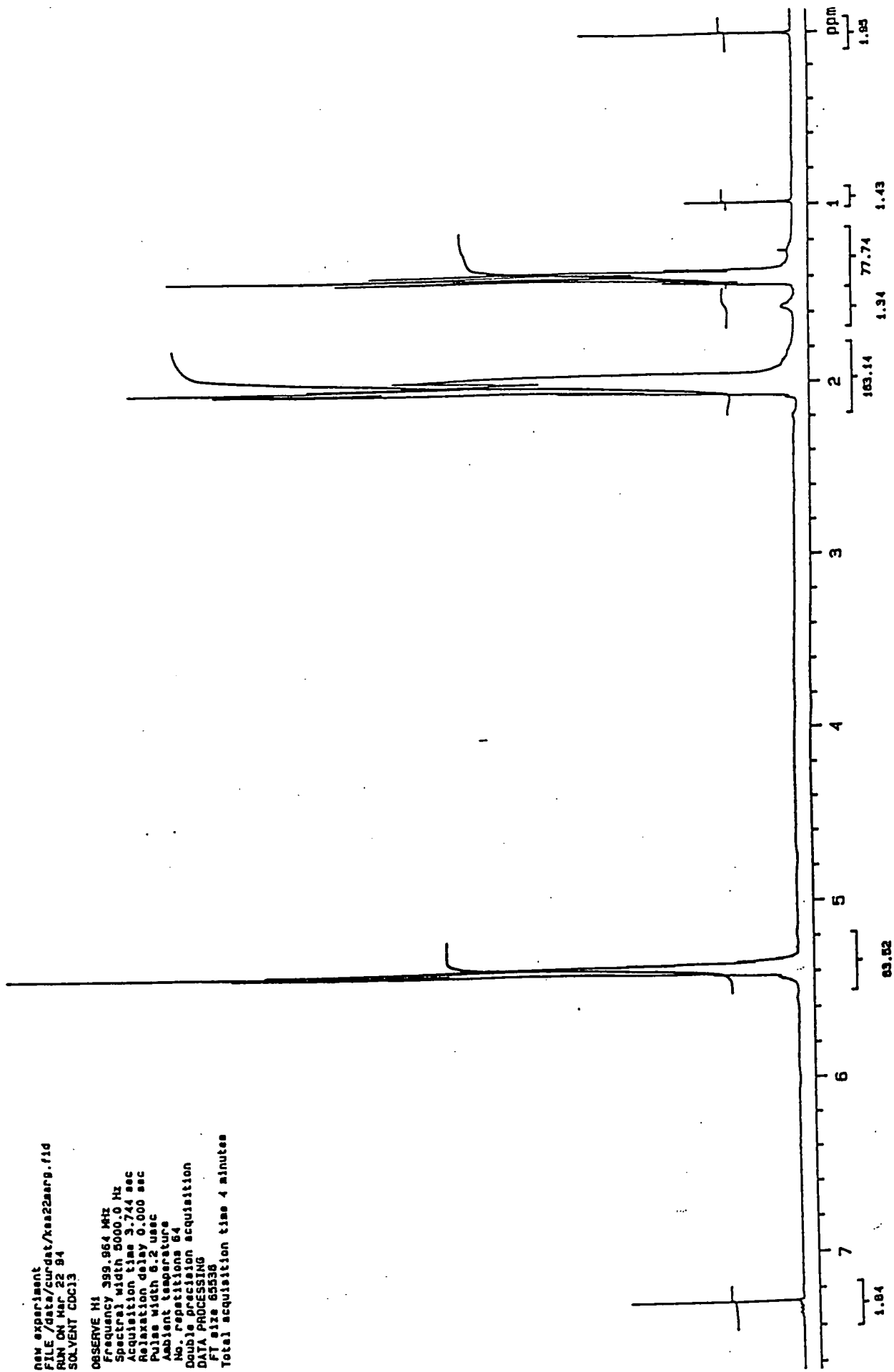
K5 9 366
 FILE /data/curdatt/ks30arc.fid
 RUN ON Mar 30 94
 SOLVENT CDC13
 OBSERVE H1
 Frequency 399.964 MHz
 Spectral width 5000.0 Hz
 Acquisition time 3.744 sec
 Relaxation delay 0.000 sec
 Pulse width 6.2 usec
 Ambient temperature
 No. repetitions 64
 Double precision acquisition
 DATA PROCESSING
 Line broadening 0.3 Hz
 FT size 65536
 Total acquisition time 4 minutes



Appendix 5.3.17. 1H n.m.r. spectrum of P5-17

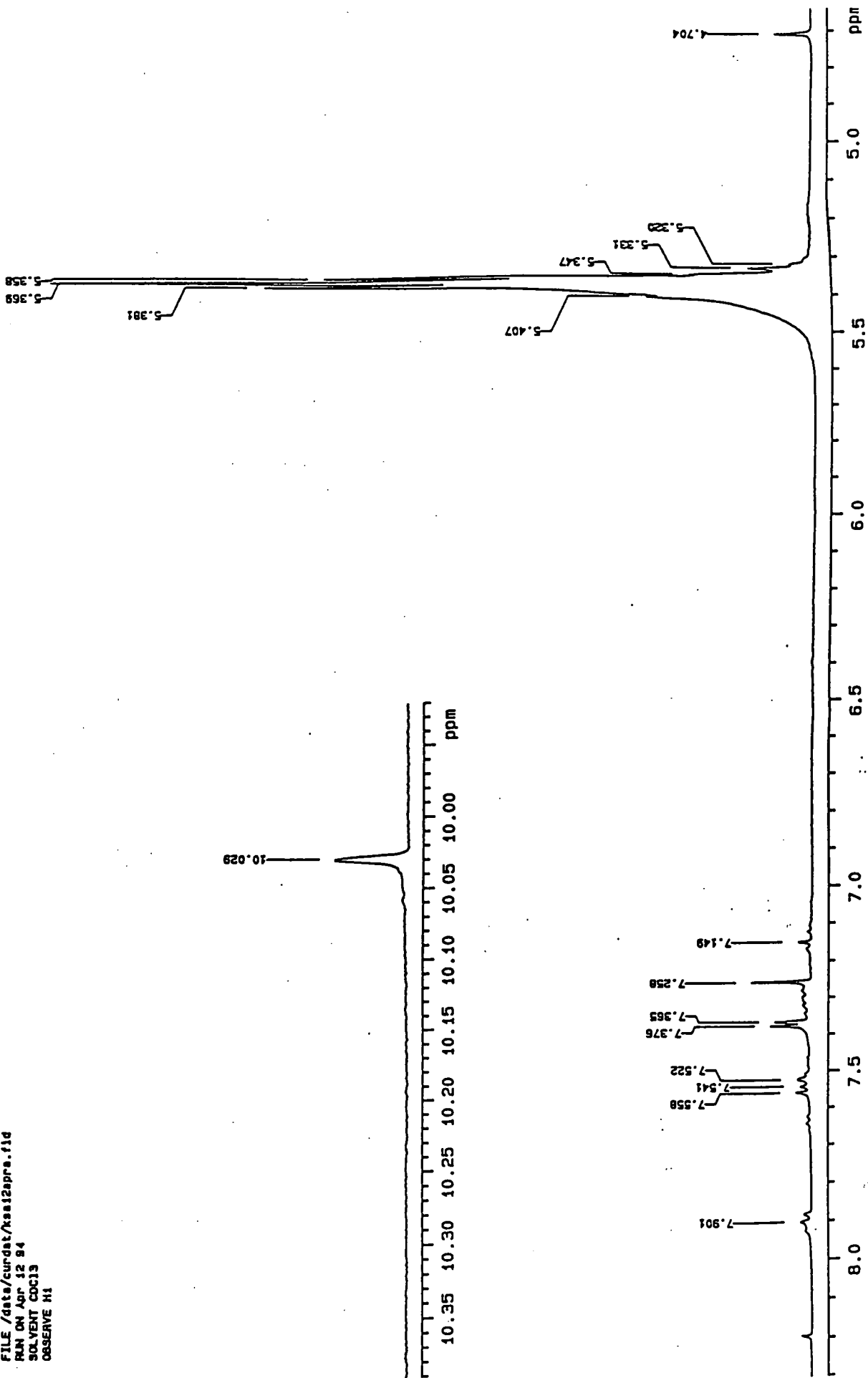
new experiment
FILE /data/curdat/ksa22aarg.fid
RUN ON Mar 22 84
SOLVENT CDC13

OBSERVE H1
Frequency 399.964 MHz
Spectral width 5000.0 Hz
Acquisition time 3.744 sec
Relaxation delay 0.000 sec
Pulse width 6.2 usec
Ambient temperature
No. repetitions 64
Double precision acquisition
DATA PROCESSING
F1 size 65536
Total acquisition time 4 minutes



Appendix 5.3.18. 1H n.m.r. spectrum of P5-18

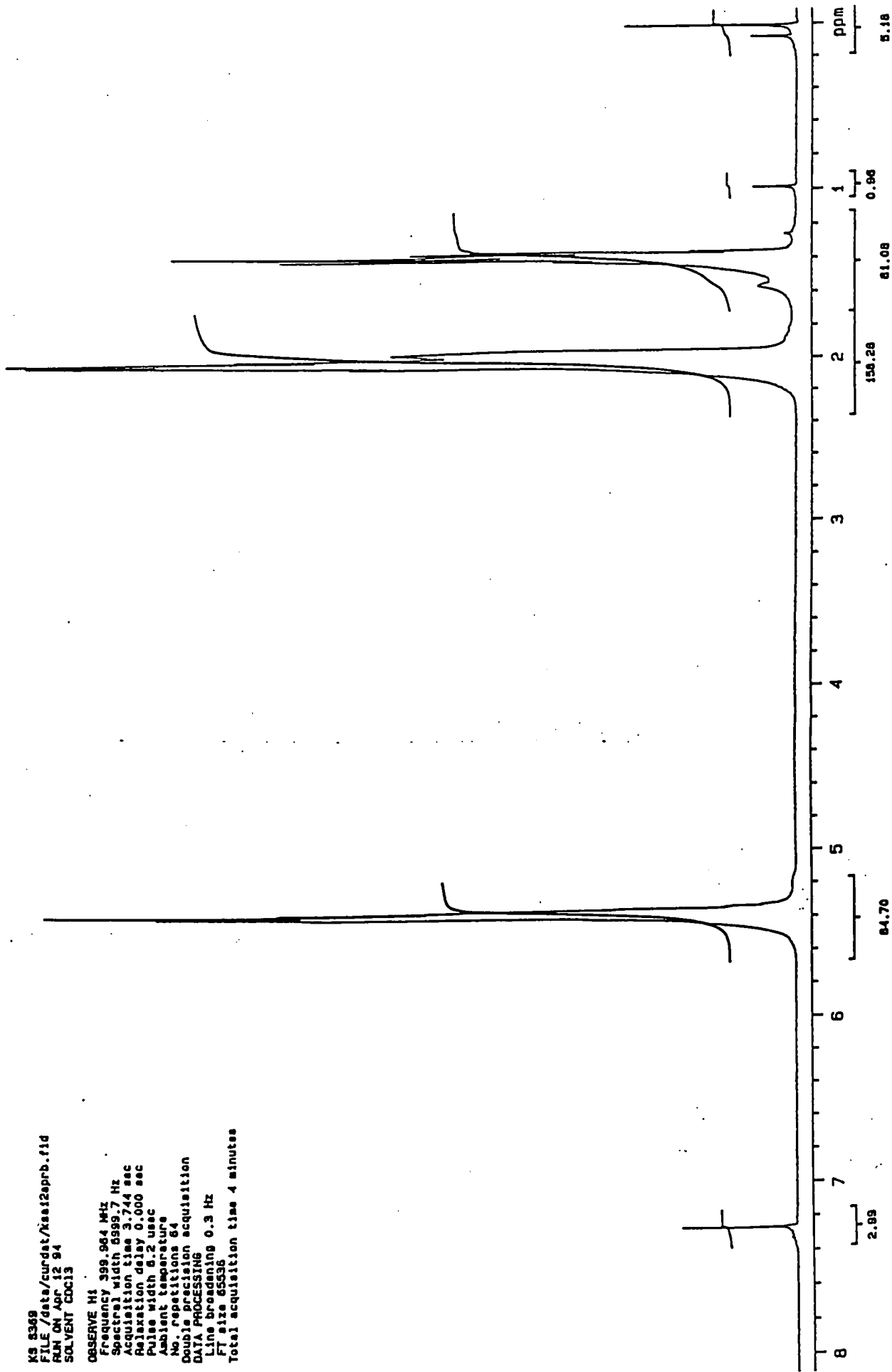
KS 9370
FILE /data/curdnt/xsai2apra.f1d
RUN ON Apr 12 84
SOLVENT CDCl3
OBSERVE H1



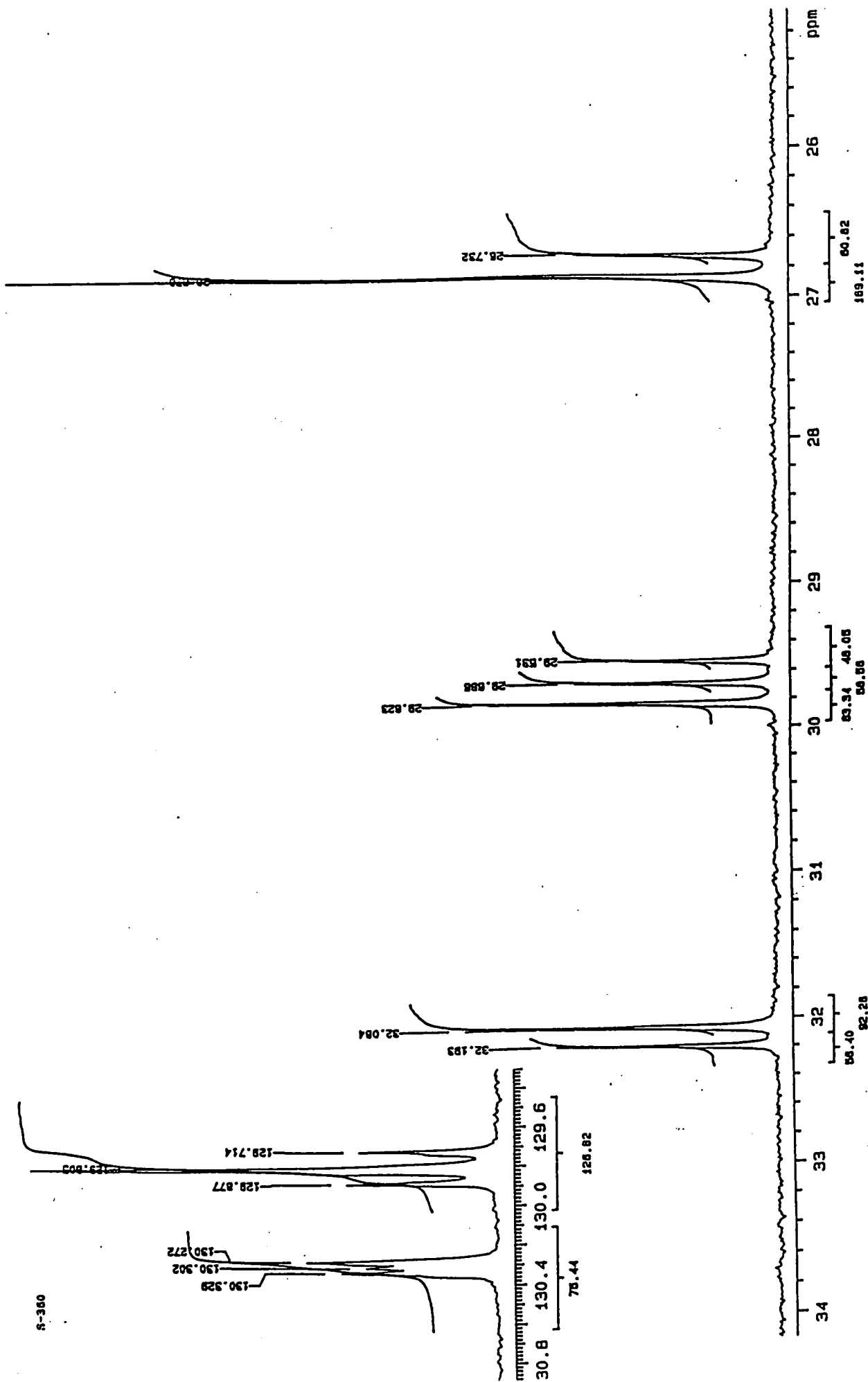
Appendix 5.3.19. ¹H n.m.r. spectrum of P5-19

K5 8369
FILE /data/curdnt/ksat2eprb.fid
RUN ON Apr 12 94
SOLVENT CDCl3

OBSERVE H1
Frequency 399.964 MHz
Spectral width 8999.7 Hz
Acquisition time 3.744 sec
Relaxation delay 0.000 sec
Pulse width 6.2 usec
Ambient temperature
No. repetitions 64
Double precision acquisition
DATA PROCESSING
Line broadening 0.3 Hz
FI size 65536
Total acquisition time 4 minutes

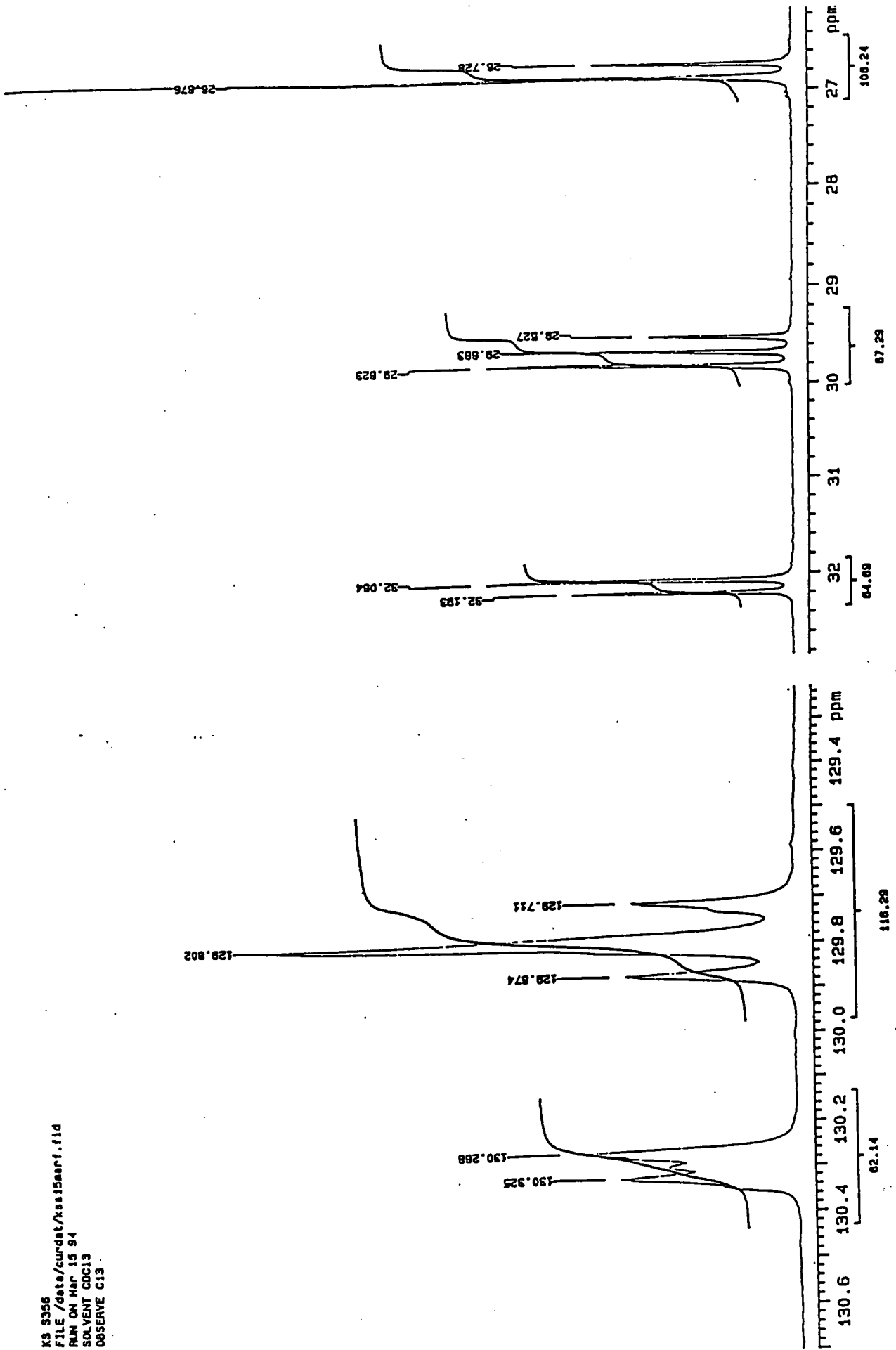


Appendix 5.3.20. ¹H n.m.r. spectrum of P5-20



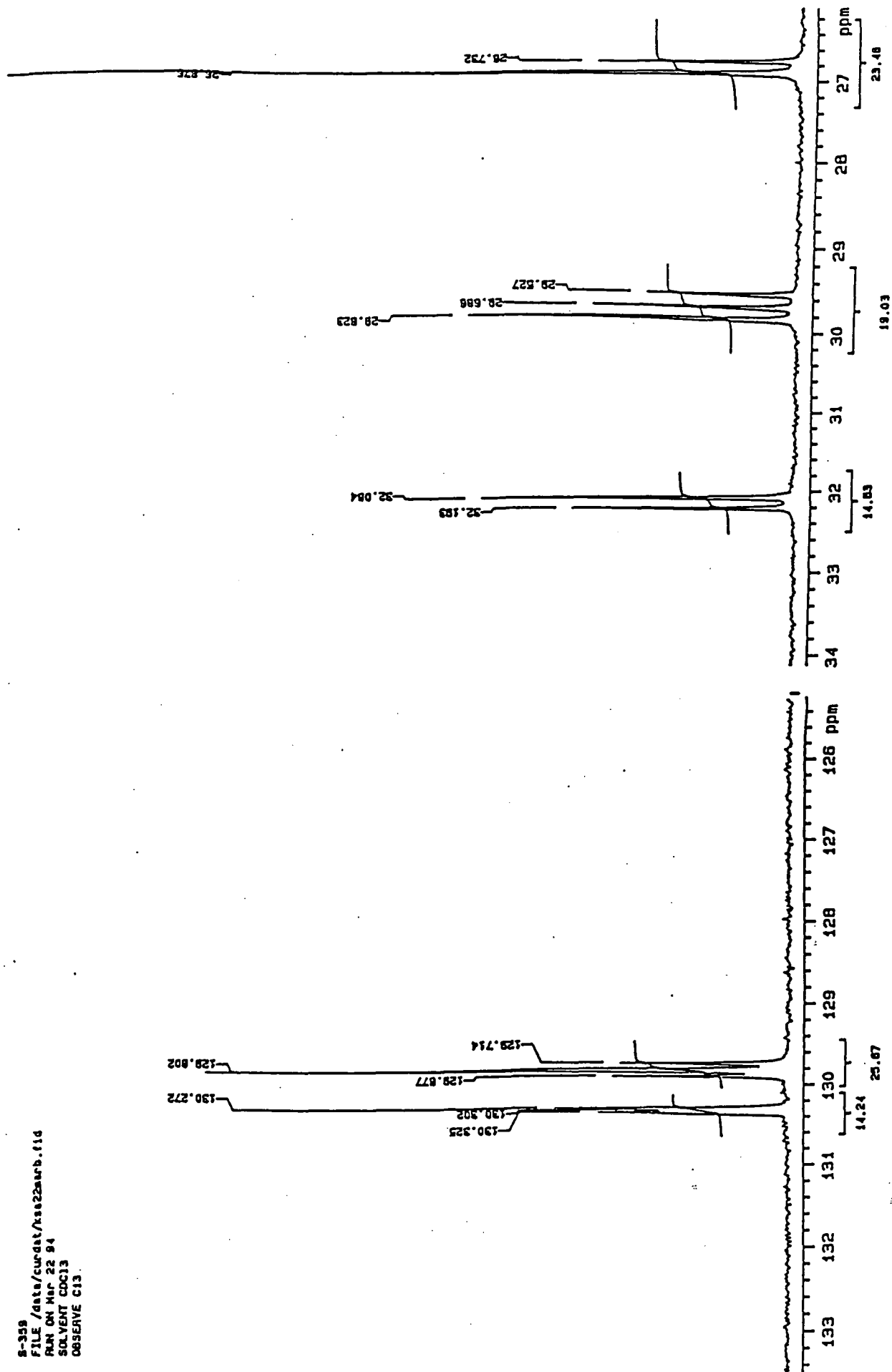
Appendix 5.4.1. ^{13}C n.m.r. spectrum of P5-1

KS S356
FILE /data/curdet/ks15marf.f1d
RUN ON Mar 15 94
SOLVENT CCl3
OBSERVE C13



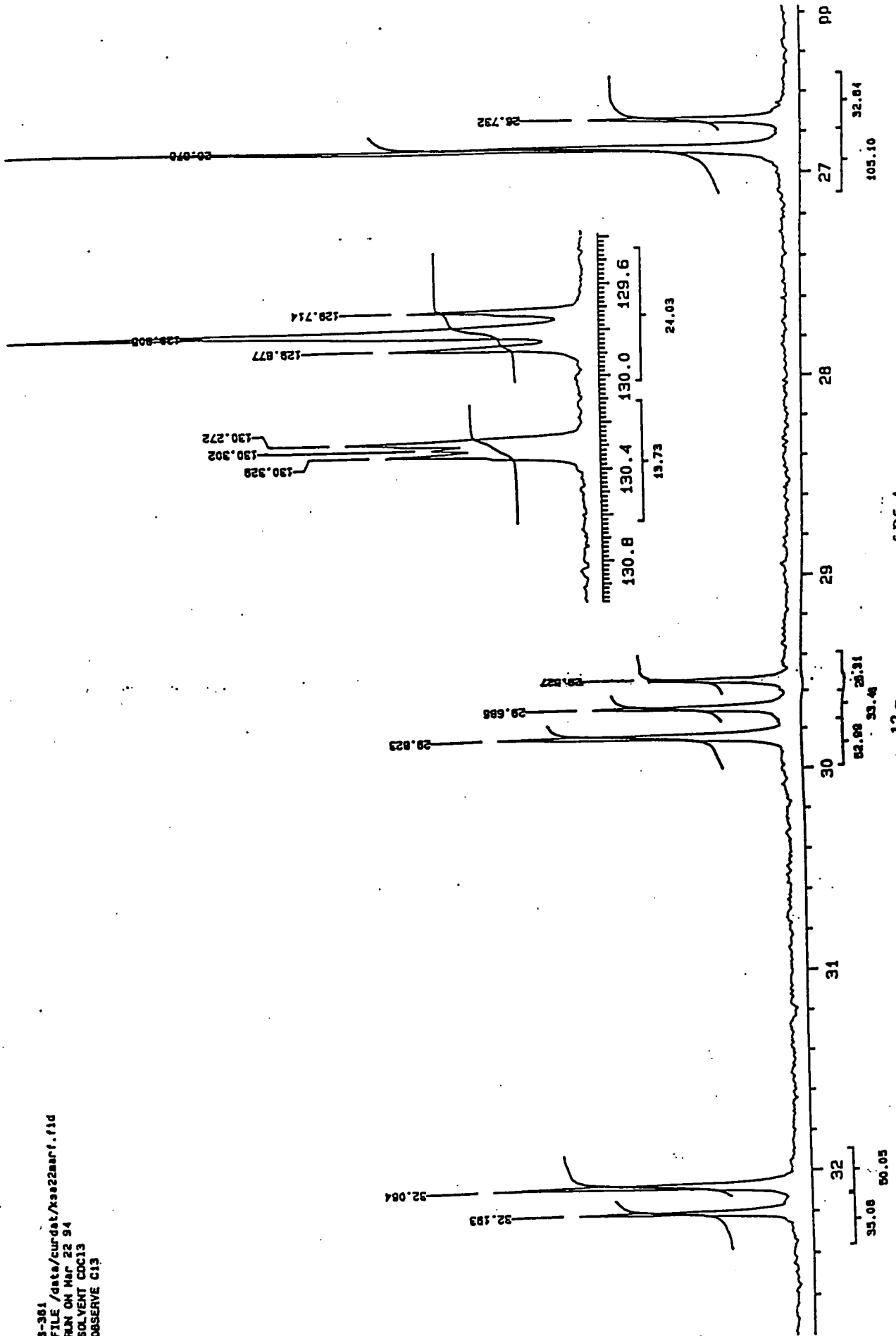
Appendix 5.4.2. ¹³C n.m.r. spectrum of P5-2

8-359
FILE /data/curdnt/lse22aarb.11d
RUN ON Mar 22 94
SOLVENT CDCl3
OBSERVE C13



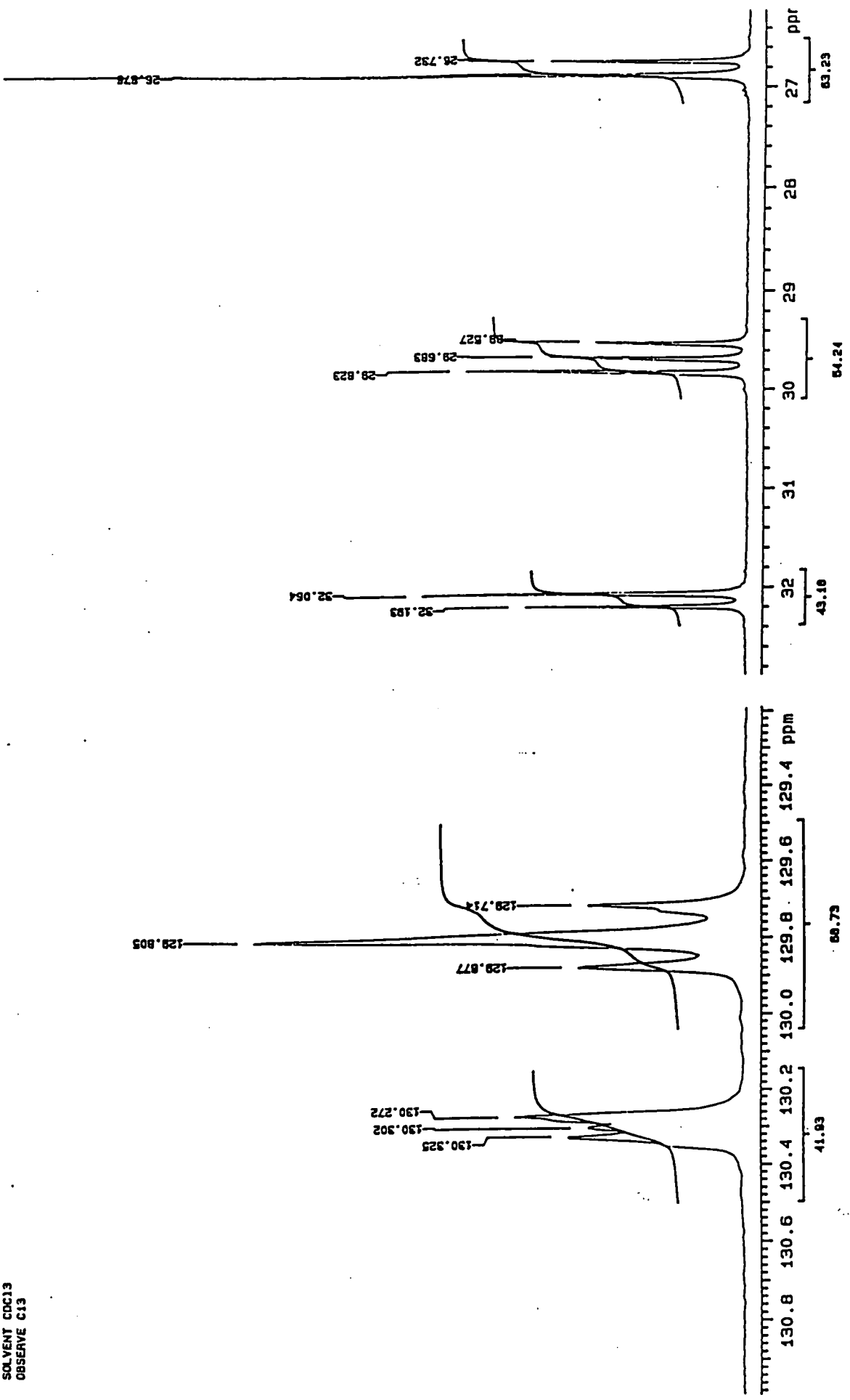
Appendix 5.4.3. ^{13}C n.m.r. spectrum of P5-3

3-361
 FILE /data/cw-dst/xss22ar.f1d
 RUN ON Mar 22 94
 SOLVENT CCl3
 OBSERVE C13



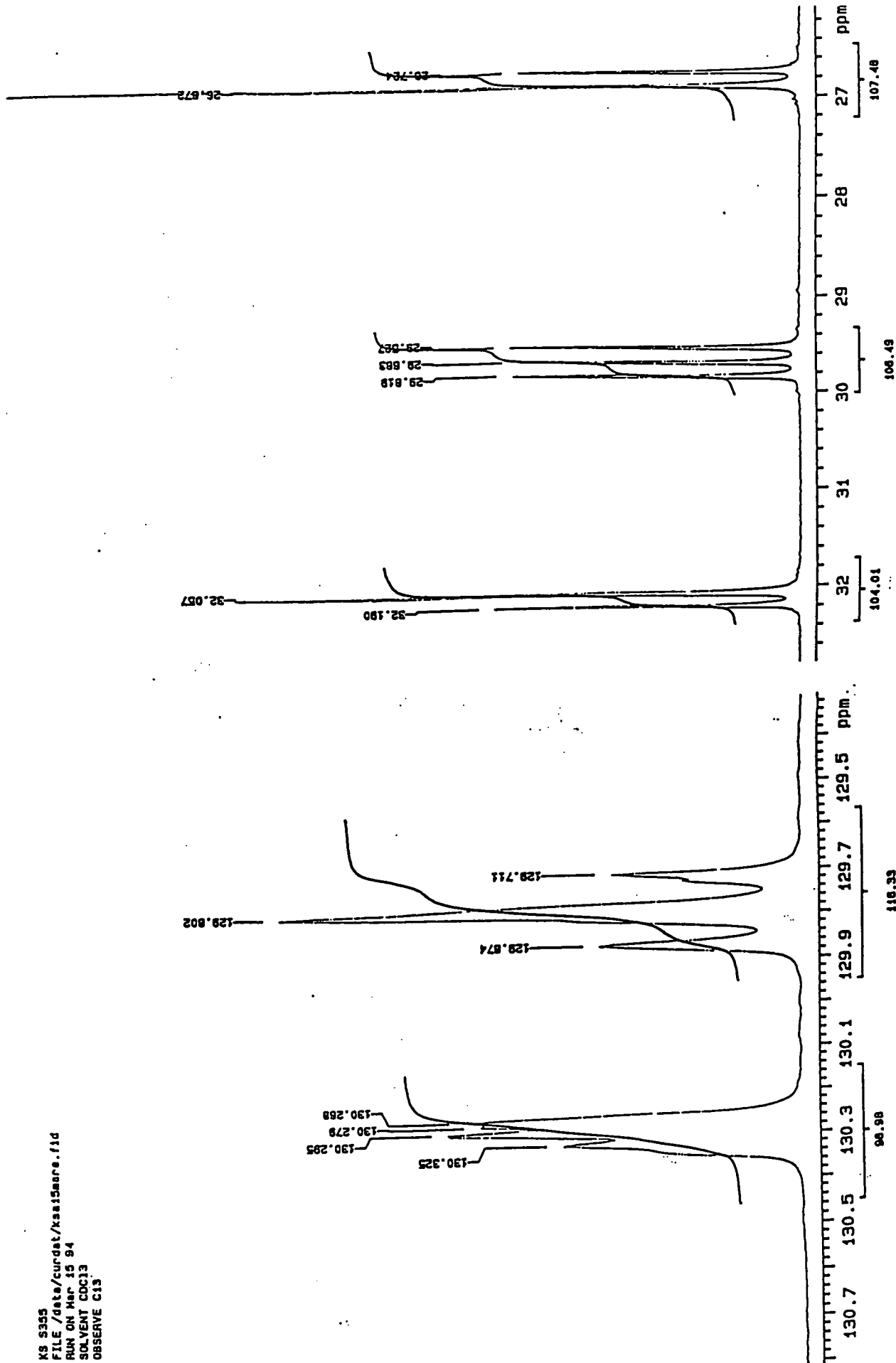
Appendix 5.4.4. ¹³C n.m.r. spectrum of P5-4

K3 3354
FILE /data/curdat/ksa15aard.fid
RUN ON Mac 15 84
SOLVENT CDCl3
OBSERVE C13

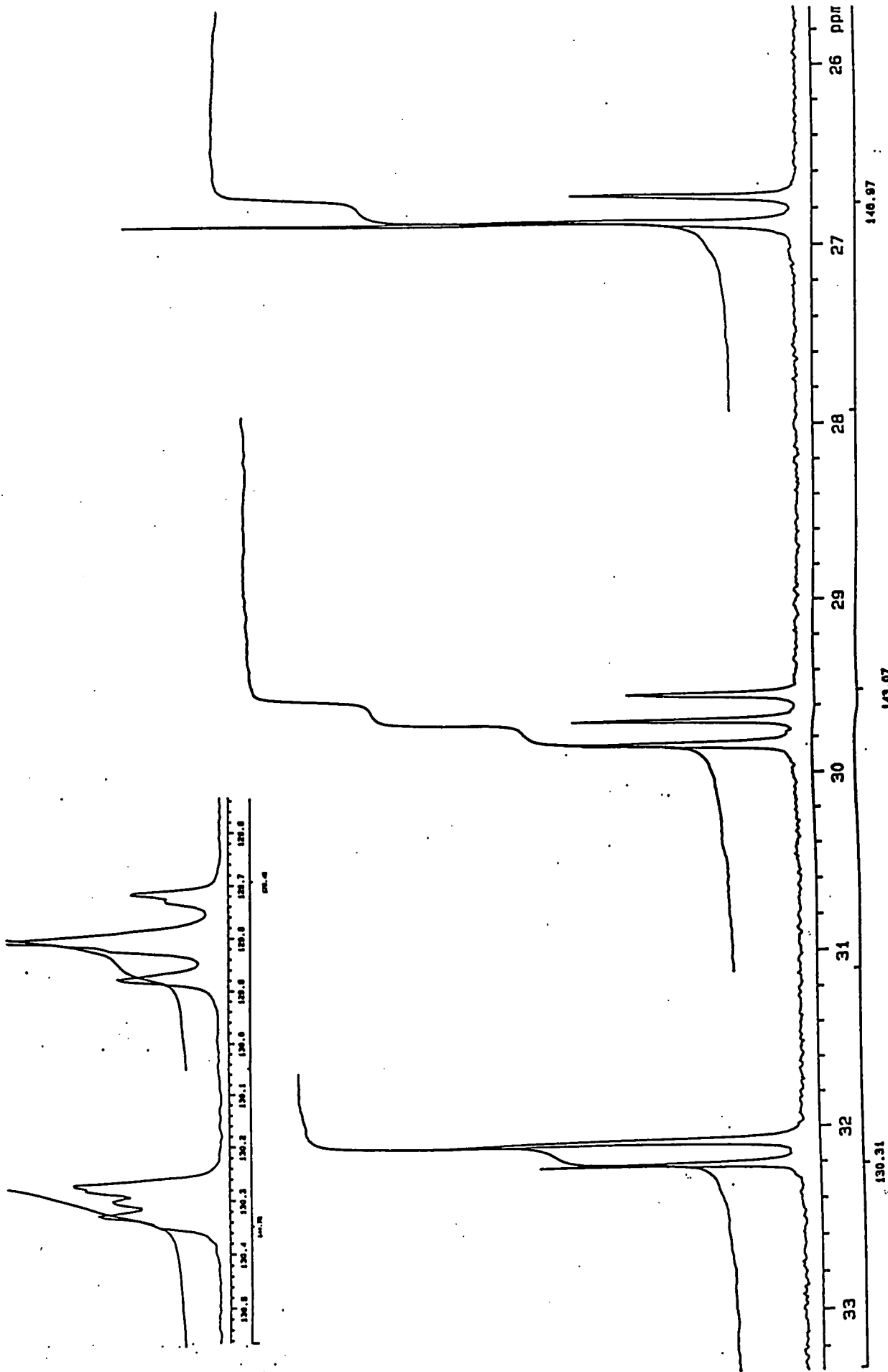


Appendix 5.4.5. ¹³C n.m.r. spectrum of P5-5

KS 5355
FILE /data/curdat/ksaismare.fid
RUN ON Mar 15 94
SOLVENT CDCl3
OBSERVE C13

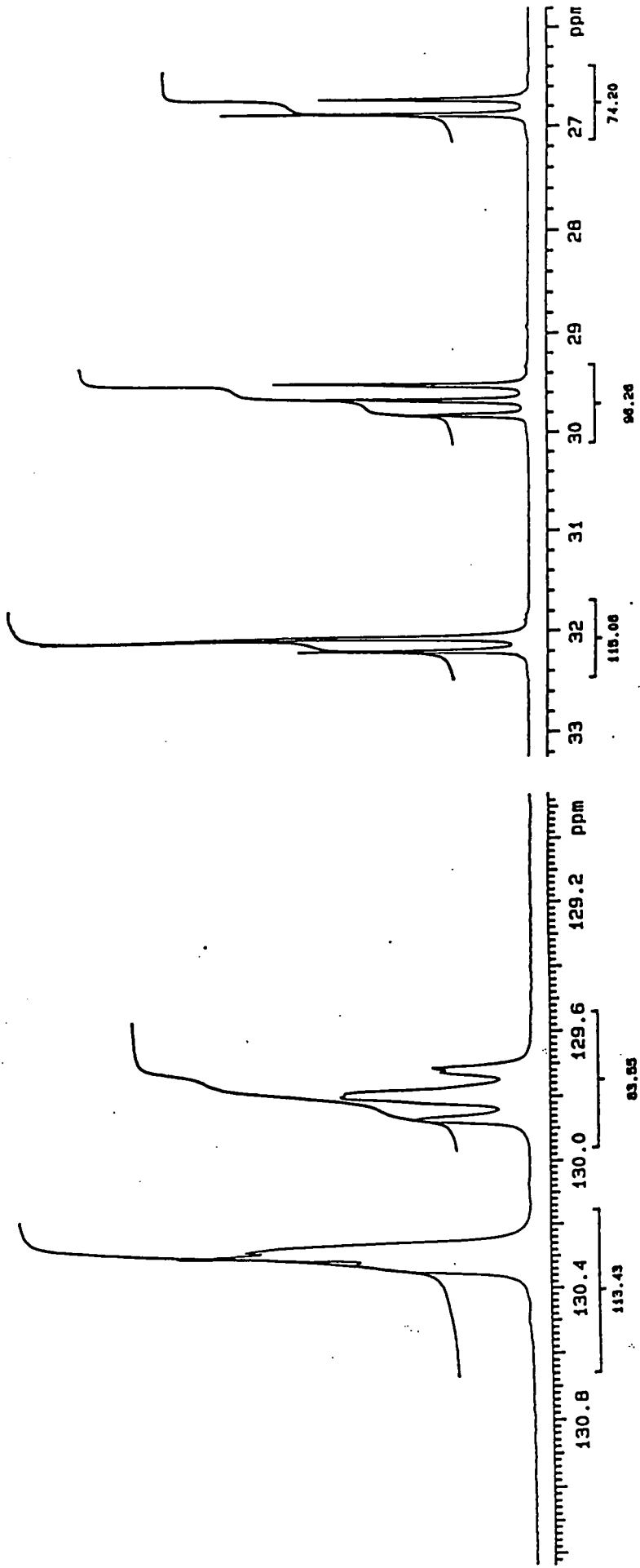


Appendix 5.4.6. ¹³C n.m.r. spectrum of P5-6



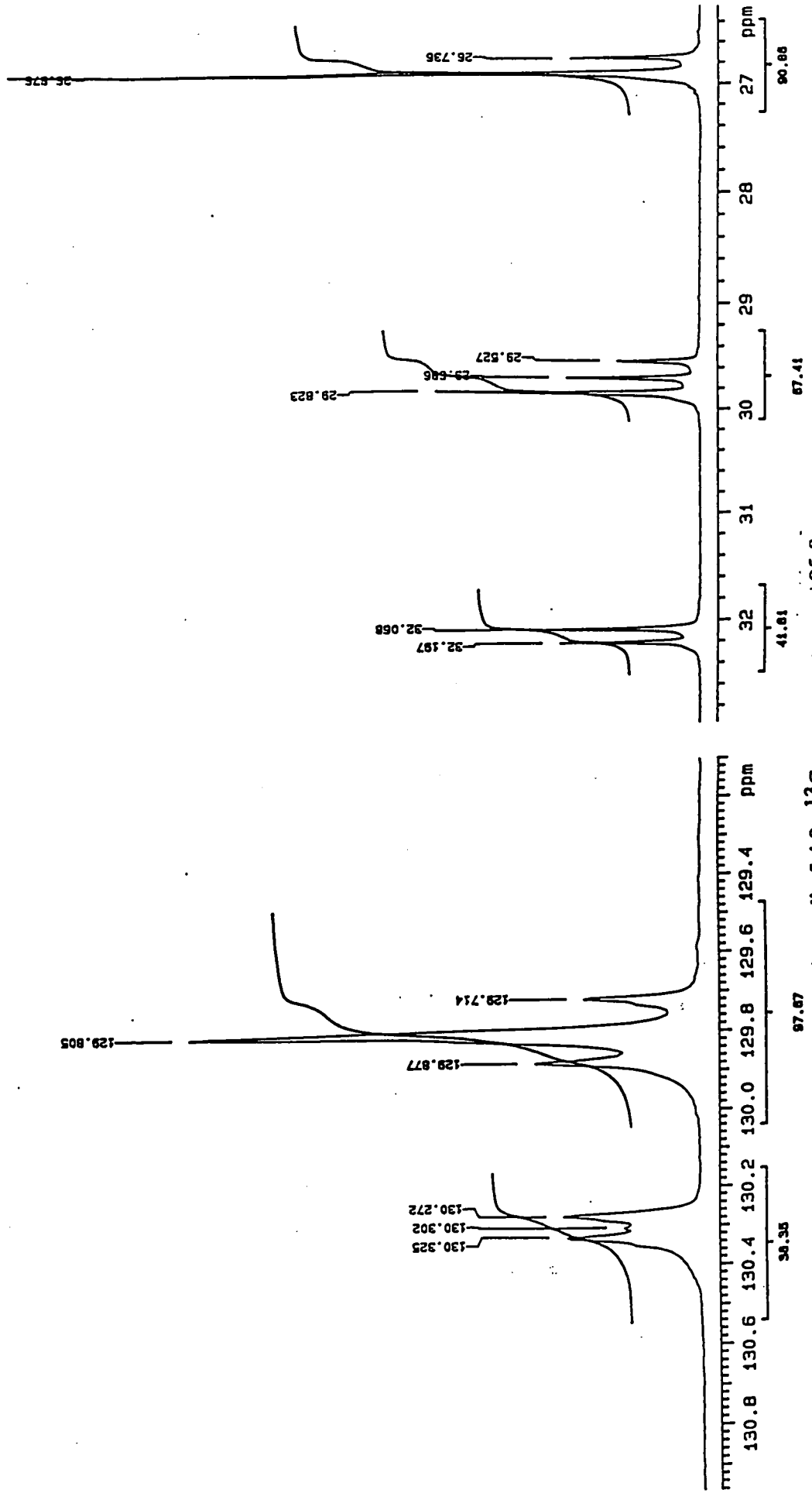
Appendix 5.4.7. ^{13}C n.m.r. spectrum of P5-7

KS 351-1
FILE /data/curdat/Kss03aarb.fid
RUN ON Mar 9 84
SOLVENT CDCl3
OBSERVE C13



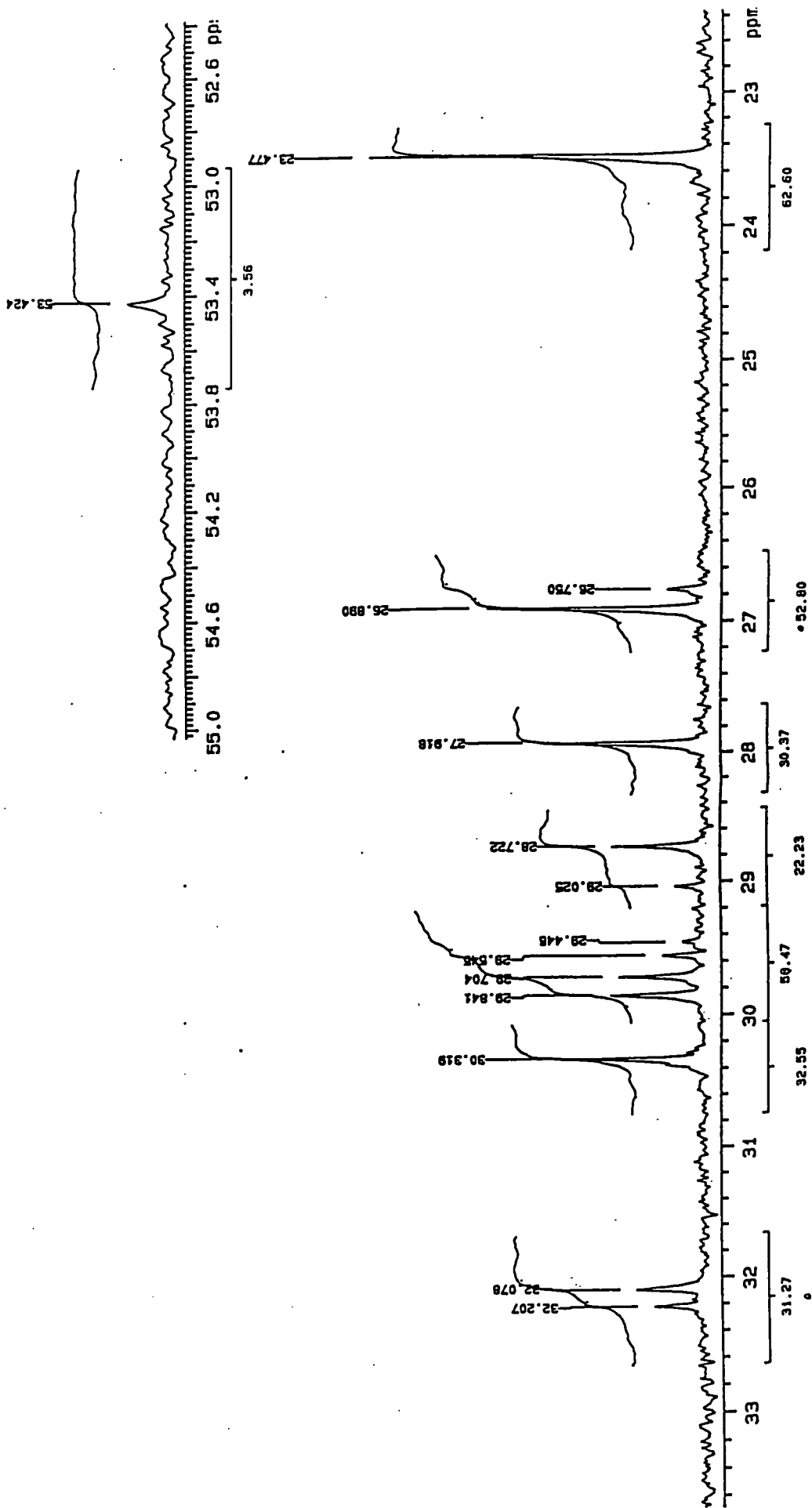
Appendix 5.4.8. ^{13}C n.m.r. spectrum of PS-8

K9_9371
FILE /data/curdet/kas14epfb.fid
RAN ON Apr 14 94
SOLVENT CCl3
OBSERVE C13



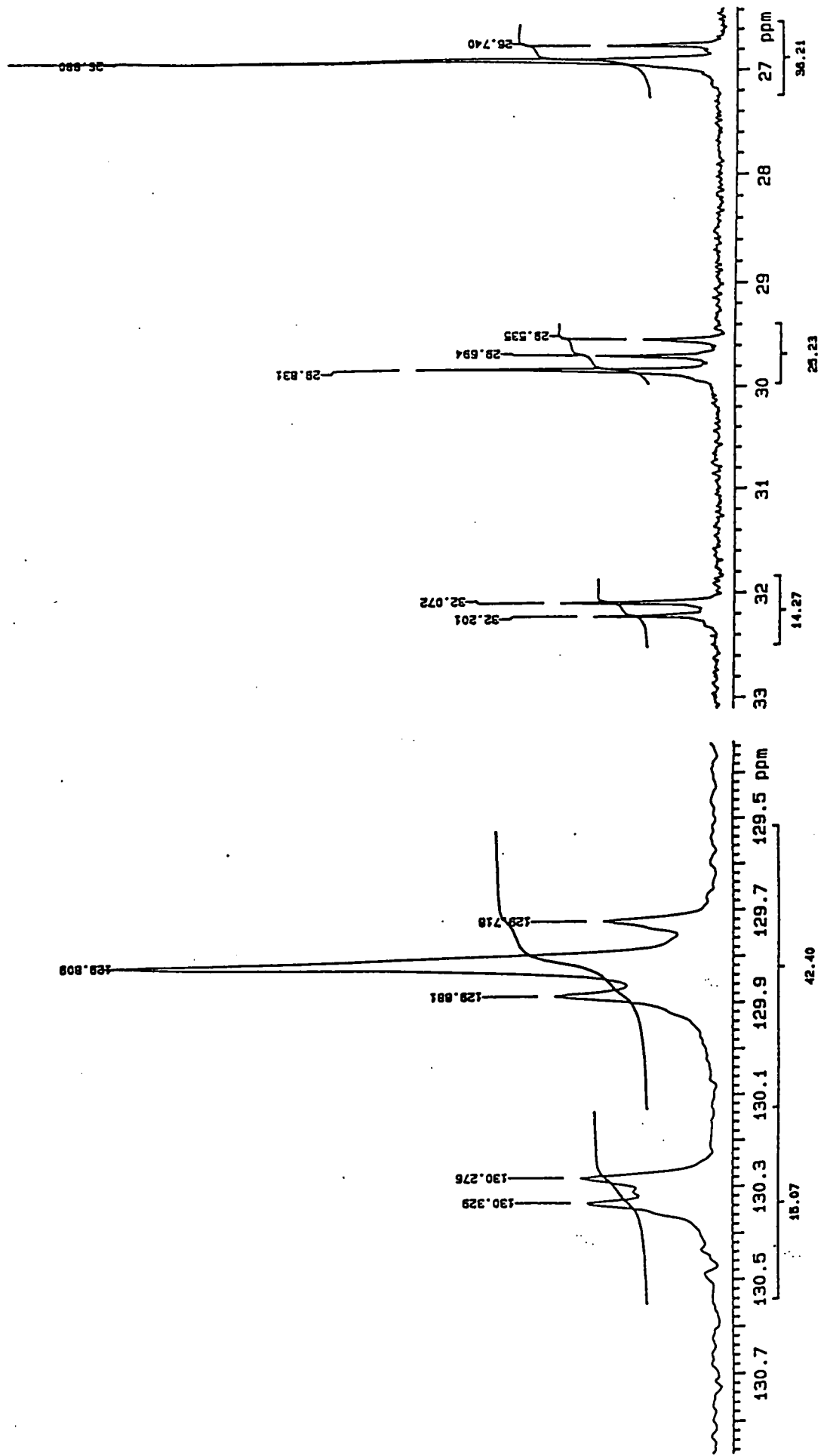
Appendix 5.4.9. ¹³C n.m.r. spectrum of P5-9

KS 8373
 FILE /data/cwrdet/ks828sprs.fid
 RUN ON Apr 28 94
 SOLVENT CDCl3
 OBSERVE C13



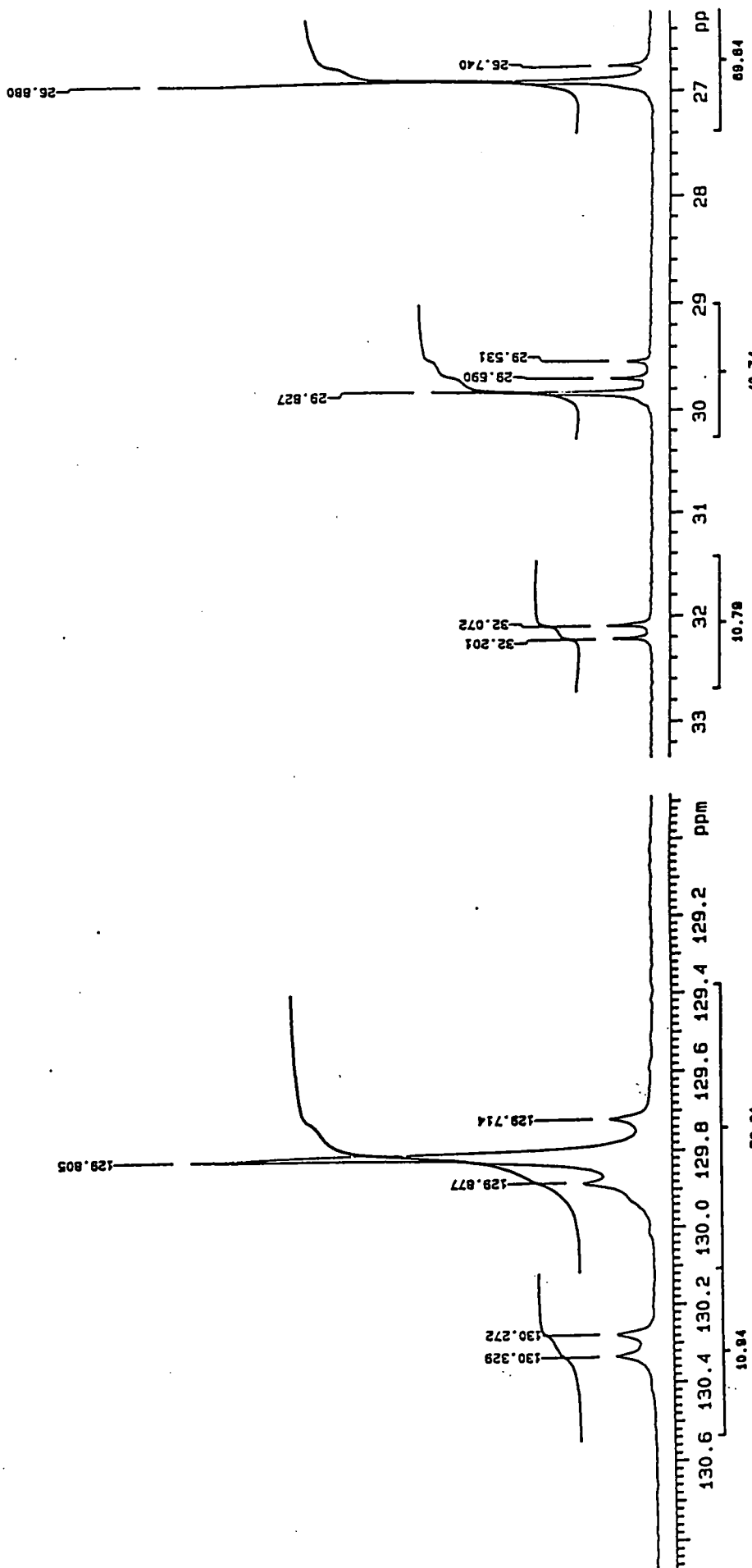
Appendix 5.4.10. ¹³C n.m.r. spectrum of P5-10

K3 3374
FILE /data/curdet/kas27apr8.f1d
RUN ON Apr 27 94
SOLVENT CDCl3
OBSERVE C13



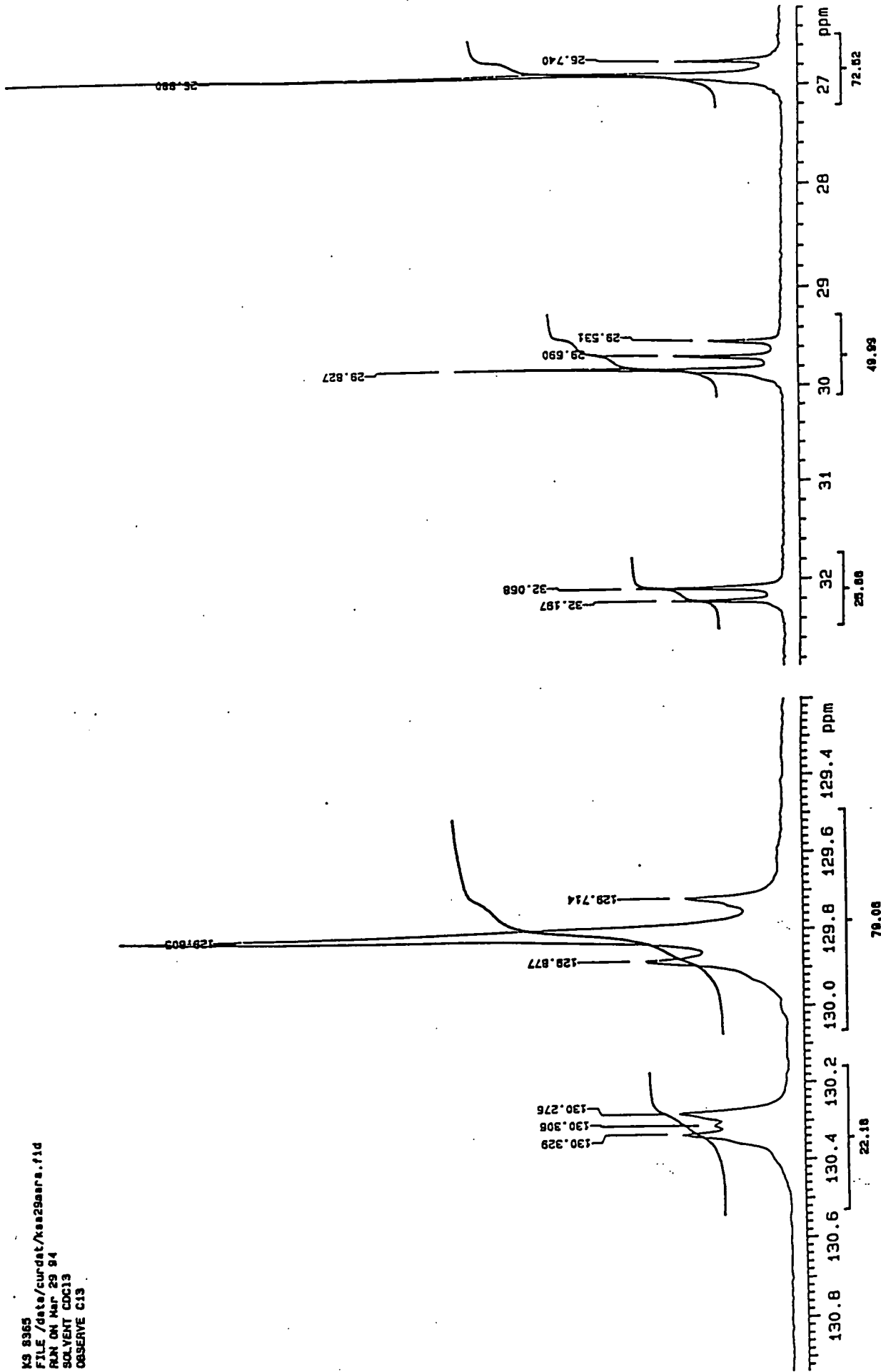
Appendix 5.4.11. ^{13}C n.m.r. spectrum of P5-11

K3 8966
FILE /data/curdnt/xas29mrd.f1d
RUN ON Mar 29 84
SOLVENT CDCl3
OBSERVE C13



Appendix 5.4.12. ^{13}C n.m.r. spectrum of P5-12

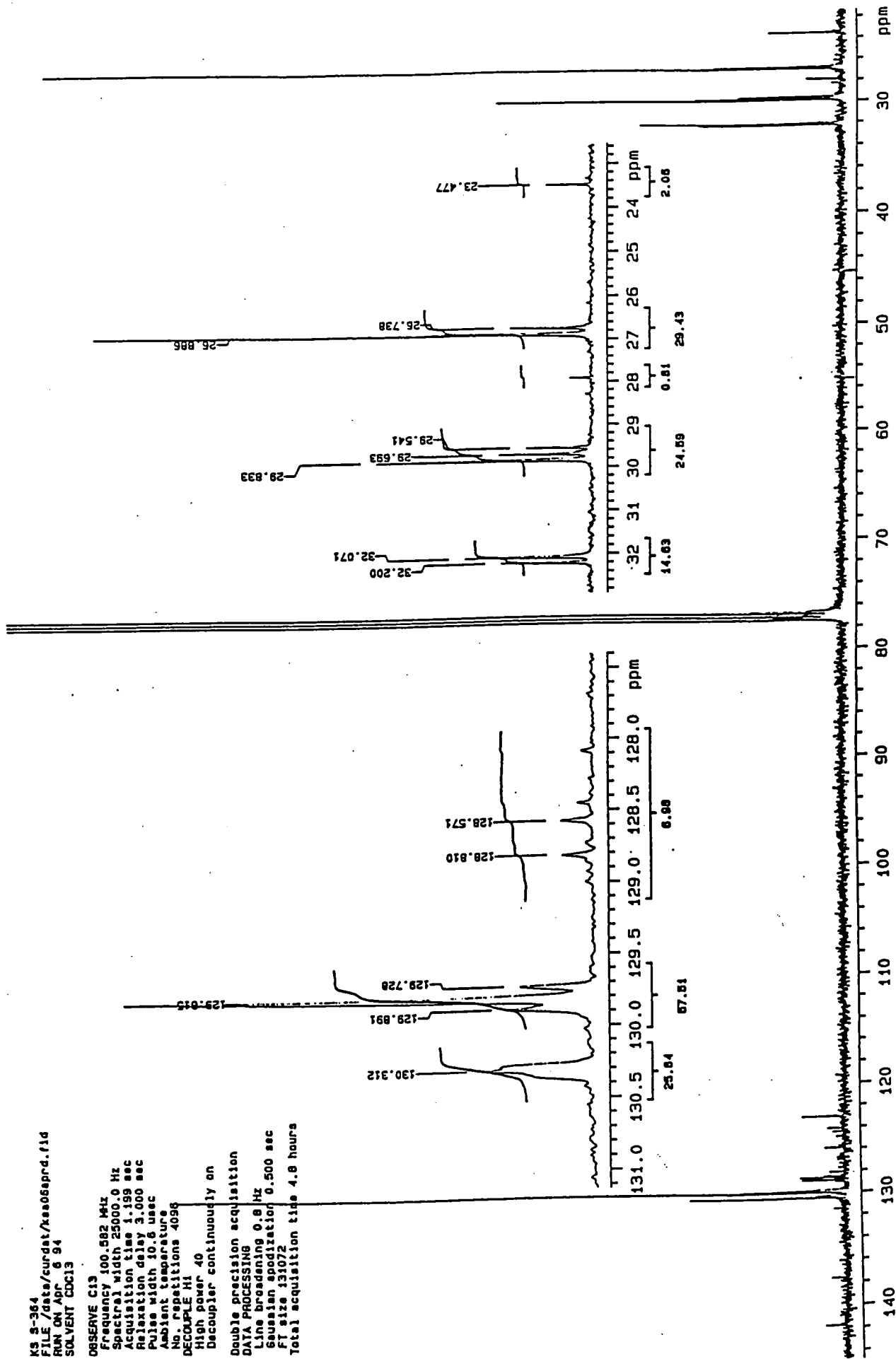
K9 8965
FILE /data/curdnt/ks29aars.11d
RUN ON Mar 29 94
SOLVENT CDCl3
OBSERVE C13



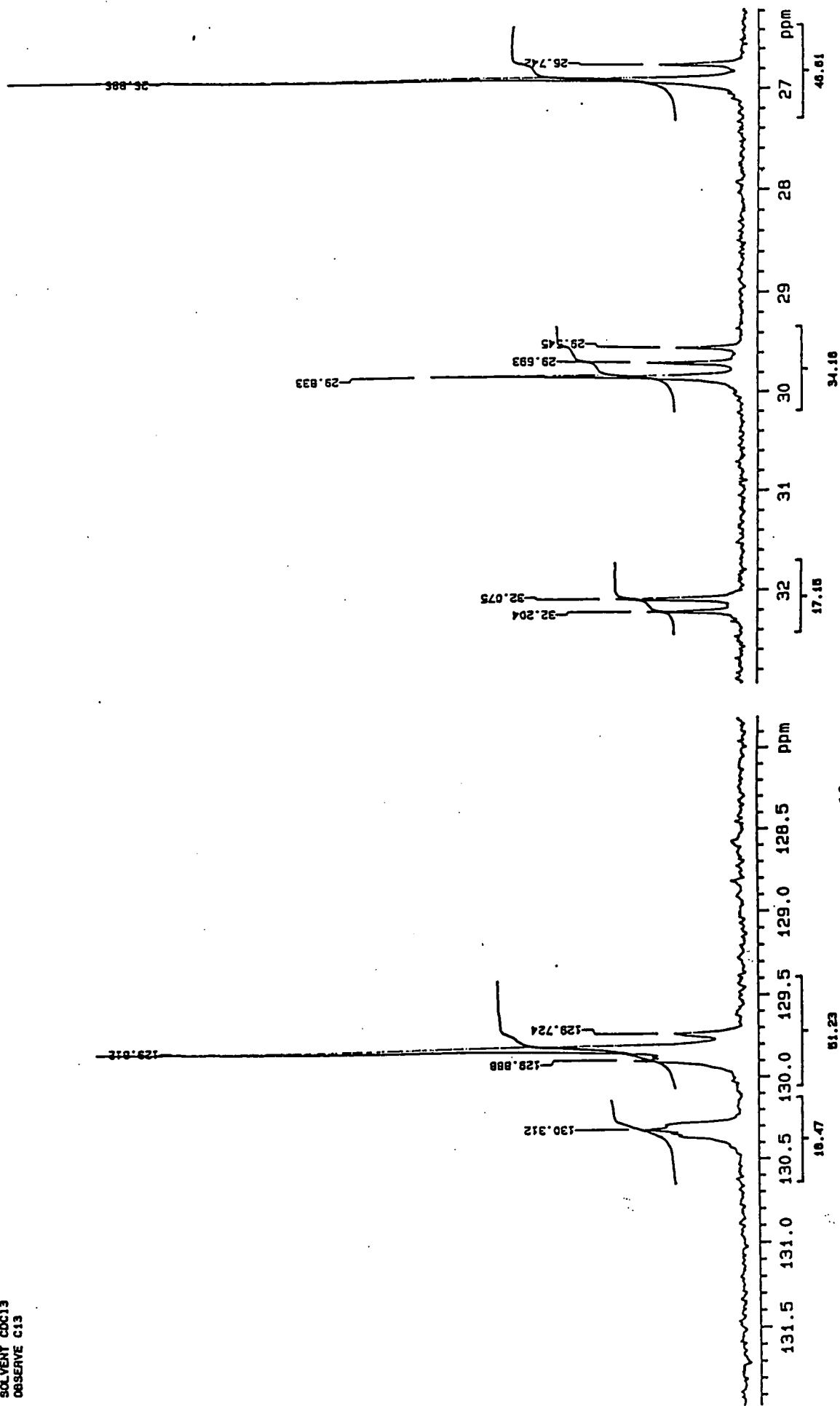
Appendix 5.4.13. ^{13}C n.m.r. spectrum of P5-13

KS 8-364
 FILE /data/curdat/ksa06sprd.fid
 RUN ON Apr 6 94
 SOLVENT CDCl3

OBSERVE C13
 Frequency 100.622 MHz
 Spectral width 25000.0 Hz
 Acquisition time 1.199 sec
 Relaxation delay 3.000 sec
 Pulse width 10.6 usec
 Ambient temperature
 No. repetitions 4098
 DECOUPLE H1
 High power 40
 Decoupler continuously on
 Double precision acquisition
 DATA PROCESSING
 Line broadening 0.8 Hz
 Gaussian apodization 0.500 sec
 FT size 131072
 Total acquisition time 4.8 hours

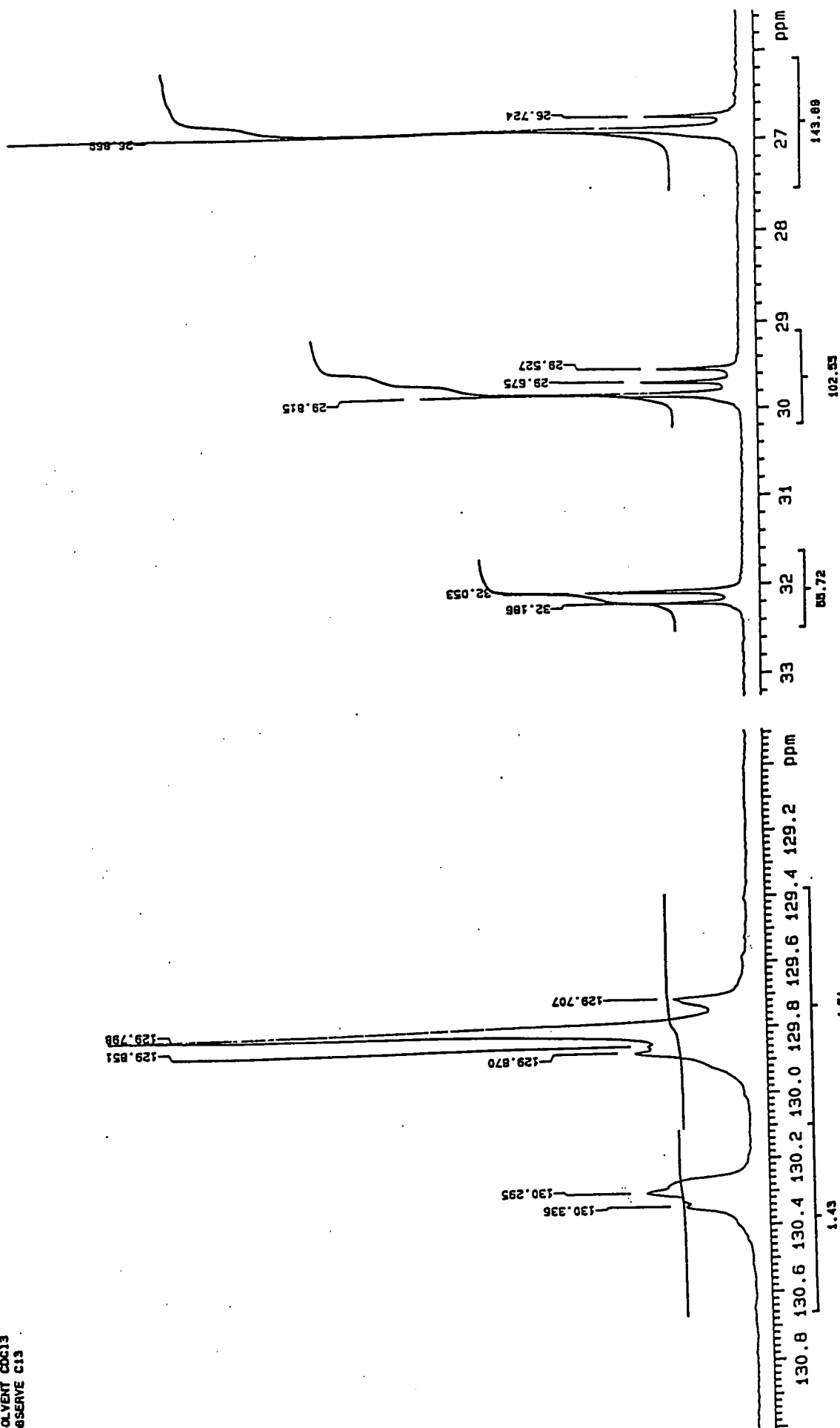


K9 8-363
FILE /data/curdat/kso06apr.b.11d
RUN ON Apr 8 84
SOLVENT CDCl3
OBSERVE C13



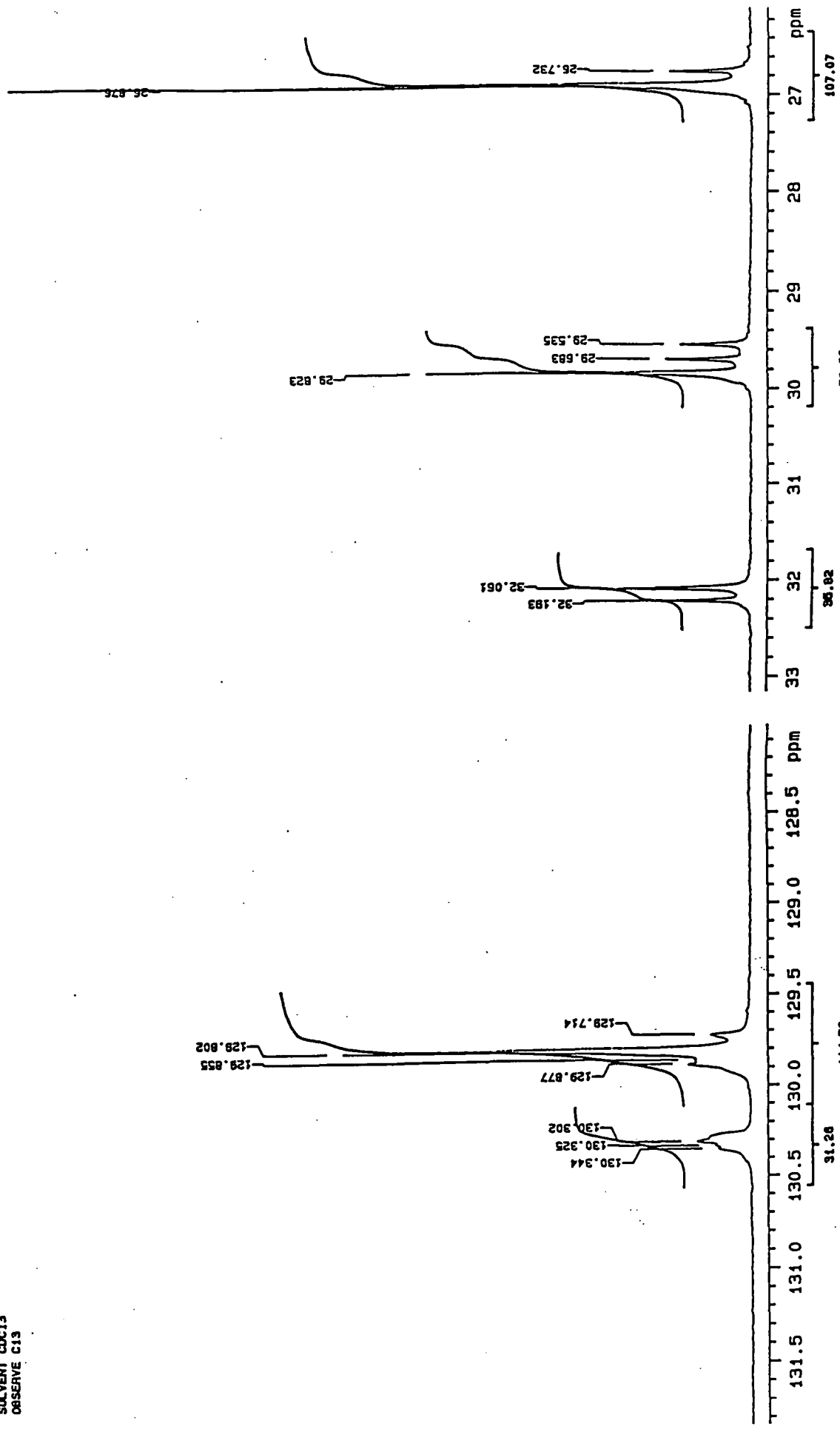
Appendix 5.4.15. ^{13}C n.m.r. spectrum of P5-15

KS 9367
FILE /data/curdet/ksa29aarc.fid
RUN ON MAR 29 94
SOLVENT CCl3
OBSERVE C13



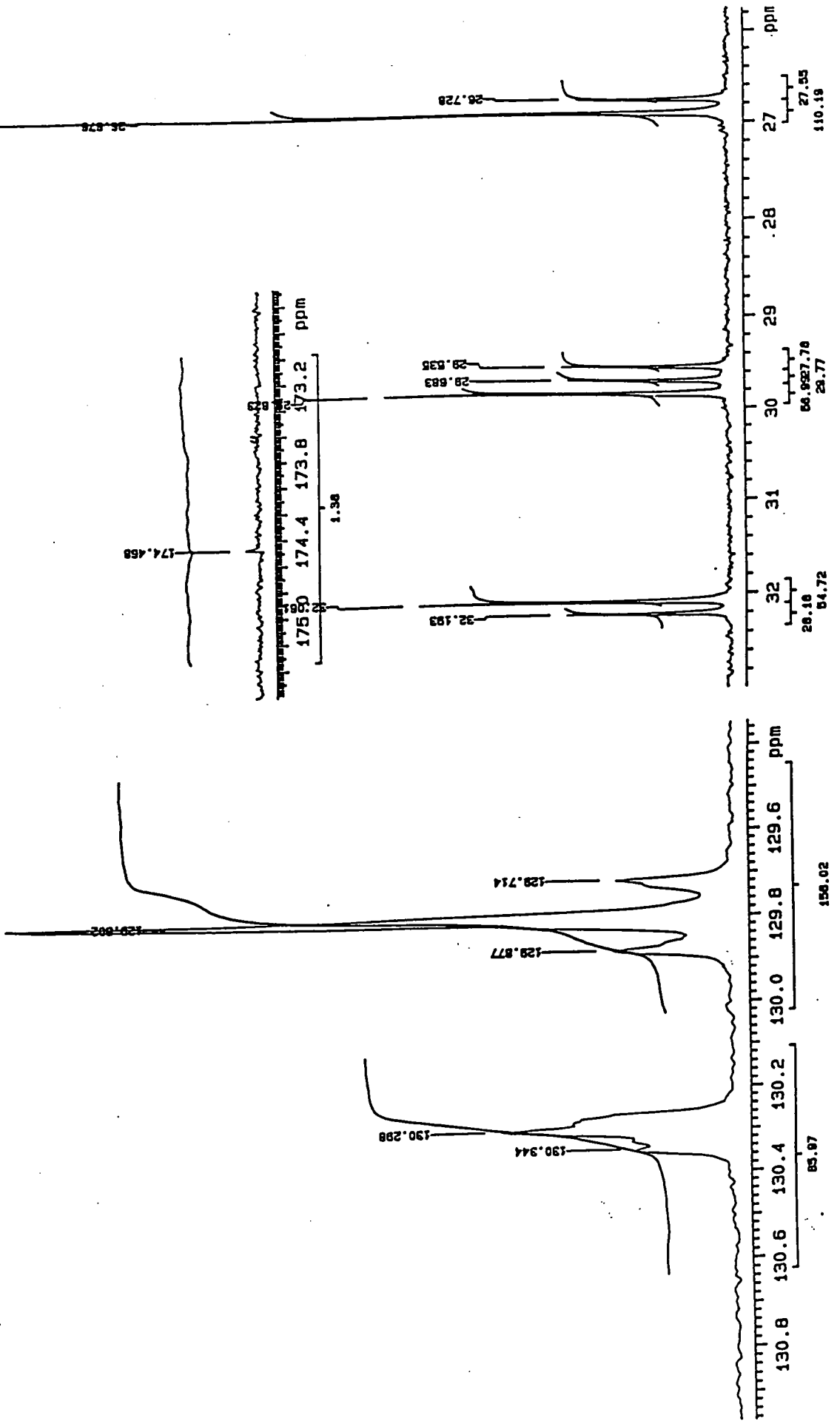
Appendix 5.4.16. ¹³C n.m.r. spectrum of P5-16

KS 5366
FILE /data/curdat/ks029marb.11d
RUN ON Mar 29 94
SOLVENT CDCl3
OBSERVE C13



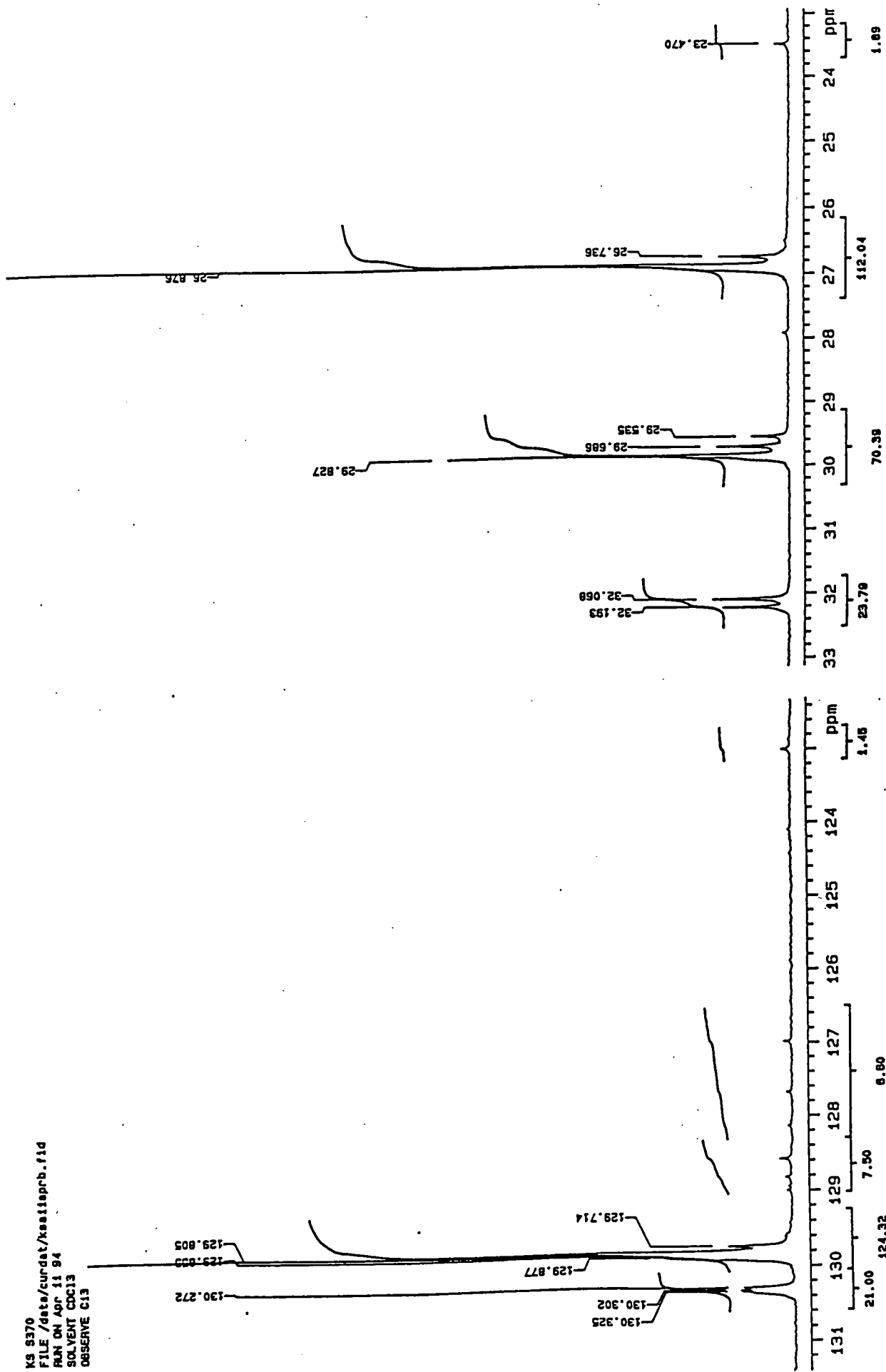
Appendix 5.4.17. ¹³C n.m.r. spectrum of P5-17

RUN ON Mar 22 94
SOLVENT CDCl3
OBSERVE C13



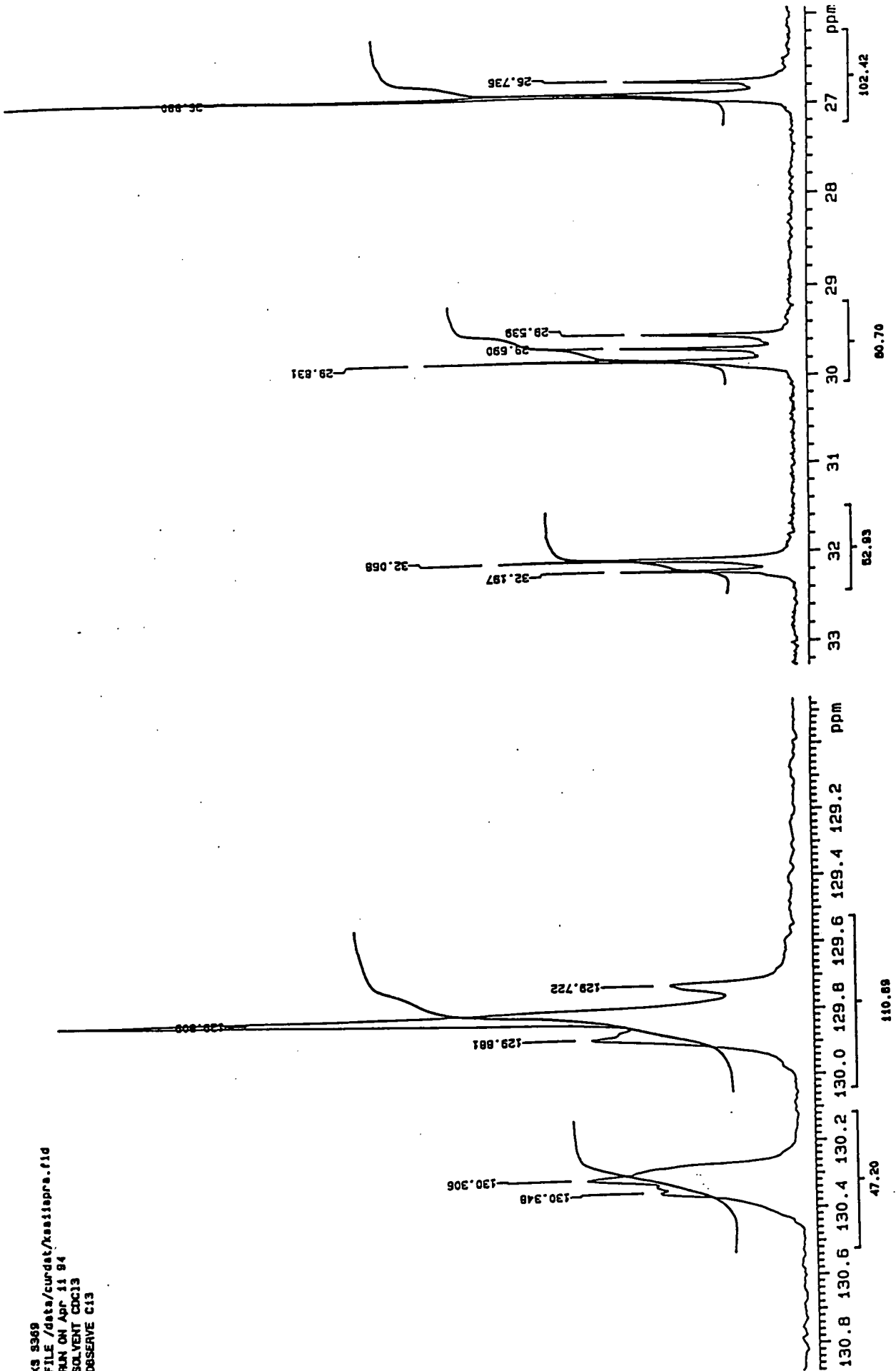
Appendix 5.4.18. ¹³C n.m.r. spectrum of P5-18

K9 8370
FILE /data/curdad/kssisprb.fid
RUN ON Apr 11 84
SOLVENT CDCl3
OBSERVE C13

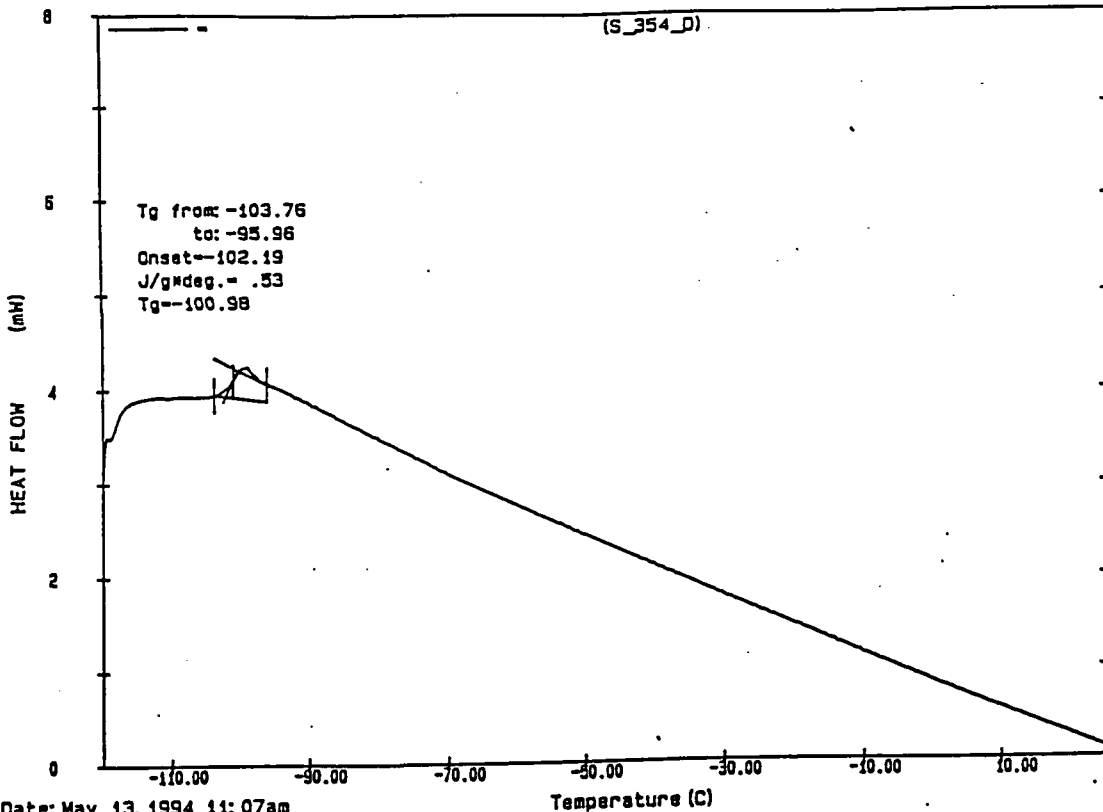


Appendix 5.4.19. ¹³C n.m.r. spectrum of PS-19

K3 9389
FILE /data/cwrdet/xos11ppra.fid
RUN ON Apr 11 94
SOLVENT CCl3
OBSERVE C13

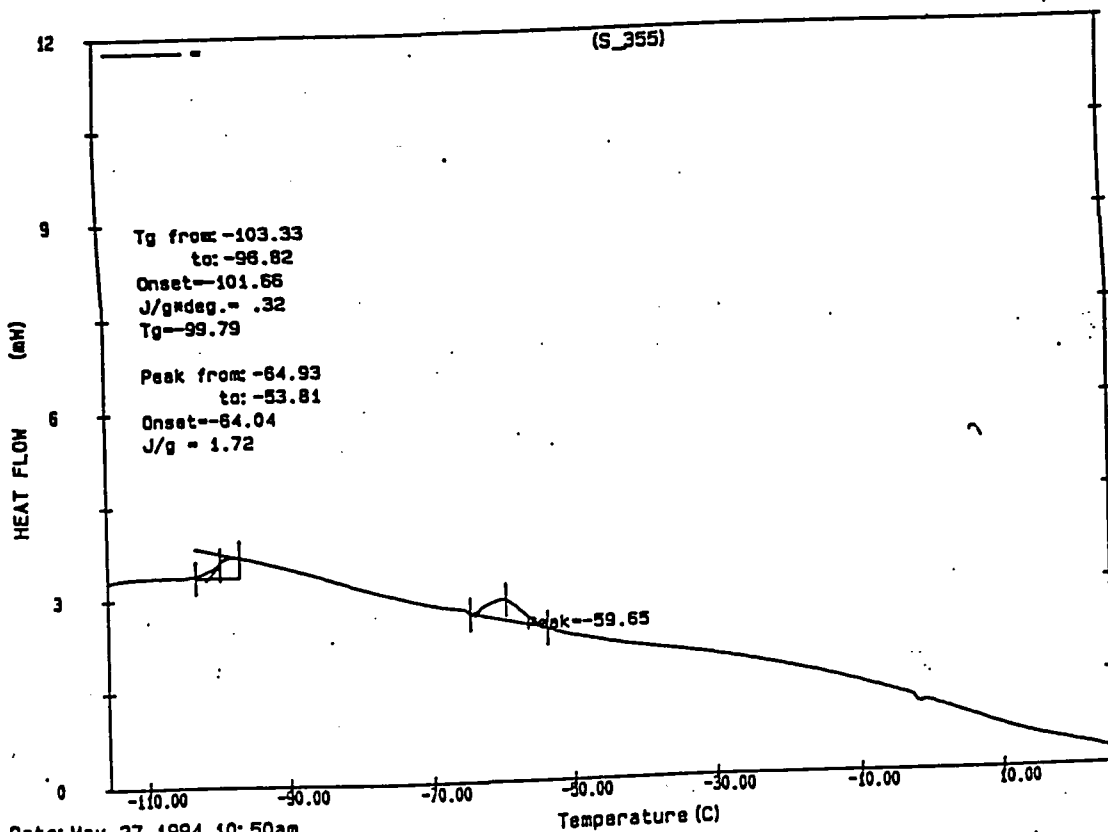


Appendix 5.4.20. ¹³C n.m.r. spectrum of P5-20



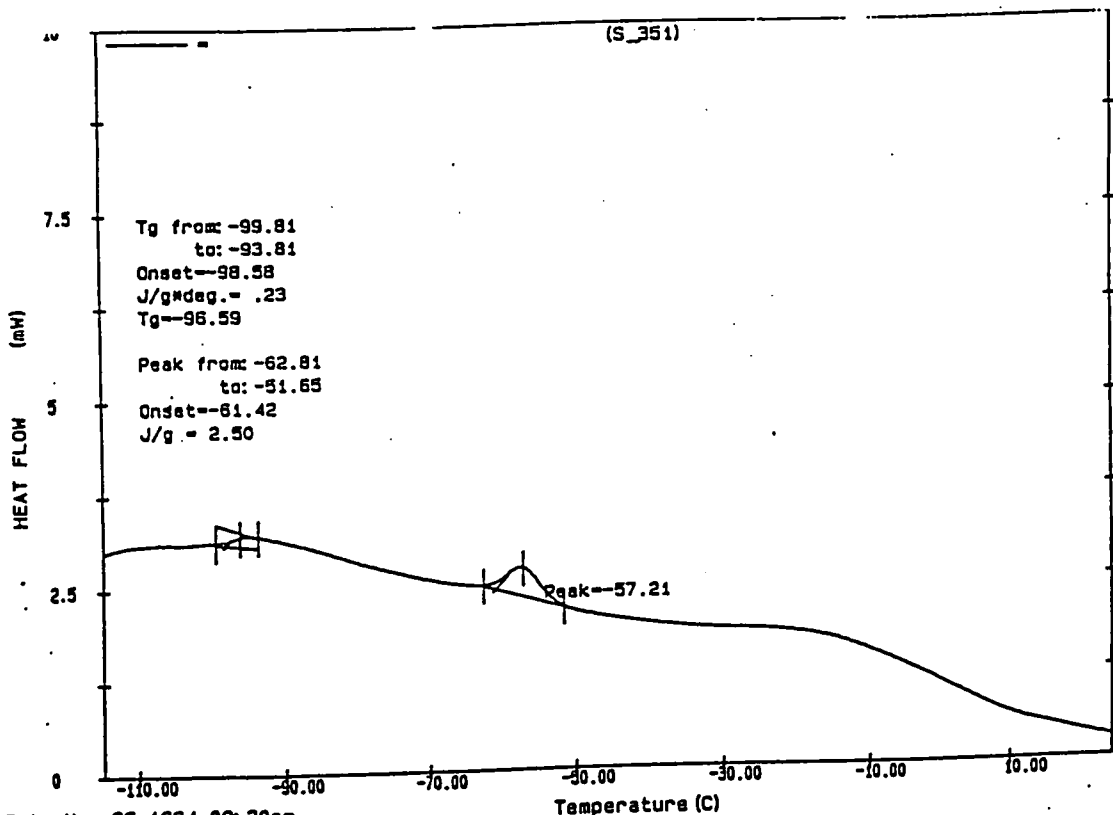
Date: May 13, 1994 11: 07am
Scanning Rate: 10.0 C/min
Sample Wt: 3.739 mg Path: \GMF\
File 1: S 354 D

Appendix 5.5.1. DSC trace of P5-5



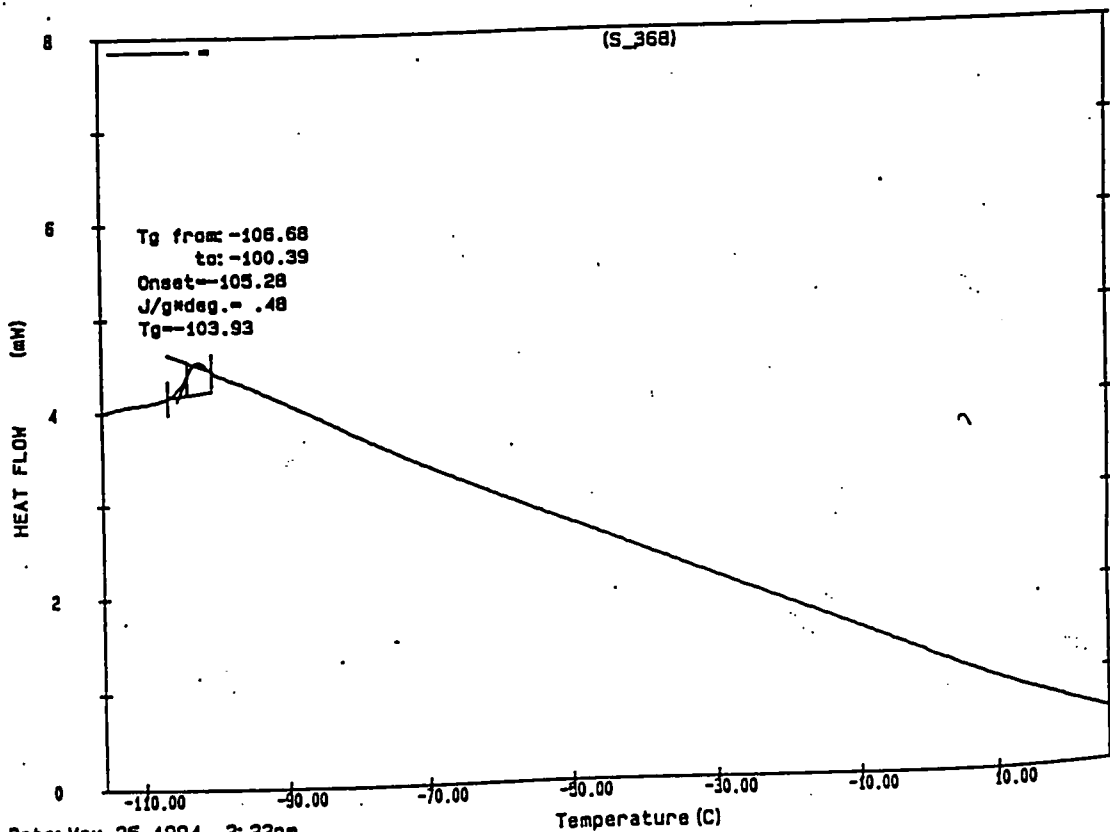
Date: May 27, 1994 10: 50am
Scanning Rate: 10.0 C/min
Sample Wt: 6.755 mg Path: \GMF\
File 1: S 355

Appendix 5.5.2. DSC trace of P5-6



Date: May 26, 1994 09: 30am
Scanning Rate: 10.0 C/min
Sample Wt: 4.863 mg Path: \GMF\
File 1: S 351

Appendix 5.5.3. DSC trace of P5-8



Date: May 25, 1994 2: 22pm
Scanning Rate: 10.0 C/min
Sample Wt: 4.517 mg Path: \GMF\
File 1: S 368

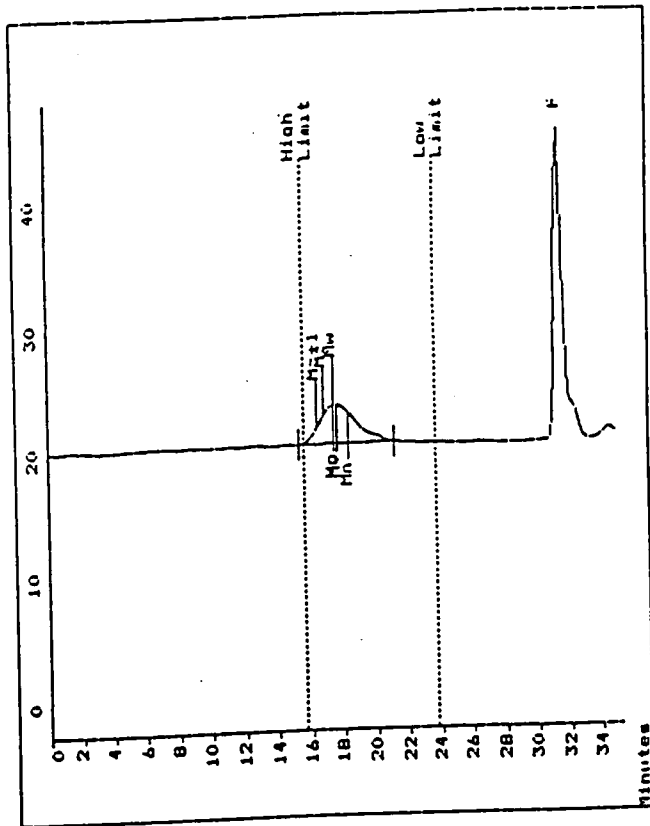
Appendix 5.5.4. DSC trace of P5-12

APPENDIX 6

Analytical data for Chapter 6

Polymer Laboratories
 GPC Data Station Ver 4.0
 15:14 Wed May 11 1994
 Unknown CC072.004 acquired GPC Data Station Ver 4.0

Concentration :
 Injection Volume :
 Solvent : TRICHLOROMETHANE
 Column Set :
 Method : 1
 Detector :
 Temperature :
 Flow Rate :
 Standards :
 Calibration Using Narrow Standards Curve Used 3rd Order Polynomial
 Calibration Limits 15.68 to 23.72 Mins
 Flow Rate Marker : TOLUENE found at 31.78Mins
 in Standards at 31.42Mins
 Broad Peak Start : 15.32 End : 21.18 Mins

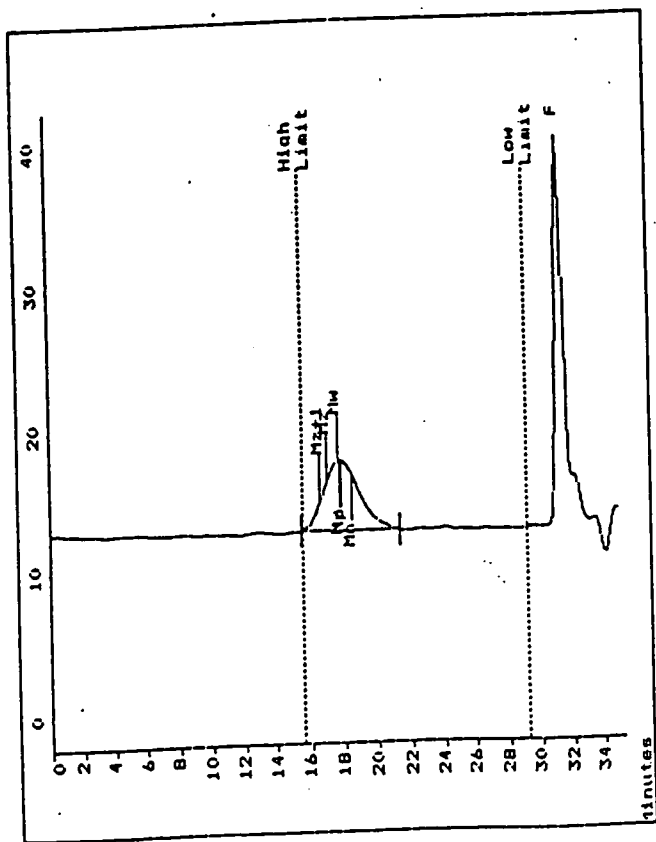


Molecular Weight Averages
 Mp = 299569.5 Mz = 518988.9
 Mn = 144688. Mz+1 = 766735.5
 Mw = 297478. MV = 270322.1
 Polydispersity = 2.056

Appendix 6.1.1. GPC trace of P6-2

Polymer Laboratories
 GPC Data Station Ver 4.0
 12:27 Thu May 05 1994
 Unknown CC071.011 acquired GPC Data Station Ver 4.0

Concentration :
 Injection Volume :
 Solvent : TRICHLOROMETHANE
 Column Set :
 Method : 1
 Detector :
 Temperature :
 Flow Rate :
 Standards :
 Calibration Using Narrow Standards Curve Used 3rd Order Polynomial
 Calibration Limits 15.63 to 29.22 Mins
 Flow Rate Marker : TOLUENE found at 31.78Mins
 in Standards at 31.57Mins
 Broad Peak Start : 15.55 End : 21.38 Mins

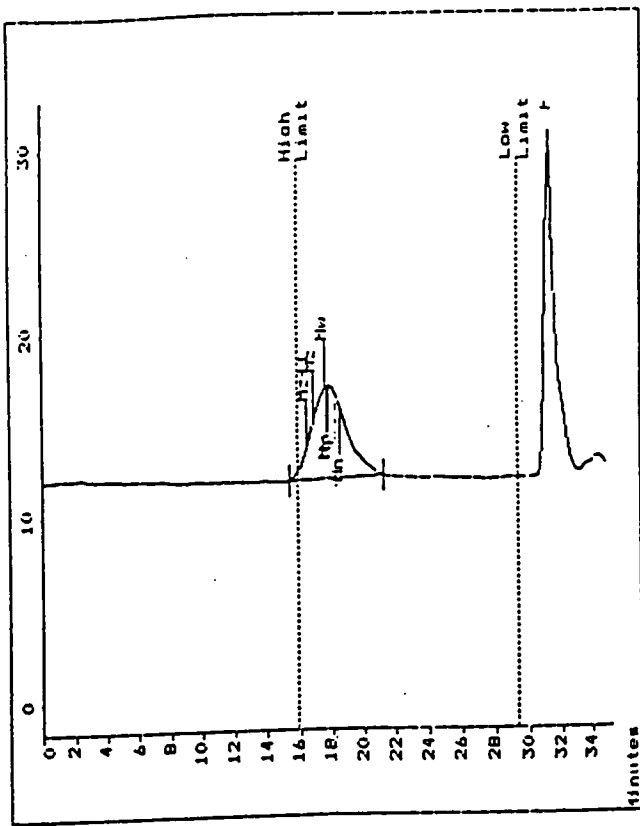


Molecular Weight Averages
 Mp = 214342.7 Mz = 423675.7
 Mn = 131080. Mz+1 = 616066.6
 Mw = 252364. MV = 231207.9
 Polydispersity = 1.925

Appendix 6.1.2. GPC trace of P6-4

Polymer Laboratories
 GPC Data Station Ver 4.0
 Unknown CC073.012 acquired GPC Data Station Ver 4.0
 10:54 Fri May 13 1994

Concentration :
 Injection Volume :
 Solvent :
 Column Set :
 Method :
 Calibration Using :
 Calibration Limits :
 Flow Rate Marker :
 Broad Peak Start :
 Detector :
 Temperature :
 Flow Rate :
 Standards :
 TRICHLOROMETHANE
 1
 Narrow Standards
 15.98 to 29.42 Mins
 TOLUENE
 15.45 End : 21.25 Mins
 Curve Used 3rd Order Polynomial
 found at 31.35Mins
 in Standards at 31.25Mins

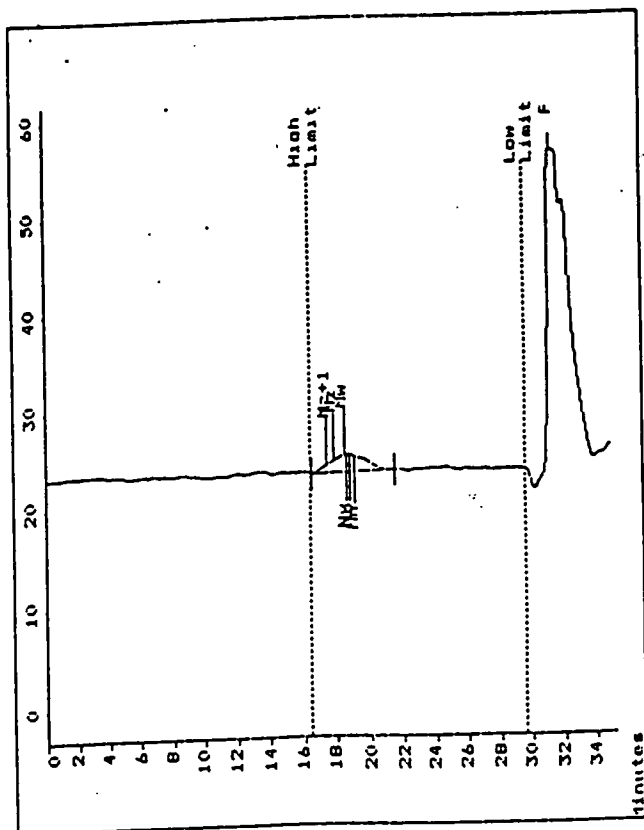


Molecular Weight Averages
 Mp = 279770.7 Mz = 653162.9
 Mn = 141992. Mz+1 = 1060306.3
 Mw = 328523. Mw = 292516.1
 Polydispersity = 2.314

Appendix 6.1.3. GPC trace of P6-5

Polymer Laboratories
 GPC Data Station Ver 4.0
 Unknown CC07801.006 acquired 13:40 Tue Jun 21 1994
 14:02 Tue Jun 21 1994

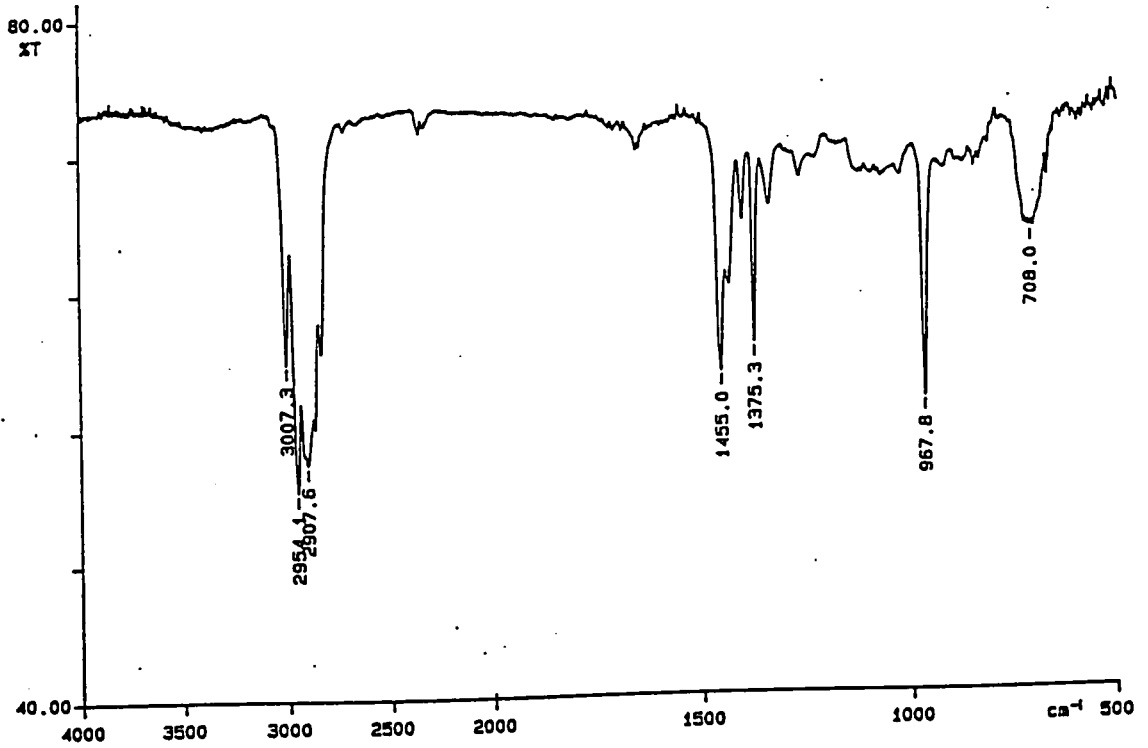
Concentration :
 Injection Volume :
 Solvent :
 Column Set :
 Method :
 Calibration Using :
 Calibration Limits :
 Flow Rate Marker :
 Broad Peak Start :
 Detector :
 Temperature :
 Flow Rate :
 Standards :
 TRICHLOROMETHANE
 1
 Narrow Standards
 16.48 to 29.37 Mins
 TOLUENE
 16.60 End : 21.33 Mins
 Curve Used 3rd Order Polynomial
 found at 31.40Mins
 in Standards at 31.40Mins



Molecular Weight Averages
 Mp = 129780.1 Mz = 274571.3
 Mn = 98757.3 Mz+1 = 388709.8
 Mw = 168641. Mw = 135668.4
 Polydispersity = 1.708

Appendix 6.1.4. GPC trace of P6-7

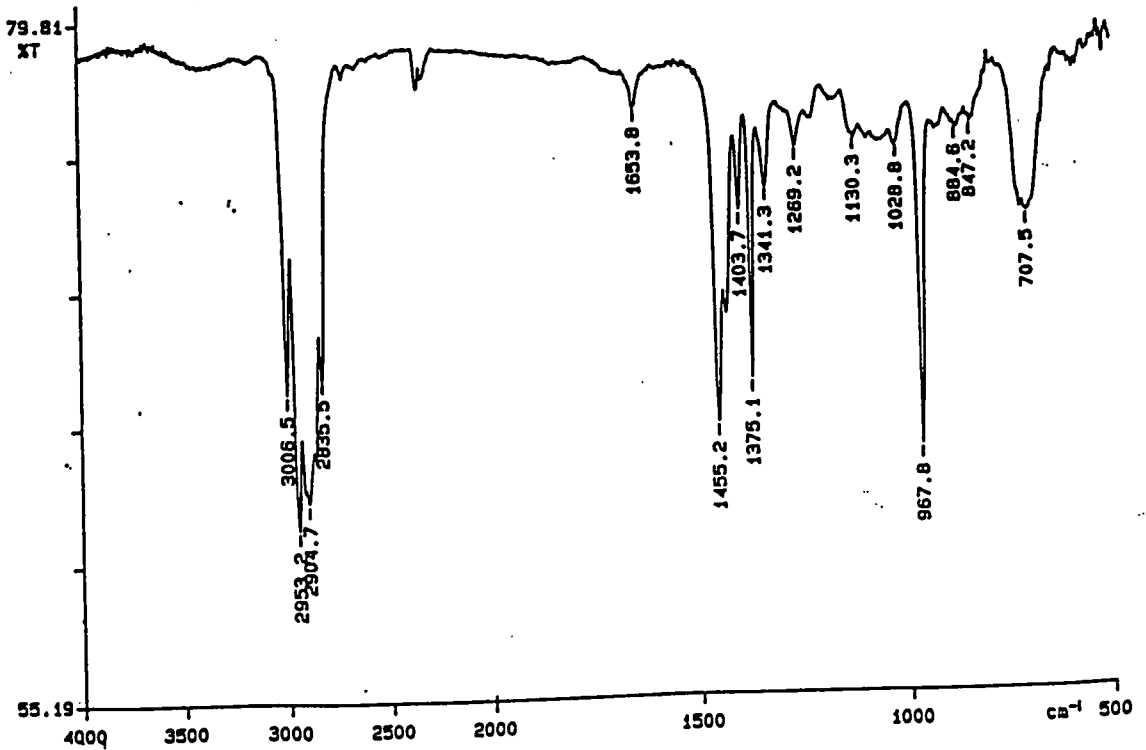
PERKIN ELMER



94/05/10 10:35 red
X: 1 scan, 4.0 cm^{-1} , flat

Appendix 6.2.1. Infrared spectrum of P6-2

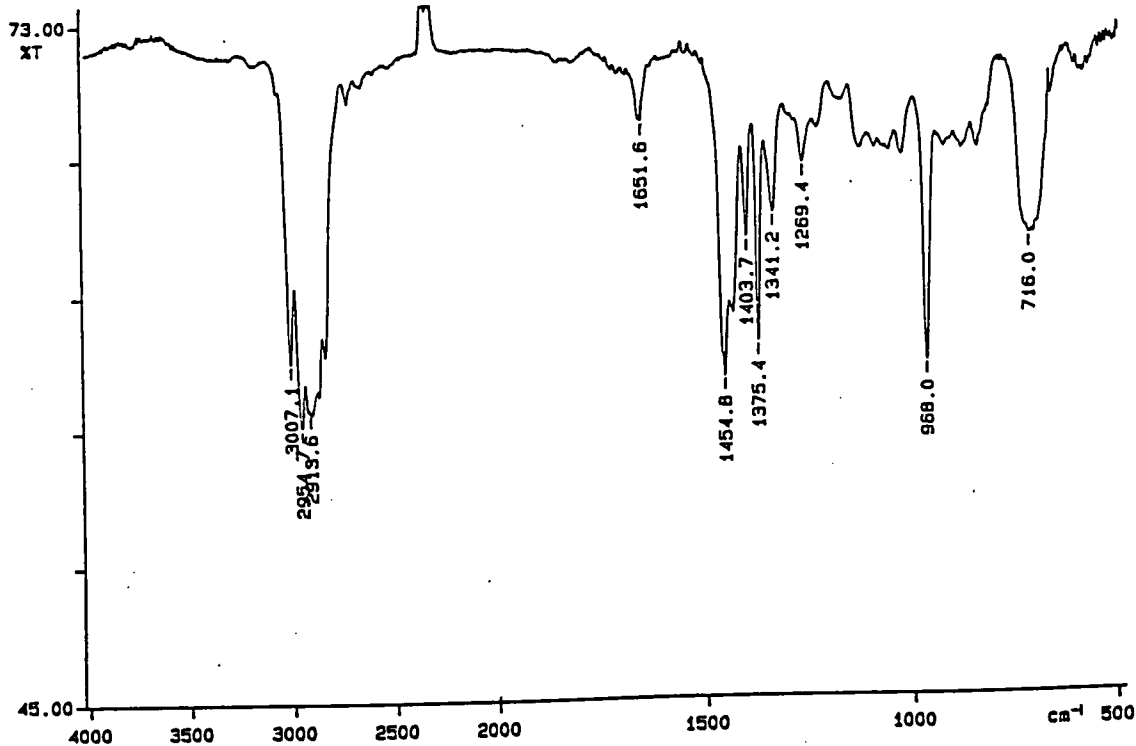
PERKIN ELMER



94/05/10 11:39 red
s-376: 4 scans, 4.0 cm^{-1} , flat
s-376

Appendix 6.2.2. Infrared spectrum of P6-4

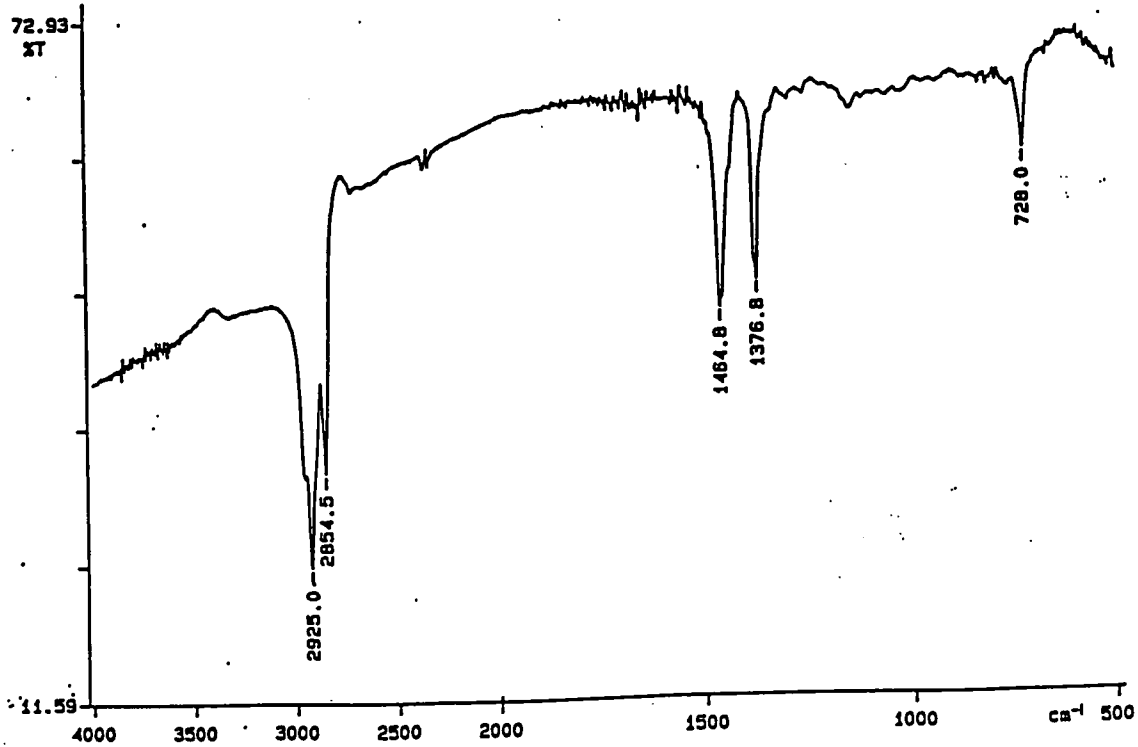
PERKIN ELMER



94/05/19 14:21 red
X: 16 scans, 4.0cm⁻¹, flat

Appendix 6.2.3. Infrared spectrum of P6-5

PERKIN ELMER

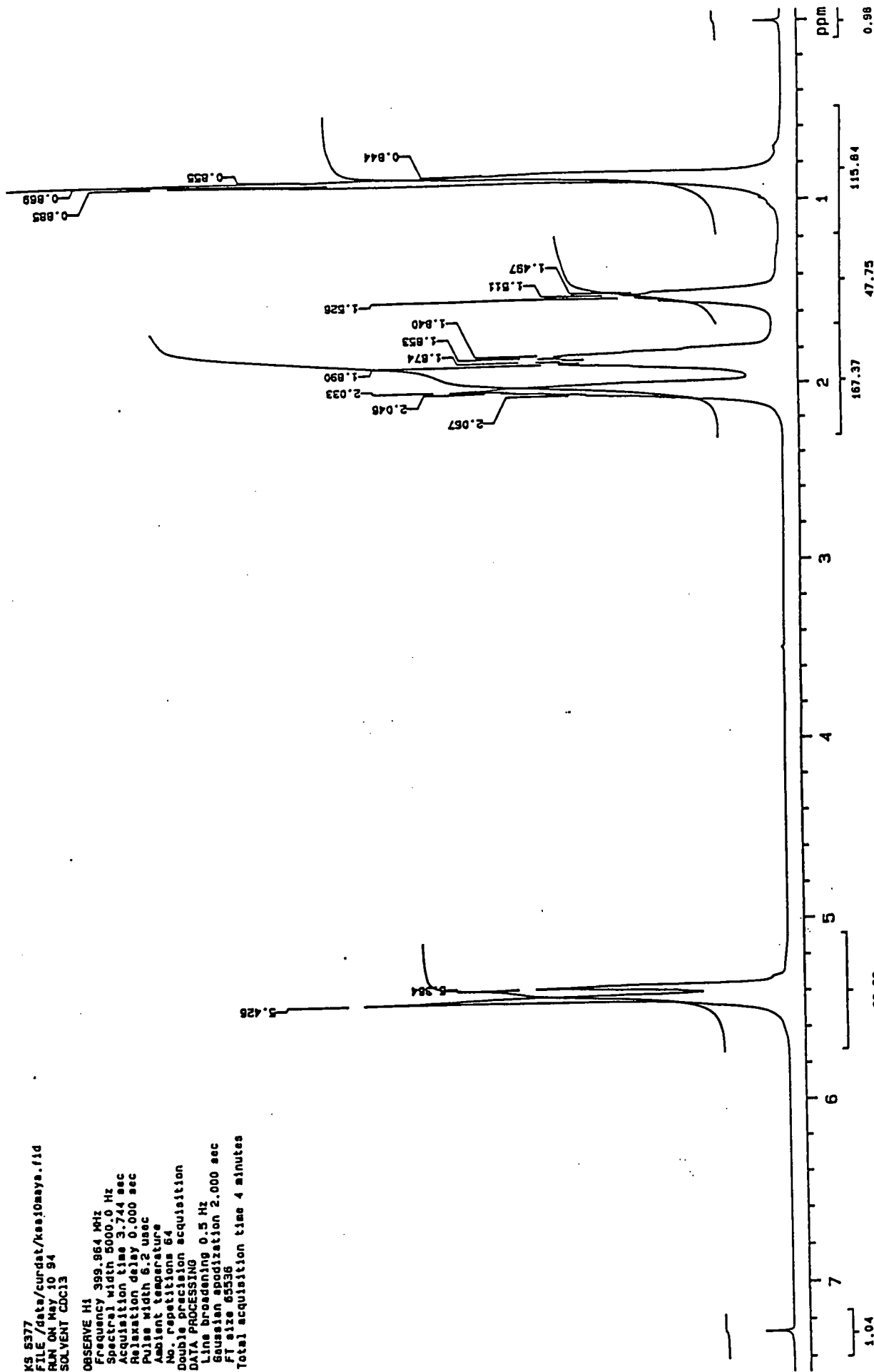


94/05/19 11:45 red
s-500-4: 4 scans, 4.0cm⁻¹
s-500-4 kbr

Appendix 6.2.4. Infrared spectrum of P6-7

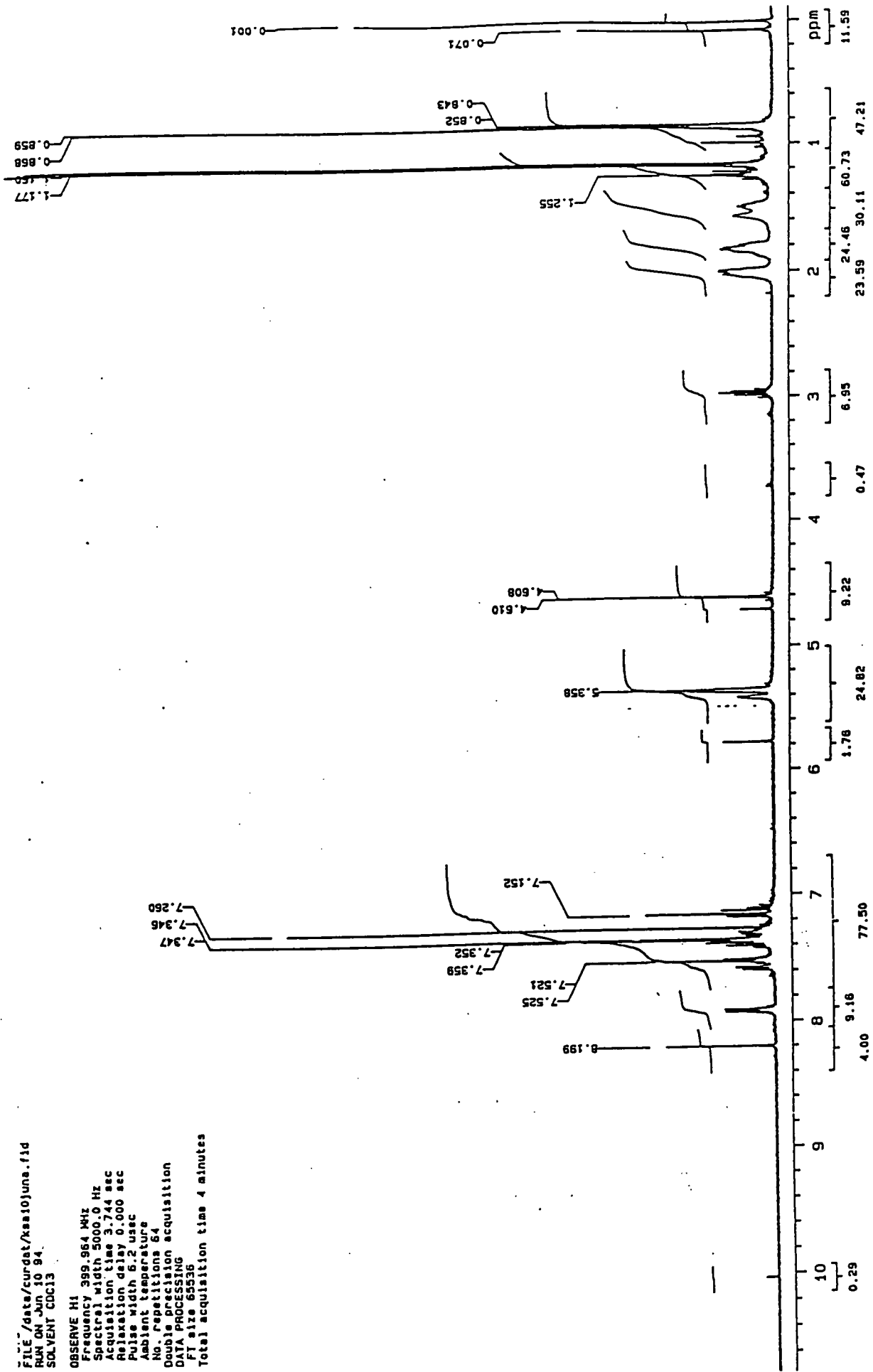
KS 5377
 FILE /data/curdatt/ks530maya.fid
 RUN ON May 10 94
 SOLVENT CDCl3

OBSERVE H1
 Frequency 399.964 MHz
 Spectral width 5000.0 Hz
 Acquisition time 3.744 sec
 Relaxation delay 0.000 sec
 Pulse width 6.2 usec
 Ambient temperature
 No. repetitions 64
 Double precision acquisition
 DATA PROCESSING
 Line broadening 0.5 Hz
 Gaussian apodization 2.000 sec
 Ff size 65236
 Total acquisition time 4 minutes



Appendix 6.3.1. ¹H n.m.r. spectrum of P6-2

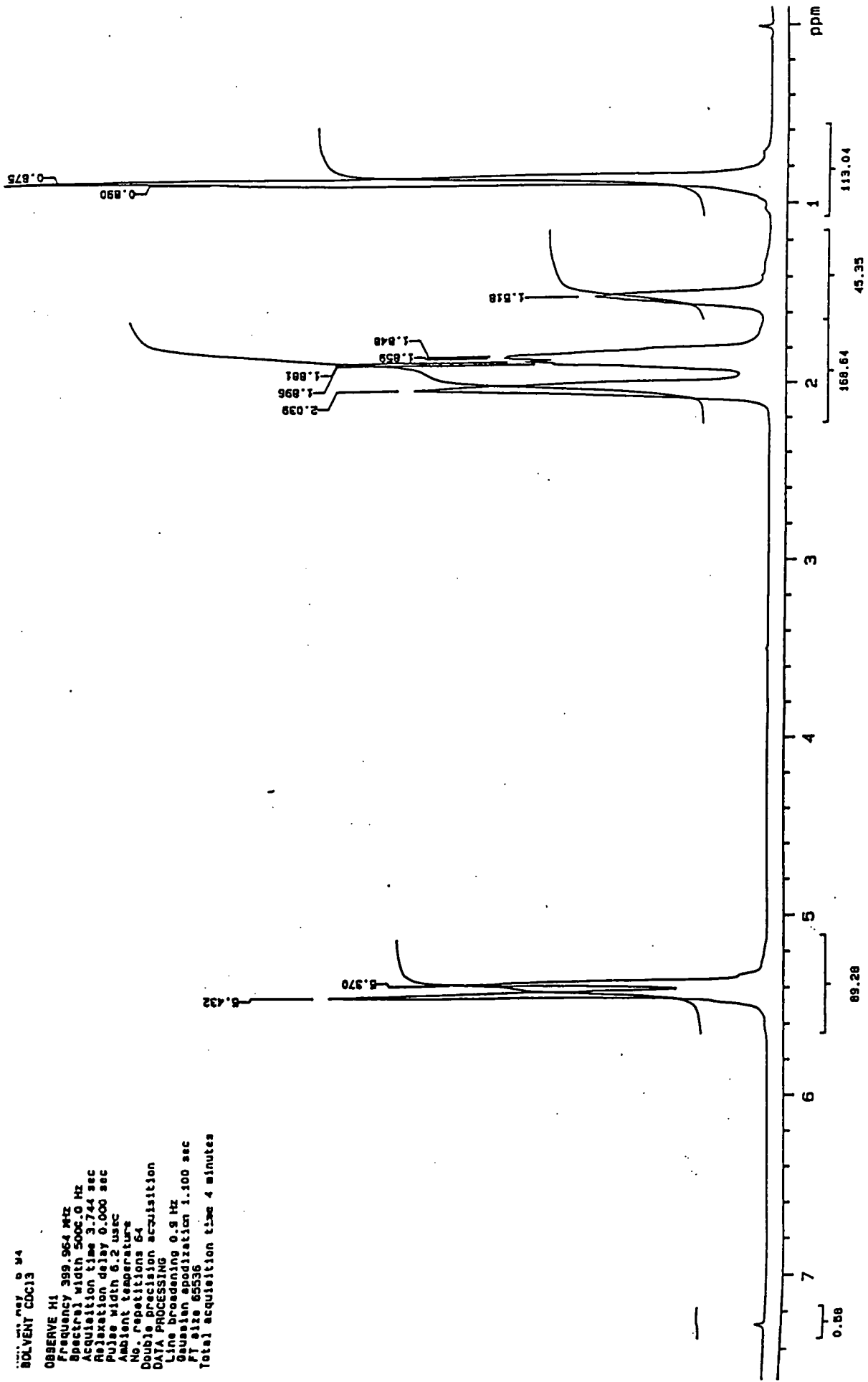
FILE //data/curdst/ksa10juna.f1d
 RUN ON Jun 10 84
 SOLVENT CDC13
 OBSERVE H1
 Frequency 399.964 MHz
 Spectral width 5000.0 Hz
 Acquisition time 3.74 sec
 Relaxation delay 0.000 sec
 Pulse width 6.2 usec
 Ambient temperature
 No. repetitions 64
 Double precision acquisition
 DATA PROCESSING
 FI size 65536
 Total acquisition time 4 minutes



Appendix 6.3.2. ¹H n.m.r. spectrum of P6-3

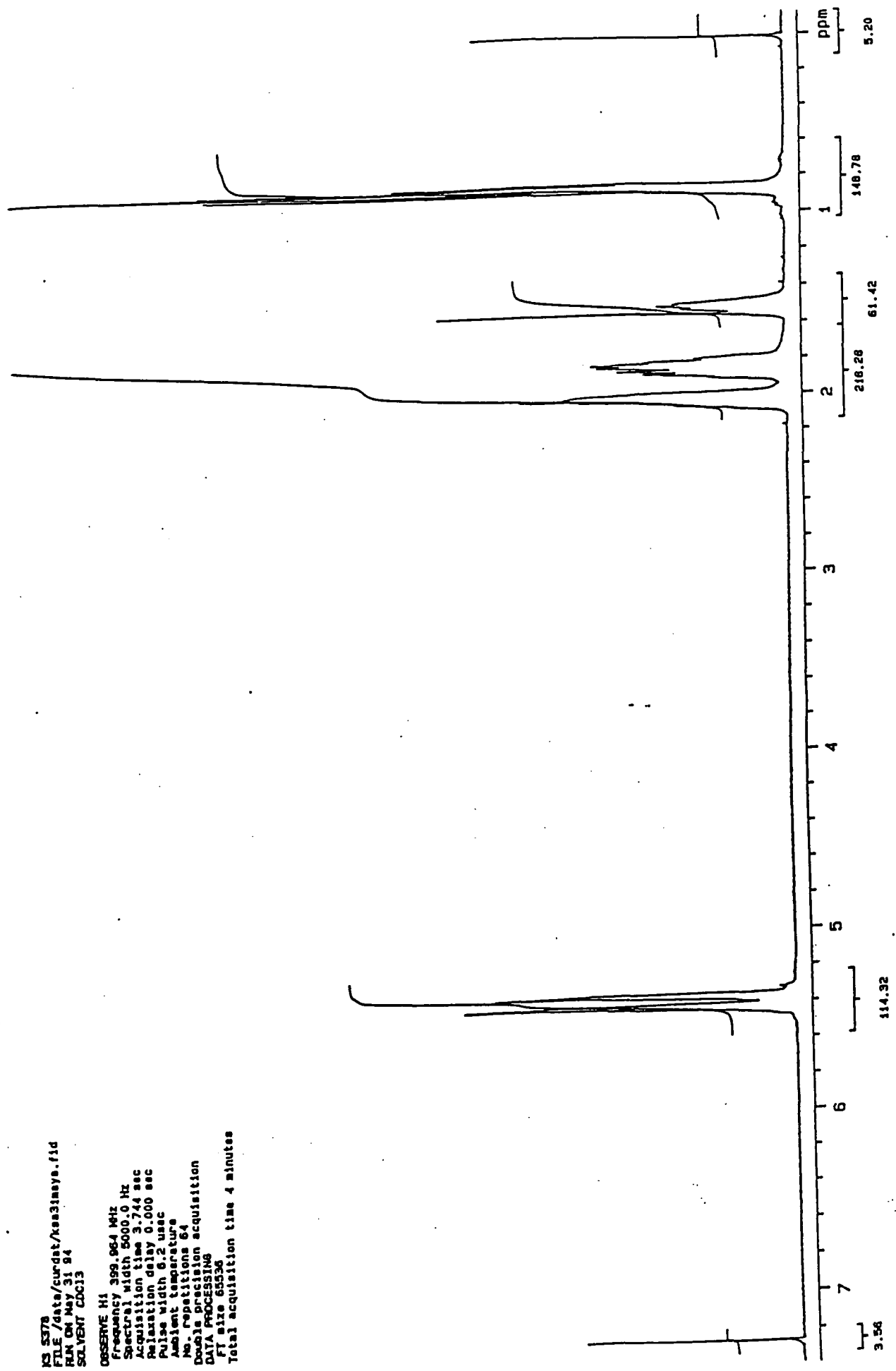
DATE: MAY 6 84
SOLVENT: CDCl3

OBSERVE: H1
Frequency: 399.964 MHz
Spectral width: 5000.0 Hz
Acquisition time: 3.744 sec
Relaxation delay: 0.000 sec
Pulse width: 6.2 usec
Ambient temperature:
No. repetitions: 64
Double precision acquisition
DATA PROCESSING
Line broadening: 0.8 Hz
Gaussian smoothing: 1.000 sec
FI size: 65536
Total acquisition time: 4 minutes



Appendix 6.3.3. ¹H n.m.r. spectrum of P6-4

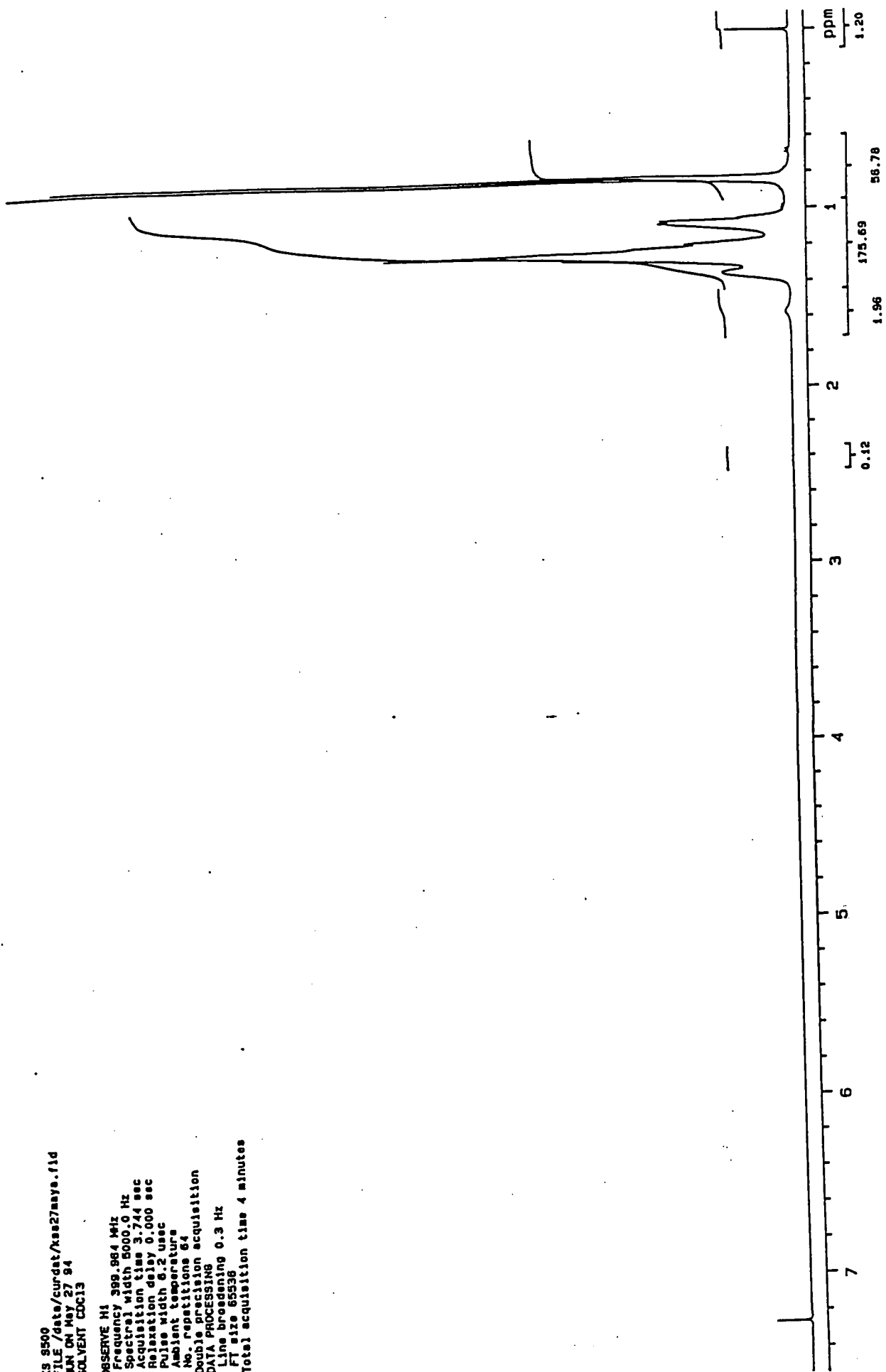
NS 5378
 FILE /data/curdnt/ksa31maye.fid
 RUN ON MAY 31 84
 SOLVENT CDCl3
 OBSERVE H1
 Frequency 399.964 MHz
 Spectral width 5000.0 Hz
 Acquisition time 3.744 sec
 Relaxation delay 0.000 sec
 Pulse width 6.2 usec
 Ambient temperature
 No. repetitions 64
 Double precision acquisition
 DATA PROCESSING
 FT size 65536
 Total acquisition time 4 minutes



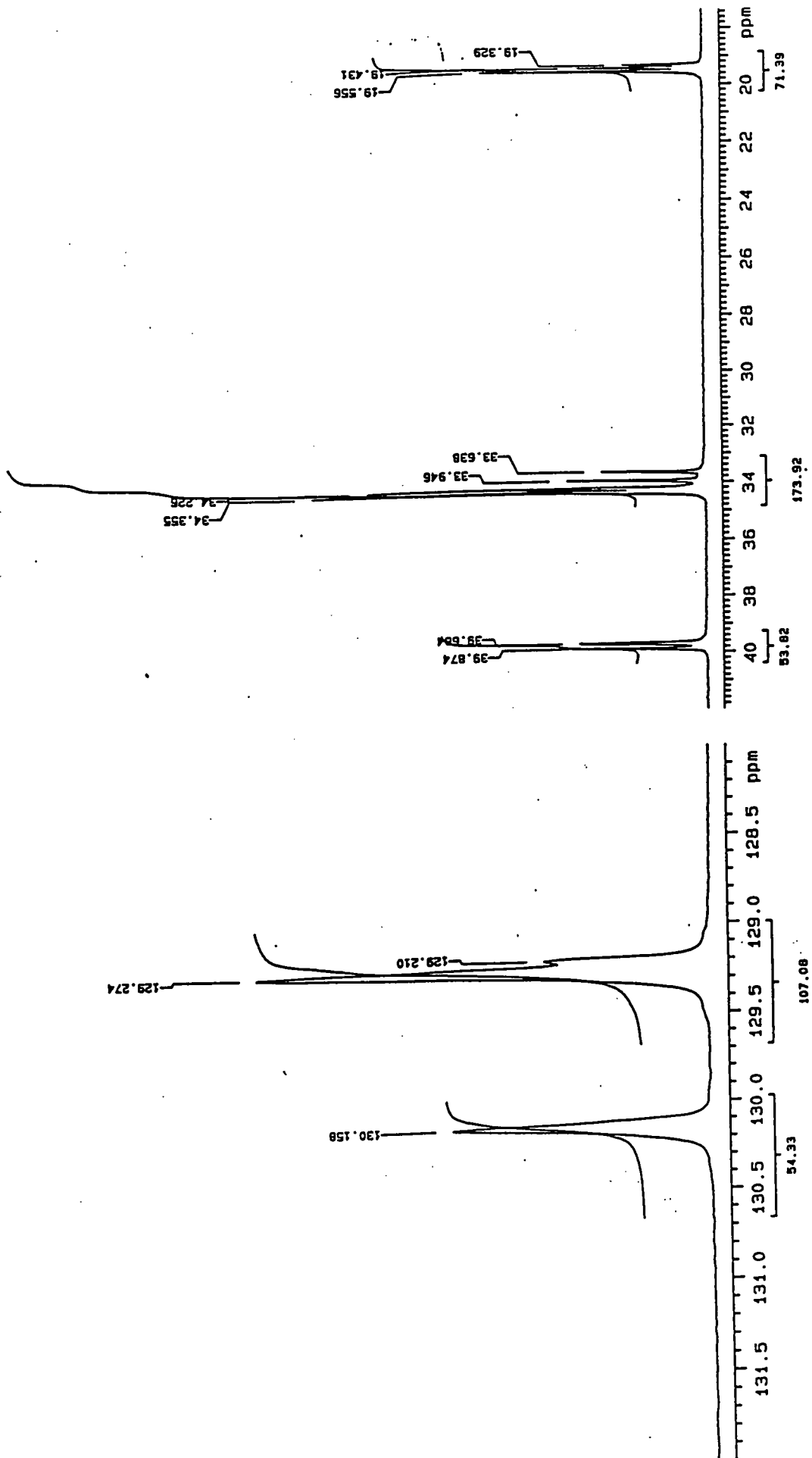
Appendix 6.3.4. 1H n.m.r. spectrum of P6-5

MS S500
FILE /date/curdatt/ksa27maye.fid
RAN ON May 27 84
SOLVENT CCl3

OBSERVE H1
Frequency 399.864 MHz
Spectral width 5000.0 Hz
Acquisition time 3.744 sec
Relaxation delay 0.000 sec
Pulse width 6.2 usec
Ambient temperature
No. repetitions 64
Double precision acquisition
DATA PROCESSING
Line broadening 0.3 Hz
FT size 65536
Total acquisition time 4 minutes

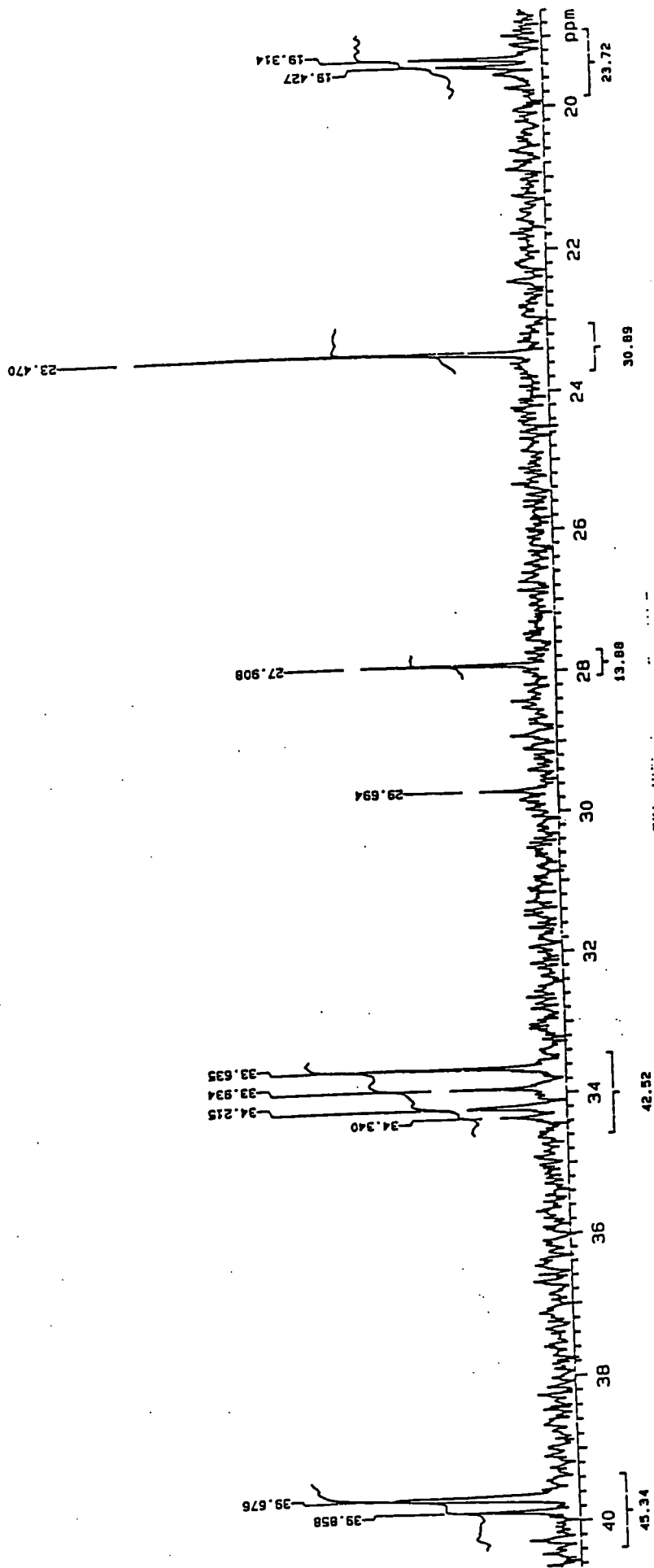


Appendix 6.3.5. 1H n.m.r. spectrum of P6-7

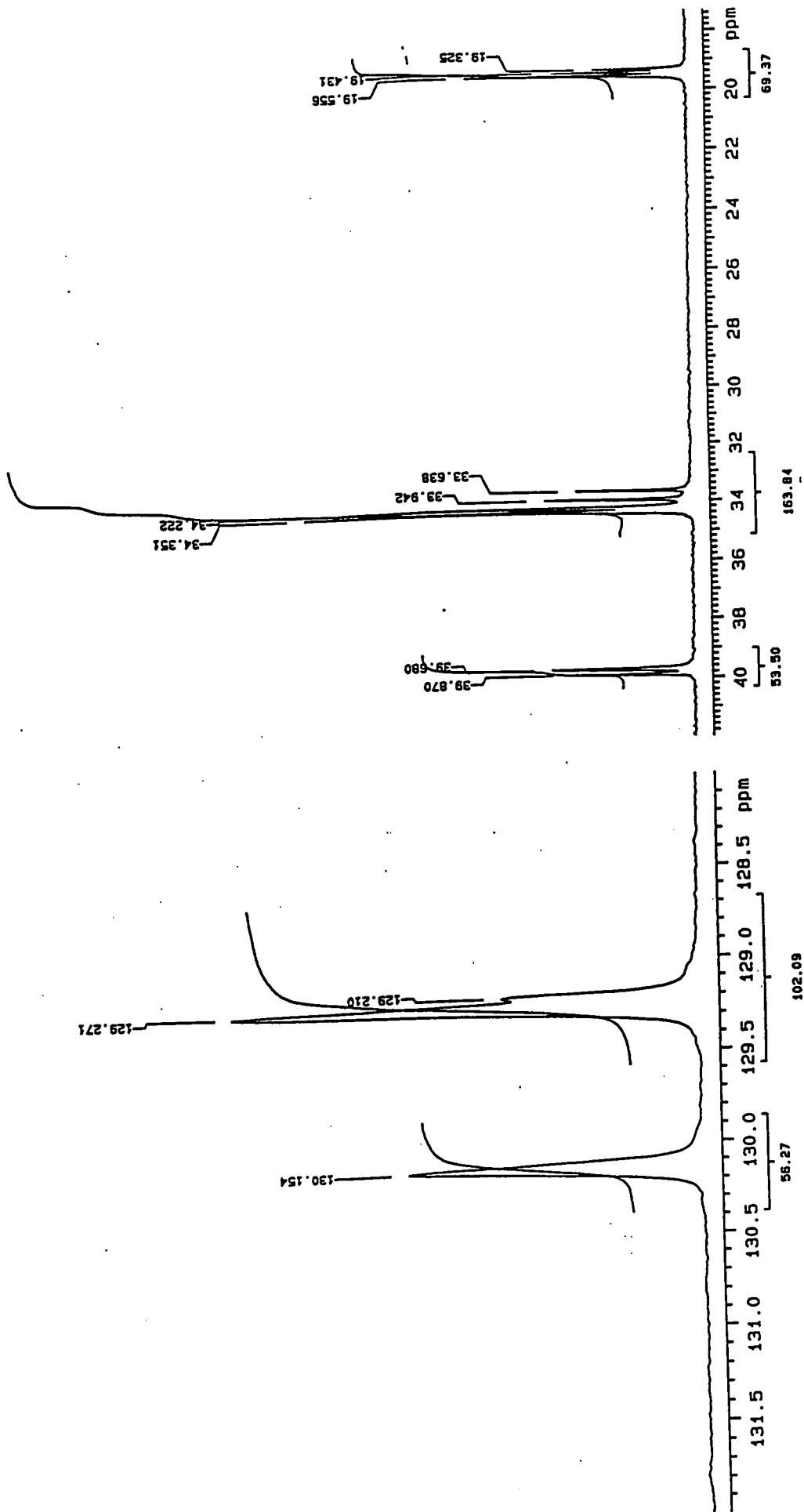


Appendix 6.4.1. ^{13}C spectrum of P6-2

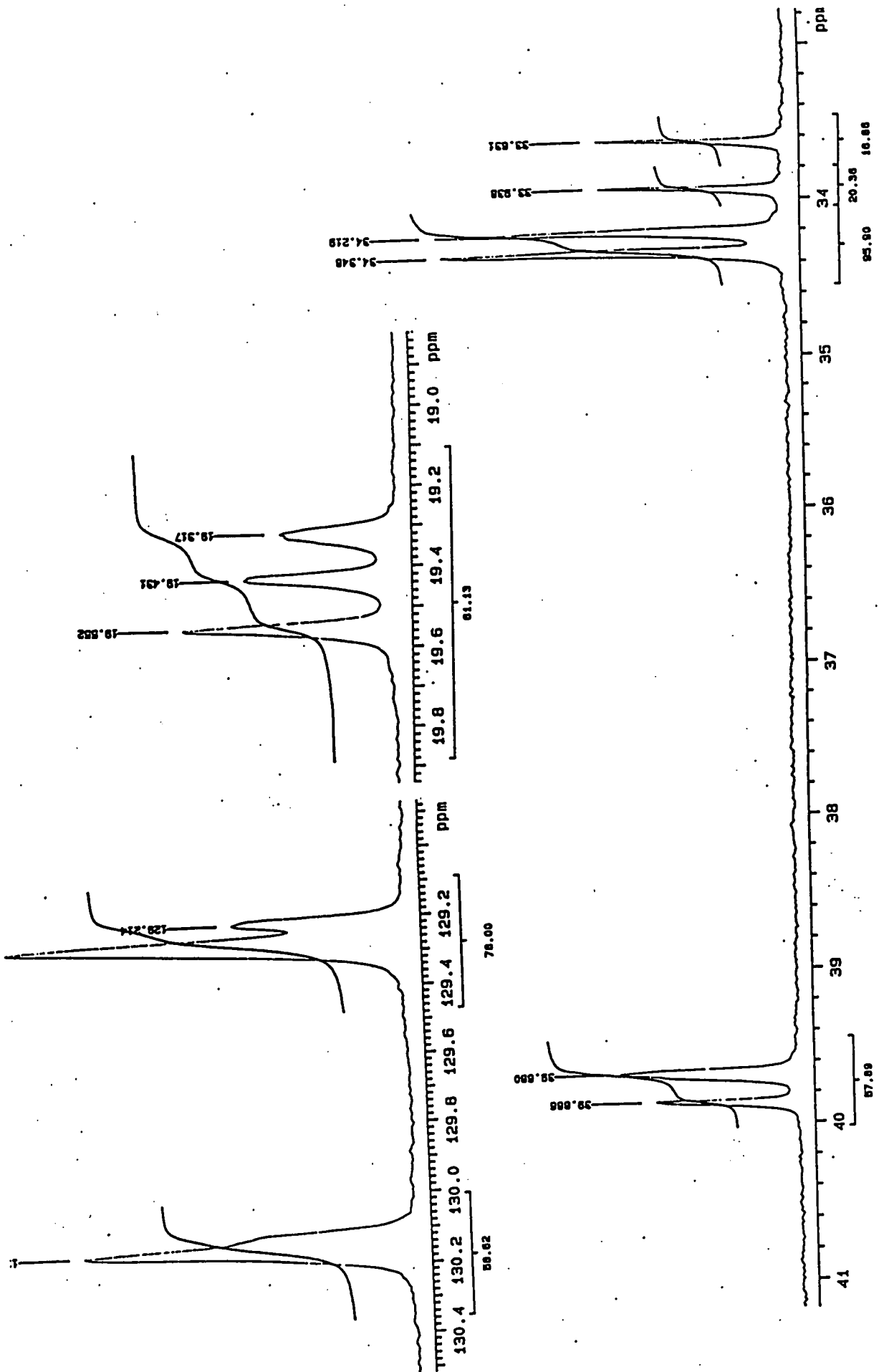
S-379
FILE /data/curdst/kss10jumb.fid
RUN ON JUN 10 94
SOLVENT CDCl3
OBSERVE C13



Appendix 6.4.2. ¹³C spectrum of P6-3



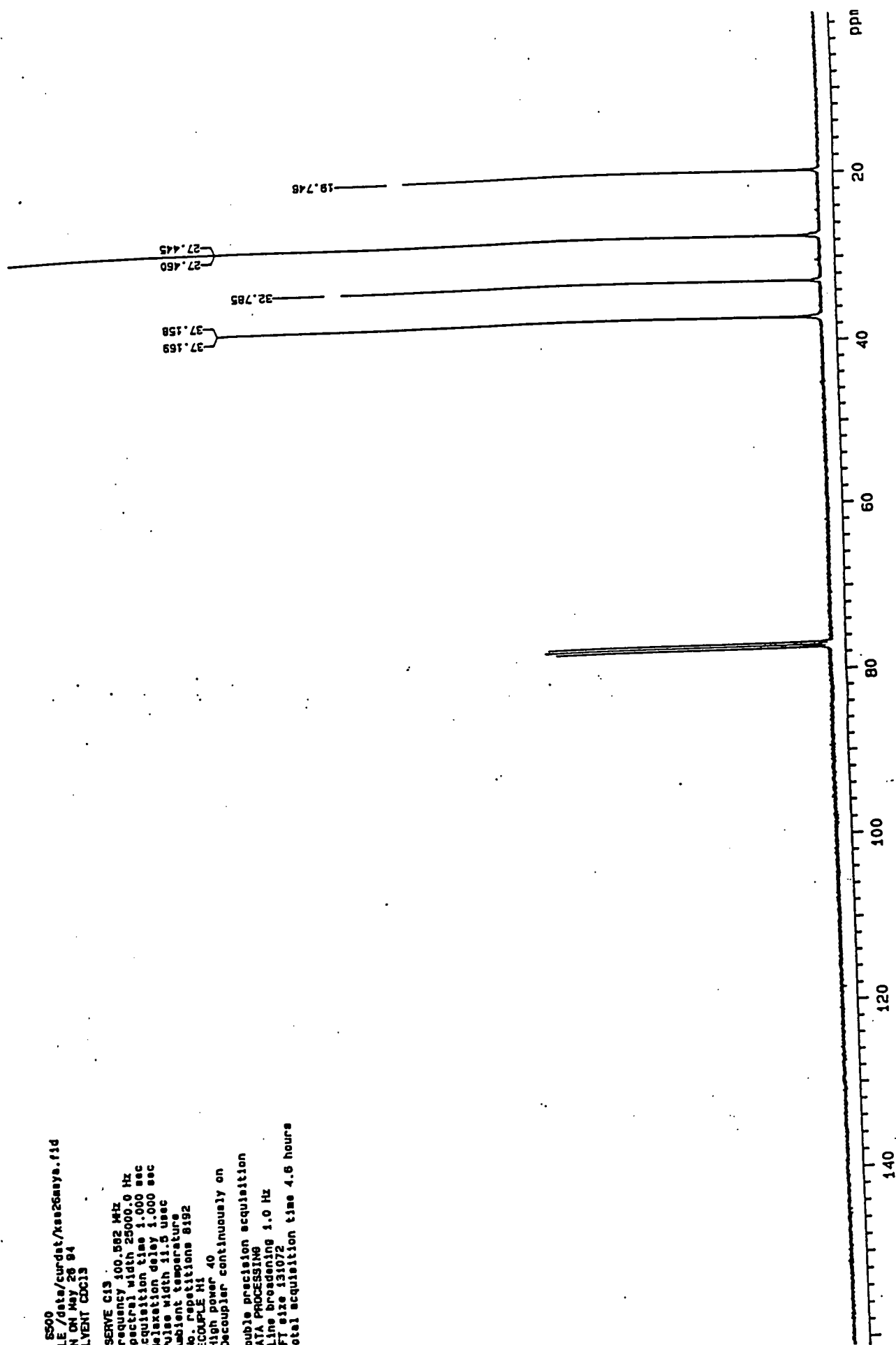
Appendix 6.4.3. ¹³C spectrum of P6-4



Appendix 6.4.4. ^{13}C spectrum of P6-5

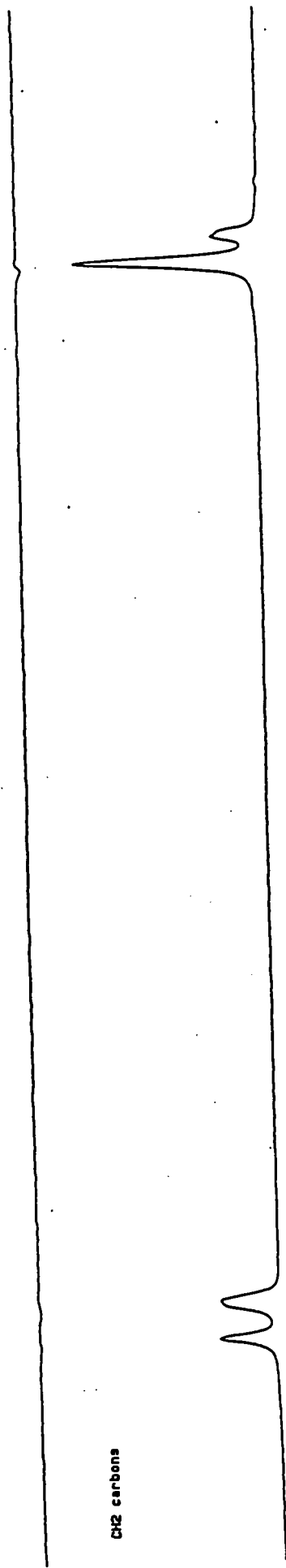
K9 8500
FILE /data/curdat/k9826m9a.fid
RUN ON May 28 84
SOLVENT CDCl3

OBSERVE C13
Frequency 100.582 MHz
Spectral width 25000.0 Hz
Acquisition time 1.000 sec
Relaxation delay 1.000 sec
Pulse width 11.5 usec
Ambient temperature
No. repetitions 8192
DECOUPLE H1
High power 40
Decoupler continuously on
Double precision acquisition
DATA PROCESSING
Line broadening 1.0 Hz
FI size 131072
Total acquisition time 4.6 hours

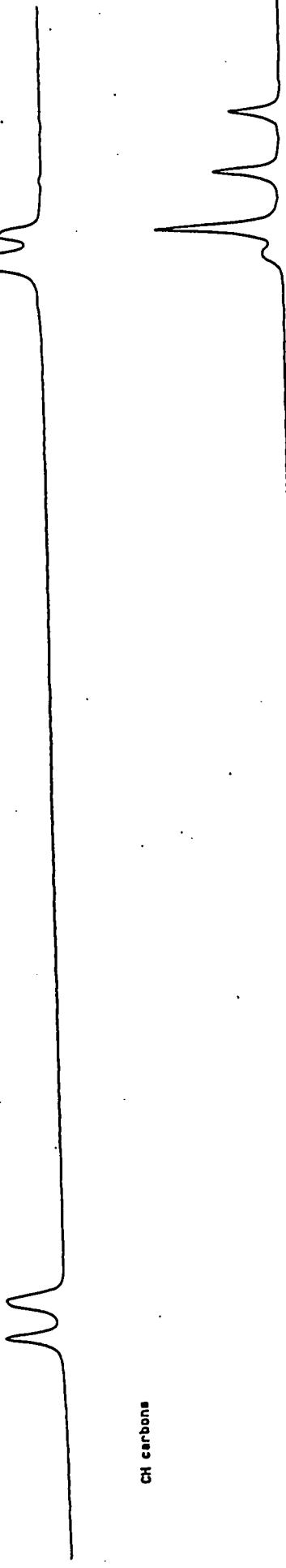


Appendix 6.4.5. ¹³C spectrum of P6-7

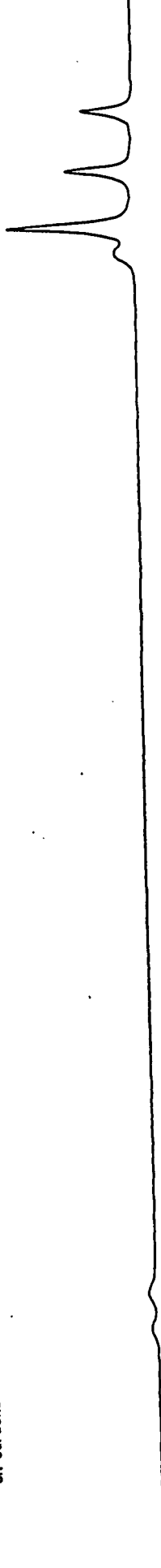
CH3 carbons



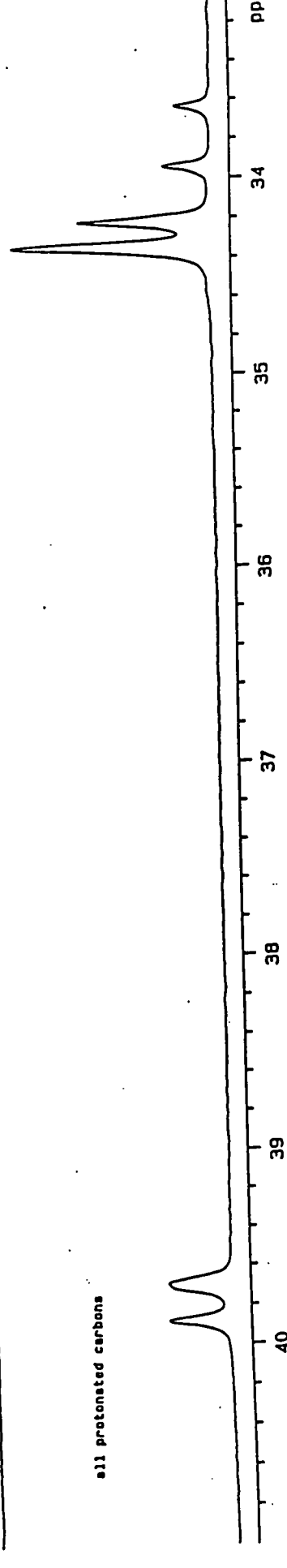
CH2 carbons



CH carbons



all protonated carbons



ppm

34

35

36

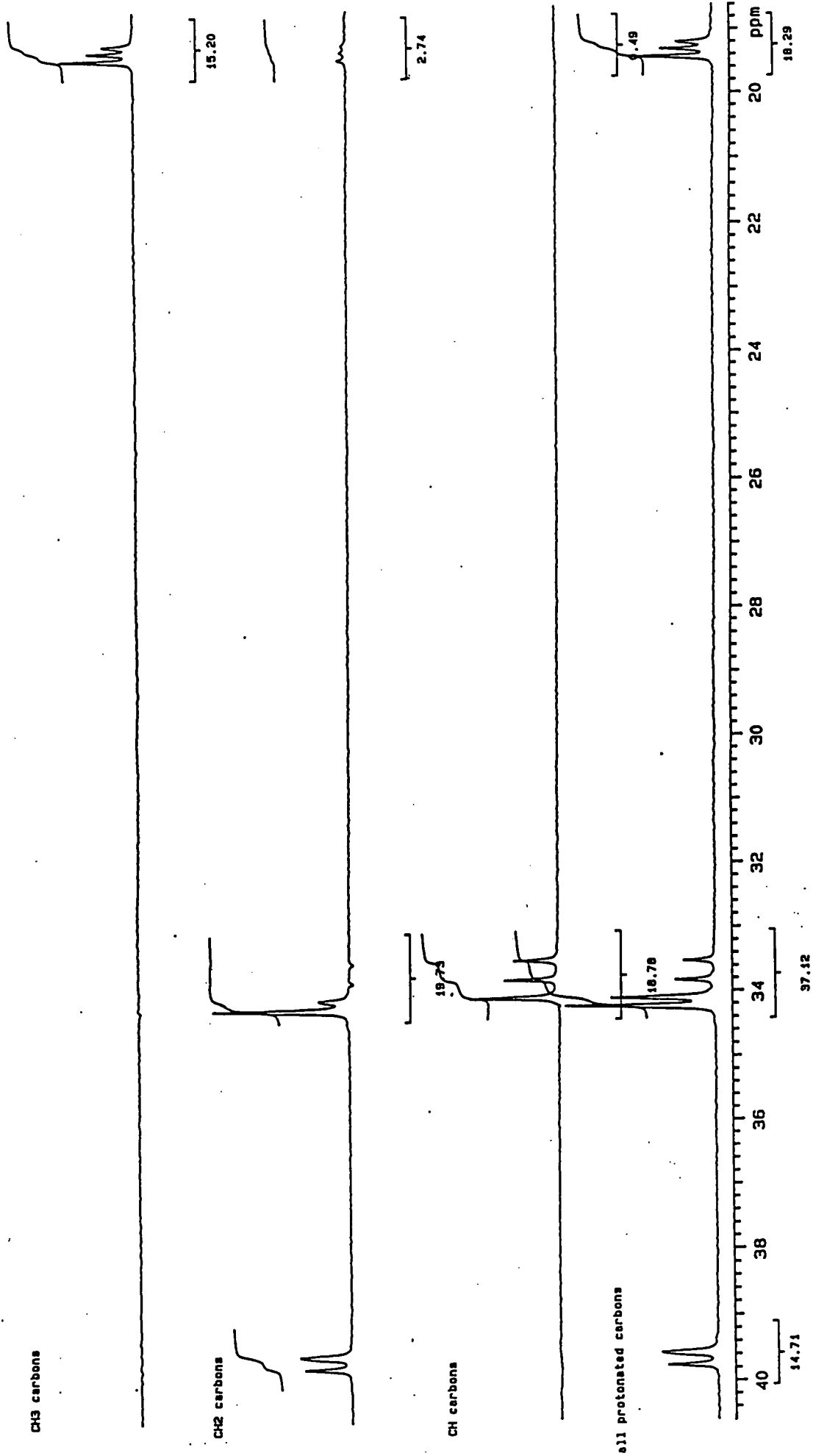
37

38

39

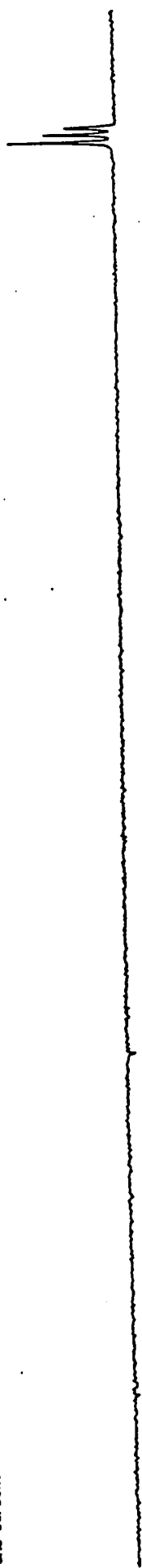
40

K9 8376
FILE /data/curdet/kas05mayb.fid
RUN ON May 5 94
SOLVENT CCl3
OBSERVE C13

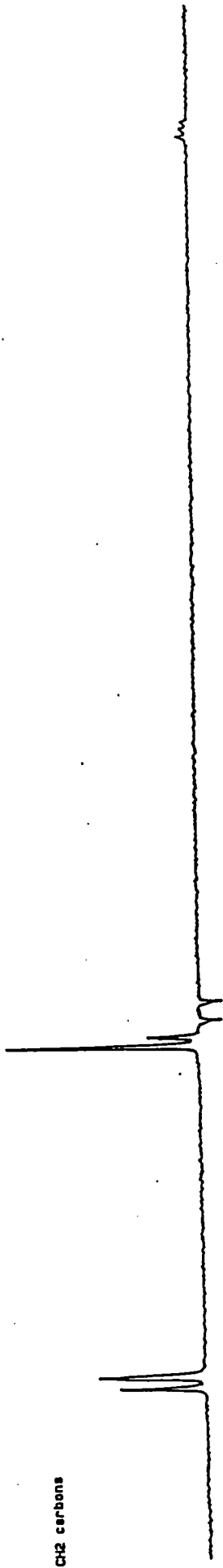


Appendix 6.5.2. DEPT spectrum of P6-4

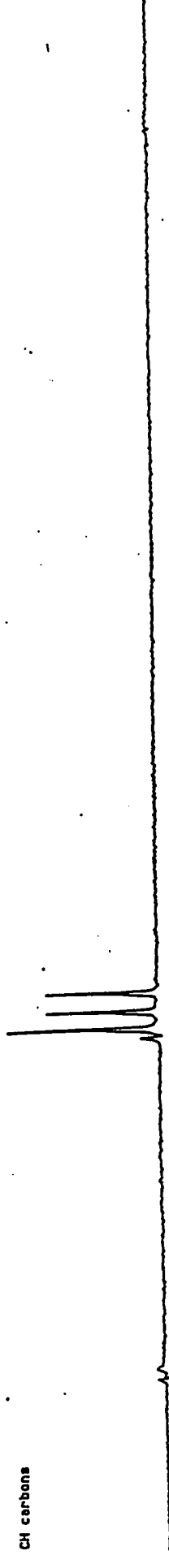
CH3 carbons



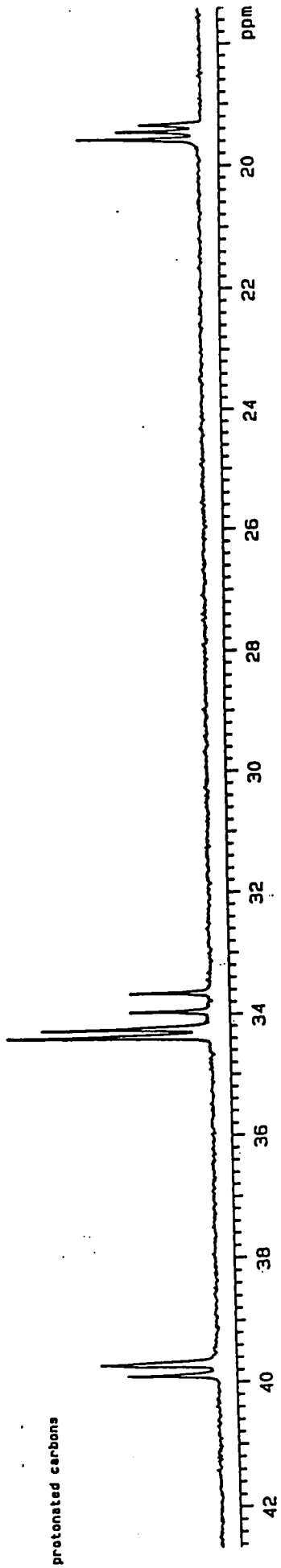
CH2 carbons



CH carbons

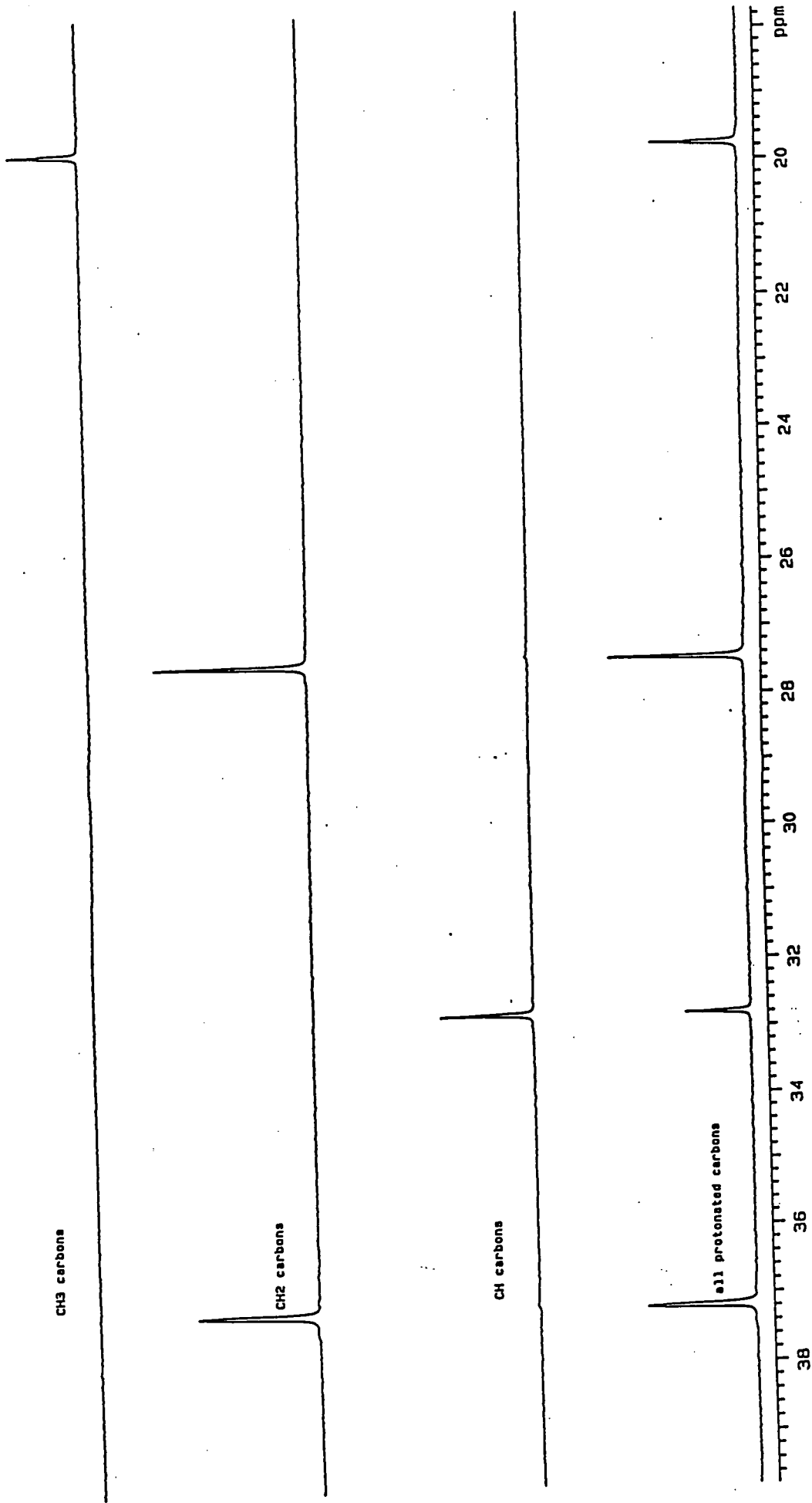


all protonated carbons

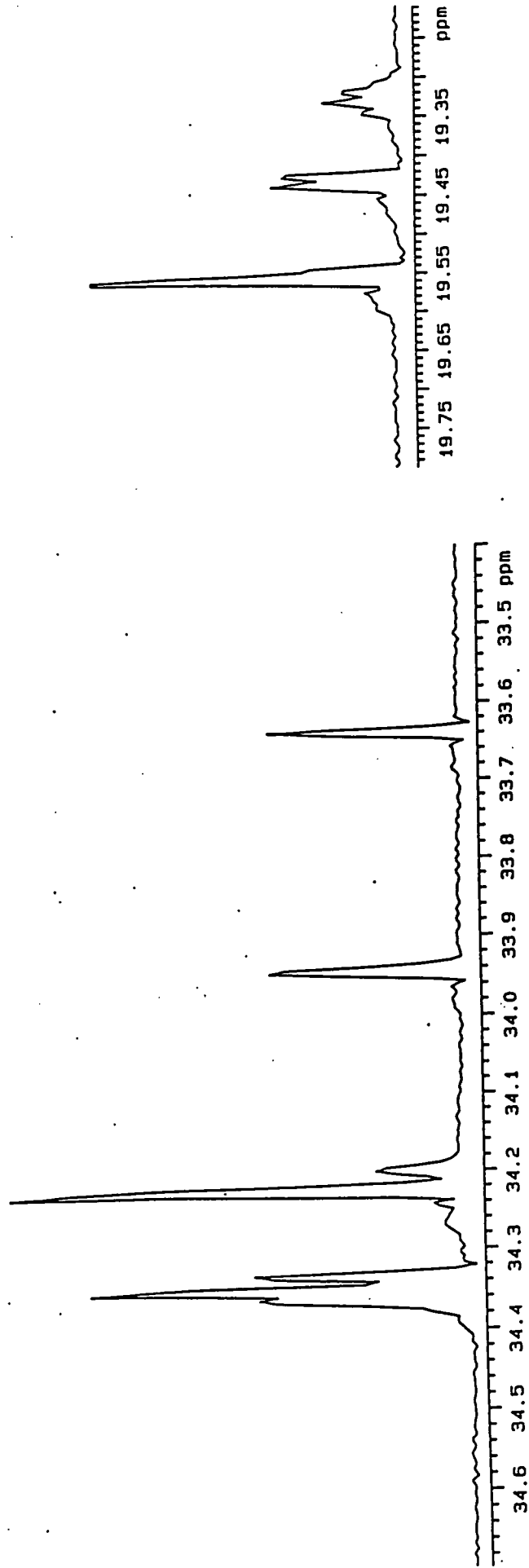
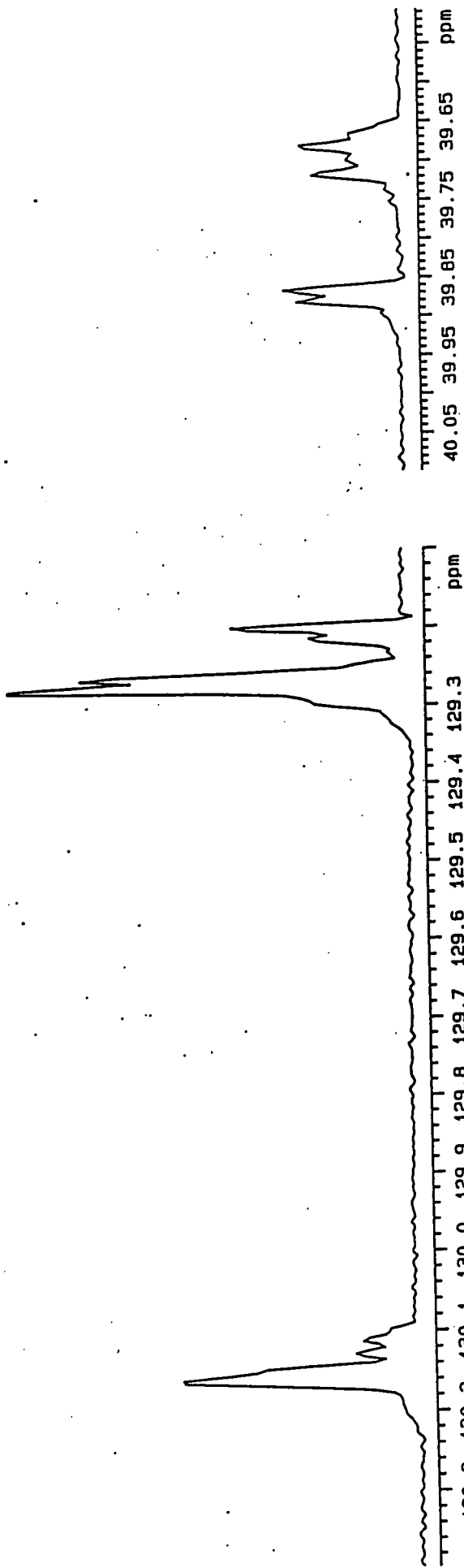


Appendix 6.5.3. DEPT spectrum of P6-5

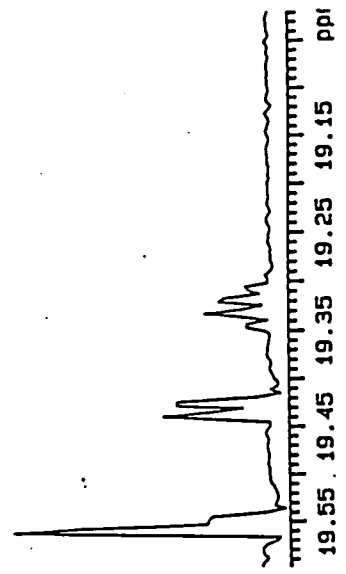
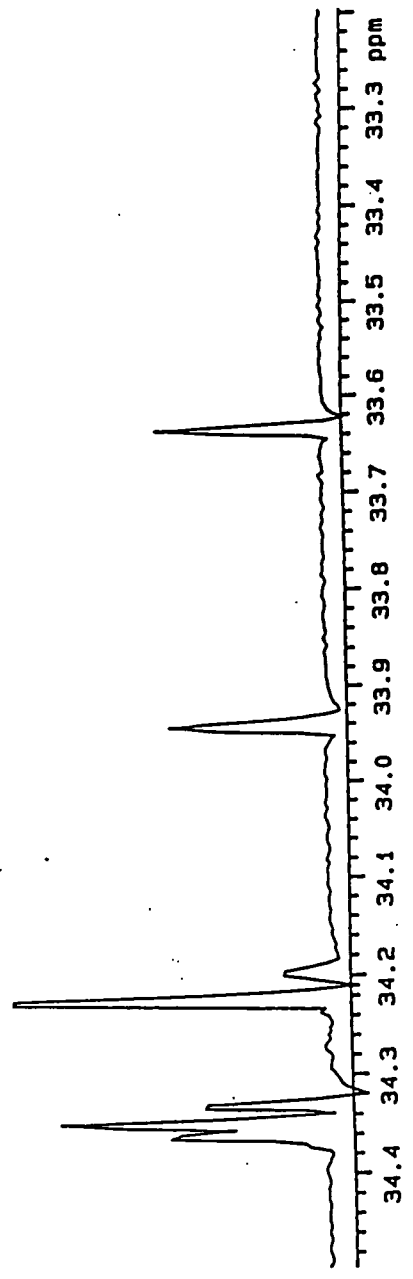
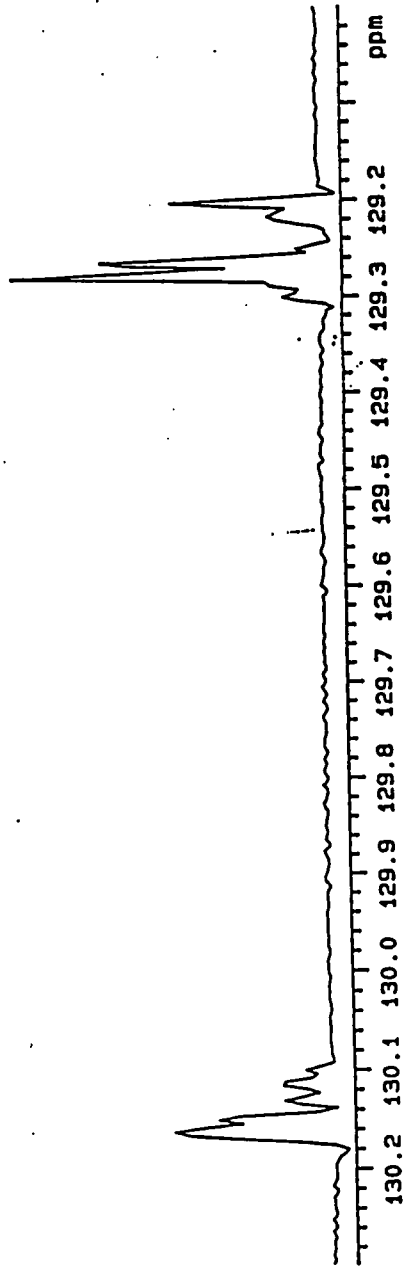
no show
FILE /data/curdatt/ks26mayb.fid
RAN ON May 28 84
SOLVENT COC13
OBSERVE C13



Appendix 6.5.4. DEPT spectrum of P6-7

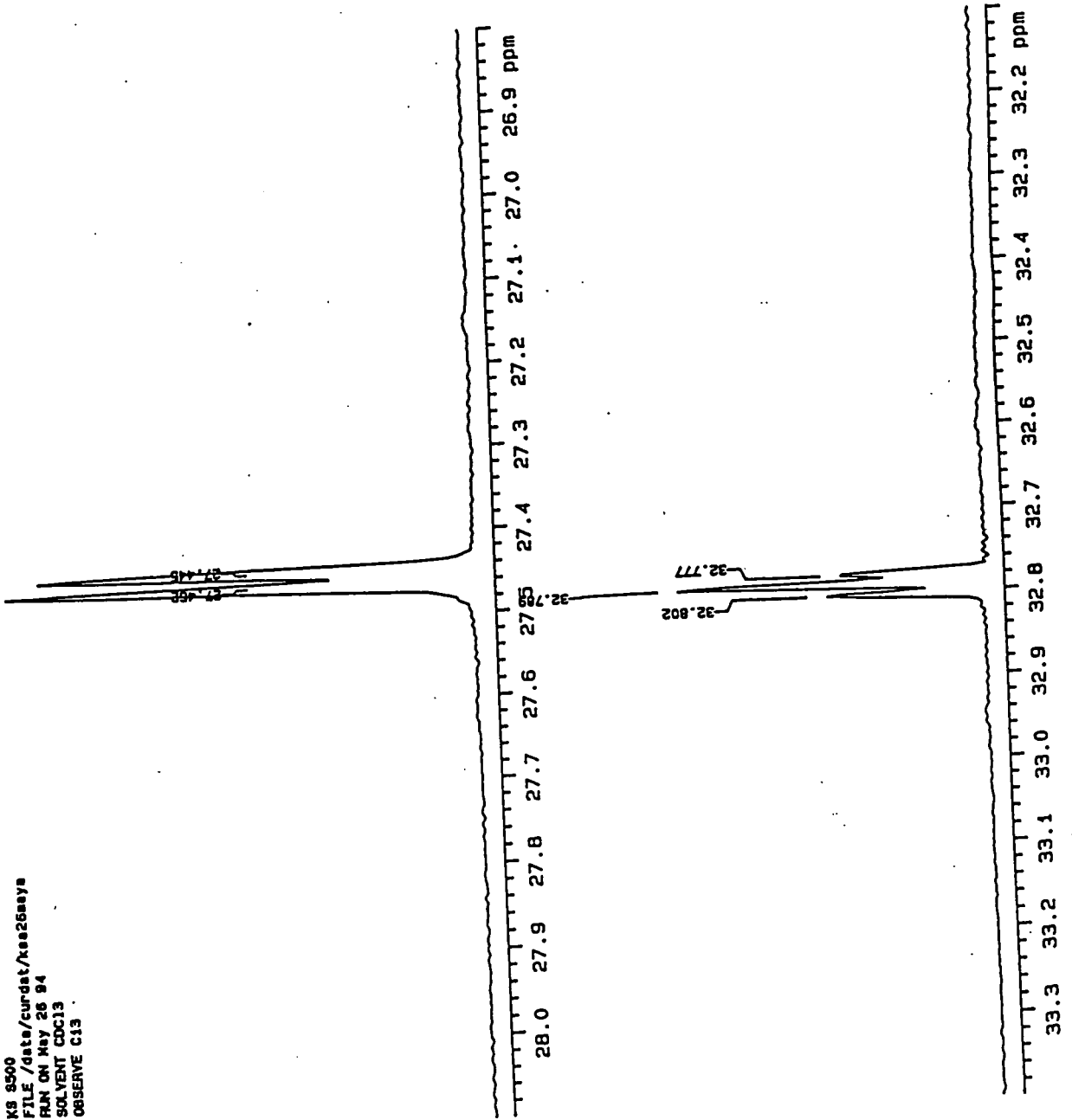


Appendix 6.6.1. Resolution enhancement ¹³C spectrum of P6-2

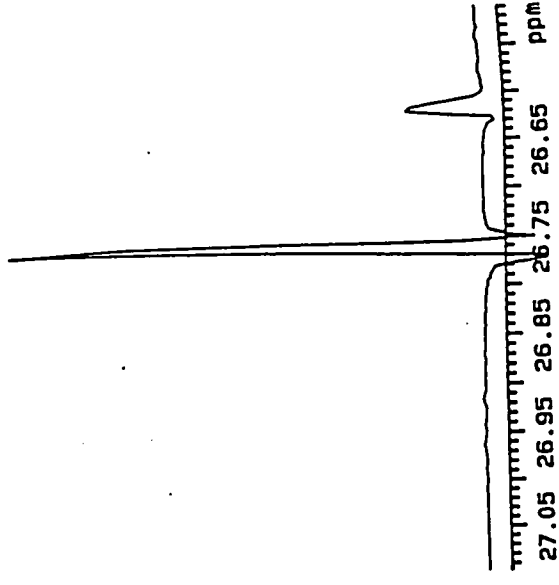
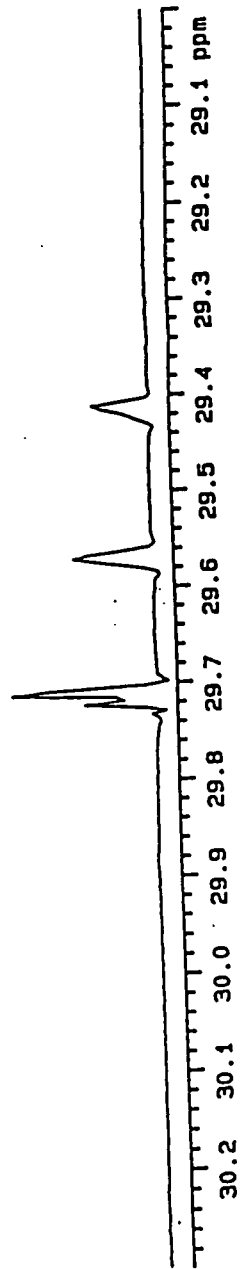
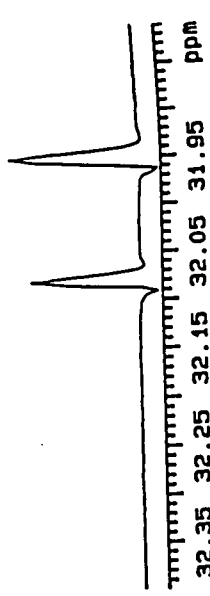
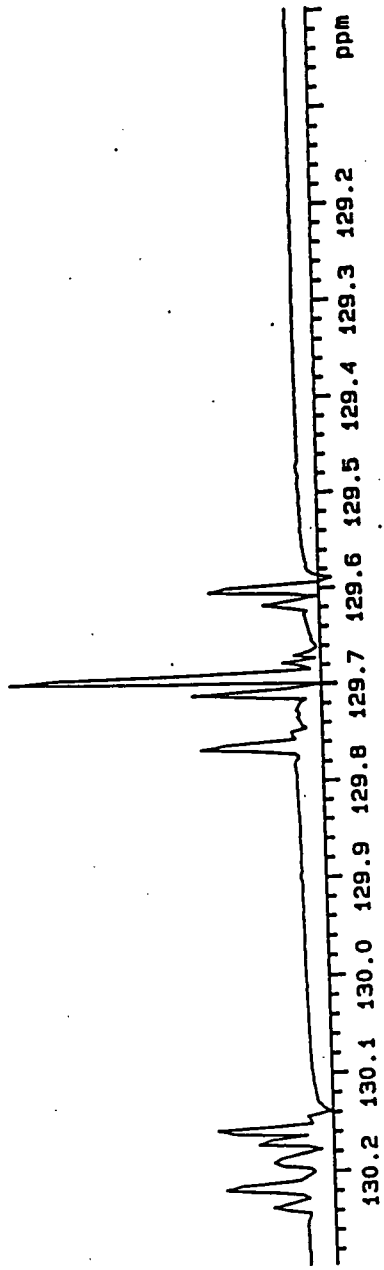


Appendix 6.6.2. Resolution enhancement ¹³C spectrum of P6-4

K3 8500
FILE /esta/curdst/has26aaya
RUN ON May 26 84
SOLVENT CDC13
OBSERVE C13

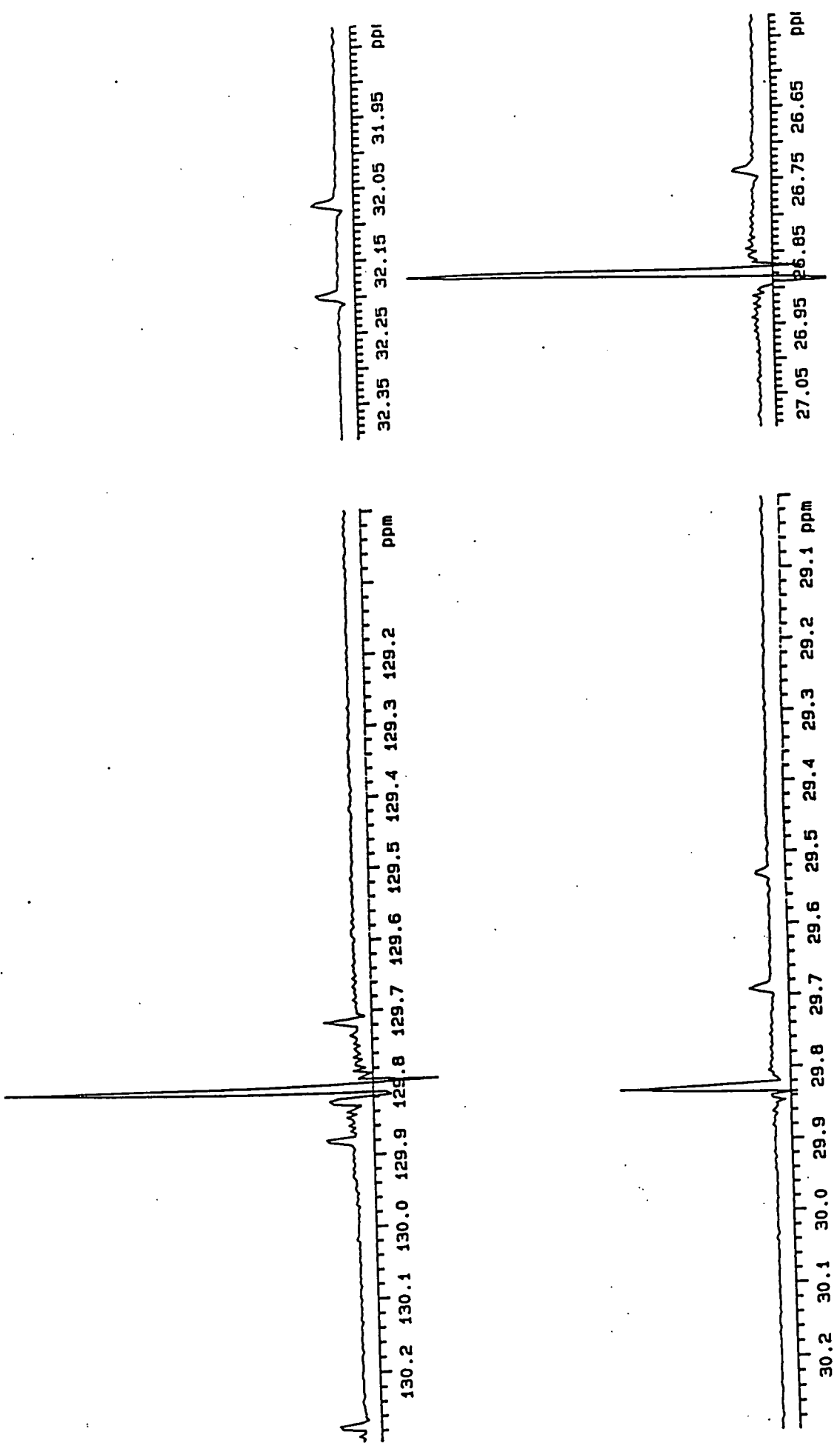


Appendix 6.6.3. Resolution enhancement ^{13}C spectrum of P6-7

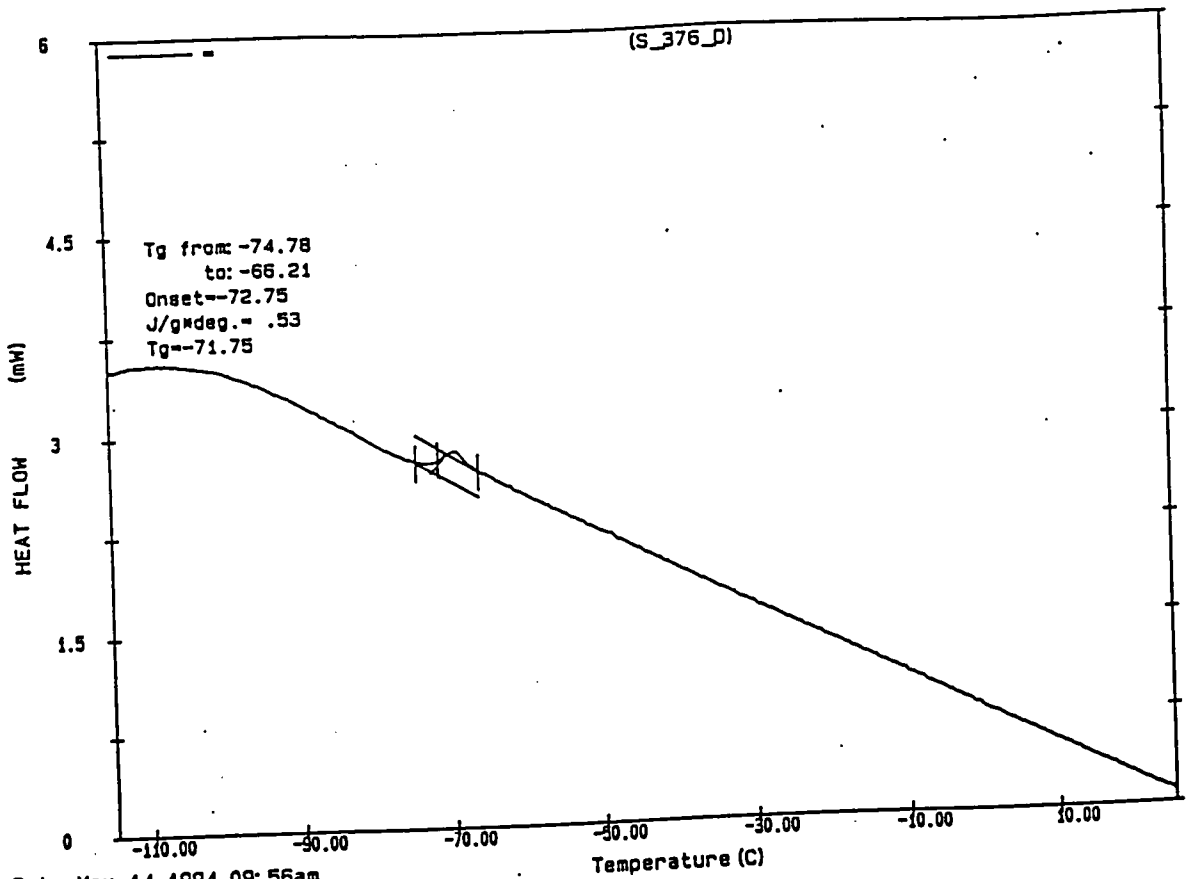


Appendix 6.6.4. Resolution enhancement ¹³C spectrum of P5-2

K9 9366
FILE /data/arch46/kas29nard
RUN ON Mar 29 94
SOLVENT CDC13
OBSERVE C13

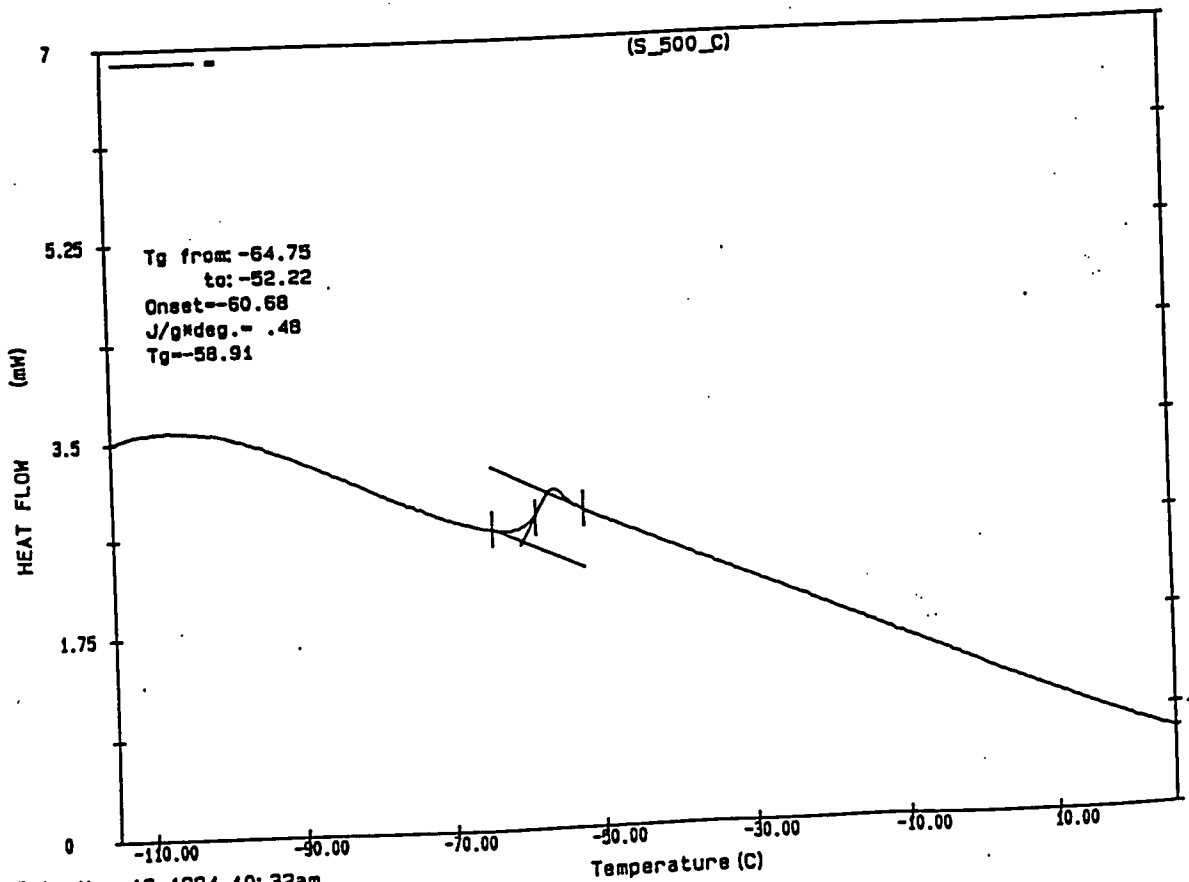


Appendix 6.6.5. Resolution enhancement ^{13}C spectrum of P5-12



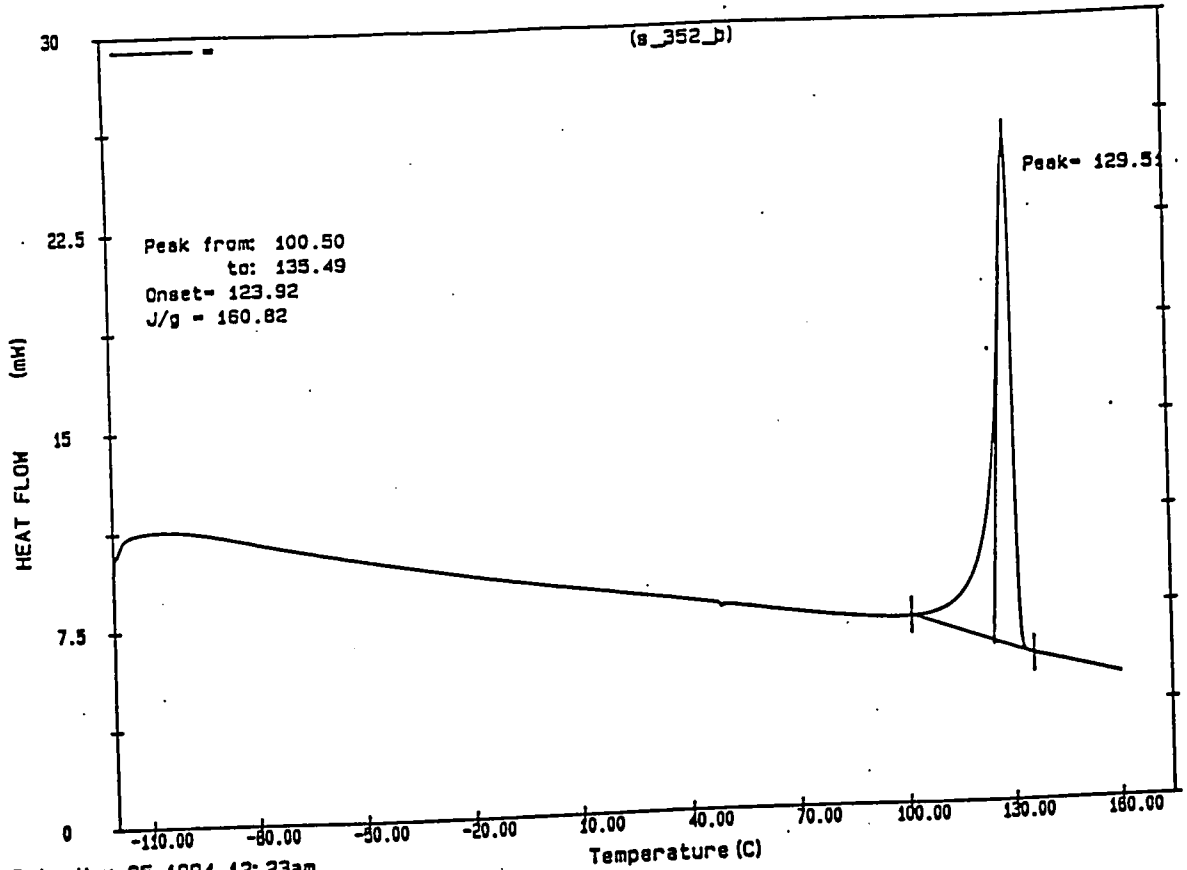
Date: May 14, 1994 09:56am
 Scanning Rate: 10.0 C/min
 Sample Wt: 2.333 mg Path: \GMF\
 File 1: S 376 D

Appendix 6.7.1. DSC trace of P6-4



Date: May 16, 1994 10:32am
 Scanning Rate: 10.0 C/min
 Sample Wt: 6.902 mg Path: \GMF\
 File 1: S 500 C

Appendix 6.7.2. DSC trace of P6-7



Date: May 25, 1994 12: 23am
Scanning Rate: 10.0 C/min
Sample Wt: 4.841 mg Path: \gmf\
File 1: 5 352 B

Appendix 6.7.3. DSC trace of P5-1H (Hydrogenated P5-1)

APPENDIX 7

References

References

1. R. L. Banks and G. C. Bailey, *Ind. Eng. Chem. Prod. Res. Develop.*, **3**, 170, (1964)
2. N. Calderon, K. W. Scott, E. A. Ofstead and W. A. Judy, *J. Am. Chem. Soc.*, **90**, 4133, (1968); *Adv. Chem. Ser.*, **91**, 399, (1968)
3. E. Wasserman, D. A. Ben-Efran and R. J. Wolovsky, *J. Am. Chem. Soc.*, **90**, 3286, (1968)
4. C. P. C. Bradshaw, E. J. Hoeman and L. Turner, *J. Catalysis*, **7**, 269, (1967)
5. A. W. Anderson and M. G. Merckling, U. S. Patent, 2,721,189, (1955)
6. J. R. Kenton, D. L. Crain and R. F. Kleinschmidt, U. S. Patent, 3,491,163
7. W. L. Truett, D. R. Johnson, I. M. Robinson and B. A. Montague, *J. Am. Chem. Soc.*, **82**, 2337, (1960)
8. D. L. Crain, *J. Catalysis*, **13**, 110, (1969)
9. H. C. Eleuterio, U. S. Patent, 3,074,918, (1963)
10. G. Dall'Asta, G. Mazzanti, G. Natta and G. Mortoni, *Macromol. Chem.*, **69**, 163, (1963)
11. G. Dall'Asta, G. Mazzanti and G. Natta, *Angew. Chem.*, **76**, 765, (1964)
12. N. Calderon, E. A. Ofstead and W. A. Judy, *J. Polym. Sci.*, **A1**, **5**, 2209, (1967)
13. N. Calderon, H. Yuchen and K. W. Scott, *Tetrahedron Lett.*, 3327, (1967)
14. W. J. Feast, and V. C. Gibson, "Olefin metathesis" in "The Chemistry of the Metal-Carbon Bond", **Vol. 5**, John Wiley & Sons Ltd., (1989)
15. G. Eastmond, A. Ledwith, S. Russo and P. Sigwalt, "Metathesis Polymerisation" in "Comprehensive Polymer Science", Pergamon Press
16. W. J. Feast, *Proc. A.C.S. Div. Polym. Mater. Sci. Eng.* **58**, 96, (1988)
17. K. J. Ivin and T. Saegusa, "Ring-Opening Polymerisation", Elsevier Applied Science Publishers, (1984)
18. V. Drugatan, A. T. Balaban, M. Dimonie, "Olefin Metathesis and Ring Opening Polymerization of Cyclo-olefins", 2nd edition, Wiley Interscience, (1985)
19. Y. Chauvin, M. Hidai and T. Tatsumi, *Bull. Chem. Soc. Japan*, **45**, 1158, (1972)
20. R. L. Banks, L. F. Heckelsberg and G. C. Bailey, *Ind. Eng. Chem. Prod. Develop.*, **7**, 29, (1968)
21. R. L. Banks, U. S. Patent, 3,261,879, (1966)
22. British Petroleum Co. Ltd., Dutch Patent, 6,511,659, (1966); K. V. Williams and L. Turner, B. P. 1,116,243, (1968)

23. R. L. Banks, L. F. Heckelsberg and G. C. Bailey, *Ind. Eng. Chem. Prod. Develop.*, **8**, 259, (1969)
24. L. F. Heckelsberg, U. S. Patent, 3,340,322, (1967)
25. T. Okuhora and K. I. Tanaka, *J. Catalysis*, **42**, 474, (1976)
26. J. I. O'Hara and C. P. C. Bradshaw, British Patent, 1,283, 348, (1972)
27. E. A. Ofstead and N. Calderon, U. S. Patent, 3,801,559, (1972)
28. E. Verkuijlen and C. Boelhouwer, *Fette. seifen-Anstrick.*, **11**, 444, (1976)
29. N. Calderon, K. W. Scott, E. A. Ofstead and W. A. Judy, A. C. S. Meeting Abs., **L54**, 155, (1968); *J. Am. Chem. Soc.*, **90**, 4133, (1968)
30. G. M. Cragg and E. McWelis, *J. Catalysis*, **38**, 482, (1975)
31. N. Calderon, "Eighth Leeds-Sheffield Symp. on Coord. and Catalysis", April (1976)
32. Y. Chauvin, D. Commerenc and D. Czuypelinck, *Makromol. Chem.*, **177**, 2637, (1976)
33. E. O. Fischer, *Adv. Organomet. Chem.*, **14**, 1, (1976)
34. E. O. Fischer and A. Maasbol, *Angew. Chem., Inter. Ed.*, **3**, 580, (1964)
35. T. J. Katz and N. Acton, *Tetrahedron Lett.*, 4251, (1976)
36. C. P. Casey and T. S. Burkhardt, *J. Am. Chem. Soc.*, **95**, 5833, (1973)
37. C. P. Casey and T. S. Burkhardt, *J. Am. Chem. Soc.*, **96**, 7808, (1974)
38. C. J. Schaverien, J. C. Dewan and R. R. Schrock, *J. Am. Chem. Soc.*, **108**, 2771, (1986)
39. J. S. Murdzek and R. R. Schrock, *Organometallics*, **6**, 1373, (1987)
40. R. R. Schrock, J. Feldman, C. F. Cannizo and R. H. Grubbs, *Macromolecules*, **20**, 1169, (1987)
41. R. R. Schrock, R. T. DePue, J. Feldman, K. B. Yap, W. M. Davies, L. Parks, M. DiMare, M. Schofield, J. Anhaus, E. Walborsky, E. Evitt, C. Kruger and P. Batz, *Organometallics*, **9**, 2262, (1990)
42. R. H. Grubbs, L. K. Johnson, B. M. Novak, D. M. McGarth, A. Benedicto, M. France, S. T. Guyen, M. Cagne, Abs of papers A. C. S., 204, August (1992)
43. T. R. Howard, J. B. Lee and R. H. Grubbs, *J. Am. Chem. Soc.*, **102**, 6876, (1980)
44. D. A. Straus and R. H. Grubbs, *J. Mol. Catal.*, **28**, 9, (1985)
45. D. A. Straus and R. H. Grubbs, *Organometallics*, **1**, 1658, (1982)
46. L. R. Gillion and R. H. Grubbs, *J. Am. Chem. Soc.*, **108**, 733, (1986)
47. M. Brooke, R. S. Matthews and A. C. young, *J. Chem. Soc., Perkin Trans. I*, 1411, (1977) ; G. M. Brooke and A. C. Young, *J. Fluorine Chem.*, 223, (1976)

48. W. J. Feast and L. A. M. Shahada, *Polymer*, 27, 1289, (1986)
49. W. J. Feast and L. A. M. Shahada, *Eur. Polym. J.*, 27, 27, (1991)
50. I. F. A. F. El-Saafin and W. J. Feast, *J. Molecular Catal.*, 15, 61, (1982)
51. G. C. Bazan, E. Khosravi, R. R. Schrock, W. J. Feast, V. C. Gibson, M. B. O'Regan, J. K. Thomas and W. M. Davis, *J. Am. Chem. Soc.*, 112, 8378, (1990)
52. G. Dall'Asta, *Makromol. Chem.*, 154, 1, (1972)
53. G. Dall'Asta and G. Motroni, *Eur. Polym. J.*, 7, 707, (1971)
54. J. L. Herrison and Y. Chauvin, *Makromol. Chem.*, 141, 161, (1970)
55. D. J. Cardin, M. J. Doyle and M. F. Lappert, *J. Chem. Soc. Chem. Comm.*, 927, (1972)
56. R. Streck, paper presented at the Fourth International Symposium on Olefin Metathesis, Belfast, September, (1981)
57. G. Natta, G. Dall'Asta, and G. Mazzanti, *Angew. Chem., Int. Ed.*, 3, 723, (1964)
58. G. Natta, G. Dall'Asta, I. W. Bassi, and G. Carella, *Makromol. Chem.*, 91, 87, (1966)
59. C. P. Casey, L. D. Albin and T. J. Burkhardt, *J. Am. Chem. Soc.*, 99, 2533, (1977)
60. J. G. Hamilton, K. J. Ivin, J. J. Rooney, *IUPAC Macro 82*, Amherst, (1982)
61. K. J. Ivin, "Olefin Metathesis", Academic press, (1983)
62. G. Martin and R. K. Hill, *Chem. Rev.*, 61, 537, (1961)
63. S. Seltzer, *Adv. Alicyclic Chem.*, 2, 1, (1968)
64. B. M. Trost, *J. Am. Chem. Soc.*, 91, 918, (1969)
65. M. P. Cava and M. J. Mitchell, *J. Am. Chem. Soc.*, 81, 5409, (1959)
66. B. Pandey and P. V. Dalvi, *Angew. Chem. Int. Ed. Engl.* 32, 1612, (1993)
67. R. Baker and T. J. Mason, *J. Chem. Soc. (c)*, 596, (1970)
68. E. Khosravi, W. J. Feast, V. C. Gibson, G. Bazan and R. R. Schrock, *Polymer*, 30, 258, (1989)
69. W. J. Feast, V. C. Gibson, E. Khosravi, E. L. Marshall and J. P. Mitchell, *Polymer*, 33, 872, (1992)
70. K. J. Ivin, D. T. Lavery and J. J. Rooney, *Makromol. Chem.*, 178, 1545, (1978)
71. K. J. Ivin, D. T. Lavery, J. J. Rooney and P. Watt, *Recl. Trav. Chim. Pays. Bas.*, 96, M.54, (1977)
72. K. J. Ivin, D. T. Lavery and J. J. Rooney, *Makromol. Chem.*, 179, 253, (1978)
73. K. J. Ivin, Grzegorz-Tapienis and J. J. Rooney, *Polymer*, 21, 436, (1980)

74. K. J. Ivin, Grzegorz-Tapienis and J. J. Rooney, *J. C. S. Chem. Comm.*, 1068, (1979)
75. K. J. Ivin, *Pure and Appl. Chem.*, 52, 1907, (1980)
76. K. J. Ivin, D. Theodore Laverty, B. S. R. Reddy and J. J. Rooney, *Maklomol. Chem. Rapid. Commun.*, 1, 467, (1980)
77. B. Strothers, *Carbon ¹³C NMR Spectroscopy*, Academic Press.
78. P. Tenney, U. S. Patent, 4,136,248, (1979)
79. W. J. Feast, V. C. Gibson and E. L. Marshall, *J. Chem. Soc. Chem. Comm.*, 1157, (1992)
80. S. Krishnamurthy, *J. Organometallic Chem.*, 156, 171, (1978)
81. D. H. R. Barton and S. W. McCombie, *J. Chem. Soc. Perkin I.*, 1975, 1574, (1975)
82. M. J. Robins, J. S. Wilson and F. Hansske, *J. Am. Chem. Soc.*, 105, 4059, (1983), K. K. Ogilvie, G. H. Hakimelahi, Z. A. Proba and N. Usman, *Tetrahedron Lett.*, 24 865, (1983)
83. K. C. Murdock and R. B. Angier, *J. Org. Chem.*, 27, 2395, (1962)
84. J. Meinwald, P. G. Gassman, and J. K. Crandall, *J. Org. Chem.*, 27, 3366, (1962) They used cis-1,4-dibromo-2-butene instead of chloride, but the yield was also poor.
85. G. H. Schmid and A. W. Wolkoff, *J. Org. Chem.*, 32, 254, (1967)
86. A. Hosomi, M. Mikami and H. Sakurai, *Bull. Chem. Soc. Jap.*, 56, 2790(1983)
87. S. E. Cremer and C. Blankenship, *J. Org. Chem.*, 47, 1626, (1982)
88. Jhonson, Keiser and Sharp *J. Org. Chem.*, 34, 862, (1969) They obtained 4-hydroxy cyclopentene by hydroboration of cyclopentadiene, but the yield was poor.
89. A. E. Greene and J.-P. Depres, *J. Org. Chem.*, 49, 928, (1984)
90. A. Hutchison, M. Grim and J. Chen, *J. Heterocyclo Chem.*, 26, 451, (1989)
91. R. O. Huchins, D. Kandasamy, F. Dux III, C. A. Maryanoff, D. Rotstein, B. Goldsmith, W. Burgoyne, J. Dalessandr and J. Puglis, *J. Org. Chem.*, 43, 2259, (1978)
92. S. Krishnamrthy, H. C. Brown. *Org Chem.*, 41, 3064, (1976), R. W. Holder and M. G. Matturro, *J. Org. Chem.*, 42, 2166, (1977)
93. S. Krishnamrthy, *Org. Chem.*, 45, 2550, (1980)
94. C. P. Casey, *Reactive Intermediates*, 2, 135, (1981)
95. G. Dall'Asta, *Rubb. Chem. Technol.*, 47, 511, (1974)
96. R. Streck, *Chem. Ztg.*, 99, 397, (1975)
97. G. Dall'Asta, *Stereo rubbers*, Wiley, New York, (1977)

98. J. J. Rooney and A. Stewart, Chem. Soc. Specialist Periodical Reports, Catalysis, 1, 277, (1977)
99. N. Calderon, J. P. Lawrence and E. A. Ofstead, Adv. Organomet. Chem., 17, 449, (1979)
100. F. Haas, K. Nutz, G. Pampus and D. Theisen, Rubber Chem. Technol., 43, 1116, (1970)
101. G. Pampus, G. Lehnert and D. Maertens, Am. Chem. Soc., Polymer Prepr., 13, 880, (1972)
102. G. Pampus and G. Lehnert, Makromol. Chem., 175, 2605, (1974)
103. I. A. Oreshkin, L. I. Red'kina, I. L. Kershenbaum, G. M. Chernenko, K. L. Makovetskii, E. I. Tinyakova, and B. A. Dolgoplosk, Europ. Polymer J., 13, 447, (1977)
104. M. K. Yakovleva, A. P. Sheinker, E. B. Kotin and A. D. Abkin, Vysokomol. Soedin., B19, 604, (1977)
105. P. Gunther, F. Haas, G. Marwede, K. Nutz, W. Oberkirch, G. Pampus, N. Schon and J. Witte, Angew. Macromol. Chem., 14, 87, (1970)
106. T. J. Katz, S. J. Lee and N. Acton, Tetrahedron Lett., 4251, (1976)
107. A. Kormer, I. A. Poletayeva and T. L. Yufa, J. Polymer. Sci. A-1, 10, 251, (1972)
108. See P. Dounis, Ph. D. Thesis, Durham University, (1994) for a review.
109. J. Carman, C. E. Wilkes, Macromolecules, 7, 40, (1974)
110. R. Streck and H. Weber, Chem. Abstr., 74, 142495, (1971)
111. Tanaka, H. Sato, K. Hatada and Y. Terawaki, Makromol. Chem., 178, 1823, (1977)
112. Pasquon and V. Giannini, "Stereoregular linear polymers" in "Encyclopedia of polymer science and engineering", 2nd edition, V.15, 632, Wiley International, (1985)
113. R. R. Schrock, S. A. Krouse, K. Knoll, J. Feldman, J. S. Murdzek and D. C. Yang, J. Molecular Catalysis, 46, 243, (1988)
114. R. R. Schrock, K. B. Yap, D. C. Yang, H. Sitzmann, L. R. Sita and G. C. Bazan, Macromolecules, 22, 3191, (1989)
115. S. J. Lee, J. McGinnis and T. J. Katz, J. Am. Chem. Soc., 98, 7818, (1976)
116. J. Levisalles, H. Rudler and D. Villemin, Rec. Trav. Chim. Pays Bas., 96, M138, (1977) 54
117. G. Dall'Asta and G. Motroni, Chim. Ind. (Milan), 972, (1968)
118. A. Ofstead, and N. Calderon, Makromol. Chem., 154, 21, (1972)

119. H. Lammens, G. Sartori, J. Siffert and N. Sprecher, *J. Polym. Sci., Polym. Lett.*, **9**, 341, (1971), and J. T. Anhaus, V. C. Gibson, W. Clegg and S. P. Collingwood, *Organometallics*, **12**, 1780, (1993)
120. J. G. Hamilton, K. J. Ivin and J. J. Rooney, *Brit. Pol. Journal*, **16**, 21, (1984)
121. H. J. Harwood, D. B. Russel, J. J. A. Verthe and J. Zymonas, *Macromol. Chem.*, **163**, 1, (1973)
122. N. J. Cusack, C. B. Reese, A. C. Risius and B. Roozpeikar, *Tetrahedron*, **32**, 2157, (1976)
123. S. Hunig, H. R. Muller and W. Thier, *Angew. Chem. Internat. Edit.*, **4**, 271, (1965)
124. J. L. Koenig, "Chemical Microstructure of Polymer Chains", John Wiley & Sons, (1980)
125. J. Brandrup, E. H. Immergut, "Polymer Handbook", 2nd ed., John Wiley & Sons, (1975)
126. V. M. Cherednichenko, *Polymer Sci. USSR.*, **A20**, 1225, (1979)

APPENDIX 8

Lectures and conferences attended by the author

UNIVERSITY OF DURHAM
Board of Studies in Chemistry
Colloquia, Lectures and Seminars given by Invited Speakers

1992

- October 28 Dr. J. K. Cockroft, (Durham University).
Recent Developments in Powder Diffraction
- October 29 Dr. J. Emsley, (Imperial College, London).
The Shocking History of Phosphorus.
- November 4 Dr. T. Kee, (University of Leeds).
Synthesis and Coordination Chemistry of Silylated Phosphites.
- November 5 Dr. C. J. Ludman, (University of Durham).
Explosions, A Demonstration Lecture.
- November 11 Prof. D. Robins, (Glasgow University).
Pyrrolizidine Alkaloids: Biological Activity, Biosynthesis and Benefits.
- November 12 Prof. M. R. Truter, (University College, London).
Luck and Logic in Host-Guest Chemistry.
- November 18 Dr. R. Nix, (Queen Mary College, London).
Characterisation of Heterogeneous Catalysts.
- November 25 Prof. Y. Vallee (University of Caen)
Reactive Thiocarbonyl Compounds.
- December 2 Dr. R. A. Aitkin, (University of St. Andrews).
The Versatile Cycloaddition Chemistry of Bu_3PCl_2 .
- December 3 Prof. P. Edwards, (Birmingham University).
SCI Lecture
What is a Metal?
- December 9 Dr. A. N. Burgess, (ICI Runcorn).
The Structure of Perfluorinated Ionomer Membranes.

1993

- January 20 Dr. D. C. Clary, (University of Cambridge).
Energy Flow in Chemical Reactions.
- January 21 Prof. L. Hall, (University of Cambridge).
NMR - A Window to the Human Body.
- February 3 Prof. S. M. Roberts, (University of Exeter).
Enzymes in Organic Synthesis.
- February 10 Dr. D. Gillies, (University of Surrey).
NMR and Molecular Motion in Solution.

- February 11 Prof. S. A. R. Knox, (Bristol University).
Tilden Lecture Organic Chemistry at Polynuclear Metal Centres.
- February 17 Dr. R. D. W. Kemmitt, (University of Leicester).
Oxatrimethylenemethane Metal Complexes.
- February 18 Dr. I. Fraser, (ICI, Wilton).
Reactive Processing of Composite Materials.
- February 22 Prof. D. M. Grant, (University of Utah).
Single Crystals, Molecular Structure and Chemical-Shift
Anisotropy
- February 24 Prof. C. J. M. Stirling, (University of Sheffield).
Chemistry on the Flat-Reactivity of Ordered Systems.
- March 3 Dr. K. J. P. Williams, (BP).
Raman Spectroscopy for Industrial Analysis.
- March 10 Dr. P. K. Baker, (University College of North Wales, Bangor).
An Investigation of the Chemistry of the Highly Versatile
7-Coordinate Complexes $[M_2(CO)_3(NCMe)_2]$ (M=Mo,W).
- March 11 Dr. R. A. Jones, (University of East Anglia).
The Chemistry of Wine Making.
- March 17 Dr. R. J. K. Taylor, (University of East Anglia).
Adventures in Natural Product Synthesis.
- March 24 Prof. I. O. Sutherland, (University of Liverpool).
Chromogenic Reagents for Chiral Amine Sensors.
- May 13 Prof. J. A. Pople, (Carnegie-Mellon University Pittsburgh).
Boys-Rahman Lecture Applications of Molecular Orbital Theory.
- May 21 Prof. L. Weber, (University of Bielefeld).
Metallo-phospha Alkenes as Synthons in Organometallic
Chemistry.
- June 1 Prof. J. P. Konopelski, (University of California, Santa Cruz).
Synthetic Adventures with Enantiomerically Pure Acetals.
- June 7 Prof. R. S. Stein, (University of Massachusetts).
Scattering Studies of Crystalline and Liquid Crystalline
Polymers.
- June 16 Prof. A. K. Covington, (University of Newcastle).
Use of Ion Selective Electrodes as Detectors in Ion
Chromatography.
- June 17 Prof. O. F. Nielsen, (H.C.Orsted Institute, University of
Copenhagen).
Low Frequency IR and Raman Studies of Hydrogen Bonded Liquids.

- October 4 Prof. F. J. Fehler, (University of California at Irvine).
Bridging the Gap Between Surfaces and Solution with
Sessilquioxanes.
- October 20 Dr. P. Quayle, (University of Manchester).
Aspects of Aqueous ROMP Chemistry.
- October 23 Prof. R. Adams, (University of S. Carolina).
The Chemistry of Metal Carbonyl Cluster Complexes
Containing Platinum and Iron, Ruthenium or Osmium and the
Development of a Cluster Based Alkyne Hydrogenation
Catalyst.
- October 27 Dr. R. A. L. Jones, (Cavendish Laboratory).
Perambulating Polymers.
- November 10 Prof. M. N. R. Ashfold, (University of Bristol).
High Resolution Photofragment Translational Spectroscopy: A
New Way to Watch Photodissociation
- November 17 Dr. A. Parker, (Laser Support Facility)
Applications of Time Resolved Resonance Raman
Spectroscopy to Chemical and Biological Problems.
- November 24 Dr. P. G. Bruce, (University of St. Andrews).
Synthesis and Applications Inorganic Materials.
- December 1 Prof. M. A. McKervy, (Queen University, Belfast).
Functionalised Calixarenes.

1994

- January 26 Prof. J. Evans, (University of Southampton).
Shining Light on Catalysts.
- February 2 Dr. A. Masters, (University of Manchester).
Modelling Water without Using Pair Potentials.
- February 9 Prof. D. Young, (University of Sussex).
Chemical and Biological Studies on the Coenzyme
Tetrahydrofolic Acid.
- February 16 Dr. R. E. Mulvey, (University of Strathclyde).
Structural Patterns in Alkali Metal Chemistry.
- March 2 Dr. C. Hunter, (University of Sheffield).
Non Covalent Interactions between Aromatic Molecules.

The author has also attended the following lectures in the IRC in Polymer Science and Technology International Seminar Series.

1992

September 21 Prof. E. L. Thomas, (MIT, Cambridge, Massachusetts), at Leeds University.
Interface Structures in Copolymer-Homopolymer Blends.

1993

April 1 Prof. H. W. Speiss, (Max-Planck Institute for Polymerforschung, Mainz), at Durham University.
Multidimensional NMR Studies of Structure and Dynamics of Polymers.

June 2 Prof. F. Ciardelli, (University of Pisa), at Durham University.
Chiral Discrimination in the Stereospecific Polymerisation of α -olefins.

June 8 Prof. B. E. Eichinger, (BIOSYM Technologies Inc. San Diego), at Leeds University.
Recent Polymer Modelling Results and a Look into the Future.

July 6 Prof. C. W. Macosko, (University of Minnesota, Minneapolis).
at Bradford University.
Morphology Development in Immiscible Polymer Blending.

CONFERENCES / MEETINGS ATTENDED BY THE AUTHOR

April 6-8 1993

Macro Group (UK) "Aspects of Contemporary Polymer Chemistry", at Lancaster University

June 27-July 2 1993

Tenth International Symposium on Olefin Metathesis, Tihany-University of Veszpre, Hungary.

April 19-21 1994

Macro Group (UK) Family Conference, "Making, Breaking and Using Chains" at Birmingham University.

